

Design and Evolution of Enzymes with New Catalytic Mechanisms

A thesis submitted to the University of Manchester for the degree of
Doctor of Philosophy in the Faculty of Science and Engineering

2021

Rebecca Crawshaw

School of Natural Sciences, Department of Chemistry

Table of Contents

Abbreviations.....	8
Abstract: Design and Evolution of Enzymes with New Catalytic Mechanisms	11
Declaration and Copyright Statement	13
Acknowledgements.....	14
Chapter 1: Introduction	15
1.1 Directed evolution	16
1.2 Repurposing Nature's Enzymes	17
1.2.1 Sitagliptin.....	17
1.2.2 Islatravir.....	19
1.2.3 MAO-N	21
1.3 Engineering Enzymes with New Function.....	22
1.3.1 Engineering Enzymes with Mechanistic Promiscuity.....	23
1.3.2 Genetic Code Expansion	27
1.4 Approaches to Enzyme Design	29
1.4.1 Catalytic antibodies.....	29
1.4.2 Computational enzyme design.....	31
1.4.2.1 Kemp eliminase.....	32
1.4.2.2 Diels-Alderase.....	35
1.4.2.3 Retro-aldolase.....	37
1.5 Morita-Baylis-Hillman reaction	40
1.5.1 <i>De novo</i> design attempt of a MBHase.....	41
1.6 References	43
Chapter 2: Aims	49
Chapter 3: An Efficient and Enantioselective <i>de novo</i> Enzyme for the Morita-Baylis-Hillman Reaction	50
3.1 Foreword.....	50
3.2 Author contributions	50
3.3 Manuscript	51
3.4 References.....	62

Chapter 4: Synthetic Utility of a <i>de novo</i> Morita-Baylis-Hillmanase	64
4.1 Foreword	64
4.2 Author contributions.....	64
4.3 Abstract	64
4.4 Introduction.....	65
4.5 Results	66
4.6 Conclusion.....	69
4.7 References	70
Chapter 5: Design and Evolution of an Enzyme with a Non-Canonical Organocatalytic Mechanism.....	72
5.1 Foreword	72
5.2 Author contributions.....	72
5.3 Manuscript.....	73
5.4 References	82
Chapter 6: Conclusions and Outlook.....	84
Chapter 7: Experimental	86
7.1 Foreword	86
7.2 Supporting Information for Chapter 3: An Efficient and Enantioselective <i>de novo</i> Enzyme for the Morita-Baylis-Hillman Reaction	86
7.2.1 Methods	86
7.2.1.1 Materials.....	86
7.2.1.2 Construction of pBbE8k_BH32 and variants	86
7.2.1.3 Protein production and purification	86
7.2.1.4 Inhibition of BH32 variants.....	87
7.2.1.5 Mass spectrometry	87
7.2.1.6 Library construction	89
7.2.1.7 Shuffling by overlap extension PCR	90
7.2.1.8 Library screening.....	90
7.2.1.9 General procedure for analytical scale biotransformations.....	91
7.2.1.10 Chromatographic analysis	92

7.2.1.11 Preparative scale biotransformation	92
7.2.1.12 Kinetic characterization	93
7.2.1.13 Preparation of product standards 3 and S1.[4].....	93
7.2.1.14 Preparation of inhibitor 4.....	93
7.2.1.15 Preparation of chiral standards	94
7.2.1.16 Crystallization, refinement and model building.....	94
7.2.1.17 Molecular Docking	94
7.2.1.18 DFT Modelling	95
7.2.1.19 References	95
7.2.2 Extended Data	97
7.2.2.1 Extended Data Figure 1.....	97
7.2.2.2 Extended Data Figure 2.....	98
7.2.2.3 Extended Data Figure 3.....	99
7.2.2.4 Extended Data Figure 4.....	100
7.2.2.5 Extended Data Figure 5.....	101
7.2.2.6 Extended Data Figure 6.....	102
7.2.2.7 Extended Data Figure 7.....	103
7.2.2.8 Extended Data Figure 8.....	104
7.2.2.9 Extended Data Table 1.....	105
7.2.3 Supplementary Information	106
7.2.3.1 BH32.10 DNA and protein sequence.....	106
7.2.3.2 Supplementary Information Table 1.....	110
7.2.3.3 Supplementary Information Table 2.....	110
7.2.3.4 Supplementary Information Table 3.....	110
7.3 Supporting Information for Chapter 4: Synthetic Utility of a <i>de novo</i> Morita-Baylis-Hillmanase	128
7.3.1 Methods	128
7.3.1.1 Materials.....	128
7.3.1.2 Protein production and purification	128

7.3.1.3 General procedure for the preparation of racemic product standards (3, 5a, 5c-k & m-t).....	128
7.3.1.4 General procedure for analytical scale biotransformations.....	133
7.3.1.5 Chromatographic analysis.	133
7.3.1.6 References.....	133
7.3.2 Supplementary Information	135
7.3.2.1 DNA and protein sequence for variants BH32.6 and BH32.10...	135
7.3.2.2 Supplementary Information Table 1	136
7.3.2.3 Supplementary Information Table 2.....	137
7.4 Supporting Information for Chapter 5: Design and Evolution of an Enzyme with a Non-Canonical Organocatalytic Mechanism	138
7.4.1 Methods	138
7.4.1.1 Materials.....	138
7.4.1.2 Construction of pBbE8k_BH32 and variants.....	138
7.4.1.3 Construction of pEVOL_PyIRS _{Me-His} /tRNA _{CUA}	138
7.4.1.4 Construction of pET29_CUT190.....	138
7.4.1.5 Protein production and purification.	138
7.4.1.6 Inhibition of BH32 and OE1 variants.....	139
7.4.1.7 Mass spectrometry	139
7.4.1.8 Library construction and screening	140
7.4.1.9 Shuffling by overlap extension PCR	140
7.4.1.10 Library screening.....	140
7.4.1.11 Steady-state kinetic assays	141
7.4.1.12 Substrate profiling of OE1 and OE1.3.....	142
7.4.1.13 General method for the synthesis of fluorescein esters from the corresponding acid chloride[4].....	142
7.4.1.14 Crystallization, refinement and model building.....	144
7.4.1.15 Data availability	144
7.4.1.16 References.....	145
7.4.2 Extended Data	146

7.4.2.1 Extended Data Figure 1.....	146
7.4.2.2 Extended Data Figure 2.....	147
7.4.2.3 Extended Data Figure 3.....	148
7.4.2.4 Extended Data Figure 4.....	149
7.4.2.5 Extended Data Figure 5.....	150
7.4.2.6 Extended Data Figure 6.....	151
7.4.2.7 Extended Data Figure 7.....	152
7.4.2.8 Extended Data Figure 8.....	153
7.4.2.9 Extended Data Table 1.....	154
7.4.2.10 Extended Data Table 2.....	155
7.4.3 Supplementary Information	156
7.4.3.1 DNA and protein sequence of the most active variant OE1.3	156
7.4.3.2 DNA and protein sequence of cutinase CUT190 S226P/R228S	157
7.4.3.3 Supplementary Information Table 1.....	158
7.4.3.4 Supplementary Information Table 2.....	160
7.4.3.5 NMR Spectra.....	161
Chapter 8: Engineering an Efficient and Enantioselective Enzyme for the Morita-Baylis-Hillman Reaction	168
8.1 Foreword.....	168
8.2 Author Contributions	168
8.3 Manuscript	169
8.4 References.....	181
8.5 Supplementary Information	184
8.5.1 Methods	184
8.5.2 Supplementary Figures	184
Chapter 9: Enzyme Design and Engineering Pave the Road to Fully Programmable Protein Catalysis	240
9.1 Foreword.....	240
9.2 Abstract.....	240
9.3 Introduction	240

9.3.1 Artificial Metalloenzymes	242
9.3.2 Enzymes with Non-Canonical Organocatalytic Groups.....	245
9.3.3 Designing Enzymes to Stabilize Rate-Limiting Transition States	246
9.3.4 A Roadmap to Better Designer Enzymes	250
9.4 References.....	254

Word count: 83,993

Abbreviations

2xYT	yeast extract and tryptone broth
AcK	acetate kinase
BpA	benzophenone-alanine
CASTing	combinatorial active site saturation testing
CPK	Corey–Pauling–Koltun
DAB	3,3'-diaminobenzidine
DABCO	1,4-diazabicyclo[2.2.2]octane
DERA	Deoxyribose 5-phosphate aldolase
DMAP	4-dimethylaminopyridine
DMSO	dimethyl sulfoxide
DNA	deoxyribonucleic acid
DFT	density functional theory
dNTP	deoxynucleotide triphosphate
<i>E. coli</i>	<i>Escherichia coli</i>
e.e	enantiomeric excess
ERED	ene reductase
FACS	fluorescence activated cell sorting
FADS	fluorescent activated droplet sorting
FDP	fructose-1,6-diphosphate
FEM	feature enhanced electron density maps
FMN	flavin mononucleotide
GluER	<i>Gluconobacter oxydans</i> ene reductase
GOase	galactose oxidase
HAD	haloacid dehalogenase
HPLC	high pressure liquid chromatography
HRP	horse radish peroxidase
HTP	High-throughput

KRED	ketoreductase
LB	lysogeny broth
LKADH	<i>Lactobacillus kefir</i> alcohol dehydrogenase
MAO-N	monoamine oxidase from <i>Aspergillus niger</i>
MBH	Morita-Baylis-Hillman
MBHase	Morita-Baylis-Hillmanase
Me-His	<i>N</i> ₆ -methylhistidine
MD	molecular dynamics
MS	mass spectrometry
NAD	nicotinamide adenine dinucleotide
NADPH	nicotinamide adenine dinucleotide phosphate
NBA	4-nitrobenzaldehyde
ncAA	non-canonical amino acid
NEM	<i>N</i> -ethylmaleimide
NMI	<i>N</i> -methylimidazole
NMR	nuclear magnetic resonance
OD	optical density
OE	Organocatalytic Esterase
P450	P450 monooxygenase
PanK	pantothenate kinase
pAF	<i>para</i> -aminophenylalanine
pAzF	<i>para</i> -azidophenylalanine
PBS	phosphate buffered saline
PCR	polymerase chain reaction
PDB	Protein Data Bank
PLP	Pyridoxal 5'-phosphate
PNP	purine nucleoside phosphorylase
PPM	Phosphopentomutase

PSP	photosensitiser protein
QM	quantum mechanic
RasADH	<i>Ralstonia</i> alcohol dehydrogenase
RDS	rate determining step
r.m.s.d.	root-mean-square deviation
s.d.	standard deviation
SDS-PAGE	sodium dodecyl sulphate polyacrylamide gel electrophoresis
sfYFP	superfolder yellow fluorescent protein
TA	Transaminase
TCEP	Tris(2-carboxyethyl)phosphine
TCTD	tetrachlorothiophene dioxide
THF	tetrahydrofuran
TSA	transition state analogue
UV	ultraviolet

Abstract: Design and Evolution of Enzymes with New Catalytic Mechanisms

A thesis submitted to The University of Manchester for the degree of Doctor of Philosophy in the Faculty of Science and Engineering (School of Natural Sciences, Department of Chemistry), 2021

Rebecca Crawshaw

The combination of computational design and directed evolution could offer a general strategy to create enzymes with new functions. To date, this approach has delivered *de novo* enzymes for a handful of model reactions, selected based on previous achievements with catalytic antibodies. In this thesis we show that new catalytic mechanisms can be engineered into proteins to accelerate valuable chemical transformations for which no natural enzymes or catalytic antibodies are known. Evolutionary optimisation of a primitive designed 'enone-binding protein' (BH32) afforded a highly efficient and enantioselective enzyme (BH32.10) that catalysed the Morita-Baylis-Hillman (MBH) reaction. BH32.10 is suitable for preparative scale transformations, accepts a broad range of aldehyde and enone coupling partners, and is able to promote highly selective mono-functionalisations of dialdehydes. Crystallographic, biochemical and computational studies reveal that evolution has led to a sophisticated catalytic mechanism comprising a His23 nucleophile paired with a fortuitously positioned Arg124. This catalytic arginine serves as a genetically encoded surrogate of privileged bidentate hydrogen bonding catalysts (e.g. thioureas), which promote a wide range of reactions in organic synthesis.

In a separate study, we have exploited an expanded genetic code to develop *de novo* hydrolases in the BH32 scaffold that employ Me-His as a non-canonical catalytic nucleophile. This study showcases how the integration of new functional components into enzyme design and evolution workflows can open up new modes of reactivity in protein active sites. Combined, the research presented in this thesis describes new approaches to generate enzymes with catalytic mechanisms not seen in Nature, which will guide the development of *de novo* enzymes for a broader range of chemical transformations in the coming years.

The research carried out during this PhD is presented as a series of manuscripts that are either published, in review or planned for submission at peer-reviewed journals. The research has been presented in this manner as the majority of the candidate's research has been published or is at a suitable stage for the preparation of draft manuscripts. Furthermore, the prepared research manuscripts lend themselves to a clear narrative and their preparation has taken equal time and consideration to that of a traditional thesis.

The contents are organised as followed:

Chapter 1: an introduction into the field of biocatalysis and enzyme engineering;

Chapter 2: aims of the PhD project;

Chapter 3: a research article describing the design and evolution of an enantioselective enzyme for the Morita-Baylis-Hillman reaction;

Chapter 4: a research article describing the substrate scope of an engineered enzyme for the Morita-Baylis-Hillman reaction;

Chapter 5: a research article describing the design and evolution of an enantioselective hydrolase with a non-canonical catalytic mechanism;

Chapter 6: conclusions of the thesis and future outlook;

Chapter 7: manuscript supporting information including materials and methods.

Chapter 8: accepted manuscript of Chapters 3 and 4, including supporting information and materials and methods.

Chapter 9: a review article discussing recent progress in the field of enzyme design and engineering.

Declaration and Copyright Statement

No portion of the work referred to in the thesis has been submitted in support of an application for another degree or qualification of this or any other university or other institute of learning.

- i. The author of this thesis (including any appendices and/or schedules to this thesis) owns certain copyright or related rights in it (the "Copyright") and s/he has given The University of Manchester certain rights to use such Copyright, including for administrative purposes.
- ii. Copies of this thesis, either in full or in extracts and whether in hard or electronic copy, may be made only in accordance with the Copyright, Designs and Patents Act 1988 (as amended) and regulations issued under it or, where appropriate, in accordance with licensing agreements which the University has from time to time. This page must form part of any such copies made.
- iii. The ownership of certain Copyright, patents, designs, trademarks and other intellectual property (the "Intellectual Property") and any reproductions of copyright works in the thesis, for example graphs and tables ("Reproductions"), which may be described in this thesis, may not be owned by the author and may be owned by third parties. Such Intellectual Property and Reproductions cannot and must not be made available for use without the prior written permission of the owner(s) of the relevant Intellectual Property and/or Reproductions.
- iv. Further information on the conditions under which disclosure, publication and commercialisation of this thesis, the Copyright and any Intellectual Property and/or Reproductions described in it may take place is available in the University IP Policy (see <http://documents.manchester.ac.uk/DocuInfo.aspx?DocID=24420>), in any relevant Thesis restriction declarations deposited in the University Library, The University Library's regulations (see <http://www.library.manchester.ac.uk/about/regulations/>) and in The University's policy on Presentation of Theses.

Acknowledgements

Firstly, I would like to thank my PhD supervisor, Dr. Anthony Green for his unwavering support during my PhD. His guidance, knowledge, motivation, and confidence in me has helped me develop into the researcher I am today, and I am forever grateful. Being in the Green group from early beginnings to where we are now has been a privilege, with the chance to work on a vast array of innovative projects that have broadened my skill set immensely. I want to also take this opportunity to thank Dr. Sarah Lovelock, who has been like a second supervisor to me. Her guidance and knowledge has taught me so much, and I would not have made many of the achievements I have without her. The Lovelock group is incredibly lucky to have you!

I would also like to thank Dr. Mary Ortmyer who supervised me during the early stages of my PhD, and for her friendship and support throughout my time in the Green group. The HPLC facility at the MIB has been essential to my work and would not be anywhere near as streamlined without the hard work and dedication of Rehana Sung- thank you for all your advice and chats! A special mention must also go to Colin Levy of the Manchester Protein Structure facility for all his patience and guidance throughout my crystallisation efforts.

I would like to acknowledge all members of the Green and Lovelock groups for making my time here so wonderful and enjoyable, the support and has been incredible both in and out of the lab. A particular special mention must go to my best friend from the beginning Ashleigh Burke- it was just us for so long! Thank you for your friendship as well as all the advice you have given me along the way, good luck in all that you do- you are going to do so well! I would also like to acknowledge Amy Crossley for all her help and support during the final stages of my PhD, I would not have achieved so much without your help, good luck in your PhD and whatever the future holds for you.

Particular thanks must also go to Ross Smithson for everything he's done for me, from proof-reading my thesis and helping me prepare for my viva, to much needed sanity checking. To Richard Obexer and Florence Hardy for proof-reading my thesis, and together with Christopher Taylor, Caitlin Swaby and Ewan Moody, for their friendships in and out of the lab. I have managed to make some friends for life during this PhD and I am incredibly grateful to you all. Finally, I must say thank you to my friends and family, especially Mum, Dad, Mabel and Nellie without whom I would not be where I am today.

Chapter 1: Introduction

In Nature, enzymes catalyse a diverse array of complex biochemical transformations with remarkable efficiency and selectivity under mild reaction conditions. These properties make enzymes highly attractive as biocatalysts for the cost-effective and sustainable production of pharmaceuticals, speciality chemicals and commodity chemicals.[1-2] Biocatalysis is now seen as a key route to the development of a greener chemical industry. Advances in DNA synthesis and sequencing services, bioinformatics tools and computational modelling methods, and workflows for high-throughput structural and biochemical enzyme characterisation, have led to the generation of enzymes which have played important roles in numerous industrial processes.[3-7] In the mid-twentieth century, pharmaceutical companies employed enzymes such as cytochrome P450 monooxygenases for the regio- and stereoselective hydroxylation of steroids such as progesterone **1** and 17 α -hydroxyprogesterone **2**, producing key aldosterone and cortisone intermediates 11-deoxycorticosterone **3** and 11-deoxycortisol **4**, respectively, (Figure 1).[8-9] However, wild-type enzymes are rarely optimal for industrial application, often displaying low solvent tolerance, stability and a poor substrate scope. To expand their practical utility, protein engineering strategies such as directed evolution have emerged as a powerful method to tailor biocatalysts to a desired application. This route also allows for the development of enzymes that promote non-natural reactions with high efficiency and selectivity, further expanding the synthetic utility of biocatalysts.

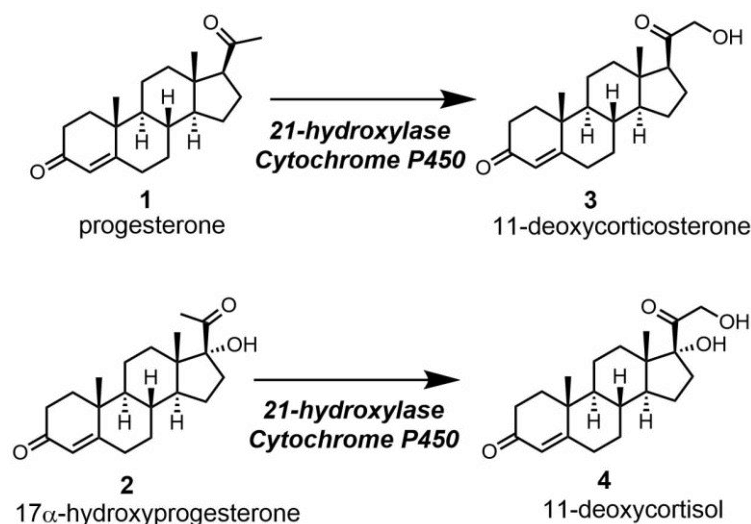


Figure 1: The hydroxylation of steroids by recombinant Cytochrome P450s. Cytochrome P450 21-hydroxylase catalyses the conversion of progesterone **1** to the aldosterone precursor 11-deoxycorticosterone **3**, and the conversion of 17 α -hydroxyprogesterone **2** to the cortisone precursor 11-deoxycortisol **4**. [8-9]

1.1 Directed evolution

Directed evolution is an iterative process that mimics Darwinian evolution *in vitro* and provides a versatile and powerful strategy for tuning and optimising enzyme properties for desired applications (Figure 2).[10,11] It comprises three main steps: the identification of a suitable enzyme displaying promiscuous activity towards a given reaction, gene diversification of the selected enzyme generating DNA libraries, and protein production and screening, which leads to the identification of variants with improved characteristics. During the transformation of host cells, such as *E.coli*, each cell takes up a single clone leading to spatial separation of library members, preserving the linkage between genotype and phenotype.

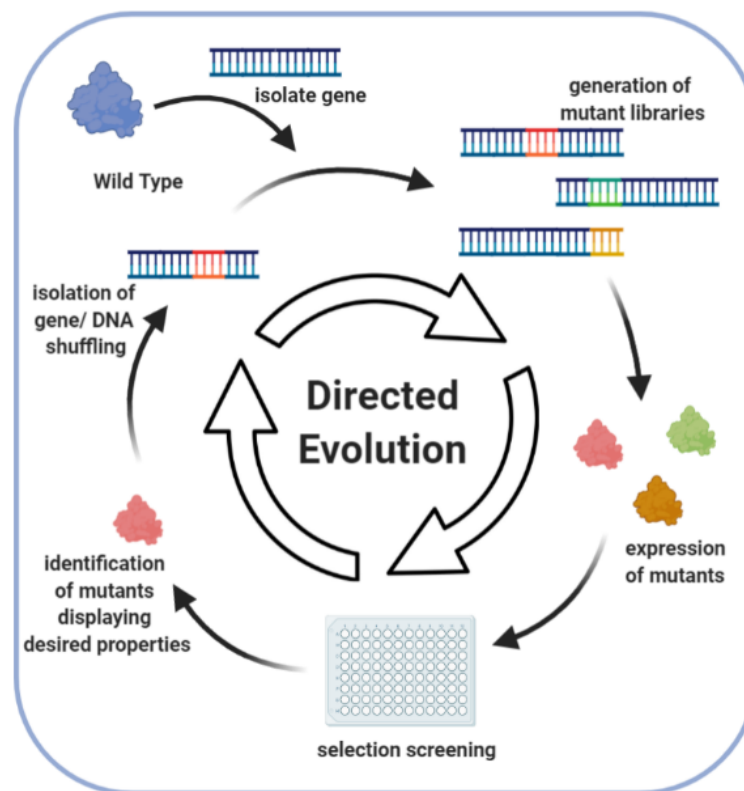


Figure 2: The directed evolution cycle. The gene coding the target protein is isolated and libraries of mutants are generated. Cells are transformed with the DNA library and variants are expressed and screened for the desired activity. Clones displaying the desired properties are isolated and characterised. The cycle is repeated until the desired properties are achieved.

Identification of a suitable starting enzyme for evolution often involves screening a panel of native enzymes identified using bioinformatics tools such as genome mining and BLAST searches. Once a template has been chosen, the gene sequence is diversified using a number of standard molecular biology methods such as random mutagenesis or site saturation mutagenesis. The chosen method of library generation depends on various factors including the availability of structural information and screening capacity. When ultra-high throughput screening methods are available, large libraries (10^5 - 10^8) are generated using techniques such as error-prone PCR[12] and DNA or gene shuffling.[13,14]

These methods are particularly attractive for the identification of catalytically important residues or 'hot-spots', which may be difficult to predict by rational design. When only medium throughput assays are available (10^2 - 10^4 variants), smaller, more focused libraries are generated, often employing computational modelling and bioinformatics to guide the selection of amino acid residues for randomisation. These libraries are generated using techniques such as saturation mutagenesis using reduced codons[15-17] or iterative combinatorial active site testing (CASTing).[18,19] Beneficial diversity is typically combined during evolutionary optimisation using DNA shuffling. These libraries are then subjected to robust screening assays and selection systems, ensuring positive hits are identified with a low number of false positives. Large libraries (10^5 - 10^8) require specialised high-throughput assays such as colony-based assays,[20] fluorescence activated cell sorting (FACS),[21] microfluidics-based screening,[22] phage display[23] and yeast display,[24] where product or by-product formation is commonly linked to a coloured or fluorescent response.

Although relatively low-throughput, arraying colonies into 96-well plates for protein production and screening offers the greatest versatility, as variants can be evaluated using a wide range of chromatographic,[4] spectrophotometric techniques.[25,26] This approach is commonly used for applications in industrial biocatalysis as the screening methods are compatible with process conditions involving high substrate loadings, high temperatures and the use of cosolvents. It is also possible to automate these workflows using colony pickers and liquid handling robots, which improve speed, accuracy and throughput.

1.2 Repurposing Nature's Enzymes

Wild-type enzymes are often not suitable for direct use in industrial applications and must first undergo optimisation to improve properties such as substrate specificity, selectivity, catalytic efficiency and stability. This section will highlight some key recent examples.

1.2.1 Sitagliptin

The redesign of a transaminase (TA) for the industrial production of Merck's antidiabetic drug Sitagliptin **7**, also called by the brand name Januvia, is a notable example (Figure 3).[3] Transaminases are pyridoxal 5'-phosphate (PLP)-dependent enzymes that catalyse the transfer of an amino group (NH_2) from an amine donor to a ketone acceptor to generate chiral amines. A panel of transaminases were screened for activity towards the pro-sitagliptin ketone **5**, however no hits were identified. An (*R*)-selective transaminase (ATA-117) had previously been developed for the (*R*)-specific transamination of methyl ketones and small cyclic ketones and this was selected as the starting scaffold for evolution. Docking studies using a homology model of ATA-117, suggested that the pro-sitagliptin ketone would not bind in the ATA-117 active site due to steric clashes in the small binding pocket.

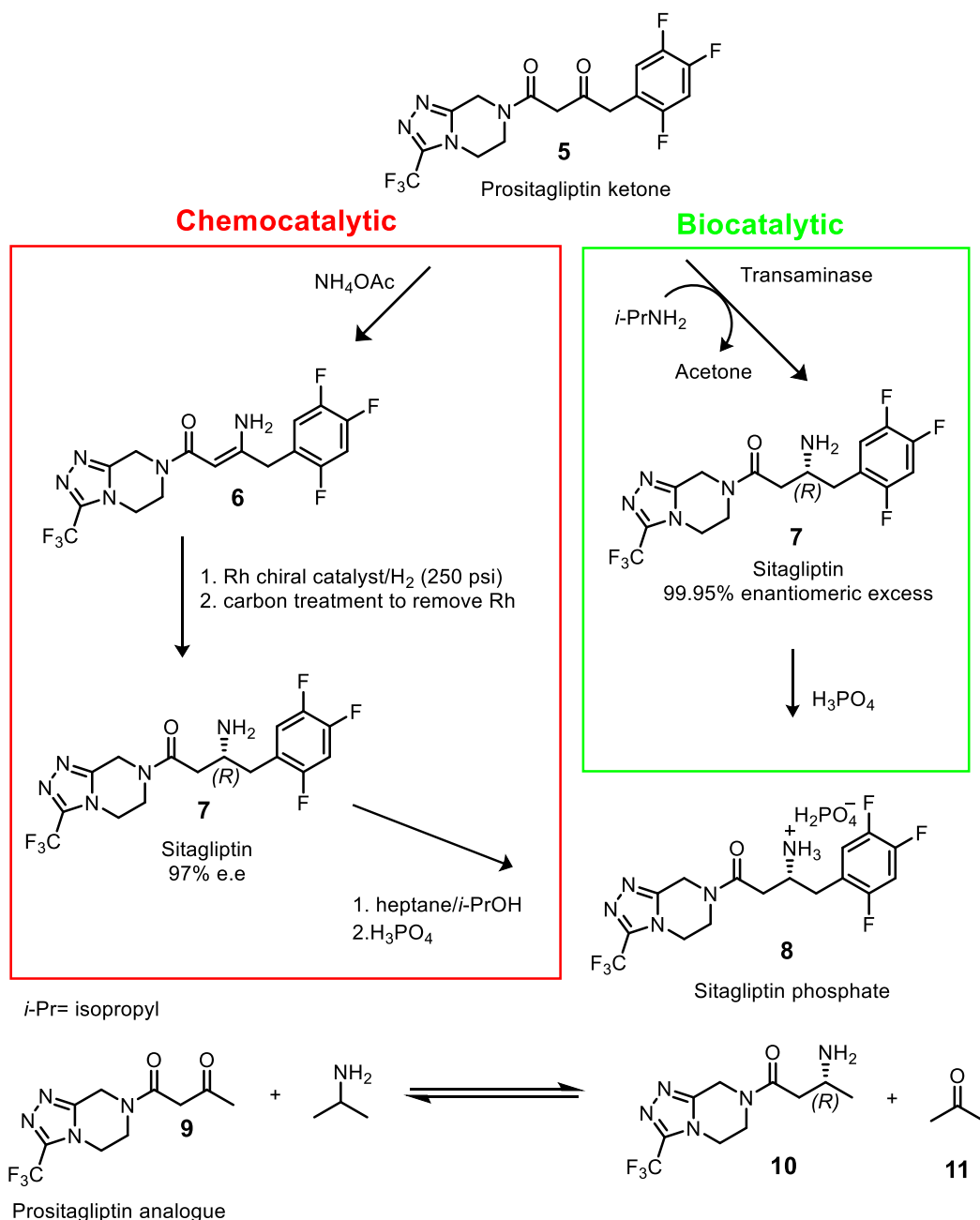


Figure 3: Chemical and enzymatic synthesis of Sitagliptin. The chemical approach utilises a rhodium-based chiral catalyst, whereas the biocatalytic route uses an engineered transaminase.[3]

The size of the substrate binding pocket was increased over 11 rounds of evolution using a substrate walking approach. Initially, libraries were screened for increased activity towards the truncated substrate **9**, and then later rounds of variants were screened towards the target substrate **5**. Libraries were arrayed in 96-well plates, and following protein production were evaluated for activity using a HPLC based assay. During evolution 27 mutations were installed using a combination of site saturation and random mutagenesis. Under optimal conditions, the final variant converted 200g/L prositagliptin ketone **5** to Sitagliptin **7** in a 92% yield and >99.95% e.e. in 50% DMSO with 6g/L biocatalyst loading. This translated to a 25,000-fold improvement in catalytic activity when compared

to the starting catalyst ATA-117. Traditional chemical synthesis of Sitagliptin **7** involved the asymmetric hydrogenation of an enamine **6** at high pressure (250 psi) using a rhodium-based chiral catalyst. This biocatalytic process outcompetes the previous chemical process and provides a 10-13% increase in yield, 53% increase in productivity (kg/L per day) and a 19% reduction in total waste.[3]

1.2.2 Islatravir

Codexis and Merck have engineered five different enzymes which form part of a nine-enzyme in vitro cascade process for the manufacture of HIV drug Islatravir **30**. [4] This new approach surpasses the previous twelve step chemoenzymatic route (Figure 4)[27] and produces the desired product in fewer than half the steps (Figure 4) and in higher yield (51% in comparison to 17%). Cascades are advantageous in comparison to chemical synthesis; they can save resources by negating the need to isolate intermediates; avoid waste generated by purifying intermediates; evade enzyme inhibition through consumption of inhibitory intermediates as they are formed; and linking reactions together can help to drive the equilibrium towards product formation.

The bacterial nucleoside salvage pathway served as inspiration for the synthesis of Islatravir **30**, which assembles nucleosides from simple building blocks when run in reverse. For the salvage pathway to become a viable route, the three enzymes making up the pathway, Purine Nucleoside Phosphorylase (PNP), Phosphopentomutase (PPM) and Deoxyribose 5-Phosphate Aldolase (DERA), needed to be repurposed to accept unnatural substrates bearing a fully substituted carbon at C-4 of the 2-deoxyribose ring. Panels of these three enzymes were screened and the most promising hits were optimised using directed evolution. The three-enzyme cascade process using optimised biocatalysts, PNP_{Rd5BB}, PPM_{Rd3BB} and DERA_{Rd3BB}, produces Islatravir **30** from **27-29** in a 76% yield. Screening of a panel of Kinases for phosphorylation activity towards **25**, led to the identification of pantothenate kinase (PanK), which showed low-level activity towards (*R*)-**25**. PanK was evolved to provide PanK_{Rd4BB} which is employed in tandem with an acetate kinase (AcK) to regenerate the adenosine triphosphate cofactor. The desymmetrising oxidation of **24** to **25** is achieved using an evolved galactose oxidase (GOase). Initially GOase favoured formation of the undesired (*S*)-enantiomer of **25** with a 40:60 *R*:*S* ratio, evolution reversed selectivity to 90:10 *R*:*S* for **25** as well as giving an 11-fold improvement in activity. Synthetic application of the engineered GOase (GOase_{Rd13BB}) required two additional redox enzymes; a peroxidase to maintain the oxidation state of copper; and catalase to catalyse the decomposition of hydrogen peroxide by-product. The fully assembled cascade yielded Islatravir **30** from relatively simple building blocks in an overall yield of 51%.[4]

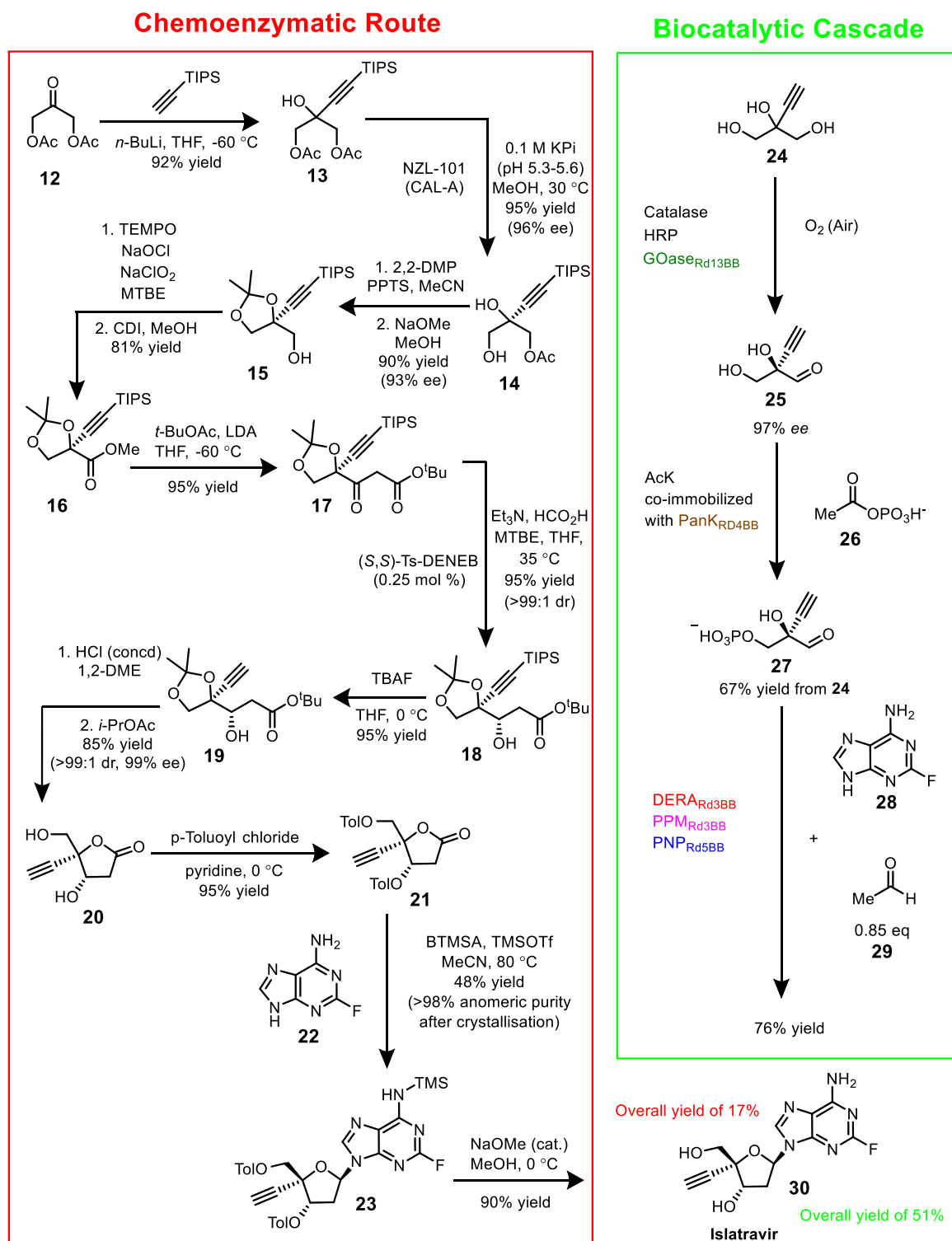


Figure 4: Chemoenzymatic and biocatalytic synthesis of Islatravir. The previous chemoenzymatic approach uses a total of 12 steps (red box),^[27] whereas the biocatalytic route using engineered enzymes is performed in three-steps (green box).^[4]

1.2.3 MAO-N

To evaluate large libraries of 10^5 - 10^8 variants specialised screening approaches such as colony based assays are required. For example, monoamine oxidase from *Aspergillus niger* (MAO-N) has been extensively engineered for the selective oxidation of a wide range of amine substrates using a colorimetric colony-based assay.[28] Monoamine oxidases (MAOs) are a family of flavin-dependent enzymes that employ molecular oxygen to catalyse the oxidation of amines to their corresponding imines. The colony-based screen (Figure 5) relies on detection H_2O_2 by-product using horse radish peroxidase (HRP) and a reactive dye, 3,3'-diaminobenzidine (DAB) **33** which is oxidised to a reddish brown polymerised quinone iminium precipitate **34**. Whilst wild-type MAO-N displays limited substrate scope and is specific for non-chiral primary amines, the substrate scope of MAO-N was expanded through directed evolution to include both secondary and tertiary amines.[29,30]

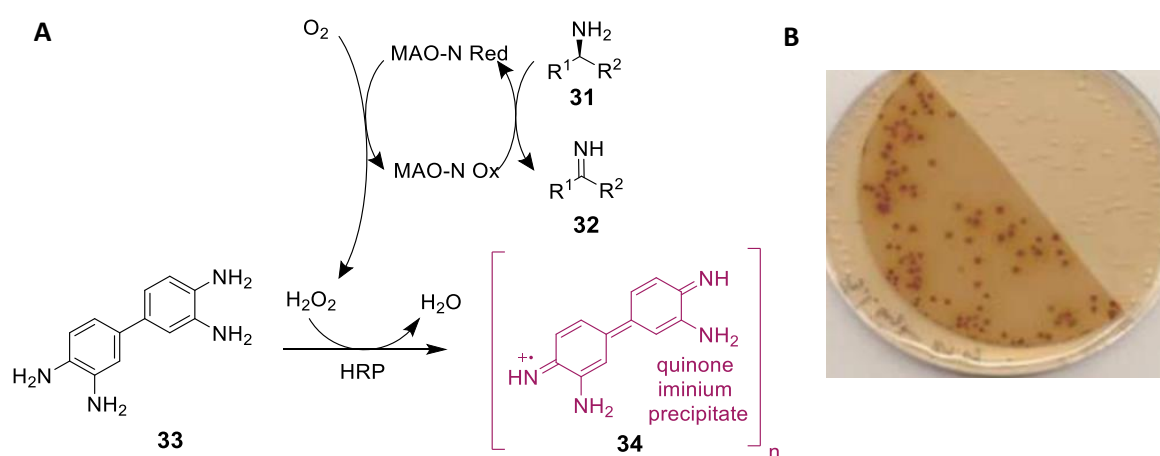


Figure 5: High-throughput colony-based screen for the evaluation of MAO-N variants. A) MAO-N catalysed conversion of amine **31** to imine **32** generating H_2O_2 as a by-product, which is detected using HRP and a reactive dye, DAB **33** which is oxidised to give a coloured precipitate **34**. B) The colony-based screen detects H_2O_2 by-product using horse radish peroxidase (HRP) and a reactive dye, 3,3'-diaminobenzidine (DAB) **33** which is oxidised to a reddish brown precipitate **34**. [28]

Engineered MAO-N variants have been employed in the preparation of pharmaceutical intermediates. For example, MAO-N variant (D5) catalyses the oxidative desymmetrisation of the prochiral bicyclic amine **35** to the corresponding imine **36**, which is a key intermediate in the production of serine protease inhibitor Telaprevir **37**, a treatment of hepatitis C (Figure 6A).[31] Imine **36** is subsequently used in a Ugi-type tri-component reaction to give the final product Teleprevir **37**. Compared to the chemical synthesis, the use of MAO-N dramatically improves both the atom and step economy of this reaction reducing the number of synthetic steps from 24 to 11.

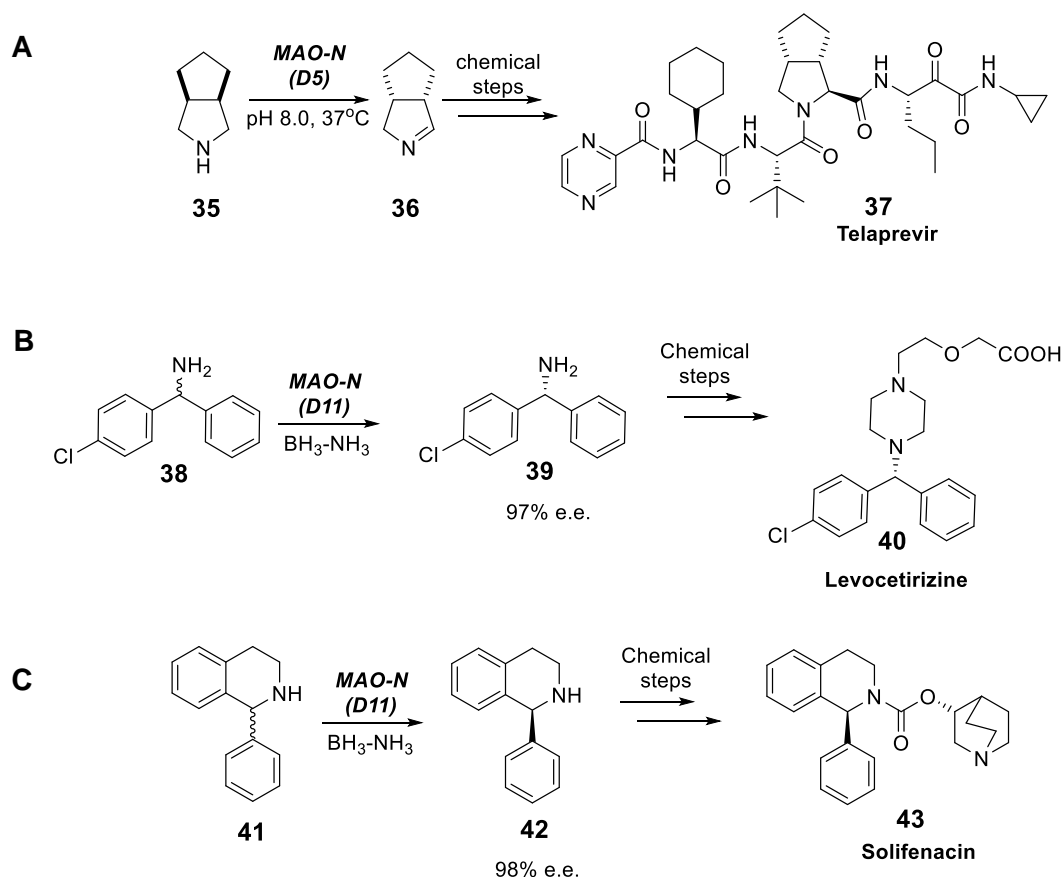


Figure 6: MAO-N catalysed deracemisation to produce key pharmaceutical intermediates. MAO-N oxidises prochiral and chiral amines **35**, **38** and **41** to their corresponding imines which are key intermediates in the synthesis of pharmaceutical compounds A) Telaprevir[31] **37**, B) Levocetirizine **40**[32] and C) Solifenacin **43**. [32]

MAO-N variants have also been employed in amine deracemisation reactions, by combining MAO-N catalysed enantioselective amine oxidation with non-selective chemical reduction of the resulting imines. For example, this process has been used in the preparative deracemisations of 4-chlorobenzhydramine **38** and phenyl tetrahydroisoquinoline **41**, which are key chiral intermediates in the synthesis of the antihistamine Levocetirizine **40** and muscarinic antagonist Solifenacin **43** respectively (Figure 6B and 6C respectively). [32]

1.3 Engineering Enzymes with New Function

While top-down engineering of natural enzymes has been hugely successful in providing access to biocatalysts for several industrial applications, [3,4,33] the approach is limited to chemical transformations represented in Nature. This section will review new approaches for the creation of enzymes with non-biological activities, including the discovery of mechanistically promiscuous enzymes, [11] the development of biocatalysts containing non-canonical catalytic residues, the generation of catalytic antibodies and the computational design of *de novo* enzymes from first principles. [34] An alternative approach to expand the functional capabilities of biocatalysts is to

harness the inherent reactivity of metal cofactors:[35, 36] however, this is outside of the scope of this introduction.

1.3.1 Engineering Enzymes with Mechanistic Promiscuity

One approach to developing biocatalysts with non-biological reactivities is to exploit the existing catalytic machinery of natural enzymes. For example, Cytochrome P450s, which utilise a heme cofactor to promote several transformations including epoxidations and hydroxylations[37], have been engineered by Arnold and others to promote non-biological carbene and nitrene transfer reactions. Carbene, nitrene and oxene transfer reactions used to functionalise C=C and C-H bonds are commonly promoted by transition-metal catalysts,[38] however these transformations are not found in Nature's biosynthetic repertoire.

By exploiting the reactivity of heme cofactors, the Arnold lab were able to promote olefin cyclopropanation using a P450 biocatalyst. The engineered variant cytochrome P450 BM3-CIS catalyses the cyclopropanation reaction between styrene **44** and ethyl diazoacetate **45** (Figure 7A)[39] and displays a strong preference for the cis products (cis:trans 71:29) **46** and **47**. Interestingly, mutation of the active site residue Ile63 to alanine switches preference of BM3-CIS to the trans products (cis:trans 19:81) **48** and **49**. Moreover, when a Thr268Ala substitution was made in cytochrome P450(BM3) wild-type, activity improved more than 60-fold from 5 turnovers to 323 turnovers with remarkable trans selectivity (cis:trans 1:99) **48** and **49**, and high enantioselectivity for the major diastereoisomer **49** (96% e.e.).[39] Cytochrome P450(BM3) Thr268Ala has been further engineered for improved activity towards *N,N*-diethyl-2-phenylacrylamide **50** and ethyl 2-diazoacetate **51** and used in the production of a chiral *cis*-cyclopropane precursor **52** an intermediate in the synthesis of the antidepressant Levomilnacipran **53** (Figure 7B).[40]

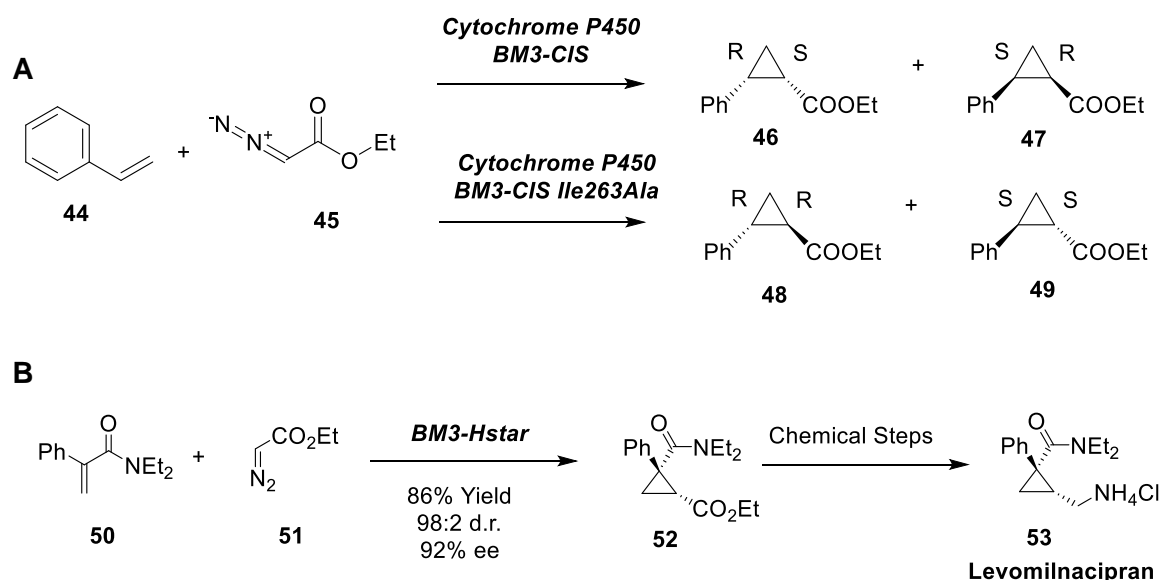


Figure 7: Cyclopropanation reactions catalysed by Cytochrome P450 catalysts BM3-CIS and BM3-Hstar. A) BM3-CIS catalyses the conversion of styrene **44** and ethyl diazoacetate **45** to cis products **46** and **47**, whereas mutant BM3-CIS Ile63Ala catalyses the conversion to trans products **48** and **49**. [39] B) Engineered BM3-Hstar catalyses the conversion of *N,N*-diethyl-2-

phenylacrylamide **50** and ethyl 2-diazoacetate **51** to **52**, an intermediate in the synthesis of Levomilnacipran **53**.^[40]

Nitrene-transfer reactions have also been added to the biocatalytic toolbox. A previously engineered panel of cytochrome 'P411' enzymes, where the axially coordinated cysteine residue is mutated to a serine, were screened for promiscuous activity towards an aryl sulfonyl azide nitrene precursor **54** (Figure 8A).^[41] These designed cytochrome 'P411' enzymes, are named due to the shift in the Soret peak of ferrous CO-bound spectrum from 450 nm for cysteine ligated enzymes to 411 nm for the serine ligated enzymes. Cytochrome P450 (BM3)-CIS Cys400Ser, displays low-level activity for C-H amination. This variant yielded product **56** in 73% yield and was able to catalyse more than 140 turnovers. Cytochrome P450 (BM3)-CIS with a cysteine axial ligand catalyses only 9 turnovers, indicating that serine-heme ligation is essential for C-H amination.

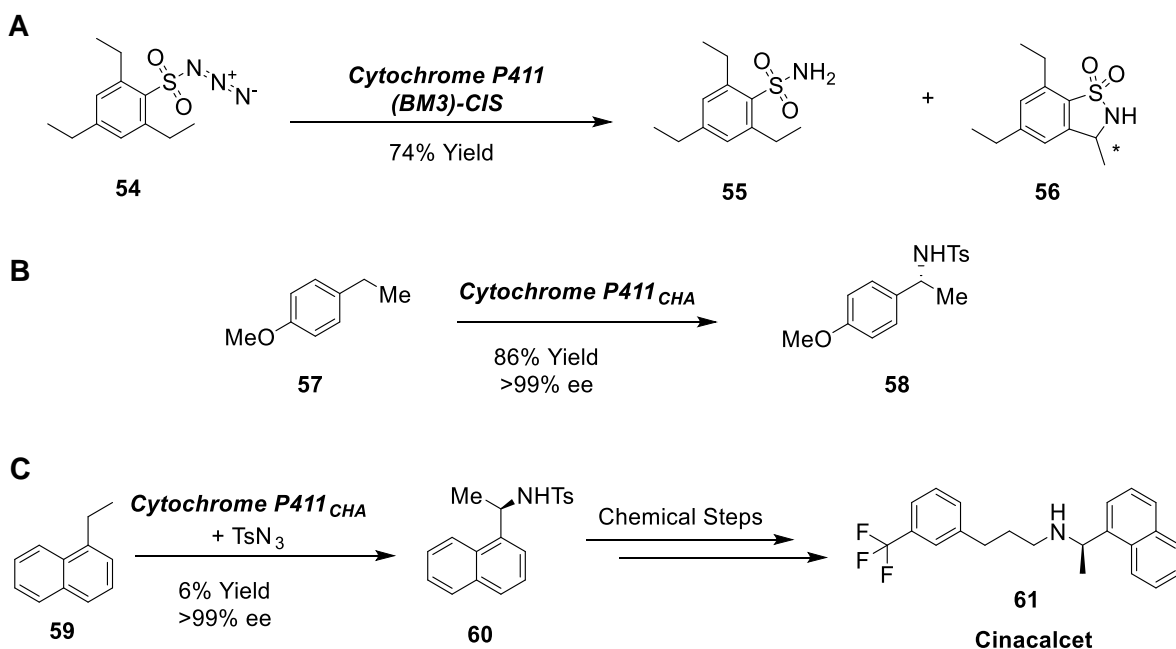


Figure 8: Cytochrome P411 variants have been engineered for nitrene-transfer and C-H amination. A) Cytochrome P411 (BM3)-CIS catalyses the conversion of aryl sulfonyl azide nitrene precursor **54** to product **56**.^[41] B) Cytochrome P411_{CHA} catalyses the conversion of alkane **57** to benzylic amine **58** by inserting a C-H bond into the alkane C) Cytochrome P411_{CHA} catalyses the amination of 1-ethylnaphthalene **59** to **60** a key intermediate in the synthesis of Cinacalcet **61**.^[42]

Intermolecular benzylic C-H amination has also been achieved biocatalytically using cytochrome P411_{CHA}.^[42] The cytochrome P411(BM3) variant P-4 which was engineered towards the imidation of allylic sulphides, displayed promiscuous activity for benzylic C-H amination. Cytochrome P411_{BM3} P-4 was engineered for improved activity towards the amination of 4-ethylanisole **57** and the most improved variant cytochrome P411_{CHA} catalyses up to 1,300 turnovers and can produce benzylic

amine **58** in 86% yield and e.e. >99%. Cytochrome P411_{CHA} has a broad substrate scope, tolerating substitution of the aromatic ring at *para*, *meta* and *ortho* positions. Notably, this enzyme can promote the amination of 1-ethylnaphthalene **59** to give the nitrogen-containing fragment **60**, a key intermediate in the synthesis of the drug Cinacalcet **61**, a treatment for hyperparathyroidism (Figure 8C).[42]

An interesting alternative approach to access new catalytic mechanisms in proteins is through photo-excitation of redox active co-factors. For example, irradiation of nicotinamide cofactor dependent ketoreductases (KREDs) with visible light leads to the enantioselective radical dehalogenation of lactones **62** (Figure 9), a challenging reaction not seen in Nature and usually promoted by small-molecule catalysts.[43] In this reaction the NAD(P)H cofactor is excited by blue LEDs (460nm) to a triplet state which serves as the single electron reductant. A substrate radical anion is formed by a single electron transfer, the C-Br bond undergoes heterolytic cleavage to give an alkyl radical and NAD(P)H⁺ then serves as the hydrogen atom donor to afford the dehalogenated lactone products (*R*)-**63** and (*S*)-**63**. [43]

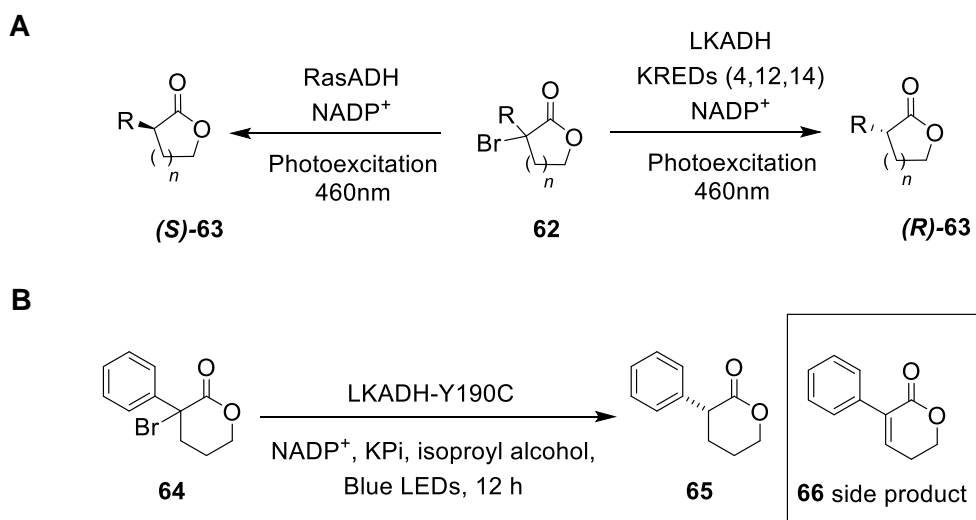


Figure 9: Radical dehalogenation of lactones using a photoenzymatic approach. A) RasADH selectively dehalogenates the halolactone **62** when irradiated by light to yield (*S*)-**63**, whilst KRED variants selectively produce (*R*)-**63**. [43] B) LKADH-Y190C and variants selectively dehalogenates the lactone **64** when irradiated by blue light to lactone **65** and side product **66**. [43]

Halogenated lactones were chosen as the target substrate, as they can bind in the active sites of ketoreductases (KREDs) without undergoing carbonyl reduction. A panel of KREDs were screened for dehalogenase activity towards halolactone **62**. Seven KREDs catalysed the formation of the desired lactone after irradiation with blue LEDs (460nm), and three variants KRED-4, KRED-12 and KRED-14 provided the (*R*)-enantiomer **63** with conversions >95%, and e.e.'s of 96% (Figure 9A). [43] In the absence of KRED, NADP⁺ or light no observable reaction occurred. It has been suggested

that a charge-transfer complex forms between the halolactone and NADPH only in the presence of the KRED active site and it is this complex, which is responsible for initial electron transfer.

The active KRED catalysts are all variants of a *Lactobacillus kefir* alcohol dehydrogenase (LKADH), and 10 of the most active variants contain a common mutation at position Tyr190, which allow the variants to reduce more sterically demanding substrates. Site saturation mutagenesis at Tyr190 in wild-type LKADH revealed that mutation of this position to cysteine activates the protein for dehalogenation activity and produces desired lactone **65** from halolactone **64** with a low yield of 3% (Figure 9B). Two further mutations Glu145Phe and Phe147Leu in the enzyme active site, increased the enzyme activity and the product **65** was produced in 72% yield and e.e. of 92%. These three mutations are hypothesised to increase the volume of the LKADH active site and therefore afford the desired dehalogenation activity. An enantiocomplimentary short-chain alcohol dehydrogenase from *Ralstonia* species (RasADH)[44] with a large active site was rationally designed to act as a biocatalyst for the dehalogenation of **64**, and afforded lactone (*S*)-**65** with a 51% yield and 85% e.e. (Figure 9B). Docking the lactone into the crystal structure of RasADH revealed interactions between the substrate carbonyl oxygen and the side chains of Tyr150 and Ser137, in a similar orientation to the natural ketone substrate. The distance between the C4 of NADPH and the α -position of the lactone was consistent for hydrogen-atom transfer. Both KRED-12 and RasADH displayed a broad substrate scope accepting halo-substituted lactones and lactones with additional stereocentres.[43]

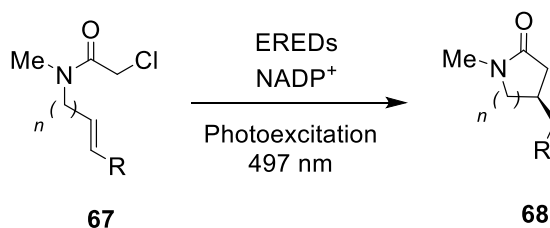


Figure 10: EREDs are able to promote asymmetric radical cyclisation reactions to produce 5-8 membered lactams through endo-trig and exo-trig ring closure. ERED GluER can promote the cyclisation of α -chloroacetamide **67** to afford γ -lactam **68** under irradiation with light.[45]

Photoexcitation of Flavin-dependent reductases have also been shown to promote asymmetric radical cyclisation reactions to generate 5-8 membered lactams through endo-trig and exo-trig ring closure.[45] Flavin-dependent “ene” reductases (EREDs) were chosen as a suitable protein scaffold due to their large active sites and substrate promiscuity, and also their ability to control radical hydrodehalogenation reactions with stereochemical outcomes.[46] A *Gluconobacter oxydans* ERED (GluER) was capable of promoting the cyclization of α -chloroacetamide **67** to afford γ -lactam **68** following irradiation with near-ultraviolet (UV) light (390nm) (Figure 10). It is hypothesised that the reaction proceeds via radical dehalogenation following single electron transfer from the photoexcited cofactor flavin mononucleotide (FMN), the substrate radical anion can then undergo intramolecular cyclisation. Optimisation of the light source revealed that cyan light (497nm) provided a higher yield and enantioselectivity.[45]

1.3.2 Genetic Code Expansion

Traditional approaches to enzyme engineering have been limited to Nature's set of 20 canonical amino acids, which contain a limited range of functional groups and restrict the range of catalytic mechanisms that can be achieved within enzyme active sites. During the course of this PhD our lab and others have shown that stop codon suppression technology can be used to genetically encode chemically-inspired, non-canonical amino acids into proteins, which can promote non-biological reactions. This approach combines the benefits of small molecule and enzyme catalysis, providing access to new chemical reactivities and increased catalytic efficiencies within an evolvable protein scaffold. We have created an enzyme with a non-canonical nucleophile, which operates via an organocatalytic mechanism. This work is presented in Chapter 5. Other examples, including the design and evolution of an enzyme for hydrazone and oxime formation, and the development of a biocatalyst for photocatalytic CO₂ reduction are described herein.

Genetic code expansion technologies allow the selective incorporation of non-canonical amino acids (ncAAs) into proteins.[47, 48] NcAA incorporation typically exploits an engineered aminoacyl tRNA synthetase and tRNA pair which is orthogonal to the hosts translation machinery. The amino acyl tRNA synthetase loads the target ncAA onto the orthogonal tRNA, and the ncAA is then incorporated into the target protein by the ribosome in response to an unassigned codon, typically UAG (Figure 11). Orthogonal translation components must be selective for the target ncAA while excluding canonical residues. To date, amino acyl tRNAs have been engineered to accept hundreds of structurally diverse amino acids including spectroscopic probes,[49, 50] bioorthogonal handles,[51, 52] photo-cross-linking amino acids[53, 54] and mimics of post-translational modifications.[55, 56]

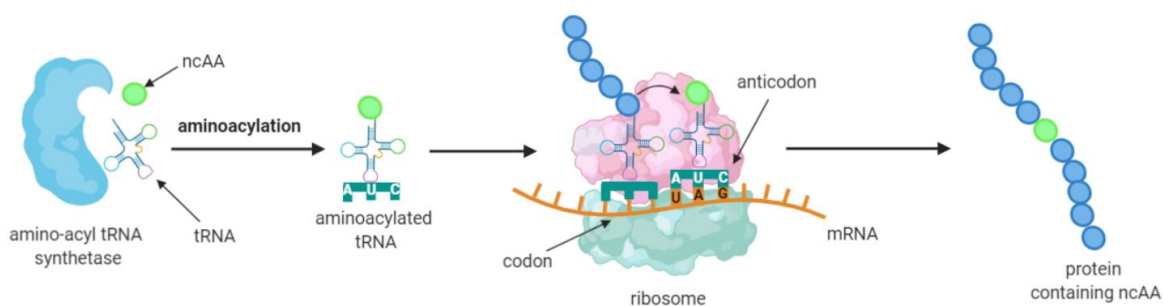


Figure 11: Genetic code expansion. An orthogonal aminoacyl tRNA synthetase loads the ncAA onto its cognate tRNA. The ncAA is then incorporated into the target protein in response to a UAG codon.

A genetically encoded *p*-azidophenylalanine (pAzF) **69** was recently introduced into the transcriptional regulator protein LmrR (Figure 12A).[57] The residue pAzF **69** was chemically reduced with tris(2-carboxyethyl)phosphine (TCEP) post translationally to generate a reactive aniline side chain (*p*-aminophenylalanine, pAF) **70**, capable of promoting hydrazone and oxime formation. Rounds of directed evolution enhanced the modest activity of LmrR_pAF for hydrazone formation between 4-hydrazino-7-nitro-2,1,3-benzoxadiazole **71** and 4-hydroxybenzaldehyde **72** (Figure 12B). The final variant LmrR_pAF_RMHL contained four mutations (A92R N19M F93H A11L) and displayed a 55-fold improvement in k_{cat} compared to the starting template LmrR_pAF and a 26,000-fold increase in k_{cat}/K_m over free aniline in solution.[58]

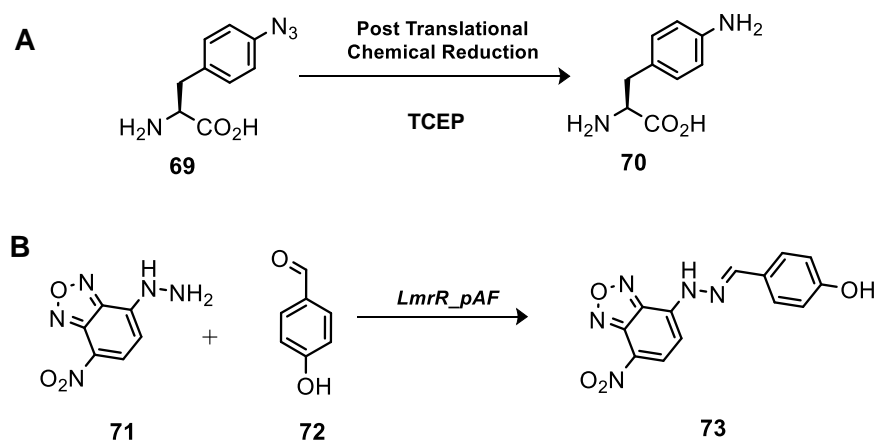


Figure 12: A genetically encoded pAzF into a transcriptional regulator protein promotes hydrazine formation. A) Post-translational chemical reduction of pAzF **69** with tris(2-carboxyethyl)phosphine affords the catalytic nucleophile pAF. **70** B) Evolved variant LmrR_pAF_RMHL catalyses hydrazine formation between 4-hydrazino-7-nitro-2,1,3-benzoxadiazole **71** and 4-hydroxybenzaldehyde **72** to yield the product **73**.^[57]

Photoresponsive elements have also been incorporated into proteins to generate enzymes for photocatalytic CO₂ reduction (Figure 13).^[59] A double mutant (Tyr203Phe, His148Glu) of the superfolder yellow fluorescent protein (sfYFP) was modified by replacing Tyr66 with benzophenone-alanine (BpA) **76**. Autocatalytic conversion of the Gly65-BpA66-Gly67 tripeptide yielded a photosensitizer protein (PSP2) with an engineered chromophore **77**. Following photochemical reduction with a suitable sacrificial reductant, super-reducing radicals (PSP2⁻) are formed which are able to drive CO₂ reduction via a nickel-terpyridine complex covalently attached to PSP2 through a Cys95 residue. This study provided a miniature CO₂ reducing enzyme with a CO₂/CO conversion quantum efficiency of 2.6%.^[59]

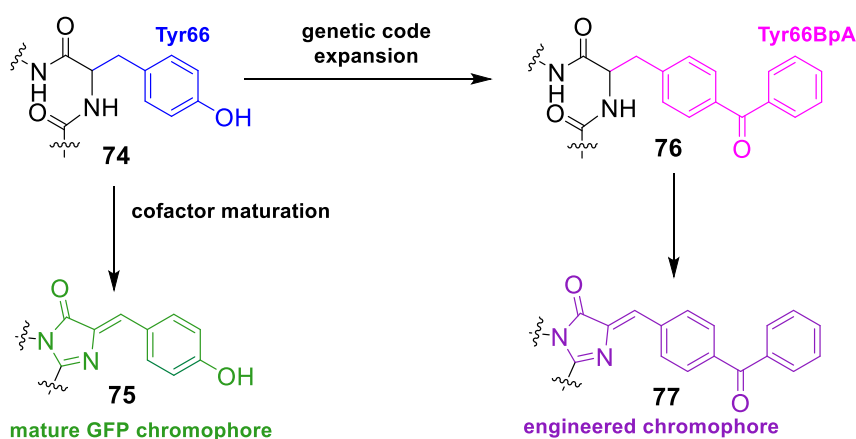


Figure 13: Design of a miniature enzyme for photocatalytic CO₂ reduction. Replacement of a Tyr66 with BpA **76** in a double mutant of sfYFP results in an engineered chromophore **77** in PSP2. When photochemical reduction is performed with a suitable sacrificial reductant the formation of

super-reducing radicals (PSP2-) can drive CO₂ reduction via a nickel-terpyridine complex covalently attached to PSP2 through a Cys95 residue.[59]

1.4 Approaches to Enzyme Design

Although many natural enzymes have been modified through protein engineering strategies to yield biocatalysts for a variety of transformations, these approaches are often insufficient. To design enzymes *de novo* –or, ‘from scratch’ has become a desirable objective in protein engineering to deliver novel biocatalysts. This section will highlight various approaches to enzyme design with key examples.

1.4.1 Catalytic antibodies

Linus Pauling proposed that enzymes can achieve such high catalytic efficiencies by selectively binding to and stabilising the transition state of a reaction to reduce the energy barrier of a particular chemical pathway.[60] Twenty years later, Jencks discovered that the mammalian immune system could raise an antibody against a transition state analogue (TSA) or ‘hapten’ to produce a catalytic antibody for a given reaction (Figure 14).[61]

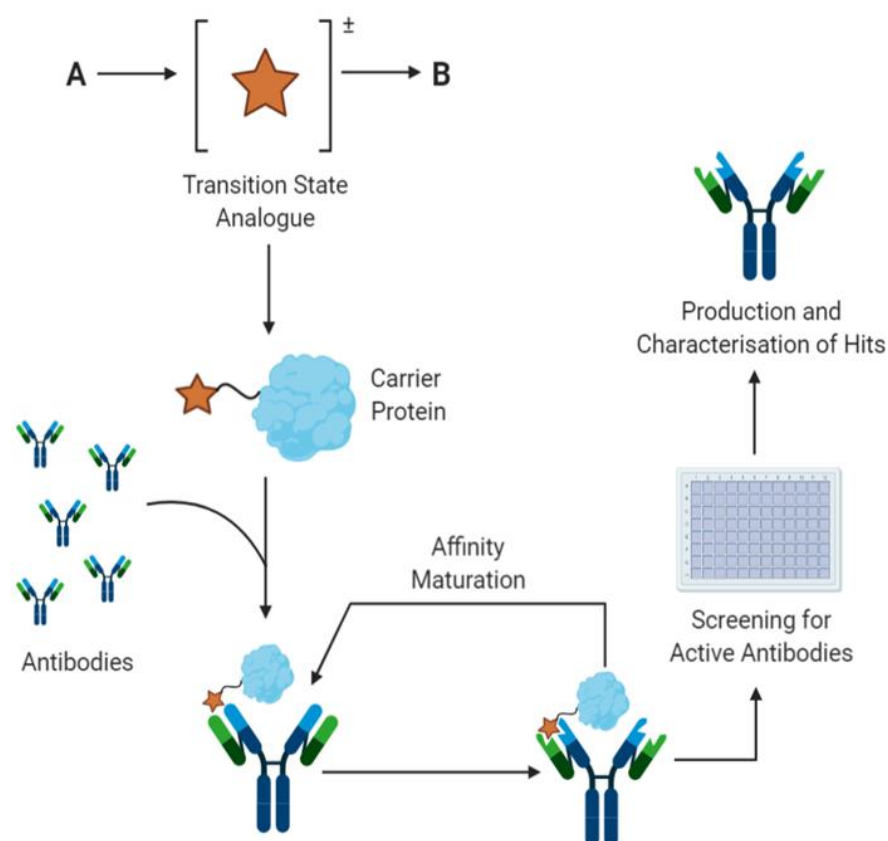


Figure 14: The generation of catalytic antibodies. Catalytic antibodies are raised against a TSA of the desired reaction linked to a carrier protein in the murine immune system. Antibodies are matured and then screened towards the desired reaction. Successful antibodies are then produced and characterised.

The first catalytic antibodies were reported in 1986 and catalysed ester hydrolysis.[62] To date, over 100 different chemical reactions have been promoted by catalytic antibodies, including aldol condensations,[63] pericyclic processes,[64] oxidation[65] and reductions.[66] Catalytic antibodies are often highly specific, with high regio- and stereoselectivity, however, their catalytic efficiency often falls far short of natural enzymes. This has been attributed to the antibody being raised against an imperfect model of the transition state analogue with no selection pressure on catalytic activity, only on affinity for the transition-state analogue.[67] Efforts to evolve catalytic antibodies have had little success and it has proved challenging to tailor antibodies to a specific reaction.

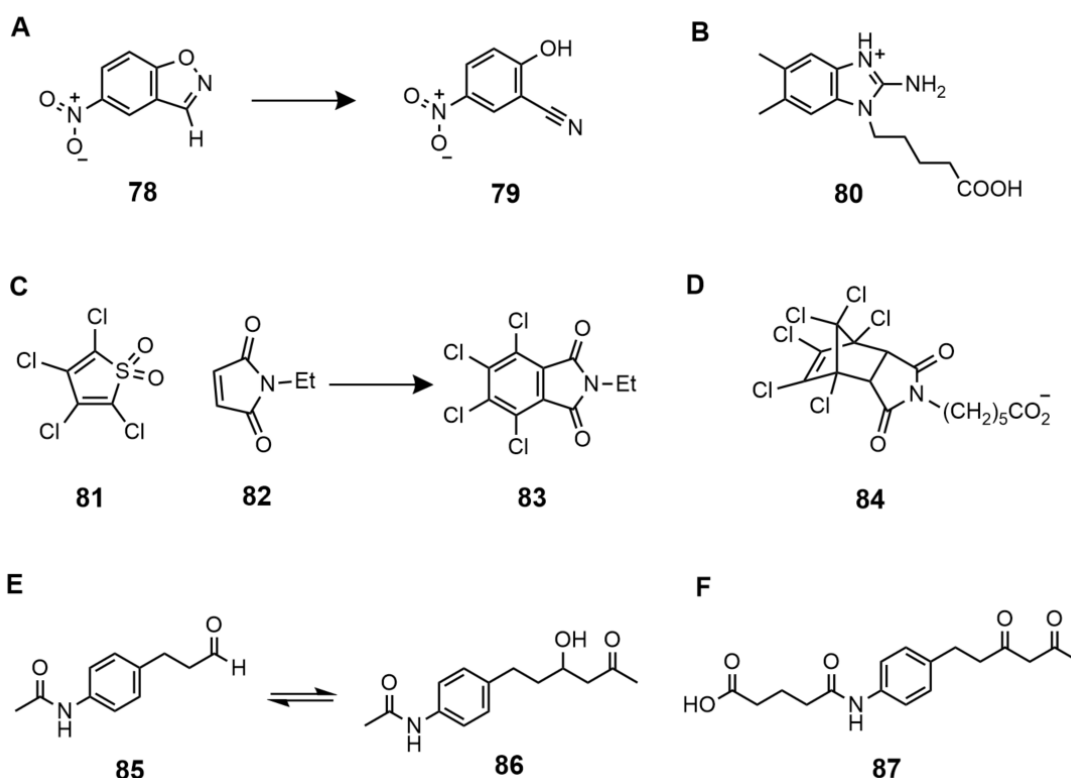


Figure 15: Reactions with catalytic antibodies. A) The Kemp Elimination reaction of 5-nitrobenzisoxazole **78** to the corresponding 5-nitro-salicylonitril **79**. B) The cationic benzimidazolium hapten **80** used to raise antibody 34E4 for the Kemp Elimination reaction.[68] C) The Diels-Alder reaction of tetrachlorothiophene dioxide **81** and *N*-ethylmaleimide **82**. D) The hapten **84** used to raise antibody 1E9 for the Diels-Alder reaction.[69] E) The retro-aldol reaction of *N*-(4-(3-oxopropyl)phenyl)acetamide **85**. F) The hapten **87** used to elicit antibody 38C2 for the retro-aldol reaction.[70]

Active catalytic antibodies have been developed for non-biological reactions including the Kemp elimination (Described in detail in Chapter 1.4.2.1), which exploits charge complementarity between the antigen and antibody. The antibody 34E4 was raised against a cationic benzimidazolium hapten **80** (Figure 15B), which mimics the transition-state geometry of all reacting bonds but has little

resemblance to the reaction product.[68] An X-ray crystal structure of 34E4 complexed with the hapten shows the negatively charged catalytic base H50E is positioned by a sophisticated hydrogen bonding network with a neighbouring asparagine and an ordered water molecule, and the substrate binds in a hydrophobic pocket positioned between two aromatic residues. This catalytic antibody promotes the cleavage of 5-nitrobenzoxazole **78** with a k_{cat}/K_m $5500 \text{ M}^{-1} \text{ s}^{-1}$. Although an impressive catalytic efficiency, it is many orders of magnitude less efficient than natural enzymes promoting proton transfer reactions, such as triose phosphate isomerase.

The first successful catalytic antibody able to promote the Diels-Alder reaction (Described in detail in Chapter 1.4.2.2) was described in 1989,[69] and was raised using the *endo* hexachloronorbornene hapten **84** (Figure 15D), a stable analogue of the bicyclic intermediate which mimicked the boat-like conformation of the transition-state. As the planar product is so different to the hapten it binds far less efficiently and therefore reduces product inhibition significantly. The most active antibody (1E9) promotes the [4+2] cycloaddition between tetrachlorothiophene dioxide **81** (TCTD) and *N*-ethylmaleimide **82** (NEM) with >50 turnovers. Spontaneous sulphur dioxide elimination leads to the formation of intermediate *N*-ethyl tetrachlorophthalimide, which is subsequently oxidised to the final product **83**. Structural studies reveal an arrangement of Van der Waals contacts, π -stacking interactions and a hydrogen bond to one of the succinimide carbonyl groups, creating a complementary pocket for the hapten **84**. The ligand is 86% buried in a snug pocket with no interfacial cavities detected, and 1E9 is able to promote the reaction by pre-organising its substrates in a complex that closely approximates the transition-state geometry.

A final notable mention is the catalytic antibody 38C2 for the retro-aldol reaction (Described in detail in Chapter 1.4.2.3), which was elicited using a mechanism-based enzyme inhibitor **87** (Figure 15F).[63] 38C2 uses an enamine mechanism, similar to natural aldolases. The ϵ -amino group of the reactive lysine residue in the binding pocket of 38C2 reacts with the ketone substrate to form a Schiff's base.[70] Hydrolytic release of the aldol product is initiated by nucleophilic attack of the enamine on the aldehyde substrate. This antibody has a broad substrate scope and accepts a wide variety of ketones.[71]

1.4.2 Computational enzyme design

The combination of computational design and directed evolution could offer a general strategy for the creation of biocatalysts with new functions. Computational enzyme design is conceptually similar to catalytic antibody technology, however, instead of using an imperfect transition-state analogue to raise a complementary antibody, active sites are designed *in silico* to stabilise a theorised rate-limiting transition state (Figure 16).[72,73]

The first step in the computational design process involves the creation of a theorised model of the rate-limiting transition state, called a theozyme. The theozyme is comprised of a quantum mechanically calculated structure of the transition state plus associated amino acid side-chains designed to stabilise the high-energy species. Programs such as Rosetta Match[74] and ORBIT[75] are used to dock the theozyme into proteins in the Protein Data Bank (PDB). Suitable scaffolds must be a sterically complementary to the theozyme with a protein backbone, which can accommodate

the amino acid functional groups. Next the active site residues are redesigned to effectively pack the theozyme using the Rosetta Design algorithm. Designs are ranked according to their calculated energies and catalytic geometries and selected designs are tested experimentally.

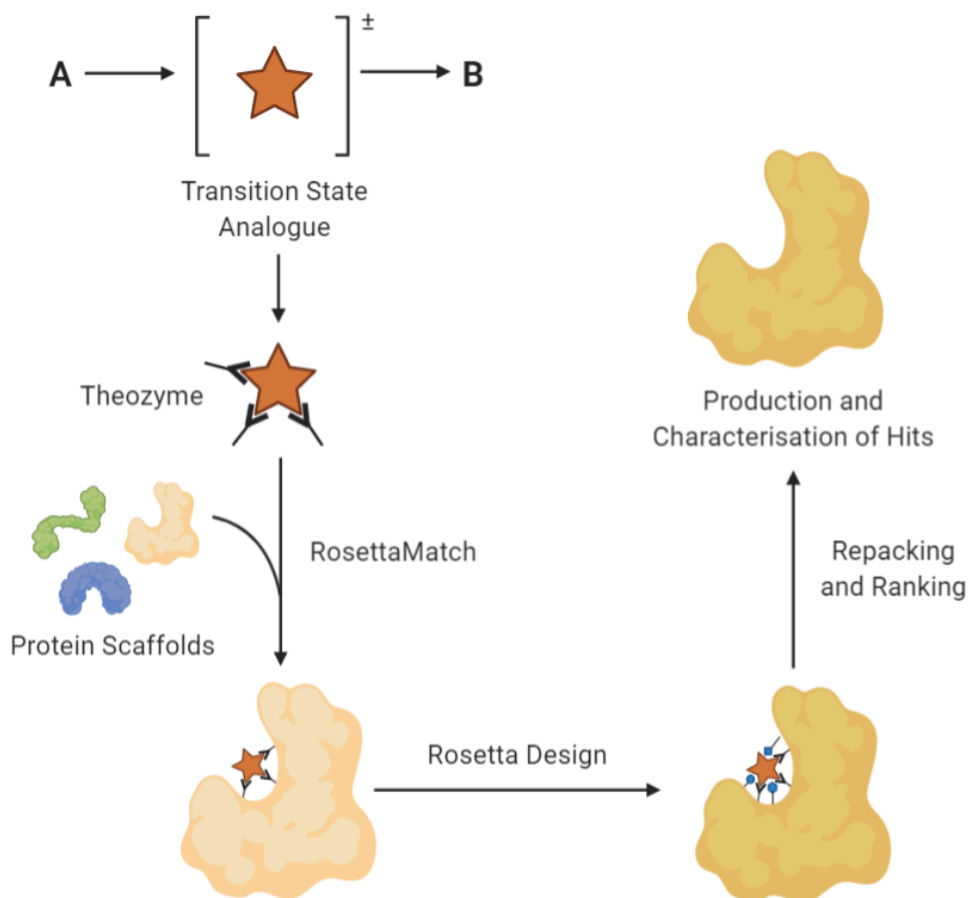


Figure 16: The generation of *de novo* enzymes. Algorithms such as RosettaMatch[74] are used to dock the theozyme into proteins in the PDB. Active site residues are then redesigned for optimal packing using algorithms such as Rosetta Design. The designs are then ranked and tested experimentally.

Although the activity of these novel designs are well below that of natural enzymes, they can be enhanced with directed evolution. This strategy has been used over the past 20 years to deliver novel enzymes for a set of well characterised transformations such as Kemp elimination[76], Diels-Alder[77] and Retro-aldol[78] reactions.

1.4.2.1 Kemp eliminase

The computational design of enzymes that can promote transformations not represented in Nature is a significant challenge. The Kemp elimination is a mechanistically simple acid/base catalysed

proton transfer reaction, which proceeds via a single transition state,[79] and several groups have attempted to design enzymes for this model transformation. The reaction of benzisoxazoles **78** to salicylonitriles **79** has served as a target reaction for these design attempts as the product of the reaction **79** is coloured, providing a convenient way of monitoring Kemp elimination reactions in high throughput. (Figure 17A).

Baker and co-workers designed *de novo* enzymes using two different theozymes with differing catalytic bases.[76] One theozyme used a carboxylate group for deprotonation mimicking antibody 34E4, whilst the other theozyme used a histidine side chain backed up by an Asp/Glu residue for stabilisation of the correct histidine tautomeric form. A hydrogen bond donor was included in both design models (Ser, Thr, Tyr, Lys, H₂O) to stabilise the growing negative charge on the phenolic oxygen, and π -stacking interactions (Phe, Tyr, Trp) were integrated for transition state stabilisation (Figure 17B).

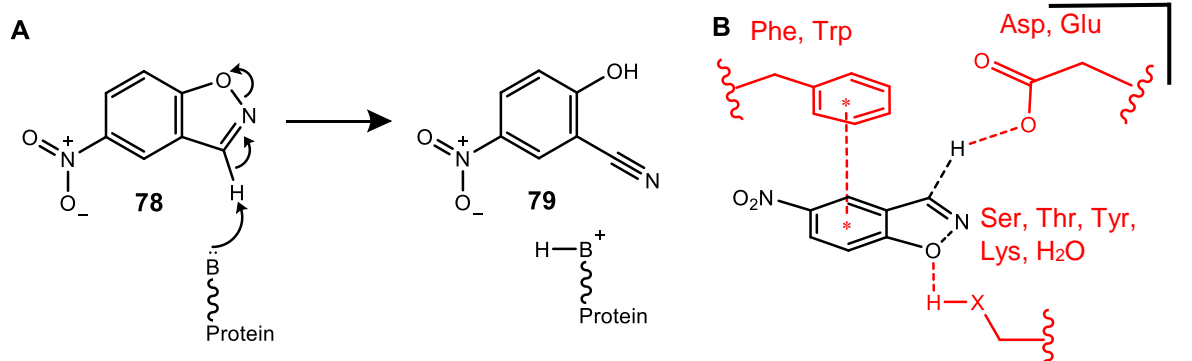


Figure 17: The Kemp elimination. A) A reaction scheme depicting the conversion of 5-nitrobenzisoxazole **78** to 5-nitro-salicylonitril **79**. B) The Kemp Elimination active site design used in the computational design process.[76]

59 of the most promising computational designs were evaluated experimentally and the most active designs displayed k_{cat}/K_m values ranging from $6 \text{ M}^{-1} \text{ s}^{-1}$ to $160 \text{ M}^{-1} \text{ s}^{-1}$. The two most active designs KE59 and KE70 were based on the same TIM barrel scaffold and employ a glutamic acid and a histidine-aspartate dyad, respectively, as the catalytic base.[76] When the catalytic bases were mutated the activity was abolished, confirming the reactions proceeded via the designed mechanisms. Out of the 59 designs evaluated only 8 showed activity towards the desired Kemp Elimination reaction and the most active variant was more than an order of magnitude less efficient than catalytic antibodies. However, this approach is compatible with further optimisation using directed evolution. The KE59 design was subsequently engineered for improved activity over 13 rounds evolution by employing error-prone mutagenesis. The most improved variant R13-3/11H demonstrated a 400-fold improvement in catalytic efficiency, with a k_{cat}/K_m of $60,000 \text{ M}^{-1} \text{ s}^{-1}$. [80] This improvement was attributed to reshaping of the substrate binding pockets, optimisation of the catalytic base placement, and increasing the base efficiency by minimising undesirable interactions with water molecules.

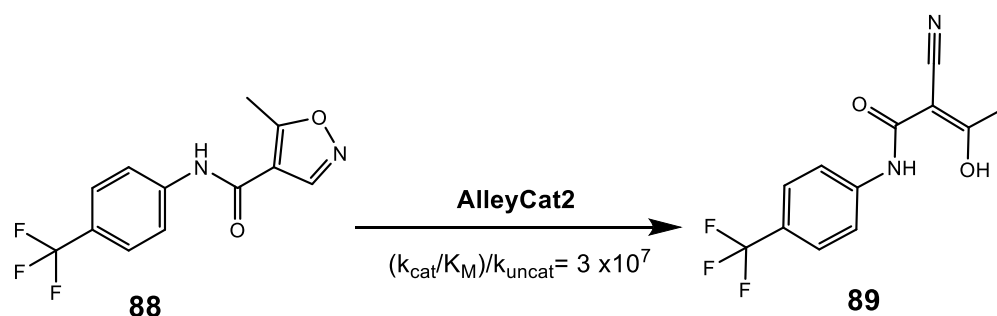


Figure 18: Catalytic activity of AlleyCat2. AlleyCat2 catalyses the conversion of immunosuppressor pro-drug leflunomide **88** to its active form teriflunomide **89**.

An alternative strategy to design an enzyme for the Kemp elimination reaction was taken by DeGrado and co-workers who used a scanning approach to place Glu or Asp residues at various positions in the active site of the calcium binding protein Calmodulin.[81] A ‘superrotamer’ library, in which the Glu/Asp carboxylate was attached to the substrate in the transition state geometry, was docked into the active site of the Glu/Asp mutants. The most promising design named AlleyCat (Phe92Glu), had very modest activity and a k_{cat}/K_M of only $6 \text{ M}^{-1} \text{ s}^{-1}$, however the design comprised of only a single mutation in a scaffold which had no prior activity for the Kemp elimination reaction. This catalytic efficiency has been improved 40-fold through directed evolution to give catalyst AlleyCat2 which facilitates the conversion of immunosuppressor pro-drug leflunomide **88** to its active form teriflunomide **89** (Figure 18).[82]

The Mayo group also designed a functional Kemp Eliminase but used a thermostable xylase as their protein scaffold.[83] Evaluation of the initial design HG-1, revealed that the catalyst was inactive. Molecular dynamics (MD) and X-ray crystallography studies revealed two potential causes, firstly the active site was too solvent exposed and secondly the designed catalytic machinery had too much rotational freedom and was found in unproductive orientations. A subsequent round of computational design, yielded the active catalyst HG-2, which promoted the Kemp elimination reaction of **78** (Figure 17A) with a k_{cat}/K_M of $122 \text{ M}^{-1} \text{ s}^{-1}$. The active site of HG-2 is less solvent exposed and buried deeper in the protein structure than HG-1 (Figure 19A). It uses a pre-existing aspartate as a catalytic base and a threonine side chain designed to stabilise the growing negative charge on the transition state. A point mutation at S265T, which was predicted by MD to provide better packing around the substrate, improved the k_{cat}/K_M 3-fold (to $430 \text{ M}^{-1} \text{ s}^{-1}$) and yielded HG-3.[83]

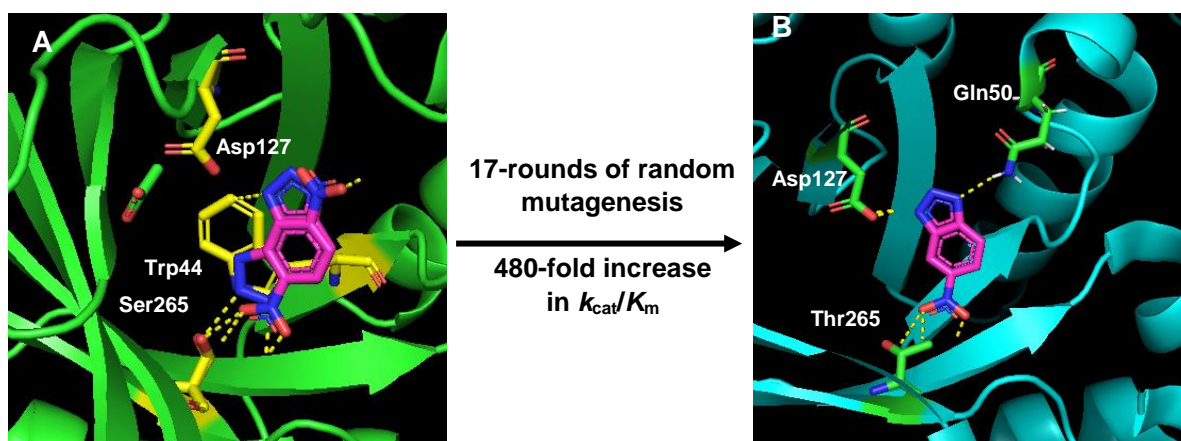


Figure 19: Biocatalysts for the Kemp elimination reaction. A) The active site of the modestly active computationally designed HG-2 in green ribbons, key active site residues are shown in yellow sticks, the two conformations of the TSA analogue are shown in magenta sticks and hydrogen bonding contacts are shown as dashed lines. PDB code: 3NYD. [83] B) HG-3 was subjected to rounds of directed evolution to yield the efficient catalyst HG3-17. The active site of HG3-17 is shown in cyan ribbons, key active site residues are shown in green sticks, the one conformation of the TSA analogue is shown in magenta sticks and hydrogen bonding contacts are shown as dashed lines. PDB code: 4BS0.[84]

HG-3 was further optimised by the Hilvert group who engineered the catalyst over 17 rounds of evolution to yield HG3.17 (Figure 19B),[84] which demonstrated a 480-fold improvement in catalytic efficiency compared to HG-3. Furthermore, the turnover number for this biocatalyst increased to 700 s^{-1} which is three orders of magnitude higher than the best catalytic antibody. The improved efficiency of the HG3.17 biocatalysts was largely attributed to the introduction of a Gln50 residue which can hydrogen bond to the developing phenoxide ion in the transition state. Mutating the Gln50 residue to Ala resulted in a 50-fold drop in activity, highlighting its importance in the Kemp elimination reaction. The combination of computational design and directed evolution has provided biocatalysts for the Kemp elimination reaction derived from a variety of enzyme engineering strategies with near enzyme-like activity.

1.4.2.2 Diels-Alderase

The Diels-Alder reaction is a [4+2]-cycloaddition between a conjugated diene and a substituted alkene to form functionalised cyclohexenes (Figure 20). In one step, two carbon-carbon bonds are formed creating up to four stereocentres. There are very few biosynthetic examples of the Diels-Alder reaction, and examples are limited to intramolecular reactions.[85-88] An enzyme for the Diels-Alder reaction between *N,N*-dimethylacrylamide **90** and 4-carboxybenzyl *trans*-1,3-butadiene-1-carbamate **91** (Figure 20) was created using a combination of computational design and directed evolution.[89]

The theozyme consisted of the theorised transition state for the reaction giving the 3*R*,4*S* endo product, a hydrogen bond donor to stabilise the diene carbamate and a hydrogen bond acceptor for

the dienophile.[77] Using RosettaMatch, the theozyme was docked into a set of 207 protein scaffolds, designs were optimised using Rosetta Design, and ranked according to their transition state binding energies, catalytic geometry, and shape complementarity. In total, 84 designs were expressed for experimental evaluation, and a total of 50 designs were found to express soluble protein. Enzymes were screened for activity using liquid chromatography-tandem mass spectrometry, and two designs were active. The most active design DA_20_00 (Figure 21A) was created from the six-bladed propeller protein scaffold diisopropylfluorophosphatase from *Loligo vulgaris* with 13 mutations built into the active site. A glutamine (Gln195) serves as the hydrogen bond donor to stabilise the diene carbamate, a tyrosine serves as a hydrogen bond acceptor for the dienophile, and the active site pocket is lined with hydrophobic residues which form a tight-complementary surface. However, this design was around 500-fold less active than the best antibody for this same reaction with a $k_{cat}/(K_{diene} \cdot K_{dienophile})$ of $0.06 \text{ M}^{-1} \text{ M}^{-1} \text{ s}^{-1}$. [77]

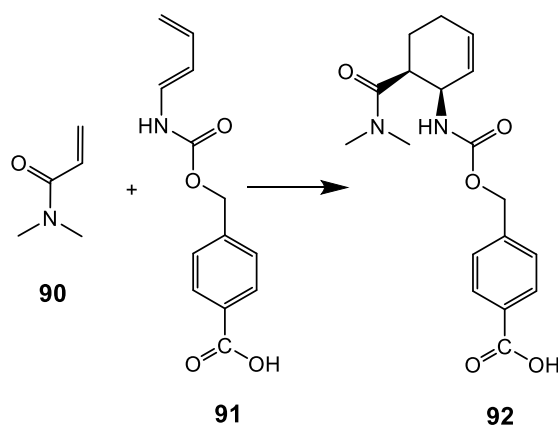


Figure 20: The Diels-Alder reaction. The reaction between *N,N*-dimethylacrylamide **90** and 4-carboxybenzyl *trans*-1,3-butadiene-1-carbamate **91** to form **92**. [77,89]

The activity of DA_20_00 for the transformation of **90** and **91** to **92** (Figure 20) was improved using directed evolution.[77] Active site residues expected to lie in close proximity to the transition state were targeted for randomisation. The most improved variant DA_20_10 contained 6 mutations, which increased the catalytic efficiency by 100-fold. Three mutations Ala74Ile, Ala21Thr and Ala173Cys, are believed to improve packing around the transition state and the catalytic residue Gln195, whilst Gln149Arg and Ser71Ala mutations are believed to improve the electrostatic complementarity with the bound substrates. Mutation of the catalytic Gln195 to a glutamate abolished activity, and mutation of the catalytic Tyr121 to phenylalanine reduced activity 27-fold, which confirms the theorised mechanism for the designed enzyme. DA_20_10 is enantioselective as well as diastereoselective, in accordance with the original design, and provides the *3R,4S endo* product **92** in >97% yield.[77]

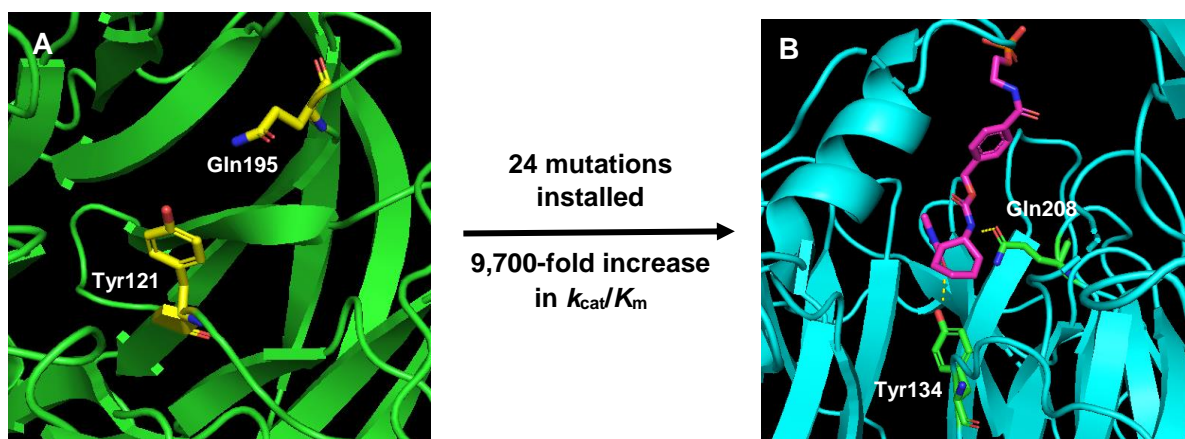


Figure 21: Design and evolution of an efficient Diels-Alderase. A) X-ray crystal structure showing the active site of the modestly active computationally designed DA_20_00 in green ribbons, key active site residues are shown in yellow sticks. PDB code: 311C.[77] B) X-ray crystal structure showing the active site of the efficient Diels-Alderase catalyst CE20. The active site of CE20 is shown in cyan ribbons, key active site residues are shown in green sticks, the Diels-Alder product analogue is shown in magenta sticks and hydrogen bonding contacts shown as dashed lines. PDB code: 4O5T.[89]

DA_20_10 was further improved over an additional eight rounds of directed evolution.[89] Error-prone PCR was used to create DNA libraries containing one to five mutations per gene and variants were evaluated using a direct MS-MS assay. A further seven mutations were installed into DA_20_10 to yield DA_20_20, which has a 5.5-fold improvement in catalytic efficiency over the starting variant. Structural analysis of DA_20_10 showed that the active site is large, open and solvent exposed. In an attempt to improve substrate binding, the computational design program Foldit was used to install an active site lid comprising of a 24-residue helix-turn-helix motif.[90] Indeed, the new design CE6 displayed a lower K_m value when compared to DA_20_20. CE6 was subjected to a further eight rounds of directed evolution to yield CE20 (Figure 21B). CE20 contains a total of 24-mutations and is 9,700-fold more active than the original DA-20_00 design.

1.4.2.3 Retro-aldolase

Aldol condensations are carbon-carbon (C-C) bond forming reactions between an enol or enolate and a carbonyl compound. In Nature, Type I aldolases catalyse the reversible aldol reaction using a catalytic lysine which forms Schiff base intermediates with the carbonyl substrates. The reaction has multiple intermediates and transition states, which makes the computational design of aldolases challenging. Nonetheless, an efficient *de novo* retro-aldolase that promotes the cleavage of 4-hydroxy-4-(6-methoxy-2-naphthyl)-2-butanone (methodol) **93** (Figure 22) has been successfully created using a combination of computational design and directed evolution.[78,91-93]

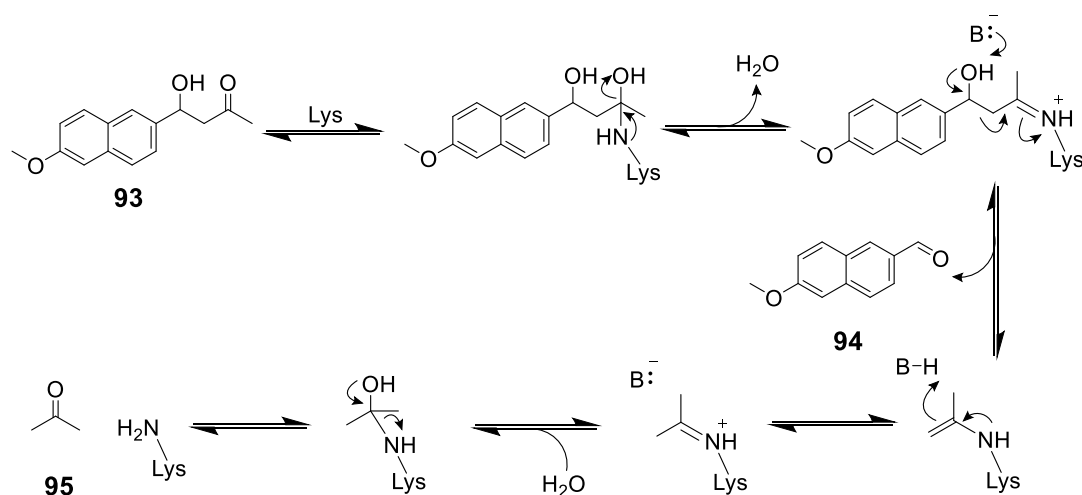


Figure 22: The retro-aldol reaction. The mechanism of the retro-aldol reaction displaying the C-C bond breaking of methodol **93** into 6-Methoxy-2-naphthaldehyde **94** and acetone **95**.

Methodol **93** was selected as the target substrate as the product of the reaction 6-Methoxy-2-naphthaldehyde **94** is a fluorescent naphthaldehyde derivative, meaning designs can be quickly evaluated using spectrophotometric methods. Retro-aldolases were designed to mimic natural type-I aldolases and exploit a catalytic lysine. Nucleophilic attack by lysine on the substrate ketone creates a carbinolamine intermediate, which is dehydrated to form the iminium species. Deprotonation of the β -alcohol triggers carbon-carbon bond cleavage and the enamine tautomerises to an imine. The imine is then hydrolysed to release the enzyme from the covalently bound product (Figure 22).

As the reaction proceeds through multiple intermediates, multiple transition states and reaction intermediates were initially used to generate a composite transition state. The original theozyme design included four different catalytic motifs to facilitate the formation of carbinolamine, elimination of water, C-C bond cleavage and subsequent product release **94**. In total, 70 designs were expressed, purified and evaluated for activity towards methodol **93** cleavage. 31 designs showed detectable retro-aldolase activity, with several designs showing rate enhancements of up to four orders of magnitude over the non-catalysed reaction.[78] However, the most active design RA61 had a catalytic efficiency (k_{cat}/K_M) of $0.74 \text{ M}^{-1} \text{ s}^{-1}$ which is well below that of natural enzymes.

The computational design process was repeated using a larger number of sidechain rotamers and designs were repacked in the presence and absence of the transition state analogue to favour designs with a pre-organised active site.[91] Out of 42 designs which were characterised experimentally, 33 showed low activity towards the cleavage of **93**.

One of the best designs however, RA95, was based on an indole-3-glycerol phosphate synthase ($\beta\alpha$)₈ barrel scaffold with 11 mutations introduced by Rosetta Design, and promotes the cleavage of **93** with a 15,000-fold rate improvement over the background reaction. The intended design features included a catalytic lysine at position 210 to promote C-C bond cleavage via Schiff base formation and an ordered water molecule coordinated by a glutamate at position 53. However, the X-ray crystal

structure of RA95 covalently bound to a mechanistic inhibitor **96** (Figure 23A) revealed that although the Lys210 side chain adopts the intended conformation, with the ϵ -amino group sitting in a relatively hydrophobic environment (Figure 23B), the Glu53 residue designed to coordinate a water for proton transfer was not in a productive conformation. Mutation of the Glu53 residue to alanine did not affect the catalytic activity confirming this hypothesis.[91]

RA95 has been extensively engineered to deliver catalysts with efficiencies approaching those of natural enzymes.[92,93] Initial rounds of evolution exploited a 96-well plate based assay with fluorescence detection and led to the identification of RA95.5-8, which contains 15 mutations and has a >4,400-fold improvement in catalytic efficiency compared to RA95.[92] RA95.5-8 was further evolved using an ultrahigh throughput droplet-based microfluidic screen[93] and a positively charged aldol substrate in replacement of methodol **93** to avoid diffusion of the fluorescent product between droplets in screening.

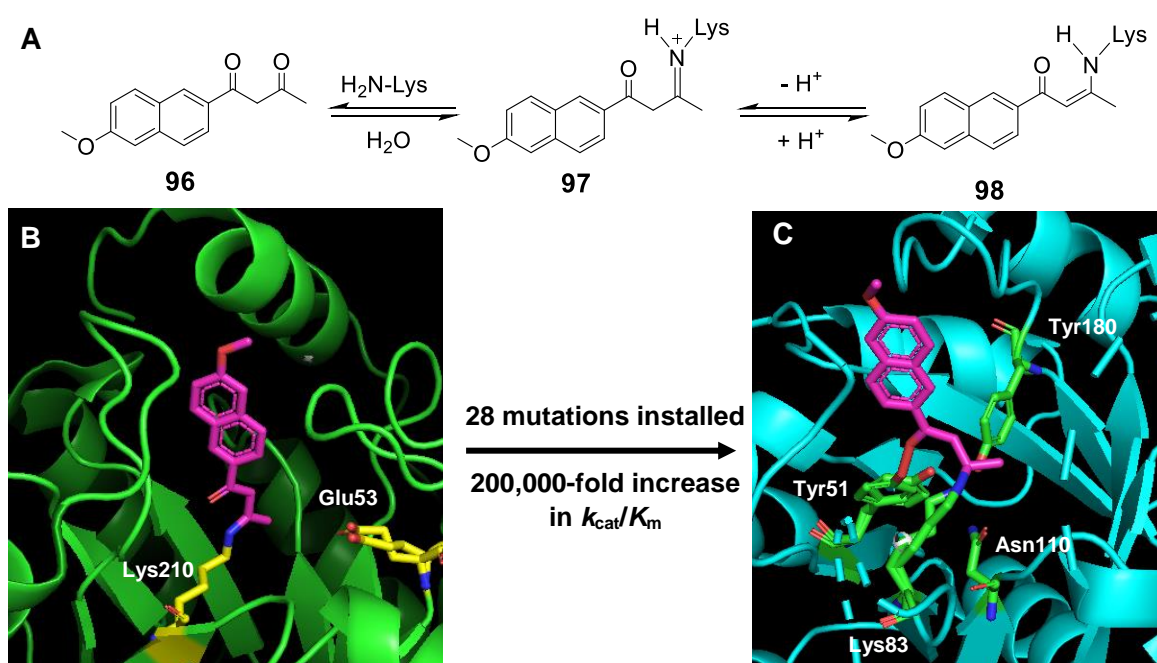


Figure 23: The Evolution of the retro-aldolase RA95. A) The mechanism of action for the 1,3-diketone mechanistic inhibitor **96** B) X-ray crystal structure showing the active site of RA95 in green ribbons covalently bound to mechanistic inhibitor **96** shown in magenta, with key residues in yellow sticks. PDB code: 4A29.[91] C) X-ray crystal structure showing the active site of RA95.5-8F in cyan ribbons covalently bound to mechanistic inhibitor **96** shown in magenta, with key residues in green sticks. PDB code: 5AN7.[93]

The most improved variant RA95.5-8F identified following 6 rounds of microfluidics screening contained an additional 13 mutations and has a k_{cat}/K_m of 34,000 $M^{-1} s^{-1}$ for the cleavage of (*R*)-methodol which is a 200,000-fold improvement compared to RA95.[93] The crystal structure of RA95.5-8F covalently bound to the 1,3-diketone mechanistic inhibitor **96** shows that the naphthyl ring binds in the original designed pocket which was conserved over the evolution trajectory. However, during evolution, the intended catalytic lysine (Lys210) has been replaced by Lys83. This

multi-step mechanism is further supported by a hydrogen bonding network consisting of residues Tyr51, Asn110 and Tyr180; which bind both the hydroxyl of the carbinolamine intermediate, and position an ordered water molecule promoting proton transfer. Interestingly, the activity of RA95.5-8F now surpasses that of previously designed catalytic antibodies (38C2) and is comparable to natural aldolases such as human fructose-1,6-diphosphate (FDP).[94, 95]

1.5 Morita-Baylis-Hillman reaction

The Morita-Baylis-Hillman (MBH) reaction involves the C-C bond formation between the α -position of an α,β -unsaturated carbonyl e.g. **99** with a carbon electrophile e.g. **100** containing an electron deficient sp^2 carbon atom, for example an aldehyde (Figure 24).[96,97] Michael addition of the nucleophile to the β -carbon of an activated alkene forms a stabilised anion, this intermediate then attacks a carbon electrophile in an aldol addition to yield a second intermediate, and subsequent proton transfer eliminates the catalyst to yield the product. Kinetic and theoretical studies suggest the rate determining step (RDS) is proton transfer and elimination of the catalyst.[98,99] The reaction is an atom efficient, multi-step transformation which leads to the generation of synthetically useful and densely functionalised products e.g., **102**. The MBH reaction is commonly catalysed by small molecule catalysts, for example, tertiary amines such as 1,4-diazabicyclo[2.2.2]octane (DABCO), 4-dimethylaminopyridine (DMAP), imidazole **101** and tertiary phosphines.

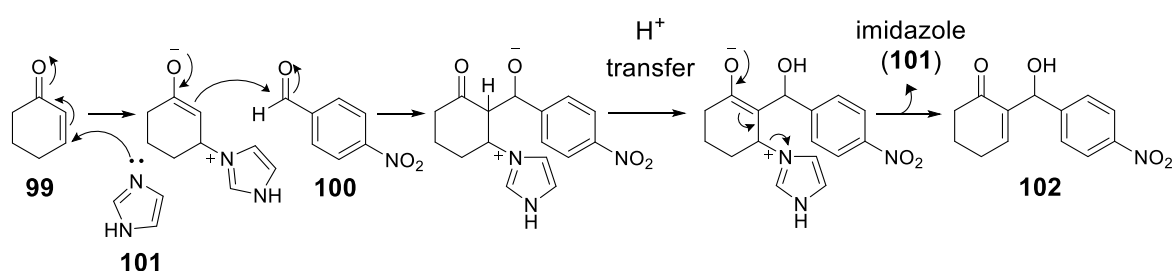


Figure 24: The model MBH reaction between 2-cyclohexenone **99 and 4-nitrobenzaldehyde **100**.** The mechanism of the model MBH reaction between 2-cyclohexen-1-one **99** and 4-nitrobenzaldehyde **100** to generate the MBH product **102**, with imidazole **101** as the nucleophile.

Co-catalysts such as thioureas have also been employed to accelerate the MBH reaction and can act as Brønsted acids stabilising the basic oxygen centre formed along the reaction coordinate, thus decreasing the energy of the RDS.[100] Enantioselective versions of the MBH reaction have also been developed by employing chiral catalysts such as quinidine derivatives, chiral DMAP surrogates or pairing catalytic nucleophiles (Lewis acids) with chiral hydrogen bond donors (Brønsted acids) such as thioureas.[101-104] The Lewis base initiates the reaction by Michael addition, and the Brønsted acid stabilises the intermediates of the reaction and promotes aldol addition and proton elimination. The first bifunctional catalyst reported for the MBH reaction was a hydroxylated chiral amine which catalysed the reaction between 4-nitrobenzaldehyde **100** and 1,1,1,3,3,3-hexafluoropropan-2-yl acrylate **103** to yield the (*R*)-enantiomer **104** in 91% e.e. (Figure 24).[105]

However, controlling the stereochemistry in MBH reactions still remains a considerable challenge. The synthetic utility of this reaction is further compromised by the low catalytic efficiency of existing systems which mean that prolonged reaction times and high catalyst loadings are required to achieve reasonable conversions.

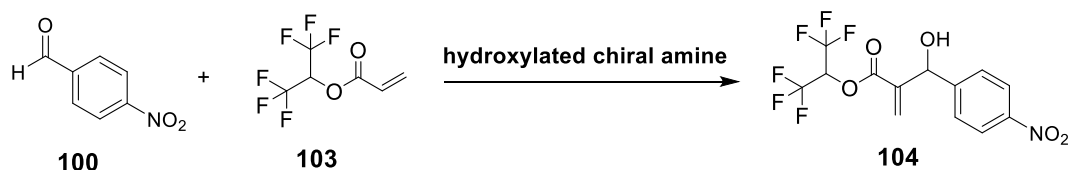


Figure 25: The MBH reaction. The MBH reaction between 4-nitrobenzaldehyde **100** and 1,1,1,3,3,3-hexafluoropropan-2-yl acrylate **103**.^[105]

1.5.1 *De novo* design attempt of a MBHase

Biocatalysis could offer a solution to address the long-standing challenges associated with the MBH reaction. However, there are no known natural enzymes or catalytic antibodies for this transformation. Only extremely low levels of promiscuous MBH activity have been reported for a handful of wild-type proteins, with non-specific protein catalysis implicated in a number of cases.^[106,107] Given the absence of wild-type enzymes for this valuable transformation, the Baker group attempted to create a *de novo* enzyme for the MBH reaction between 2-cyclohexen-1-one **99** and 4-nitrobenzaldehyde **100**.^[108] This bimolecular reaction is a demanding transformation with multiple high energy transition states and represents the most complex *de novo* design to date. The theozyme design used a composite transition state for the reaction generated by MD simulations and Quantum Mechanic (QM) modelling and included a histidine or cysteine nucleophile and two hydrogen bond donors to stabilise oxyanion intermediates **Int 1** and **Int 2** (Figure 26).

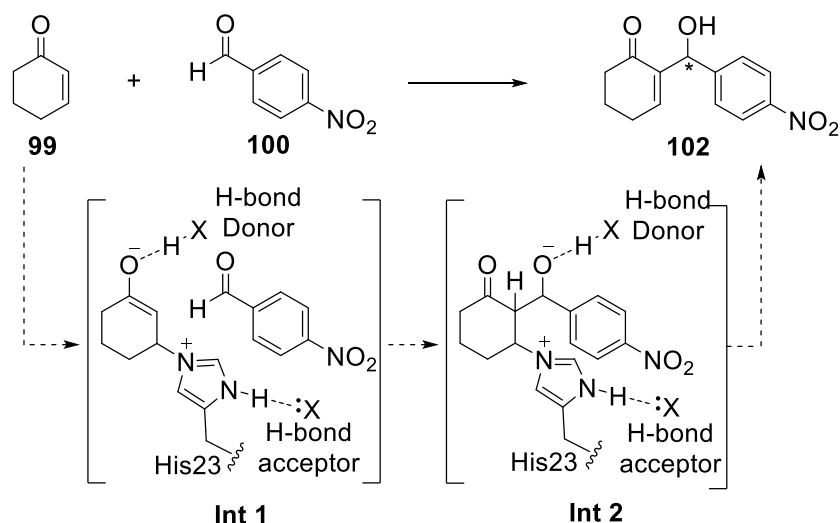


Figure 26: The model MBH reaction between 2-cyclohexenone **99 and 4-nitrobenzaldehyde **100**.** A scheme of the model MBH reaction between 2-cyclohexen-1-one **99** and 4-nitrobenzaldehyde **100** to generate the MBH product **102**, showing the two proposed intermediates formed along the reaction pathway, **Int1** and **Int2**.

48 computational designs were selected for experimental evaluation and enzymes were screened as cell free lysates using a high-pressure liquid chromatography (HPLC) analysis. Two designs, BH25 and BH32, showed activity towards the MBH reaction. The BH25 design utilised a nucleophilic cysteine (Cys39) supported by a lysine residue (Lys285) built into an alanine racemase from *Geobacillus stearothermophilus*. The BH32 design utilised a nucleophilic histidine (His23) positioned by hydrogen-bonding to glutamic acid (Glu46) built into a haloacid dehalogenase from *Pyrococcus horikoshii*. Despite intensive design efforts, the most active design BH32 had very modest activity and promoted the coupling of 2-cyclohexen-1-one **99** with 4-nitrobenzaldehyde **100** with a turnover of $<1 \text{ day}^{-1}$ and was described by the authors as an 'enone-binding protein'. The activity of BH32 was dependent on the His23 nucleophile and mutation of His23 to alanine significantly reduced catalytic activity. However, comparison of the X-ray crystal structure of BH32 to the design model showed that other intended features including the Glu46-His23 hydrogen bond, and residues required for oxyanion stabilisation were not accurately positioned leading to unproductive interactions.[108] Although the BH32 design had very low-level activity, it represents the most complex enzyme design to date and provides a starting point for further optimisation using directed evolution.

1.6 References

1. Bornscheuer, U. T. et al. Engineering the third wave of biocatalysis. *Nature* **485**, 185-194 (2012).
2. Turner, N. J. Directed evolution of enzymes for applied biocatalysis. *Trends Biotechnol.* **21**, 474-478 (2003).
3. Savile, C. K. et al. Biocatalytic asymmetric synthesis of chiral amines from ketones applied to sitagliptin manufacture. *Science* **329**, 305-309 (2010).
4. Huffman, M. A. et al. Design of an in vitro biocatalytic cascade for the manufacture of islatravir. *Science* **366**, 1255-1259 (2019).
5. Jungmann, V. et al. Biocatalytic conversion of avermectin to 4"-oxo-avermectin: characterization of biocatalytically active bacterial strains and of cytochrome p450 monooxygenase enzymes and their genes. *Appl. Environ. Microbiol.* **71**, 6968-6976 (2005).
6. Shaw, A. J. et al. Metabolic engineering of a thermophilic bacterium to produce ethanol at high yield. *Proc. Natl. Acad. Sci. U. S. A.* **105**, 13769-13774 (2008).
7. Kopetzki, E., Lehnert, K. & Buckel, P. Enzymes in diagnostics: achievements and possibilities of recombinant DNA technology. *Clin. Chem.* **40**, 688-704 (1994).
8. Hogg, J. A. Steroids, the steroid community, and Upjohn in perspective: a profile of innovation. *Steroids* **57**, 593-616 (1992).
9. Barnes, H. J., Arlotto, M. P. & Waterman, M. R. Expression and enzymatic activity of recombinant cytochrome P450 17 alpha-hydroxylase in *Escherichia coli*. *Proc. Natl. Acad. Sci. U. S. A.* **88**, 5597-5601 (1991).
10. Jackel, C., Kast, P. & Hilvert, D. Protein design by directed evolution. *Annu. Rev. Biophys.* **37**, 153-173 (2008).
11. Arnold, F. H. Directed Evolution: Bringing New Chemistry to Life. *Angew. Chem. Int. Ed. Engl.* **57**, 4143-4148 (2018).
12. Cadwell, R. C. & Joyce, G. F. Randomization of genes by PCR mutagenesis. *PCR Methods Appl.* **2**, 28-33 (1992).
13. Stemmer, W. P. Rapid evolution of a protein in vitro by DNA shuffling. *Nature* **370**, 389-391 (1994).
14. Zhao, H., Giver, L., Shao, Z., Affholter, J. A. & Arnold, F. H. Molecular evolution by staggered extension process (StEP) in vitro recombination. *Nat. Biotechnol.* **16**, 258-261 (1998).
15. Reetz, M. T. & Wu, S. Greatly reduced amino acid alphabets in directed evolution: making the right choice for saturation mutagenesis at homologous enzyme positions. *Chem. Commun. (Camb.)* **43**, 5499-5501 (2008).
16. Kille, S. et al. Reducing codon redundancy and screening effort of combinatorial protein libraries created by saturation mutagenesis. *ACS Synth. Biol.* **2**, 83-92 (2013).
17. Reetz, M. T., Kahakeaw, D. & Lohmer, R. Addressing the numbers problem in directed evolution. *Chembiochem* **9**, 1797-1804 (2008).
18. Reetz, M. T. et al. Expanding the substrate scope of enzymes: combining mutations obtained by CASTing. *Chemistry* **12**, 6031-6038 (2006).

19. Reetz, M. T., Wang, L. W. & Bocola, M. Directed evolution of enantioselective enzymes: iterative cycles of CASTing for probing protein-sequence space. *Angew. Chem. Int. Ed. Engl.* **45**, 1236-1241 (2006).
20. Delagrave, S. et al. Application of a very high-throughput digital imaging screen to evolve the enzyme galactose oxidase. *Protein Eng.* **14**, 261-267 (2001).
21. Mastrobattista, E. et al. High-throughput screening of enzyme libraries: in vitro evolution of a beta-galactosidase by fluorescence-activated sorting of double emulsions. *Chem. Biol.* **12**, 1291-1300 (2005).
22. Agresti, J. J. et al. Ultrahigh-throughput screening in drop-based microfluidics for directed evolution. *Proc. Natl. Acad. Sci. U S A* **107**, 4004-4009 (2010).
23. Fernandez-Gacio, A., Uguen, M. & Fastrez, J. Phage display as a tool for the directed evolution of enzymes. *Trends Biotechnol.* **21**, 408-414 (2003).
24. Lipovsek, D. et al. Selection of horseradish peroxidase variants with enhanced enantioselectivity by yeast surface display. *Chem. Biol.* **14**, 1176-1185 (2007).
25. Abrahamson, M. J., Vazquez-Figueroa, E., Woodall, N. B., Moore, J. C. & Bommarius, A. S. Development of an amine dehydrogenase for synthesis of chiral amines. *Angew. Chem. Int. Ed. Engl.* **51**, 3969-3972 (2012).
26. Khan, N. U., Kamath, A. V. & Vaidyanathan, C. S. Study of interfering substances in a simple, new spectrophotometric assay for phenylalanine ammonia-lyase. *Biochem. Int.* **14**, 451-455 (1987).
27. McLaughlin, M. et al. Enantioselective Synthesis of 4'-Ethynyl-2-fluoro-2'-deoxyadenosine (EFdA) via Enzymatic Desymmetrization. *Org. Lett.* **19**, 926-929 (2017).
28. Alexeeva, M., Enright, A., Dawson, M. J., Mahmoudian, M. & Turner, N. J. Deracemization of alpha-methylbenzylamine using an enzyme obtained by in vitro evolution. *Angew. Chem. Int. Ed. Engl.* **41**, 3177-3180 (2002).
29. Carr, R. et al. Directed evolution of an amine oxidase for the preparative deracemisation of cyclic secondary amines. *ChemBiochem* **6**, 637-639 (2005).
30. Dunsmore, C. J., Carr, R., Fleming, T. & Turner, N. J. A chemo-enzymatic route to enantiomerically pure cyclic tertiary amines. *J. Am. Chem. Soc.* **128**, 2224-2225 (2006).
31. Znabet, A. et al. A highly efficient synthesis of telaprevir by strategic use of biocatalysis and multicomponent reactions. *Chem. Commun. (Camb.)* **46**, 7918-7920 (2010).
32. Ghislieri, D. et al. Engineering an enantioselective amine oxidase for the synthesis of pharmaceutical building blocks and alkaloid natural products. *J. Am. Chem. Soc.* **135**, 10863-10869 (2013).
33. Schober, M. et al. Chiral synthesis of LSD1 inhibitor GSK2879552 enabled by directed evolution of an imine reductase. *Nat. Catal.* **2**, 909-915 (2019).
34. Hilvert, D. Design of protein catalysts. *Annu. Rev. Biochem.* **82**, 447-470 (2013).
35. Hyster, T. K., Knorr, L., Ward, T. R. & Rovis, T. Biotinylated Rh(III) complexes in engineered streptavidin for accelerated asymmetric C-H activation. *Science* **338**, 500-503 (2012).

36. Mirts, E. N., Petrik, I. D., Hosseinzadeh, P., Nilges, M. J. & Lu, Y. A designed heme-[4Fe-4S] metalloenzyme catalyzes sulfite reduction like the native enzyme. *Science* **361**, 1098-1101 (2018).
37. Guengerich, F. P. Common and uncommon cytochrome P450 reactions related to metabolism and chemical toxicity. *Chem. Res. Toxicol.* **14**, 611-650 (2001).
38. Labinger, J. A. & Bercaw, J. E. Understanding and exploiting C-H bond activation. *Nature* **417**, 507-514 (2002).
39. Coelho, P. S., Brustad, E. M., Kannan, A. & Arnold, F. H. Olefin cyclopropanation via carbene transfer catalyzed by engineered cytochrome P450 enzymes. *Science* **339**, 307-310 (2013).
40. Wang, Z. J. et al. Improved cyclopropanation activity of histidine-ligated cytochrome P450 enables the enantioselective formal synthesis of levomilnacipran. *Angew. Chem. Int. Ed. Engl.* **53**, 6810-6813 (2014).
41. McIntosh, J. A. et al. Enantioselective intramolecular C-H amination catalyzed by engineered cytochrome P450 enzymes in vitro and in vivo. *Angew. Chem. Int. Ed. Engl.* **52**, 9309-9312 (2013).
42. Prier, C. K., Zhang, R. K., Buller, A. R., Brinkmann-Chen, S. & Arnold, F. H. Enantioselective, intermolecular benzylic C-H amination catalysed by an engineered iron-haem enzyme. *Nat. Chem.* **9**, 629-634 (2017).
43. Emmanuel, M. A., Greenberg, N. R., Oblinsky, D. G. & Hyster, T. K. Accessing non-natural reactivity by irradiating nicotinamide-dependent enzymes with light. *Nature* **540**, 414-417 (2016).
44. Man, H. et al. Structures of alcohol dehydrogenases from *Ralstonia* and *Sphingobium* spp. reveal the molecular basis for their recognition of 'bulky-bulky' ketones. *Top. Catal.* **57**, 356-365 (2014).
45. Biegasiewicz, K. F. et al. Photoexcitation of flavoenzymes enables a stereoselective radical cyclization. *Science* **364**, 1166-1169 (2019).
46. Sandoval, B. A., Meichan, A. J. & Hyster, T. K. Enantioselective Hydrogen Atom Transfer: Discovery of Catalytic Promiscuity in Flavin-Dependent 'Ene'-Reductases. *J. Am. Chem. Soc.* **139**, 11313-11316 (2017).
47. Davis, L. & Chin, J. W. Designer proteins: applications of genetic code expansion in cell biology. *Nat. Rev. Mol. Cell. Biol.* **13**, 168-182 (2012).
48. Liu, C. C. & Schultz, P. G. Adding new chemistries to the genetic code. *Annu. Rev. Biochem.* **79**, 413-444 (2010).
49. Schultz, K. C. et al. A genetically encoded infrared probe. *J. Am. Chem. Soc.* **128**, 13984-13985 (2006).
50. Chatterjee, A., Guo, J., Lee, H. S. & Schultz, P. G. A genetically encoded fluorescent probe in mammalian cells. *J. Am. Chem. Soc.* **135**, 12540-12543 (2013).
51. Lang, K. et al. Genetically encoded norbornene directs site-specific cellular protein labelling via a rapid bioorthogonal reaction. *Nat. Chem.* **4**, 298-304 (2012).
52. Blizzard, R. J. et al. Ideal Bioorthogonal Reactions Using A Site-Specifically Encoded Tetrazine Amino Acid. *J. Am. Chem. Soc.* **137**, 10044-10047 (2015).

53. Chin, J. W., Martin, A. B., King, D. S., Wang, L. & Schultz, P. G. Addition of a photocrosslinking amino acid to the genetic code of Escherichia coli. *Proc. Natl. Acad. Sci. U. S. A.* **99**, 11020-11024 (2002).
54. Chou, C. et al. Genetically encoding an aliphatic diazine for protein photocrosslinking. *Chem. Sci.* **2**, 480-483 (2011).
55. Rogerson, D. T. et al. Efficient genetic encoding of phosphoserine and its nonhydrolyzable analog. *Nat. Chem. Biol.* **11**, 496-503 (2015).
56. Neumann, H., Peak-Chew, S. Y. & Chin, J. W. Genetically encoding N(epsilon)-acetyllysine in recombinant proteins. *Nat. Chem. Biol.* **4**, 232-234 (2008).
57. Drienovska, I., Mayer, C., Dulson, C. & Roelfes, G. A designer enzyme for hydrazone and oxime formation featuring an unnatural catalytic aniline residue. *Nat. Chem.* **10**, 946-952 (2018).
58. Mayer, C., Dulson, C., Reddem, E., Thunnissen, A. W. H. & Roelfes, G. Directed Evolution of a Designer Enzyme Featuring an Unnatural Catalytic Amino Acid. *Angew. Chem. Int. Ed. Engl.* **58**, 2083-2087 (2019).
59. Liu, X. et al. A genetically encoded photosensitizer protein facilitates the rational design of a miniature photocatalytic CO₂-reducing enzyme. *Nat. Chem.* **10**, 1201-1206 (2018).
60. Pauling, L. Nature of forces between large molecules of biological interest. *Nature* **161**, 707-709 (1948).
61. Jencks, W. P. *Catalysis in chemistry and enzymology.* (McGraw-Hill, 1969).
62. Tramontano, A., Janda, K. D. & Lerner, R. A. Catalytic antibodies. *Science* **234**, 1566-1570 (1986).
63. Wagner, J., Lerner, R. A. & Barbas, C. F., 3rd. Efficient aldolase catalytic antibodies that use the enamine mechanism of natural enzymes. *Science* **270**, 1797-1800 (1995).
64. Gouverneur, V. E. et al. Control of the exo and endo pathways of the Diels-Alder reaction by antibody catalysis. *Science* **262**, 204-208 (1993).
65. Wentworth, P., Jr. et al. Antibody catalysis of the oxidation of water. *Science* **293**, 1806-1811 (2001).
66. Hsieh, L. C., Yonkovich, S., Kochersperger, L. & Schultz, P. G. Controlling chemical reactivity with antibodies. *Science* **260**, 337-339 (1993).
67. Hilvert, D. Critical analysis of antibody catalysis. *Annu. Rev. Biochem.* **69**, 751-793 (2000).
68. Thorn, S. N., Daniels, R. G., Auditor, M. T. & Hilvert, D. Large rate accelerations in antibody catalysis by strategic use of haptenic charge. *Nature* **373**, 228-230 (1995).
69. Hilvert, D. et al. Antibody catalysis of the Diels-Alder reaction. *J. Am. Chem. Soc.* **111**, 9261-9262 (1989).
70. Bjornestedt, R. et al. Copying Nature's Mechanism for the Decarboxylation of β -Keto Acids into Catalytic Antibodies by Reactive Immunization. *J. Am. Chem. Soc.* **118**, 11720-11724 (1996).
71. Hoffmann, T. et al. Aldolase Antibodies of Remarkable Scope. *J. Am. Chem. Soc.* **120**, 2768-2779 (1998).
72. Kiss, G., Celebi-Olcum, N., Moretti, R., Baker, D. & Houk, K. N. Computational enzyme design. *Angew. Chem. Int. Ed. Engl.* **52**, 5700-5725 (2013).

73. Kries, H., Blomberg, R. & Hilvert, D. *De novo* enzymes by computational design. *Curr. Opin. Chem. Biol.* **17**, 221-228 (2013).
74. Zanghellini, A. et al. New algorithms and an in silico benchmark for computational enzyme design. *Protein Sci.* **15**, 2785-2794 (2006).
75. Dahiyat, B. I. & Mayo, S. L. Protein design automation. *Protein Sci.* **5**, 895-903 (1996).
76. Rothlisberger, D. et al. Kemp elimination catalysts by computational enzyme design. *Nature* **453**, 190-195 (2008).
77. Siegel, J. B. et al. Computational design of an enzyme catalyst for a stereoselective bimolecular Diels-Alder reaction. *Science* **329**, 309-313 (2010).
78. Jiang, L. et al. *De novo* computational design of retro-aldol enzymes. *Science* **319**, 1387-1391 (2008).
79. Casey, M.L. et al. The Physical Organic Chemistry of Benzisoxazoles. I. The Mechanism of the Base-Catalyzed Decomposition of Benzisoxazoles. *J. Org. Chem.* **38**, 2294-2301 (1973).
80. Khersonsky, O. et al. Bridging the gaps in design methodologies by evolutionary optimization of the stability and proficiency of designed Kemp eliminase KE59. *Proc. Natl. Acad. Sci. U. S. A.* **109**, 10358-10363 (2012).
81. Korendovych, I. V. et al. Design of a switchable eliminase. *Proc. Natl. Acad. Sci. U. S. A.* **108**, 6823-6827 (2011).
82. Caselle, E. A. et al. Kemp Eliminases of the AlleyCat Family Possess High Substrate Promiscuity. *ChemCatChem* **11**, 1425-1430 (2019).
83. Privett, H. K. et al. Iterative approach to computational enzyme design. *Proc. Natl. Acad. Sci. U. S. A.* **109**, 3790-3795 (2012).
84. Blomberg, R. et al. Precision is essential for efficient catalysis in an evolved Kemp eliminase. *Nature* **503**, 418-421 (2013).
85. Katayama, K., Kobayashi, T., Oikawa, H., Honma, M. & Ichihara, A. Enzymatic activity and partial purification of solanapyrone synthase: first enzyme catalyzing Diels-Alder reaction. *Biochim. Biophys. Acta.* **1384**, 387-395 (1998).
86. Auclair K. et al. Lovastatin nonaketide synthase catalyzes an intramolecular Diels-Alder reaction of a substrate analogue. *J. Am. Chem. Soc.* **122**, 11519-11520 (2000).
87. Stocking, E. M. & Williams, R. M. Chemistry and biology of biosynthetic Diels-Alder reactions. *Angew. Chem. Int. Ed. Engl.* **42**, 3078-3115 (2003).
88. Kim, H. J., Ruzsyczky, M. W., Choi, S. H., Liu, Y. N. & Liu, H. W. Enzyme-catalysed [4+2] cycloaddition is a key step in the biosynthesis of spinosyn A. *Nature* **473**, 109-112 (2011).
89. Preiswerk, N. et al. Impact of scaffold rigidity on the design and evolution of an artificial Diels-Alderase. *Proc. Natl. Acad. Sci. U S A* **111**, 8013-8018 (2014).
90. Eiben, C. B. et al. Increased Diels-Alderase activity through backbone remodeling guided by Foldit players. *Nat. Biotechnol.* **30**, 190-192 (2012).
91. Althoff, E. A. et al. Robust design and optimization of retroaldol enzymes. *Protein Sci.* **21**, 717-726 (2012).
92. Giger, L. et al. Evolution of a designed retro-aldolase leads to complete active site remodeling. *Nat. Chem. Biol.* **9**, 494-498 (2013).

93. Obexer, R. et al. Emergence of a catalytic tetrad during evolution of a highly active artificial aldolase. *Nat. Chem.* **9**, 50-56 (2017).
94. Esposito, G. et al. Structural and functional analysis of aldolase B mutants related to hereditary fructose intolerance. *FEBS Lett.* **531**, 152-156 (2002).
95. Heine, A. et al. Observation of covalent intermediates in an enzyme mechanism at atomic resolution. *Science* **294**, 369-374 (2001).
96. Morita, K. et al. A Tertiary Phosphine-catalyzed Reaction of Acrylic Compounds with Aldehydes. *Bull. Chem. Soc. Japan* **41**, 2815 (1968).
97. Baylis, A. B. & Hillman, M. E. D. German patent 2155113. *Chem. Abstr.* **77** (1972).
98. Price, K. E., Broadwater, S. J., Jung, H. M. & McQuade, D. T. Baylis-Hillman mechanism: a new interpretation in aprotic solvents. *Org. Lett.* **7**, 147-150 (2005).
99. Price, K. E., Broadwater, S. J., Walker, B. J. & McQuade, D. T. A new interpretation of the Baylis-Hillman mechanism. *J. Org. Chem.* **70**, 3980-3987 (2005).
100. Iwabuchi, Y. et al. Chiral Amine-Catalyzed Asymmetric Baylis-Hillman Reaction: A Reliable Route to Highly Enantiomerically Enriched (α -Methylene- β -hydroxy)esters. *J. Am. Chem. Soc.* **121**, 10219-10220 (1999).
101. Doyle, A. G. & Jacobsen, E. N. Small-molecule H-bond donors in asymmetric catalysis. *Chem. Rev.* **107**, 5713-5743 (2007).
102. Taylor, M. S. & Jacobsen, E. N. Asymmetric catalysis by chiral hydrogen-bond donors. *Angew. Chem. Int. Ed. Engl.* **45**, 1520-1543 (2006).
103. Shi, M. & Liu, X.-G. Asymmetric Morita-Baylis-Hillman reaction of arylaldehydes with 2-cyclohexen-1-one and 2-cyclopenten-1-one catalyzed by chiral bis(thio)urea and DABCO. *Org. Lett.* **10**, 1043-1046 (2008).
104. Wei, Y. & Shi, M. Recent advances in organocatalytic asymmetric Morita-Baylis-Hillman/aza-Morita-Baylis-Hillman Reactions. *Chem. Rev.* **113**, 6659-6690 (2013).
105. Ciganek, E. The Catalyzed α -Hydroxyalkylation and α -Aminoalkylation of Activated Olefins (The Morita-Baylis-Hillman Reaction). *Org. React.* **51**, 201-350 (1997).
106. Reetz, M. T., Mondière, R. & Carballeira, J. D. Enzyme promiscuity: first protein-catalyzed Morita-Baylis-Hillman reaction. *Tetrahedron Lett.* **48**, 1679-1681 (2007).
107. López-Iglesias, M., Busto, E., Gotor, V. & Gotor-Fernández, V. Use of protease from *Bacillus licheniformis* as promiscuous catalyst for organic synthesis: applications in C-C and C-N bond formation reactions. *Adv. Synth. Catal.* **353**, 2345-2353 (2011).
108. Bjelic, S. et al. Computational design of enone-binding proteins with catalytic activity for the Morita-Baylis-Hillman reaction. *ACS Chem. Biol.* **8**, 749-757 (2013).

Chapter 2: Aims

The primary aim of this thesis is to develop an efficient and enantioselective *de novo* enzyme of the Morita-Baylis-Hillman reaction, a valuable C-C bond forming reaction not observed in Nature, by subjecting the primitive computational design BH32 to iterative rounds of laboratory evolution. A second objective is to prepare and characterise variants of BH32 with the catalytic His23 residue replaced by a non-canonical *N*₅-methylhistidine, to investigate whether the introduction of 'organocatalytic groups' into *de novo* active sites can open up new channels of reactivity and generate biocatalysts with augmented properties.

The specific aims of this project are as follows:

1. Characterise the primitive computational design BH32 and assess its catalytic activity for the MBH reaction.
2. Develop robust high-throughput (HTP) assays that report on MBH activity to underpin directed evolution efforts.
3. Subjected BH32 to iterative rounds of laboratory evolution to optimise catalytic activity.
4. Perform structural, kinetic and biochemical characterization of optimised variants to gain insights into the catalytic mechanism and the origins of improved function.
5. Investigate the synthetic scope of evolved BH32 variants.
6. Prepare and characterise variants of BH32 with the His23 nucleophile replaced with a non-canonical Me-His residue.

Chapter 3: An Efficient and Enantioselective *de novo* Enzyme for the Morita-Baylis-Hillman Reaction

Rebecca Crawshaw¹, Amy E. Crossley¹, Linus Johannissen¹, Ashleigh J. Burke¹, Sam Hay¹, Colin Levy¹, David Baker^{2,3,4}, Sarah L. Lovelock^{1*} and Anthony P. Green^{1*}

¹Manchester Institute of Biotechnology, School of Chemistry, 131 Princess Street, University of Manchester, Manchester M1 7DN, UK. ²Department of Biochemistry, University of Washington, Seattle, WA 98195. ³Institute for Protein Design, University of Washington, Seattle, WA 98195. ⁴Howard Hughes Medical Institute, University of Washington, Seattle, WA 98195.

3.1 Foreword

This chapter consists of a research article submitted to Nature on 15th December 2020 and describes the design and evolution of an enantioselective biocatalyst for the Morita-Baylis-Hillman reaction.

3.2 Author contributions

The research presented in this chapter was a collaborative effort between the doctoral candidate and the following researchers: Amy E. Crossley, Linus Johannissen, Ashleigh J. Burke, Sam Hay, Colin Levy, David Baker, Sarah L. Lovelock and Anthony P. Green. The doctoral candidate carried out molecular biology, assay development, protein production and purification, directed evolution, crystallization and kinetic characterization. The doctoral candidate, Ashleigh J. Burke and Amy E. Crossley developed spectrophotometric assays and carried out organic synthesis and enzyme-inhibition experiments. Linus Johannissen and Sam Hay carried out molecular docking and DFT calculations. Sarah L. Lovelock and Sam Hay interpreted and analysed kinetic data. Colin Levy interpreted, analysed and presented structural data. David Baker provided the BH32 design model. All authors discussed the results and participated in writing the manuscript.

3.3 Manuscript

The combination of computational design and directed evolution could offer a general strategy to create enzymes with new functions. To date, this approach has delivered *de novo* enzymes for a handful of model reactions, selected based on previous achievements with catalytic antibodies. Here we show that design offers a viable route to biocatalysts for more challenging chemical transformations. Evolutionary optimisation of a primitive design afforded a highly efficient and enantioselective enzyme for a bimolecular Morita-Baylis-Hillman reaction. A sophisticated catalytic mechanism has emerged comprising a His23 nucleophile paired with a judiciously positioned Arg124, which shuttles between conformational states to stabilise multiple oxyanion intermediates and serves as a genetically encoded surrogate of privileged bidentate hydrogen bonding catalysts. Our study demonstrates that elaborate catalytic devices can be built from scratch, where multiple functional components operate in tandem to accelerate demanding multi-step processes.

The ability to reliably design enzymes would have significant impacts across the chemical industry, allowing the rapid delivery of *de novo* biocatalysts in response to diverse societal challenges. Computational enzyme design is conceptually similar to catalytic antibody technology; in that it aims to generate protein catalysts based on fundamental principles of transition state stabilisation.[1] However, in principle computational design offers a far more flexible approach, as it is not limited to the antibody fold or reliant on the availability of an imperfect transition state mimic. Thus far, computational algorithms have enabled the design of primitive catalysts for a handful of transformations that have been optimised through laboratory evolution to deliver enzymes with efficiencies approaching natural systems.[2-7] Naturally, early efforts targeted simple model transformations selected based on previous achievements in the catalytic antibody field.[8-10] If we are to establish 'bottom up' enzyme design as a reliable source of biocatalysts for practical applications, we must move beyond the functional capabilities of antibodies and develop enzymes for demanding multi-step chemical processes.

The Morita-Baylis-Hillman (MBH) reaction (Fig. 1A), involving the coupling of α,β -unsaturated carbonyl compounds (e.g. **1**) with electrophilic aldehydes (e.g. **2**), is an iconic transformation in organic synthesis.[11] These reactions are typically promoted by small catalytic nucleophiles such as 4-dimethylaminopyridine (DMAP), 1,4-diazabicyclo[2.2.2]octane (DABCO) and imidazole. Enantioselective versions of the MBH reaction have been developed by employing chiral DMAP surrogates or by pairing catalytic nucleophiles with chiral hydrogen bond donors such as thioureas;[12] however achieving high levels of stereo-control remains a considerable challenge. Despite the great synthetic potential, the practical utility of MBH reactions is further compromised by the low efficiencies achieved by existing catalytic systems, which results in prolonged reaction times and the requirement for high catalyst loadings. Given the enormous rate accelerations achieved by enzymes, biological catalysts could offer a plausible solution to these long-standing challenges. However, there are no catalytic antibodies or known natural enzymes for the MBH reaction. Only extremely low levels of promiscuous activity have been reported with a handful of proteins,[13,14] with unspecific protein catalysis implicated in a number of these cases. In the absence of a suitable

natural enzyme, we elected to push the boundaries of *de novo* enzyme design and engineering to tackle the challenge of efficient MBH catalysis.

A primitive computational design (BH32) was selected as a starting template for evolutionary optimisation.[15] BH32 utilises a histidine nucleophile (His23) built into the cap domain of haloacid dehalogenase from *Pyrococcus horikoshii* by introducing 12 active site mutations predicted by the Rosetta software suite. Other intended design features (Fig. 1A) include: Glu46 to position and activate the His23 catalytic nucleophile through hydrogen bonding; an aromatic aldehyde binding pocket shaped by Phe132 and Leu10; Gln128 to serve as an oxyanion-hole to stabilise the first covalent enzyme-substrate intermediate formed upon reaction with 2-cyclohexen-1-one (Int 1); and an ordered water molecule bound through Ser22 designed to stabilise Int 2, formed following C-C bond formation, through hydrogen bonding. BH32 promotes the coupling of 2-cyclohexen-1-one **1** with 4-nitrobenzaldehyde **2** with extremely low efficiency ($k_{\text{cat}}/K_{\text{enone}} \cdot K_{\text{aldehyde}} = 2.21 \pm 0.18 \text{ M}^{-2}\text{s}^{-1}$). This activity is dependent on the His23 nucleophile, however comparison of the design model with the structurally characterised protein reveals discrepancies, which compromise the intended design features and likely contribute towards low efficiency.

A high-throughput spectrophotometric assay was developed to allow rapid evaluation of large libraries of BH32 derivatives during evolution. This was achieved by modifying the MBH product **3** through acetylation of the C3 secondary alcohol to generate a dual function mechanistic inhibitor and spectroscopic probe **4** (Fig. 1B). Upon reaction with the His23 nucleophile, it was expected that E1cB elimination of the acetoxy group would generate a stable, conjugated product suitable for spectrophotometric detection. Indeed, incubation of BH32 with **4** resulted in the anticipated time resolved spectral changes. The spectroscopic changes were made more pronounced to improve assay sensitivity, by introducing a 4-OMe substituent to increase the degree of conjugation upon inhibition. The formation of a stable 1:1 protein-inhibitor complex was confirmed by MS analysis of the intact protein (Extended Data Table 1). No spectral or mass changes were observed with the BH32 H23A variant, confirming the His23 catalytic nucleophile as the site of covalent attachment. Although this assay doesn't report on overall catalytic turnover, we anticipated that it would provide a useful tool for MBHase engineering capable of reporting on key features of MBH catalysis, including nucleophilicity of His23, stabilisation of C1 oxyanion intermediates and shape complementarity between the active site and the MBH product.

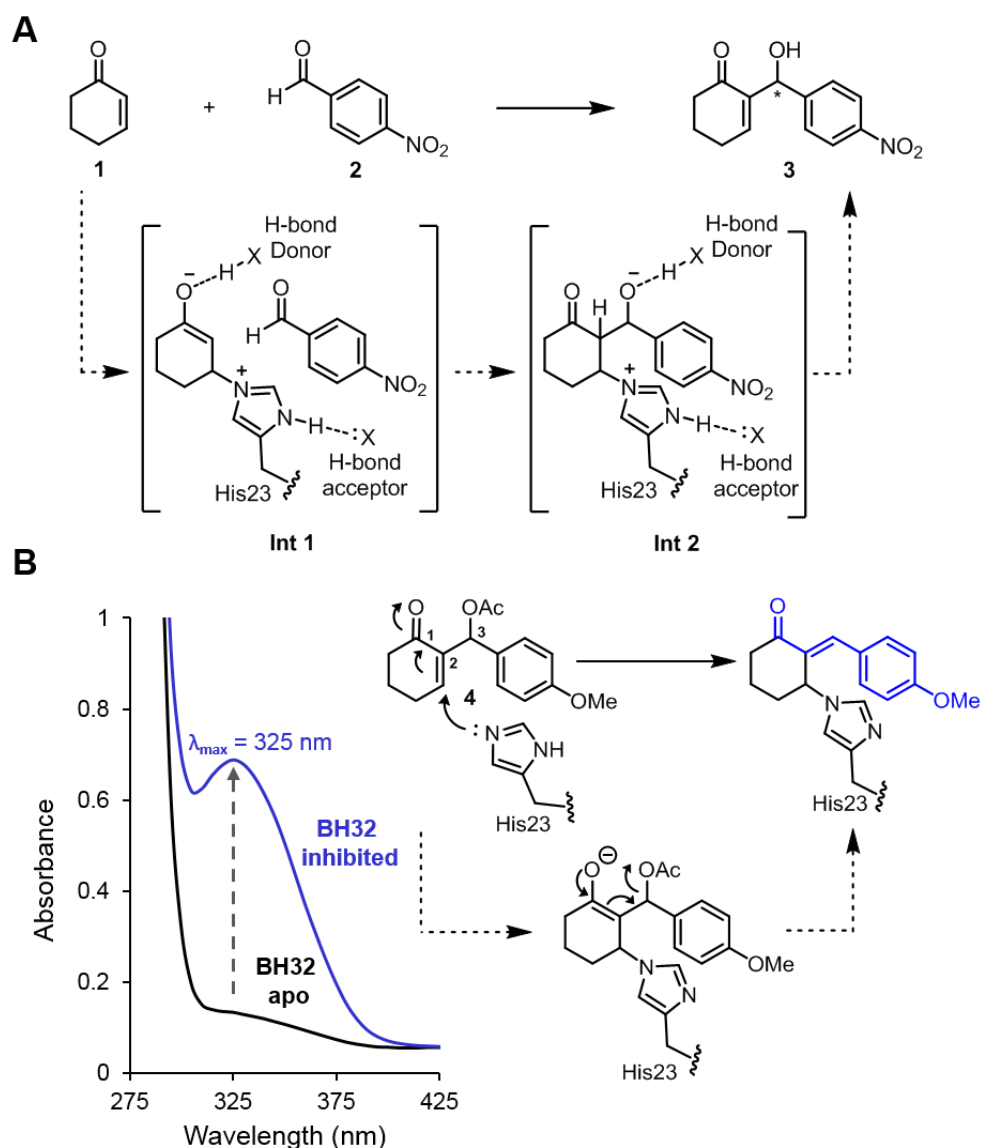
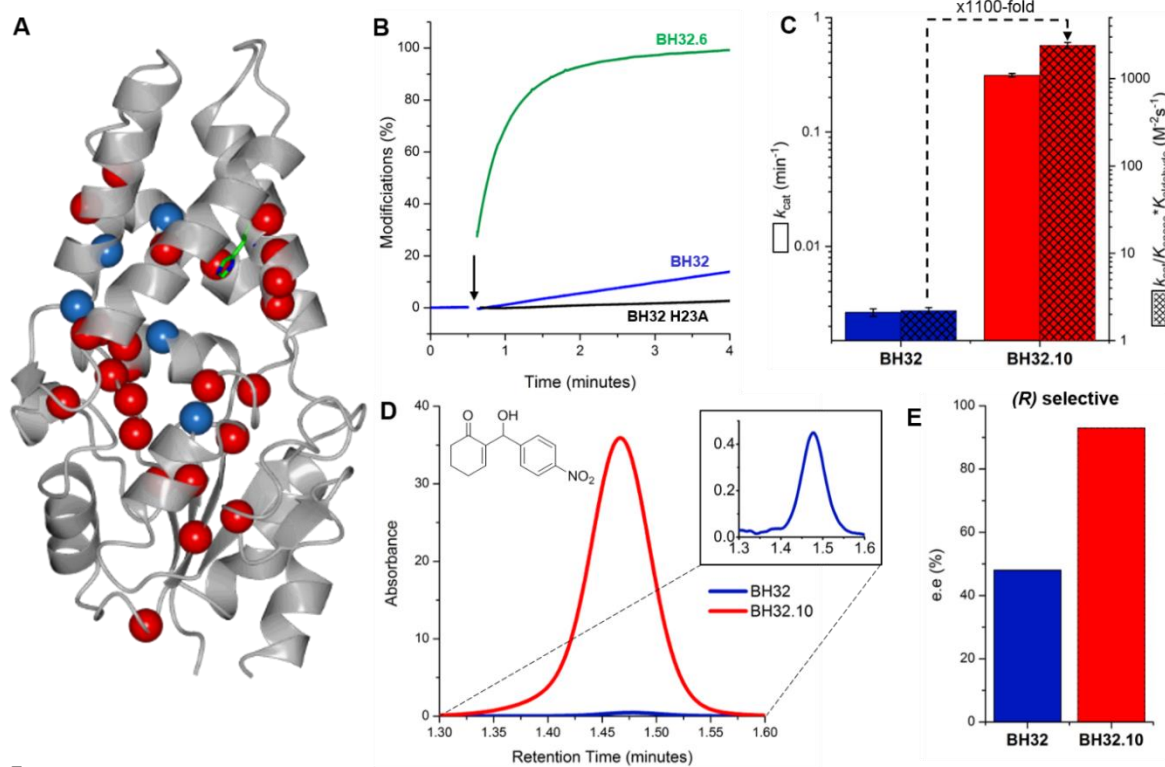


Figure 1: A designed enzyme for the Morita-Baylis-Hillman (MBH) reaction and the development of a dual function mechanistic inhibitor. (A) Chemical scheme of the MBH reaction between **1** and **2** catalysed by the computationally designed enzyme BH32.[15] Intended design features include a His23 nucleophile positioned by a hydrogen bond acceptor, and hydrogen bond donors for oxyanion stabilisation. (B) Chemical scheme of BH32 inhibition with the mechanistic inhibitor **4**. Addition of the His23 nucleophile is followed by E1cB elimination of the acetoxy group, generating a conjugated π -system, which can be monitored by an increase in absorbance at 325 nm. The stereochemistry of the exocyclic double bond in the inhibited complex is unknown. The wavelength scan shows the spectral changes that occur when BH32 (25 μM) is incubated with inhibitor **4** (250 μM) for 40 minutes.

The evolutionary strategy used for BH32 optimisation included both local and global mutagenesis (Extended Data Fig. 1): error-prone PCR was used to target the entire gene sequence leading to the identification of 'hot spots' that were further interrogated as small focused libraries (Rounds 1-2, 8 & 10); iterative cassette mutagenesis was used to individually randomise twenty positions per round (Rounds 3-4, 6-7 & 9); and combinatorial active site saturation mutagenesis (CASTing) was used to target active site residues (Round 5). Beneficial diversity identified along the evolutionary coordinate was combined by DNA shuffling. The aforementioned spectrophotometric assay was used to rapidly evaluate libraries during rounds 1-6. The most active (ca. 1%) clones identified during each round were further evaluated as purified enzymes for MBH activity using HPLC analysis. The correlation between increased rate of reaction with inhibitor **4**, and improving MBH activity was generally excellent. While the reaction of BH32 with inhibitor **4** takes > 60 minutes to reach completion, under identical conditions selective modification of BH32.6 is essentially complete within 1.5 minutes (Fig. 2B and Extended Data Table 1). To further refine the catalytic mechanism, BH32.6 was subjected to an additional four rounds of evolution using a UPLC assay to monitor the formation of MBH product **3** catalysed by individual variants arrayed as cell lysates in 96-well plates.

The most active variant to emerge following 10 rounds of evolution (BH32.10) contains 24 mutations (Fig. 2A) and is 1100-fold more efficient than the starting design ($k_{\text{cat}}/K_{\text{enone}} \cdot K_{\text{aldehyde}} = 2399 \pm 200 \text{ M}^{-2}\text{s}^{-1}$ and $2.21 \pm 0.18 \text{ M}^{-2}\text{s}^{-1}$ for BH32.10 and BH32, respectively) (Fig. 2C and Extended Data Fig. 2). This improvement in catalytic performance is achieved through a substantial 120-fold increase in turnover number ($k_{\text{cat}} = 0.31 \pm 0.01 \text{ min}^{-1}$ and $0.16 \pm 0.01 \text{ hr}^{-1}$ for BH32.10 and BH32, respectively) combined with improved affinity for **1** ($K_{\text{enone}} = 2.6 \pm 0.2 \text{ mM}$ and $9.6 \pm 0.9 \text{ mM}$, respectively) and **2** ($K_{\text{aldehyde}} = 0.8 \pm 0.07 \text{ mM}$ and $2.1 \pm 0.2 \text{ mM}$, respectively).



MIRAVFFDSWGLISVEGTYKVFHFKIMEEVLGDYPLNPKTLLDEYEKLAAREAFSNNAGKPY
 RPLRDILERVMRKLAEKYGFKYPENLWEISLRMAQRYGELYPEVVEVLKSLKGYHVGVIL
 NRDTLSTAFDLALGIKDLFDSITTSEEAGFSKPHPRIFELALKKAGVKGEKAVCVGPNPVK
 DAGGSKNLGMTSILLDRKGEKREFWDKADFIIVSDLREVIVDELNGQGSLEWSPQFEK

Figure 2: Characterization of BH32, BH32.10 and selected variants. (A) Structure showing the amino acid positions mutated in BH32.10 (represented as spheres). Twenty-four mutations introduced during directed evolution are shown in red. Computationally designed residues remaining following evolution are shown in blue. The His23 catalytic nucleophile is shown in stick representation. (B) Time course for the inhibition of BH32.6 (25 μ M, green), BH32 (25 μ M, blue) and BH32 H23A (25 μ M, black) with inhibitor **4** (250 μ M). The black arrow indicates the time of protein addition. (C) Bar chart comparing the turnover number (k_{cat} , solid colour) and catalytic efficiency ($k_{cat}/K_{enone} \cdot K_{aldehyde}$, hatched) of BH32 (blue) and BH32.10 (red) for the MBH reaction between **1** and **2**. Steady state kinetic data (average of measurements made in triplicate at each substrate concentration) were fitted globally using a kinetic model for two substrates with randomly ordered binding to extract kinetic constants and associated errors (shown as error bars). Representative Michaelis-Menten plots at fixed concentrations of **1** or **2** are shown in Extended Data Fig. 2. (D) HPLC traces showing product **3** formation in the reaction of **1** (3 mM) with **2** (0.6 mM) catalysed by BH32.10 (20 μ M, red) and BH32 (20 μ M, blue) following 22 hours incubation. (E) Bar chart showing the enantiomeric excess of product **3** formed following BH32 (blue) and BH32.10 (red) catalysed MBH reactions. Reaction conditions are as described in D. (F) Protein sequence of evolved variant BH32.10 highlighting the nucleophilic histidine (green), computationally designed residues (blue) and positions mutated (red).

With 3 mol% BH32, the reaction of **1** (3 mM) and **2** (0.6 mM) gave <0.5% conversion to product (**3**) after 4.5 hours (Table 1, Entry 1), which increased to only 1% following incubation for 22 h (Fig. 2D). Furthermore, product formation was accompanied by a substantial proportion of a competing aldol by-product **S1** (5:1 ratio of **3**:**S1**, Extended Data Fig. 3). In contrast, under identical reaction conditions BH32.10 afforded **3** as the sole product in 56% (Table 1, Entry 2) and 83% conversion (Fig. 2D) after 4.5 hours and 22 hours, respectively. For comparison, with commonly employed small molecule catalytic nucleophiles imidazole, DMAP and DABCO, low but detectable conversions (<0.5%) are only achieved using high catalyst loadings and prolonged reaction times (Table 1, Entry 6-7), further highlighting the efficiency of BH32.10. Significantly, the activity gains observed during evolution correlated with substantial improvements in enantioselectivity, with reactions catalysed by BH32.10 affording (*R*)-**3** in 93% e.e. (Fig. 2E).

Table 1: The MBH reactions of **1** and **2** catalysed by small molecule nucleophiles, BH32, BH32.10 and selected variants.

Entry	Catalyst	Catalyst Loading (mol%)	Time (h)	Conversion (%)
1	BH32	3	4.5	<0.5
2	BH32.10	3	4.5	56
3	BH32.10 H23A	3	4.5	<0.5
4	BH32.10 R124A	3	4.5	<1
5	BH32.10 W10A	3	4.5	3.8
6	Imidazole	167	22	<0.5
7	DMAP	167	22	<0.5
8	BH32.10	0.5	19	94

Entries 1-7 were carried out using **1** (3 mM) and **2** (0.6 mM) in PBS (pH 7.4) with 3% DMSO as a cosolvent. Conversion to product was determined by HPLC analysis. Entry 8 was performed on a preparative scale using **1** (50 mM) and **2** (10 mM) in PBS (pH 7.4) with 20% DMSO as a cosolvent. Conversion to product was determined by HPLC analysis. The final product was isolated in 90% yield following extraction into organic solvent and chromatographic purification.

We also explored the utility of BH32.10 for preparative scale biotransformations (Table 1, Entry 8). Significantly, the enzyme readily tolerates 20% DMSO as an organic cosolvent, which allows reactions to be performed with increased substrate loadings (10 mM concentration of **2**). High conversions (94%) and isolated yields (90%) are obtained within 19 h using only 0.5 mol% catalyst loading to allow synthesis of several hundred milligrams of MBH product **3** (Extended Data Fig. 4). The high degree of solvent tolerance and mutational flexibility of the BH32 scaffold (12% of the

protein was mutated during computational design and evolution) is noteworthy, and likely reflects the stability of the starting scaffold, which originates from a hyperthermophilic organism that grows optimally at 98 °C.

To understand the origins of improved efficiency, crystal structures of several evolved BH32 variants were solved for comparison to the original design. The most active variant, BH32.10, proved challenging to crystallise; however, we were able to solve the apo structure of BH32.9, which contains 21 out of 24 mutations present in BH32.10, to 2.3 Å resolution (Supplementary Information Table 1). The BH32.9 and BH32 structures superimpose well, with a root-mean-square-deviation of 0.8 Å. However, evolution has resulted in extensive remodelling of the active site, including a ~30% reduction in volume (Fig. 3). The designed His23 nucleophile has been preserved and is essential for catalytic activity in BH32.10 (Table 1, Entry 3). In contrast Gln128 and Ser22, intended to stabilise key oxanion intermediates through hydrogen bonding interactions, have been abandoned during evolution. Instead, an active site Arg124 has emerged which is critical for effective catalysis (Table 1, Entry 4). This catalytic residue emerged in the early rounds of evolutionary optimisation, and in the crystal structure of BH32.3 (resolution 1.5 Å, Supplementary Information Table 1) adopts a conformation which places the guanidinium motif in close proximity to the amide side chain of the originally designed Gln128. However, subsequent active site remodelling resulted in a substantial repositioning of the arginine side chain leading to a ~5 Å displacement of the guanidinium ion in BH32.9 (Extended Data Fig. 5). The originally designed aldehyde binding site is occluded in BH32.9 by residues Trp10, Leu122, Arg124 & Ser129 which emerged during evolution. Molecular docking of substrates **1** and **2** reveals the presence of a new aldehyde binding pocket shaped by Trp10, Val22, Ile26, Leu64, Trp88, Ser91, Leu92, Phe132, Arg124 & Ser129, and a 2-cyclohexen-1-one binding mode suitable for nucleophilic attack by His23 (Fig. 3).

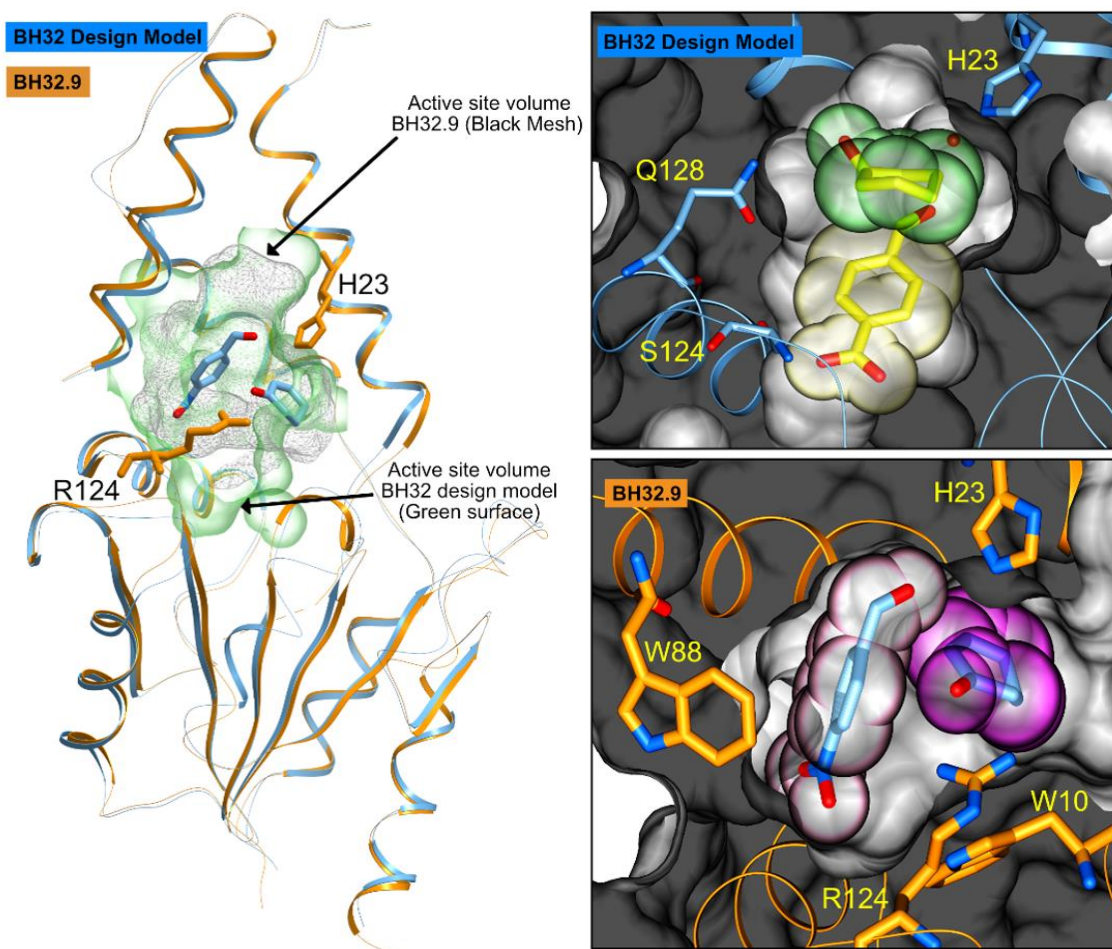


Figure 3: Crystal structures of BH32 and BH32.9. A ribbon representation of the superimposed coordinates of the BH32 design model (blue) and the evolved variant BH32.9 (orange). The His23 nucleophile and catalytic Arg124 from BH32.9 are shown in orange stick representation. Substrates docked into BH32.9 are shown in all atom-coloured stick representation. The active site surface volume of the BH32 design model is shown as a green transparency whilst the equivalent active site surface volume for BH32.9 is shown as a grey mesh. The right-hand panels show a close-up representation of the active sites. The top panel shows the substrate binding pocket of BH32 design model highlighting the spatial arrangement of the designed residues Gln128, Ser124 and His23. The protein backbone is shown in ribbon representation (blue) with the protein surface shown in grey. The substrates are derived from the original composite transition state model[15] with the aldehyde shown in stick representation and transparent yellow CPK spheres. 2-Cyclohexen-1-one is also shown in stick representation with accompanying transparent green CPK spheres. The bottom panel shows the aldehyde and enone binding pocket of BH32.9 highlighting the spatial arrangement of key residues Trp88, Trp10, Arg124 and His23 (stick representation – orange carbon atoms). The protein backbone is shown in ribbon representation (orange) with the protein surface shown in grey. The substrate positions depicted are those obtained from initial docking studies prior to DFT calculations. The aldehyde substrate is shown in stick representation with accompanying transparent pink CPK spheres. 2-Cyclohexen-1-one is shown in stick representation with transparent magenta CPK spheres.

To shed light on the catalytic mechanism, an active site 'cluster' model comprising 270 atoms was constructed from the BH32.9 crystal structure and docked substrates, with peripheral atoms fixed to maintain the crystal structure geometry (Extended Data Fig. 6). Relaxed potential energy scans were performed to model each chemical step (Extended Data Figures 7 and 8). During energy minimisation of the reactant state, the aromatic aldehyde forms an edge to face π -stacking interaction with Trp88. Aldehyde binding is further supported by a hydrogen bonding network involving the *para*-nitro substituent, Ser129 and Trp10, two residues that emerged during the latter stages of evolution. Trp10 packs closely with Phe132 and likely participates in additional cation- π interactions with the catalytic Arg124. Mutation of the Trp10 of BH32.10 to alanine leads to a substantial reduction in activity (Table 1, Entry 5), underscoring the importance of this residue to the catalytic mechanism. Nucleophilic addition of His23 to the *si*-face of **1** generates the first oxyanion intermediate (Int1) which is stabilised by a bidentate hydrogen bond to the side chain of Arg124 ($R(\text{O-N}) = 2.68$ and 2.72 Å). Similar interactions have been observed in both natural[16] and *de novo* hydrolases[17-19] and are the hallmark of small molecule hydrogen bonding catalysts such as thiourea and guanidinium ions.[20,21] The transition from the reactant state to Int1 has a potential energy barrier of 38.4 kJ mol⁻¹ and proceeds with rotation of the 2-cyclohexen-1-one ring, which allows Arg124 to interact with the developing negative charge in the *p*-orbital of the C1-oxygen and positions the enolate of Int1 in a near ideal geometry for subsequent addition to aldehyde **2**. Diastereoselective carbon-carbon bond formation generates a second oxyanion intermediate (Int2), with the (*R*)-configuration at the C3-position, and proceeds with transfer of negative charge to the C3-oxygen. Remarkably, Arg124 is ideally positioned to support this charge transfer and shuttles between bidentate hydrogen bonding modes to stabilise Int1 and Int2 ($R(\text{O-N}) = 2.62$ and 2.72 Å), via a bridging mode at the transition state involving a single hydrogen bond to each oxygen atom. The resulting potential energy barrier is only 16.0 kJ mol⁻¹, with Int1 and Int2 states that are almost isoenergetic ($\Delta E = -4.6$ kJ mol⁻¹), suggesting that this step is highly reversible. The third chemical step involves proton transfer from C2 to the C3 alkoxide leading to the generation of a third oxyanion intermediate (Int 3), which again is stabilised by bidentate hydrogen bonding to Arg124 ($R(\text{O-N}) = 2.71$ and 2.75 Å). Based on previous models of thiourea promoted MBH reactions,[22] a water molecule was included in the calculation to facilitate proton transfer, leading to a concerted process with a potential energy barrier of 60.9 kJ mol⁻¹. The final chemical step involves elimination of the His23 nucleophile to generate MBH product (*R*)-**3**, and proceeds with a potential energy barrier of 43.3 kJ mol⁻¹.

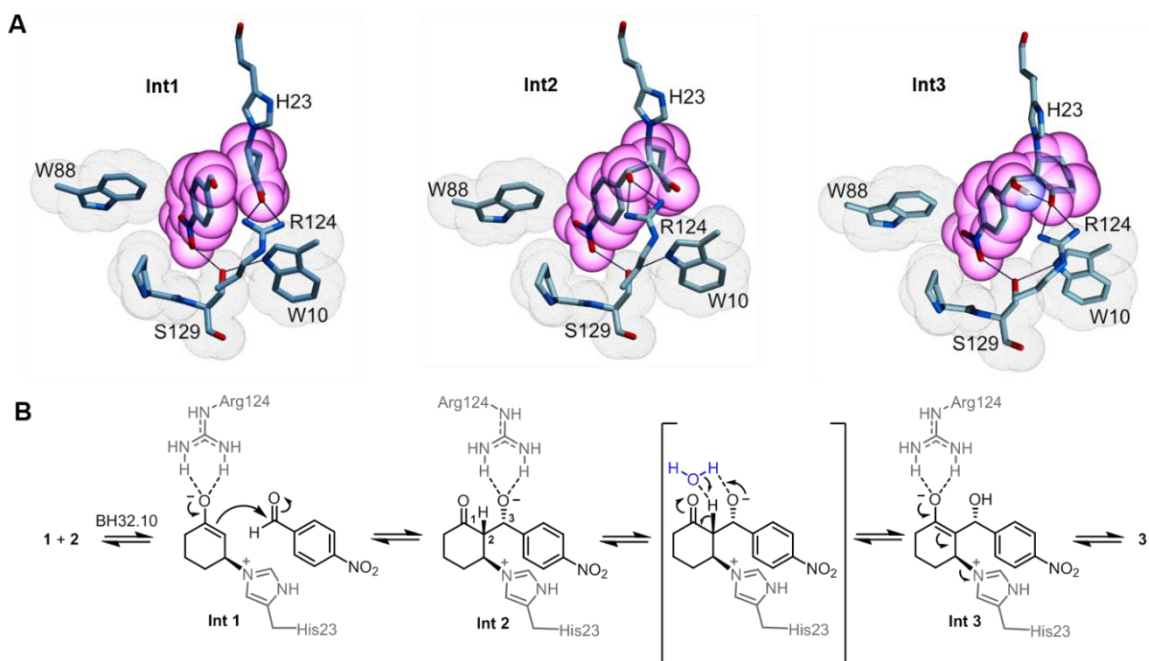


Figure 4: Proposed Catalytic mechanism of a *de novo* MBHase. (A) DFT states for intermediates 1, 2 & 3 are shown in all atom-coloured stick representation. The images presented show only a subset of the atoms used in the full DFT calculation for greater visual clarity. Atoms derived from several residues that form close packing interactions with substrates **1** and **2** during catalysis (Trp10, Trp88, Phe128 & Ser129) are highlighted with grey dot surfaces. Heavy atoms from the substrates are highlighted with magenta transparent CPK spheres whilst protons (Int3) are highlighted with purple transparent CPK spheres. Atoms from the His23 nucleophile and catalytic Arg124 are shown in all atom-coloured stick representation. The hydrogen bonding network that emerged during evolution between Trp10, Ser129 and the aldehyde substrate are shown as black dashed lines. In addition, hydrogen bonds between Arg124 and each intermediate state are shown. (B) The BH32.10 catalytic mechanism showing the role played by Arg124 in stabilising three intermediates covalently bound through His23. A catalytic water molecule is shown in blue to facilitate proton transfer from C2 to the C3 alkoxide.

These studies show how the interplay of computational design and laboratory evolution has delivered a highly sophisticated active site capable of processing the Morita-Baylis-Hillman reaction with high efficiency and selectivity. BH32.10 employs two key catalytic motifs, a nucleophilic histidine and a multi-functional arginine, in a catalytic mechanism with strong similarities to that observed with small molecule systems.[20,21] This suggests that in cases where no natural enzyme or catalytic antibodies are available to serve as a blueprint for theozyme design, we should turn to small molecule catalysis for inspiration. In particular, the realization that an appropriately positioned arginine can serve as a genetically encoded surrogate of privileged bidentate hydrogen bonding catalysts should open the door to a wealth of new chemistries in designed active sites.[20,21,23,24] The range of accessible chemistries can be further extended by developing engineered cellular translation components to introduce new functional amino acids inspired by small molecule catalytic

motifs.[25,26] In contrast to small molecule systems which are challenging to optimise, the efficiency of protein catalysts can be enhanced by orders of magnitude through laboratory evolution.[27-29] As highlighted in this study, a bottom up approach to enzyme development provides a remarkable glimpse into the evolution of new active site environments, where multiple components work in concert to fine tune and accurately position key functional groups, substrates and intermediates to deliver complex catalytic devices reminiscent of natural enzymes. The next key challenge for design is to learn how to build such sophisticated active sites *in silico*, to allow the rapid delivery of efficient and selective *de novo* biocatalysts in response to diverse societal challenges.

3.4 References

1. Hilvert, D. Design of protein catalysts. *Annu. Rev. Biochem.* **82**, 447-470 (2013).
2. Röthlisberger, D. et al. Kemp elimination catalysts by computational enzyme design. *Nature* **453**, 190-195 (2008).
3. Jiang, L. et al. *De novo* computational design of retro-aldol enzymes. *Science* **319**, 1387-1391 (2008).
4. Siegel, J. B. et al. Computational design of an enzyme catalyst for a stereoselective bimolecular Diels-Alder reaction. *Science* **329**, 309-313 (2010).
5. Eiben, C. B. et al. Increased Diels-Alderase activity through backbone remodeling guided by Foldit players. *Nat. Biotechnol.* **30**, 190-192 (2012).
6. Blomberg, R. et al. Precision is essential for efficient catalysis in an evolved Kemp eliminase. *Nature* **503**, 418-421 (2013).
7. Obexer, R. et al. Emergence of a catalytic tetrad during evolution of a highly active artificial aldolase. *Nat. Chem.* **9**, 50-56 (2017).
8. Gouverneur, V. E. et al. Control of the exo and endo pathways of the Diels-Alder reaction by antibody catalysis. *Science* **262**, 204-208 (1993).
9. Stewart, J. D. & Benkovic, S. J. Transition-state stabilization as a measure of the efficiency of antibody catalysis. *Nature* **375**, 388-391 (1995).
10. Barbas, C. F., 3rd et al. Immune versus natural selection: antibody aldolases with enzymic rates but broader scope. *Science* **278**, 2085-2092 (1997).
11. Basavaiah, D., Rao, A. J. & Satyanarayana, T. Recent advances in the Baylis-Hillman reaction and applications. *Chem. Rev.* **103**, 811-892 (2003).
12. Wei, Y. & Shi, M. Recent advances in organocatalytic asymmetric Morita-Baylis-Hillman/aza-Morita-Baylis-Hillman reactions. *Chem. Rev.* **113**, 6659-6690 (2013).
13. Reetz, M.T., Mondière, R., Carballeira, J.D. Enzyme promiscuity: first protein-catalyzed Morita-Baylis-Hillman reaction. *Tetrahedron Lett.* **48**, 1679-1681 (2007).
14. López-Iglesias, M., Busto, E., Gotor, V., Gotor-Fernández, V. Use of protease from *Bacillus licheniformis* as promiscuous catalyst for organic synthesis: applications in C-C and C-N bond formation reactions. *Adv. Synth. Catal.* **353**, 2345 – 2353 (2011).
15. Bjelic, S. et al. Computational design of enone-binding proteins with catalytic activity for the Morita-Baylis-Hillman reaction. *ACS Chem. Biol.* **8**, 749-757 (2013).
16. Phillips, M. A., Fletterick, R. & Rutter, W. J. Arginine 127 stabilizes the transition state in carboxypeptidase. *J. Biol. Chem.* **265**, 20692-20698 (1990).
17. Janda, K. D., Schloeder, D., Benkovic, S. J. & Lerner, R. A. Induction of an antibody that catalyzes the hydrolysis of an amide bond. *Science* **241**, 1188-1191 (1988).
18. Roberts, V. A., Stewart, J., Benkovic, S. J. & Getzoff, E. D. Catalytic antibody model and mutagenesis implicate arginine in transition-state stabilization. *J. Mol. Biol.* **235**, 1098-1116 (1994).
19. Studer, S. et al. Evolution of a highly active and enantiospecific metalloenzyme from short peptides. *Science* **362**, 1285-1288 (2018).

20. Doyle, A. G. & Jacobsen, E. N. Small-molecule H-bond donors in asymmetric catalysis. *Chem. Rev.* **107**, 5713-5743 (2007).
21. Taylor, M. S. & Jacobsen, E. N. Asymmetric catalysis by chiral hydrogen-bond donors. *Angew. Chem. Int. Ed. Engl.* **45**, 1520-1543 (2006).
22. Amarante, G. W. et al. Bronsted acid catalyzed Morita-Baylis-Hillman reaction: a new mechanistic view for thioureas revealed by ESI-MS(/MS) monitoring and DFT calculations. *Chemistry* **15**, 12460-12469 (2009).
23. Knowles, R. R., Lin, S. & Jacobsen, E. N. Enantioselective thiourea-catalyzed cationic polycyclizations. *J. Am. Chem. Soc.* **132**, 5030-5032 (2010).
24. Park, Y. et al. Macrocyclic bis-thioureas catalyze stereospecific glycosylation reactions. *Science* **355**, 162-166 (2017).
25. Drienovska, I., Mayer, C., Dulson, C. & Roelfes, G. A designer enzyme for hydrazone and oxime formation featuring an unnatural catalytic aniline residue. *Nat. Chem.* **10**, 946-952 (2018).
26. Burke, A. J. et al. Design and evolution of an enzyme with a non-canonical organocatalytic mechanism. *Nature* **570**, 219-223 (2019).
27. Bornscheuer, U. T. et al. Engineering the third wave of biocatalysis. *Nature* **485**, 185-194 (2012).
28. Arnold, F. H. Directed Evolution: Bringing New Chemistry to Life. *Angew. Chem. Int. Ed. Engl.* **57**, 4143-4148 (2018).
29. Qu, G., Li, A., Acevedo-Rocha, C. G., Sun, Z. & Reetz, M. T. The Crucial Role of Methodology Development in Directed Evolution of Selective Enzymes. *Angew. Chem. Int. Ed. Engl.* **59**, 13204-13231 (2020).

Chapter 4: Synthetic Utility of a *de novo* Morita-Baylis-Hillmanase

Rebecca Crawshaw¹, Amy E. Crossley¹, Sarah L. Lovelock¹ and Anthony P. Green^{1*}

¹Manchester Institute of Biotechnology, School of Chemistry, 131 Princess Street, University of Manchester, Manchester M1 7DN, UK.

4.1 Foreword

This chapter consists of a research article describing the substrate scope of a *de novo* enzyme for the Morita-Baylis-Hillman reaction.

4.2 Author contributions

The research presented in this chapter was a collaborative effort between the doctoral candidate and the following researchers: Amy E. Crossley, Sarah L. Lovelock and Anthony P. Green. The doctoral candidate carried out biotransformations and HPLC/SFC analysis. The doctoral candidate and Amy E. Crossley carried out organic synthesis. The doctoral candidate, Amy E. Crossley and Sarah L. Lovelock interpreted and analysed the data. The manuscript was edited by Anthony P. Green.

4.3 Abstract

Computational enzyme design has delivered a handful of primitive enzymes from scratch, which can be optimised through laboratory evolution to deliver biocatalysts for chemical transformation not observed in Nature. We have recently reported the development of a *de novo* enzyme, BH32.10, which promotes the model Morita-Baylis-Hillman reaction of 2-cyclohexen-1-one and 4-nitrobenzaldehyde with high efficiency and selectivity. Here, we show that BH32.10 accepts a broad range of enone and aldehyde coupling partners, including notoriously challenging MBH substrates such as unsaturated lactones, and is also able to promote highly selective mono-functionalisations of dialdehyde substrates to generate densely functionalised chiral molecules from simple building blocks. Our study allows us to add the Morita-Baylis-Hillman reaction to the restricted repertoire of biocatalysts available for C-C bond formations and makes us optimistic about the prospects of designing *de novo* enzymes for complex and valuable chemical transformations.

4.4 Introduction

The ability to reliably design enzymes would have a significant impact across the chemical industry, allowing for the rapid delivery of *de novo* biocatalysts in response to diverse societal challenges. Computational enzyme design is conceptually similar to catalytic antibody technology; in that it aims to generate protein catalysts based on fundamental principles of transition state stabilisation.[1] However, in principle computational design offers a far more flexible approach, as it is not limited to the antibody fold or reliant on the availability of an imperfect transition state mimic. Thus far, computational algorithms have enabled the design of primitive catalysts for a handful of transformations that have been optimised through laboratory evolution to deliver enzymes with efficiencies approaching natural systems.[2-7] Naturally, early efforts targeted simple model transformations previously achieved with catalytic antibodies.[8-10] For example, highly effective antibodies and *de novo* enzymes have been created for the retro-aldol reaction,[3,7,10] which employ reactive lysine residues reminiscent of natural type I aldolases. If we are to establish 'bottom up' enzyme design as a reliable source of biocatalysts for practical applications, we must move beyond the functional capabilities of antibodies, and develop enzymes for complex bimolecular chemical processes. To this end we have recently combined computational design[11] and directed evolution to yield a biocatalyst for the Morita-Baylis-Hillman (MBH) reaction.[12]

The Morita-Baylis-Hillman (MBH) reaction (Fig. 1A), involving the coupling of activated alkenes (e.g. α,β -unsaturated carbonyl compounds) with carbon electrophiles (e.g. aldehydes), is an iconic transformation in organic synthesis.[13-15] This reaction provides a versatile and atom economical approach to generate densely functionalised chiral building blocks for synthesis. MBH reactions are typically promoted by small catalytic nucleophiles such as 1,4-diazabicyclo[2.2.2]octane (DABCO), 4-dimethylaminopyridine (DMAP) and imidazole. Enantioselective versions of the MBH reaction have been developed by employing quinidine derivatives, chiral DMAP surrogates or by pairing catalytic nucleophiles with chiral hydrogen bond donors such as thioureas;[15] however achieving high levels of stereo-control remains a considerable challenge. Despite the great synthetic potential, the practical utility of MBH reactions is further compromised by the low efficiencies achieved by existing catalytic systems, which results in prolonged reaction times and the requirement for high catalyst loadings. To address these long-standing challenges, we have recently used a combination of computational enzyme design and directed evolution to develop the *de novo* enzyme BH32.10[12] that promotes the model MBH reaction of 2-cyclohexen-1-one **1** and 4-nitrobenzaldehyde **2** with high efficiency and selectivity that compares favourably with modest selectivities achieved by chiral small molecule catalysts[16,17] (Fig. 1A). Structural and biochemical analysis reveals that BH32.10 employs a sophisticated catalytic mechanism which combines a His23 nucleophile with a multifunctional catalytic Arg124 which shuttles between conformational states to stabilise multiple oxyanion intermediates along the complex reaction coordinate (Fig. 1B). Here we show that despite its intricate mechanism, BH32.10 can couple a broad range of enone and aldehyde coupling partners to provide highly functionalised chiral molecules from simple chemical building blocks.

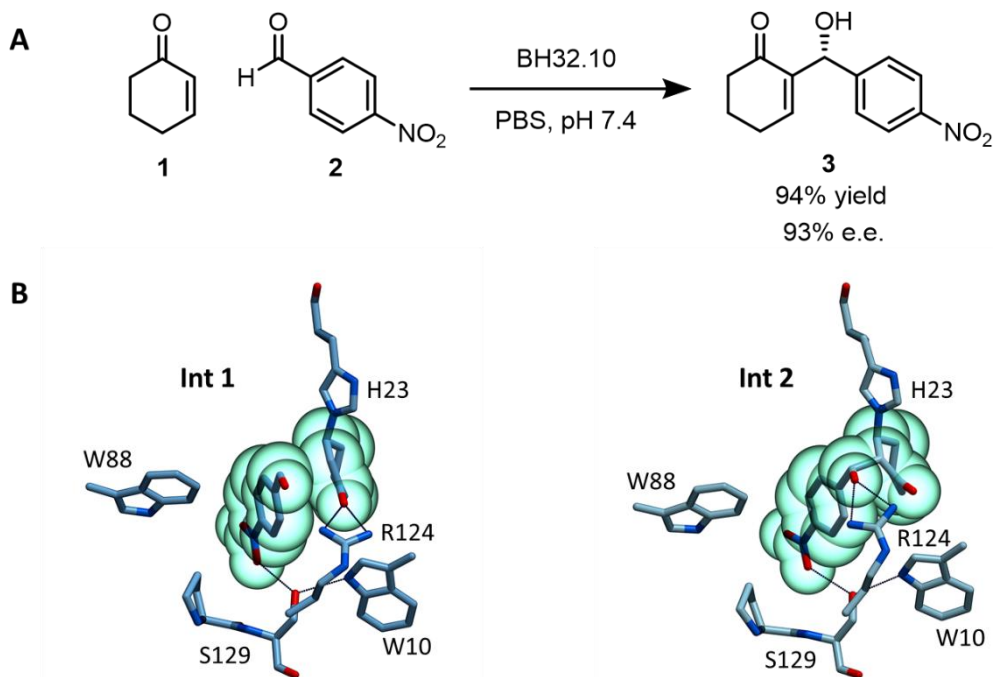


Figure 1: A designed evolved enzyme for the Morita-Baylis-Hillman (MBH) reaction. A) BH32.10 promotes the MBH reaction of **1** and **2** with high efficiency and selectivity.[12] **B)** DFT states for intermediates (Int 1 and Int 2) formed along the reaction coordinate, showing the roles of key catalytic residues His23 and Arg124. Heavy atoms from the substrates **1** and **2** are highlighted with aqua transparent CPK spheres. Atoms derived from several residues that form close packing interactions with substrates **1** and **2** during catalysis (Trp10, Trp88, Arg124 & Ser129) shown in all atom coloured stick representation, as well as atoms from the His23 nucleophile. The hydrogen bonding network that emerged during evolution between Trp10, Ser129 and the aldehyde substrate are shown as black dashed lines. In addition, hydrogen bonds between Arg124 and both intermediate states are shown.

4.5 Results

We first investigated BH32.10 activity towards a small panel of cyclic alkenes in combination with **2** as the aldehyde reaction partner. In addition to 2-cyclohexen-1-one **1**, BH32.10 efficiently couples cyclopentenone and the functionalised cyclopentenone (3a*S*,6a*S*)-2,2-dimethyl-3a,6a-dihydro-4H-cyclopenta[*d*][1,3]dioxol-4-one with appreciable levels of stereocontrol (Fig. 2). In contrast to the high activity displayed with the *S,S*-isomer of 2,2-dimethyl-3a,6a-dihydro-4H-cyclopenta[*d*][1,3]dioxol-4-one, activity with the *R,R*-enantiomer is modest, demonstrating that BH32.10 can discriminate between enantiomeric starting materials, thus providing opportunities to develop kinetic resolution processes. Testament to its catalytic power, BH32.10 can even promote enantioselective transformations of unsaturated lactones, which are notoriously challenging as MBH substrates.[18,19] To our knowledge, this is the first example of an enantioselective MBH transformation with this challenging class of substrate.

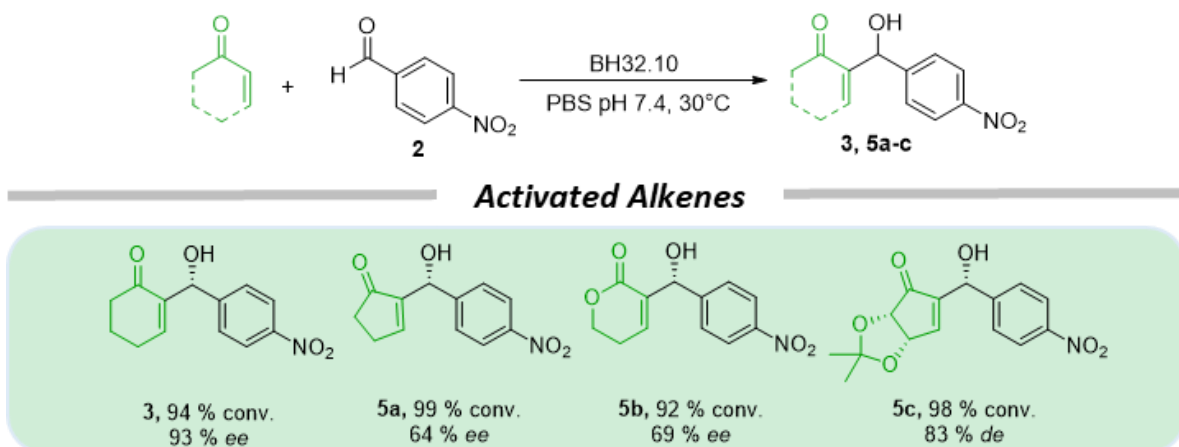


Figure 2: Substrate scope of *de novo* MBHase. BH32.10 accepts a range of activated cyclic alkenes to deliver MBH adducts with appreciable levels of stereocontrol. Reported conversions and selectivities are an average from biotransformations performed in triplicate. The stereochemistry of **5a-c** are assigned by analogy to the (*R*)-**3** product formed by BH32.10 mediated biotransformations. Reaction conditions for the synthesis of **3** and **5a-c** are reported in Supplementary Table 1 (Chapter 7.3.2.2).

We next explored the aldehyde substrate scope in combination with 2-cyclohexen-1-one **1** as a coupling partner. BH32.10 couples a broad range of mono- and di- substituted aromatic aldehydes with high levels of stereocontrol (Fig. 3). In many cases, the MBH adducts contain useful functional groups that can serve as handles for further chemical modifications. While BH32.10 displays a clear preference for para-substituted derivatives, the less highly evolved BH32.6 accepts a broader range of substituents at the 2- and 3- positions, including the activated ketone isatin (product **5i**), albeit with reduced efficiency and minimal selectivity. These results suggest BH32.10 has been highly specialised through evolution to operate efficiently and selectively on specific classes of substrate, whereas its ancestor BH32.6 is more promiscuous and thus provides an attractive starting template for engineering MBHases to produce a broader range of target structures.

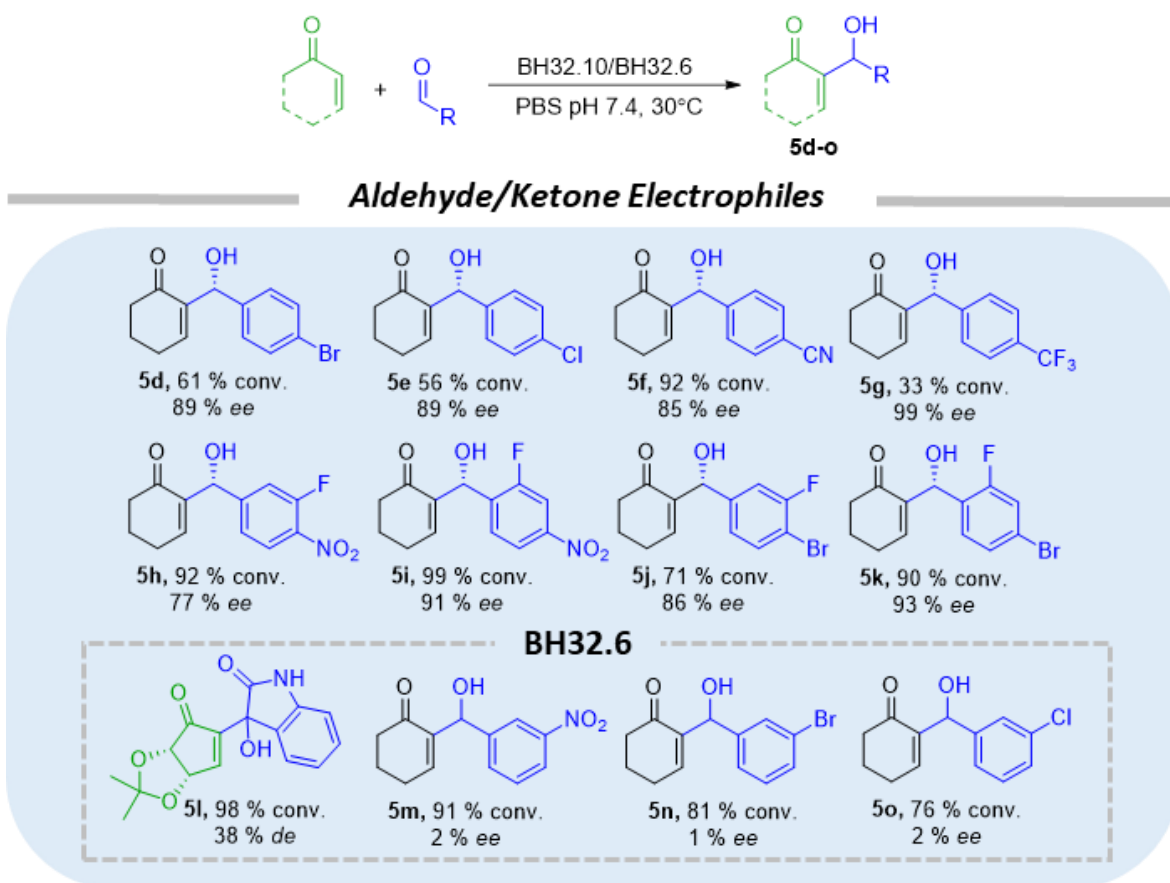


Figure 3: Substrate scope of *de novo* MBHases. BH32.10 tolerates a range of aldehydes and as substrates, leading to the production of densely functionalised MBH adducts with high conversions and selectivities. The less highly evolved BH32.6 accepts a broader range of substituents at the 2- and 3- positions, albeit with reduced efficiency and minimal enantioselectivity. Reported conversions and selectivities are an average from biotransformations performed in triplicate. The stereochemistry of **5d-k** are assigned by analogy to the (*R*)-**3** product formed by BH32.10 mediated biotransformations. Reaction conditions for the synthesis of **5d-o** are reported in Supplementary Table 1 (Chapter 7.3.2.2).

We also recognised the opportunity to perform selective mono-functionalisations of aromatic and heteroaromatic dialdehydes to deliver functionalised chiral products from simple chemical building blocks. Indeed, biotransformations of the symmetrical dialdehydes terephthalaldehyde, thiophene-2,5-dicarboxaldehyde and furan-2,5-dicarboxaldehyde proceed with excellent conversions and selectivities to chiral mono-functionalised MBH adducts (**5p-t**). Presumably the high selectivity for the mono-functionalised adducts arises due to the aldehyde products being too sterically encumbered to be accommodated in the aromatic binding pocket of BH32.10. Reaction of 2-cyclohexen-1-one **1** with the unsymmetrical dialdehyde, thiophene-2,4-dicarboxaldehyde, delivered enantioenriched mono-substituted products **5s** and **5t** with modest (ca. 2:1) regiocontrol, which could likely be improved through additional rounds of evolution.

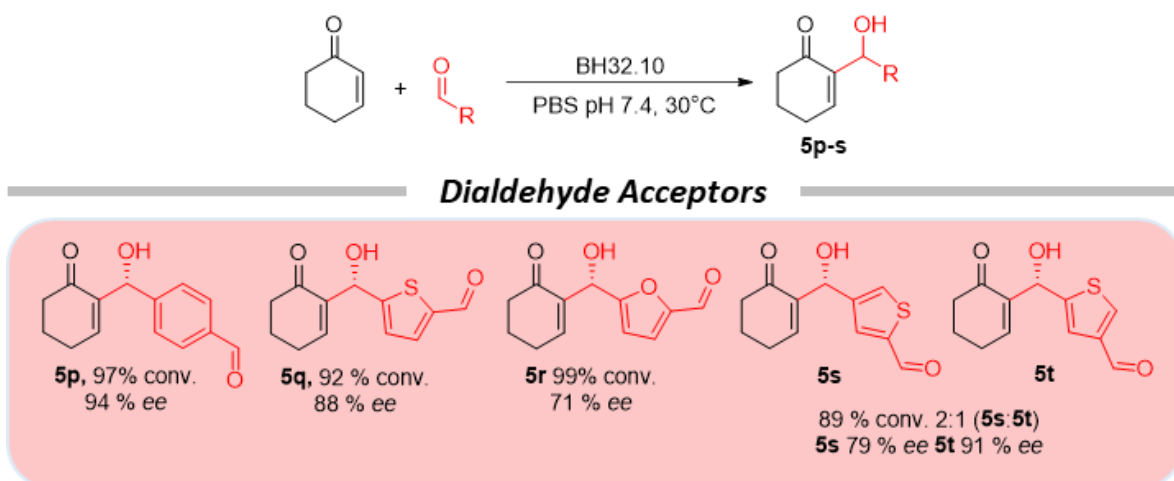


Figure 4: Selective mono-functionalisations of dialdehydes BH32.10 promotes enantioselective mono-functionalisations of aromatic and heteroaromatic dialdehydes with high conversions. Reported conversions and selectivities are an average from biotransformations performed in triplicate. The stereochemistry of **5p-t** are assigned by analogy to the (*R*)-**3** product formed by BH32.10 mediated biotransformations. Reaction conditions for the synthesis of **5p-t** are reported in Supplementary Table 1 (Chapter 7.3.2.2).

4.6 Conclusion

In conclusion we have demonstrated that the recently developed *de novo* MBHase BH32.10[12] can promote a broad array of Morita-Baylis-Hillman transformations with selectivities and efficiencies that cannot be achieved with existing chemical catalysts.[18,19] This study shows how *de novo* enzymes can augment the biocatalytic toolbox to allow access to important chemical transformations not found in Nature.

4.7 References

1. Hilvert, D. Design of protein catalysts. *Annu. Rev. Biochem.* **82**, 447-470 (2013).
2. Röthlisberger, D. et al. Kemp elimination catalysts by computational enzyme design. *Nature* **453**, 190-195 (2008).
3. Jiang, L. et al. *De novo* computational design of retro-aldol enzymes. *Science* **319**, 1387-1391 (2008).
4. Siegel, J. B. et al. Computational design of an enzyme catalyst for a stereoselective bimolecular Diels-Alder reaction. *Science* **329**, 309-313 (2010).
5. Eiben, C. B. et al. Increased Diels-Alderase activity through backbone remodelling guided by Foldit players. *Nat. Biotechnol.* **30**, 190-192 (2012).
6. Blomberg, R. et al. Precision is essential for efficient catalysis in an evolved Kemp eliminase. *Nature* **503**, 418-421 (2013).
7. Obexer, R. et al. Emergence of a catalytic tetrad during evolution of a highly active artificial aldolase. *Nat. Chem.* **9**, 50-56 (2017).
8. Gouverneur, V. E. et al. Control of the exo and endo pathways of the Diels-Alder reaction by antibody catalysis. *Science* **262**, 204-208 (1993).
9. Stewart, J. D. & Benkovic, S. J. Transition-state stabilization as a measure of the efficiency of antibody catalysis. *Nature* **375**, 388-391 (1995).
10. Barbas III, C. F. et al. Immune versus natural selection: antibody aldolases with enzymic rates but broader scope. *Science* **278**, 2085-2092 (1997).
11. Bjelic, S. et al. Computational design of enone-binding proteins with catalytic activity for the Morita-Baylis-Hillman reaction. *ACS Chem. Biol.* **8**, 749-757 (2013).
12. Crawshaw, R. et al., An Efficient and Enantioselective *de novo* Enzyme for the Morita-Baylis-Hillman Reaction. *In Review: Nature* (2020).
13. Basavaiah, D., Rao, A. J. & Satyanarayana, T. Recent advances in the Baylis-Hillman reaction and applications. *Chem. Rev.* **103**, 811-892 (2003).
14. Basavaiah, D., Reddy, B. S. Badsara, S. S. Recent contributions from the Baylis-Hillman Reaction to Organic Chemistry. *Chem. Rev.* **9**, 5447-5674 (2010).
15. Wei, Y. & Shi, M. Recent advances in organocatalytic asymmetric Morita-Baylis-Hillman/aza-Morita-Baylis-Hillman Reactions. *Chem. Rev.* **113**, 6659-6690 (2013).
16. Shi, M. & Liu, X.- G. Asymmetric Morita-Baylis-Hillman reaction of arylaldehydes with 2-cyclohexen-1-one and 2-cyclopenten-1-one catalyzed by chiral bis(thio)urea and DABCO. *Org. Lett.* **10**, 1043-1046 (2008).
17. Nakayama, Y., Gotanda, T. & Ito, K. Asymmetric Morita-Baylis-Hillman reactions of 2-cyclohexen-1-one catalyzed by chiral biaryl-based bis(thiourea) organocatalysts. *Tetrahedron Lett.* **52**, 6234-6237 (2011).
18. Aggarwal, V. K., Emme, I. & Fulford, S. Y. Correlation between p*K*_a and reactivity of quinuclidine-based catalysts in the Baylis-Hillman reaction: Discovery of quinuclidine as optimum catalyst leading to substantial enhancement of scope. *J. Org. Chem.* **3**, 692-700 (2003).

19. Karur, S., Hardin, J., Headley, A. & Li, G. A novel approach to Morita–Baylis–Hillman (MBH) lactones via the Lewis acid-promoted couplings of α,β -unsaturated lactone with aldehydes. *Tetrahedron Lett.* **44**, 2991-2994 (2003).

Chapter 5: Design and Evolution of an Enzyme with a Non-Canonical Organocatalytic Mechanism

Nature **570**, 219-223 (2019).

Ashleigh J. Burke^{1,2}, Sarah L. Lovelock^{1,2}, Amina Frese¹, Rebecca Crawshaw¹, Mary Ortmyer¹, Mark Dunstan¹, Colin Levy¹ & Anthony P. Green^{1*}

¹Manchester Institute of Biotechnology, School of Chemistry, 131 Princess Street, University of Manchester, Manchester M1 7DN, UK.

²These authors contributed equally: Ashleigh J. Burke and Sarah L. Lovelock.

5.1 Foreword

This chapter consists of a research article published in *Nature* on 27th May 2019 and describes the design and evolution of an enantioselective hydrolase with a non-canonical catalytic mechanism.

5.2 Author contributions

The research presented in this chapter was a collaborative effort between the doctoral candidate and the following researchers: Ashleigh J. Burke, Sarah L. Lovelock, Amina Frese, Mary Ortmyer, Mark Dunstan, Colin Levy and Anthony P. Green. The doctoral candidate and Ashleigh J. Burke installed the non-canonical amino acid *N*_ε-methylhistidine into BH32 variants and developed biochemical assays to investigate the impact of the non-canonical nucleophile on hydrolytic activity. Ashleigh J. Burke and Sarah L. Lovelock carried out molecular biology, assay development, directed evolution, and protein production, purification and kinetic characterisation. The doctoral candidate, Ashleigh J. Burke and Sarah L. Lovelock carried out enzyme-inhibition experiments and protein crystallisation. Ashleigh J. Burke carried out substrate synthesis, evaluation of substrates **2-7**, and the final round of evolution (OE1.3 to OE1.4). Mark Dunstan automated the directed-evolution workflow. Amina Frese, Mary Ortmyer, Mark Dunstan and Colin Levy interpreted and analysed structural data. All authors discussed the results and participated in writing the manuscript.

5.3 Manuscript

The combination of computational design and laboratory evolution is a powerful and potentially versatile strategy for the development of enzymes with new functions.[1-4] However, the limited functionality presented by the genetic code restricts the range of catalytic mechanisms that are accessible in designed active sites. Inspired by mechanistic strategies from small-molecule organocatalysis,[5] here we report the generation of a hydrolytic enzyme that uses *N*₆-methylhistidine as a non-canonical catalytic nucleophile. Histidine methylation is essential for catalytic function because it prevents the formation of unreactive acyl-enzyme intermediates, which has been a long-standing challenge when using canonical nucleophiles in enzyme design.[6-10] Enzyme performance was optimised using directed evolution protocols adapted to an expanded genetic code, affording a biocatalyst capable of accelerating ester hydrolysis with greater than 9,000-fold increased efficiency over free *N*₆-methylhistidine in solution. Crystallographic snapshots along the evolutionary trajectory highlight the catalytic devices that are responsible for this increase in efficiency. *N*₆-methylhistidine can be considered to be a genetically encodable surrogate of the widely employed nucleophilic catalyst 4-dimethylaminopyridine,[11] and its use will create opportunities to design and engineer enzymes for a wealth of valuable chemical transformations.

Designing hydrolytic enzymes with sophisticated catalytic machineries reminiscent of those found in nature presents a formidable challenge.[6-9,12] Natural hydrolases often use a catalytic triad containing an activated nucleophile paired with hydrogen-bond donors to stabilise oxyanion intermediates.[13-15] Although computational approaches have enabled the accurate design of histidine, cysteine and serine nucleophiles, the formation of unreactive acyl-enzyme intermediates has compromised catalytic function.[6-9] Synthetic mimics of hydrolytic enzymes and self-assembled α -helical barrels derived from synthetic peptides are compromised by similar limitations.[10,16]

To create a functional hydrolase we selected a computationally designed enzyme for the Morita–Baylis–Hillman reaction, denoted BH32, as a template for catalytic remodelling. BH32 uses a histidine nucleophile (His23) built into the cap domain (HAD superfamily nomenclature) of haloacid dehalogenase from *Pyrococcus horikoshii* by introducing 12 active-site mutations predicted by the Rosetta software suite.[17] The catalytic activity of BH32 for its designed Morita–Baylis–Hillman reaction is modest (less than 1 turnover per day). Nevertheless, we were attracted by the potential to unlock new catalytic functions within the BH32 template by harnessing the reactivity of the designed histidine nucleophile. The hydrolytic activity of BH32 towards a series of monoacylated fluorescein derivatives was evaluated by monitoring the formation of the fluorescein product at 500 nm. Consistent with previously designed catalysts for ester hydrolysis, the reaction profile (product formation over time) exhibits biphasic behaviour, with an initial ‘burst’ phase correlating to fast enzyme acylation followed by slow hydrolytic turnover (Fig. 1a, b). Using fluorescein 2-phenylacetate (**1**) as a substrate, an observed rate constant (k_{obs}) of $1.3 \pm 0.03 \text{ min}^{-1}$ was determined for the formation of the acyl-enzyme intermediate (Extended Data Fig. 1). A His23Ala mutation abolishes the burst phase, suggesting that acylation proceeds via the designed His23 nucleophile. Following the initial burst, the rate of substrate hydrolysis by BH32 is indistinguishable from that of the His23Ala variant and from background chemical hydrolysis (Fig. 1b, Extended Data Fig. 5d). These

observations suggest that the His23-acyl intermediate is stable and resistant to hydrolysis, thus compromising the catalytic function of BH32.

To gain further insights into the reaction mechanism, BH32 was alkylated with the mechanistic inhibitor 2-bromoacetophenone to provide a structural analogue of the acyl-enzyme intermediate. The X-ray crystal structure of the inhibited protein was solved to a resolution of 2.0 Å and revealed that the nucleophilic histidine reacts via the N_ε atom as originally designed for the Morita–Baylis–Hillman reaction (Extended Data Fig. 7). The stability of the acyl-imidazole intermediate, which accumulates during ester hydrolysis by BH32, probably arises from the loss of a proton on the non-coordinating N_δ atom following acylation to form a neutral species (Fig. 1a). We postulated that a more reactive acyl-imidazolium intermediate could be generated by replacing His23 with a non-canonical N_δ-methylhistidine (Me-His) nucleophile (Fig. 1a). An engineered pyrrolysyl-tRNA synthetase/pyrrolysyl-tRNA pair was used to introduce a Me-His23 residue in response to a UAG stop codon.[18] This genetically encoded modification leads to a substantial increase in the rate of hydrolytic turnover (Fig. 1b), affording a functional esterase that operates via a non-canonical organocatalytic mechanism (organocatalytic esterase, OE1). This observation supports our hypothesis that the poor turnover displayed by previously designed hydrolases can be attributed to the challenges of accurately creating networks of residues that activate neutral acyl-enzyme species.

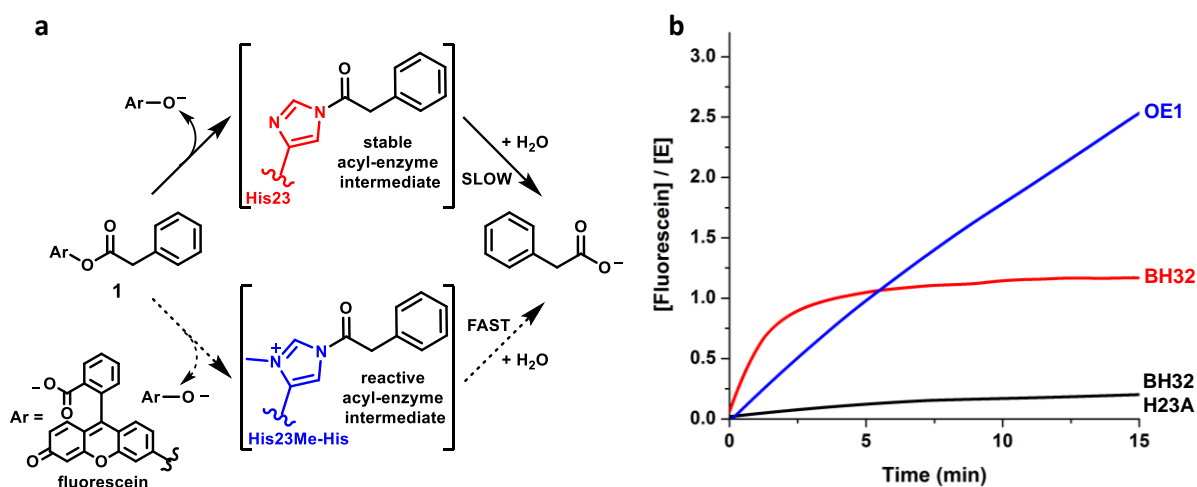


Figure 1: Characterisation of BH32 containing nucleophilic His23 and Me-His23 residues. a) Reaction scheme for the hydrolysis of fluorescein 2-phenylacetate (**1**) catalysed by BH32 (His23) and BH32(His23Me-His) (OE1). Acylation of the Me-His nucleophile leads to the generation of a reactive acyl-imidazolium intermediate. b) Time course of the hydrolysis of fluorescein 2-phenylacetate (100 μM) catalysed by BH32 (red), BH32(His23Ala) (black) and OE1 (blue). Reactions were monitored by an increase in absorbance at 500 nm due to the formation of fluorescein. The biphasic reaction profile of BH32 is consistent with rapid acylation of the His23 nucleophile followed by slow hydrolysis of the acyl-imidazole intermediate. Following the initial burst phase, the rate of substrate hydrolysis by BH32 is indistinguishable from that of the His23Ala variant. The introduction of a non-canonical Me-His23 nucleophile substantially increases the rate of hydrolytic turnover.

Directed evolution has proven to be an invaluable tool for tailoring the catalytic functions of enzymes.[19,20] To demonstrate that this technology can be adapted to optimise designed enzymes with non-canonical mechanisms, we subjected OE1 to laboratory evolution using a spectrophotometric assay based on fluorescein detection. The evolutionary strategy used included both local and global mutagenesis (Fig. 2a, Extended Data Fig. 2): early rounds used combinatorial active-site-saturation mutagenesis (CASTing)[21] to target active-site residues, including those in close proximity to the Me-His nucleophile; error-prone PCR was used to target the entire gene, leading to the identification of 'hot spots' that were further interrogated as small, focused libraries. A further 21 residues were selected and individually randomised via saturation mutagenesis. Beneficial diversity identified along the evolutionary coordinate was combined by DNA shuffling.

The most active variant (OE1.3) to emerge after the evaluation of more than 12,000 OE1 descendants contains six mutations distributed around the active site, and hydrolyses fluorescein 2-phenylacetate with a catalytic efficiency ($k_{\text{cat}}/K_{\text{M}}$, where k_{cat} is the turnover number and K_{M} is the Michaelis constant) of $3,190 \text{ M}^{-1} \text{ s}^{-1}$, representing a 15-fold improvement over the parent template OE1. Notably, this increased efficiency was primarily achieved through a more than 10-fold increase in turnover number ($k_{\text{cat}} = 0.77 \pm 0.07 \text{ min}^{-1}$ and $7.8 \pm 0.4 \text{ min}^{-1}$ for OE1 and OE1.3, respectively; Fig. 2b). OE1.3 is greater than 9,000-fold more efficient than free Me-His in solution ($k_{\text{Me-His}} = 0.35 \text{ M}^{-1} \text{ s}^{-1}$; Extended Data Fig. 5a), and approximately 2,800-fold more efficient than the commonly used organocatalysts 4-dimethylaminopyridine (DMAP) ($k_{\text{DMAP}} = 1.13 \text{ M}^{-1} \text{ s}^{-1}$; Extended Data Fig. 5b) and *N*-methylimidazole (NMI) ($k_{\text{NMI}} = 1.16 \text{ M}^{-1} \text{ s}^{-1}$; Extended Data Fig. 5c). In contrast to previous designs that operate via canonical nucleophiles,[6-10] OE1.3 is not compromised by slow hydrolysis of the acyl-enzyme catalytic intermediate. The time course of fluorescein 2-phenylacetate hydrolysis by OE1.3 shows a reaction profile that is essentially linear for more than 40 turnovers. Replacement of the Me-His23 nucleophile with either alanine (OE1.3(Me-His23Ala)) or histidine (OE1.3(Me-His23His)) effectively abolishes hydrolytic activity, demonstrating that catalytic function is strictly dependent on the presence of the non-canonical residue (Fig. 2c). We also compared the activity of OE1.3 to that of a promiscuous natural hydrolase, CUT190, in which a classical Ser-His-Asp catalytic triad is paired with an oxyanion hole and embedded in an open active site.[22] Notably, OE1.3 and CUT190 display similar binding affinities for fluorescein 2-phenylacetate ($K_{\text{M}} = 41 \pm 5$ and $K_{\text{M}} = 39 \pm 4$ for OE1.3 and CUT190, respectively) and catalyse its hydrolysis with comparable turnover numbers ($k_{\text{cat}} = 7.8 \pm 0.4 \text{ min}^{-1}$ and $k_{\text{cat}} = 4.5 \pm 0.4 \text{ min}^{-1}$ for OE1.3 and CUT190 respectively, Extended Data Fig. 3d, g, h).

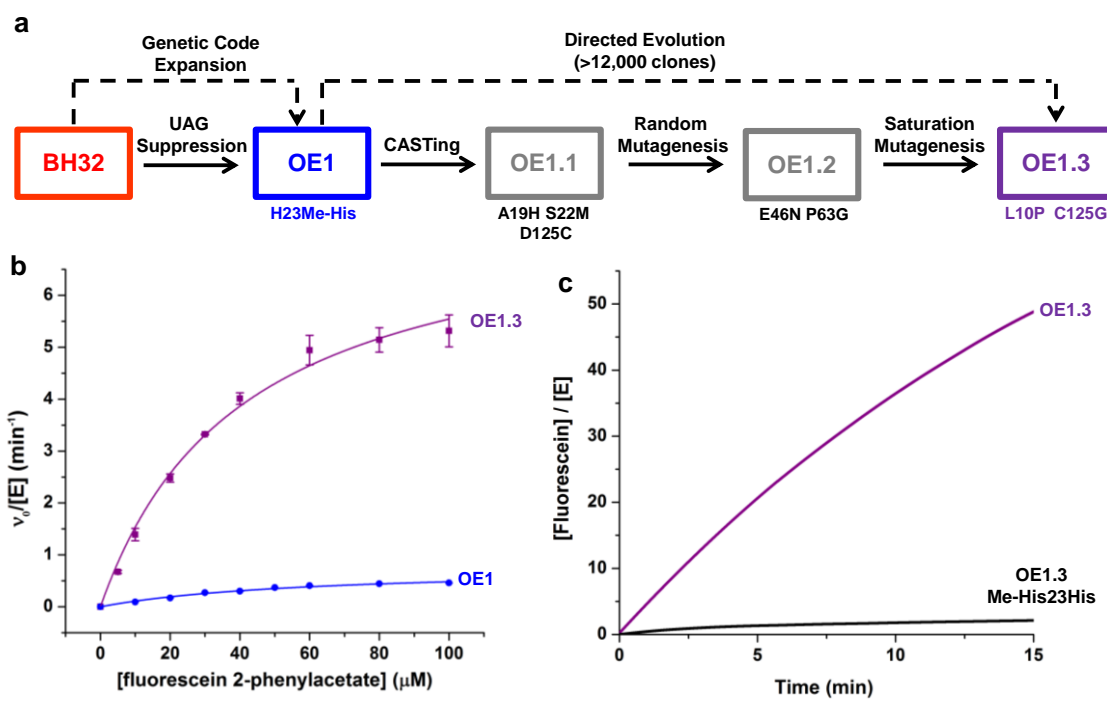


Figure 2: Evolution and characterisation of OE1.3. a) Design and evolution workflow used to generate OE1.3. BH32 (red) is a computationally designed enone-binding protein that is generated by introducing 12 mutations into a haloacid dehalogenase from *Pyrococcus horikoshii*. [17] Replacement of the His23 nucleophile of BH32 by a non-canonical Me-His residue afforded hydrolytic enzyme OE1 (blue). Six additional mutations were accumulated during laboratory evolution to afford OE1.3 (purple). Position 125 was mutated twice during evolution. From OE1, each arrow indicates the evolutionary strategy used during each round of optimisation. After each round, beneficial diversity was combined by DNA shuffling. b) Michaelis–Menten plots of the hydrolysis of fluorescein 2-phenylacetate by OE1 (blue) and OE1.3 (purple). Data are mean \pm s.d. of measurements made in triplicate. Michaelis–Menten plots for OE1.1 and OE1.2 are shown in Extended Data Fig. 3. c) Time course of the hydrolysis of fluorescein 2-phenylacetate (100 μM) catalysed by OE1.3 (purple) and OE1.3(Me-His23His) (black). Replacement of the Me-His catalytic nucleophile of OE1.3 with His abolishes hydrolytic turnover.

To gain insights into the origins of improved catalytic activity along the evolutionary trajectory, X-ray structures of OE1 and OE1.3 were solved and refined to resolutions of 2.0 Å and 1.9 Å, respectively (Fig. 3a). The Me-His residue adopts a single, well-defined conformation in both structures, with the methyl group extending into a small pocket within the protein bounded by the side chains of residues Ile26, Met27, Leu42, Tyr45 and Phe87. Compared with OE1, a small rotation of approximately 15° is observed in the plane of the Me-His imidazole ring in OE1.3. The Ala19His and Ser22Met mutations lie above and beneath the plane of the ring, respectively, and reduce the degree of rotational freedom available to the Me-His. Glu46, which was originally designed to form a hydrogen bond with the histidine nucleophile of BH32, is mutated to asparagine in OE1.3. The amide side chain of Asn46 forms hydrogen bonds with two ordered water molecules, placing them in close proximity to Me-His23 and His19. This, in combination with the phenolic side chain of Tyr45, creates a network

of polar interactions that may have a role in mechanistically important proton transfers and/or water delivery along the esterase reaction coordinate. Indeed, the Tyr45Phe and Asn46Glu mutations in OE1.3 result in 4.3- and 3.7-fold reductions in k_{cat} , respectively (Extended Data Fig. 3e, f, h), which shows that these residues are functionally important but are not essential for esterase activity. The final mutation installed during evolution (Leu10Pro), which gave a 3-fold increase in k_{cat} , expands the active-site pocket and induces a backbone rearrangement in the protein extending from residue Phe7 through to Leu13. Alkylation of OE1.3 with 2-bromoacetophenone results in complete enzyme deactivation due to selective modification of Me-His23 (Fig. 3b, Extended Data Table 2), further confirming its role as the catalytic nucleophile. Notably, OE1.3 was found to undergo a global conformational change upon inhibition, which is caused by an adjustment in the relative orientations of two domains (residues 1–15, 57–63 and 90–228 in domain 1 (core), and residues 16–56 and 64–89 in domain 2 (cap)). The individual core and cap domains can be superimposed onto the apo-OE1.3 structure with a root-mean-square deviation (r.m.s.d.) of 0.83 Å and 0.81 Å, respectively. Upon inhibition the two domains open by approximately 9°, modulated through hinge residues located at positions 15–22, 56–57, 63–64 and 89–90, which leads to a substantial increase in solvent-accessible surface (Fig. 3b). We note that this domain reorientation is not observed upon Me-His alkylation in the intermediate variant OE1.2, which lacks the Leu10Pro mutation (Extended Data Fig. 8). Although further investigation is needed to elucidate the functional importance of this domain motion to the catalytic cycle of OE1.3, similar conformational changes between the cap and core domains of members of the HAD superfamily have been described previously and are thought to be coupled to their reaction coordinate.[23] Our observations thus raise the possibility that functionally relevant conformational dynamics have emerged during OE1.3 evolution.

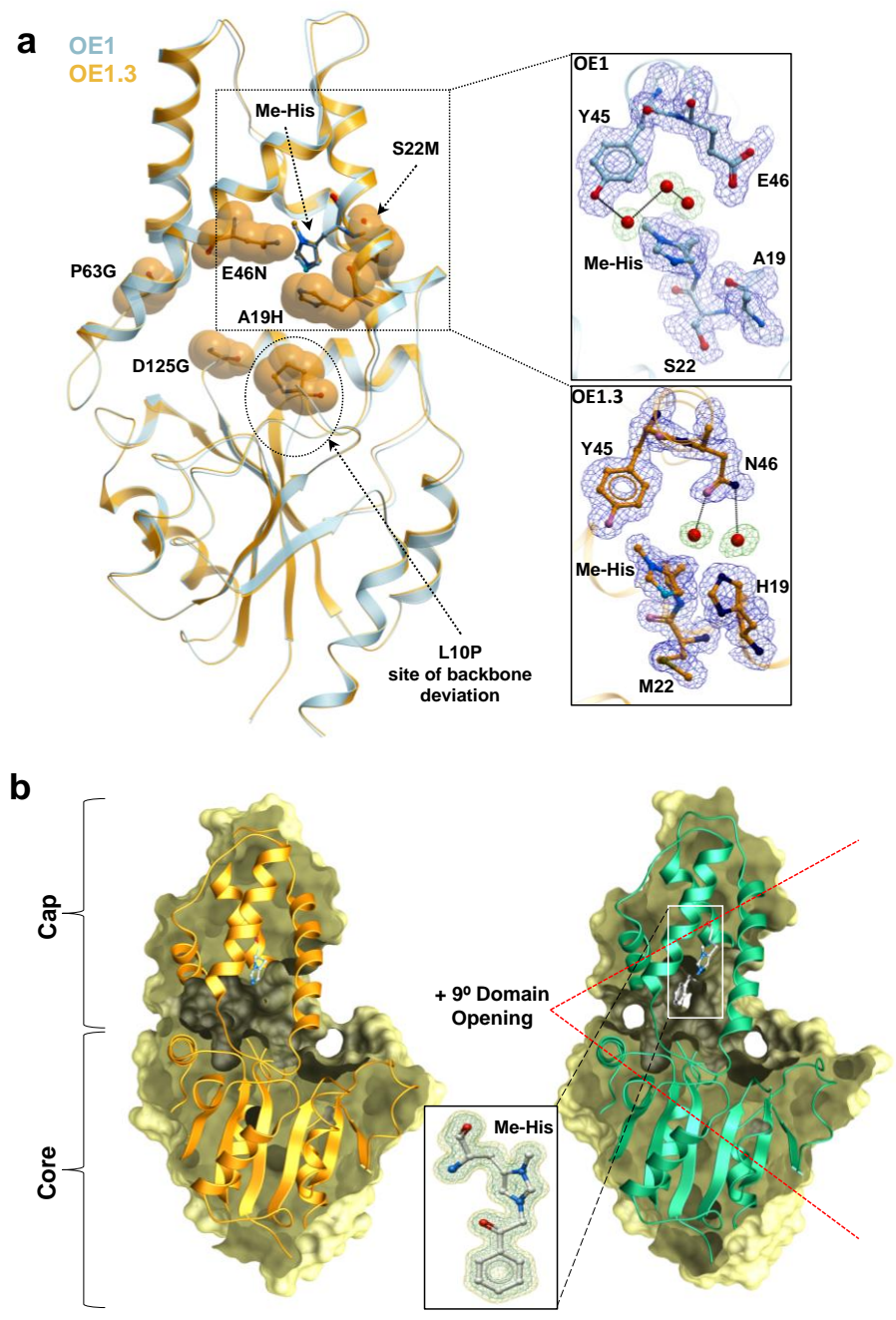


Figure 3: Crystal structures of OE1, OE1.3 and inhibited OE1.3. a) A global superposition of OE1 and OE1.3 based on backbone positions (r.m.s.d. of 0.48 Å). Ribbon representations of OE1 and OE1.3 are shown in light blue and orange, respectively. Me-His residues are shown in ball-and-stick representation, coloured by atom type, with Ca colouring consistent with the ribbon representation. Sites of mutation in OE1.3 are shown in both ball-and-stick representation and Corey–Pauling–Koltun (CPK) spheres. The right-hand panels show an expanded view of the two Me-His environments with associated mutations. The top panel shows Me-His for structure OE1 with associated feature enhanced electron density maps (FEM) contoured at 3σ . Electron density for the protein is shown in blue, whereas ordered water molecules are shown with green electron density for clarity (FEM, 3σ). The lower panel shows a similar expanded view of the OE1.3 Me-His environment, highlighting the hydrogen bonding between Asn46 and two ordered water molecules.

b) A ribbon and surface representation of apo- (left) and inhibited- (right) OE1.3. The orientation of the protein in both images is identical. The Me-His and alkylated Me-His residues are shown in ball and stick representation coloured by atom type. Alkylation of OE1.3 with 2-bromoacetophenone induces a 9° opening between the two domains. Electron density of the alkylated Me-His is shown in yellow and green ($F_o - F_c$ omit map contoured at 1σ (green) and 3σ (yellow)). Apo- and inhibited forms of OE1.3 were solved as their Cys186Ala/Cys212Ala variants to avoid additional alkylations during inhibition. These substitutions had no effect on esterase activity (Extended Data Fig. 6).

We next evaluated the activities of OE1 and OE1.3 towards a series of fluorescein esters (**2–6**). Substrates with electron-donating (**2**) and electron-withdrawing (**3**) phenyl substituents, heterocycles (**4** and **6**), and a sterically demanding naphthyl group (**5**) were all well tolerated. Notably, directed evolution resulted in substantial rate accelerations with all substrates tested, with initial velocities between 33-fold and 8-fold greater with OE1.3 than with OE1 (Fig. 4a). However, the introduction of an α -methyl substituent (*(R)*-**7** and *(S)*-**7**) led to substantial reductions in activity compared with achiral substrates **2–6**. Furthermore, the more active OE1.3 displays only modest levels of enantioselectivity (1:1.5 in favour of the *(R)*-enantiomer). To demonstrate that our designed hydrolases can be tailored to promote enantioselective transformations, OE1.3 was subjected to further rounds of evolution.

Libraries were generated by individually randomising 20 residues (see Extended Data Fig. 2 for details) and screened for improved activity towards fluorescein *(R)*-2-phenylpropanoate (*(R)*-**7**). The most active variants from each library were subjected to a second round of screening towards both *(R)*- and *(S)*-enantiomers of **7**, leading to the identification of five clones that showed improved activity and selectivity. Combining this beneficial diversity by DNA shuffling led to the identification of a triple mutant OE1.4 (OE1.3(N14Q/S124L/D180F)). This variant preferentially hydrolyses *(R)*-**7** with a k_{cat} of $12 \pm 2.6 \text{ min}^{-1}$, which is 8-fold higher than its activity towards the *(S)*-enantiomer ($k_{cat} = 1.5 \pm 0.2 \text{ min}^{-1}$) and represents a 15-fold improvement over the parent template OE1.3 ($k_{cat} = 0.8 \pm 0.09 \text{ min}^{-1}$; Fig. 4b). Although disparate in sequence, the Asn14Gln, Ser124Leu and Asp180Phe mutations are clustered around the Pro10 residue that was installed during the previous round of evolution. This shows that our artificial enzymes can be readily adapted to perform new functions by installing a relatively small number of mutations, making us optimistic about future efforts to utilise our approaches to create enzymes with broad synthetic utility.

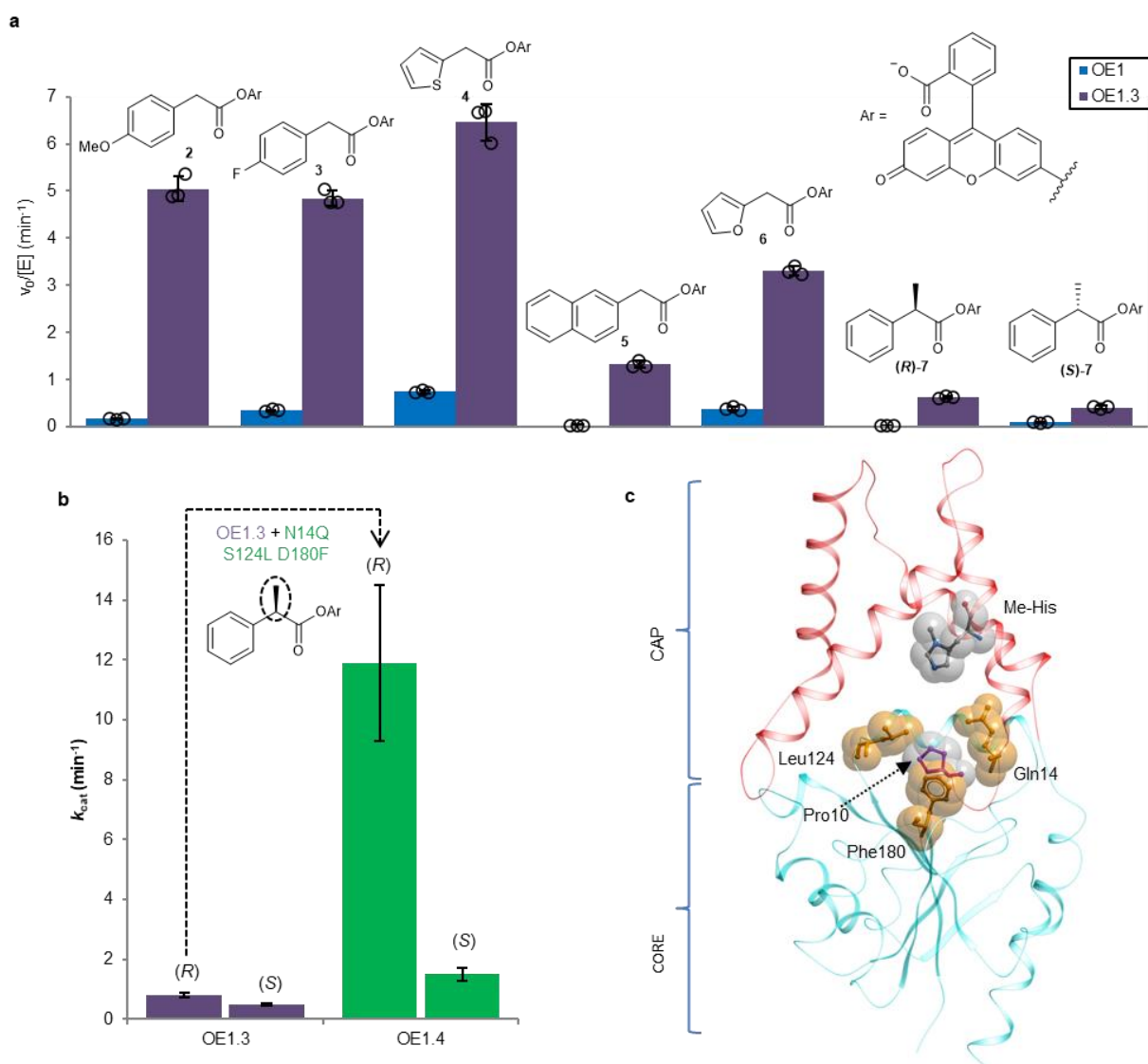


Figure 4: Substrate promiscuity of OE1.3 and engineering of an enantioselective hydrolase OE1.4. a) Bar chart showing the initial rate of fluorescein ester hydrolysis ($100 \mu\text{M}$) catalysed by OE1 and OE1.3. The evolved variant OE1.3 is more active than OE1 towards all substrates screened. Data are mean \pm s.d. of measurements made in triplicate, with individual data points shown as circles. b) Bar chart comparing the k_{cat} of OE1.3 and OE1.4 for the hydrolysis of fluorescein (*R*)-2-phenylpropanoate and fluorescein (*S*)-2-phenylpropanoate. The corresponding Michaelis–Menten plots are shown in Extended Data Fig. 4. c) A model of the engineered OE1.4 structure derived from in silico mutagenesis and energy minimisation of the OE1.3 scaffold (ICM Pro). The core and cap domains are shown as cyan and red ribbons, respectively, with Pro10 and MeHis highlighted with grey CPK spheres. The Asn14Gln, Ser124Leu and Asp180Phe mutations are highlighted with orange CPK spheres.

Genetic-code expansion has emerged as a powerful technology for modifying protein structure and function.[24-28] The ability to encode non-canonical functionality also presents new opportunities to generate *de novo* protein catalysts. Early examples include the use of genetically encoded para-azidophenylalanine as a reactive handle for the generation of artificial metalloenzymes, or as a precursor to a reactive aniline group that is capable of promoting hydrazone formations.[29,30] We have now exploited an expanded genetic code to generate an enzyme that operates via a non-canonical organocatalytic mechanism. Introduction of the reactive Me-His nucleophile directly through the cellular translation machinery allowed us to optimise enzyme performance via laboratory evolution. This study takes the first steps towards the 'bottom-up' generation of hydrolytic enzymes that are tailored towards specific applications, for example to degrade and recycle anthropogenic contaminants to prevent their accumulation in the environment. The design of more efficient biocatalysts that are capable of hydrolysing non-activated substrates will probably be achieved by developing more sophisticated mechanisms that pair non-canonical nucleophiles with oxyanion holes. More generally, our study will inspire the development of translation components to encode new families of functional amino acids with diverse modes of reactivity. We anticipate that integrating such 'chemically inspired' catalytic functionality into computational-design algorithms will provide a powerful and versatile strategy to generate enzymes with functions that are not accessible to nature.

5.4 References

1. Röthlisberger, D. et al. Kemp elimination catalysts by computational enzyme design. *Nature* **453**, 190-195 (2008).
2. Siegel, J. B. et al. Computational design of an enzyme catalyst for a stereoselective bimolecular Diels–Alder reaction. *Science* **329**, 309-313 (2010).
3. Blomberg, R. et al. Precision is essential for efficient catalysis in an evolved Kemp eliminase. *Nature* **503**, 418-421 (2013).
4. Obexer, R. et al. Emergence of a catalytic tetrad during evolution of a highly active artificial aldolase. *Nat. Chem.* **9**, 50-56 (2017).
5. Jencks, W. P., Salvesen, K. & Oakenfull, D. G. Reactions of acetylimidazole and acetylimidazolium ion with nucleophilic reagents. Mechanisms of catalysis. *J. Am. Chem. Soc.* **93**, 188-194 (1971).
6. Bolon, D. N. & Mayo, S. L. Enzyme-like proteins by computational design. *Proc. Natl Acad. Sci. USA* **98**, 14274-14279 (2001).
7. Richter, F. et al. Computational design of catalytic dyads and oxyanion holes for ester hydrolysis. *J. Am. Chem. Soc.* **134**, 16197-16206 (2012).
8. Rajagopalan, S. et al. Design of activated serine-containing catalytic triads with atomic-level accuracy. *Nat. Chem. Biol.* **10**, 386-391 (2014).
9. Moroz, Y. S. et al. New tricks for old proteins: single mutations in a nonenzymatic protein give rise to various enzymatic activities. *J. Am. Chem. Soc.* **137**, 14905-14911 (2015).
10. Burton, A. J., Thomson, A. R., Dawson, W. M., Brady, R. L. & Woolfson, D. N. Installing hydrolytic activity into a completely *de novo* protein framework. *Nat. Chem.* **8**, 837-844 (2016).
11. Wurz, R. P. Chiral dialkylaminopyridine catalysts in asymmetric synthesis. *Chem. Rev.* **107**, 5570-5595 (2007).
12. Studer, S. et al. Evolution of a highly active and enantiospecific metalloenzyme from short peptides. *Science* **362**, 1285-1288 (2018).
13. Brady, L. et al. A serine protease triad forms the catalytic centre of a triacylglycerol lipase. *Nature* **343**, 767-770 (1990).
14. Smith, A. J. T. et al. Structural reorganization and preorganization in enzyme active sites: comparisons of experimental and theoretically ideal active site geometries in the multistep serine esterase reaction cycle. *J. Am. Chem. Soc.* **130**, 15361-15373 (2008).
15. Buller, A. R. & Townsend, C. A. Intrinsic evolutionary constraints on protease structure, enzyme acylation, and the identity of the catalytic triad. *Proc. Natl Acad. Sci. USA* **110**, E653-E661 (2013).
16. Breslow, R. & Dong, S. D. Biomimetic reactions catalyzed by cyclodextrins and their derivatives. *Chem. Rev.* **98**, 1997-2012 (1998).
17. Bjelic, S. et al. Computational design of enone-binding proteins with catalytic activity for the Morita–Baylis–Hillman reaction. *ACS Chem. Biol.* **8**, 749-757 (2013).
18. Xiao, H. et al. Genetic incorporation of histidine derivatives using an engineered pyrrolysyl-tRNA synthetase. *ACS Chem. Biol.* **9**, 1092-1096 (2014).
19. Bornscheuer, U. T. et al. Engineering the third wave of biocatalysis. *Nature* **485**, 185-194 (2012).

20. Arnold, F. H. Directed evolution: bringing new chemistry to life. *Angew. Chem. Int. Ed. Engl.* **57**, 4143-4148 (2018).
21. Reetz, M. T., Bocola, M., Carballeira, J. D., Zha, D. & Vogel, A. Expanding the range of substrate acceptance of enzymes: combinatorial active-site saturation test. *Angew. Chem. Int. Ed. Engl.* **44**, 4192-4196 (2005).
22. Kawai, F. et al. A novel Ca²⁺-activated, thermostabilized polyesterase capable of hydrolyzing polyethylene terephthalate from *Saccharomonospora viridis* AHK190. *Appl. Microbiol. Biotechnol.* **98**, 10053-10064 (2014).
23. Grifn, J. L. et al. Near attack conformers dominate β -phosphoglucomutase complexes where geometry and charge distribution reflect those of substrate. *Proc. Natl Acad. Sci. USA* **109**, 6910-6915 (2012).
24. Liu, C. C. & Schultz, P. G. Adding new chemistries to the genetic code. *Annu. Rev. Biochem.* **79**, 413-444 (2010).
25. Chin, J. W. Expanding and reprogramming the genetic code. *Nature* **550**, 53-60 (2017).
26. Ugwumba, I. N. et al. Improving a natural enzyme activity through incorporation of unnatural amino acids. *J. Am. Chem. Soc.* **133**, 326-333 (2011).
27. Agostini, F. et al. Biocatalysis with unnatural amino acids: enzymology meets xenobiology. *Angew. Chem. Int. Ed. Engl.* **56**, 9680-9703 (2017).
28. Windle, C. L. et al. Extending enzyme molecular recognition with an expanded amino acid alphabet. *Proc. Natl Acad. Sci. USA* **114**, 2610-2615 (2017).
29. Yang, H. et al. Evolving artificial metalloenzymes via random mutagenesis. *Nat. Chem.* **10**, 318-324 (2018).
30. Drienovská, I., Mayer, C., Dulson, C. & Roelfes, G. A designer enzyme for hydrazone and oxime formation featuring an unnatural catalytic aniline residue. *Nat. Chem.* **10**, 946-952 (2018).

Chapter 6: Conclusions and Outlook

We have entered an era where protein structures can be designed with near atomic level precision based on fundamental biophysical principles. However, embedding new catalytic sites and substrate binding pockets with similar levels of accuracy remains a formidable challenge. Prior to this thesis, *de novo* enzyme design had delivered primitive enzymes for handful of well-studied transformations that have previously been achieved with catalytic antibodies (e.g. Kemp Elimination). These designs have been optimised through laboratory evolution to deliver efficiencies approaching natural enzymes. If we are to establish 'bottom-up' enzyme design as a reliable resource of biocatalysts for practical applications, we must move beyond simple model transformations to more complex and mechanistically challenging reactions that have no biological counterpart.

During this PhD, the strategy of evolving a primitive computational design has been exploited to create an efficient biocatalyst for the MBH reaction, a valuable C-C bond forming reaction for which no effective protein catalysts were previously known. This work has moved beyond prior work in the field, demonstrating that the combination of *de novo* design and laboratory evolution can be adapted to tackle more demanding multi-step chemical transformations, where multiple functional active site components are required to operate in concert to achieve efficient and selective catalysis. Through extensive laboratory evolution, a biocatalyst with a 1,100-fold increase in catalytic efficiency over the starting design has been developed. Investigation of the synthetic utility of BH32.10 revealed the biocatalyst accepted a broad array of activated alkene and aldehyde/ketone coupling partners, further reinforcing the versatility of this biocatalyst. The substrate scope of the predecessor BH32.6 was also assessed, revealing a more promiscuous activity in comparison to BH32.10, which could provide an interesting starting point for the further engineering of MBHases to produce a broader range of target structures. Cascade biocatalysis employs several enzymes which work consecutively to generate high-value molecules from simple building blocks. By combining the engineered MBHase in a cascade with other biocatalysts, for example a transaminase, further densely functionalised products with distinct motifs could be accessed with high efficiency and selectivity to deliver an array of new molecules.

BH32.10 is orders of magnitude more efficient than small molecule catalysts for the MBH reaction and promotes reactions with high levels of stereocontrol that surpasses other known MBH catalysts. BH32.10 delivers the (*R*)-enantiomer of the MBH product from the reaction of 2-cyclohexen-1-one and 4-nitrobenzaldehyde in 93% e.e., which compares favourably with the modest selectivities achieved with small molecule catalysts such as DABCO paired with chiral bis(thio)urea. Structural characterization of BH32.9 combined with DFT modelling reveals that a sophisticated array of catalytic machinery has been installed and refined along the evolution trajectory, which pairs a His23 catalytic nucleophile with a judiciously positioned Arg124. This catalytic arginine shuttles between conformational states to stabilise multiple transition states and oxyanion intermediates along the complex reaction coordinate. Arg124 can be likened to privileged bidentate hydrogen bonding catalysts such as thioureas which promote a wealth of important transformations in organic synthesis. The observation that Arg can serve as a genetically encoded surrogate of bidentate

hydrogen bonding catalysts should therefore inspire the future design of biocatalysts for a broad range of non-biological transformations.

Enzyme design and engineering strategies are typically reliant on Nature's alphabet of 20 canonical amino acids, which contain a narrow range of functional groups. Under these constraints, important modes of catalysis have proven challenging to design. Most notably, efforts to employ catalytic Cys, Ser or His nucleophiles to accelerate hydrolysis or acyl-transfer reactions have proven challenging due to the stability of acyl-enzyme catalytic intermediates. Here we have exploited an expanded genetic code to develop *de novo* hydrolases (OE1-OE1.4) in the BH32 scaffold, that exploit Me-His as a non-canonical catalytic nucleophile. Histidine methylation leads to the generation of reactive acyl-imidazolium intermediates which are susceptible to hydrolytic turnover. Significantly we have demonstrated *de novo* enzymes with non-canonical amino acids can be optimised using directed evolution workflows adapted to an expanded genetic code. This combination of GCE and laboratory evolution delivered OE1.3, which is *ca.* 4 orders of magnitude more efficient than equivalent small molecule catalysts in promoting ester hydrolysis, and OE1.4 which can promote enantioselective transformations. We anticipate that the integration of non-canonical functional groups into enzyme design and engineering workflows will greatly expand the repertoire of chemical transformation accessible in *de novo* active sites in the coming years.

Chapter 7: Experimental

7.1 Foreword

This chapter contains the supporting information for the research presented in Chapters 3-5.

7.2 Supporting Information for Chapter 3: An Efficient and Enantioselective *de novo* Enzyme for the Morita-Baylis-Hillman Reaction

7.2.1 Methods

7.2.1.1 Materials

All chemicals and biological materials were obtained from commercial suppliers. Lysozyme, DNase I and kanamycin were purchased from Sigma-Aldrich; polymyxin B sulfate from AlfaAesar; LB agar, LB media, 2×YT media and arabinose from Formedium; *Escherichia coli* (*E. coli*) 5α, Q5 DNA polymerase, T4 DNA ligase and restriction enzymes from New England BioLabs; and oligonucleotides were synthesised by Integrated DNA Technologies.

7.2.1.2 Construction of pBbE8k_BH32 and variants

The original BH32 design[1] was modified to introduce C186A and C212A mutations to avoid any non-specific alkylations of these positions. These substitutions had no effects on MBH activity. The C186A and C212A double mutant is referred to as BH32 throughout this study. BH32 was subcloned, using *NdeI* and *XhoI* restriction sites, into a pBbE8k vector[2] modified to include a 6×His tag or Strep-tag following the *XhoI* restriction site to yield pBbE8k_BH32_6His or pBbE8k_BH32_Strep. The H23A mutation was introduced into the pBbE8k_BH32 constructs using QuikChange site-directed mutagenesis.

7.2.1.3 Protein production and purification

For expression of BH32 and variants, chemically competent *E. coli* 5α were transformed with the relevant pBbE8k_BH32 constructs. Single colonies of freshly transformed cells were cultured for 18 h in 10 mL LB medium containing 25 μg mL⁻¹ kanamycin. Starter cultures (500 μL) were used to inoculate 50 mL 2×YT medium supplemented with 25 μg mL⁻¹ kanamycin. Cultures were grown at 37 °C, 200 r.p.m. to an optical density at 600 nm (OD₆₀₀) of around 0.5. Protein expression was induced with the addition of L-arabinose to a final concentration of 10 mM. Induced cultures were incubated for 20 h at 25 °C and the cells were subsequently collected by centrifugation (3,220g for 10 min). For His-tagged variants, pelleted cells were resuspended in lysis buffer (50 mM HEPES, 300 mM NaCl, pH 7.5 containing 20 mM imidazole) and lysed by sonication. Cell lysates were cleared by centrifugation (27,216g for 30 min), and supernatants were subjected to affinity chromatography using Ni-NTA Agarose (Qiagen). Purified protein was eluted using 50 mM HEPES, 300 mM NaCl, pH 7.5 containing 250 mM imidazole. For Strep-tagged variants, pelleted cells were resuspended in Buffer NP (50 mM NaH₂PO₄, 300 mM NaCl, pH 8) and lysed by sonication. Cell lysates were cleared by centrifugation (27,216g for 30 min), supernatants were subjected to a *Strep*-Tactin® Superflow Plus resin (Qiagen) and purified protein was eluted using 50 mM NaH₂PO₄, 300 mM NaCl, 2.5 mM desthiobiotin at pH 8.0. Proteins were desalted using 10DG desalting columns (Bio-Rad) with PBS

pH 7.4 and analysed by SDS-PAGE. Proteins were further purified by size-exclusion chromatography using a Superdex 200 column (GE Healthcare) in PBS pH 7.4. Proteins were aliquoted, flash-frozen in liquid nitrogen and stored at $-80\text{ }^{\circ}\text{C}$. Protein concentrations were determined by measuring the absorbance at 280 nm and assuming an extinction coefficient of $25,900\text{ M}^{-1}\text{ cm}^{-1}$ for BH32-BH32.6, and $29,910\text{ M}^{-1}\text{ cm}^{-1}$ for BH32.10.

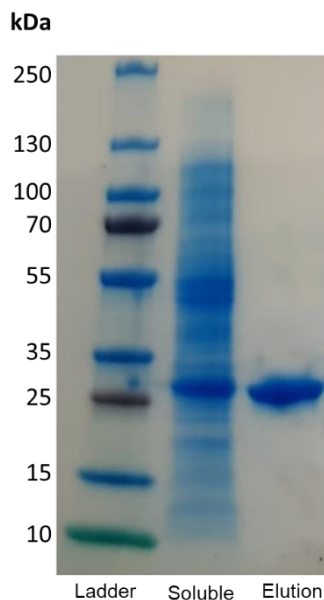


Figure S1: SDS-PAGE of BH32 purified by affinity chromatography using Ni-NTA Agarose.

Lane 1: molecular weight marker, Lane 2: soluble fraction, Lane 3: elution of Ni-NTA resin.

7.2.1.4 Inhibition of BH32 variants

Strep-tagged BH32 variants, excluding BH32.6 which instead contained a his-tag, ($25\text{ }\mu\text{M}$) were inhibited following incubation at room temperature with 4-methoxyphenyl-(6-oxocyclohex-1-en-1-yl)methyl acetate, **4** ($250\text{ }\mu\text{M}$) in PBS pH 7.4 with 3% (v/v) acetonitrile. Formation of the covalently modified protein was monitored spectrophotometrically at 325 nm. Samples were diluted in PBS pH 7.4, excess inhibitor was removed using a Vivaspin® 10k MWCO (Sartorius) and inhibited proteins were characterised by mass spectrometry (Figure S2, Figure S3, Table S1).

7.2.1.5 Mass spectrometry

Purified protein samples were buffer exchanged into 0.1% acetic acid using a 10k MWCO Vivaspin (Sartorius) and diluted to a final concentration of 0.5 mg mL^{-1} . Mass spectrometry was performed using a 1200 series Agilent LC, with a $5\text{ }\mu\text{L}$ injection into 5% acetonitrile (with 0.1% formic acid) and desalted inline for 1 min. Protein was eluted over 1 min using 95% acetonitrile with 5% water. The resulting multiply charged spectrum was analysed using an Agilent QTOF 6510 and deconvoluted using Agilent MassHunter Software.

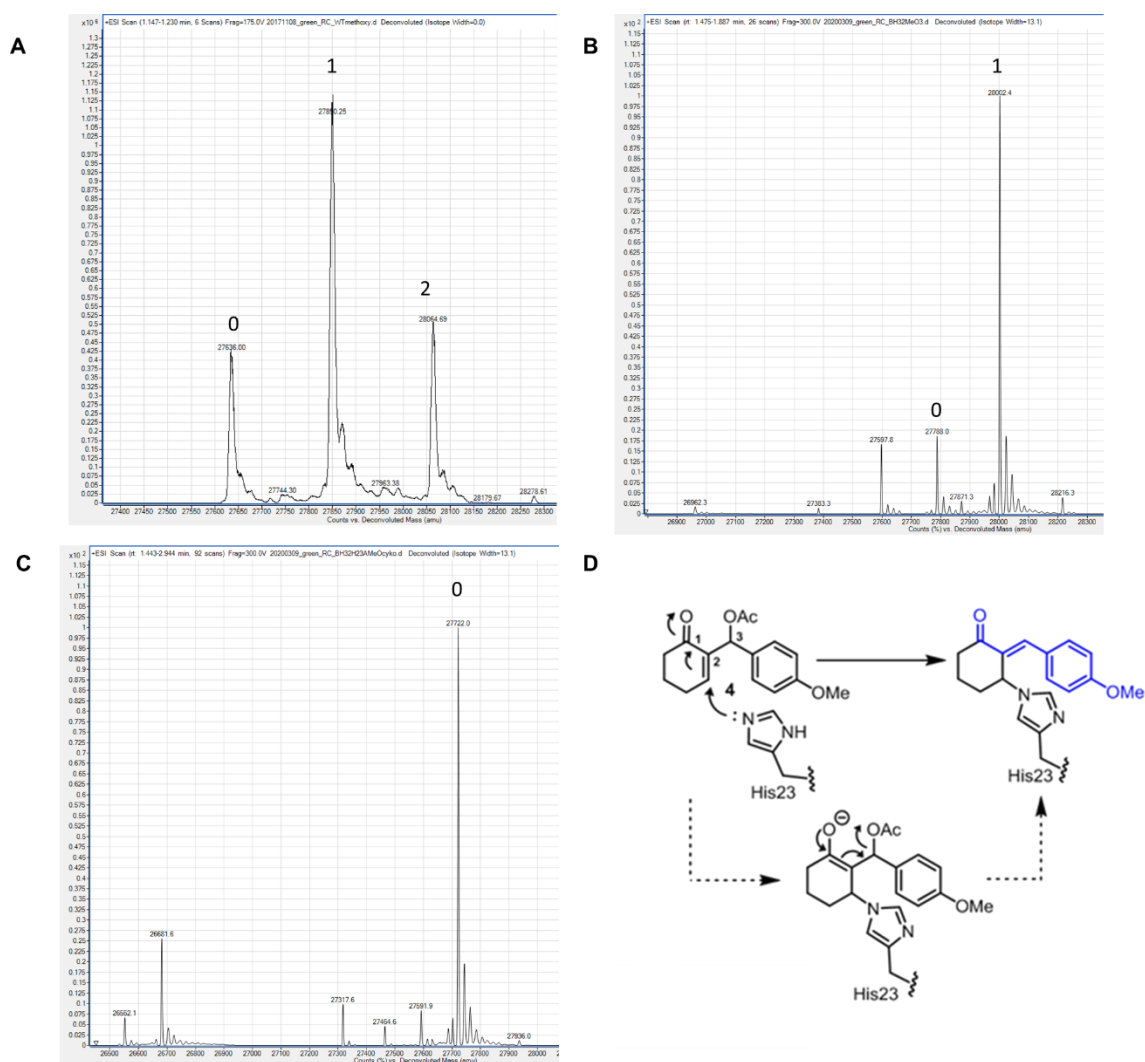


Figure S2: Mass Spectrum of BH32 variants inhibited with the Mechanistic Inhibitor. BH32 variants (25 μ M His-tagged) were inhibited following incubation with 4-methoxyphenyl-(6-oxocyclohex-1-en-1-yl)methyl acetate, **4** (250 μ M) in PBS pH 7.4 with 3% (v/v) acetonitrile at room temperature for 40 minutes. Formation of the covalently modified protein was monitored spectrophotometrically at 325 nm. Samples were diluted in PBS pH 7.4, excess inhibitor was removed using a Vivaspin® 10k MWCO and then characterised by mass spectrometry. **A**) The inhibited BH32 design mass spectrum showed multiple modifications with the mechanistic inhibitor. **B**) The BH32 design was modified to introduce C186A and C212A mutations to avoid any non-specific alkylations of these positions, displaying a single modification at H23. **C**) The nucleophile knockout BH32 H23A (C186A C212A) showed no modifications with the mechanistic inhibitor. **D**) Chemical scheme of BH32 inhibition with the mechanistic inhibitor **4**.

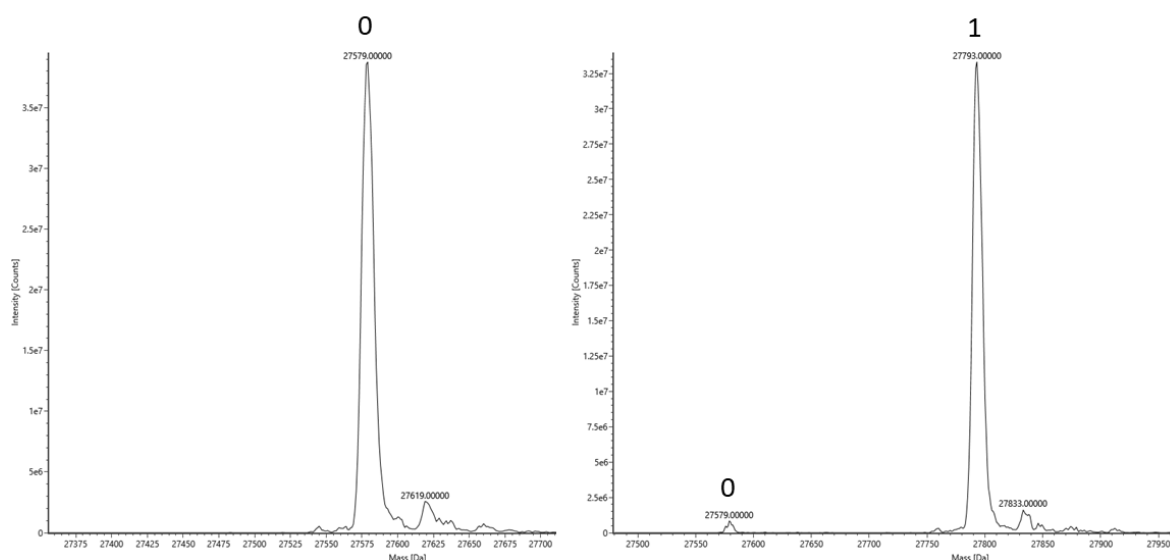


Figure S3: Mass Spectrum of BH32.6 inhibited with the Mechanistic Inhibitor. BH32.6 (25 μ M) was inhibited following incubation with 4-methoxyphenyl-(6-oxocyclohex-1-en-1-yl)methyl acetate, **4** (250 μ M) in PBS pH 7.4 with 3% (v/v) acetonitrile at room temperature for 10 minutes. Formation of the covalently modified protein was monitored spectrophotometrically at 325 nm. Samples were diluted in PBS pH 7.4, excess inhibitor was removed using a Vivaspin® 10k MWCO and then characterised by mass spectrometry. **A)** BH32.6 mass spectrum without inhibition. **B)** BH32.6 inhibited with the mechanistic inhibitor displaying a single modification at H23.

7.2.1.6 Library construction

Rounds 1, 2, 8 & 10: *random mutagenesis using error-prone PCR followed by saturation mutagenesis of identified 'hot spots'*. Random libraries were generated by error-prone PCR of the entire gene using a JBS Error-Prone Kit (Jena Bioscience) according to the manufacturer's protocol. PCR conditions were adjusted to generate an average of 2.5 mutations per gene. The linear library fragments and the modified pBbE8k vector were digested using *NdeI* and *XhoI* endonucleases, gel-purified and subsequently ligated using T4 DNA ligase. Variants with improved activity were sequenced and identified 'hot spots' were subsequently individually randomised using overlap extension PCR and NNK degenerate primers.

Rounds 3, 4, 6, 7 & 9: *saturation mutagenesis*. In each round, twenty positions located in the active site and on flexible loops were individually randomised using cassette mutagenesis. DNA libraries were constructed by overlap extension PCR using degenerate primer pairs (NNK codons). Genes were cloned as described above.

Round 5: *saturation mutagenesis*. Two libraries were generated each containing two simultaneously randomised positions (Thr122/Met130 and Ser22/Ser95). Libraries were generated by overlap extension PCR using pBbE8k_BH32.4 as a template and degenerate primer pairs (22 codons).[3] Genes were cloned as described above.

7.2.1.7 Shuffling by overlap extension PCR

After each round of evolution, beneficial diversity was combined by DNA shuffling of fragments generated by overlap extension PCR. Primers were designed that encoded either the parent amino acid or the identified mutation. These primers were used to generate short fragments (up to 6) which were gel-purified and mixed appropriately in overlap extension PCR to generate genes containing all possible combinations of mutations. Genes were cloned as described above.

7.2.1.8 Library screening

For protein expression and screening, all transfer and aliquotting steps were performed using Hamilton liquid-handling robots. Chemically competent *E. coli* 5 α cells were transformed with the ligated libraries. Freshly transformed clones were used to inoculate 180 μ L of 2xYT medium supplemented with 25 μ g mL⁻¹ kanamycin in Corning® Costar® 96-well microtitre round bottom plates. For reference, each plate contained 6 freshly transformed clones of the parent template and 2 clones containing an empty pBbE8k vector. Plates were incubated overnight at 30 °C, 80 % humidity in a shaking incubator at 900 r.p.m. 20 μ L of overnight culture was used to inoculate 480 μ L 2xYT medium supplemented with 25 μ g mL⁻¹ kanamycin. The cultures were incubated at 30 °C, 80 % humidity with shaking at 900 r.p.m. until an OD₆₀₀ of about 0.5 was reached, and L-arabinose was added to a final concentration of 10 mM. Induced plates were incubated for 20 h at 30 °C, 80 % humidity with shaking at 900 r.p.m. Cells were harvested by centrifugation at 2,900 g for 5 min. The supernatant was discarded and the pelleted cells were resuspended in 400 μ L of lysis buffer (PBS pH 7.4 buffer supplemented with 1.0 mg mL⁻¹ lysozyme, 0.5 mg mL⁻¹ polymixin B and 10 μ g mL⁻¹ DNase I) and incubated for 2 h at 30 °C, 80 % humidity with shaking at 900 r.p.m. Cell debris was removed by centrifugation at 2,900 g for 5 min.

Rounds 1-6: 100 μ L Clarified lysate was transferred to 96-well microtitre plates containing 80 μ L PBS buffer pH 7.4. Reactions were initiated with the addition of 20 μ L inhibitor **4** (Rounds 1-4: 250 μ M final concentration, Rounds 5-6: 100 μ M final concentration) in PBS pH 7.4 containing acetonitrile (3% (v/v) final concentration). Inhibition was monitored spectrophotometrically at 325 nm, over 15 minutes using a CLARIOstar plate reader (BMG Labtech). Reaction rates of individual variants were normalised to the average of the 6 parent clones.

Rounds 7-10: 75 μ L Clarified lysate was transferred to 96-well polypropylene microtitre plates and the reaction was initiated with the addition of 25 μ L assay mix containing 4-nitrobenzaldehyde (0.6 mM final concentration) and 2-cyclohexen-1-one (3 mM final concentration) in PBS pH 7.4. Reactions were heat-sealed and incubated for 18 h at 30 °C, 80 % humidity with shaking at 900 r.p.m. Reactions were quenched with the addition of 100 μ L acetonitrile and incubated for a further 2 h at 30 °C, 80 % humidity with shaking at 900 r.p.m. Precipitated proteins were removed by centrifugation at 2,900g for 10 min. 100 μ L of the clarified reaction was transferred to 96-well polypropylene microtitre plates and heat-sealed with pierceable foil. Reactions were evaluated by HPLC analysis as described below.

Following each round, the most active variants were rescreened as purified proteins using the HPLC assay. Proteins were produced and purified as described above, however starter cultures were inoculated from glycerol stocks prepared from the original overnight cultures.

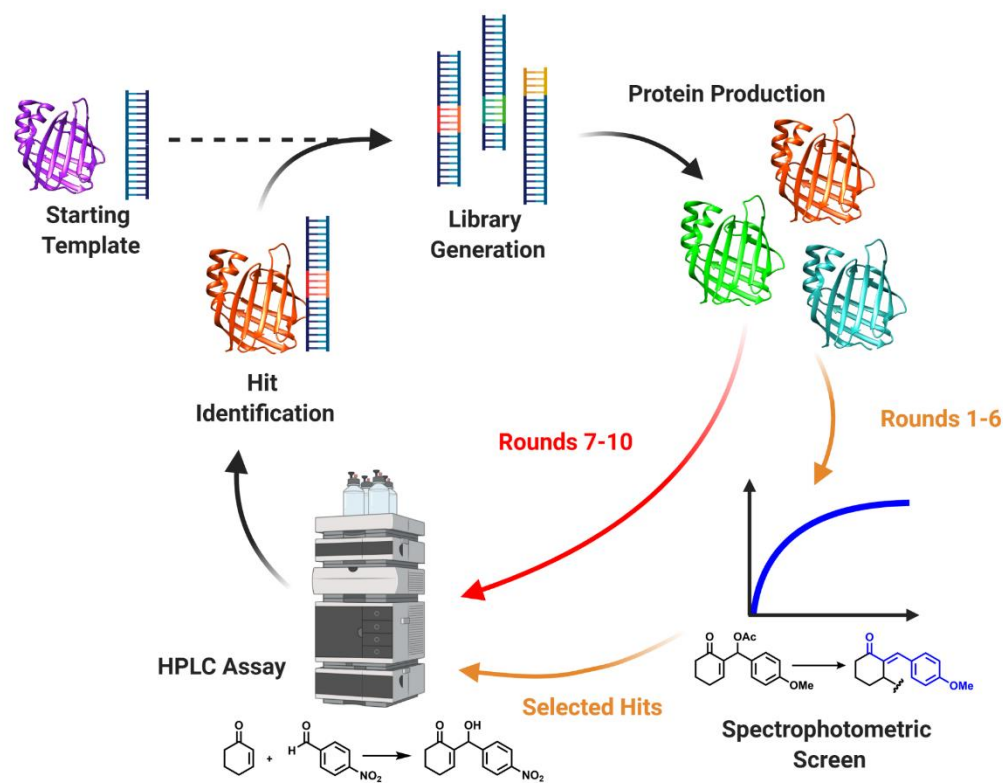


Figure S4: Directed Evolution Workflow. Schematic diagram showing the evolution workflow used to generate and evaluate libraries. Rounds 1-6 used a spectrophotometric screen to evaluate libraries, selected hits were then purified and screened for MBH activity using a HPLC assay. Rounds 7-10 evaluated libraries for MBH activity in lysate using a HPLC assay, selected hits were then purified and screened.

7.2.1.9 General procedure for analytical scale biotransformations

To compare the activity of BH32, BH32.10 and its variants (Table 1), analytical scale biotransformations were performed using **1** (3 mM), **2** (0.6 mM) and the relevant biocatalyst (18 μ M) in PBS (pH 7.4) with 3 % DMSO as a cosolvents (1 mL). For comparison, reactions were also performed at varying concentrations of small molecule catalytic nucleophiles imidazole, DMAP and DABCO (18 μ M, 60 μ M and 1 mM). Reactions were incubated at 25 $^{\circ}$ C with shaking (800 r.p.m.). For HPLC analysis, reactions were quenched at the stated time points with the addition of 1 mL acetonitrile. Samples were vortexed and precipitated proteins were removed by centrifugation (14,000 g for 5 minutes). For SFC analysis, the substrates and products were extracted with 3 volumes of ethyl acetate. Precipitated proteins were cleared by centrifugation (14,000 g for 5 minutes), the organic phase was separated and analysed by SFC.

7.2.1.10 Chromatographic analysis

HPLC analysis was performed on a 1290 Infinity II Agilent LC system with a Kinetex® 5 µm XB-C18 100 Å LC Column, 50 x 2.1 mm (Phenomenex), using an isocratic method with 25% acetonitrile in water at 1 mL min⁻¹ for 1.5 minutes. Peak areas were integrated using Agilent OpenLab software and conversion was calculated at 280 nm using the extinction coefficient 600 mM⁻¹ cm⁻¹ for both **3** and **4**.

Chiral analysis was performed using an SFC 1290 Infinity II Agilent system with a Daicel 80S82 CHIRALPAK® IA-3 SFC column, 3 mm, 50 mm, 3 µm, using an isocratic method with 35% methanol in CO₂ at 1 mL min⁻¹ for 1 minute. Peak areas were integrated using Agilent OpenLabs software.

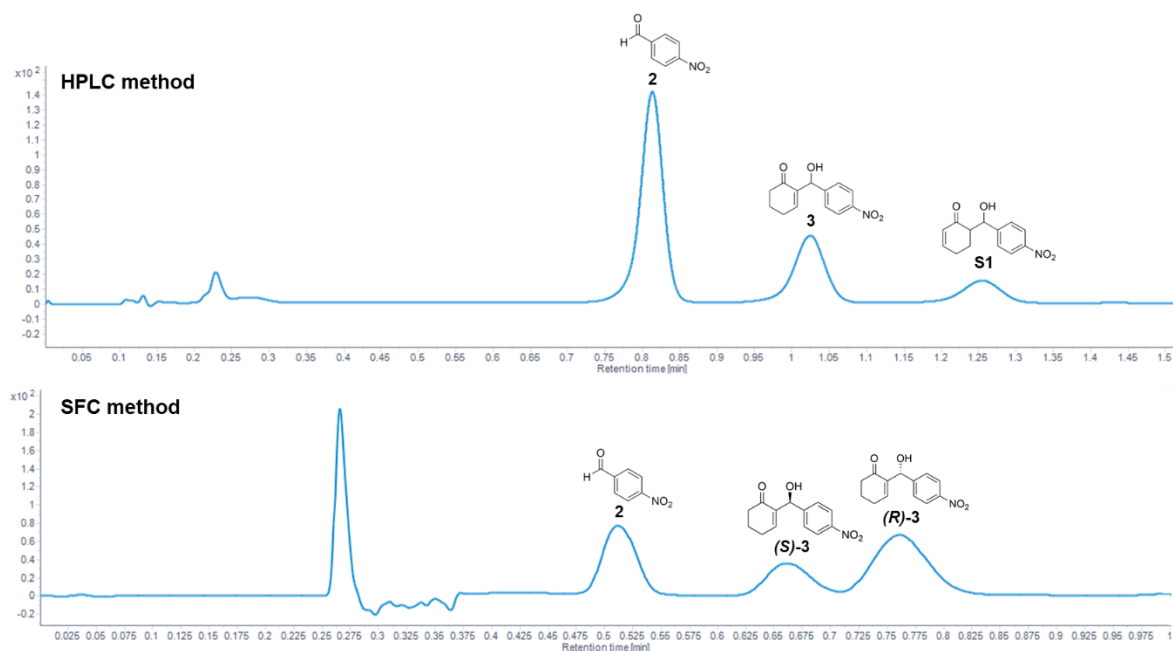


Figure S5: Analytical Methods for MBH reaction between 2-cyclohexen-1-one and 4-nitrobenzaldehyde. A) HPLC trace showing the 1.5 minute method used to evaluate MBH activity. B) SFC trace showing the 1 minute method used to evaluate enantioselectivity for the MBH reaction.

7.2.1.11 Preparative scale biotransformation

A preparative scale biotransformation was performed using **1** (50 mM), **2** (10 mM), strep-tag purified BH32.10 (50 µM) in PBS (pH 7.4, 72 mL) with 20 % DMSO (18 mL) as a cosolvent. The reaction was incubated at 30 °C with shaking at 100 r.p.m. for 19 hours. An aliquot (100 µL) was removed and quenched with acetonitrile for HPLC analysis, which showed the reaction had proceeded to 94 % conversion. The reaction mixture was extracted with ethyl acetate (2 x 400 mL), dried over MgSO₄, filtered and the solvent was removed *in vacuo*. The crude product (Fig. S4) was purified by flash column chromatography (5:1 cyclohexane:ethyl acetate) to give 2-(hydroxy(4-nitrophenyl)methyl)cyclohex-2-en-1-one, **3** as a light-yellow solid (201 mg, 90%). Spectral data is consistent with literature values.[3] δ_H (400 MHz, CDCl₃): 8.21 (m, 2H), 7.56 (m, 2H), 6.82 (t, *J* = 4.1 Hz, 1H), 5.62 (d, *J* = 6.1 Hz, 1 H), 3.51 (d, *J* = 6.0 Hz, 1H), 2.46 (m, 4H), 2.03 (m, 2H). ¹³C NMR (100 MHz, CDCl₃) δ 200.1, 149.3, 148.1, 147.2, 140.2, 127.1, 123.5, 72.0, 38.4, 25.8, 22.3. ESI-MS *m/z* = 270 [M + Na]⁺

7.2.1.12 Kinetic characterization

Kinetic assays were performed using strep-tagged purified enzyme (60 μ M BH32 or 10 μ M BH32.10) in PBS pH 7.4 with 3% acetonitrile and either, a fixed concentration of **1** (25 mM) and varying concentrations of **2** (0.25-2 mM for BH32 and 0.05-2 mM for BH32.10) or using a fixed concentration of **2** (2 mM) and varying concentrations of **1** (1-25 mM for BH32 and 0.5-25 mM for BH32.10). Reactions were incubated at 30 °C, 800 r.p.m. Samples were taken at 10-minute intervals for BH32.10 (for one hour), and at 24 h, 40 h, 49 h, 68 h and 94 h for BH32 and analysed by HPLC as described above. Linear fits of conversion vs time allowed determination of initial velocities (V_0) at each condition. The combined V_0 vs [4-nitrobenzaldehyde] and V_0 vs [2-cyclohexen-1-one] steady state kinetic data were fitted globally using a kinetic model for two-substrates with randomly ordered binding[6] $V_0 = k_{cat}[E][A][B]/((K_{enone}+[A])(K_{aldehyde}+[B]))$ where k_{cat} is the turnover number, [E] is the total enzyme concentration, [A] and [B] are the initial 2-cyclohexen-1-one and 4-nitrobenzaldehyde concentrations respectively, and K_{enone} and $K_{aldehyde}$ are the corresponding apparent Michaelis constants.

7.2.1.13 Preparation of product standards **3** and **S1**. [4]

4-nitrobenzaldehyde (1.5 g, 10 mmol), 2-cyclohexen-1-one (970 μ L, 10 mmol) and imidazole (681 mg, 10 mmol) were stirred in 1M NaHCO₃ (40 mL) and THF (10 mL) for 40 hours at room temperature. The reaction was acidified with 1M HCl and extracted with ethyl acetate (150 mL). The organic layer was dried over MgSO₄, filtered and the solvent was removed *in vacuo*. The reaction yielded a mixture of the Morita-Baylis-Hillman adduct **3** and aldol adduct **S1** which were separated by flash column chromatography (5:1 cyclohexane:ethyl acetate).

2-(hydroxy(4-nitrophenyl)methyl)cyclohex-2-en-1-one **3** (562 mg, 23%). See characterization data above ('preparative scale biotransformation').

6-(hydroxy(4-nitrophenyl)methyl)cyclohex-2-en-1-one **S1** (180 mg, 7%) as a 4:1 mixture of diastereoisomers. Spectral data is consistent with literature values.[5] δ_H (400 MHz, CDCl₃): 8.26-8.20 (m, 2H), 7.57-7.51 (m, 2H), 7.10-6.97 (m, 1H), 6.13-6.08 (m, 1H), 5.70 (d, $J = 2.3$ Hz, 1H_{maj}), 4.99 (d, $J = 8.7$ Hz, 1H_{min}), 4.95 (br s, OH_{min}), 2.95 (br s, OH_{maj}), 2.72-2.65 (m, 1H_{maj}), 2.62-2.53 (m, 1H_{min}), 2.48-2.25 (m, 2H), 2.06-1.93 (m, 1H), 1.57-1.46 (m, 1H). ESI-MS $m/z = 270$ [M + Na]⁺

7.2.1.14 Preparation of inhibitor **4**

Anisaldehyde (1.36 g, 10 mmol), 2-cyclohexen-1-one (970 μ L, 10 mmol) and imidazole (681 mg, 10 mmol) were stirred in 1M NaHCO₃ (40 mL) and THF (10 mL) 48 hours at room temperature. The reaction was acidified with 1M HCl and extracted with ethyl acetate (150 mL). The organic layer was dried over MgSO₄, filtered and the solvent was removed *in vacuo*. The product was purified by flash column chromatography (5:1 cyclohexane:ethyl acetate) to yield 2-(hydroxy(4-methoxyphenyl)methyl)cyclohex-2-en-1-one (440 mg, 19%). Spectral data is consistent with literature values.[6] δ_H (400 MHz; CDCl₃) 7.28 (m, 2H), 6.90 (m, 2H), 6.78 (t, $J = 4.1$ Hz, 1H), 5.53 (s, 1H); 3.81 (s, 3H); 3.43 (s, 1H), 2.44 (m, 4H), 2.02 (m, 2H). ¹³C NMR (100 MHz, CDCl₃) δ 200.4, 158.9, 147.0, 141.1, 133.8, 127.7, 113.7, 72.0, 55.2, 38.5, 25.7, 22.5. ESI-MS $m/z = 255$ [M + Na]⁺

2-(hydroxy(4-methoxyphenyl)methyl)cyclohex-2-en-1-one (50 mg, 0.25 mmol) and acetic anhydride (50 μ L) were stirred in pyridine (1 mL) overnight at room temperature. The reaction was diluted in ethyl acetate (30 mL) and washed with 1M NaHCO₃ (2 x 10 mL), 10% CuSO₄ (2 x 10 mL) and then brine (10 mL). The organic layer was dried over MgSO₄, filtered and the solvent removed *in vacuo*. The product was purified by flash column chromatography (5:1 cyclohexane:ethyl acetate) to give the product (4-methoxyphenyl)(6-oxocyclohex-1-en-1-yl)methyl acetate, **4** (49 mg, 84%); δ_{H} (400 MHz; CDCl₃) 7.29 (m, 2H), 6.98 (t, $J = 4.0$ Hz, 1H), 6.87 (m, 2H), 6.69 (s, 1H), 3.80 (s, 3H), 2.44 (m, 4H), 2.10 (s, 3H), 2.02 (m, 2H). ^{13}C NMR (100 MHz, CDCl₃) δ 197.0, 169.5, 159.3, 145.3, 138.9, 130.9, 128.6, 113.7, 71.4, 55.2, 38.3, 25.7, 22.5, 21.2. ESI-MS $m/z = 297$ [M + Na]⁺

7.2.1.15 Preparation of chiral standards

The enantiomers of **3** were separated by preparative chiral HPLC by Reach Separations (Nottingham) to afford (*R*)-**3** (99.5% *e.e*) and (*S*)-**3** (99.9% *e.e*) as white solids. The absolute stereochemistry was determined by measuring the optical rotation ((*R*)-**3** (-52.5°) and (*S*)-**3** (+50.0°) at 0.008 g mL⁻¹ in DCM at 27 °C) and comparison to literature values.[7]

7.2.1.16 Crystallization, refinement and model building

Crystals of BH32 and BH32 variants were prepared by mixing 200 nL of 20 mg mL⁻¹ protein in PBS buffer pH 7.4 with equal volumes of precipitant. All trials were conducted by sitting-drop vapour diffusion and incubated at 4 °C. Protein crystallization conditions are given in Table S3. BH32.3 crystals were flash cooled in liquid nitrogen whilst BH32.9 crystals were first cryoprotected by the addition of 10 % PEG 200 to the mother liquor prior to flash cooling. Data were collected from single crystals at Diamond Light Source and subsequently scaled and reduced with Xia2[8]. Preliminary phasing was performed by molecular replacement in Phaser using a search model derived from wild-type BH32 (PDB code: 3U26). Iterative cycles of rebuilding and refinement were performed in COOT[9] and Phenix.refine[10], respectively. Structure validation with MolProbity and PDBREDO were integrated into the iterative rebuild and refinement process. Complete data collection and refinement statistics can be found in Table S2. Coordinates and structure factors have been deposited in the Protein Data Bank under accession numbers 6Z1K & 6Z1L. All figures and surface representations were generated in ICM Pro (Molsoft).

7.2.1.17 Molecular Docking

To generate starting structures for DFT modelling, molecular docking was performed with Autodock Vina[11], using AutoDockTools[12] to assign to the crystal structure and generate input files. The protein was kept rigid during docking, but all substrate bonds were rotatable. For the product, the highest-scoring pose was selected. For the reactant state, 2-cyclohexen-1-one was docked first and the pose which showed the best overlap with the corresponding fragment of the docked product was selected (this had an estimated binding energy only 0.2 kcal mol⁻¹ higher than the lowest energy pose, which was very similar but rotated around the keto group). The aldehyde was then docked into the 2-cyclohexen-1-one bound structure, and again the binding mode with the best overlap to the corresponding fragment in the docked product was selected (this had an estimated binding energy of 0.8 kcal mol⁻¹ higher than the lowest binding mode).

7.2.1.18 DFT Modelling

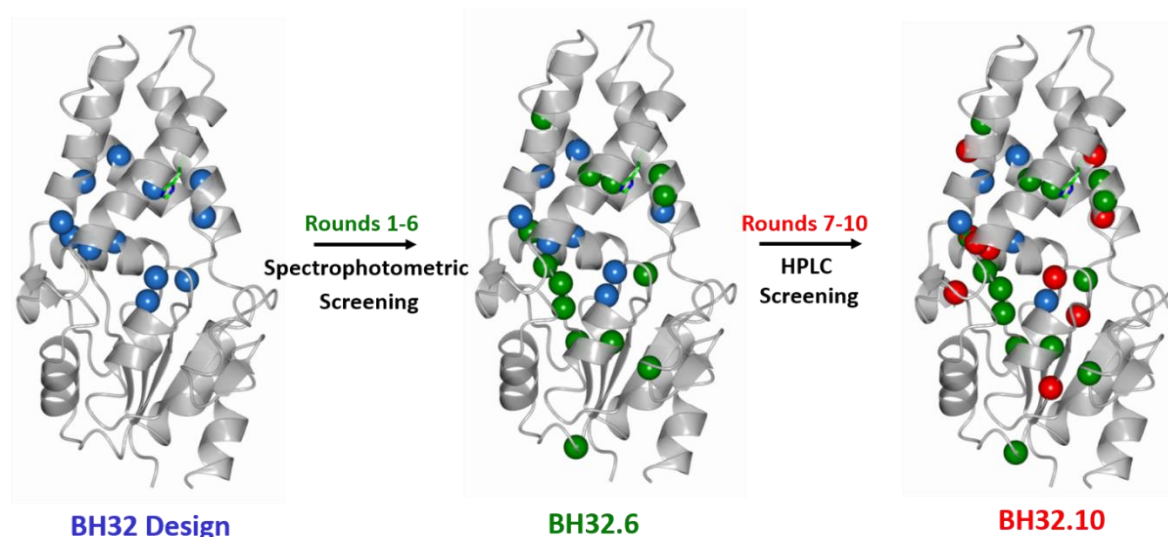
A cluster model was constructed using the docked conformations for the substrates, including the first-shell amino acids around the substrates (Trp10, Ile14, Ala19, Val22, His23, Ile26, Leu64, Trp88, Ser91, Leu92, Ala95, Arg124, Phe128, Ser129, Phe132). Residues were truncated at the C_β unless their backbone atoms are in near contact with the substrates or involved in hydrogen bonding with the substrates or other amino acids. The models contained a total of 270 atoms (or 273 when including an extra water molecule for the proton transfer step) shown in Fig. S6. The coordinates for all energy minimised ground and transition state structures are provided in the supplementary materials. Calculations were performed using Gaussian16 revision A03[13], using the B3LYP functional[14] and the 6-31G(d,p) basis sets[15,16] for all atoms except for the Arg124 guanidino nitrogens and the C=O groups of 2-cyclohexen-1-one and aldehyde, for which 6-311+G(d,p) was used. Grimme's D3 dispersion correction with Becke-Johnson damping was employed[17] and implicit solvation was treated using the polarizable conductor calculation model (CPCM)[18,19] with a dielectric constant $\epsilon = 5.7$ to mimic the enzyme environment.[20,21] All models have a net charge of +1 (from Arg124) and spin multiplicity 1. Sixteen peripheral atoms were kept fixed during the calculations: the C_α of residues whose backbone was included, and C_β for residues truncated at C_β (atom numbers 16, 26, 31, 36, 43, 52, 54, 57, 60, 71, 77, 85, 89, 97, 104, 245). Each chemical step was modelled by performing a relaxed potential energy scan of the making/breaking bond for steps 1, 2 and 4. For step 3 a water molecule was added to promote proton transfer, and a simple reaction coordinate, z was scanned: $z = R(\text{C-H}) - R(\text{O-H})$, where R is distance, C and H are the carbon and hydrogen atoms of the breaking bond and O is the oxygen atom of the water molecule. In each case, the transition state was selected as the structure with the highest potential energy along the scanned coordinate, to within ± 0.02 Å of the maximum for the breaking/forming bond for steps 1, 2 and 4, and within ± 0.03 Å along z for step 3.

7.2.1.19 References

1. Bjelic, S. et al. Computational design of enone-binding proteins with catalytic activity for the Morita-Baylis-Hillman reaction. *ACS Chem. Biol.* **8**, 749-757 (2013).
2. Lee, T. S. et al. BglBrick vectors and datasheets: A synthetic biology platform for gene expression. *J. Biol. Eng.* **5**, 12 (2011).
3. Kille, S. et al. Reducing codon redundancy and screening effort of combinatorial protein libraries created by saturation mutagenesis. *ACS Synth. Biol.* **2**, 83-92 (2013).
4. Luo, S., Wang, P. G. & Cheng, J.-P. Remarkable rate acceleration of imidazole-promoted Baylis-Hillman reaction involving cyclic enones in basic water solution. *J. Org. Chem.* **69**, 555-558 (2004).
5. Kataoka, T., Iwama, T., Tsujiyama, S., Iwamura, T. & Watanabe, S. The Chalcogeno-Baylis-Hillman reaction: a new preparation of allylic alcohols from aldehydes and electron-deficient alkenes. *Tetrahedron* **54**, 11813-11824 (1998).
6. Vazquez-Chavez, J. et al. Effect of chiral N-substituents with methyl and trifluoromethyl groups on the catalytic performance of mono- and bifunctional thioureas. *Org. Biomol. Chem.* **17**, 10045-10051 (2019).

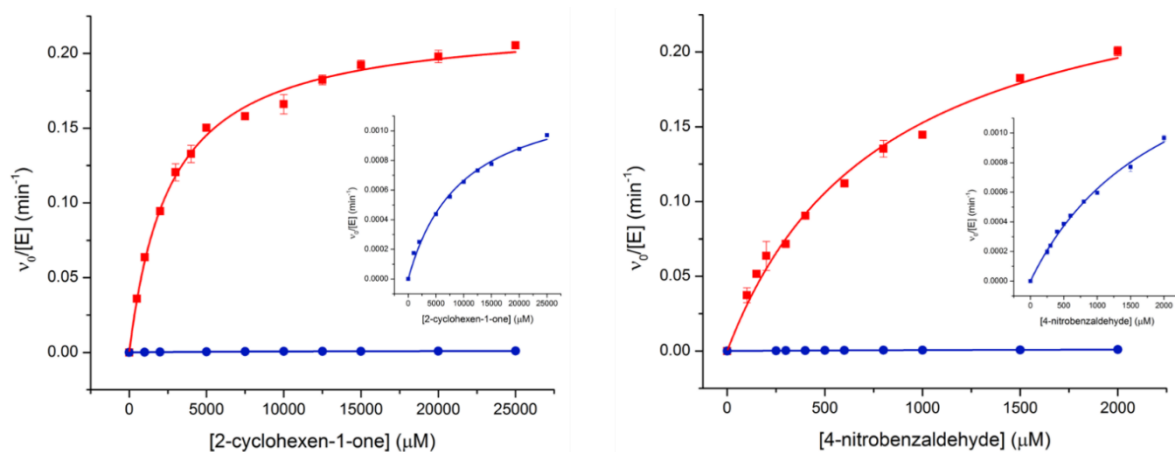
7. Wang, F. et al. A highly efficient kinetic resolution of Morita–Baylis–Hillman adducts achieved by N–Ar axially chiral Pd-complexes catalyzed asymmetric allylation. *Chem. Commun.* **47**, 12813–12815 (2011).
8. Winter, G. et al. DIALS: implementation and evaluation of a new integration package. *Acta Crystallogr. D* **74**, 85–97 (2018).
9. Emsley, P., Lohkamp, B., Scott, W. G. & Cowtan, K. Features and development of Coot. *Acta Crystallogr. D Biol. Crystallogr.* **66**, 486–501 (2010).
10. Afonine, P. V. et al. Towards automated crystallographic structure refinement with phenix.refine. *Acta Crystallogr. D Biol. Crystallogr.* **68**, 352–67 (2012).
11. Trott, O. & Olson, A. J. AutoDock Vina: improving the speed and accuracy of docking with a new scoring function, efficient optimization, and multithreading. *J Comput. Chem.* **31**, 455–61 (2010).
12. Morris, G. M. et al. AutoDock4 and AutoDockTools4: Automated docking with selective receptor flexibility. *J Comput. Chem.* **30**, 2785–91 (2009).
13. Frisch, M. J. et al. *Gaussian 16* Rev A.03, Wallingford, CT (2016).
14. Becke, A. D. Density-functional thermochemistry. III. The role of exact exchange. *J. Chem. Phys.* **98**, 5648–5652 (1993).
15. Hehre, W., Ditchfield, R. & Pople, J. Further extensions of gaussian-type basis sets for use in molecular orbital studies of organic molecules. *J. Chem. Phys.* **56**, 2257–2261 (1972).
16. Francl, M. et al. Self-consistent molecular orbital methods. XXIII. A polarization-type basis set for 2nd-row elements. *J. Chem. Phys.* **77**, 3654–3665 (1982).
17. Grimme, S., Ehrlich, S. & Goerigk, L. Effect of the damping function in dispersion corrected density functional theory. *J. Comput. Chem.* **32**, 1456–65 (2011).
18. Barone, V. & Cossi, M. Quantum calculation of molecular energies and energy gradients in solution by a conductor solvent model. *J. Phys. Chem.* **102**, 1995–2001 (1998).
19. Cossi, M., Rega, N., Scalmani, G. & Barone, V. Energies, structures, and electronic properties of molecules in solution with the C-PCM solvation model. *J. Comput. Chem.* **24**, 669–681 (2003).
20. Shaik, S., Kumar, D., de Visser, S. P., Altun, A. & Thiel, W. Theoretical perspective on the structure and mechanism of cytochrome P450 enzymes. *Chem. Rev.* **105**, 2279–2328 (2005).
21. Heyes, D. J., Sakuma, M., de Visser, S. P. & Scrutton, N. S. Nuclear quantum tunneling in the light-activated enzyme protochlorophyllide oxidoreductase. *J. Biol. Chem.* **284**, 3762–3767 (2009).

7.2.2 Extended Data

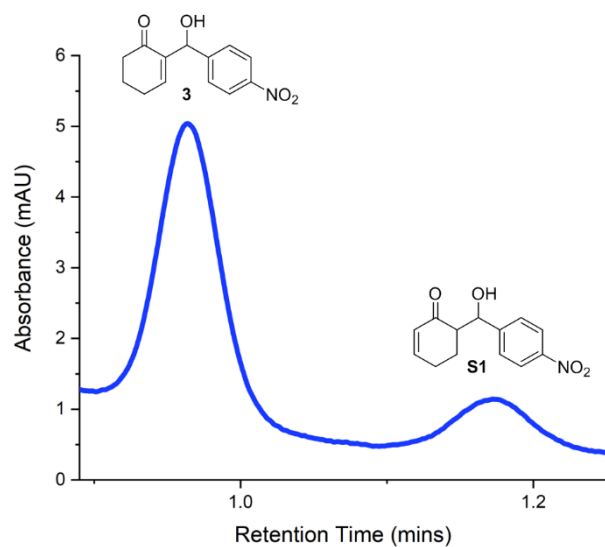


Round	Description	Clones Screened	Beneficial mutations	Best Variant
1	Random mutagenesis of the entire gene Saturation mutagenesis of 'hotspots': Y45/T49 and F87/F88 (two sites simultaneously randomized), T49, R50	3,780	T49A/M, A52V, F87L/T, Q96R, M120L, K167I, V226G	BH32.1 = BH32+ T49A_F87L
2	Random mutagenesis of the entire gene Saturation mutagenesis of 'hotspots': N14, M130, E174	2,070	N14Y, M130K, E174G	BH32.2 = BH32.1 + N14Y_M103T
3	Saturation mutagenesis of active site positions and flexible loop regions: L10, A19, P38, L42, Y45, E46, P60, P63, F81, S91, Q96, S124, D125, Q128, M130, L133, F154, K167, E174, K202	1800	P63C, S124R, D125Q, Q128P, E174K	BH32.3 = BH32.2 + S124R_Q128P_E174K
4	Saturation mutagenesis of active site positions and flexible loop regions: V16, E17, G32, Y34, L36, Y61, L64, L68, M120, T122, D123, D125, T126, Q128, E149, G152, L199, E204, K205, E207	1800	D123N, P128L, E204G	BH32.4 = BH32.3 + D123N
5	Saturation mutagenesis of positions: S22/S95 and M120/T122 (two sites simultaneously randomized)	2700	S22V_S95A, M120V_T122L	BH32.5 = BH32.4 + S22V_S95A_M120V_T122L
6	Saturation mutagenesis of active site positions and flexible loop regions: L10, A20, L24, M27, L42, T45, P63, L64, S91, L92, Q96, D125, E127, A129, I145, T147	1440	A20Y, A129G	BH32.6 = BH32.5 + A20Y
7	Saturation mutagenesis of active site positions and flexible loop regions: L10, L24, L42, E46, A129	450	L10W, L24F, L42V, A129S	BH32.7 = BH32.6 + L10W_L24F_A129S
8	Saturation mutagenesis of F154	90	F154S	BH32.8 = BH32.7 + F154S
9	Saturation mutagenesis of active site positions and flexible loop regions: Y20, V30, K47, Y56, I67, E70, F87, S91, R97, F153, K155, F161, L165, K171, V176, Y177, D180, S196, D210, L219, I223	1890	K47E, Y56N, Y177C, D180P, D210G,	BH32.9 = BH32.8 + Y56N_Y177C_D180P
10	Random mutagenesis of the entire gene Saturation mutagenesis of 'hotspots': V16, A19, E70, M72, E89, P128, S154	2,430	V16A/P/G, A19T, E70R, P128L/M, S154A/G	BH32.10 = BH32.9 + A19T_E70R_P128L

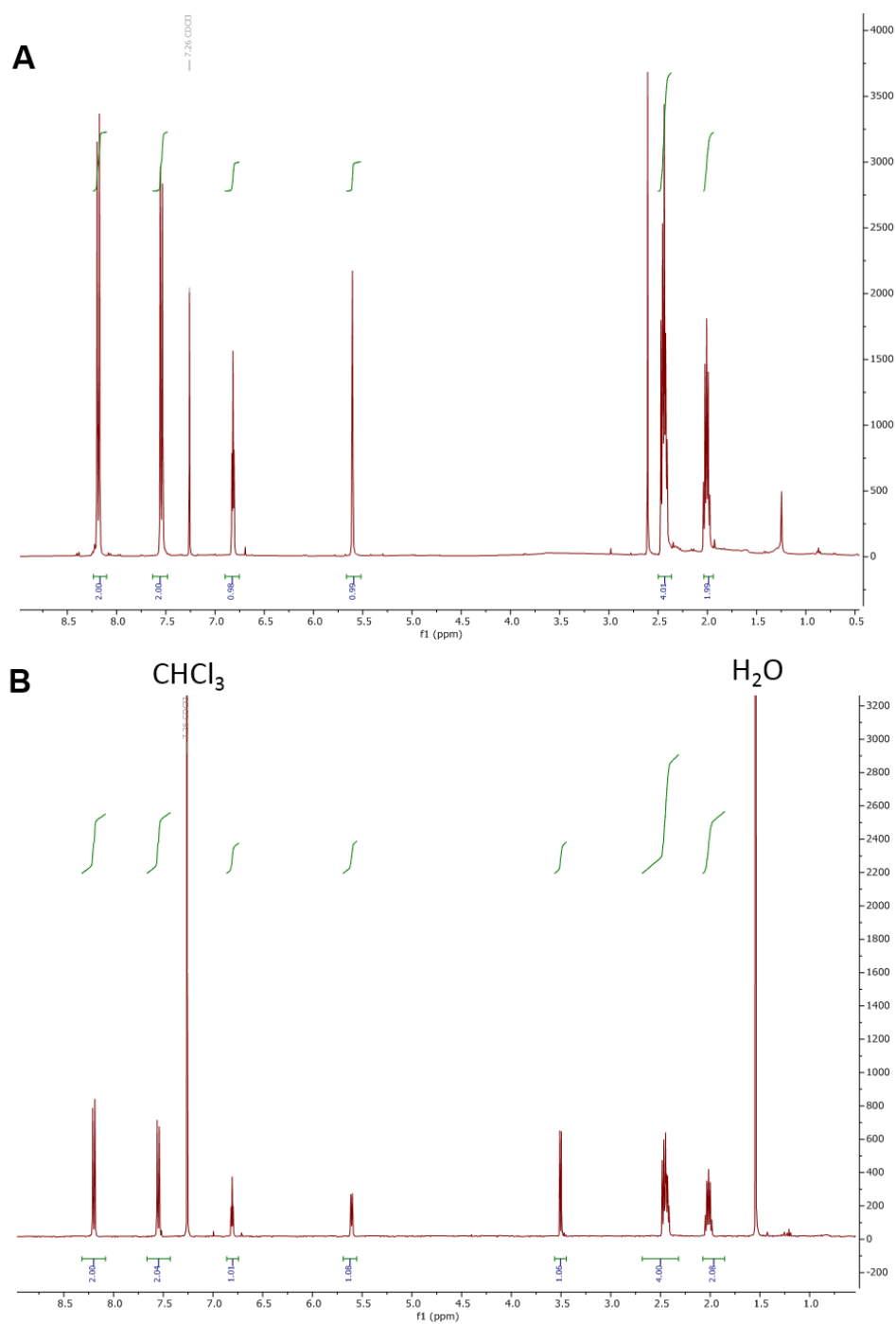
7.2.2.1 Extended Data Figure 1: Directed evolution of BH32.10. Structures showing the amino acid positions mutated throughout evolution (represented as spheres). The original design contains twelve active site mutations (shown in blue) built into the cap domain of a haloacid dehalogenase from *Pyrococcus horikoshii*. Fifteen mutations (shown in green) were introduced during the first six rounds of evolution, which exploited a spectrophotometric assay. Rounds 7-10 exploited a HPLC assay and led to the accumulation of a further nine mutations (shown in red). The final variant BH32.10 contains 29 mutations, 5 that remain from the initial computational design and 24 that were installed during evolution. The table shows the mutations for selected BH32 variants.



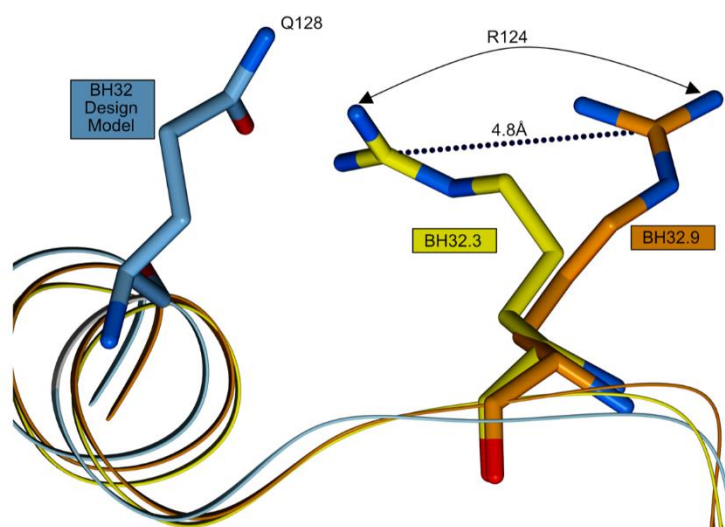
7.2.2.2 Extended Data Figure 2: Kinetic characterization of BH32 and BH32.10 towards the MBH reaction with **1** and **2**. Michaelis-Menten plots for the MBH reaction with **1** and **2** catalysed by BH32 (60 μM, blue) or BH32.10 (10 μM, red). Kinetic assays were performed at either a fixed concentration of **1** (25 mM) and various concentrations of **2**, or using a fixed concentration of **2** (2 mM) and various concentrations of **1**. The plots show the averaged initial rates which were fitted to the Michaelis–Menten equation using Origin software. Data are mean ± s.d. of measurements made in triplicate. To derive the rate constants the combined V_0 vs [**1**] and V_0 vs [**2**] steady state kinetic data were fitted globally using a kinetic model for two substrates with randomly ordered binding.



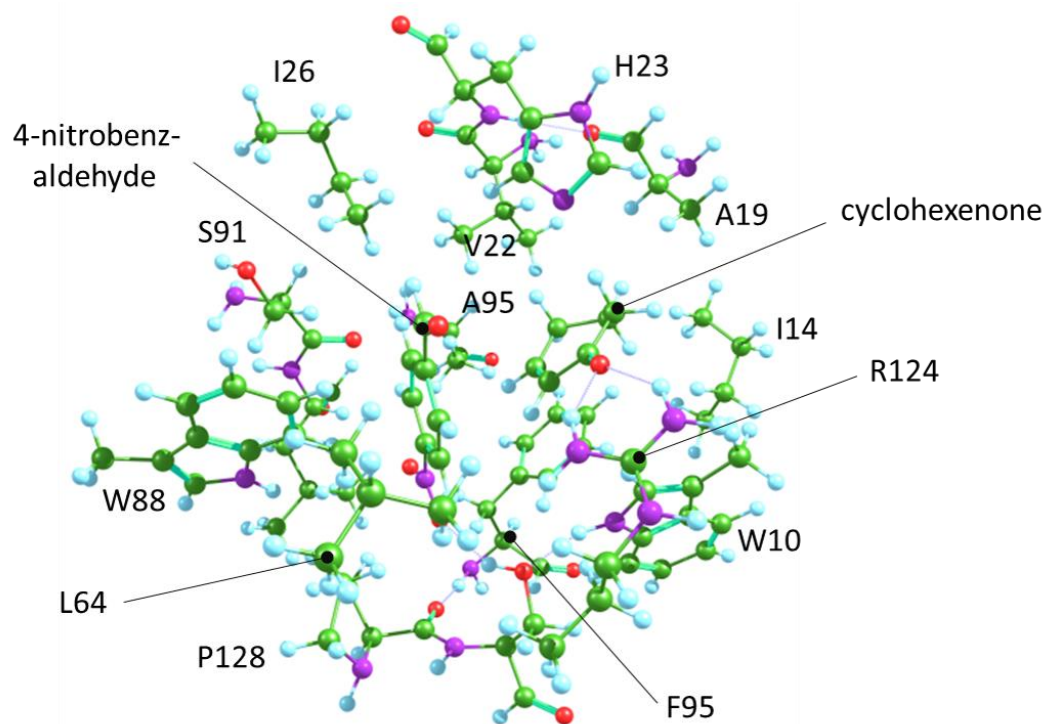
7.2.2.3 Extended Data Figure 3: HPLC analysis of the BH32 catalysed MBH reaction. HPLC trace showing product **3** and aldol by-product **S1** (5:1 ratio of **3**:**S1**), formed during the BH32 (3 mol%) catalysed reaction of **1** (3 mM) and **2** (0.6 mM) following 22 hours incubation.



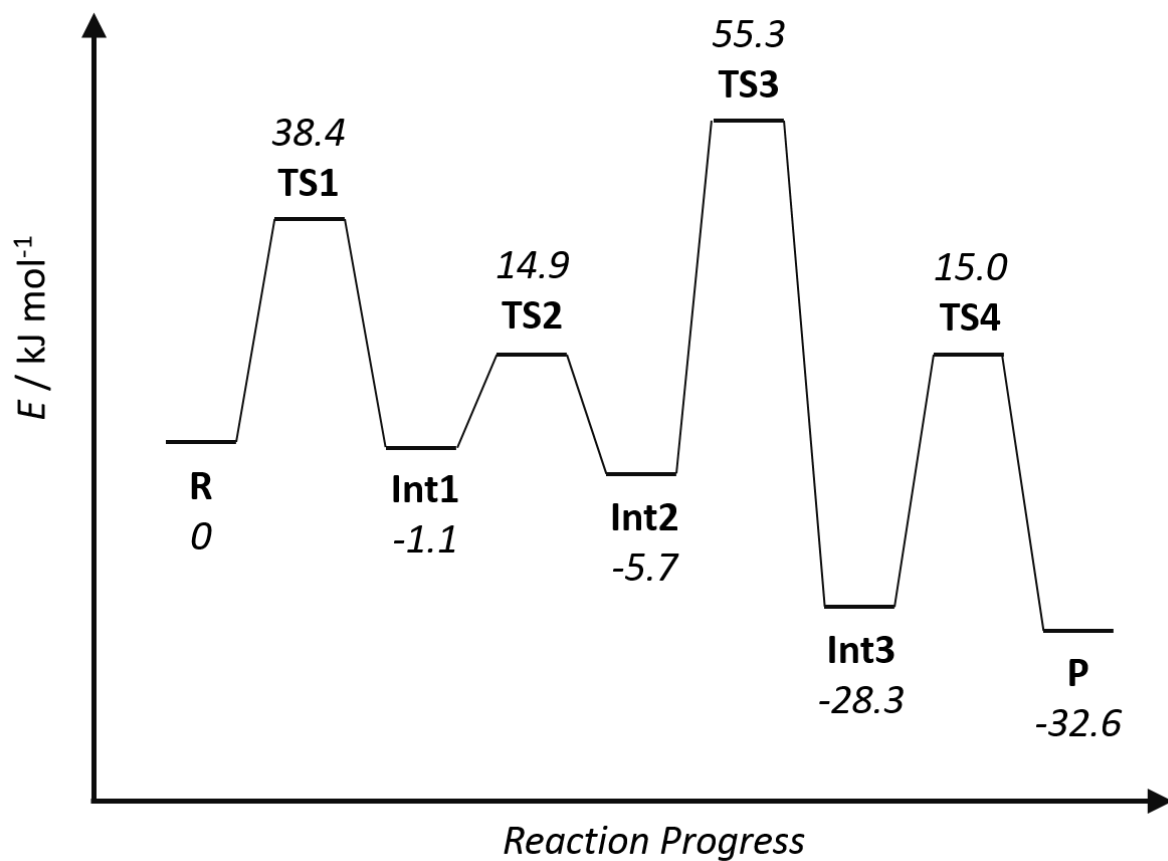
7.2.2.4 Extended Data Figure 4: Characterization of product 3 produced from a preparative scale biotransformation. NMR traces (400 MHz; CDCl₃) showing **A**) crude product extracted from the BH32.10 (50 μM) catalysed MBH reaction of **1** (50 mM) and **2** (10 mM) in PBS (pH 7.4) with 20% DMSO as a cosolvent and **B**) product isolated following purification by flash column chromatography.



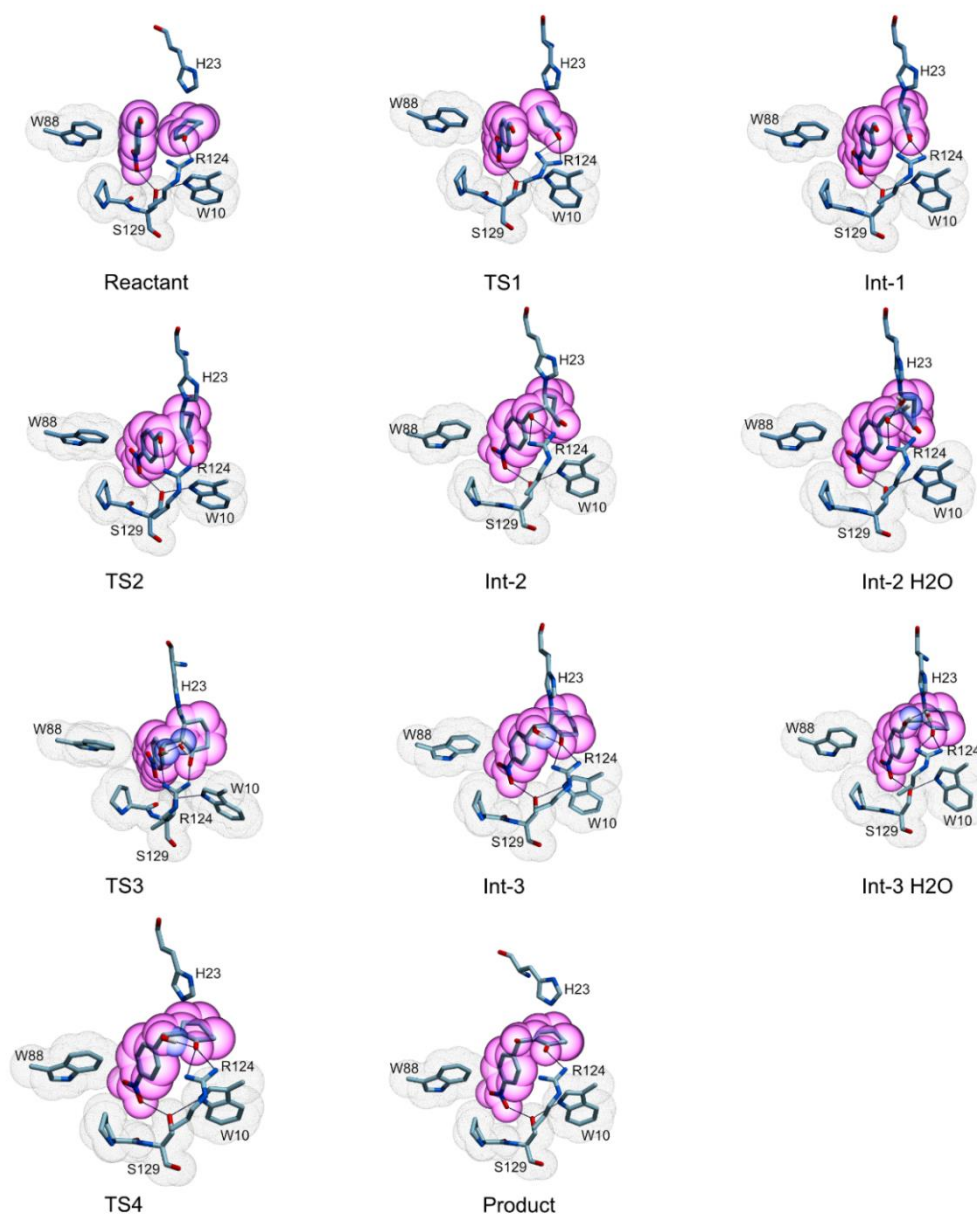
7.2.2.5 Extended Data Figure 5: Structural characterization of residues responsible for oxyanion intermediate stabilisation in BH32, BH32.3 and BH32.9. Three superimposed structures are displayed, the BH32 Design Model in blue, BH32.3 in yellow and BH32.9 in orange. Backbone atoms are displayed in cartoon ribbon representation whilst residues are shown as all atom-coloured stick models. The catalytic Arg124 in BH32.3 adopts an orientation that places the guanidinium motif in close proximity to the amide side chain of Gln128 designed to interact with the oxyanion of **Int1**. During the evolution process, Arg124 reorientates to adopt a pose ideal to support charge transfer during catalysis (BH32.9 orange).



7.2.2.6 Extended Data Figure 6: Cluster model used for DFT modelling



7.2.2.7 Extended Data Figure 7: Computed reaction profile for the complete MBH mechanism. For step 3 (**Int2** → **Int3**) the barrier for proton transfer was calculated with a water molecule not present for the other steps, and the potential energy of the ground state (**Int2** + H₂O molecule) was normalised to the energy of Int2.



7.2.2.8 Extended Data Figure 8: DFT states showing reactants, transition states and intermediates formed along the reaction coordinate. Stick representations of the complete DFT progression from reactant through to products are presented in all atom colours. For clarity, a subset of atoms that form close packing interactions with the substrates are shown along with atoms derived from the His23 nucleophile and catalytic Arg124. Atoms derived from residues that provide close packing contacts (Trp10, Trp88, Pro128 & Ser129) are shown with additional dot surfaces (black) whilst substrate derived heavy atoms are shown with semi-transparent CPK spheres (magenta). Substrate derived proton atoms, relevant to catalysis, are highlighted with purple CPK spheres whilst hydrogen bonds are shown as black dashed lines.

7.2.2.9 Extended Data Table 1: Experimental and calculated masses of apo and inhibited enzymes. Mass spectrometry data for BH32 and variants. Enzymes were inhibited with mechanistic inhibitor **4**.

Variant	Observed Mass	Expected Mass
BH32	27788	27788
BH32 inhibited (60 minutes incubation)	28003 (80% single modification)	28002
BH32 H23A	27721	27722
BH32 H23A inhibited (60 minutes incubation)	27721 (no modification)	27722
BH32.6*	27580	27579
BH32.6 inhibited* (15 minutes incubation)	27795 (100% single modification)	27793
BH32.10	27806	27806
BH32.10 H23A	27740	27739
BH32.10 W10A	27691	27690
BH32.10 R124A	27721	27720

*Variants highlighted contain a C-terminal His-tag. All other proteins contain a strep-tag.

7.2.3 Supplementary Information

7.2.3.1 BH32.10 DNA and protein sequence

Mutations from the BH32 Design: L10W, N14I, A19T, A20Y, S22V, L24F, T49A, Y56N, E70R, F87L, S95A, M120V, T122L, D123N, S124R, Q128L, A129S, M130T, F154S, E174K, Y177C, D180P, C186A, C212A

```
ATGATTCGTGCGGTATTCTTTGATAGCTGGGGTACTCTGATTAGCGTTGAAGGCACTTATAAA
GTGCATTTTAAAATTATGGAGGAAGTGCTGGGTGACTATCCGCTGAACCCGAAAACCCTGCTG
GACGAATACGAGAACTGGCTCGCGAAGCGTTCTCTAACAATGCGGGCAAACCGTATCGTCC
GCTGCGTGATATCCTGGAACGTGTAATGCGTAACTGGCGGAAAAGTACGGTTTTCAAATACCC
TGAAAACCTTGTTGGGAAATCTCCCTGCGTATGGCGCAACGCTACGGCGAGCTGTACCCGGAAG
TGGTGAAGTACTGAAATCTCTGAAAGGTAATATCACGTTGGCGTGATCCTGAATAGGGATA
CCGAGCTGTCTACGGCATTCTGGACGCACTGGGCATCAAAGACCTGTTCCGACTCCATCACC
ACGTCTGAAGAAGCTGGTTTTCTCTAAACCGCACCCACGCATCTTCGAACTGGCTCTGAAGAAA
GCCGGCGTTAAAGGCGAGAAAGCAGTGTGTGTTGGTCCTAACCCGGTCAAAGACGCGGGTG
GTTCTAAGAACCTGGGTATGACTAGCATCCTGCTGGATCGTAAAGGTGAGAAACGTGAATTCT
GGGATAAGGCGGACTTTATCGTCTCCGACCTGCGCGAAGTTATTAAGATTGTTGACGAACTGA
ACGGTCAGGGCTCTCTCGAGTGGAGTCACCCACAGTTTGAGAAA
```

```
MIRAVFFDSWGT LISVEGTYKVHFKIMEEVLGDYPLNPKTLLDEYEKLAREAFSNNAGKPYRPLRDI
LERVMRKLAEKYGFKYPENLWEISLRMAQRYGELYPEVVEVLKSLKGKYHVGVILNRDTELSTAFI
DALGIKDLFDSITTSEEAGFSKPHPRIFELALKKAGVKGEKAVCVGPNPVKDAGGSKNLGMTSILLD
RKGEKREFWDKADFI VSDLREVIKIVDELNGQGSLEWSHPQFEK
```

7.2.3.2 Supplementary Information Table 1. Data collection and refinement statistics

	BH32.3	BH32.9
Wavelength	0.976	0.9795
Resolution range	55.26 - 1.48 (1.533 - 1.48)	42.71 - 2.29 (2.372 - 2.29)
Space group	P 31 2 1	P 31 2 1
Unit cell	71.689 71.689 121.272 90 90 120	70.9666 70.9666 118.768 90 90 120
Total reflections	578916 (56870)	158031 (15120)
Unique reflections	60772 (5941)	16121 (1571)
Multiplicity	9.5 (9.6)	9.8 (9.6)
Completeness (%)	99.90 (99.13)	99.55 (98.66)
Mean I/sigma(I)	14.64 (1.19)	10.51 (1.21)
Wilson B-factor	26.4	65.35
R-merge	0.05985 (1.411)	0.0806 (1.617)
R-meas	0.0634 (1.491)	0.08509 (1.708)
R-pim	0.02062 (0.4776)	0.02701 (0.5474)
CC1/2	0.997 (0.679)	0.999 (0.603)
CC*	0.999 (0.899)	1 (0.867)
Reflections used in refinement	60762 (5939)	16120 (1551)
Reflections used for R-free	3039 (305)	824 (95)
R-work	0.1572 (0.2272)	0.2226 (0.3236)
R-free	0.1771 (0.2647)	0.2616 (0.4293)
CC(work)	0.964 (0.872)	0.946 (0.681)
CC(free)	0.966 (0.831)	0.925 (0.403)
Number of non-hydrogen atoms	2210	1890
macromolecules	1950	1838
ligands	18	9
solvent	242	43
Protein residues	448	226
RMS(bonds)	0.009	0.006
RMS(angles)	1.12	1.08

Ramachandran favoured (%)	98.69	97.75
Ramachandran allowed (%)	1.31	1.35
Ramachandran outliers (%)	0	0.9
Rotamer outliers (%)	1.43	2.02
Clash score	2.76	8.59
Average B-factor	35.89	75.73
macromolecules	34.02	75.73
ligands	60.92	80.84
solvent	49.14	74.73
Number of TLS groups	0	1

7.2.3.3 Supplementary Information Table 2: Mother liquor composition used for protein crystallization of BH32.3 and BH32.9

Variant	Crystallisation conditions (200+200nl drops incubated at 4°C)
BH32.3	0.06M Divalents [0.3M Magnesium chloride hexahydrate; 0.3M calcium chloride dihydrate] 0.1 M BS1 pH 6.5 [Imidazole; MES monohydrate (acid)] 30% Precipitant mix 2 [40% v/v Ethylene glycol; 20% w/v PEG 8K] Morpheus screen condition A2 (Molecular Dimensions)
BH32.9	0.1M SPG pH 9.0 25% w/v PEG 1500 PACT premier Eco condition A6 (Molecular Dimensions)

7.2.3.4 Supplementary Information Table 3: Coordinates of energy minimised DFT models.

R			TS1				
C	1.205779000	-2.863845000	1.892888000	C	1.246923000	-3.376484000	2.169459000
C	2.444330000	-3.567453000	1.412983000	C	1.204173000	-3.602055000	0.668822000
C	2.487783000	-3.743882000	-0.107648000	C	1.244245000	-2.275339000	-0.097920000
C	2.188395000	-2.421433000	-0.818007000	C	2.466448000	-1.450296000	0.316060000
C	0.930507000	-1.803581000	-0.291170000	C	2.584020000	-1.325937000	1.828996000
C	0.471607000	-2.027166000	0.956834000	C	1.887418000	-2.225835000	2.657684000
O	0.846890000	-2.958537000	3.077223000	O	0.650826000	-4.194292000	2.933671000
C	1.456163000	1.483631000	3.247011000	C	0.449266000	0.386731000	3.832148000
C	0.412169000	1.368710000	2.201293000	C	-0.202703000	0.544787000	2.515315000
C	-0.879998000	0.922907000	2.527912000	C	-1.461201000	-0.030572000	2.289533000
C	-1.842899000	0.793407000	1.536503000	C	-2.102206000	0.156814000	1.076473000
C	-1.492707000	1.142947000	0.227177000	C	-1.463313000	0.921805000	0.096135000
C	-0.231482000	1.620000000	-0.117410000	C	-0.200478000	1.486582000	0.277295000
C	0.728879000	1.720814000	0.885135000	C	0.424777000	1.290969000	1.507578000
O	1.282748000	1.191320000	4.411943000	O	-0.035529000	-0.227420000	4.762626000
C	-1.134051000	-6.911329000	2.308724000	C	-1.620509000	-6.924619000	1.842646000
C	-2.023619000	-5.962772000	1.570389000	C	-2.417559000	-5.883623000	1.122594000
C	-2.241432000	-4.630281000	1.841702000	C	-2.374547000	-4.515465000	1.284606000
C	-2.857790000	-6.285321000	0.439474000	C	-3.403189000	-6.141419000	0.103717000
N	-3.169049000	-4.107564000	0.958660000	N	-3.275659000	-3.909737000	0.425146000
C	-3.566095000	-5.099851000	0.089102000	C	-3.915321000	-4.881096000	-0.316598000
C	-3.058761000	-7.451307000	-0.320641000	C	-3.887897000	-7.314341000	-0.502520000
C	-4.451998000	-5.058721000	-0.993494000	C	-4.877191000	-4.769202000	-1.327107000
C	-3.935386000	-7.409018000	-1.399396000	C	-4.846456000	-7.207534000	-1.503370000
C	-4.624005000	-6.222464000	-1.733103000	C	-5.333025000	-5.946632000	-1.910346000
C	2.218324000	-8.110624000	-1.481338000	C	1.638245000	-8.134262000	-2.025149000
C	0.767577000	-7.630711000	-1.308787000	C	0.327026000	-7.524383000	-1.504376000
C	3.110809000	-7.126187000	-2.245270000	C	2.347405000	-7.261509000	-3.066350000
C	-0.022679000	-7.530019000	-2.616764000	C	-0.759821000	-7.358858000	-2.570955000
N	7.307856000	-5.904231000	-0.771808000	N	6.505870000	-6.687033000	0.098692000
C	6.512532000	-4.895487000	-0.056828000	C	6.164695000	-5.357047000	-0.409131000
C	7.456213000	-3.931019000	0.629109000	C	6.790050000	-4.275051000	0.444557000
O	7.715744000	-2.811631000	0.218794000	O	7.485895000	-3.364051000	0.027032000
C	5.585704000	-5.574283000	0.947763000	C	4.644213000	-5.167390000	-0.421775000
N	8.223065000	-1.356695000	-2.510486000	N	8.135158000	-1.830445000	-2.588360000
C	7.265827000	-0.257786000	-2.314788000	C	7.278745000	-0.657184000	-2.368267000
C	7.773561000	0.681145000	-1.214546000	C	7.822733000	0.195678000	-1.223845000
O	7.902205000	1.898051000	-1.383564000	O	7.940147000	1.421125000	-1.306919000
C	5.805495000	-0.698870000	-2.010562000	C	5.774549000	-0.964881000	-2.102932000
C	4.886919000	0.509016000	-1.786369000	C	4.962246000	0.324753000	-1.937007000
C	5.271950000	-1.598339000	-3.130534000	C	5.183330000	-1.841474000	-3.211287000
N	8.025910000	0.109612000	-0.010211000	N	8.092294000	-0.470290000	-0.071322000
C	8.232245000	0.941645000	1.160687000	C	8.326386000	0.238788000	1.173991000
C	9.482117000	1.799249000	1.011553000	C	9.744337000	0.809209000	1.211058000
O	9.659614000	2.813228000	1.651936000	O	10.403162000	0.901594000	2.224698000
C	8.334481000	0.065710000	2.420610000	C	8.069128000	-0.670436000	2.375797000
C	7.119174000	-0.792797000	2.601426000	C	6.661203000	-1.163265000	2.418637000
N	7.128148000	-1.937070000	3.374225000	N	6.257468000	-2.207183000	3.234370000
C	5.842515000	-0.733499000	2.083566000	C	5.529773000	-0.782572000	1.738829000
C	5.894040000	-2.512047000	3.296587000	C	4.933691000	-2.427864000	3.045370000
N	5.089094000	-1.805385000	2.521850000	N	4.481910000	-1.583102000	2.138002000
C	6.857653000	4.842869000	0.543925000	C	7.258706000	4.266757000	0.811640000
C	5.718111000	4.176447000	-0.238244000	C	6.052741000	3.743238000	0.018440000
C	6.499664000	6.179869000	1.201343000	C	7.003323000	5.582613000	1.554205000
C	4.622525000	3.569015000	0.644772000	C	4.919720000	3.196149000	0.893897000
C	-3.877362000	3.037519000	7.473589000	C	-3.624581000	2.898592000	7.358658000
C	-2.560194000	2.324103000	7.148775000	C	-2.340783000	2.065043000	7.266898000
C	-2.803480000	0.843634000	6.821187000	C	-2.652928000	0.629252000	6.823116000
C	-1.828860000	3.014213000	5.988614000	C	-1.327419000	2.723176000	6.320057000
C	-2.578112000	9.498149000	1.302792000	C	-1.791584000	9.577676000	1.891184000
C	-2.514960000	8.027468000	1.017280000	C	-1.879923000	8.161897000	1.409595000
C	-3.125956000	7.346600000	-0.007382000	C	-2.558587000	7.698548000	0.309349000
C	-1.814767000	7.036383000	1.799149000	C	-1.279518000	7.005418000	2.030982000
N	-2.854007000	5.988682000	0.092482000	N	-2.418544000	6.322167000	0.207912000
C	-2.054517000	5.767473000	1.195435000	C	-1.639170000	5.867687000	1.250716000
C	-1.019976000	7.101549000	2.956539000	C	-0.485483000	6.821853000	3.176266000
C	-1.544364000	4.580861000	1.731855000	C	-1.234010000	4.573082000	1.590829000
C	-0.504335000	5.925027000	3.487882000	C	-0.084174000	5.535907000	3.520265000
C	-0.770788000	4.678378000	2.884678000	C	-0.458439000	4.424797000	2.736686000
N	2.347591000	7.061582000	-1.502187000	N	2.999909000	6.920640000	-1.167900000
C	2.238330000	5.654928000	-1.134549000	C	2.719574000	5.538035000	-0.799690000
C	1.326416000	4.742580000	-1.931932000	C	1.680407000	4.751007000	-1.574821000

O	1.409919000	3.510190000	-1.818249000	O	1.576204000	3.524531000	-1.422027000
C	1.800639000	5.611590000	0.346062000	C	2.317144000	5.539599000	0.690763000
O	2.713387000	6.330660000	1.152893000	O	3.326380000	6.146725000	1.475282000
N	0.395726000	5.357368000	-2.684518000	N	0.866716000	5.476668000	-2.363075000
C	-0.650965000	4.632051000	-3.377491000	C	-0.234954000	4.887169000	-3.094801000
C	-0.097910000	4.251837000	-4.758714000	C	0.305820000	4.476770000	-4.471927000
O	-0.607290000	4.582278000	-5.810352000	O	-0.158104000	4.860517000	-5.527504000
C	-1.961474000	5.422133000	-3.439402000	C	-1.452933000	5.812247000	-3.172284000
C	-3.230069000	4.550657000	-3.357065000	C	-2.808156000	5.078916000	-3.379315000
C	-4.473418000	5.443073000	-3.452241000	C	-3.948577000	6.101839000	-3.209455000
C	-3.283271000	3.443027000	-4.416971000	C	-2.965694000	4.020476000	-4.234834000
N	2.570428000	1.966571000	-4.457892000	N	2.711698000	2.066748000	-4.233304000
C	2.226336000	0.546879000	-4.394914000	C	2.321075000	0.665414000	-4.379315000
C	1.577367000	0.113117000	-5.699116000	C	1.642396000	0.461418000	-5.722937000
O	1.578468000	-1.028280000	-6.115038000	O	1.673201000	-0.575249000	-6.354749000
C	1.198143000	0.317306000	-3.275307000	C	1.290345000	0.301463000	-3.295169000
C	-5.811703000	-1.988094000	4.844381000	C	-5.909910000	-1.827394000	4.699926000
C	-4.667209000	-3.000421000	4.802624000	C	-4.824999000	-2.900282000	4.596682000
C	-3.758375000	-2.849120000	6.028540000	C	-3.882671000	-2.870759000	5.804761000
N	-2.567641000	-3.701729000	5.985474000	N	-2.924344000	-3.982146000	5.794603000
C	-1.485004000	-3.441531000	5.247947000	C	-1.819137000	-4.029213000	5.039580000
N	-0.474791000	-4.318561000	5.188918000	N	-1.252748000	-5.210524000	4.753544000
N	-1.370809000	-2.293437000	4.573998000	N	-1.237465000	-2.923593000	4.569835000
N	-7.667045000	2.323039000	0.377813000	N	-7.212247000	2.863988000	0.591590000
C	-7.095007000	2.161045000	-0.974931000	C	-6.855553000	2.771976000	-0.839020000
C	-6.828472000	0.688502000	-1.307165000	C	-6.785156000	1.315046000	-1.318920000
O	-6.427762000	0.337272000	-2.418483000	O	-6.599904000	1.023820000	-2.502512000
C	-5.772224000	2.968891000	-0.966026000	C	-5.464711000	3.446360000	-0.962067000
C	-5.430937000	3.065329000	0.527461000	C	-4.907199000	3.353663000	0.464996000
C	-6.811163000	3.237033000	1.164171000	C	-6.154180000	3.599292000	1.315982000
N	-7.054233000	-0.157404000	-0.276334000	N	-6.915507000	0.417618000	-0.314344000
C	-6.935439000	-1.594613000	-0.374547000	C	-6.986941000	-1.015939000	-0.480915000
C	-8.315695000	-2.241394000	-0.427095000	C	-8.387781000	-1.498977000	-0.117918000
O	-8.593587000	-3.287185000	0.118363000	O	-8.614229000	-2.491348000	0.540395000
C	-6.082366000	-2.162224000	0.759133000	C	-5.923322000	-1.728324000	0.346985000
O	-4.713996000	-1.790780000	0.642863000	O	-4.616208000	-1.466581000	-0.157033000
H	-0.442893000	-1.569091000	1.314382000	H	1.868413000	-2.058381000	3.730721000
H	3.289630000	-2.942225000	1.748445000	H	2.062821000	-4.225978000	0.387249000
H	2.522539000	-4.520201000	1.945649000	H	0.303152000	-4.176769000	0.438403000
H	1.741393000	-4.485297000	-0.414522000	H	0.326473000	-1.712526000	0.108659000
H	3.464790000	-4.125353000	-0.414153000	H	1.266064000	-2.453661000	-1.175978000
H	3.015722000	-1.713328000	-0.662297000	H	3.368613000	-1.928432000	-0.076882000
H	2.101800000	-2.562308000	-1.898243000	H	2.425650000	-0.450642000	-0.124841000
H	0.372933000	-1.143562000	-0.947076000	H	2.701854000	-0.313682000	2.202084000
H	2.431949000	1.862315000	2.894528000	H	1.427021000	0.887476000	3.942387000
H	-1.111334000	0.690162000	3.561011000	H	-1.931665000	-0.616037000	3.069525000
H	-0.02328000	1.930569000	-1.126298000	H	0.264299000	2.088176000	-0.496851000
H	1.719262000	2.085201000	0.634379000	H	1.397108000	1.739651000	1.685125000
H	-0.396314000	-7.375127000	1.643050000	H	-1.298802000	-7.714210000	1.155656000
H	-0.586877000	-6.399396000	3.105762000	H	-0.721340000	-6.492847000	2.288426000
H	-1.795553000	-4.002437000	2.596716000	H	-1.750774000	-3.923999000	1.937818000
H	-3.528399000	-3.155855000	0.947141000	H	-3.458588000	-2.916264000	0.337377000
H	-2.528504000	-8.366855000	-0.074406000	H	-3.512476000	-8.287024000	-0.197345000
H	-4.968533000	-4.145455000	-1.261920000	H	-5.246879000	-3.808674000	-1.662133000
H	-4.091235000	-8.299633000	-2.000673000	H	-5.225978000	-8.104564000	-1.983530000
H	-5.281599000	-6.200464000	-2.595226000	H	-6.074672000	-5.889386000	-2.701450000
H	2.652267000	-8.287756000	-0.488701000	H	2.313692000	-8.302353000	-1.176406000
H	0.767968000	-6.653254000	-0.804945000	H	0.540974000	-6.547802000	-1.046255000
H	0.243314000	-8.316777000	-0.631340000	H	-0.060019000	-8.158721000	-0.697345000
H	4.148113000	-7.474937000	-2.284307000	H	3.312874000	-7.689263000	-3.355679000
H	3.111020000	-6.143925000	-1.759580000	H	2.533320000	-6.255258000	-2.671229000
H	2.770300000	-6.983672000	-3.275733000	H	1.749776000	-7.150420000	-3.976394000
H	0.424014000	-6.810913000	-3.310052000	H	-0.453352000	-6.667944000	-3.361828000
H	-1.052303000	-7.212654000	-2.427638000	H	-1.682535000	-6.969688000	-2.132191000
H	-0.056689000	-8.501147000	-3.124297000	H	-0.992333000	-8.321266000	-3.042040000
H	7.870825000	-6.446697000	-0.118871000	H	6.134792000	-6.821065000	1.037397000
H	7.948093000	-5.461393000	-1.426905000	H	7.514306000	-6.808419000	0.152863000
H	5.937433000	-4.326229000	-0.795335000	H	6.561979000	-5.253354000	-1.424267000
H	7.984253000	-4.335735000	1.517570000	H	6.593373000	-4.373144000	-1.532033000
H	4.923012000	-6.270859000	0.427829000	H	4.182725000	-5.989045000	-0.974800000
H	4.983112000	-4.837062000	1.482573000	H	4.371035000	-4.220971000	-0.896357000
H	6.165294000	-6.139180000	1.686671000	H	4.244002000	-5.171976000	0.598532000
H	8.054783000	-2.082783000	-1.815756000	H	7.893435000	-2.573582000	-1.933918000
H	8.055054000	-1.785581000	-3.416013000	H	7.957583000	-2.200492000	-3.517390000
H	7.262490000	0.351127000	-3.224456000	H	7.347232000	-0.021327000	-3.256574000
H	5.834906000	-1.289073000	-1.084283000	H	5.724690000	-1.531160000	-1.162463000
H	4.838410000	1.139793000	-2.681243000	H	5.019049000	0.940148000	-2.841178000

H	5.226641000	1.137753000	-0.959765000	H	5.317925000	0.939593000	-1.107207000
H	3.867854000	0.183320000	-1.557033000	H	3.909840000	0.094278000	-1.757718000
H	5.873877000	-2.504351000	-3.243273000	H	5.706944000	-2.797778000	-3.294271000
H	5.275906000	-1.069405000	-4.091285000	H	5.242600000	-1.337939000	-4.183664000
H	4.243783000	-1.909305000	-2.924324000	H	4.128662000	-2.055934000	-3.009391000
H	7.901783000	-0.887416000	0.120561000	H	7.992800000	-1.478073000	-0.025609000
H	7.393320000	1.639418000	1.278588000	H	7.658857000	1.112621000	1.202792000
H	10.238680000	1.404869000	0.302722000	H	10.124262000	1.146714000	0.228657000
H	8.484009000	0.731218000	3.277914000	H	8.320728000	-0.115039000	3.284277000
H	9.224861000	-0.571670000	2.351450000	H	8.756937000	-1.523627000	2.335159000
H	7.914898000	-2.289307000	3.901094000	H	6.848840000	-2.711811000	3.881072000
H	5.434480000	0.001342000	1.405325000	H	5.403184000	-0.013893000	0.994575000
H	5.639795000	-3.421305000	3.821458000	H	4.343927000	-3.166700000	3.565766000
H	7.229685000	4.144574000	1.305625000	H	7.576479000	3.497367000	1.530064000
H	6.147719000	3.393037000	-0.869115000	H	6.401317000	2.959836000	-0.658907000
H	5.275333000	4.918367000	-0.917760000	H	5.670104000	4.557258000	-0.612956000
H	6.210659000	6.919394000	0.444945000	H	6.751938000	6.381963000	0.847167000
H	7.348606000	6.586485000	1.760382000	H	7.886123000	5.900151000	2.118707000
H	5.656772000	6.080539000	1.893308000	H	6.166962000	5.497739000	2.254931000
H	3.842167000	3.105495000	0.029810000	H	4.093259000	2.818748000	0.280205000
H	4.145914000	4.328034000	1.270797000	H	4.514737000	3.969594000	1.551393000
H	5.038684000	2.792720000	1.299426000	H	5.276464000	2.368547000	1.519918000
H	-3.706276000	4.087956000	7.731476000	H	-3.414248000	3.917203000	7.701598000
H	-4.553174000	3.011916000	6.609781000	H	-4.108057000	2.970521000	6.376419000
H	-1.915228000	2.372684000	8.037113000	H	-1.890751000	2.019547000	8.268559000
H	-3.443469000	0.751674000	5.933462000	H	-3.096554000	0.628225000	5.818715000
H	-3.302105000	0.325050000	7.647542000	H	-3.363910000	0.147757000	7.503579000
H	-1.860175000	0.324900000	6.613774000	H	-1.743414000	0.021180000	6.786568000
H	-0.874680000	2.522053000	5.769251000	H	-0.393406000	2.153573000	6.280641000
H	-1.622960000	4.066651000	6.210148000	H	-1.090729000	3.744732000	6.636432000
H	-2.435218000	2.984916000	5.074775000	H	-1.728027000	2.778908000	5.300015000
H	-3.178719000	10.020677000	0.553267000	H	-2.342438000	10.253684000	1.231594000
H	-3.021996000	9.695137000	2.285808000	H	-2.204820000	9.683996000	2.901282000
H	-3.748440000	7.721705000	-0.807206000	H	-3.142891000	8.243894000	-0.417988000
H	-3.174218000	5.282302000	-0.550367000	H	-2.814822000	5.750439000	-0.519924000
H	-0.818351000	8.057601000	3.430804000	H	-0.194801000	7.673057000	3.784999000
H	-1.751494000	3.622795000	1.270918000	H	-1.517457000	3.718858000	0.986757000
H	0.106541000	5.959196000	4.384656000	H	0.525813000	5.379354000	4.404597000
H	-0.373868000	3.777958000	3.338065000	H	-0.130929000	3.435001000	3.031675000
H	2.749098000	7.207970000	-2.421916000	H	3.410994000	7.017756000	-2.089847000
H	1.466076000	7.562610000	-1.430694000	H	2.188545000	7.527840000	-1.089357000
H	3.236699000	5.215609000	-1.198727000	H	3.652556000	4.976285000	-0.890431000
H	0.781839000	6.022693000	0.429552000	H	1.354379000	6.063894000	0.800736000
H	1.771148000	4.579905000	0.697997000	H	2.177486000	4.515751000	1.039377000
H	2.973461000	7.097016000	0.613773000	H	3.666179000	6.872291000	0.923933000
H	0.453615000	6.358188000	-2.806158000	H	1.077440000	6.453771000	-2.506177000
H	-0.786546000	3.694725000	-2.824082000	H	-0.479363000	3.957409000	-2.566714000
H	0.837438000	3.658560000	-4.727987000	H	1.184759000	3.803267000	-4.435254000
H	-1.980907000	6.001373000	-4.369371000	H	-1.390811000	6.403756000	-4.092616000
H	-1.974411000	6.136252000	-2.609052000	H	-1.409706000	6.511651000	-2.331198000
H	-3.226155000	4.053251000	-2.374436000	H	-2.870143000	4.544981000	-2.173258000
H	-4.491509000	5.969966000	-4.412909000	H	-3.908715000	6.645635000	-4.159851000
H	-4.495686000	6.200528000	-2.660800000	H	-3.889286000	6.844783000	-2.406156000
H	-5.391056000	4.852406000	-3.380506000	H	-4.924979000	5.613052000	-3.146874000
H	-3.265819000	3.868378000	-5.425066000	H	-2.864208000	4.472087000	-5.226064000
H	-4.198984000	2.853102000	-4.305419000	H	-3.952845000	3.550603000	-4.377010000
H	-2.441946000	2.750548000	-4.329469000	H	-2.222483000	3.224697000	-4.146009000
H	3.484015000	2.108713000	-4.877925000	H	3.618682000	2.245309000	-4.653605000
H	2.582212000	2.377022000	-3.527225000	H	2.761089000	2.330467000	-3.252403000
H	3.083242000	-0.116656000	-4.218893000	H	3.158533000	-0.042359000	-4.321353000
H	1.055379000	0.933820000	-6.238258000	H	1.067150000	1.346609000	-6.073666000
H	0.301041000	0.922704000	-3.437561000	H	0.397165000	0.926474000	-3.377679000
H	1.636923000	0.610515000	-2.317754000	H	1.724021000	0.472719000	-2.305396000
H	0.903904000	-0.731691000	-3.234467000	H	0.993248000	-0.745230000	-3.377010000
H	-5.433028000	-0.961051000	4.804171000	H	-5.473357000	-0.823420000	4.743067000
H	-6.488993000	-2.130532000	3.998405000	H	-6.578030000	-1.865808000	3.834690000
H	-4.086691000	-2.869564000	3.881791000	H	-4.240536000	-2.769981000	3.677704000
H	-5.058286000	-4.023413000	4.777278000	H	-5.286463000	-3.893042000	4.537515000
H	-3.439856000	-1.809956000	6.161190000	H	-3.339419000	-1.924743000	5.860051000
H	-4.299569000	-3.116423000	6.938433000	H	-4.447289000	-2.956146000	6.736426000
H	-2.625317000	-4.609541000	6.420948000	H	-3.283535000	-4.875280000	6.099841000
H	-0.529172000	-5.207128000	5.658523000	H	-1.808262000	-6.050509000	4.788045000
H	0.301540000	-4.134966000	4.561030000	H	-0.455846000	-5.194209000	4.120658000
H	-0.578846000	-2.197887000	3.933316000	H	-0.387487000	-3.075459000	4.022706000
H	-2.138001000	-1.646693000	4.521474000	H	-1.371480000	-2.015788000	4.989877000
H	-8.628883000	2.640269000	0.341025000	H	-8.127526000	3.277857000	0.724815000
H	-7.765963000	2.525274000	-1.759988000	H	-7.587313000	3.265718000	-1.486423000

H	-4.999653000	2.491653000	-1.570296000	H	-4.839796000	2.962429000	-1.714375000
H	-5.957650000	3.967660000	-1.369643000	H	-5.595921000	4.494426000	-1.244821000
H	-4.756739000	3.891748000	0.765725000	H	-4.117197000	4.077778000	0.674422000
H	-4.966601000	2.135990000	0.871462000	H	-4.508271000	2.351546000	0.653037000
H	-6.831423000	2.966202000	2.224464000	H	-6.055780000	3.224170000	2.639465000
H	-7.137381000	4.283468000	1.076402000	H	-6.364146000	4.677278000	1.369501000
H	-7.442953000	0.305065000	0.546915000	H	-7.125852000	0.862793000	0.581577000
H	-6.452177000	-1.796904000	-1.339246000	H	-6.850158000	-1.243492000	-1.544517000
H	-9.061851000	-1.667269000	-1.014473000	H	-9.202642000	-0.852980000	-0.505643000
H	-6.120854000	-3.252072000	0.733353000	H	-6.076749000	-2.806169000	0.298000000
H	-6.495915000	-1.834228000	1.722191000	H	-6.002570000	-1.419317000	1.397599000
H	-4.630108000	-0.851962000	0.419408000	H	-4.527870000	-0.526202000	-0.380121000
H	-4.392460000	2.562127000	8.315294000	H	-4.343490000	2.449688000	8.052532000
H	-6.400441000	-2.091754000	5.761927000	H	-6.518927000	-1.966707000	5.599195000
H	-1.579392000	9.950818000	1.307709000	H	-0.752195000	9.924470000	1.934632000
H	7.701409000	5.002069000	-0.139334000	H	8.102888000	4.400591000	0.124138000
H	2.217678000	-9.081804000	-1.993921000	H	1.431479000	-9.123376000	-2.455076000
H	-1.705880000	-7.728142000	2.765915000	H	-2.199592000	-7.417631000	-3.395077000
N	-5.463703000	-0.812987000	-4.995084000	N	-5.320470000	0.014989000	-5.172458000
C	-4.436529000	-1.767945000	-4.565339000	C	-4.501123000	-1.112658000	-4.678433000
C	-5.100324000	-2.926769000	-3.849988000	C	-5.188352000	-1.616535000	-3.435029000
O	-5.171100000	-4.066624000	-4.265488000	O	-5.994597000	-2.531716000	-3.395634000
C	-3.409891000	-1.057514000	-3.663519000	C	-3.077506000	-0.603337000	-4.388123000
C	-2.252382000	-1.963057000	-3.317792000	C	-2.098708000	-1.675223000	-3.960945000
C	-1.223405000	-2.181128000	-4.245533000	C	-1.065096000	-2.068357000	-4.821149000
C	-2.223114000	-2.666042000	-2.107212000	C	-2.193208000	-2.299820000	-2.706114000
C	-0.203073000	-3.094653000	-3.981786000	C	-0.148885000	-3.052898000	-4.444651000
C	-1.213154000	-3.595925000	-1.844132000	C	-1.293834000	-3.300547000	-2.334660000
C	-0.205709000	-3.816707000	-2.784805000	C	-0.264077000	-3.676861000	-3.200974000
H	-5.929151000	-0.411593000	-4.181298000	H	-5.506395000	0.660005000	-4.02137000
H	-6.167074000	-1.280157000	-5.562290000	H	-6.232956000	-0.338385000	-5.454693000
H	-5.613671000	-2.629781000	-2.908430000	H	-4.989249000	-1.002874000	-2.541408000
H	-3.913525000	-0.703376000	-2.758688000	H	-3.147180000	0.171447000	-3.615255000
H	-1.218265000	-1.627838000	-5.180610000	H	-0.960149000	-1.583420000	-5.787130000
H	-3.000811000	-2.487946000	-1.371216000	H	-2.967784000	-2.002923000	-2.006299000
H	-1.220073000	-4.147949000	-0.911126000	H	-1.397383000	-3.779646000	-1.366967000
H	0.575869000	-4.542095000	-2.585048000	H	0.443151000	-4.445531000	-2.905077000
H	0.594419000	-3.228423000	-4.705764000	H	0.657405000	-3.320125000	-5.120733000
H	-3.931485000	-2.174489000	-5.448613000	H	-4.488452000	-1.900008000	-5.438020000
H	-3.068386000	-0.169240000	-4.203858000	H	-2.719807000	-0.109244000	-5.295650000
H	-2.840906000	0.439998000	1.758397000	H	-3.065726000	-0.293935000	0.896172000
N	-2.503414000	1.046575000	-0.828175000	N	-2.168404000	1.179092000	-1.161278000
O	-3.593427000	0.535392000	-0.549033000	O	-3.350376000	0.821717000	-1.257348000
O	-2.228150000	1.489009000	-1.939862000	O	-1.566766000	1.754448000	-2.062970000

Int1

C	1.019605000	-2.648063000	2.158226000
C	0.690327000	-2.859037000	0.688602000
C	1.560490000	-2.052060000	-0.279248000
C	3.017325000	-2.043414000	0.177563000
C	3.100513000	-1.357552000	1.545399000
C	2.128389000	-1.923461000	2.527333000
O	0.193624000	-3.152394000	3.009117000
C	0.748077000	0.254112000	3.554094000
C	0.007488000	0.422506000	2.284444000
C	-1.265498000	-0.152990000	2.146608000
C	-2.010888000	0.072366000	1.002109000
C	-1.474080000	0.891398000	0.002436000
C	-0.203270000	1.464599000	0.101224000
C	0.534843000	1.218299000	1.255159000
O	0.245757000	-0.202995000	4.567639000
C	-1.465090000	-6.987847000	1.838270000
C	-2.285223000	-5.976216000	1.104038000
C	-2.311579000	-4.611520000	1.292106000
C	-3.218153000	-6.263515000	0.044743000
N	-3.207686000	-4.034455000	0.409377000
C	-3.776825000	-5.020690000	-0.369554000
C	-3.622536000	-7.445314000	-0.601112000
C	-4.712778000	-4.935119000	-1.406054000
C	-4.551629000	-7.364218000	-1.632785000
C	-5.089175000	-6.120791000	-2.028868000
C	1.838145000	-8.092716000	-2.023238000
C	0.383151000	-7.797041000	-1.622764000
C	2.567547000	-6.879152000	-2.610970000
C	-0.540427000	-7.467951000	-2.800118000

TS2

C	1.228231000	-2.745316000	2.095015000
C	0.888600000	-2.949954000	0.629236000
C	1.745889000	-2.140717000	-0.348313000
C	3.189247000	-2.069050000	0.147691000
C	3.210578000	-1.272810000	1.457555000
C	2.212302000	-1.770423000	2.484593000
O	0.593033000	-3.398310000	2.944773000
C	1.169567000	-0.219606000	3.197094000
C	0.233237000	0.120486000	2.073527000
C	-1.036705000	-0.479711000	2.019292000
C	-1.929435000	-0.158232000	1.011320000
C	-1.546619000	0.779974000	0.046442000
C	-0.292001000	1.394747000	0.064968000
C	0.588454000	1.057977000	1.089513000
O	0.690211000	-0.543552000	4.338505000
C	-1.048486000	-7.052707000	1.923997000
C	-1.914067000	-6.093525000	1.175790000
C	-2.079218000	-4.748490000	1.417117000
C	-2.761014000	-6.417073000	0.056152000
N	-2.982956000	-4.215757000	0.514704000
C	-3.418632000	-5.214788000	-0.331104000
C	-3.020842000	-7.600117000	-0.657867000
C	-4.315908000	-5.174347000	-1.402929000
C	-3.907754000	-7.560012000	-1.728927000
C	-4.547309000	-6.356913000	-2.096559000
C	2.294342000	-7.988558000	-1.947968000
C	0.796433000	-7.764879000	-1.681711000
C	3.020696000	-6.730915000	-2.439774000
C	-0.030073000	-7.479212000	-2.939443000

N	7.251145000	-6.264678000	-0.730203000	N	7.549570000	-5.743023000	-0.948061000
C	6.288060000	-5.214780000	-0.371006000	C	6.568255000	-4.827429000	-0.349460000
C	6.985188000	-4.236561000	0.545531000	C	7.320698000	-3.832698000	0.502780000
O	7.336169000	-3.111034000	0.227087000	O	7.504786000	-2.662477000	0.204222000
C	5.061696000	-5.833515000	0.296183000	C	5.545576000	-5.615590000	0.465797000
N	8.132246000	-1.673727000	-2.455635000	N	8.195644000	-1.184893000	-2.490291000
C	7.293662000	-0.476561000	-2.296499000	C	7.269698000	-0.054631000	-2.323693000
C	7.809897000	0.386837000	-1.147278000	C	7.731476000	0.848253000	-1.182232000
O	7.900238000	1.614240000	-1.224371000	O	7.730094000	2.078259000	-1.265653000
C	5.782191000	-0.771185000	-2.078113000	C	5.789831000	-0.468573000	-2.087370000
C	4.967994000	0.513595000	-1.888257000	C	4.874148000	0.741722000	-1.873773000
C	5.214305000	-1.612170000	-3.225827000	C	5.275560000	-1.344319000	-3.234721000
N	8.082645000	-0.279961000	0.004632000	N	8.062778000	0.209718000	-0.029128000
C	8.304082000	0.422275000	1.255618000	C	8.243091000	0.937746000	1.213819000
C	9.730862000	0.969968000	1.308717000	C	9.637151000	1.564294000	1.257770000
O	10.429387000	0.930304000	2.298554000	O	10.352499000	1.545628000	2.236055000
C	8.026915000	-0.487821000	2.452274000	C	8.018328000	0.031957000	2.425591000
C	6.632639000	-1.012110000	2.439706000	C	6.674106000	-0.610500000	2.403169000
N	6.238539000	-2.132369000	3.151053000	N	6.382432000	-1.774065000	3.093226000
C	5.516844000	-0.594748000	1.768992000	C	5.525932000	-0.285876000	1.735707000
C	4.940233000	-2.389542000	2.926594000	C	5.117221000	-2.149050000	2.857728000
N	4.485854000	-1.458306000	2.088208000	N	4.577235000	-1.247135000	2.034674000
C	7.139131000	4.425096000	0.913646000	C	6.832372000	4.858132000	0.843150000
C	5.952206000	3.878462000	0.108419000	C	5.676852000	4.235507000	0.047115000
C	6.848408000	5.729708000	1.663179000	C	6.466210000	6.149293000	1.582796000
C	4.829111000	3.295852000	0.973350000	C	4.602698000	3.579986000	0.921770000
C	-3.792719000	2.492191000	7.753153000	C	-3.694445000	2.829069000	7.541631000
C	-2.429099000	1.946885000	7.314666000	C	-2.528878000	1.856843000	7.325847000
C	-2.540912000	0.481331000	6.864919000	C	-2.848285000	0.478205000	7.917029000
C	-1.822282000	2.806197000	6.196140000	C	-2.176335000	1.743380000	5.834826000
C	-2.043771000	9.504455000	1.987842000	C	-2.639213000	9.373625000	1.929043000
C	-2.071740000	8.135696000	1.379199000	C	-2.613640000	8.022292000	1.279808000
C	-2.645955000	7.775750000	0.185092000	C	-3.195281000	7.676800000	0.084975000
C	-1.515930000	6.926319000	1.941068000	C	-1.988824000	6.820659000	1.786641000
N	-2.472121000	6.418511000	-0.038222000	N	-2.958616000	6.339698000	-0.193165000
C	-1.790874000	5.867707000	1.026130000	C	-2.228732000	5.784789000	0.836183000
C	-0.830031000	6.631393000	3.132337000	C	-1.269753000	6.510241000	2.954642000
C	-1.404932000	4.546318000	1.274328000	C	-1.771953000	4.475286000	1.021655000
C	-0.455785000	5.316497000	3.388920000	C	-0.829214000	5.205078000	3.151848000
C	-0.743308000	4.285527000	2.470356000	C	-1.078500000	4.197977000	2.195706000
N	2.816003000	7.003288000	-1.003587000	N	2.339117000	7.152292000	-1.054286000
C	2.576671000	5.594264000	-0.708864000	C	2.197516000	5.729619000	-0.761197000
C	1.585070000	4.818106000	-1.558788000	C	1.256254000	4.890090000	0.868800000
O	1.579160000	3.577456000	-1.544809000	O	1.333197000	3.651516000	-1.599310000
C	2.137691000	5.513715000	0.767646000	C	1.775251000	5.616830000	0.717065000
O	3.108506000	6.115625000	1.604307000	O	2.710963000	6.279093000	1.548785000
N	0.690677000	5.540994000	-2.261333000	N	0.313498000	5.550310000	-2.309554000
C	-0.351605000	4.885005000	-3.020510000	C	-0.694715000	4.820192000	-3.048098000
C	0.262390000	4.185295000	-4.237627000	C	-0.042751000	4.111311000	-4.237472000
O	-0.274758000	3.281146000	-4.839121000	O	-0.509076000	3.133008000	-4.779826000
C	-1.478647000	5.873731000	-3.406529000	C	-1.854392000	5.748444000	-3.484313000
C	-2.904498000	5.288403000	-3.323716000	C	-3.254670000	5.102572000	-3.421441000
C	-3.936900000	6.420676000	-3.403131000	C	-4.332287000	6.185627000	-3.565902000
C	-3.206010000	4.218283000	-4.378658000	C	-3.480457000	3.986681000	-4.447429000
N	2.798859000	2.115337000	-4.241819000	N	2.639159000	2.231877000	-4.294112000
C	2.313118000	0.735712000	-4.320094000	C	2.212612000	0.830460000	-4.326948000
C	1.645401000	0.518579000	-5.667026000	C	1.529483000	0.552909000	-5.655004000
O	1.706881000	-0.515371000	-6.305477000	O	1.643578000	-0.482369000	-6.284489000
C	1.251444000	0.483111000	-3.235034000	C	1.191968000	0.556595000	-3.207737000
C	-5.890719000	-2.016117000	4.708755000	C	-5.755091000	-2.335635000	4.777411000
C	-4.798285000	-3.077456000	4.619118000	C	-4.469918000	-3.160238000	4.799563000
C	-4.115102000	-3.303240000	5.972683000	C	-3.802505000	-3.116208000	6.180566000
N	-2.976734000	-4.225667000	5.874962000	N	-2.467306000	-3.715565000	6.192563000
C	-1.862822000	-3.911440000	5.188772000	C	-1.396903000	-3.142630000	5.616691000
N	-1.085996000	-4.881074000	4.676626000	N	-0.240860000	-3.829171000	5.505648000
N	-1.481402000	-2.648708000	5.035098000	N	-1.438962000	-1.888121000	5.186981000
N	-7.202623000	2.676737000	0.642678000	N	-7.396228000	2.244832000	0.672873000
C	-6.927091000	2.593092000	-0.805709000	C	-7.104164000	2.149409000	-0.771724000
C	-6.838382000	1.140265000	-1.294469000	C	-6.919064000	0.697030000	-1.223923000
O	-6.705689000	0.859113000	-2.487653000	O	-6.783715000	0.397900000	-2.412026000
C	-5.571086000	3.321481000	-1.015608000	C	-5.813123000	2.985591000	-0.994075000
C	-4.944573000	3.303982000	0.385870000	C	-5.226141000	3.117656000	0.418858000
C	-6.160768000	3.499437000	1.291601000	C	-6.478138000	3.223411000	1.288801000
N	-6.902004000	0.233712000	-0.291283000	N	-6.925048000	-0.200046000	-0.210763000
C	-6.966260000	-1.198937000	-0.471209000	C	-6.909066000	-1.634189000	-0.402215000
C	-8.358463000	-1.696446000	-0.095643000	C	-8.261159000	-2.215385000	-0.001084000
O	-8.570353000	-2.702278000	0.547078000	O	-8.397182000	-3.232476000	0.644163000

C	-5.886219000	-1.912024000	0.335516000	C	-5.766028000	-2.292359000	0.360982000
O	-4.584916000	-1.622464000	-0.164087000	O	-4.501674000	-1.943269000	-0.190637000
H	2.328500000	-1.786761000	3.584676000	H	2.613942000	-1.946054000	3.476898000
H	0.776896000	-3.934555000	0.483369000	H	1.004055000	-4.024596000	0.442584000
H	-0.366469000	-2.614635000	0.549370000	H	-0.176616000	-2.741311000	0.497666000
H	1.198435000	-1.019629000	-0.332830000	H	1.349528000	-1.125753000	-0.454389000
H	1.482284000	-2.458288000	-1.290535000	H	1.705971000	-2.591174000	-1.341854000
H	3.390460000	-3.069623000	0.272345000	H	3.579536000	-3.077925000	0.326303000
H	0.186624000	-1.525499000	-0.541085000	H	3.837741000	-1.589475000	-0.586060000
H	2.972952000	-0.275223000	1.395679000	H	3.018955000	-0.222622000	1.210054000
H	1.772242000	0.662923000	3.560397000	H	2.069068000	0.418338000	3.185951000
H	-1.657668000	-0.771926000	2.943273000	H	-1.316477000	-1.205057000	2.771745000
H	0.186624000	2.103976000	-0.682453000	H	-0.014380000	2.128649000	-0.682732000
H	1.513216000	1.675349000	1.367118000	H	1.550530000	1.558410000	1.137960000
H	-1.010425000	-7.706360000	1.147153000	H	-0.333765000	-7.553982000	1.259834000
H	-0.646569000	-6.514944000	2.389439000	H	-0.475603000	-6.541891000	2.704201000
H	-1.722131000	-4.001790000	1.964269000	H	-1.586945000	-4.125300000	2.150833000
H	-3.429635000	-3.047615000	0.328574000	H	-3.278282000	-3.247853000	-0.444455000
H	-3.210823000	-8.405095000	-0.301443000	H	-2.530189000	-8.528842000	-0.380156000
H	-5.124182000	-3.986880000	-1.727849000	H	-4.807710000	-4.258999000	-1.698924000
H	-4.869439000	-8.268397000	-2.143525000	H	-4.111931000	-8.465354000	-2.292906000
H	-5.808810000	-6.083708000	-2.841286000	H	-5.228563000	-6.341881000	-2.941326000
H	2.386158000	-8.446776000	-1.140584000	H	2.772882000	-8.338293000	-1.024159000
H	0.369354000	-6.963253000	-0.906322000	H	0.676872000	-6.934214000	-0.971335000
H	-0.020750000	-8.665248000	-1.086048000	H	0.386159000	-8.651495000	-1.181556000
H	3.614956000	-7.109657000	-2.832998000	H	4.093432000	-6.910899000	-2.568664000
H	2.553415000	-6.038068000	-1.906682000	H	2.904126000	-5.909178000	-1.721900000
H	2.102118000	-6.538217000	-3.541249000	H	2.628170000	-6.385807000	-3.401733000
H	-0.235616000	-6.552443000	-3.315528000	H	0.287725000	-6.558793000	-3.437885000
H	-1.570115000	-7.325140000	-2.459808000	H	-1.089762000	-7.369567000	-2.691918000
H	-0.537217000	-8.280517000	-3.536299000	H	0.066417000	-8.298018000	-3.662211000
H	7.544264000	-6.786537000	0.093668000	H	8.039397000	-6.273011000	-0.229492000
H	8.086132000	-5.866625000	-1.153527000	H	8.248753000	-5.232337000	-1.482096000
H	6.002385000	-4.679065000	-1.282302000	H	6.074924000	-4.274291000	-1.155645000
H	7.243769000	-4.638604000	1.547875000	H	7.785416000	-4.255415000	1.418435000
H	4.626916000	-6.584613000	-0.367201000	H	5.079464000	-6.371428000	-0.170435000
H	4.303987000	-5.075593000	0.512839000	H	4.763343000	-4.961930000	0.861497000
H	5.335186000	-6.322445000	1.237958000	H	6.025380000	-6.123698000	1.309782000
H	7.794106000	-2.415738000	-1.844428000	H	7.907552000	-1.956315000	-1.890511000
H	8.040785000	-2.022845000	-3.404698000	H	8.137228000	-1.529025000	-3.443735000
H	7.405608000	0.140550000	-3.193327000	H	7.323487000	0.567754000	-3.222137000
H	5.719133000	-1.369814000	-1.159171000	H	5.792263000	-1.076877000	-1.172658000
H	5.035560000	1.152184000	-2.774300000	H	4.851377000	1.377620000	-2.764005000
H	5.313192000	1.106835000	-1.039045000	H	5.195932000	1.370260000	-1.040802000
H	3.910283000	0.285344000	-1.731453000	H	3.847162000	0.420596000	-1.677446000
H	5.572269000	-2.557021000	-3.340468000	H	5.882300000	-2.245020000	-3.360671000
H	5.277109000	-1.069364000	-4.176186000	H	5.287894000	-0.792299000	-4.181686000
H	4.161115000	-1.850071000	-3.045326000	H	4.244725000	-1.661956000	-3.047419000
H	8.029433000	-1.290814000	0.032120000	H	8.096437000	-0.802128000	0.001674000
H	7.647384000	1.303931000	1.272424000	H	7.537252000	1.780615000	1.216062000
H	10.078411000	1.412791000	0.356846000	H	9.945179000	2.040564000	0.308359000
H	8.228064000	0.070677000	3.370941000	H	8.153775000	0.624034000	3.335258000
H	8.729885000	-1.327978000	2.439907000	H	8.789362000	-0.745695000	2.446030000
H	6.830313000	-2.676268000	3.765812000	H	7.022305000	-2.275759000	3.696139000
H	5.367174000	0.230069000	1.094578000	H	5.301777000	0.533641000	1.075776000
H	4.361502000	-3.191843000	3.351381000	H	4.629171000	-3.018043000	3.264922000
H	7.469265000	3.658586000	1.629709000	H	7.210106000	4.118822000	1.564200000
H	6.325239000	3.110642000	-0.573417000	H	6.091783000	3.493267000	-0.638593000
H	5.551957000	4.686902000	-0.518955000	H	5.218956000	5.016673000	-0.575182000
H	6.583204000	6.527662000	0.959666000	H	6.157142000	6.925537000	0.872961000
H	7.719588000	6.063916000	2.235939000	H	7.315584000	6.537191000	2.154492000
H	6.009682000	5.619907000	2.357880000	H	5.633558000	5.996480000	2.276676000
H	4.027289000	2.880543000	0.351449000	H	3.825015000	3.112179000	0.306474000
H	4.385350000	4.057731000	1.618715000	H	4.114557000	4.310105000	1.571804000
H	5.210525000	2.490692000	1.614153000	H	5.043861000	2.802231000	1.558241000
H	-3.713455000	3.528288000	8.098968000	H	-3.459319000	3.824321000	7.149774000
H	-4.502855000	2.472503000	6.917245000	H	-4.595140000	2.471811000	7.027102000
H	-1.750964000	1.983147000	8.178581000	H	-1.649635000	2.255373000	7.851069000
H	-3.217765000	0.400087000	6.003718000	H	-3.738569000	0.053831000	7.434394000
H	-2.936735000	-0.152575000	7.666562000	H	-3.056352000	0.538986000	8.990402000
H	-1.560912000	0.094099000	6.564309000	H	-2.016364000	-0.220815000	7.774979000
H	-0.838284000	2.429839000	5.895859000	H	-1.304923000	1.098879000	5.674681000
H	-1.705566000	3.848973000	6.509869000	H	-1.951080000	2.722991000	5.398388000
H	-2.466320000	2.798223000	5.307949000	H	-3.019556000	1.321943000	5.270878000
H	-2.552728000	10.230001000	1.347482000	H	-3.200835000	10.089107000	1.322357000
H	-2.536348000	9.517970000	2.967436000	H	-3.106509000	9.334254000	2.920264000
H	-3.173454000	8.385838000	-0.534267000	H	-3.767162000	8.285337000	-0.601123000

H	-2.855473000	5.904193000	-0.813989000	H	-3.347731000	5.831052000	-0.969820000
H	-0.603355000	7.419106000	3.844978000	H	-1.067582000	7.278249000	3.695653000
H	-1.614734000	3.757608000	0.561010000	H	-1.954277000	3.710710000	0.275266000
H	0.066710000	5.074768000	4.309436000	H	-0.276574000	4.954679000	4.052399000
H	-0.433848000	3.271331000	2.695106000	H	-0.711643000	3.192170000	2.371089000
H	3.211497000	7.155777000	-1.925128000	H	2.714507000	7.332647000	-1.979215000
H	1.983508000	7.576940000	-0.895798000	H	1.470209000	7.667430000	-0.938374000
H	3.528217000	5.066607000	-0.806781000	H	3.182029000	5.267783000	-0.866550000
H	1.157776000	6.003517000	0.875809000	H	0.767037000	6.041927000	0.833139000
H	2.021198000	4.471335000	1.067400000	H	1.728982000	4.568500000	1.015091000
H	3.439706000	6.874721000	1.094499000	H	2.985684000	7.061011000	1.040043000
H	0.785748000	6.545103000	-2.297446000	H	0.328951000	6.558929000	-2.336499000
H	-0.771441000	4.090749000	-2.394917000	H	-1.088889000	4.033727000	-2.397853000
H	1.256641000	4.570249000	-4.540886000	H	0.905987000	4.566834000	-4.585420000
H	-1.308311000	6.286663000	-4.408419000	H	-1.676298000	6.146646000	-4.491049000
H	-1.416546000	6.717423000	-2.709753000	H	-1.848173000	6.609290000	-2.805916000
H	-2.998073000	4.791629000	-2.344884000	H	-3.353498000	4.632602000	-2.430670000
H	-3.884418000	6.918454000	-4.377871000	H	-4.277096000	6.650606000	-4.556580000
H	-3.774760000	7.186203000	-2.636495000	H	-4.221894000	6.985022000	-2.824558000
H	-4.952046000	6.030361000	-3.282614000	H	-5.332498000	5.755940000	-3.454381000
H	-3.111796000	4.637006000	-5.387513000	H	-3.368208000	4.372820000	-5.467430000
H	-4.232398000	3.855492000	-4.259989000	H	-4.495277000	3.587721000	-4.342800000
H	-2.526305000	3.370255000	-4.302238000	H	-2.772805000	3.168357000	-4.317819000
H	3.764440000	2.181390000	-4.546259000	H	3.598308000	2.331074000	-4.609412000
H	2.737655000	2.469974000	-3.291156000	H	2.567996000	2.612433000	-3.354288000
H	3.105082000	-0.017293000	-4.221025000	H	3.041040000	0.117215000	-4.229409000
H	1.057624000	1.393456000	-6.014209000	H	0.881775000	1.384775000	-5.999472000
H	0.404836000	1.163698000	-3.353969000	H	0.302568000	1.179596000	-3.330418000
H	1.689727000	0.660739000	-2.248443000	H	1.640668000	0.799318000	-2.240133000
H	0.887195000	-0.544601000	-3.280189000	H	0.890221000	-0.491810000	-3.206953000
H	-5.474504000	-1.044886000	4.998076000	H	-5.548645000	-1.278105000	4.975727000
H	-6.395614000	-1.891810000	3.746439000	H	-6.248601000	-2.405222000	3.803716000
H	-4.046142000	-2.776273000	3.880659000	H	-3.773488000	-2.783991000	4.041446000
H	-5.215627000	-4.029568000	4.271709000	H	-4.676790000	-4.204340000	4.539495000
H	-3.777263000	-2.356987000	6.406518000	H	-3.729385000	-2.088384000	6.551032000
H	-4.810589000	-3.736615000	6.694492000	H	-4.400783000	-3.658495000	6.915589000
H	-3.197631000	-5.209645000	5.924679000	H	-2.414456000	-4.708808000	6.360443000
H	-1.506223000	-5.778803000	4.491760000	H	-0.280136000	-4.820602000	5.691594000
H	-0.372272000	-4.553538000	4.016161000	H	0.336636000	-3.573143000	4.693141000
H	-0.698414000	-2.461575000	4.393753000	H	-0.586929000	-1.395510000	4.817311000
H	-1.924244000	-1.891947000	5.527671000	H	-2.275137000	-1.343644000	5.313897000
H	-8.135699000	3.027536000	0.825867000	H	-8.368903000	2.475820000	0.841797000
H	-7.712823000	3.059265000	-1.409588000	H	-7.919312000	2.539525000	-1.391538000
H	-4.957703000	2.833856000	-1.775237000	H	-5.133234000	2.512259000	-1.703352000
H	-5.755236000	4.352577000	-1.332962000	H	-6.082960000	3.972198000	-1.383220000
H	-4.188640000	4.077490000	0.534453000	H	-4.564210000	3.978059000	0.533400000
H	-4.481426000	2.331377000	0.581516000	H	-4.664393000	2.215732000	0.681276000
H	-5.989488000	3.163611000	2.319137000	H	-6.296195000	2.971640000	2.338311000
H	-6.436636000	4.563626000	1.325037000	H	-6.877831000	4.247812000	1.250717000
H	-7.070477000	0.666341000	0.619050000	H	-7.103553000	0.224476000	0.700440000
H	-6.840621000	-1.413720000	-1.538815000	H	-6.796671000	-1.802829000	-1.480311000
H	-9.182655000	-1.047550000	-0.458542000	H	-9.130220000	-1.616620000	-0.344129000
H	-6.024911000	-2.990854000	0.263749000	H	-5.855207000	-3.377092000	0.295329000
H	-5.967613000	-1.628403000	1.393324000	H	-5.821261000	-2.011517000	1.421187000
H	-4.496703000	-0.672796000	-0.346686000	H	-4.438792000	-0.982337000	-0.325186000
H	-4.218258000	1.895606000	8.567264000	H	-3.936404000	2.932208000	8.604825000
H	-6.651405000	-2.287631000	5.448587000	H	-6.465834000	-2.684789000	5.534115000
H	-1.017042000	9.856946000	2.143658000	H	-1.628102000	9.774167000	2.070188000
H	7.985097000	4.583202000	0.233520000	H	7.665099000	5.061187000	0.158582000
H	1.853548000	-8.917884000	-2.747580000	H	2.415335000	-8.795519000	-2.682774000
H	-2.063065000	-7.573003000	2.549983000	H	-1.638211000	-7.842914000	2.405678000
N	-5.318979000	-0.112325000	-5.163713000	N	-5.452744000	-0.521294000	-4.938923000
C	-4.461938000	-1.207993000	-4.659079000	C	-4.431287000	-1.528935000	-4.606937000
C	-5.148176000	-1.725933000	-3.421204000	C	-5.048667000	-2.521499000	-3.649277000
O	-5.921076000	-2.669870000	-3.385708000	O	-5.541796000	-3.587231000	-3.974241000
C	-3.061379000	-0.645524000	-4.358584000	C	-3.199278000	-0.828460000	-4.008461000
C	-2.043723000	-1.681829000	-3.934998000	C	-2.057730000	-1.776254000	-3.719636000
C	-0.967490000	-1.992902000	-4.776111000	C	-1.008882000	-1.924701000	-4.636265000
C	-2.142850000	-2.353502000	-2.704979000	C	-2.040204000	-2.555267000	-2.552453000
C	-0.012819000	-2.942206000	-4.405394000	C	0.032532000	-2.823390000	-4.397567000
C	-1.207315000	-3.324184000	-2.342633000	C	-1.017103000	-3.476948000	-2.322488000
C	-0.134401000	-3.617002000	-3.189315000	C	0.026545000	-3.608915000	-3.242472000
H	-5.529642000	0.531522000	-4.398531000	H	-5.805977000	-0.085899000	-4.085082000
H	-6.217966000	-0.499408000	-5.445234000	H	-6.248939000	-0.978976000	-5.378101000
H	-4.986581000	-1.095671000	-2.531620000	H	-5.101158000	-2.165713000	-2.601335000
H	-3.165895000	0.121796000	-3.581940000	H	-3.511641000	-0.311960000	-3.094705000
H	-0.858766000	-1.470049000	-5.721401000	H	-0.994061000	-1.317957000	-5.536852000

H	-2.948447000	-2.117617000	-2.017026000	H	-2.831420000	-2.441986000	-1.819563000
H	-1.315408000	-3.844544000	-1.397342000	H	-1.038676000	-4.087901000	-1.426281000
H	0.602288000	-4.359589000	-2.898309000	H	0.830997000	-4.314074000	-3.056311000
H	0.827904000	-3.138358000	-5.063496000	H	0.851316000	-2.889455000	-5.106841000
H	-4.415039000	-1.997140000	-5.415332000	H	-4.154718000	-2.063382000	-5.522210000
H	-2.718420000	-0.131718000	-5.260822000	H	-2.887198000	-0.056646000	-4.718097000
H	-2.984493000	-0.379237000	0.889740000	H	-2.900989000	-0.627785000	0.971554000
N	-2.288278000	1.197998000	-1.165283000	N	-2.497487000	1.153694000	-0.981298000
O	-3.434561000	0.726530000	-1.232776000	O	-3.607912000	0.596459000	-0.999717000
O	-1.819705000	1.926926000	-2.038634000	O	-2.184950000	2.020340000	-1.799045000

Int2

C	1.500090000	-3.107772000	1.885288000
C	1.122213000	-3.223687000	0.421848000
C	2.001271000	-2.385736000	-0.515764000
C	3.415165000	-2.272448000	0.057896000
C	3.339458000	-1.416699000	1.324576000
C	2.329996000	-1.934523000	2.367892000
O	1.151394000	-3.963374000	2.682098000
C	1.449102000	-0.743078000	2.985614000
C	0.423420000	-0.240320000	1.967277000
C	-0.838274000	-0.853622000	1.910033000
C	-1.800060000	-0.430354000	1.006310000
C	-1.492321000	0.626520000	0.142768000
C	-0.254150000	1.272859000	0.175717000
C	0.690667000	0.832387000	1.101478000
O	0.903498000	-1.119312000	4.166158000
C	-0.853035000	-7.011315000	2.034630000
C	-1.750651000	-6.102392000	1.263445000
C	-1.986875000	-4.766117000	1.491814000
C	-2.565959000	-6.474180000	0.135196000
N	-2.906122000	-4.284453000	0.576860000
C	-3.279690000	-5.309460000	-0.266922000
C	-2.756856000	-7.672969000	-0.574525000
C	-4.166538000	-5.320666000	-1.348588000
C	-3.631945000	-7.683502000	-1.655616000
C	-4.328574000	-6.516732000	-2.037866000
C	2.496984000	-7.879045000	-1.847036000
C	0.976581000	-7.787005000	-1.636239000
C	3.149232000	-6.532900000	-2.186910000
C	0.183758000	-7.475439000	-2.909127000
N	7.560452000	-5.382828000	-1.150138000
C	6.677374000	-4.569231000	-0.303090000
C	7.531522000	-3.567072000	0.437130000
O	7.584709000	-2.376672000	0.166304000
C	5.896828000	-5.472133000	0.649212000
N	8.193280000	-0.881344000	-2.505295000
C	7.217113000	0.203816000	-2.326927000
C	7.649872000	1.129391000	-1.192163000
O	7.583302000	2.357124000	-1.278762000
C	5.762209000	-0.278478000	-2.079925000
C	4.789655000	0.883548000	-1.851377000
C	5.280465000	-1.171991000	-3.227975000
N	8.031362000	0.513844000	-0.041484000
C	8.177530000	1.260861000	1.195360000
C	9.551720000	1.928442000	1.240699000
O	10.279850000	1.907363000	2.209419000
C	7.967366000	0.371026000	2.422709000
C	6.686728000	-0.390635000	2.366867000
N	6.506287000	-1.589327000	3.033512000
C	5.521862000	-0.177710000	1.681748000
C	5.295902000	-2.094608000	2.765321000
N	4.675254000	-1.241557000	1.944305000
C	6.641716000	5.130995000	0.795102000
C	5.502394000	4.477524000	-0.001096000
C	6.238928000	6.417157000	1.524398000
C	4.463535000	3.766001000	0.872416000
C	-3.813457000	2.816907000	7.325923000
C	-2.585247000	1.899339000	7.359081000
C	-2.965635000	0.496198000	7.847054000
C	-1.908750000	1.843697000	5.981565000
C	-2.961843000	9.355914000	1.891214000
C	-2.892785000	7.997176000	1.259072000

Int2 (with H₂O molecule)

C	1.322429000	-2.987617000	1.754141000
C	1.112427000	-3.079478000	0.261183000
C	2.340221000	-2.654619000	-0.579286000
C	3.590021000	-2.463932000	0.285780000
C	3.284970000	-1.417625000	1.361154000
C	2.213040000	-1.906425000	2.335118000
O	0.787230000	-3.776334000	2.514964000
C	1.386779000	-0.709382000	2.992238000
C	0.353462000	-0.181601000	2.002898000
C	-0.928959000	-0.752194000	1.966117000
C	-1.873602000	-0.324888000	1.044718000
C	-1.527035000	0.689353000	0.146357000
C	-0.266904000	1.292244000	0.159724000
C	0.660822000	0.850103000	1.101431000
O	0.860102000	-1.093293000	4.195542000
C	-0.986892000	-7.037084000	1.802028000
C	-1.879948000	-6.103738000	1.052846000
C	-2.092144000	-4.766842000	1.303004000
C	-2.719103000	-6.447412000	-0.6067098000
N	-3.019587000	-4.259609000	0.411618000
C	-3.421203000	-5.265972000	-0.441448000
C	-2.939016000	-7.631919000	-0.792082000
C	-4.323412000	-5.246617000	-1.509647000
C	-3.829545000	-7.612414000	-1.860587000
C	-4.513694000	-6.429603000	-2.214743000
C	2.282701000	-7.893309000	-2.150056000
C	0.768868000	-7.757837000	-1.916083000
C	2.993551000	-6.547544000	-2.342917000
C	-0.016461000	-7.280245000	-3.141306000
N	7.268300000	-5.471679000	-1.634985000
C	6.555316000	-4.702987000	-0.606939000
C	7.519502000	-3.734344000	0.036921000
O	7.480682000	-2.523373000	-0.120934000
C	5.945274000	-5.649772000	0.425200000
N	8.162815000	-0.953561000	-2.782265000
C	7.163089000	0.098596000	-2.541944000
C	7.601749000	0.981551000	-1.379278000
O	7.577641000	2.211969000	-1.439626000
C	5.719417000	-0.426239000	-2.314778000
C	4.731703000	0.699797000	-1.986476000
C	5.232867000	-1.239930000	-3.518448000
N	7.950777000	0.327219000	-0.238415000
C	8.200598000	1.062474000	0.985028000
C	9.612192000	1.652912000	0.965542000
O	10.331326000	1.712490000	1.939444000
C	7.990911000	0.210445000	2.234891000
C	6.594036000	-0.288854000	2.369500000
N	6.084637000	-0.796116000	3.554482000
C	5.591346000	-0.434890000	1.456550000
C	4.832074000	-1.241624000	3.380343000
N	4.516889000	-1.034009000	2.093991000
C	6.740423000	4.971153000	0.688232000
C	5.583560000	4.378883000	-0.132924000
C	6.376062000	6.249987000	1.450009000
C	4.550371000	3.619297000	0.707080000
C	-3.672230000	2.715959000	7.407766000
C	-2.448074000	1.795806000	7.333454000
C	-2.776202000	0.401919000	7.882785000
C	-1.915422000	1.708446000	5.895331000
C	-2.754126000	9.369889000	2.024751000
C	-2.722372000	8.021643000	1.368087000

C	-3.479842000	7.617910000	0.077176000	C	-3.332846000	7.674794000	0.188070000
C	-2.213901000	6.824402000	1.766178000	C	-2.061702000	6.826781000	1.846349000
N	-3.197044000	6.288553000	-0.192870000	N	-3.081604000	6.344527000	-0.107710000
C	-2.428771000	5.771425000	0.828257000	C	-2.311162000	5.794441000	0.894229000
C	-1.464983000	6.549792000	2.924779000	C	-1.303205000	6.517713000	2.989813000
C	-1.917958000	4.481654000	1.014683000	C	-1.825600000	4.491412000	1.052787000
C	-0.970525000	5.264188000	3.123753000	C	-0.833461000	5.218904000	3.161052000
C	-1.194339000	4.240809000	2.178398000	C	-1.091894000	4.216126000	2.202550000
N	2.065000000	7.262896000	-1.104244000	N	2.164714000	7.239347000	-1.079308000
C	1.973148000	5.840204000	-0.791326000	C	2.063277000	5.808977000	-0.807724000
C	1.042520000	4.961500000	-1.611040000	C	1.099728000	4.966556000	-1.627585000
O	1.145796000	3.725692000	-1.574585000	O	1.178780000	3.728477000	-1.619626000
C	1.586551000	5.732791000	0.696299000	C	1.716037000	5.658902000	0.686084000
O	2.520791000	6.430241000	1.500618000	O	2.681568000	6.316583000	1.486754000
N	0.083313000	5.586815000	-2.322950000	N	0.141040000	5.626369000	-2.308708000
C	-0.901071000	4.817698000	-3.053010000	C	-0.866968000	4.893097000	-3.042995000
C	-0.230193000	4.127955000	-4.243361000	C	-0.225550000	4.222782000	-4.260323000
O	-0.663260000	3.130070000	-4.777797000	O	-0.685515000	3.248351000	-4.333913000
C	-2.102564000	5.692879000	-3.484552000	C	-2.060905000	5.797348000	-3.433388000
C	-3.473499000	4.990655000	-3.386848000	C	-3.441243000	5.115453000	-3.324352000
C	-4.598008000	6.022116000	-3.548328000	C	-4.551253000	6.168117000	-3.443126000
C	-3.662304000	3.835380000	-4.376112000	C	-3.667181000	3.984723000	-4.333974000
N	2.514224000	2.321842000	-4.287213000	N	2.500272000	2.346830000	-4.404700000
C	2.123943000	0.909370000	-4.309941000	C	2.055377000	0.949830000	-4.427764000
C	1.432490000	0.612762000	-5.629574000	C	1.320685000	0.693566000	-5.731978000
O	1.572193000	-0.416424000	-6.264165000	O	1.420682000	-0.325459000	-6.390177000
C	1.128119000	0.615674000	-3.173538000	C	1.082924000	0.686215000	-3.263897000
C	-5.690894000	-2.417454000	4.869554000	C	-5.682149000	-2.403233000	4.806824000
C	-4.306908000	-3.037213000	4.691349000	C	-4.357299000	-3.148448000	4.668827000
C	-3.625275000	-3.249375000	6.047675000	C	-3.686539000	-3.330251000	6.035541000
N	-2.237176000	-3.693833000	5.937814000	N	-2.323602000	-3.850682000	5.945023000
C	-1.236604000	-2.914116000	5.499821000	C	-1.288160000	-3.132749000	5.483828000
N	-0.035493000	-3.442383000	5.212662000	N	-0.108414000	-3.740009000	5.246660000
N	-1.375425000	-1.596747000	5.367429000	N	-1.370973000	-1.822099000	5.294385000
N	-7.502677000	2.073441000	0.728819000	N	-7.475989000	2.207295000	0.785997000
C	-7.210716000	1.968458000	-0.714842000	C	-7.197242000	2.127020000	-0.661908000
C	-6.988424000	0.517090000	-1.148824000	C	-7.004148000	0.680968000	-1.128056000
O	-6.870047000	0.208729000	-2.336469000	O	-6.894706000	0.396111000	-2.322257000
C	-5.939988000	2.835047000	-0.947951000	C	-5.912749000	2.974559000	-0.887709000
C	-5.370616000	3.026801000	0.465497000	C	-5.325501000	3.120708000	0.523946000
C	-6.632467000	3.106545000	1.323524000	C	-6.577176000	3.206509000	1.396345000
N	-6.939714000	-0.368287000	-0.126117000	N	-6.969782000	-0.226732000	-0.124200000
C	-6.894128000	-1.803285000	-0.310606000	C	-6.954346000	-1.658266000	-0.338847000
C	-8.224397000	-2.415458000	0.116701000	C	-8.297603000	-2.251425000	0.073995000
O	-8.324704000	-3.445016000	0.748500000	O	-8.419840000	-3.290358000	0.686289000
C	-5.720423000	-2.437538000	0.424475000	C	-5.795022000	-2.332194000	0.383522000
O	-4.478887000	-2.072869000	-0.167147000	O	-4.545182000	-1.971125000	-0.191594000
H	2.849140000	-2.296270000	3.255785000	H	2.688962000	-2.401882000	3.179946000
H	1.184055000	-4.288121000	0.174994000	H	0.801315000	-4.104075000	0.049108000
H	0.065196000	-2.956135000	0.328930000	H	0.250897000	-2.444357000	0.026199000
H	1.581241000	-1.382880000	-0.646564000	H	2.130220000	-1.721555000	-1.111871000
H	2.025571000	-2.840460000	-1.506985000	H	2.540915000	-3.408512000	-1.343401000
H	3.807540000	-3.268427000	0.294454000	H	3.877279000	-3.404828000	0.769693000
H	4.097986000	-1.812394000	-0.655817000	H	4.430644000	-2.146935000	-0.333541000
H	3.056326000	-0.407497000	1.020227000	H	2.953303000	-0.502657000	0.861784000
H	2.197806000	0.067829000	3.100336000	H	2.140123000	0.091893000	3.115414000
H	-1.062285000	-1.660030000	2.597477000	H	-1.181610000	-1.536408000	2.668068000
H	-0.035612000	2.098295000	-0.493066000	H	-0.019972000	2.088254000	-0.534554000
H	1.642604000	1.351874000	1.159406000	H	1.632280000	1.333687000	1.141326000
H	-0.134718000	-7.517466000	1.378079000	H	-0.281425000	-7.544681000	1.132786000
H	-0.281941000	-6.454708000	2.783025000	H	-0.402714000	-6.499429000	2.554615000
H	-1.552443000	-4.117794000	2.238633000	H	-1.625937000	-4.132968000	2.042371000
H	-3.244942000	-3.331900000	0.491118000	H	-3.341884000	-3.299254000	0.349439000
H	-2.222798000	-8.573824000	-0.285781000	H	-2.414305000	-8.545102000	-0.525588000
H	-4.701614000	-4.432165000	-1.652143000	H	-4.849767000	-4.345995000	-1.792926000
H	-3.783182000	-8.601015000	-2.216504000	H	-4.002516000	-8.518668000	-2.433453000
H	-4.990840000	-6.540775000	-2.890768000	H	-5.196806000	-6.431074000	-3.058044000
H	2.960581000	-8.277837000	-0.935658000	H	2.732178000	-8.411965000	-1.293762000
H	0.763380000	-7.020518000	-0.877559000	H	0.593910000	-7.065948000	-1.080032000
H	0.615794000	-8.734818000	-1.216896000	H	0.368470000	-8.727640000	-1.594427000
H	4.236645000	-6.624644000	-2.282716000	H	4.074596000	-6.674133000	-2.465871000
H	2.944836000	-5.793404000	-1.402075000	H	2.831471000	-5.897815000	-1.473346000
H	2.770792000	-6.125083000	-3.129931000	H	2.622774000	-6.015761000	-3.225464000
H	0.460536000	-6.507851000	-3.337367000	H	0.297296000	-6.284161000	-3.466232000
H	-0.889731000	-7.446627000	-2.701881000	H	-1.086979000	-7.231793000	-2.922242000
H	0.362169000	-8.239299000	-3.675082000	H	0.126864000	-7.964339000	-3.986015000
H	8.218953000	-5.916939000	-0.586160000	H	8.016234000	-6.026305000	-1.222843000

H	8.101234000	-4.800379000	-1.784786000	H	7.688516000	-4.857657000	-2.328381000
H	5.996516000	-4.011530000	-0.954576000	H	5.773639000	-4.116867000	-1.100633000
H	8.192154000	-3.993089000	1.220886000	H	8.335417000	-4.198225000	0.628875000
H	5.348045000	-6.219326000	0.071198000	H	5.264226000	-6.342422000	-0.075009000
H	5.181566000	-4.901989000	1.248356000	H	5.391459000	-5.099719000	1.191437000
H	6.572792000	-5.994546000	1.335213000	H	6.725536000	-6.233803000	0.925451000
H	7.938580000	-1.671728000	-1.916325000	H	7.946615000	-1.769466000	-2.213596000
H	8.153710000	-1.215511000	-3.463168000	H	8.104609000	-1.258850000	-3.748942000
H	7.233890000	0.829033000	-1.225034000	H	7.159414000	0.764354000	-3.410576000
H	5.806974000	-0.889020000	-1.168589000	H	5.784693000	-1.112441000	-1.460621000
H	4.708197000	1.509140000	-2.745353000	H	4.628514000	1.388125000	-2.830976000
H	5.098605000	1.536929000	-1.032636000	H	5.037039000	1.297343000	-1.123676000
H	3.787289000	0.507153000	-1.625526000	H	3.739449000	0.288373000	-1.777428000
H	5.921947000	-2.047623000	-3.357652000	H	5.891565000	-2.087248000	-3.727081000
H	5.268868000	-0.616817000	-4.173000000	H	5.187413000	-0.615189000	-4.418029000
H	4.262959000	-1.530277000	-3.041397000	H	4.229345000	-1.636527000	-3.334487000
H	8.129611000	-0.494110000	-0.010124000	H	8.057922000	-0.681285000	-0.231081000
H	7.446130000	2.080776000	1.173209000	H	7.517998000	1.923459000	0.992929000
H	9.834377000	2.434158000	0.298415000	H	9.929447000	2.029511000	-0.025363000
H	8.009456000	0.996874000	3.318961000	H	8.269744000	0.810929000	3.104478000
H	8.799714000	-0.335708000	2.504249000	H	8.680441000	-0.643065000	2.217875000
H	7.187585000	-2.033616000	3.636504000	H	6.570301000	-0.818454000	4.442084000
H	5.225195000	0.625968000	1.030736000	H	5.561050000	-0.184874000	0.414938000
H	4.902969000	-3.018394000	3.153990000	H	4.196277000	-1.637124000	4.175805000
H	7.034673000	4.405243000	1.521670000	H	7.103359000	4.212511000	1.396472000
H	5.935186000	3.762021000	-0.703598000	H	5.996725000	3.702706000	-0.884456000
H	5.008492000	5.252206000	-0.603464000	H	5.089704000	5.195655000	-0.676897000
H	5.924859000	7.183958000	0.806603000	H	6.115474000	7.052667000	0.750250000
H	7.071427000	6.824970000	2.107091000	H	7.209505000	6.601606000	2.067054000
H	5.398692000	6.249861000	2.205608000	H	5.510044000	6.098171000	2.102172000
H	3.686451000	3.296644000	0.257667000	H	3.739253000	3.233200000	0.078485000
H	3.968903000	4.461908000	1.554323000	H	4.100014000	4.263366000	1.466724000
H	4.937689000	2.979921000	1.474461000	H	5.016527000	2.762863000	1.211136000
H	-3.543870000	3.829999000	7.009440000	H	-3.435582000	3.722024000	7.045696000
H	-4.561517000	2.434759000	6.620206000	H	-4.488807000	2.322204000	6.789884000
H	-1.863507000	2.320275000	8.072727000	H	-1.656481000	2.228536000	7.960912000
H	-3.702034000	0.042635000	7.169085000	H	-3.579557000	-0.061619000	7.293934000
H	-3.421174000	0.527250000	8.842166000	H	-3.122185000	0.450217000	8.920491000
H	-2.091496000	-0.161870000	7.899683000	H	-1.902372000	-0.258077000	7.850315000
H	-0.993873000	1.241739000	6.007327000	H	-1.007887000	1.097200000	5.839895000
H	-1.641089000	2.844536000	5.625767000	H	-1.677260000	2.699338000	5.493245000
H	-2.584652000	1.405195000	5.235180000	H	-2.667013000	1.261074000	5.230924000
H	-3.560849000	10.039548000	1.283611000	H	-3.346908000	10.076690000	1.437901000
H	-3.411847000	9.312336000	2.890237000	H	-3.191146000	9.317768000	3.029115000
H	-4.085619000	8.197787000	-0.604677000	H	-3.935073000	8.278529000	-0.475966000
H	-3.576288000	5.759265000	-0.960452000	H	-3.481627000	5.836119000	-0.878795000
H	-1.280912000	7.330200000	3.657546000	H	-1.092811000	7.282005000	3.732411000
H	-2.081572000	3.704736000	0.276436000	H	-2.015257000	3.731053000	0.303662000
H	-0.392980000	5.043312000	4.016401000	H	-0.249089000	4.971067000	4.042094000
H	-0.785176000	3.250597000	2.353846000	H	-0.701537000	3.215034000	2.356598000
H	2.419395000	7.443646000	-2.037355000	H	2.501364000	7.444855000	-2.013842000
H	1.181939000	7.751335000	-0.979718000	H	1.290584000	7.733740000	-0.920309000
H	2.969285000	5.407730000	-0.911911000	H	3.050359000	5.368851000	-0.968514000
H	0.569744000	6.131196000	0.829108000	H	0.708871000	6.066544000	0.859161000
H	1.576036000	4.687149000	1.006500000	H	1.699110000	4.603778000	0.962228000
H	2.760104000	7.215384000	0.979313000	H	2.916034000	7.116554000	0.986370000
H	0.079543000	6.594512000	-2.375040000	H	0.156766000	6.634889000	-2.337927000
H	-1.255465000	4.018293000	-2.395664000	H	-1.224417000	4.082726000	-2.400630000
H	0.699773000	4.615538000	-4.598804000	H	0.709385000	4.701500000	-4.615317000
H	-1.957726000	6.079503000	-4.501041000	H	-1.928759000	6.202556000	-4.444303000
H	-2.120081000	6.565365000	-2.821499000	H	-2.051175000	6.655956000	-2.752390000
H	-3.540842000	4.545065000	-2.382461000	H	-3.497380000	4.649884000	-2.328261000
H	-4.573393000	6.461022000	-4.552021000	H	-4.538419000	6.626953000	-4.438081000
H	-4.513487000	6.845728000	-2.830469000	H	-4.439144000	6.975401000	-2.710644000
H	-5.577756000	5.553847000	-3.413078000	H	-5.535999000	5.713368000	-3.298341000
H	-3.580071000	4.193654000	-5.408961000	H	-3.599175000	4.363908000	-5.360347000
H	-4.656512000	3.394315000	-4.250443000	H	-4.665597000	3.556310000	-4.198297000
H	-2.916219000	3.053795000	-4.233023000	H	-2.930873000	3.188871000	-4.222400000
H	3.466329000	2.446459000	-4.614474000	H	3.448864000	2.437116000	-4.752920000
H	2.442336000	2.705345000	-3.348759000	H	2.465457000	2.723792000	-3.461620000
H	2.972299000	0.218438000	-4.221575000	H	2.879727000	0.227315000	-4.368472000
H	0.755638000	1.424826000	-5.964381000	H	0.654629000	1.526939000	-6.033725000
H	0.217467000	1.208573000	-3.289409000	H	0.185353000	1.302560000	-3.356341000
H	1.582302000	0.884441000	-2.215451000	H	1.570465000	0.946948000	-2.320061000
H	0.859663000	-0.441441000	-3.156456000	H	0.787517000	-0.363204000	-3.235239000
H	-5.623451000	-1.430441000	5.339969000	H	-5.527034000	-1.394856000	5.206003000
H	-6.195309000	-2.295163000	3.906528000	H	-6.183373000	-2.307185000	3.839330000

H	-3.684729000	-2.387627000	4.065066000	H	-3.686750000	-2.596181000	4.000463000
H	-4.375455000	-3.999495000	4.171665000	H	-4.509999000	-4.132795000	4.212588000
H	-3.659502000	-2.333127000	6.647765000	H	-3.669399000	-2.385734000	6.590833000
H	-4.154863000	-4.008419000	6.627152000	H	-4.253154000	-4.030787000	6.652268000
H	-2.049724000	-4.682295000	6.004422000	H	-2.194690000	-4.847221000	6.028694000
H	0.002291000	-4.404319000	4.912133000	H	-0.126997000	-4.730461000	5.054833000
H	0.589180000	-2.783470000	4.712400000	H	0.538413000	-3.213514000	4.662687000
H	-0.590512000	-1.103786000	4.878943000	H	-0.553626000	-1.342271000	4.823209000
H	-2.214533000	-1.122984000	5.651114000	H	-2.207864000	-1.319383000	5.533592000
H	-8.485309000	2.258057000	0.897929000	H	-8.452601000	2.411726000	0.966650000
H	-8.034766000	2.330649000	-1.339848000	H	-8.019632000	2.516811000	-1.272238000
H	-5.236701000	2.360983000	-1.633517000	H	-5.226671000	2.503799000	-1.592860000
H	-6.233545000	3.800515000	-1.371178000	H	-6.191668000	3.955700000	-1.283903000
H	-4.742923000	3.914950000	0.560876000	H	-4.678006000	3.992941000	0.633713000
H	-4.776634000	2.154434000	0.754739000	H	-4.747416000	2.229483000	0.786800000
H	-6.449739000	2.891821000	2.381090000	H	-6.388868000	2.962312000	2.446512000
H	-7.073567000	4.112325000	1.253350000	H	-6.996846000	4.222926000	1.354904000
H	-7.120046000	0.058001000	0.783673000	H	-7.139707000	0.184203000	0.794674000
H	-6.798093000	-1.970425000	-1.391110000	H	-6.860515000	-1.804313000	-1.422526000
H	-9.113208000	-1.828479000	-0.194845000	H	-9.173767000	-1.641139000	-0.228422000
H	-5.794994000	-3.523868000	0.365646000	H	-5.886556000	-3.415243000	0.294408000
H	-5.748836000	-2.153414000	1.484875000	H	-5.823812000	-2.077115000	1.451160000
H	-4.414107000	-1.106780000	-0.257848000	H	-4.469106000	-1.004914000	-0.268826000
H	-4.287564000	2.884291000	8.310840000	H	-4.043193000	2.803915000	8.434439000
H	-6.329781000	-3.045350000	5.499812000	H	-6.366130000	-2.928516000	5.482042000
H	-1.965419000	9.798148000	2.010640000	H	-1.747062000	9.789082000	2.137847000
H	7.471835000	5.351066000	0.112624000	H	7.583079000	5.181973000	0.018266000
H	2.709760000	-8.603827000	-2.643954000	H	2.458830000	-8.532539000	-3.025337000
H	-1.416248000	-7.798486000	2.551619000	H	-1.556332000	-7.823309000	2.313716000
N	-5.524960000	-0.712358000	-4.832272000	N	-5.651477000	-0.527583000	-4.879729000
C	-4.443556000	-1.661070000	-4.529740000	C	-4.567117000	-1.479057000	-4.593651000
C	-5.007166000	-2.767569000	-3.666072000	C	-5.122685000	-2.581091000	-3.719503000
O	-5.330618000	-3.870830000	-4.066847000	O	-5.487270000	-3.671007000	-4.122027000
C	-3.283638000	-0.923740000	-3.838265000	C	-3.395241000	-0.741112000	-3.924975000
C	-2.088370000	-1.820310000	-3.614639000	C	-2.205410000	-1.641441000	-3.687017000
C	-1.045534000	-1.863024000	-4.548588000	C	-1.163930000	-1.711417000	-4.620653000
C	-2.029082000	-2.675867000	-2.504996000	C	-2.145036000	-2.466481000	-2.554681000
C	0.031790000	-2.734987000	-4.381686000	C	-0.081546000	-2.571497000	-4.425248000
C	-0.970027000	-3.571605000	-2.348234000	C	-1.080490000	-3.349753000	-2.368505000
C	0.067077000	-3.598489000	-3.284275000	C	-0.038271000	-3.395177000	-3.297947000
H	-5.920166000	-0.335900000	-3.969181000	H	-6.027339000	-0.147952000	-4.009453000
H	-6.279351000	-1.195084000	-5.315684000	H	-6.416421000	-1.009995000	-5.346549000
H	-5.185553000	-2.466540000	-2.612993000	H	-5.257406000	-2.290160000	-2.657191000
H	-3.646850000	-0.517196000	-2.888091000	H	-3.747635000	-0.312094000	-2.980425000
H	-1.067202000	-1.198799000	-5.407602000	H	-1.187519000	-1.074137000	-5.499745000
H	-2.820058000	-2.644160000	-1.764485000	H	-2.937910000	-2.420149000	-1.817026000
H	-0.963012000	-4.249455000	-1.501211000	H	-1.074404000	-4.001092000	-1.501533000
H	0.897859000	-4.285655000	-3.157201000	H	0.800715000	-4.066550000	-3.144219000
H	0.844291000	-2.719940000	-5.100862000	H	0.731403000	-2.573558000	-5.144070000
H	-4.094366000	-2.108819000	-5.466579000	H	-4.236134000	-1.930420000	-5.535362000
H	-3.016974000	-0.070155000	-4.468791000	H	-3.124018000	0.097352000	-4.573488000
H	-2.766666000	-0.910252000	0.966869000	H	-2.854137000	-0.776976000	1.015240000
N	-2.501067000	1.081725000	-0.796082000	N	-2.516300000	1.146300000	-0.814363000
O	-3.612237000	0.526672000	-0.796047000	O	-3.636650000	0.611408000	-0.818580000
O	-2.232582000	2.010927000	-1.558838000	O	-2.220418000	2.057012000	-1.588414000
				O	2.869398000	-2.065615000	5.514367000
				H	2.054267000	-1.627327000	5.109174000
				H	2.987336000	-1.658770000	6.381931000

TS3 (with H₂O molecule)

C	1.252542000	-3.120875000	1.589714000
C	1.608465000	-3.929824000	0.358214000
C	2.539776000	-3.189160000	-0.595513000
C	3.731760000	-2.672100000	0.199306000
C	3.279821000	-1.619299000	1.215709000
C	2.122089000	-2.066954000	2.094786000
O	0.242707000	-3.455439000	2.229910000
C	1.422211000	-0.861254000	2.801532000
C	0.363038000	-0.239210000	1.917785000
C	-0.946554000	-0.747111000	1.879912000
C	-1.880732000	-0.239201000	0.990748000
C	-1.504519000	0.797440000	0.132404000
C	-0.221339000	1.350032000	0.158943000
C	0.700859000	0.823015000	1.061082000

Int3

C	1.439554000	-2.904352000	2.375676000
C	1.799472000	-4.088668000	1.499267000
C	2.364144000	-3.643841000	0.149873000
C	3.547286000	-2.708017000	0.372496000
C	3.146061000	-1.473774000	1.209916000
C	2.003786000	-1.677864000	2.146655000
O	0.550408000	-3.122654000	3.311295000
C	1.479761000	-0.416079000	2.819207000
C	0.378521000	0.119402000	1.918489000
C	-0.918449000	-0.422136000	1.964231000
C	-1.877872000	-0.049040000	1.038025000
C	-1.537223000	0.890064000	0.056244000
C	-0.269585000	1.473818000	0.001408000
C	0.678833000	1.080958000	0.940713000

O	0.889512000	-1.207904000	4.077652000	O	1.061048000	-0.635653000	4.163707000
C	-1.164811000	-7.029533000	1.540979000	C	-1.081165000	-7.116798000	1.585753000
C	-2.104387000	-6.163638000	0.755769000	C	-1.890062000	-6.049964000	0.920578000
C	-2.189716000	-4.788057000	0.769527000	C	-1.964976000	-4.705363000	1.221168000
C	-3.095638000	-6.621100000	-0.185325000	C	-2.785429000	-6.271735000	-0.185299000
N	-3.168079000	-4.363348000	-0.112024000	N	-2.858960000	-4.083244000	0.366770000
C	-3.742503000	-5.463823000	-0.712778000	C	-3.375318000	-5.017366000	-0.504720000
C	-3.484501000	-7.891014000	-0.646734000	C	-3.132024000	-7.405432000	-0.942486000
C	-4.753743000	-5.550172000	-1.676755000	C	-4.293173000	-4.875250000	-1.830762000
C	-4.491738000	-7.981249000	-1.600781000	C	-4.039086000	-7.265173000	-1.986523000
C	-5.116671000	-6.822352000	-2.109199000	C	-4.613909000	-6.010640000	-2.284562000
C	2.113371000	-7.806047000	-2.421114000	C	2.267307000	-7.884701000	-2.318190000
C	0.761413000	-7.529090000	-1.745604000	C	0.897515000	-7.383721000	-1.830762000
C	3.061872000	-6.602020000	-2.405624000	C	3.180001000	-6.769322000	-2.839984000
C	-0.092001000	-6.472246000	-2.451903000	C	0.004253000	-6.813706000	-2.936666000
N	7.166589000	-5.401940000	-1.845486000	N	7.509536000	-5.518805000	-1.431813000
C	6.449153000	-4.784069000	-0.721098000	C	6.549687000	-4.818652000	-0.564570000
C	7.389245000	-3.821635000	-2.036023000	C	7.331894000	-3.861259000	0.304198000
O	7.296047000	-2.605389000	-0.107784000	O	7.381910000	-2.654298000	0.120227000
C	5.956588000	-5.864763000	0.238747000	C	5.762886000	-5.836368000	0.257582000
N	8.142516000	-1.008188000	-2.737695000	N	8.208880000	-1.079375000	-2.521868000
C	7.185743000	0.074227000	-2.459894000	C	7.274467000	0.038130000	-2.312658000
C	7.661406000	0.897598000	-1.266730000	C	7.723077000	0.874546000	-1.118622000
O	7.715630000	2.129007000	-1.292230000	O	7.765928000	2.105620000	-1.151181000
C	5.721432000	-0.390979000	-2.233875000	C	5.790809000	-0.393520000	-2.148527000
C	4.782781000	0.779896000	-1.919009000	C	4.865425000	0.797660000	-1.873605000
C	5.200095000	-1.198492000	-3.426476000	C	5.309044000	-1.185162000	-3.368899000
N	7.951593000	0.191274000	-0.141315000	N	8.001913000	0.175907000	0.015344000
C	8.217974000	0.873015000	1.109510000	C	8.243245000	0.860572000	1.269358000
C	9.660612000	1.381779000	1.126940000	C	9.706576000	1.294305000	1.350291000
O	10.382182000	1.332397000	2.099722000	O	10.387848000	1.196823000	2.348043000
C	7.944206000	0.002148000	2.332385000	C	7.860527000	0.016571000	2.484231000
C	6.553778000	-0.530036000	2.386478000	C	6.435988000	-0.425845000	2.480083000
N	6.131916000	-1.374156000	3.402817000	N	5.858287000	-1.065856000	3.566411000
C	5.495850000	-0.443119000	1.528351000	C	5.471614000	-0.422262000	1.509607000
C	4.883934000	-1.803506000	3.172921000	C	4.606866000	-1.446149000	3.268397000
N	4.476307000	-1.240543000	2.028373000	N	4.357937000	-1.063777000	2.015468000
C	6.852543000	4.825744000	0.955508000	C	6.848861000	4.799689000	1.078665000
C	5.692500000	4.280886000	0.108245000	C	5.712970000	4.254633000	0.199435000
C	6.512556000	6.081810000	1.764832000	C	6.485964000	6.056462000	1.876880000
C	4.623387000	3.541146000	0.920321000	C	4.629714000	3.501445000	0.979995000
C	-3.928296000	1.979867000	7.651071000	C	-3.981067000	1.994978000	7.645064000
C	-2.460524000	1.611766000	7.405927000	C	-2.539702000	1.537323000	7.393628000
C	-2.342408000	0.199279000	6.812917000	C	-2.513316000	0.161034000	6.709364000
C	-1.777823000	2.639149000	6.492383000	C	-1.770361000	2.570270000	6.558412000
C	-2.545352000	9.394736000	2.399884000	C	-2.607587000	9.297775000	2.352661000
C	-2.542702000	8.073866000	1.689072000	C	-2.601564000	7.988050000	1.622940000
C	-3.149206000	7.793103000	0.489623000	C	-3.181937000	7.727109000	0.406231000
C	-1.919725000	6.842444000	2.123609000	C	-2.001869000	6.746183000	2.058647000
N	-2.929827000	6.470273000	0.140480000	N	-2.966067000	6.406079000	0.046592000
C	-2.185604000	5.858055000	1.126260000	C	-2.254315000	5.775611000	1.044863000
C	-1.183797000	6.464659000	3.261330000	C	-1.298884000	6.349485000	3.210444000
C	-1.735257000	4.537225000	1.233849000	C	-1.823123000	4.448866000	1.151654000
C	-0.751083000	5.147499000	3.382703000	C	-0.886620000	5.025669000	3.330583000
C	-1.023066000	4.193853000	2.378789000	C	-1.146128000	4.084898000	2.311569000
N	2.347302000	7.271292000	-0.750406000	N	2.334322000	7.207289000	-0.675809000
C	2.208288000	5.833815000	-0.538336000	C	2.221351000	5.763548000	-0.493627000
C	1.238851000	5.049585000	-1.407242000	C	1.299477000	4.974736000	-1.408412000
O	1.297924000	3.811604000	-1.460963000	O	1.402814000	3.741184000	-1.499533000
C	1.829886000	5.633997000	0.942223000	C	1.793578000	5.528879000	0.968957000
O	2.793601000	6.240706000	1.784292000	O	2.712100000	6.141879000	1.855743000
N	0.294486000	5.757574000	-2.058927000	N	0.341521000	5.666380000	-2.054532000
C	-0.725154000	5.077557000	-2.828305000	C	-0.668922000	4.973420000	-2.826811000
C	-0.091636000	4.445337000	-4.069813000	C	-0.016756000	4.307150000	-4.039371000
O	-0.574411000	3.511229000	-4.672512000	O	-0.483528000	3.347942000	-4.614521000
C	-1.894265000	6.025965000	-3.188431000	C	-1.807528000	5.938143000	-3.239575000
C	-3.292011000	5.374808000	-3.121908000	C	-3.218596000	5.313879000	-3.239173000
C	-4.373922000	6.460215000	-3.200943000	C	-4.273545000	6.422721000	-3.354375000
C	-3.538072000	4.298868000	-4.185274000	C	-3.439848000	4.254413000	-4.324280000
N	2.593167000	2.508011000	-4.278572000	N	2.658687000	2.434104000	-4.215658000
C	2.113703000	1.123049000	-4.348153000	C	2.225890000	1.035871000	-4.283789000
C	1.403309000	0.933747000	-5.677272000	C	1.535841000	0.797116000	-5.615842000
O	1.565961000	-0.023250000	-6.412901000	O	1.669004000	-0.207176000	-6.289771000
C	1.112314000	0.857225000	-3.211808000	C	1.211366000	0.732249000	-3.167565000
C	-5.772554000	-2.407193000	4.695402000	C	-5.776083000	-2.518856000	4.645499000
C	-4.613434000	-3.369029000	4.451717000	C	-4.866609000	-3.703876000	4.329317000
C	-3.862381000	-3.682432000	5.752021000	C	-4.177948000	-4.223646000	5.602013000

N	-2.627014000	-4.434888000	5.519752000	N	-2.969935000	-5.004492000	5.329353000
C	-1.540834000	-3.900764000	4.944360000	C	-1.843240000	-4.452469000	4.869055000
N	-0.532512000	-4.694609000	4.531716000	N	-0.794717000	-5.203452000	4.503819000
N	-1.421705000	-2.583784000	4.804341000	N	-1.712285000	-3.125111000	4.796116000
N	-7.425901000	2.397504000	0.848006000	N	-7.457405000	2.236337000	0.740150000
C	-7.136850000	2.370873000	-0.600059000	C	-7.094245000	2.225250000	-0.691713000
C	-6.964545000	0.940375000	-1.122218000	C	-6.876672000	0.799742000	-1.220723000
O	-6.844624000	0.702493000	-2.325437000	O	-6.645914000	0.567965000	-2.409331000
C	-5.834999000	3.201095000	-0.781577000	C	-5.798468000	3.073648000	-0.498573000
C	-5.245918000	3.255328000	0.635448000	C	-5.260681000	3.084224000	0.635107000
C	-6.496477000	3.334250000	1.510283000	C	-6.542427000	3.141562000	1.466193000
N	-6.959584000	-0.007520000	-0.154518000	N	-6.966580000	-0.148366000	-0.259046000
C	-6.985087000	-1.428991000	-0.426246000	C	-6.914921000	-1.572259000	-0.498573000
C	-8.346035000	-1.998880000	-0.040510000	C	-8.280002000	-2.190028000	-0.215541000
O	-8.500993000	-3.059118000	0.526268000	O	-8.441865000	-3.241473000	0.365751000
C	-5.847261000	-2.172576000	0.269753000	C	-5.818119000	-2.237334000	0.331674000
O	-4.578001000	-1.816558000	-0.264959000	O	-4.521249000	-1.821619000	-0.080132000
H	2.494295000	-2.712374000	3.166938000	H	2.515812000	-4.736739000	2.024488000
H	2.091526000	-4.852342000	0.710940000	H	0.885460000	-4.673922000	1.361026000
H	0.668366000	-4.241971000	-0.104292000	H	1.583963000	-3.131126000	-0.423246000
H	2.014458000	-2.353526000	-1.073519000	H	2.682071000	-4.507885000	-0.442390000
H	2.875628000	-3.852585000	-1.396323000	H	4.328415000	-3.248745000	0.915620000
H	4.199116000	-3.499702000	0.744271000	H	3.985165000	-2.384604000	-0.575479000
H	4.493927000	-2.242646000	-0.451123000	H	2.970727000	-0.614828000	0.551543000
H	3.022036000	-0.702597000	0.673126000	H	2.271411000	0.338858000	2.860432000
H	2.206582000	-0.108882000	2.952160000	H	-1.164309000	-1.159217000	2.716479000
H	-1.227666000	-1.561060000	2.529615000	H	-0.023105000	2.215250000	-0.748297000
H	0.050586000	2.167964000	-0.499152000	H	1.665970000	1.532239000	0.907261000
H	1.695705000	1.256275000	1.101088000	H	-0.640692000	-7.793751000	0.846193000
H	-0.667424000	-7.763659000	0.897989000	H	-0.252795000	-6.698233000	2.164638000
H	-0.385782000	-6.425369000	2.015923000	H	-1.428845000	-4.130681000	1.963124000
H	-1.592731000	-4.081712000	1.327044000	H	-3.156315000	-3.113533000	0.387223000
H	-3.459040000	-3.400232000	-0.247153000	H	-2.691972000	-8.373097000	-0.718261000
H	-3.002654000	-8.786579000	-0.263835000	H	-4.735574000	-3.920249000	-1.789739000
H	-5.2114141000	-4.666364000	-2.105979000	H	-4.310889000	-8.130641000	-2.583477000
H	-4.801152000	-8.955842000	-1.966915000	H	-5.315976000	-5.919908000	-3.107647000
H	-5.892844000	-6.923206000	-2.862149000	H	2.771956000	-8.401884000	-1.492077000
H	2.598570000	-8.649651000	-1.914282000	H	1.048645000	-6.620606000	-1.053817000
H	0.942100000	-7.214943000	-0.708611000	H	0.369702000	-8.212853000	-1.342351000
H	0.192947000	-8.465887000	-1.685353000	H	4.161596000	-7.157904000	-3.130637000
H	4.045285000	-6.853521000	-2.815931000	H	3.341503000	-6.005266000	-2.069812000
H	3.211586000	-6.243765000	-1.380080000	H	2.750850000	-6.268225000	-3.713343000
H	2.665079000	-5.767251000	-2.992496000	H	0.458517000	-5.945396000	-3.422143000
H	0.396429000	-5.494490000	-2.455162000	H	-0.962506000	-6.498907000	-2.534118000
H	-1.059672000	-6.354592000	-1.957515000	H	-0.183339000	-7.566794000	-3.7111059000
H	-0.275398000	-6.749422000	-3.496646000	H	8.160772000	-6.073922000	-0.879705000
H	7.975955000	-5.927356000	-1.520440000	H	8.057743000	-4.862393000	-1.982294000
H	7.498497000	-4.699491000	-2.501836000	H	5.880825000	-4.228634000	-1.199626000
H	5.612345000	-4.212650000	-1.130190000	H	7.949668000	-4.333941000	1.095788000
H	8.245475000	-4.290592000	0.491444000	H	5.263395000	-6.536997000	-0.415654000
H	5.333028000	-6.576506000	-0.306357000	H	5.008357000	-5.351788000	0.882559000
H	5.372240000	-5.436254000	1.057989000	H	6.431134000	-6.405639000	0.913179000
H	6.800918000	-6.410107000	0.674718000	H	7.909882000	-1.879857000	-1.968015000
H	7.920901000	-1.818280000	-2.163045000	H	8.166511000	-1.375531000	-3.492271000
H	8.035150000	-1.310069000	-3.701572000	H	7.350714000	0.710181000	-3.172899000
H	7.209096000	0.766444000	-3.307281000	H	5.767625000	-1.075936000	-1.288449000
H	5.755813000	-1.063027000	-1.368913000	H	4.837736000	1.476437000	-2.731232000
H	4.696167000	1.455206000	-2.775815000	H	5.178625000	1.391416000	-1.011438000
H	5.125001000	1.384205000	-1.074770000	H	3.841939000	0.455270000	-1.694103000
H	3.777238000	0.414066000	-1.688309000	H	5.921210000	-2.074416000	-3.541494000
H	5.816003000	-2.081491000	-3.618061000	H	5.343266000	-0.567760000	-4.273972000
H	5.187381000	-0.588709000	-4.337353000	H	4.275184000	-1.516400000	-3.228169000
H	4.177388000	-1.541724000	-3.239483000	H	8.032438000	-0.837326000	0.006479000
H	7.954578000	-0.823180000	-0.148163000	H	7.656409000	1.789070000	1.246303000
H	7.586837000	1.772699000	1.132065000	H	10.103148000	1.708202000	0.403184000
H	9.999534000	1.804000000	0.162145000	H	8.080427000	0.596636000	3.384833000
H	8.169177000	0.592610000	3.225232000	H	8.504814000	-0.870411000	2.527893000
H	8.644202000	-0.842464000	2.343388000	H	6.299568000	-1.209162000	4.465693000
H	6.674618000	-1.624329000	4.219264000	H	5.491190000	-0.044158000	0.507286000
H	5.391763000	0.083114000	0.598351000	H	3.915393000	-1.960208000	3.914736000
H	4.290189000	-2.461544000	3.810548000	H	7.176570000	4.009645000	1.769793000
H	7.199868000	4.035145000	1.636292000	H	6.143580000	3.586905000	-0.550662000
H	6.101562000	3.605194000	-0.646983000	H	5.260563000	5.093418000	-0.347473000
H	5.231826000	5.118303000	-0.433687000	H	6.252913000	6.887597000	1.201026000
H	6.257324000	6.912735000	1.096726000	H	7.310914000	6.372288000	2.523775000
H	7.357106000	6.398568000	2.385478000	H	5.604429000	5.895291000	2.505937000
H	5.651248000	5.919645000	2.420713000	H	3.842870000	3.139196000	0.308104000

H	3.817882000	3.177527000	0.271534000	H	4.155567000	4.142085000	1.727866000
H	4.171513000	4.192017000	1.672983000	H	5.057457000	2.630339000	1.491951000
H	5.057413000	2.672770000	1.432115000	H	-4.007177000	2.963399000	8.155801000
H	-4.018275000	2.975141000	8.098774000	H	-4.522209000	2.103010000	6.696935000
H	-4.487033000	1.986812000	6.706986000	H	-2.036163000	1.440981000	8.365648000
H	-1.939535000	1.614783000	8.373284000	H	-3.007355000	0.212634000	5.729917000
H	-2.854835000	0.156976000	5.841580000	H	-3.035162000	-0.592946000	7.309963000
H	-2.799548000	-0.548082000	7.471671000	H	-1.485056000	-0.182670000	6.548832000
H	-1.293802000	-0.077941000	6.657471000	H	-0.731696000	2.259550000	6.399752000
H	-0.721294000	2.394013000	6.337211000	H	-1.758354000	3.549811000	7.048311000
H	-1.831271000	3.647160000	6.917029000	H	-2.233988000	2.698244000	5.572288000
H	-2.261208000	2.668011000	5.507939000	H	-3.153487000	10.058331000	1.787867000
H	-3.113273000	10.140388000	1.837003000	H	-3.081015000	9.206730000	3.337583000
H	-2.993658000	9.313801000	3.397354000	H	-3.739076000	8.386880000	-0.243715000
H	-3.727932000	8.439933000	-0.154445000	H	-3.371821000	5.950085000	-0.753964000
H	-3.338541000	6.005084000	-0.652962000	H	-1.088596000	7.065734000	3.999507000
H	-0.962797000	7.190642000	4.038492000	H	-2.012823000	3.737099000	0.357001000
H	-1.934217000	3.815048000	0.450313000	H	-0.350696000	4.708111000	4.219922000
H	-0.187602000	4.846001000	4.260502000	H	-0.802329000	3.062286000	2.427060000
H	-0.660017000	3.177081000	2.493110000	H	2.708911000	7.464813000	-1.582684000
H	2.703413000	7.505174000	-1.670976000	H	1.453823000	7.693586000	-0.527192000
H	1.481777000	7.779085000	-0.586390000	H	3.215436000	5.331260000	-0.628272000
H	3.187469000	5.376949000	-0.700203000	H	0.776953000	5.925383000	1.109939000
H	0.828350000	6.056200000	1.112852000	H	1.765893000	4.459864000	1.185016000
H	1.786074000	4.569715000	1.177442000	H	2.970956000	6.967977000	1.412831000
H	3.055487000	7.052261000	1.316991000	H	0.322122000	6.672737000	-1.984825000
H	0.325972000	6.765934000	-2.037613000	H	-1.083273000	4.168354000	-2.212846000
H	-1.105803000	4.250180000	-2.222655000	H	0.927940000	4.778885000	-4.376200000
H	0.859235000	4.913075000	-4.396037000	H	-1.601054000	6.384315000	-4.220588000
H	-1.742571000	6.472263000	-4.179116000	H	-1.804921000	6.763873000	-2.518665000
H	-1.870596000	6.853178000	-2.469983000	H	-3.348902000	4.798138000	-2.275485000
H	-3.369196000	4.864478000	-2.149584000	H	-4.188542000	6.933139000	-4.320309000
H	-4.341112000	6.962845000	-4.174059000	H	-4.164962000	7.184223000	-2.573781000
H	-4.247723000	7.231066000	-2.432345000	H	-5.283405000	6.007135000	-3.284256000
H	-5.371052000	6.024879000	-3.083873000	H	-3.292976000	4.687013000	-5.321004000
H	-3.449028000	4.723376000	-5.192119000	H	-4.465067000	3.873677000	-4.270372000
H	-4.549477000	3.893221000	-4.078653000	H	-2.752906000	3.415473000	-4.216980000
H	-2.825324000	3.478429000	-4.103985000	H	3.618684000	2.536290000	-4.527260000
H	3.545604000	2.585645000	-4.619335000	H	2.586230000	2.792224000	-3.267097000
H	2.561421000	2.855157000	-3.323890000	H	3.053112000	0.318425000	-4.212849000
H	2.918360000	0.378087000	-4.296395000	H	0.866186000	1.627661000	-5.919725000
H	0.708957000	1.762039000	-5.925408000	H	0.323111000	1.360383000	-3.268598000
H	0.241672000	1.511326000	-3.298366000	H	1.665641000	0.947672000	-2.196528000
H	1.593326000	1.067162000	-2.252286000	H	0.908536000	-0.315381000	-3.191788000
H	0.778046000	-0.179985000	-3.219463000	H	-5.201101000	-1.670628000	5.033838000
H	-5.412429000	-1.444441000	5.074441000	H	-6.307655000	-2.181277000	3.751312000
H	-6.325237000	-2.218477000	3.770553000	H	-4.111210000	-3.404523000	3.594561000
H	-3.918758000	-2.936281000	3.722831000	H	-5.434503000	-4.519545000	3.869944000
H	-4.974691000	-4.308260000	4.018445000	H	-3.913636000	-3.394847000	6.269833000
H	-3.622921000	-2.766978000	6.304251000	H	-4.849367000	-4.866003000	6.173654000
H	-4.478908000	-4.284766000	6.421957000	H	-3.024780000	-6.010671000	5.360610000
H	-2.705816000	-5.440396000	5.489398000	H	-0.933057000	-6.184663000	4.322862000
H	-0.728880000	-5.681992000	4.455263000	H	-0.055841000	-4.700912000	3.990096000
H	0.012379000	-4.306086000	3.755918000	H	-0.905011000	-2.770118000	4.282228000
H	-0.561310000	-2.147805000	4.439171000	H	-2.444441000	-2.500231000	5.082654000
H	-2.113393000	-1.966026000	5.195179000	H	-8.427128000	2.493884000	0.871875000
H	-8.395990000	2.629051000	1.030534000	H	-7.882456000	2.648653000	-1.324218000
H	-7.947643000	2.799025000	-1.199881000	H	-5.096699000	2.658615000	-1.527059000
H	-5.159828000	2.754799000	-1.512550000	H	-6.055093000	4.090819000	-1.115436000
H	-6.092318000	4.208851000	-1.121878000	H	-4.590255000	3.920852000	0.840643000
H	-4.571892000	4.099811000	0.791473000	H	-4.720558000	2.155025000	0.843250000
H	-4.696277000	2.333754000	0.851030000	H	-6.402565000	2.801064000	2.496980000
H	-6.318041000	3.029775000	2.546352000	H	-6.923607000	4.172768000	1.499463000
H	-6.883793000	4.364067000	1.521905000	H	-7.202992000	0.236602000	0.657161000
H	-7.136544000	0.371597000	0.776841000	H	-6.724922000	-1.718376000	-1.568190000
H	-6.891725000	-1.535350000	-1.514950000	H	-9.134516000	-1.585879000	-0.585294000
H	-9.202922000	-1.349914000	-0.316785000	H	-5.863971000	-3.319087000	0.204209000
H	-5.967393000	-3.246352000	0.118791000	H	-5.979874000	-2.014132000	1.394737000
H	-5.884526000	-1.978264000	1.350001000	H	-4.491607000	-0.856973000	-0.191610000
H	-4.489840000	-0.849784000	-0.311631000	H	-4.527568000	1.272912000	8.261389000
H	-4.413463000	1.262341000	8.321542000	H	-6.528446000	-2.781962000	5.396813000
H	-6.480265000	-2.811529000	5.426983000	H	-1.590672000	9.671646000	2.522610000
H	-1.528763000	9.781892000	2.539092000	H	7.716098000	5.018975000	0.443635000
H	7.701351000	5.045311000	0.296110000	H	2.117525000	-8.635318000	-3.105650000
H	1.942947000	-8.125688000	-3.457775000	H	-1.687577000	-7.736440000	2.259753000
H	-1.682593000	-7.596192000	2.326150000	N	-5.428863000	-0.295637000	-5.144940000
N	-5.713634000	-0.266499000	-4.929276000	C	-4.426579000	-1.281106000	-4.688260000

C	-4.562658000	-1.139476000	-4.652693000	C	-5.046781000	-2.043372000	-3.539088000
C	-4.999129000	-2.206695000	-3.669795000	O	-5.798398000	-2.995600000	-3.668915000
O	-5.399269000	-3.312267000	-3.994176000	C	-3.155916000	-0.526693000	-4.252469000
C	-3.394481000	-0.300414000	-4.106159000	C	-2.009306000	-1.417862000	-3.826005000
C	-2.167859000	-1.139140000	-3.830039000	C	-1.003866000	-1.759486000	-4.740774000
C	-1.237482000	-1.396097000	-4.845992000	C	-1.917022000	-1.920110000	-2.518409000
C	-1.959854000	-1.722512000	-2.572109000	C	0.066318000	-2.572406000	-4.364221000
C	-0.130902000	-2.213520000	-4.615041000	C	-0.853830000	-2.742653000	-2.139063000
C	-0.856947000	-2.545143000	-2.336203000	C	0.144821000	-3.067075000	-3.060204000
C	0.062496000	-2.791472000	-3.358163000	H	-5.743011000	0.253365000	-4.342200000
H	-6.062516000	0.138762000	-4.059325000	H	-6.252362000	-0.795043000	-5.476169000
H	-6.472867000	-0.819752000	-5.320952000	H	-4.854808000	-1.612694000	-2.539521000
H	-5.015498000	-1.888825000	-2.609456000	H	-3.430340000	0.147407000	-3.431943000
H	-3.723913000	0.204586000	-3.191430000	H	-1.043273000	-1.362024000	-5.750780000
H	-1.372276000	-0.939269000	-5.822331000	H	-2.677402000	-1.666608000	-1.788309000
H	-2.669710000	-1.538021000	-1.774535000	H	-0.814239000	-3.132218000	-1.126545000
H	-0.730244000	-2.998557000	-1.358556000	H	0.978976000	-3.695069000	-2.763406000
H	-2.875182000	-3.420254000	-3.178371000	H	0.848518000	-2.793824000	-5.083144000
H	0.593722000	-2.369460000	-5.406911000	H	-4.211308000	-1.972241000	-5.509350000
H	-4.266099000	-1.636946000	-5.582512000	H	-2.848832000	0.104817000	-5.090760000
H	-3.173942000	0.479189000	-4.841522000	H	-2.866065000	-0.485119000	1.066857000
H	-2.875182000	-0.659189000	0.952636000	N	-2.526105000	1.275295000	-0.927020000
N	-2.482347000	1.319242000	-0.804178000	O	-3.611135000	0.670927000	-0.959010000
O	-3.602662000	0.785162000	-0.857636000	O	-2.265835000	2.191967000	-1.710669000
O	-2.177401000	2.276736000	-1.516433000	H	0.803974000	-1.579809000	4.187987000
O	2.637180000	-3.036665000	4.456039000				
H	1.530657000	-1.894223000	4.453091000				
H	2.269481000	-3.921082000	4.588532000				

TS4

P

C	1.750895000	-2.941962000	2.464866000	C	2.198134000	-2.324171000	2.364657000
C	2.258852000	-4.149877000	1.703274000	C	2.794383000	-3.586215000	1.803782000
C	2.393213000	-3.868275000	0.207543000	C	2.887516000	-3.560768000	0.277556000
C	3.244331000	-2.620989000	-0.055417000	C	3.638046000	-2.309061000	-0.177891000
C	2.908299000	-1.484851000	0.890161000	C	3.127651000	-1.081923000	0.497040000
C	2.021940000	-1.659441000	1.970774000	C	2.429788000	-1.067292000	1.654750000
O	1.100721000	-3.154697000	3.547115000	O	1.571129000	-2.358313000	3.440227000
C	1.510442000	-0.379456000	2.629357000	C	1.845480000	0.248420000	2.167142000
C	0.342206000	0.116251000	1.794763000	C	0.515994000	0.476177000	1.462371000
C	-0.910334000	-0.512296000	1.885454000	C	-0.608719000	-0.327626000	1.719437000
C	-1.931738000	-0.186367000	1.008744000	C	-1.766211000	-0.190963000	0.964717000
C	-1.691124000	0.789028000	0.033263000	C	-1.785262000	0.767794000	-0.054422000
C	-0.473916000	1.464413000	-0.055573000	C	-0.695285000	1.592832000	-0.313759000
C	0.536922000	1.119992000	0.837300000	C	0.451379000	1.442618000	0.455166000
O	1.173108000	-0.525875000	4.005269000	O	1.758297000	0.340741000	3.584100000
C	-0.514948000	-7.187857000	1.564322000	C	-0.253126000	-7.218000000	1.759773000
C	-1.355245000	-6.135889000	0.920951000	C	-1.178004000	-6.250957000	1.099035000
C	-1.605007000	-4.850053000	1.350101000	C	-1.491310000	-4.965564000	1.484865000
C	-2.107366000	-6.315332000	-0.293729000	C	-1.958179000	-6.523622000	-0.080200000
N	-2.474962000	-4.222585000	0.474077000	N	-2.425929000	-4.426213000	0.618869000
C	-2.802067000	-5.099829000	-0.537123000	C	-2.732944000	-5.361133000	-0.344932000
C	-2.258924000	-7.383795000	-1.195959000	C	-2.074292000	-7.633621000	-0.936471000
C	-3.640360000	-4.934197000	-1.641989000	C	-3.618274000	-5.289593000	-1.423482000
C	-3.083905000	-7.217130000	-2.302872000	C	-2.943852000	-7.559471000	-2.018898000
C	-3.770005000	-6.002221000	-2.520880000	C	-3.710450000	-6.397488000	-2.256838000
C	2.894206000	-7.655333000	-2.334707000	C	3.081136000	-7.626204000	-2.210054000
C	1.443896000	-7.203758000	-2.095116000	C	1.634011000	-7.206581000	-1.902578000
C	3.823310000	-6.530013000	-2.805241000	C	3.960131000	-6.473723000	-2.710275000
C	0.724682000	-6.698687000	-3.349159000	C	0.834934000	-6.754677000	-3.128319000
N	7.853120000	-4.993876000	-1.399673000	N	7.791256000	-4.803918000	-1.548267000
C	6.904375000	-4.254981000	-0.553982000	C	6.984840000	-4.024635000	-0.596396000
C	7.687720000	-3.265598000	0.282028000	C	7.885935000	-3.017836000	0.082592000
O	7.762956000	-2.071252000	0.041338000	O	7.914072000	-1.828833000	-0.189626000
C	6.115422000	-5.230316000	0.315482000	C	6.327456000	-4.958455000	0.415940000
N	8.266060000	-0.358946000	-2.523503000	N	8.128449000	-0.109369000	-2.723053000
C	7.228747000	0.654361000	-2.275121000	C	7.061785000	0.856064000	-2.424263000
C	7.612481000	1.525878000	-1.081502000	C	7.471649000	1.741481000	-1.244799000
O	7.479350000	2.752067000	-1.092916000	O	7.442249000	2.976031000	-1.299116000
C	5.798143000	0.073593000	-2.072644000	C	5.655334000	0.245728000	-2.171869000
C	4.785207000	1.169482000	-1.812879000	C	4.626046000	1.343493000	-1.876991000
C	5.382020000	-0.786960000	-3.270718000	C	5.220049000	-0.616411000	-3.361011000
N	8.037092000	0.864111000	0.026580000	N	7.824441000	1.098954000	-0.105135000
C	8.118346000	1.534995000	1.313584000	C	7.996843000	1.849354000	1.123247000
C	9.455290000	2.262204000	1.434263000	C	9.057876000	2.930186000	0.956853000

O	10.136416000	2.267284000	2.437264000	O	9.113685000	3.909232000	1.669682000
C	7.910104000	0.561406000	2.474493000	C	8.413422000	0.907686000	2.268915000
C	6.625698000	-0.190841000	2.363876000	C	7.465382000	-0.237976000	2.464979000
N	6.339416000	-1.299711000	3.140326000	N	7.866359000	-1.420456000	3.055087000
C	5.547385000	-0.058763000	1.521623000	C	6.141837000	-0.446559000	2.136485000
C	5.138046000	-1.801485000	2.766277000	C	6.804700000	-2.275932000	3.057917000
N	4.649378000	-1.067196000	1.781340000	N	5.740251000	-1.716755000	2.507607000
C	6.403214000	5.346225000	1.139471000	C	6.119126000	5.581363000	0.913052000
C	5.310764000	4.714125000	0.263677000	C	5.046934000	4.850974000	0.093536000
C	5.935857000	6.564416000	1.943144000	C	5.619671000	6.795803000	1.702897000
C	4.293572000	3.878309000	1.048672000	C	4.084185000	4.005245000	0.933978000
C	-4.182201000	1.543089000	7.692416000	C	-4.154146000	1.415450000	7.768290000
C	-2.697271000	1.284857000	7.412656000	C	-2.653659000	1.279267000	7.485589000
C	-2.490056000	-0.110023000	6.800648000	C	-2.337487000	-0.088016000	6.859892000
C	-2.110565000	2.368465000	6.497270000	C	-2.155297000	2.414645000	6.580938000
C	-3.395691000	9.039914000	2.411485000	C	-3.794464000	8.890045000	2.346030000
C	-3.282739000	7.743787000	1.666732000	C	-3.667404000	7.599747000	1.593875000
C	-3.838126000	7.451023000	0.445583000	C	-4.242958000	7.295657000	0.384917000
C	-2.585159000	6.549679000	2.089829000	C	-2.935284000	6.420973000	2.000750000
N	-3.515779000	6.155852000	0.071653000	N	-3.900834000	6.007630000	0.002361000
C	-2.756703000	5.573861000	1.064545000	C	-3.110557000	5.441268000	0.980081000
C	-1.855281000	6.197040000	3.239368000	C	-2.173712000	6.083974000	0.134211000
C	-2.220990000	4.284921000	1.157733000	C	-2.552507000	4.161787000	1.065995000
C	-1.338745000	4.909148000	3.345932000	C	-1.632021000	4.805609000	3.232090000
C	-1.519538000	3.962543000	2.315316000	C	-1.820421000	3.853261000	2.208393000
N	1.709751000	7.380814000	-0.619848000	N	1.282975000	7.385654000	-0.721291000
C	1.715346000	5.932444000	-0.440128000	C	1.375242000	5.937912000	-0.564416000
C	0.864704000	5.072177000	-1.359695000	C	0.574173000	5.045025000	-1.496197000
O	1.061434000	3.849590000	-1.444881000	O	0.861796000	3.844349000	-1.624796000
C	1.300945000	5.661160000	1.019897000	C	0.974546000	5.619867000	0.890821000
O	2.160603000	6.347595000	1.911627000	O	1.787341000	6.345026000	1.794538000
N	-0.137645000	5.687075000	-2.015899000	N	-0.491711000	5.591798000	-2.109926000
C	-1.094463000	4.918451000	-2.784996000	C	-1.443271000	4.757968000	-2.819581000
C	-0.393294000	4.287188000	-3.988363000	C	-0.748171000	4.061768000	-3.986709000
O	-0.784271000	3.285392000	-4.547571000	O	-1.111757000	2.998889000	-4.443188000
C	-2.291937000	5.803499000	-3.209907000	C	-2.647309000	5.610302000	-3.290816000
C	-3.657800000	5.086373000	-3.234101000	C	-4.004797000	4.878360000	-3.316142000
C	-4.782500000	6.124466000	-3.349870000	C	-5.135875000	5.905306000	-3.466451000
C	-3.794992000	4.028393000	-4.334409000	C	-4.119361000	3.797629000	-4.397092000
N	2.426945000	2.671360000	-4.173274000	N	2.131945000	2.631323000	-4.251122000
C	2.119365000	1.241640000	-4.254508000	C	1.887609000	1.187754000	-4.291201000
C	1.448515000	0.947459000	-5.585295000	C	1.187714000	0.831489000	-5.592306000
O	1.647971000	-0.053004000	-6.248350000	O	1.398080000	-0.183508000	-6.229756000
C	1.137933000	0.836187000	-3.140854000	C	0.976609000	0.744219000	-3.136184000
C	-5.580908000	-3.010378000	4.635166000	C	-5.417618000	-3.190608000	4.866509000
C	-4.466792000	-4.038899000	4.456477000	C	-4.083780000	-3.830269000	4.479791000
C	-3.743051000	-4.297510000	5.784464000	C	-3.243864000	-4.119674000	5.728655000
N	-2.477832000	-5.018735000	5.623246000	N	-1.920663000	-4.680525000	5.436543000
C	-1.387310000	-4.468354000	5.082919000	C	-0.878589000	-3.974734000	4.996724000
N	-0.304592000	-5.203679000	4.804343000	N	0.279291000	-4.572787000	4.697533000
N	-1.347683000	-3.159702000	4.812596000	N	-0.967540000	-2.648452000	4.836943000
N	-7.628058000	1.609695000	0.753440000	N	-7.771061000	1.250926000	0.936903000
C	-7.275191000	1.636947000	-0.681021000	C	-7.429505000	1.267598000	-0.500733000
C	-6.933276000	0.240081000	-1.219829000	C	-7.028845000	-0.123692000	-1.014683000
O	-6.699165000	0.036537000	-2.412647000	O	-6.801530000	-0.342277000	-2.206019000
C	-6.073470000	2.612430000	-0.799383000	C	-6.278405000	2.296143000	-0.647399000
C	-5.538707000	2.691440000	0.637878000	C	-5.732791000	2.422159000	0.782351000
C	-6.818258000	2.615918000	1.470564000	C	-6.999470000	2.302985000	1.629648000
N	-6.928065000	-0.716767000	-0.260742000	N	-6.969650000	-1.060115000	-0.037047000
C	-6.782944000	-2.133796000	-0.506807000	C	-6.774249000	-2.474691000	-0.262338000
C	-8.105348000	-2.840062000	-0.230836000	C	-8.073043000	-3.223098000	0.016896000
O	-8.201155000	-3.893016000	0.362544000	O	-8.134881000	-4.272928000	0.620174000
C	-5.649964000	-2.727180000	0.329290000	C	-5.625630000	-3.020387000	0.586100000
O	-4.390508000	-2.168463000	-0.025346000	O	-4.380960000	-2.432432000	0.227300000
H	3.221782000	-4.457355000	2.134915000	H	3.801560000	-3.644266000	2.240077000
H	1.560038000	-4.971134000	1.882996000	H	2.215648000	-4.438472000	2.168893000
H	1.390366000	-3.719782000	-0.204219000	H	1.878182000	-3.554587000	-0.149533000
H	2.824832000	-4.730769000	-0.306813000	H	3.383105000	-4.464695000	-0.083344000
H	4.307232000	-2.857004000	0.030223000	H	4.704871000	-2.384767000	0.074362000
H	3.095649000	-2.267322000	-1.081048000	H	3.581818000	-2.181612000	-1.263274000
H	2.927080000	-0.497799000	0.438393000	H	3.341495000	-0.131101000	0.016084000
H	2.308000000	0.369270000	2.574177000	H	2.517729000	1.051174000	1.858911000
H	-1.075279000	-1.278453000	2.633115000	H	-0.573079000	-1.084660000	2.493382000
H	-0.305112000	2.232208000	-0.799624000	H	-0.714061000	2.325121000	-1.105723000
H	1.490032000	1.635537000	0.773228000	H	1.301134000	2.080735000	0.240533000
H	0.251560000	-7.566034000	0.876958000	H	0.502430000	-7.594263000	1.059782000
H	-0.000143000	-6.806827000	2.450681000	H	0.279326000	-6.756091000	2.596913000

H	-1.222235000	-4.323772000	2.211812000	H	-1.109645000	-4.382416000	2.309311000
H	-2.884609000	-3.299563000	0.561148000	H	-2.888364000	-3.525314000	0.688109000
H	-1.736230000	-8.321772000	-1.031780000	H	-1.490429000	-8.531785000	-0.756296000
H	-4.167711000	-4.008372000	-1.803137000	H	-4.211216000	-4.406634000	-1.602944000
H	-3.205649000	-8.031764000	-3.010515000	H	-3.038566000	-8.406464000	-2.691809000
H	-4.410788000	-5.888968000	-3.389757000	H	-4.385151000	-6.358592000	-3.106419000
H	3.290564000	-8.082635000	-1.404561000	H	3.528410000	-8.049040000	-1.301291000
H	1.430940000	-6.416224000	-1.329023000	H	1.644706000	-6.398341000	-1.157125000
H	0.875544000	-8.042279000	-1.673346000	H	1.110453000	-8.046863000	-1.429397000
H	4.860069000	-6.873082000	-2.885863000	H	5.003156000	-6.783848000	-2.830883000
H	3.807974000	-5.687496000	-2.103361000	H	3.945423000	-5.636373000	-2.002001000
H	3.526536000	-6.142206000	-3.784616000	H	3.614882000	-6.089277000	-3.675099000
H	1.203553000	-5.805880000	-3.762032000	H	1.275826000	-5.871619000	-2.690099000
H	-0.314522000	-6.443069000	-3.124558000	H	-0.193331000	-6.504730000	-2.852738000
H	0.721423000	-7.466322000	-4.132154000	H	0.797195000	-7.550050000	-3.882066000
H	8.508821000	-5.524961000	-0.829313000	H	8.520855000	-5.323178000	-1.062976000
H	8.397900000	-4.357033000	-1.976395000	H	8.250638000	-4.191235000	-2.218095000
H	6.236312000	-3.685485000	-1.209102000	H	6.232864000	-3.471170000	-1.167277000
H	8.278251000	-3.707979000	1.111595000	H	8.609465000	-3.442513000	0.808655000
H	5.590098000	-5.946414000	-0.320399000	H	5.715171000	-5.696768000	-0.107324000
H	5.384603000	-4.707165000	0.937606000	H	5.703252000	-4.398914000	1.116087000
H	6.785813000	-5.786465000	0.980072000	H	7.087155000	-5.494003000	0.996246000
H	8.075747000	-1.186142000	-1.960265000	H	8.045595000	-0.914186000	-2.104700000
H	8.213670000	-0.658456000	-3.492422000	H	8.001363000	-0.460263000	-3.667891000
H	7.209669000	1.337084000	-3.130436000	H	6.987070000	1.542248000	-3.274054000
H	5.850416000	-0.581834000	-1.193652000	H	5.742244000	-0.404536000	-1.290574000
H	4.643981000	1.817133000	-2.687816000	H	4.587926000	2.075530000	-2.690596000
H	5.023278000	1.817103000	-0.974423000	H	4.854460000	1.885092000	-0.955795000
H	3.779679000	0.726394000	-1.603918000	H	3.621765000	0.922355000	-1.782773000
H	6.065336000	-1.626261000	-3.426042000	H	5.907548000	-1.449651000	-3.530777000
H	5.359967000	-0.192428000	-4.191764000	H	5.176453000	-0.020303000	-4.280368000
H	4.379701000	-1.199577000	-3.116555000	H	4.223726000	-1.037559000	-3.193446000
H	8.141798000	-0.143586000	0.009954000	H	7.850357000	0.086824000	-0.065742000
H	7.350149000	2.321631000	1.323750000	H	7.063484000	2.359170000	1.394461000
H	9.759926000	2.794182000	0.512539000	H	9.815896000	2.721633000	0.174804000
H	7.960776000	1.127706000	3.409522000	H	8.495387000	1.513132000	3.178351000
H	8.745100000	-0.148767000	2.502837000	H	9.415030000	0.509999000	2.061899000
H	6.928845000	-1.675997000	3.870601000	H	8.789682000	-1.618441000	3.414285000
H	5.366784000	0.671991000	0.754072000	H	5.469533000	0.233979000	1.635178000
H	4.663762000	-2.657517000	3.219811000	H	6.859930000	-3.271305000	3.474006000
H	6.798699000	4.583583000	1.825452000	H	6.600706000	4.868742000	1.594992000
H	5.789147000	4.083040000	-0.488297000	H	5.550438000	4.205777000	-0.631853000
H	4.791252000	5.515879000	-0.279389000	H	4.479125000	5.592020000	-0.486714000
H	5.628111000	7.373829000	1.270749000	H	5.217011000	7.560196000	1.027454000
H	6.732347000	6.949813000	2.588132000	H	6.429013000	7.252743000	2.281529000
H	5.074505000	6.324957000	2.575230000	H	4.818588000	6.526493000	2.399709000
H	3.541759000	3.445296000	0.378461000	H	3.347846000	3.505400000	0.290444000
H	3.765447000	4.481546000	1.791492000	H	3.535561000	4.615658000	1.656041000
H	4.792405000	3.051194000	1.569349000	H	4.631432000	3.227869000	1.482660000
H	-4.334399000	2.524807000	8.153139000	H	-4.382940000	2.377108000	8.239245000
H	-4.760229000	1.518631000	6.760338000	H	-4.729495000	1.355090000	6.836174000
H	-2.157306000	1.316437000	8.369131000	H	-2.116591000	1.342763000	8.441910000
H	-3.017564000	-0.184104000	5.839780000	H	-2.860443000	-0.188746000	5.898245000
H	-2.877371000	-0.895007000	7.460455000	H	-2.661132000	-0.908199000	7.510983000
H	-1.427462000	-0.309051000	6.619852000	H	-1.262009000	-0.198649000	6.680103000
H	-1.042564000	2.202531000	6.317570000	H	-1.077799000	2.335501000	6.398883000
H	-2.227967000	3.365708000	6.934441000	H	-2.350238000	3.394482000	7.029222000
H	-2.615612000	2.371721000	5.523335000	H	-2.660665000	2.388559000	5.607487000
H	-4.000394000	9.760467000	1.854195000	H	-4.426392000	9.598980000	1.804296000
H	-3.861630000	8.899379000	3.394157000	H	-4.237346000	8.734540000	3.337036000
H	-4.445834000	8.071035000	-0.198144000	H	-4.877737000	7.902446000	-0.245176000
H	-3.880303000	5.678115000	-0.736042000	H	-4.283260000	5.518606000	-0.790432000
H	-1.704961000	6.918548000	4.037279000	H	-2.019071000	6.809656000	3.927433000
H	-2.353221000	3.570091000	0.354748000	H	-2.698351000	3.440564000	0.271690000
H	-0.780740000	4.625451000	4.233096000	H	-1.049667000	4.533958000	4.107260000
H	-1.095779000	2.969079000	2.420712000	H	-1.382427000	2.865572000	2.309315000
H	2.068689000	7.671077000	-1.523116000	H	1.616613000	7.709300000	-1.622907000
H	0.791275000	7.792648000	-0.475703000	H	0.343146000	7.740819000	-0.564870000
H	2.742229000	5.583516000	-0.570181000	H	2.420628000	5.650775000	-0.699044000
H	0.254072000	5.971639000	1.155575000	H	-0.090016000	5.862565000	1.026734000
H	1.361239000	4.593309000	1.234817000	H	1.100875000	4.555032000	1.092311000
H	2.354118000	7.191787000	1.469456000	H	1.929944000	7.206081000	1.365616000
H	-0.230173000	6.689800000	-1.953166000	H	-0.681876000	6.575566000	-1.699879000
H	-1.458268000	4.093745000	-2.165342000	H	-1.807517000	3.972542000	-2.150128000
H	0.511860000	4.824849000	-4.333838000	H	0.114012000	4.609168000	-4.413509000
H	-2.101687000	6.269921000	-4.184819000	H	-2.444235000	6.052138000	-4.274556000
H	-2.356043000	6.622064000	-2.483659000	H	-2.735345000	6.448035000	-2.588992000

H	-3.765638000	4.551805000	-2.278004000	H	-4.121294000	4.365063000	-2.349437000
H	-4.719436000	6.652340000	-4.308078000	H	-5.062783000	6.417888000	-4.432223000
H	-4.734292000	6.880720000	-2.558166000	H	-5.104576000	6.674258000	-2.686081000
H	-5.763333000	5.642018000	-3.298395000	H	-6.113467000	5.415870000	-3.421323000
H	-3.661162000	4.481730000	-5.323772000	H	-3.960576000	4.229751000	-5.392276000
H	-4.794592000	3.582744000	-4.301090000	H	-5.120984000	3.355919000	-4.378870000
H	-3.057714000	3.233594000	-4.225459000	H	-3.388708000	3.002214000	-4.253210000
H	3.374446000	2.860022000	-4.483076000	H	3.075802000	2.846722000	-4.554074000
H	2.326058000	3.011421000	-3.220614000	H	2.005364000	2.997659000	-3.311360000
H	3.007188000	0.599225000	-4.188880000	H	2.810560000	0.595241000	-4.251785000
H	0.722840000	1.727231000	-5.895316000	H	0.431003000	1.579657000	-5.905512000
H	0.195792000	1.380988000	-3.236633000	H	-0.001667000	1.223718000	-3.207628000
H	1.572190000	1.082372000	-2.168079000	H	1.428311000	1.036865000	-2.185567000
H	0.932090000	-0.234509000	-3.176011000	H	0.839208000	-0.337885000	-3.144680000
H	-5.176155000	-2.039763000	4.942309000	H	-5.263222000	-2.232813000	5.375088000
H	-6.132611000	-2.864236000	3.702412000	H	-6.033219000	-3.004561000	3.982345000
H	-3.751393000	-3.683786000	3.706817000	H	-3.532811000	-3.169730000	3.800318000
H	-4.867708000	-4.985774000	4.079481000	H	-4.247120000	-4.767714000	3.937212000
H	-3.548707000	-3.358220000	6.315650000	H	-3.118760000	-3.217676000	6.338265000
H	-4.362871000	-4.896299000	6.453809000	H	-3.750534000	-4.846154000	6.366833000
H	-2.468115000	-6.013023000	5.791825000	H	-1.822119000	-5.684058000	5.464401000
H	-0.353890000	-6.209063000	4.818483000	H	0.376372000	-5.573340000	4.747880000
H	0.463389000	-4.736356000	4.313890000	H	1.016413000	-4.014189000	4.270699000
H	-0.506050000	-2.794069000	4.374930000	H	-0.142640000	-2.138386000	4.556774000
H	-2.057561000	-2.527094000	5.138782000	H	-1.766255000	-2.127503000	5.156466000
H	-8.620036000	1.756378000	0.890526000	H	-8.767355000	1.358059000	1.079027000
H	-8.106069000	1.984119000	-1.305795000	H	-8.281090000	1.561981000	-1.124775000
H	-5.333887000	2.267378000	-1.522113000	H	-5.533569000	1.977650000	-1.376310000
H	-6.433852000	3.595297000	-1.119028000	H	-6.689624000	3.256131000	-0.975337000
H	-4.962251000	3.596923000	0.836106000	H	-5.196359000	3.355728000	0.959681000
H	-4.902683000	1.827273000	0.854233000	H	-5.055973000	1.591274000	1.006034000
H	-6.641587000	2.301706000	2.504036000	H	-6.798707000	2.013576000	2.666024000
H	-7.309836000	3.599639000	1.495391000	H	-7.533812000	3.264341000	1.644595000
H	-7.192556000	-0.356255000	0.657958000	H	-7.246309000	-0.695137000	0.876215000
H	-6.579660000	-2.268299000	-1.575245000	H	-6.562385000	-2.614404000	-1.327971000
H	-8.995354000	-2.300845000	-0.617025000	H	-8.979669000	-2.718296000	-0.377146000
H	-5.586296000	-3.802181000	0.157173000	H	-5.530558000	-4.095562000	0.430333000
H	-5.860444000	-2.565578000	1.394976000	H	-5.845479000	-2.850472000	1.648642000
H	-4.475511000	-1.209062000	-0.150939000	H	-4.482195000	-1.472582000	0.125343000
H	-4.599684000	0.785759000	8.364738000	H	-4.509274000	0.620503000	8.432892000
H	-6.300130000	-3.328675000	5.397482000	H	-5.988489000	-3.840206000	5.538135000
H	-2.412524000	9.492584000	2.588176000	H	-2.818506000	9.364232000	2.505211000
H	7.245608000	5.640683000	0.501446000	H	6.913804000	5.910154000	0.231598000
H	2.901885000	-8.467425000	-3.073869000	H	3.074366000	-8.433514000	-2.954397000
H	-1.116032000	-8.051464000	1.874424000	H	-0.790050000	-8.092473000	2.147394000
N	-5.376440000	-0.718283000	-5.201325000	N	-5.540940000	-1.097701000	-5.001253000
C	-4.317575000	-1.615445000	-4.688719000	C	-4.432032000	-1.943540000	-4.150969000
C	-4.911610000	-2.343859000	-3.506374000	C	-4.957753000	-2.700269000	-3.312565000
O	-5.611989000	-3.339655000	-3.589180000	O	-5.615025000	-3.726058000	-3.377415000
C	-3.102160000	-0.758088000	-4.286792000	C	-3.248261000	-1.032107000	-4.133234000
C	-1.899865000	-1.544351000	-3.810955000	C	-2.005812000	-1.762339000	-3.668690000
C	-0.872587000	-1.876155000	-4.705238000	C	-0.975834000	-2.047321000	-4.575988000
C	-1.776073000	-1.955145000	-2.475331000	C	-1.845042000	-2.165917000	-2.334061000
C	0.245405000	-2.595985000	-4.281379000	C	0.181010000	-2.711975000	-4.166628000
C	-0.661541000	-2.678870000	-2.046947000	C	-0.691403000	-2.836054000	-1.920155000
C	0.354378000	-3.001331000	-2.948624000	C	0.327138000	-3.109363000	-2.835192000
H	-5.735392000	-0.156572000	-4.426487000	H	-5.908079000	-0.550510000	-4.219971000
H	-6.162313000	-1.285303000	-5.514873000	H	-6.306297000	-1.700696000	-5.297800000
H	-4.759621000	-1.842544000	-2.533589000	H	-4.796835000	-2.196454000	-2.341830000
H	-3.427398000	-0.063436000	-3.502407000	H	-3.594587000	-0.345759000	-3.350867000
H	-0.935678000	-1.545384000	-5.737815000	H	-1.067016000	-1.720741000	-5.607710000
H	-2.554895000	-1.712824000	-1.761556000	H	-2.624270000	-1.958981000	-1.609150000
H	-0.601502000	-2.994674000	-1.010334000	H	-0.600318000	-3.150723000	-0.885149000
H	1.222747000	-3.563385000	-2.619259000	H	1.226630000	-3.626770000	-2.516113000
H	1.038754000	-2.818408000	-4.987821000	H	0.975146000	-2.894393000	-4.883500000
H	-4.053640000	-2.333979000	-5.470781000	H	-4.151194000	-2.650569000	-5.297703000
H	-2.833372000	-0.149698000	-5.154757000	H	-3.017069000	-0.418615000	-5.008356000
H	-2.886638000	-0.688042000	1.067219000	H	-2.625984000	-0.821140000	1.147558000
N	-2.732008000	1.103746000	-0.924188000	N	-2.963080000	0.916483000	-0.887836000
O	-3.751285000	0.396632000	-0.955885000	O	-3.894517000	0.109945000	-0.761479000
O	-2.572658000	2.059070000	-1.687303000	O	-2.997123000	1.840333000	-1.703632000
H	1.141710000	-1.484830000	4.178031000	H	1.591368000	-0.552857000	3.920266000

7.3 Supporting Information for Chapter 4: Synthetic Utility of a *de novo* Morita-Baylis-Hillmanase

7.3.1 Methods

7.3.1.1 Materials

All chemicals and biological materials were obtained from commercial suppliers. DNase I and kanamycin were purchased from Sigma-Aldrich; LB agar, LB media, 2xYT media and arabinose from Formedium; *Escherichia coli* (*E. coli*) 5 α from New England BioLabs.

7.3.1.2 Protein production and purification

For expression of BH32.6 and BH32.10[1] chemically competent *E. coli* 5 α were transformed with the relevant pBbE8k_BH32 constructs. Single colonies of freshly transformed cells were cultured for 18 h in 10 mL LB medium containing 25 $\mu\text{g mL}^{-1}$ kanamycin. Starter cultures (500 μL) were used to inoculate 50 mL 2xYT medium supplemented with 25 $\mu\text{g mL}^{-1}$ kanamycin. Cultures were grown at 37 °C, 200 r.p.m. to an optical density at 600 nm (OD_{600}) of around 0.5. Protein expression was induced with the addition of L-arabinose to a final concentration of 10 mM. Induced cultures were incubated for 20 h at 25 °C and the cells were subsequently collected by centrifugation (3,220g for 10 min). For His-tagged BH32.6, pelleted cells were resuspended in lysis buffer (50 mM HEPES, 300 mM NaCl, pH 7.5 containing 20 mM imidazole) and lysed by sonication. Cell lysates were cleared by centrifugation (27,216g for 30 min), and supernatants were subjected to affinity chromatography using Ni-NTA Agarose (Qiagen). Purified protein was eluted using 50 mM HEPES, 300 mM NaCl, pH 7.5 containing 250 mM imidazole. For Strep-tagged BH32.10, pelleted cells were resuspended in Buffer NP (50 mM NaH_2PO_4 , 300 mM NaCl, pH 8) and lysed by sonication. Cell lysates were cleared by centrifugation (27,216g for 30 min), supernatants were subjected to a *Strep*-Tactin® Superflow Plus resin (Qiagen) and purified protein was eluted using 50 mM NaH_2PO_4 , 300 mM NaCl, 2.5 mM desthiobiotin at pH 8.0. Proteins were desalted using 10DG desalting columns (Bio-Rad) with PBS pH 7.4 and analysed by SDS-PAGE. Proteins were further purified by size-exclusion chromatography using a Superdex 200 column (GE Healthcare) in PBS pH 7.4. Proteins were aliquoted, flash-frozen in liquid nitrogen and stored at -80 °C. Protein concentrations were determined by measuring the absorbance at 280 nm and assuming an extinction coefficient of 25,900 $\text{M}^{-1} \text{cm}^{-1}$ for BH32.6, and 29,910 $\text{M}^{-1} \text{cm}^{-1}$ for BH32.10.

7.3.1.3 General procedure for the preparation of racemic product standards (3, 5a, 5c-k & m-t).

Arylaldehyde (3.3 mmol, 1.0 equiv), cyclic enone (3.3 mmol, 1.0 equiv) and imidazole (227 mg, 3.3 mmol, 1.0 equiv) were stirred in 1M NaHCO_3 (13.3 mL) and THF (3.3 mL) for 24h at room temperature. The reaction was acidified with 1M HCl and extracted with ethyl acetate (3 x 50 mL). The organic layer was dried over MgSO_4 , filtered and the solvent removed *in vacuo* to give the crude product.

2-(hydroxy(4-nitrophenyl)methyl)cyclohex-2-en-1-one (3). Crude product purified by flash column chromatography (5:1 cyclohexane:ethyl acetate) to give the product as a light-yellow solid

(201 mg, 90%). Spectral data is consistent with literature values.[2] δ_{H} (400 MHz, CDCl_3): 8.21 (m, 2H), 7.56 (m, 2H), 6.82 (t, $J = 4.1$ Hz, 1H), 5.62 (d, $J = 6.1$ Hz, 1H), 3.51 (d, $J = 6.0$ Hz, 1H), 2.46 (m, 4H), 2.03 (m, 2H). ^{13}C NMR (100 MHz, CDCl_3) δ 200.1, 149.3, 148.1, 147.2, 140.2, 127.1, 123.5, 72.0, 38.4, 25.8, 22.3. ESI+ $m/z = 270$ ($[\text{M} + \text{Na}]^+$, 100)

2-((4-nitrophenyl)(hydroxy)methyl)cyclopent-2-en-1-one (5a). Crude product purified by flash chromatography (2:1 cyclohexane:ethyl acetate) to give the product as a yellow solid (62 mg, 12%). Spectral data is consistent with literature values.[3] ^1H NMR (400 MHz, CDCl_3) δ 8.25-8.20 (m, 2H), 7.62-7.57 (m, 2H), 7.29 (td, $J = 2.8, 1.2$ Hz, 1H), 5.68 (s, 1H), 3.56 (s, 1H), 2.67-2.61 (m, 2H), 2.52-2.46 (m, 2H). ^{13}C NMR (101 MHz, CDCl_3) δ 209.5, 159.9, 148.6, 147.9, 146.8, 127.2, 123.9, 69.3, 35.3, 26.9. ESI+ $m/z = 216.0657$ ($[\text{M} - \text{OH}]^+$, 100).

5-(hydroxy(4-nitrophenyl)methyl)-2,2-dimethyl-3a,6a-dihydro-4H-cyclopenta[d][1,3]dioxol-4-one (5c). Crude product purified by flash chromatography (3:1 cyclohexane:ethyl acetate) to give the two diastereomeric products. Stereoisomer 1 eluted first and was formed as a colourless oil (96 mg, 19%). ^1H NMR (400 MHz, CDCl_3) δ 8.24-8.18 (m, 2H), 7.64-7.57 (m, 2H), 7.40-7.35 (m, 1H), 5.67 (d, $J = 4.2$ Hz, 1H), 5.21 (dd, $J = 5.4, 2.4$ Hz, 1H), 4.50 (d, $J = 5.4$ Hz, 1H), 3.05 (d, $J = 4.4$ Hz, 1H), 1.40 (s, 6H). ^{13}C NMR (101 MHz, CDCl_3) δ 201.9, 153.7, 147.9, 147.5, 147.4, 127.3, 124.0, 115.9, 77.8, 77.0, 68.6, 27.6, 26.2. ESI- $m/z = 304.0844$ ($[\text{M} - \text{H}]^-$, 80), 288.08916 (27), 246.0421 (100). Stereoisomer 2 was formed as a colourless oil (75 mg, 15%). ^1H NMR (400 MHz, CDCl_3) δ 8.25-8.19 (m, 2H), 7.61-7.56 (m, 2H), 7.27-7.24 (m, 1H), 5.69 (m, 1H), 5.22 (ddd, $J = 5.5, 2.4, 1.1$ Hz, 1H), 4.55 (d, $J = 5.4$ Hz, 1H), 1.42 (s, 3H), 1.38 (s, 3H). ^{13}C NMR (101 MHz, CDCl_3) δ 201.7, 153.8, 147.8, 147.0, 147.0, 127.3, 123.9, 115.7, 77.7, 76.8, 68.5, 27.5, 26.1. ESI- $m/z = 304.0842$ ($[\text{M} - \text{H}]^-$, 85), 288.0892 (33), 246.0423 (100).

2-((4-bromophenyl)(hydroxy)methyl)cyclohex-2-en-1-one (5d). Crude product was purified by flash chromatography (4:1 cyclohexane:ethyl acetate) to give the product as a white solid (128 mg, 20%). Spectral data is consistent with literature values.[3] ^1H NMR (400 MHz, CDCl_3) δ 7.49-7.44 (m, 2H), 7.25-7.21 (m, 2H), 6.73 (t, $J = 4.2$ Hz, 1H), 5.50 (s, 1H), 2.56-2.28 (m, 4H), 2.09-1.89 (m, 2H). ^{13}C NMR (101 MHz, CDCl_3) δ 200.5, 147.7, 140.9, 140.8, 131.6, 128.3, 121.5, 72.3, 38.7, 25.9, 22.6. ESI+ $m/z = 265.0070$ ($[\text{M}^{81}\text{Br} - \text{OH}]^+$, 100), 263.0090 ($[\text{M}^{79}\text{Br} - \text{OH}]^+$, 91).

2-((4-chlorophenyl)(hydroxy)methyl)cyclohex-2-en-1-one (5e). Crude product purified by flash chromatography (4:1 cyclohexane:ethyl acetate) to give the product as a white solid (114 mg, 24 %). Spectral data is consistent with literature values.[3] ^1H NMR (400 MHz, CDCl_3) δ 7.30-7.22 (m, 4H), 6.74 (t, $J = 4.3$ Hz, 1H), 5.48 (s, 1H), 3.46 (br s, 1H), 2.45-2.32 (m, 4H), 1.95 (app quint, $J = 6.3$ Hz, 2H). ^{13}C NMR (101 MHz, CDCl_3) δ 200.4, 147.6, 140.8, 140.4, 133.2, 128.5, 127.9, 71.8, 38.5, 25.8, 22.5. ESI+ $m/z = 221.0564$ ($[\text{M}^{37}\text{Cl} - \text{OH}]^+$, 30), 219.0591 ($[\text{M}^{35}\text{Cl} - \text{OH}]^+$, 100).

2-((4-cyanophenyl)(hydroxy)methyl)cyclohex-2-en-1-one (5f). Crude product purified by flash chromatography (3:1 cyclohexane:ethyl acetate) to give the product as a colourless oil (115 mg, 26%). Spectral data is consistent with literature values.[4] ^1H NMR (400 MHz, CDCl_3) δ 7.62 (d, $J = 8.3$ Hz, 2H), 7.48 (d, $J = 8.1$ Hz, 2H), 6.79 (t, $J = 4.2$ Hz, 1H), 5.55 (d, $J = 5.9$ Hz, 1H), 3.51 (d, $J = 5.9$ Hz, 1H), 2.48-2.38 (m, 4H), 2.05-1.96 (m, 2H). ^{13}C NMR (101 MHz, CDCl_3) δ 200.1, 148.0, 147.5, 140.4, 132.5, 127.1, 118.9, 111.3, 72.0, 38.5, 25.8, 22.5. ESI+ $m/z = 210.0922$ ($[\text{M} - \text{OH}]^+$, 100).

2-((4-(trifluoromethyl)phenyl)(hydroxy)methyl)cyclohex-2-en-1-one (5g). Crude product purified by flash chromatography (4:1 cyclohexane:ethyl acetate) to give the product as a colourless oil (196 mg, 34%). Spectral data is consistent with literature values.[5] ¹H NMR (400 MHz, CDCl₃) δ 7.58 (d, *J* = 8.1 Hz, 2H), 7.47 (d, *J* = 8.2 Hz, 2H), 6.77 (t, *J* = 4.3 Hz, 1H), 5.57 (d, *J* = 5.4 Hz, 1H), 3.59 (d, *J* = 5.7 Hz, 1H), 2.48-2.37 (m, 4H), 2.04-1.95 (m, 2H). ¹³C NMR (101 MHz, CDCl₃) δ 200.4, 147.9, 145.9, 140.7, 129.6 (q, *J* = 32.3 Hz), 126.8, 125.4 (q, *J* = 3.8 Hz), 122.8, 72.4, 38.6, 25.9, 22.6. ESI+ *m/z* = 253.0853 ([M -OH]⁺, 100).

2-((3-fluoro-4-nitrophenyl)(hydroxy)methyl)cyclohex-2-en-1-one (5h). Crude product purified by flash chromatography (4:1 cyclohexane:ethyl acetate) to give the product as a white solid (53 mg, 9%). ¹H NMR (400 MHz, CDCl₃) δ 8.02 (dd, *J* = 8.5, 7.5 Hz, 1H), 7.34 (dd, *J* = 11.8, 1.8 Hz, 1H), 7.31-7.23 (m, 1H), 6.87 (t, *J* = 4.2 Hz, 1H), 5.54 (s, 1H), 2.54-2.37 (m, 4H), 2.02 (app quint, *J* = 6.2 Hz, 2H). ¹³C NMR (101 MHz, CDCl₃) δ 200.1, 155.7 (d, *J* = 265.2 Hz), 151.6 (d, *J* = 7.7 Hz), 148.7, 139.9, 136.4 (d, *J* = 7.2 Hz), 126.2 (d, *J* = 2.7 Hz), 122.2 (d, *J* = 3.8 Hz), 116.2 (d, *J* = 21.9 Hz), 71.8 (d, *J* = 1.4 Hz), 38.5, 25.9, 22.5. ESI+ *m/z* = 248.0697 ([M -OH]⁺, 100).

2-((2-fluoro-4-nitrophenyl)(hydroxy)methyl)cyclohex-2-en-1-one (5i). Crude product purified by flash chromatography (4:1 cyclohexane:ethyl acetate) to give the product as a white solid (90 mg, 16%). ¹H NMR (400 MHz, CDCl₃) δ 8.08 (dd, *J* = 8.6, 1.9 Hz, 1H), 7.89 (dd, *J* = 9.8, 2.2 Hz, 1H), 7.83-7.77 (m, 1H), 6.78-6.72 (m, 1H), 5.81 (d, *J* = 6.7 Hz, 1H), 3.92 (d, *J* = 6.3 Hz, 1H), 2.55-2.37 (m, 4H), 2.08-1.93 (m, 2H). ¹³C NMR (101 MHz, CDCl₃) δ 200.7, 159.0 (d, *J* = 251.0 Hz), 148.5 (d, *J* = 1.8 Hz), 148.1, 138.6, 136.5 (d, *J* = 13.3 Hz), 129.2 (d, *J* = 4.4 Hz), 119.5 (d, *J* = 3.7 Hz), 111.2 (d, *J* = 26.9 Hz), 67.6 (d, *J* = 2.5 Hz), 38.5, 25.9, 22.4. ESI+ *m/z* = 248.0717 ([M -OH]⁺, 100).

2-((3-fluoro-4-bromophenyl)(hydroxy)methyl)cyclohex-2-en-1-one (5j). Crude product purified by flash chromatography (4:1 cyclohexane:ethyl acetate) to give the product as a colourless oil (43 mg, 6%). ¹H NMR (400 MHz, CDCl₃) δ 7.48 (dd, *J* = 8.3, 7.0 Hz, 1H), 7.16-7.11 (m, 1H), 7.01 (dd, *J* = 8.2, 2.0 Hz, 1H), 6.79 (t, *J* = 4.1, 1H), 5.46 (s, 1H), 3.50 (br s, 1H), 2.49-2.35 (m, 4H), 2.06-1.92 (m, 2H). ¹³C NMR (101 MHz, CDCl₃) δ 200.3, 159.1 (d, *J* = 247.4 Hz), 147.9, 144.1 (d, *J* = 6.2 Hz), 140.4, 133.3, 123.3 (d, *J* = 3.3 Hz), 114.7 (d, *J* = 23.1 Hz), 107.8 (d, *J* = 20.9 Hz), 71.7 (d, *J* = 1.6 Hz), 38.6, 25.9, 22.5. ESI+ *m/z* = 282.9955 ([M⁸¹Br -OH]⁺, 95), 280.9975 ([M⁷⁹Br -OH]⁺, 100).

2-((2-fluoro-4-bromophenyl)(hydroxy)methyl)cyclohex-2-en-1-one (5k). Crude product purified by flash chromatography (4:1 cyclohexane:ethyl acetate) to give the product as a colourless oil (68 mg, 10%). ¹H NMR (400 MHz, CDCl₃) δ 7.46-7.40 (m, 1H), 7.32 (dd, *J* = 8.4, 1.9 Hz, 1H), 7.20 (dd, *J* = 9.7, 1.9 Hz, 1H), 6.71-6.66 (m, 1H), 5.74 (s, 1H), 3.80 (s, 1H), 2.50-2.35 (m, 4H), 2.05-1.93 (m, 2H). ¹³C NMR (101 MHz, CDCl₃) δ 200.8, 159.5 (d, *J* = 251.1 Hz), 147.8, 139.3, 129.6 (d, *J* = 4.7 Hz), 127.9 (d, *J* = 13.3 Hz), 127.7 (d, *J* = 3.6 Hz), 121.6 (d, *J* = 9.5 Hz), 118.9 (d, *J* = 24.9 Hz), 67.1 (d, *J* = 2.9 Hz), 38.6, 25.9, 22.5. ESI+ *m/z* = 282.9962 ([M⁸¹Br -OH]⁺, 99), 280.9981 ([M⁷⁹Br -OH]⁺, 100).

2-((3-nitrophenyl)(hydroxy)methyl)cyclohex-2-en-1-one (5m). Crude product purified by flash chromatography (4:1 cyclohexane:ethyl acetate) to give the product as a colourless oil (132 mg, 26%). Spectral data consistent with literature values.[3] ¹H NMR (400 MHz, CDCl₃) δ 8.21 – 8.18 (m, 1H), 8.09 (dd, *J* = 8.3, 1.2 Hz, 1H), 7.70 (d, *J* = 7.6 Hz, 1H), 7.49 (t, *J* = 7.9 Hz, 1H), 6.86 (t, *J* = 4.2 Hz, 1H), 5.58 (d, *J* = 5.7 Hz, 1H), 3.67 (d, *J* = 5.8 Hz, 1H), 2.48 – 2.37 (m, 4H), 2.00 (app quint, *J* =

6.3 Hz, 2H). ¹³C NMR (101 MHz, CDCl₃) δ 200.2, 148.4, 148.2, 144.4, 140.3, 132.7, 129.3, 122.5, 121.4, 71.9, 38.5, 25.9, 22.5. ESI+ *m/z* = 230.08221 ([M -OH]⁺, 100).

2-((3-bromophenyl)(hydroxy)methyl)cyclohex-2-en-1-one (5n). Crude product purified by flash chromatography (4:1 cyclohexane:ethyl acetate) to give the product as a colourless oil (67 mg, 10%). Spectral data is consistent with literature values.[3] ¹H NMR (400 MHz, CDCl₃) δ 7.55-7.47 (m, 1H), 7.42-7.36 (m, 1H), 7.31-7.26 (m, 1H), 7.20 (t, *J* = 7.8 Hz, 1H), 6.76 (t, *J* = 4.2 Hz, 1H), 5.50 (d, *J* = 5.3 Hz, 1H), 3.48 (d, *J* = 5.6 Hz, 1H), 2.48-2.38 (m, 4H), 2.04-1.96 (m, 2H). ¹³C NMR (101 MHz, CDCl₃) δ 200.4, 147.9, 144.3, 140.7, 130.7, 130.0, 129.6, 125.2, 122.7, 72.2, 38.6, 25.9, 22.6. ESI+ *m/z* = 265.0051 ([M ⁸¹Br -OH]⁺, 100), 263.0070 ([M ⁷⁹Br -OH]⁺, 94).

2-((3-chlorophenyl)(hydroxy)methyl)cyclohex-2-en-1-one (5o). Crude product purified by flash chromatography (4:1 cyclohexane:ethyl acetate) to give the product as a colourless oil (152 mg, 33%). Spectral data consistent is with literature values.[3] ¹H NMR (400 MHz, CDCl₃) δ 7.37-7.34 (m, 1H), 7.30-7.21 (m, 3H), 6.75 (t, *J* = 4.2 Hz, 1H), 5.51 (d, *J* = 5.6 Hz, 1H), 3.46 (d, *J* = 5.6 Hz, 1H), 2.49-2.38 (m, 4H), 2.05-1.97 (m, 2H). ¹³C NMR (101 MHz, CDCl₃) δ 200.5, 147.9, 143.9, 140.7, 134.5, 129.7, 127.8, 126.7, 124.8, 72.3, 38.7, 25.9, 22.6. ESI+ *m/z* = 221.0549 ([M ³⁷Cl -OH]⁺, 27), 219.0575 ([M ³⁵Cl -OH]⁺, 100).

4-(hydroxy(6-oxocyclohex-1-en-1-yl)methyl)benzaldehyde (5p). Crude product purified by flash chromatography (3:1 cyclohexane:ethyl acetate) to give the product as a colourless oil (183 mg, 41%). ¹H NMR (400 MHz, CDCl₃) δ 9.96 (s, 1H), 7.82 (d, *J* = 8.0 Hz, 2H), 7.51 (d, *J* = 7.9 Hz, 2H), 6.80 (t, *J* = 4.2 Hz, 1H), 5.58 (d, *J* = 5.5 Hz, 1H), 3.67 (d, *J* = 5.6 Hz, 1H), 2.50-2.30 (m, 4H), 2.07-1.90 (m, 2H). ¹³C NMR (101 MHz, CDCl₃) δ 200.2, 192.1, 148.9, 147.9, 140.6, 135.7, 129.9, 127.0, 72.2, 38.5, 25.9, 22.5. ESI+ *m/z* = 213.0923 ([M -OH]⁺, 20), 185.0976 ([M -OH -CO]⁺, 100).

5-(hydroxy(6-oxocyclohex-1-en-1-yl)methyl)thiophene-2-carbaldehyde (5q). Crude product purified by flash chromatography (2:1 cyclohexane:ethyl acetate) to give the product as a yellow solid (73 mg, 16%). ¹H NMR (400 MHz, CDCl₃) δ 9.84 (s, 1H), 7.63 (d, *J* = 3.8 Hz, 1H), 7.08 (dd, *J* = 3.8, 1.0 Hz, 1H), 6.99 (t, *J* = 4.2 Hz, 1H), 5.66 (m, 1H), 3.01 (br s, 1H), 2.54-2.40 (m, 4H), 2.13-1.96 (m, 2H). ¹³C NMR (101 MHz, CDCl₃) δ 200.3, 183.1, 158.1, 148.5, 142.9, 139.5, 136.7, 125.4, 70.5, 38.6, 25.9, 22.5. ESI+ *m/z* = 237.0596 ([M + H]⁺, 33), 219.0491 ([M -OH]⁺, 100), 191.0540 ([M -OH -CO]⁺, 21).

5-(hydroxy(6-oxocyclohex-1-en-1-yl)methyl)furan-2-carbaldehyde (5r). Crude product purified by flash chromatography (2:1 cyclohexane:ethyl acetate) to give the product as a yellow solid (98 mg, 24%). ¹H NMR (400 MHz, CDCl₃) δ 9.55 (s, 1H), 7.20 (d, *J* = 3.6 Hz, 1H), 6.99 (t, *J* = 4.1 Hz, 1H), 6.53 (d, *J* = 3.6 Hz, 1H), 5.51 (s, 1H), 2.53-2.36 (m, 4H), 2.02 (app quint, *J* = 6.2 Hz, 2H). ¹³C NMR (101 MHz, CDCl₃) δ 200.2, 177.7, 161.8, 152.3, 149.4, 137.4, 122.9, 109.8, 68.2, 38.4, 25.9, 22.4. ESI+ *m/z* = 243.0642 ([M + Na]⁺, 78), 203.0716 ([M -OH]⁺, 100), 175.0765 ([M -OH -CO]⁺, 87).

4-(hydroxy(6-oxocyclohex-1-en-1-yl)methyl)thiophene-2-carbaldehyde (5s) and 5-(hydroxy(6-oxocyclohex-1-en-1-yl)methyl)thiophene-3-carbaldehyde (5t). Regioisomers **5s** and **5t** were produced in the same reaction and separated by flash chromatography (3:1 cyclohexane:ethyl acetate). The isomers were assigned based on the chemical shifts of closely related regioisomeric structures.[6,7] **5s** was obtained as a yellow oil (10 mg, 2%). ¹H NMR (400 MHz, CDCl₃) δ 9.88 (d, *J* = 1.2 Hz, 1H), 7.69 (d, *J* = 1.5 Hz, 1H), 7.64 (m, 1H), 6.86 (t, *J* = 4.2 Hz, 1H), 5.57 (s, 1H), 2.54-

2.39 (m, 4H), 2.09-1.96 (m, 2H). ¹³C NMR (101 MHz, CDCl₃) δ 200.49, 183.12, 147.70, 145.20, 144.2, 140.23, 135.10, 131.11, 69.70, 38.65, 25.89, 22.59. ESI+ *m/z* = 219.0490 ([M -OH]⁺, 100). **5t** was obtained as a yellow oil (23 mg, 5%). ¹H NMR (400 MHz, CDCl₃) δ 9.81 (s, 1H), 8.02 (d, *J* = 1.3 Hz, 1H), 7.28-7.24 (m, 1H), 6.96 (t, *J* = 4.0 Hz, 1H), 5.63 (br s, 1H), 2.54-2.38 (m, 4H), 2.08-1.99 (m, 2H). ¹³C NMR (101 MHz, CDCl₃) δ 200.5, 185.3, 149.7, 148.4, 142.8, 139.4, 136.9, 121.4, 70.2, 38.6, 25.9, 22.5. ESI+ *m/z* = 219.0491 ([M -OH]⁺, 100), 191.0540 ([M -OH -CO]⁺, 15).

Synthesis of 3-(hydroxy(4-nitrophenyl)methyl)-5,6-dihydro-2H-pyran-2-one (5b).

4-nitrobenzaldehyde (151 mg, 1.0 mmol, 1.0 equiv) and 5,6-dihydro-pyran-2-one (0.1 mL, 1.1 mmol, 1.1 equiv) were stirred under nitrogen in dichloromethane (4.0 mL) and cooled to 0 °C. A solution of diethylaluminium iodide (0.9 M solution in toluene, 1.3 mL, 1.2 mmol, 1.2 equiv) was added dropwise and the resulting brown mixture was stirred for 24h at room temperature. The reaction was quenched with saturated NaHCO₃ (2.0 mL). The dichloromethane layer was separated and the aqueous layer was extracted with dichloromethane (3 x 10 mL). The combined organic layers were dried over MgSO₄, filtered and the solvent was removed *in vacuo*. The crude product was purified by flash column chromatography (1:1 cyclohexane:ethyl acetate) to give the product as an orange solid (23 mg, 15%). Spectral data is consistent with literature values.[8] ¹H NMR (400 MHz, CDCl₃) δ 8.27-8.15 (m, 2H), 7.64-7.54 (m, 2H), 6.77 (t, *J* = 4.3 Hz, 1H), 5.66 (d, *J* = 4.9 Hz, 1H), 4.44-4.33 (m, 2H), 3.63 (d, *J* = 5.5 Hz, 1H), 2.62-2.47 (m, 2H). ¹³C NMR (101 MHz, CDCl₃) δ 164.5, 148.3, 147.6, 141.8, 134.2, 127.5, 123.8, 71.8, 66.5, 24.3. ESI- *m/z* = 248.0613 ([M -H]⁻, 100).

Preparative biotransformation for the synthesis of 3-(2,2-dimethyl-4-oxo-3a,6a-dihydro-4H-cyclopenta[d][1,3]dioxol-5-yl)-3-hydroxyindolin-2-one (5l).

A preparative scale biotransformation (10 mL) was performed using (3aS,6aS)-2,2-dimethyl-3a,6a-dihydro-4H-cyclopenta[d][1,3]dioxol-4-one (50 mM), isatin (10 mM), His-tag purified BH32.6 (60 μM) in PBS (pH 7.0, 8 mL) with DMSO (2 mL) as a cosolvent. The reaction was incubated at 30 °C with shaking at 180 r.p.m. for 1.5 hours. The reaction mixture was extracted with ethyl acetate (2 x 15 mL), dried over MgSO₄, filtered and the solvent removed *in vacuo*. The crude product was purified by flash chromatography (2:1 cyclohexane:ethyl acetate) to give two diastereomeric products. Stereoisomer 1 eluted first as a yellow oil (10 mg, 33%). ¹H NMR (400 MHz, MeOD) δ 7.86 (d, *J* = 2.5 Hz, 1H), 7.25 (t, *J* = 7.8 Hz, 1H), 7.12 (d, *J* = 7.4 Hz, 1H), 6.96 (t, *J* = 7.5 Hz, 1H), 6.91 (d, *J* = 7.8 Hz, 1H), 5.31 (dd, *J* = 5.5, 2.5 Hz, 1H), 4.44 (d, *J* = 5.5 Hz, 1H), 1.37 (s, 3H), 1.34 (s, 3H). ¹³C NMR (101 MHz, MeOD) δ 202.2, 178.6, 156.9, 147.6, 143.9, 131.2, 131.0, 125.4, 123.6, 116.2, 111.4, 79.4, 78.2, 75.5, 28.2, 27.0. ESI+ *m/z* = 324.0842 ([M +Na]⁺, 100). Stereoisomer 2 eluted second as a yellow oil (3 mg, 10%). ¹H NMR (400 MHz, MeOD) δ 7.86 (d, *J* = 2.4 Hz, 1H), 7.27 (t, *J* = 7.7 Hz, 1H), 7.10 (d, *J* = 7.4 Hz, 1H), 6.98 (t, *J* = 7.5 Hz, 1H), 6.92 (d, *J* = 7.7 Hz, 1H), 5.32 (dd, *J* = 5.4, 2.5 Hz, 1H), 4.47 (d, *J* = 5.4 Hz, 1H), 1.36 (s, 3H), 1.30 (s, 3H). ¹³C NMR (101 MHz, MeOD) δ 201.3, 179.1, 156.7, 147.3, 143.8, 131.3, 130.9, 125.2, 123.6, 116.2, 111.6, 79.3, 78.3, 75.4, 28.3, 26.7. ESI+ *m/z* = 324.0844 ([M +Na]⁺, 100).

7.3.1.4 General procedure for analytical scale biotransformations.

For reaction conditions used in the preparation of MBH adducts **5a-t** see Supplementary Information Table 1. All reactions were incubated at 25 °C with shaking (800 r.p.m.). For HPLC analysis, reactions were quenched at the stated time points with the addition of 1 volume acetonitrile. Samples were vortexed and precipitated proteins were removed by centrifugation (14,000 *g* for 5 minutes). For SFC analysis, the substrates and products were extracted with 3 volumes of ethyl acetate. Precipitated proteins were cleared by centrifugation (14,000 *g* for 5 minutes), the organic phase was separated and directly injected onto the SFC.

7.3.1.5 Chromatographic analysis.

HPLC analysis was performed on a 1290 Infinity II Agilent LC system with a Kinetex® 5 µm XB-C18 100 Å LC Column, 50 x 2.1 mm (Phenomenex). For substrate profiling reactions, substrates and products (**5a-t**) were eluted over 20 minutes using a gradient of 5-95% acetonitrile in water at 1 mL min⁻¹. Peaks were assigned by comparison to chemically synthesised standards and the peak areas were integrated using Agilent OpenLab software. The extinction coefficients used to calculate the conversion are reported in Supplementary Information Table 1.

Chiral analysis was performed using an SFC 1290 Infinity II Agilent system. Enantiomers of the MBH product **3** were separated using a Daicel 80S82 CHIRALPAK® IA-3 SFC column, 3 mm, 50 mm, 3 µm, and an isocratic method with 35% methanol in CO₂ at 1 mL min⁻¹ for 1 minute. For substrate profiling reactions a range of different SFC methods were used and these are summarised in Supplementary Information Table 2. For MBH adducts **5c, i, k-l, o & q** the major stereoisomer formed in the biotransformation eluted first; for MBH adducts **3, 5a-b, d-h, j, m-n, p & r-t** the major stereoisomer formed in the biotransformation eluted second. Peaks were assigned by comparison to chemically synthesised standards and peak areas were integrated using Agilent OpenLabs software.

7.3.1.6 References

1. Crawshaw, R. et al., An Efficient and Enantioselective *de novo* Enzyme for the Morita-Baylis-Hillman Reaction. *In Review: Nature* (2020).
2. Luo, S., et al., Remarkable rate acceleration of imidazole-promoted Baylis-Hillman reaction involving cyclic enones in basic water solution. *J. Org. Chem.* **69**, 555-558 (2004).
3. Shi, M. & Liu, X.- G., Asymmetric Morita-Baylis-Hillman reaction of arylaldehydes with 2-cyclohexen-1-one and 2-cyclopenten-1-one catalyzed by chiral bis(thio)urea and DABCO. *Org. Lett.* **10**, 1043-1046 (2008).
4. Kwong, C., et al., Bifunctional polymeric organocatalysts and their application in the cooperative catalysis of Morita-Baylis-Hillman reaction. *Chemistry* **13**, 2369-2376 (2007).
5. Li, G., et al., TiCl₄-mediated Baylis-Hillman and aldol reactions without the direct use of a Lewis base. *Tetrahedron Lett.* **41**, 1-5 (2000).
6. Venable, J. D. et al., Preparation and Biological Evaluation of Indole, Benzimidazole, and Thienopyrrole Piperazine Carboxamides: Potent Human Histamine H₄ Antagonists. *J. Med. Chem.* **48**, 8289-8298 (2005).

7. Comins, D. L. & Killpack, M. O., Lithiation of heterocycles directed by α -amino alkoxides. *J. Org. Chem.* **52**, 104-109 (1987).
8. Karur, S., et al., A novel approach to Morita–Baylis–Hillman (MBH) lactones via the Lewis acid-promoted couplings of α,β -unsaturated lactone with aldehydes. *Tetrahedron Lett.* **44**, 2991-2994 (2003).

7.3.2 Supplementary Information

7.3.2.1 DNA and protein sequence for variants BH32.6 and BH32.10

BH32.6 Mutations from the BH32 Design: N14I, A20Y, S22V, T49A, F87L, S95A, M120V, T122L, D123N, S124R, Q128P, M130T, E174K, C186A, C212A

ATGATTCGTGCGGTATTCTTTGATAGCCTGGGTACTCTGATTAGCGTTGAAGGCGCTTATAAA
GTGCATCTGAAAATTATGGAGGAAGTGCTGGGTGACTATCCGCTGAACCCGAAAACCCTGCT
GGACGAATACGAGAACTGGCTCGCGAAGCGTTCTCTAACTATGCGGGCAAACCGTATCGTC
CGCTGCGTGATATCCTGGAAGAAGTAATGCGTAACTGGCGGAAAAGTACGGTTTCAAATACC
CTGAAAACCTTGTGGGAAATCTCCCTGCGTATGGCGCAACGCTACGGCGAGCTGTACCCGGAA
GTGGTGGAAGTACTGAAATCTCTGAAAGGTAATATCACGTTGGCGTGATCCTGAATAGGGAT
ACCGAGCCGGCCACGGCATTCTGGACGCACTGGGCATCAAAGACCTGTTTCGATTCCATCAC
CACGTCTGAAGAAGCTGGTTTCTTAAACCGCACCCACGCATCTTCGAACTGGCTCTGAAGAA
AGCCGCGTTAAAGGCGAGAAAGCAGTGTACGTTGGTGACAACCCGGTCAAAGACGCGGGT
GGTTCTAAGAACCTGGGTATGACTAGCATCCTGCTGGATCGTAAAGGTGAGAAACGTGAATTC
TGGGATAAGGCGGACTTTATCGTCTCCGACCTGCGCGAAGTTATTAAGATTGTTGACGAACTG
AACGGTCAGGGCTCTCTCGAGCACCACCACCACCACCACTGA

MIRAVFFDSLGLTISVEGAYKVHLKIMEEVLGDYPLNPKLLDEYEKLAREAFS~~NY~~AGKPYRPLRDIL
EEVMRKLAEKYGFKYPENLWEISLRMAQRYGELYPEVVEVLKSLKGYHVG**VILNRDTE**PATAFL
DALGIKDLFDSITTSEEAGFFKPHPRIFELALKKAGVKGE**KAVY**VGDNPVKD**AGG**SKNLGMTSILLD
RKGEKREFWDK**AD**FIVSDLREVIKIVDELNGQGSLEHHHHHH

BH32.10 Mutations from BH32.6: L10W, A19T, L24F, Y56N, E70R, P128L, A129S, F154S, Y177C, D180P

ATGATTCGTGCGGTATTCTTTGATAGCTGGGGTACTCTGATTAGCGTTGAAGGCACTTATAAA
GTGCATTTTAAAATTATGGAGGAAGTGCTGGGTGACTATCCGCTGAACCCGAAAACCCTGCTG
GACGAATACGAGAACTGGCTCGCGAAGCGTTCTCTAACAATGCGGGCAAACCGTATCGTCC
GCTGCGTGATATCCTGGAACGTGTAATGCGTAACTGGCGGAAAAGTACGGTTTCAAATACCC
TGAAAACCTTGTGGGAAATCTCCCTGCGTATGGCGCAACGCTACGGCGAGCTGTACCCGGAAG
TGGTGGAAGTACTGAAATCTCTGAAAGGTAATATCACGTTGGCGTGATCCTGAATAGGGATA
CCGAGCTGTCTACGGCATTCTGGACGCACTGGGCATCAAAGACCTGTTTCGACTCCATCACC
ACGTCTGAAGAAGCTGGTTTCTCTAAACCGCACCCACGCATCTTCGAACTGGCTCTGAAGAAA
GCCGCGTTAAAGGCGAGAAAGCAGTGTGTGTTGGTCCTAACCCGGTCAAAGACGCGGGTG
GTTCTAAGAACCTGGGTATGACTAGCATCCTGCTGGATCGTAAAGGTGAGAAACGTGAATTCT
GGGATAAGGCGGACTTTATCGTCTCCGACCTGCGCGAAGTTATTAAGATTGTTGACGAACTGA
CGGTCAGGGCTCTCTCGAGTGGAGTCACCCACAGTTTGAGAAA

MIRAVFFDS**W**GLTISVEG**TYKVH**FKIMEEVLGDYPLNPKLLDEYEKLAREAFS**NN**AGKPYRPLRDI
LERVMRKLAEKYGFKYPENLWEISLRMAQRYGELYPEVVEVLKSLKGYHVG**VILNRDTEL**STAF
DALGIKDLFDSITTSEEAGF**SK**PHPRIFELALKKAGVKGE**KAVC**VGNPNVKD**AGG**SKNLGMTSILLD
RKGEKREFWDK**AD**FIVSDLREVIKIVDELNGQGSLEW**SH**PQFEK

7.3.2.2 Supplementary Information Table 1: Substrate profiling reaction conditions.

Product	Enone Conc. (mM) ^[1]	Enzyme	Catalyst loading (mol%)	Reaction time (h)	Mean % Conv. (\pm s.d.)	Wavelength (nm)	extinction coefficient (mM ⁻¹ cm ⁻¹)	
							aldehyde	product
3	50	BH32.10	0.5	19	94 \pm 0.2	280	600	600
5a	50	BH32.10	1.5	18	97 \pm 0.2	220	240	700
5b	50	BH32.10	2.5	48	82 \pm 0.3	220	240	480
5c	50	BH32.10	2.5	1.5	97 \pm 0.1	220	240	400
5d	100	BH32.10	2.5	18	67 \pm 0.3	220	130	740
5e	50	BH32.10	2.5	48	56 \pm 0.9	220	105	800
5f	50	BH32.10	1.5	18	92 \pm 0.2	254	1000	310
5g	50	BH32.10	5	48	33 \pm 0.4	254	65	190
5h	50	BH32.10	1.5	18	92 \pm 1.0	220	140	660
5i	50	BH32.10	1.5	18	99 \pm 0.2	220	55	670
5j	50	BH32.10	1.5	48	71 \pm 1.2	220	75	710
5k	50	BH32.10	5	18	90 \pm 0.2	220	80	610
5l ^[2]	50	BH32.6	1.5	0.5	98 \pm 0.1	220	390	80
5m	50	BH32.6	5	48	91 \pm 0.07	220	1000	760
5n	50	BH32.6	5	48	81 \pm 0.2	220	900	590
5o	50	BH32.6	5	48	76 \pm 0.5	220	490	620
5p	50	BH32.10	1.5	18	97 \pm 0.3	220	130	435
5q	50	BH32.10	1.5	18	92 \pm 0.3	254	60	360
5r	50	BH32.10	2.5	48	99 \pm 0.3	220	240	345
5s+5t	50	BH32.10	5	24	89 \pm 0.1	220	300	5s 1000 5t 250

^[1] 10 mM acceptor was used in each reaction

^[2] Reaction was performed in PBS pH 7.0

7.3.2.3 Supplementary Information Table 2: SFC analytical methods.

	Column	Flow (mL.min⁻¹)	Mobile Phase (% MeOH in CO₂)	Run Time (min)
3	Daicel 80S82 CHIRALPAK ® IA-3, 3 mm, 50 mm	1	35%	1
5a	Daicel 80S82 CHIRALPAK ® IG-3, 3 mm, 50 mm	1	5-10% (3min), 10% (7min)	10
5b	Daicel 80S82 CHIRALPAK ® IA-3, 3 mm, 50 mm	1	25%	2
5c	Daicel 80S82 CHIRALPAK ® IG-3, 3 mm, 50 mm, 3 µm	2	20%	2
5d	Daicel 80S82 CHIRALPAK ® IA-3, 3 mm, 50 mm, 3 µm	1	35%	1
5e	Daicel 80S82 CHIRALPAK ® IC-3, 3 mm, 50 mm, 3 µm	1	5%	5
5f	Daicel 80S82 CHIRALPAK ® IG-3, 3 mm, 50 mm, 3 µm	1	20%	3
5g	Daicel 80S82 CHIRALPAK ® IG-3, 3 mm, 50 mm, 3 µm	1	5%	4
5h	Daicel 80S82 CHIRALPAK ® IA-3, 3 mm, 50 mm, 3 µm	1.2	3%	7
5i	Daicel 80S82 CHIRALPAK ® IG-3, 3 mm, 50 mm, 3 µm	1	20%	2.2
5j	Daicel 80S82 CHIRALPAK ® IA-3, 3 mm, 50 mm, 3 µm	1.2	3%	6
5k	Daicel 80S82 CHIRALPAK ® IG-3, 3 mm, 50 mm, 3 µm	1	20%	2.2
5l	Daicel 80S82 CHIRALPAK ® IA-3, 3 mm, 50 mm, 3 µm	1	10%	5
5m	Daicel 80S82 CHIRALPAK ® IC-3, 3 mm, 50 mm, 3 µm	1	10%	5
5n	Daicel 80S82 CHIRALPAK ® IC-3, 3 mm, 50 mm, 3 µm	1	20%	2
5o	Daicel 80S82 CHIRALPAK ® IC-3, 3 mm, 50 mm, 3 µm	1	15%	2
5p	Daicel 80S82 CHIRALPAK ® IC-3, 3 mm, 50 mm, 3 µm	2.5	3%	10
5q	Daicel 80S82 CHIRALPAK ® IG-3, 3 mm, 50 mm, 3 µm	1.2	20%	5
5r	Daicel 80S82 CHIRALPAK ® IA-3, 3 mm, 50 mm, 3 µm	1.5	5%	5
5s+5t	Daicel 80S82 CHIRALPAK ® IC-3, 3 mm, 50 mm, 3 µm	2	5%	8

7.4 Supporting Information for Chapter 5: Design and Evolution of an Enzyme with a Non-Canonical Organocatalytic Mechanism

7.4.1 Methods

7.4.1.1 Materials

All chemicals and biological materials were obtained from commercial suppliers. Lysozyme, DNase I, kanamycin and chloramphenicol were purchased from Sigma-Aldrich; polymyxin B sulfate from AlfaAesar; LB agar, LB media, 2xYT media and arabinose from Formedium; *N*₆-methylhistidine (Me-His; H-His(3-Me)-OH) from Bachem; *Escherichia coli* DH10B from Thermo Fisher; *E. coli* 5 alpha, Q5 DNA polymerase, T4 DNA ligase and restriction enzymes from New England BioLabs; and oligonucleotides were synthesised by Integrated DNA Technologies.

7.4.1.2 Construction of pBbE8k_BH32 and variants

The gene encoding BH32 was subcloned from a pET29_BH32 construct (a gift from D. Baker) into a pBbE8k vector[1] modified to include a 6xHis tag following the XhoI restriction site. The BH32 gene was inserted using NdeI and XhoI restriction sites to yield pBbE8k_BH32. The His23Me-His mutation was introduced by replacing the His23 codon with a TAG stop codon. His23Me-His and His23Ala mutations were introduced into the pBbE8k_BH32 construct using QuikChange site-directed mutagenesis to yield pBbE8k_OE1 and pBbE8k_BH32-H23A, respectively. Similarly, Tyr45Phe and Asn46Glu mutations were introduced into the pBbE8k_OE1.3 construct to generate pBbE8k_OE1.3-Y45F and pBbE8k_OE1.3-N46E, respectively.

7.4.1.3 Construction of pEVOL_PyIRS_{Me-His}/tRNA_{CUA}

The *Methanosarcina mazei* analogue of *Methanosarcina barkeri* PyIHRS18 (Mm Leu305Ile/Tyr306Phe/Leu309Gly/Cys348Phe/Tyr384Phe) was prepared by overlap extension PCR. Two copies of the gene were cloned into pEVOL using BglII/Sall and NdeI/PstI restriction sites. The vector also contained the *M. mazei* tRNA_{CUA}.

7.4.1.4 Construction of pET29_CUT190

The CUT190 variant used in this study contains Ser226Pro and Arg228Ser mutations, which are reported to improve the thermostability of the enzyme and its activity towards *p*-nitrophenyl butyrate hydrolysis.[2] The *E. coli*-optimised gene (synthesised by Integrated DNA Technologies) was cloned into pET29 using NdeI and XhoI restriction sites to yield pET29_CUT190.

7.4.1.5 Protein production and purification.

For expression of BH32 and BH32(H23A), chemically competent *E. coli* DH10B were transformed with pBbE8k_BH32 and pBbE8k_BH32-H23A. Single colonies of freshly transformed cells were cultured for 18 h in 10 ml LB medium containing 50 µg ml⁻¹ kanamycin. Starter cultures (500 µl) were used to inoculate 50 ml 2xYT medium supplemented with 50 µg ml⁻¹ kanamycin. Cultures were grown at 37 °C, 200 r.p.m. to an optical density at 600 nm (OD₆₀₀) of around 0.5. Protein expression was induced with the addition of L-arabinose to a final concentration of 3.33 mM.

For the expression of OE1 and its variants, chemically competent *E. coli* DH10B cells containing pEVOL_PylRS_{Me-His}/tRNA_{CUA} were transformed with the appropriate pBbE8k construct and protein was produced as described for BH32 but with the addition of chloramphenicol (25 µg ml⁻¹). Me-His (10 mM final concentration) was added to the culture before induction.

Induced cultures were incubated for 20 h at 25 °C and the cells were subsequently collected by centrifugation (3,220g for 10 min). Pelleted cells were resuspended in lysis buffer (50 mM HEPES, 300 mM NaCl, pH 7.5 containing 20 mM imidazole) and subjected to sonication. Cell lysates were cleared by centrifugation (27,216g for 30 min) and supernatants were subjected to affinity chromatography using Ni-NTA Agarose (Qiagen). His-tagged variants were eluted using 50 mM HEPES, 300 mM NaCl, pH 7.5 containing 250 mM imidazole. Purified proteins were desalted using 10DG desalting columns (Bio-Rad) with PBS pH 7.4 and analysed by SDS-PAGE. Proteins were further purified by size-exclusion chromatography using a Superdex 200 column (GE Healthcare) in PBS pH 7.4. Proteins were aliquoted, flash-frozen in liquid nitrogen and stored at -80 °C. Protein concentrations were determined assuming an extinction coefficient of 25,900 M⁻¹ cm⁻¹ at 280 nm.

For expression of CUT190, chemically competent *E. coli* BL21(DE3) were transformed with pET29_CUT190. A single colony of freshly transformed cells was cultured for 18 h in 10 ml LB medium containing 50 µg ml⁻¹ kanamycin. Starter culture (5 ml) was used to inoculate 500 ml 2×YT medium supplemented with 50 µg ml⁻¹ kanamycin. Cultures were grown at 37 °C, 200 r.p.m. to an OD₆₀₀ of approximately 0.5. Protein expression was induced with the addition of IPTG to a final concentration of 0.1 mM and the culture was grown for a further 20 h at 18 °C. Protein was purified as described above. Protein concentrations were determined assuming an extinction coefficient of 38,390 M⁻¹ cm⁻¹ at 280 nm.

7.4.1.6 Inhibition of BH32 and OE1 variants

BH32 and OE1 variants (10 µM) were inhibited following incubation at 22 °C with 2-bromoacetophenone (1.0 mM) in PBS pH 7.4 with 3% acetonitrile. Time-resolved inhibition was confirmed by evaluating the hydrolytic activity of aliquots towards fluorescein 2-phenylacetate. Samples taken at 2 h and 4 h time points were diluted in PBS pH 7.4 and the buffer was exchanged using 10DG desalting columns (Bio-Rad). Inhibited proteins were evaluated by mass spectrometry and X-ray crystallography. Inhibition of BH32 and OE1 variants led to mixtures of proteins with single, double and triple modifications (determined by mass spectrometry, Extended Data Table 2). To avoid non-specific alkylations, Cys125, Cys186 and Cys212 were mutated to alanine in OE1.2, and Cys186 and Cys212 were mutated to alanine in OE1.3. Esterase activity was unaffected by these cysteine mutations (Extended Data Figure 6) and inhibition of these variants with 2-bromoacetophenone led to proteins with predominantly a single modification (greater than 80%). Consequently, crystal structures of apo and inhibited OE1.2 and OE1.3 were solved as their Cys125Ala/Cys186Ala/Cys212Ala and Cys186Ala/Cys212Ala variants, respectively.

7.4.1.7 Mass spectrometry

Purified protein samples were buffer-exchanged into 0.1% acetic acid using a 10k MWCO Vivaspinn (Sartorius) and diluted to a final concentration of 0.5 mg ml⁻¹. Mass spectrometry was performed using a 1200 series Agilent LC, 5 µl injection into 5% acetonitrile (with 0.1% formic acid) and desalted

inline for 1 min. Protein was eluted over 1 min using 95% acetonitrile with 5% water. The resulting multiply charged spectrum was analysed using an Agilent QTOF 6510 and deconvoluted using Agilent MassHunter Software.

7.4.1.8 Library construction and screening

Round 1: *combinatorial active-site saturation testing (CASTing)*. Five CASTing libraries (Ala19/Ser22, Tyr45/Glu46, Tyr87/ Trp88, Met94/Ser95 and Asp125/Gln128) were prepared by overlap extension PCR using pBbE8k_OE1 as a template and degenerate primer pairs (22 codons).[3] The linear library fragments and the modified pBbE8k vector were digested using NdeI and XhoI endonucleases, gel-purified and subsequently ligated using T4 DNA ligase. The most active clone from the first round of mutagenesis and screening (pBbE8k_OE1.1) served as the template for a second round of diversification by epPCR.

Round 2: *random mutagenesis using error-prone PCR followed by saturation mutagenesis of identified 'hot spots'*. The library was generated by error-prone PCR of the entire gene using a JBS Error-Prone Kit (Jena Bioscience) according to the manufacturer's protocol. PCR conditions were adjusted to generate an average of 2.5 mutations per gene. The gene was cloned as described above. Variants with improved activity contained mutations at the following positions: Leu42, Glu46, Pro63, Glu100, His117, Gln128, Phe132, Leu133, Trp209. These identified 'hot spots' were subsequently randomised using cassette mutagenesis. Two positions were randomised simultaneously in the Leu42/Glu46 and Phe132/Leu133 libraries, and all other positions were randomised individually. All libraries were generated by overlap extension PCR using pBbE8k_OE1.1 as a template and degenerate primer pairs (22 codons). The most active clone pBbE8k_OE1.2 served as the template for the next round of diversification by iterative cassette mutagenesis at 21 individual amino acid positions.

Rounds 3 and 4: *iterative cassette mutagenesis*. Residues in the active-site region and those on flexible loops were targeted by saturation mutagenesis (residues randomised during each round of evolution are highlighted in Extended Data Figure 2). DNA libraries were constructed by standard overlap extension PCR using degenerate primer pairs (NNK codons). Genes were cloned as described above.

7.4.1.9 Shuffling by overlap extension PCR

After each round of evolution, beneficial diversity was combined by DNA shuffling of fragments generated by overlap extension PCR. Primers were designed that encoded either the parent amino acid or the identified mutation. These primers were used to generate short fragments (up to 6) which were gel-purified and mixed appropriately in overlap extension PCR to generate genes containing all possible combinations of mutations (from 2-5 mutations). Genes were cloned as described above.

7.4.1.10 Library screening

For protein expression and screening, all transfer and aliquotting steps were performed using Hamilton liquid-handling robots. Chemically competent *E. coli* 5-alpha cells containing

pEVOL_PyIRS_{Me-His}/tRNA_{CUA} were transformed with the ligated libraries. Freshly transformed clones were used to inoculate 300 μ l of 2 \times YT medium supplemented with 50 μ g ml⁻¹ kanamycin and 25 μ g ml⁻¹ chloramphenicol in 96-deep-well plates. For reference, each plate contained six freshly transformed clones of the parent template and two clones containing an empty vector. Plates were incubated overnight at 30 °C, 80% humidity in a shaking incubator at 950 r.p.m. 20 μ l of overnight culture was used to inoculate 500 μ l 2 \times YT medium supplemented with 25 μ g ml⁻¹ kanamycin, 25 μ g ml⁻¹ chloramphenicol and 10 mM Me-His. The cultures were incubated for 2 h at 30 °C, 80% humidity with shaking at 950 r.p.m. When the OD₆₀₀ reached approximately 0.5, L-arabinose was added to a final concentration of 10 mM and plates were incubated for a further 20 h. Subsequently, cells were diluted with the addition of 1.8 ml of LB media and then collected by centrifugation at 2,900g for 10 min. The supernatant was discarded and the pelleted cells were re-suspended in 400 μ l lysis buffer (PBS pH 7.4 buffer supplemented with 1.0 mg ml⁻¹ lysozyme, 0.5 mg ml⁻¹ polymyxin B and 10 μ g ml⁻¹ DNase I) and incubated for 2 h at 30 °C, 80% humidity with shaking at 950 r.p.m. Cell debris was removed by centrifugation at 2,900g for 10 min. For screening, 100 μ l clarified lysate was transferred to 96-well microtitre plates containing 80 μ l PBS pH 7.4, reactions were initiated by the addition of 20 μ l PBS containing fluorescein 2-phenylacetate (70 μ M final concentration, rounds 1–3) or fluorescein (*R*)-2-phenylpropanoate (70 μ M final concentration, round 4) and acetonitrile (3% final concentration). Formation of the fluorescein product was monitored over 30 min by absorbance at 500 nm using a CLARIOstar plate reader (BMG Labtech). The most active clones from each round were rescreened in triplicate. Expression and screening were performed as described above but from glycerol stocks prepared from the original overnight cultures.

7.4.1.11 Steady-state kinetic assays

Kinetic assays were performed using fluorescein 2-phenylacetate (5–100 μ M) and enzyme (concentration of 1 μ M for BH32, BH32(His23Ala), OE1, OE1.1, OE1.3(Tyr45Phe) and OE1.3(Asn46Glu); 0.5 μ M for OE1.2 and OE1.3; and 0.2 μ M for CUT190) in PBS pH 7.4 with 3% DMSO as a co-solvent. Initial rates were measured at 500 nm using a Cary 50Bio UV-vis spectrophotometer (Varian) at 22 °C, using a $\Delta\epsilon_{500}$ (change in molar extinction coefficient at 500 nm) of 43.5 mM⁻¹ cm⁻¹ (as determined from standard curves of fluorescein and fluorescein 2-phenylacetate) to convert absorbance into product concentration. The data were corrected for the buffer-catalysed background reaction measured under the same conditions (Extended Data Figure 5d). Assays with BH32, OE1 and variants were performed in triplicate and the averaged initial rates were fitted to the Michaelis-Menten equation using Origin software (Extended Data Figure 3). CUT190 assays were also performed in triplicate but the averaged initial rates were fitted to a Hill equation using the Origin software (Extended Data Figure 3). Representative time courses for the hydrolysis of 100 μ M fluorescein 2-phenylacetate are shown in Figures 1b, 2c.

Kinetic assays were performed using single enantiomers of fluorescein 2-phenylpropanoate (5–60 μ M for OE1.3 and 1.25–60 μ M for OE1.4) and enzyme (concentration of 1 μ M for OE1.3 and 0.5 μ M for OE1.4) in PBS pH 7.4 with 3% DMSO as a co-solvent. Initial rates were measured at 500 nm at 22 °C using a $\Delta\epsilon_{500} = 47.0$ mM⁻¹ cm⁻¹ (as determined from standard curves of fluorescein and fluorescein 2-phenylpropanoate) to convert absorbance into product concentration. Averaged initial rates for OE1.3 were fitted to a Michaelis-Menten equation and the rates for OE1.4 were fitted to a

Michaelis-Menten equation with substrate inhibition ($y = k_{\text{cat}} \times x / (K_M + x(1 + x/K_i))$) using Origin software (Extended Data Figure 4).

To determine the rate constant of fluorescein 2-phenylacetate hydrolysis catalysed by the nucleophiles Me-His, DMAP and *N*-methylimidazole, reactions were performed using a fixed concentration of fluorescein 2-phenylacetate (50 μM) and varying concentrations of nucleophile (0.5–1 mM). Linear fits of averaged initial rates versus nucleophile concentration were used to derive bimolecular rate constants $k_{\text{Me-His}}$, k_{DMAP} and k_{NMI} (Extended Data Figure 5).

7.4.1.12 Substrate profiling of OE1 and OE1.3

Assays were performed using fluorescein esters 2–7 (100 μM) and purified enzyme in PBS pH 7.4 with 3% DMSO as a co-solvent. Initial rates were measured at 500 nm using a Cary 50Bio UV-vis spectrophotometer at 22 $^{\circ}\text{C}$, using a $\Delta\epsilon_{500}$ to convert absorbance into product concentration. The data was corrected for the buffer-catalysed background reaction measured under the same conditions. For details of enzyme concentrations, extinction coefficients and the rates of background hydrolysis for each substrate, see Extended Data Table 1.

7.4.1.13 General method for the synthesis of fluorescein esters from the corresponding acid chloride[4]

Fluorescein sodium salt (0.53 mmol, 1 equiv.) and zinc chloride (0.13 mmol, 0.25 equiv.) were stirred in dry DMF (10 ml) at room temperature. The corresponding acid chloride (0.53 mmol, 1 equiv.) was added dropwise and the reaction was stirred overnight at room temperature. The reaction mixture was diluted with ethyl acetate (70 ml) and washed with 1 M HCl (2 \times 50 ml) and brine (1 \times 50 ml). The organic layer was dried over MgSO_4 , filtered and the solvent removed in vacuo to give the crude product.

Fluorescein 2-phenylacetate (1)

The crude product was purified by flash column chromatography (1:1 ethyl acetate:cyclohexane) to give the product as a yellow oil (118 mg, 49%). EI-MS $m/z = 451$ $[\text{M} + \text{H}]^+$. ^1H NMR (400 MHz, CDCl_3) δ 8.02 (1H, d, $J = 7.8$ Hz, CH), 7.63 (2H, m, 2 \times CH), 7.35 (5H, m, Ph), 7.09 (1H, d, $J = 6.9$ Hz, CH), 7.03 (1H, d, $J = 1.3$ Hz, CH), 6.76 (2H, m, 2 \times CH), 6.66 (1H, d, $J = 2.4$ Hz, CH), 6.57 (1H, d, $J = 8.7$ Hz, CH), 6.50 (1H, dd, $J = 8.7, 2.4$ Hz, CH), 3.89 (2H, s, CH_2); ^{13}C NMR (100 MHz, CDCl_3) δ 170.0, 170.0, 158.1, 153.0, 152.1, 151.8, 151.8, 135.3, 132.9, 129.9, 129.3, 129.1, 129.1, 128.8, 127.5, 126.3, 125.1, 124.0, 117.2, 116.6, 112.6, 110.4, 110.3, 103.1, 83.0, 41.3.

Fluorescein 4-methoxyphenylacetate (2)

The crude product was purified by flash column chromatography (1:1 ethyl acetate: cyclohexane) to give the product as a yellow oil (45 mg, 18%). EI-MS $m/z = 481$ $[\text{M} + \text{H}]^+$. ^1H NMR (400 MHz, CDCl_3) δ 8.02 (1H, d, $J = 7.1$ Hz, CH), 7.64 (2H, m, 2 \times CH), 7.29 (2H, d, $J = 8.6$ Hz, 2 \times CH), 7.12 (1H, d, $J = 7.3$ Hz, CH), 7.04 (1H, d, $J = 1.6$ Hz, CH), 6.91 (2H, d, $J = 8.6$ Hz, 2 \times CH), 6.76 (2H, m, 2 \times CH), 6.69 (1H, d, $J = 2.3$ Hz, CH), 6.61 (1H, d, $J = 8.8$ Hz, CH), 6.52 (1H, dd, $J = 8.9, 2.3$ Hz, CH), 5.65 (1H, br s, OH), 3.82 (3H, s, CH_3), 3.82 (2H, s, CH_2); ^{13}C NMR (100 MHz, CDCl_3) δ 170.0, 169.5, 159.0, 157.7, 153.0, 152.2, 151.9, 151.8, 135.2, 130.3, 129.9, 129.3, 129.0, 126.4, 125.1, 125.0, 124.0, 117.3, 116.7, 114.2, 112.5, 111.0, 110.3, 103.1, 82.6, 55.3, 40.5.

Fluorescein 4-fluorophenylacetate (3)

The crude product was purified by flash column chromatography (1:1 ethyl acetate: cyclohexane) to give the product as a yellow oil (73 mg, 29%). Electron ionization mass spectrometry (EI-MS) $m/z = 469 [M + H]^+$. ¹H NMR (400 MHz, CDCl₃) δ 8.02 (1H, d, $J = 7.2$ Hz, CH), 7.64 (2H, m, 2 \times CH), 7.35 (2H, dd, $J = 8.4$ Hz, 5.4 Hz, 2 \times CH), 7.07 (4H, m, 4 \times CH), 6.76 (2H, m, 2 \times CH), 6.67 (1H, d, $J = 2.2$ Hz, CH), 6.58 (1H, d, $J = 8.7$ Hz, CH), 6.51 (1H, dd, $J = 8.4, 2.3$ Hz, CH), 3.86 (2H, s, CH₂); ¹³C NMR (100 MHz, CDCl₃) δ 169.9, 169.7, 162.2 (d, $J = 245$ Hz, C–F), 158.0, 153.0, 152.1, 151.8, 151.8, 135.3, 130.9 (d, $J = 8$ Hz, C–F), 129.9, 129.2, 129.1, 128.6 (d, $J = 3$ Hz, C–F), 126.3, 125.1, 124.0, 117.1, 116.7, 115.7 (d, $J = 22$ Hz, C–F), 112.6, 110.5, 110.2, 103.1, 82.9, 40.4.

Fluorescein 2-thiopheneacetate (4)

The crude product was purified by flash column chromatography (1:1 ethyl acetate:cyclohexane) to give the product as a yellow oil (116 mg, 48%). EI-MS $m/z = 457 [M + H]^+$. ¹H NMR (400 MHz, CDCl₃) δ 8.03 (1H, d, $J = 7.2$ Hz, CH), 7.65 (2H, m, 2 \times CH), 7.28 (1H, m, CH), 7.12 (1H, d, $J = 7.3$ Hz, CH), 7.06 (2H, m, 2 \times CH), 7.01 (1H, m, CH), 6.79 (2H, s, 2 \times CH), 6.69 (1H, d, $J = 2.3$ Hz, CH), 6.60 (1H, d, $J = 8.4$ Hz, CH), 6.52 (1H, dd, $J = 8.7, 2.4$ Hz, CH), 6.30 (1H, br s, OH), 4.11 (2H, s, CH₂); ¹³C NMR (100 MHz, CDCl₃) δ 170.0, 168.8, 158.1, 153.0, 152.1, 151.8, 151.7, 135.3, 133.8, 129.9, 129.2, 129.1, 127.3, 127.0, 126.3, 125.5, 125.1, 124.0, 117.1, 116.7, 112.6, 110.4, 110.2, 103.1, 83.0, 35.5.

Fluorescein naphthalen-2-yl-acetate (5)

The crude product was purified by flash column chromatography (1:1 ethyl acetate:cyclohexane) to give the product as a yellow oil (106 mg, 40%). EI-MS $m/z = 501 [M + H]^+$. ¹H NMR (400 MHz, CDCl₃) δ 8.02 (1H, d, $J = 6.7$ Hz, CH), 7.85 (4H, m, 4 \times CH), 7.62 (2H, m, 2 \times CH), 7.50 (3H, m, 3 \times CH), 7.07 (1H, d, $J = 6.9$ Hz, CH), 7.03 (1H, s, CH), 6.76 (2H, s, 2 \times CH), 6.64 (1H, d, $J = 2.3$ Hz, CH), 6.57 (1H, d, $J = 8.7$ Hz, CH), 6.52 (1H, br s, OH), 6.49 (1H, dd, $J = 8.7, 2.5$ Hz, CH), 4.05 (2H, s, CH₂); ¹³C NMR (100 MHz, CDCl₃) δ 170.0, 170.0, 158.1, 153.0, 152.0, 151.8, 151.8, 135.3, 133.4, 132.6, 130.3, 129.9, 129.1, 129.1, 128.5, 128.2, 127.7, 127.7, 127.1, 126.3, 126.3, 126.1, 125.1, 124.0, 117.2, 116.6, 112.6, 110.3, 110.3, 103.1, 83.1, 41.5.

General method for the synthesis of fluorescein esters from the corresponding carboxylic acid

Acid (1 mmol, 1 equiv.) was dissolved in dry acetonitrile (10 ml), dicyclohexylcarbodiimide (1.1 mmol, 1.1 equiv.) was added and the mixture was cooled to 0 °C. Fluorescein (1.2 mmol, 1.2 equiv.) was added and the reaction mixture was stirred for 15 min at 0 °C, then at room temperature overnight. The reaction was diluted with ethyl acetate (70 ml), washed with 1 M HCl (2 \times 50 ml) and then brine (1 \times 50 ml). The organic layer was dried over MgSO₄, filtered and the solvent removed in vacuo to yield the crude product.

Fluorescein 2-furanacetate (6)

The crude product was purified by flash column chromatography (1:1 ethyl acetate:cyclohexane) to give the product as a yellow oil (24 mg, 6%). EI-MS $m/z = 441 [M + H]^+$. ¹H NMR (400 MHz, CDCl₃) δ 8.03 (1H, d, $J = 7.1$, CH), 7.66 (2H, m, 2 \times CH), 7.42 (1H, d, $J = 1.0$ Hz, CH), 7.16 (1H, d, $J = 7.5$, CH), 7.10 (1H, s, CH), 6.80 (2H, d, $J = 1.1$ Hz, 2 \times CH), 6.73 (1H, d, $J = 2.4$ Hz, CH), 6.65 (1H, d, $J = 8.6$ Hz, CH), 6.55 (1H, dd, $J = 8.4, 2.4$ Hz, CH), 6.37 (2H, m, 2 \times CH), 3.96 (2H, s, CH₂); ¹³C NMR

(100 MHz, CDCl₃) δ 169.6, 167.5, 157.8, 153.0, 152.1, 151.8, 151.7, 146.5, 142.5, 135.2, 129.9, 129.3, 129.1, 126.4, 125.1, 124.0, 117.2, 116.8, 112.5, 110.9, 110.7, 110.3, 108.6, 103.1, 82.6, 34.2.

(R)- and (S)-Fluorescein 2-phenylpropanoate (7)

The crude products were purified by flash column chromatography (1:1 ethyl acetate:cyclohexane) to give (*R*)-**7** (42 mg, 9%) and (*S*)-**7** (51 mg, 11%) as yellow oils. EI-MS m/z = 465 [M + H]⁺. ¹H NMR (400 MHz, CDCl₃) δ 8.01 (1H, d, J = 7.5 Hz, CH), 7.64 (2H, m, 2 \times CH), 7.34 (5H, m, Ph), 7.07 (1H, m, CH), 6.96 (1H, m, CH), 6.76–6.63 (3H, m, 3 \times CH), 6.58 (1H, dd, J = 8.7 Hz, 1.2 Hz, CH), 6.51 (1H, m, CH), 3.99 (1H, q, J = 7.1 Hz, CH), 1.63 (3H, dd, J = 7.2, 1.5 Hz, CH₃); ¹³C NMR (100 MHz, CDCl₃) δ 173.0, 169.9, 158.1, 153.0, 152.1, 151.9, 151.8, 139.5, 135.3, 129.9, 129.1, 129.0, 128.9, 128.9, 127.6, 127.5, 127.5, 126.3, 125.1, 124.0, 117.1, 117.1, 116.5, 112.6, 110.4, 110.2, 110.2, 103.1, 83.0, 45.6, 45.6, 18.4, 18.4.

7.4.1.14 Crystallization, refinement and model building

Crystals of OE1 variants were prepared by mixing 200 nl of 10 mg ml⁻¹ protein in PBS buffer pH 7.4 with equal volumes of precipitant. All trials were conducted by sitting-drop vapour diffusion and incubated at 4 °C. Protein crystallization conditions are given in Supplementary Table 2. All crystals were cryoprotected by the addition of 10% PEG 200 to the mother liquor and flash-cooled in liquid nitrogen. Data were collected from single crystals at Diamond Light Source and subsequently scaled and reduced with Xia2. Preliminary phasing was performed by molecular replacement in Phaser using a search model derived from wild-type BH32 (PDB code: 2UW6). Iterative cycles of rebuilding and refinement were performed in COOT and Phenix.refine,[5] respectively. Structure validation with MolProbity and PDBREDO were integrated into the iterative rebuild and refinement process. Complete data collection and refinement statistics can be found in the Supplementary information. Coordinates and structure factors have been deposited in the Protein Data Bank under accession numbers 6Q7N, 6Q7O, 6Q7P, 6Q7Q and 6Q7R. In silico mutagenesis was performed using ICM Pro to derive model of engineered OE1.4.

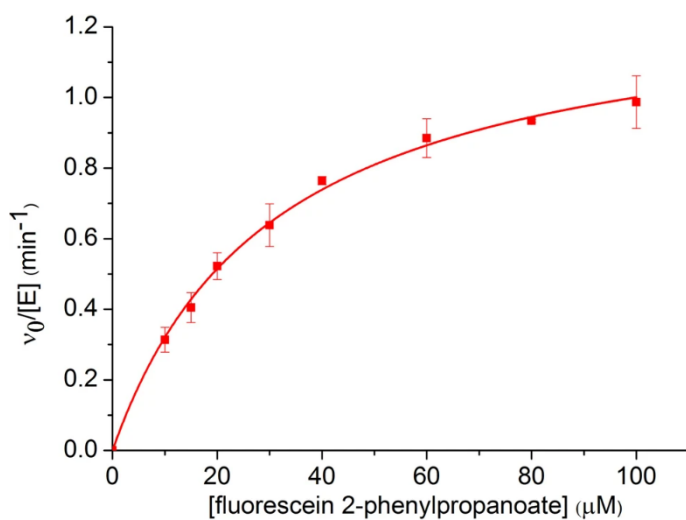
7.4.1.15 Data availability

Coordinates and structure factors have been deposited in the Protein Data Bank under accession numbers 6Q7N, 6Q7O, 6Q7P, 6Q7Q and 6Q7R.

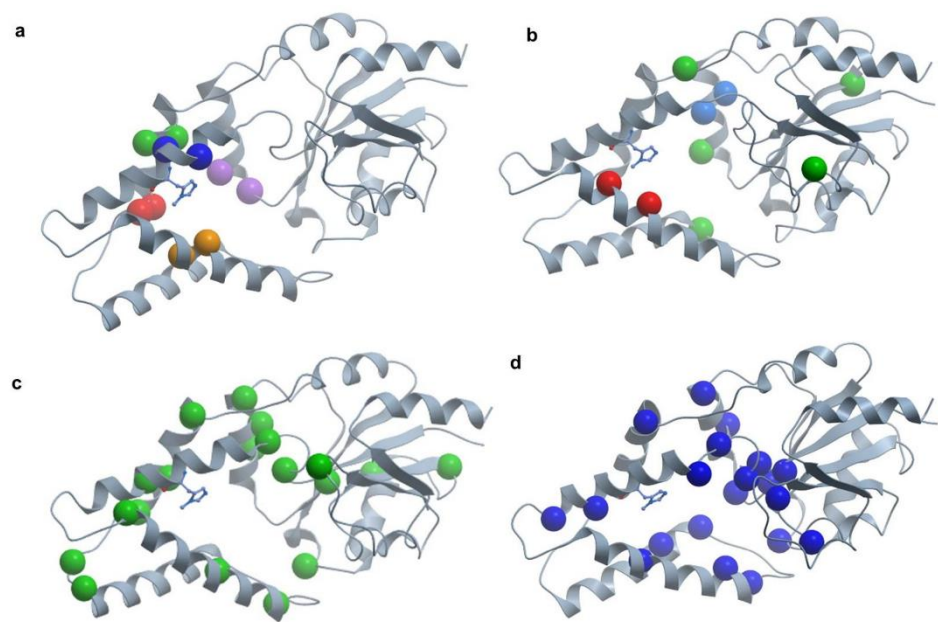
7.4.1.16 References

1. Lee, T. S. et al. BglBrick vectors and datasheets: A synthetic biology platform for gene expression. *J. Biol. Eng.* **5**, 12 (2011).
2. Kawai, F. et al. A novel Ca²⁺-activated, thermostabilized polyesterase capable of hydrolyzing polyethylene terephthalate from *Saccharomonospora viridis* AHK190. *Appl. Microbiol. Biotechnol.* **98**, 10053-10064 (2014).
3. Kille, S. et al. Reducing codon redundancy and screening effort of combinatorial protein libraries created by saturation mutagenesis. *ACS Synth. Biol.* **2**, 83-92 (2013).
4. Yang, Y., Babiak, P. & Reymond, J. New monofunctionalized fluorescein derivatives for the efficient high-throughput screening of lipases and esterases in aqueous media. *Helv. Chim. Acta* **89**, 404-415 (2006).
5. Adams, P. D. et al. PHENIX: a comprehensive Python-based system for macromolecular structure solution. *Acta Crystallogr. D* **66**, 213-221 (2010).

7.4.2 Extended Data



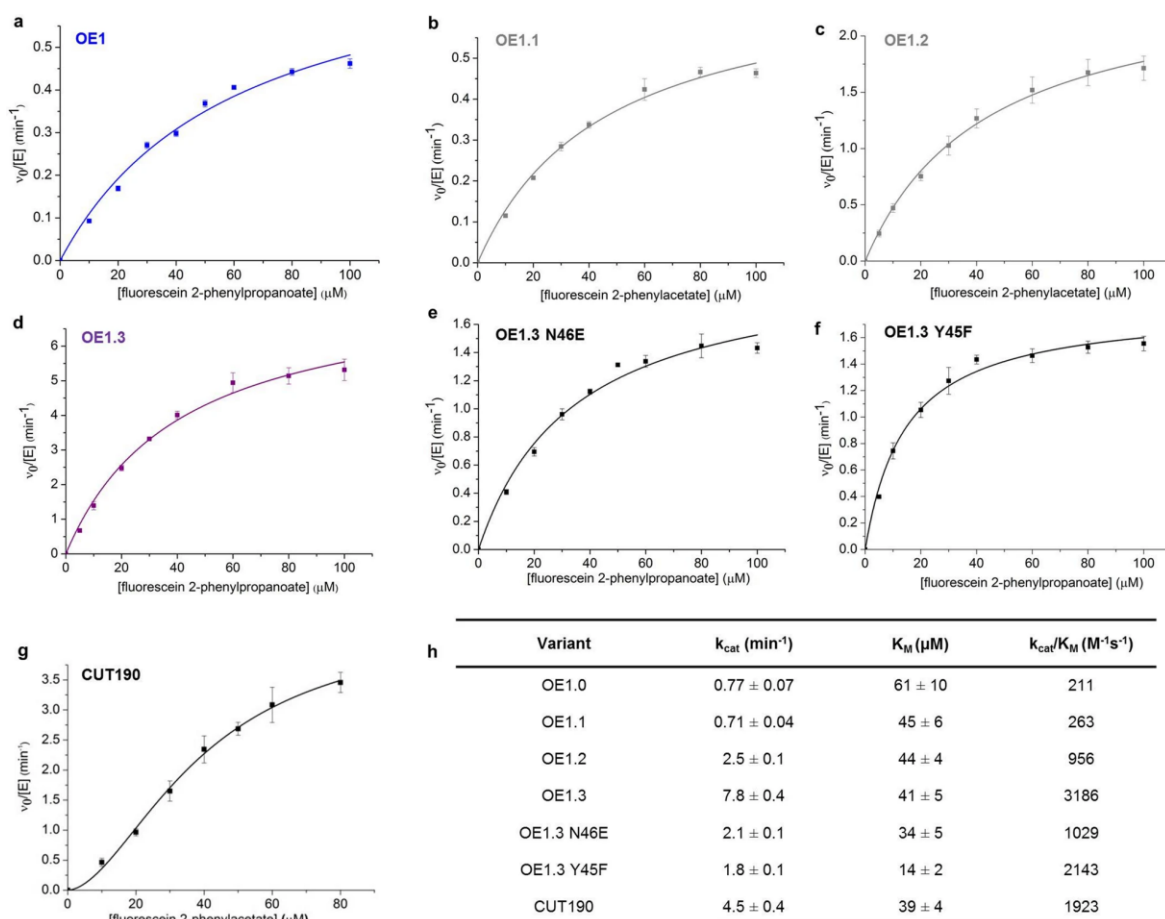
7.4.2.1 Extended Data Figure 1: Kinetic characterization of BH32. Michaelis–Menten plot showing the rate of His23 acylation (the ‘burst phase’) with varying concentrations of fluorescein 2-phenylacetate. Averaged initial rates were fitted to the Michaelis–Menten equation to derive rate constant k_{obs} $1.3 \pm 0.03 \text{ min}^{-1}$ and the enzyme–substrate dissociation constant K_s $30.9 \pm 1.8 \mu\text{M}$ ($R^2 = 0.99$). Data are mean \pm s.d. of measurements made in triplicate.



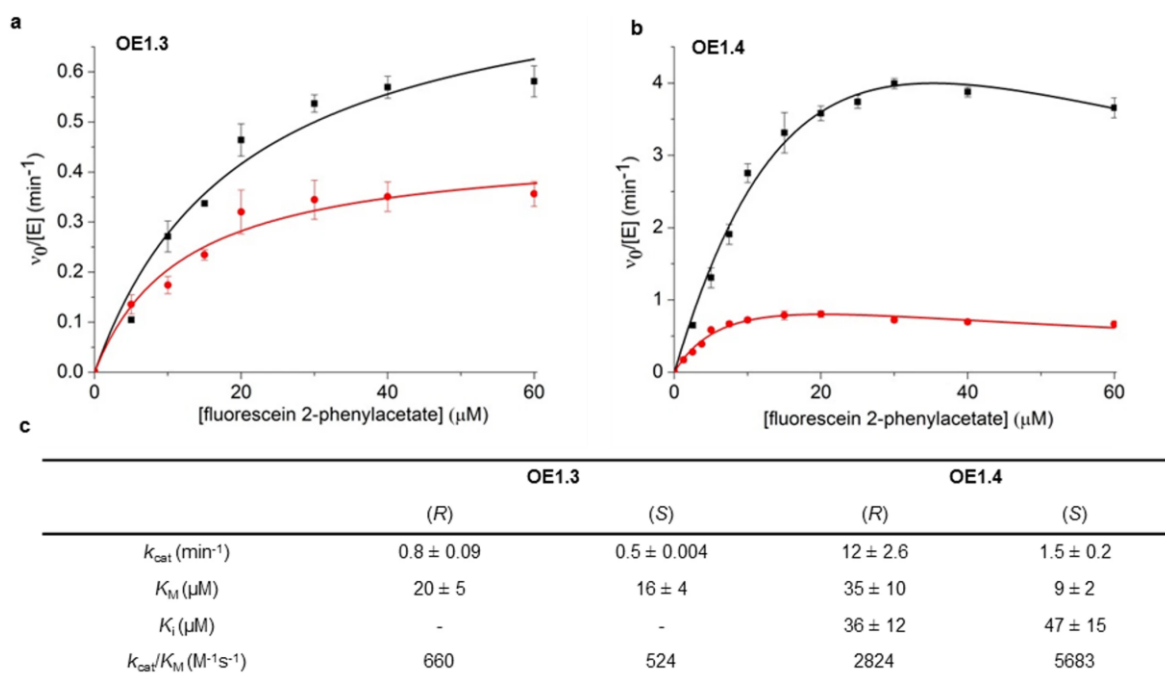
Round	Description	Positions Mutated	Most active variant following gene shuffling
1	CASTing targeting the active site	A19/S22 (blue), Y45/E46 (orange), Y87/W88 (red), M94/S95 (green), D125/Q128 (purple)	A19H S22M H23Me-His D125C
2	Random mutagenesis followed by saturation mutagenesis at identified 'hotspots'	Random mutagenesis: entire gene Saturation mutagenesis: L42/E46 (red), F132/L133 (blue), P63, E100, H117, Q128, W209 (green)	A19H S22M H23Me-His E46N P63G D125C
3	Saturation mutagenesis targeting active site positions and residues in flexible loop regions	D8, L10, N14, I26, P38, T49, F56, Y79, F87, F81, S91, Q96, Y98, D125, M130, L133, L136, F154, K167, E174, K202	L10P A19H S22M H23Me-His E46N P63G D125G
4	Saturation mutagenesis targeting active site positions and residues in flexible loop regions	D8, S9, G11, N14, V16, M27, L31, Y45, F53, Y56, L64, L68, Y98, T122, S124, M130, L136, F154, D180, P182	L10P N14Q A19H S22M H23Me-His E46N P63G S124L D125G D180F

7.4.2.2 Extended Data Figure 2: Evolutionary strategy used to generate OE1.3 and OE1.4.

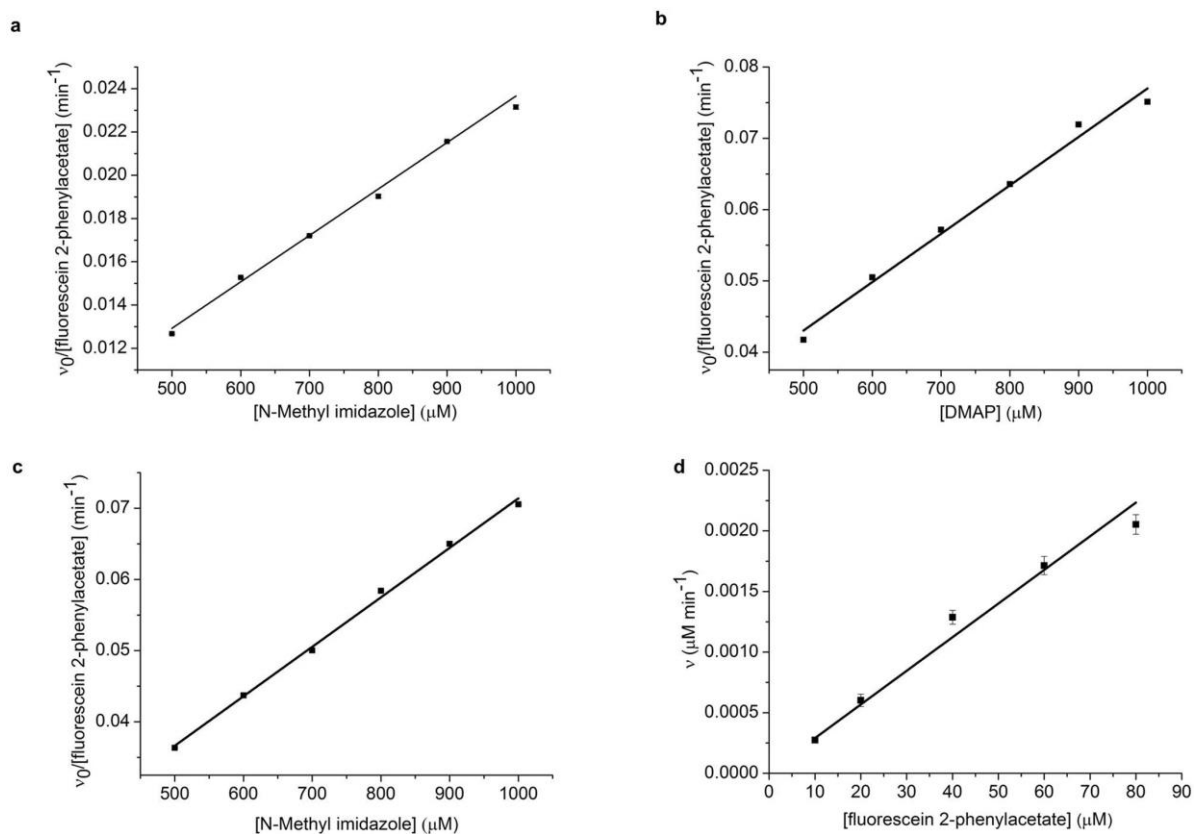
Structures showing the amino acid positions randomised during each round of evolution. The Me-His residue is shown in ball-and-stick representation and targeted residues are represented as spheres. a) The round 1 library was prepared by randomising active-site residues in pairs Ala19/Ser22 (blue) Tyr45/Glu46 (orange) Tyr87/Trp88 (red) Met94/Ser95 (green) and Asp125/Gln128 (purple). b) The round 2 library was prepared by random mutagenesis of the entire gene. Variants with improved activity enabled the identification of 'hot spots', which were further interrogated using saturation mutagenesis. Residues Leu42/Glu46 (red) and Phe132/Leu133 (blue) were randomised simultaneously; all other positions were randomised individually (green). c) The round 3 library was prepared by saturation mutagenesis, using NNK degenerate codons to individually randomise 21 positions (see table). d) The round 4 library was prepared by saturation mutagenesis, using NNK degenerate codons to individually randomise 20 positions (see table). Libraries generated during rounds 1-3 were screened for activity towards fluorescein 2-phenylacetate. The round 4 library was screened for activity towards fluorescein (*R*)-2-phenylpropanoate.



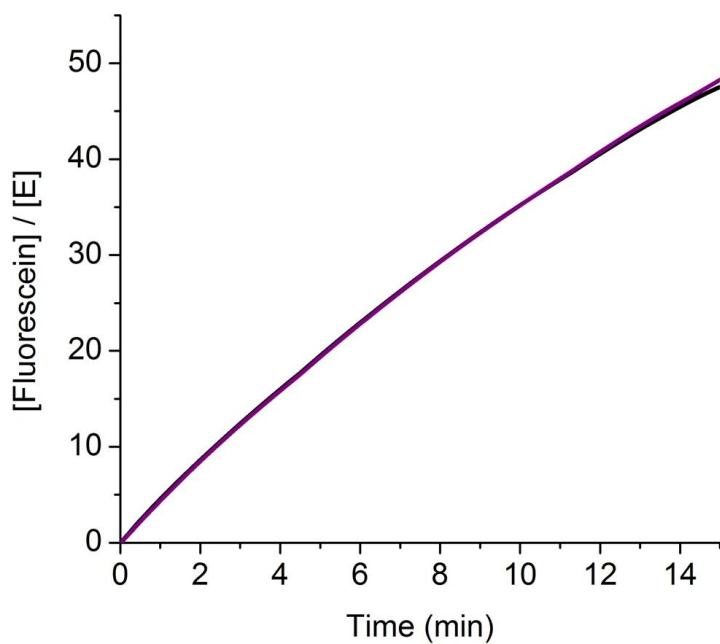
7.4.2.3 Extended Data Figure 3: Kinetic characterization of OE1, OE1 variants and CUT190. a-f) Michaelis-Menten plots of fluorescein 2-phenylacetate hydrolysis catalysed by OE1 (a), OE1.1 (b), OE1.2 (c), OE1.3 (d), OE1.3(N46E) (e) and OE1.3(Y45F) (f). g) A Hill plot of fluorescein 2-phenylacetate hydrolysis catalysed by CUT190, $n = 2.3 \pm 0.4$. Data are mean \pm s.d. of measurements made in triplicate. h) A table summarizing the kinetic parameters of OE1 and its variants, and the cutinase variant Ser226Pro/Arg228Ser (CUT190).



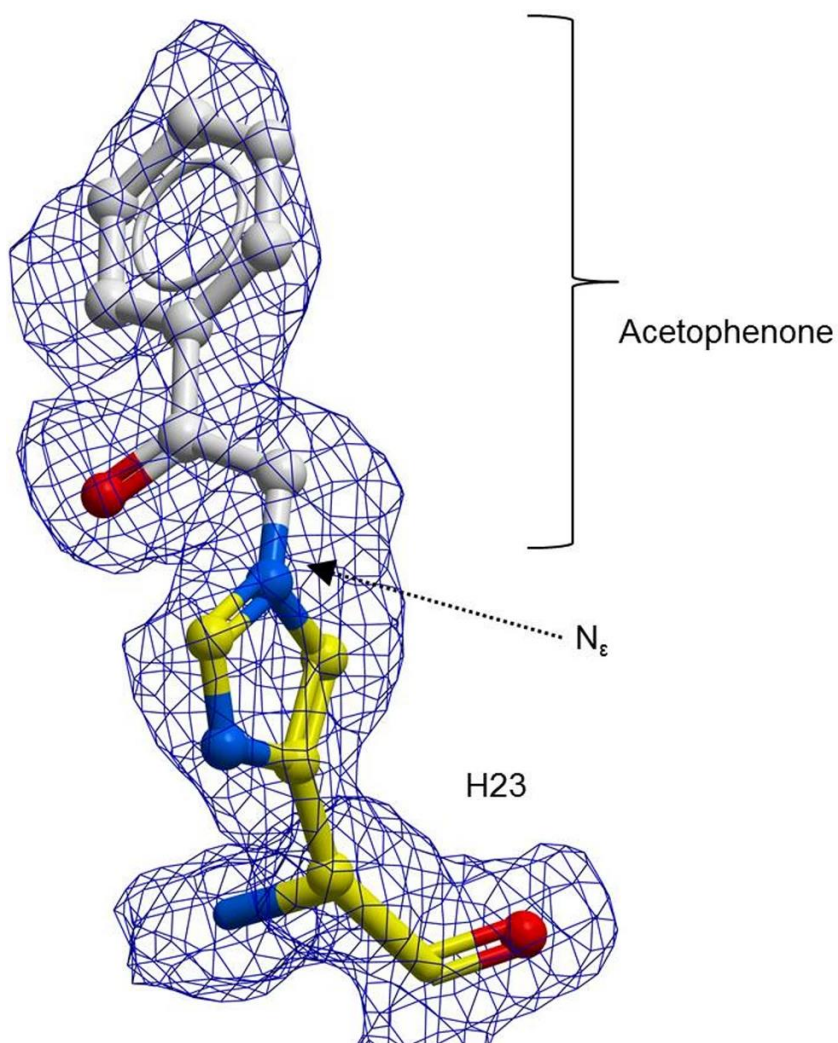
7.4.2.4 Extended Data Figure 4: Kinetic characterization of OE1.3 and OE1.4 towards the hydrolysis of (R)- and (S)- fluorescein 2-phenylpropanoate. a) Michaelis-Menten plots of fluorescein (R)-2-phenylpropanoate and fluorescein (S)-2-phenylpropanoate hydrolysis (shown in black and red, respectively), catalysed by OE1.3. The averaged initial rates were fitted to the Michaelis-Menten equation using Origin software. b) Michaelis-Menten plots of fluorescein (R)-2-phenylpropanoate and fluorescein (S)-2-phenylpropanoate hydrolysis (shown in black and red, respectively) catalysed by OE1.4. The averaged initial rates were fitted to the equation for Michaelis-Menten with substrate inhibition using Origin software. Data are mean \pm s.d. of measurements made in triplicate. c) Table summarizing the kinetic parameters for the hydrolysis of both enantiomers of fluorescein 2-phenylpropanoate catalysed by OE1.3 and OE1.4. Data are mean \pm s.d. of measurements made in triplicate.



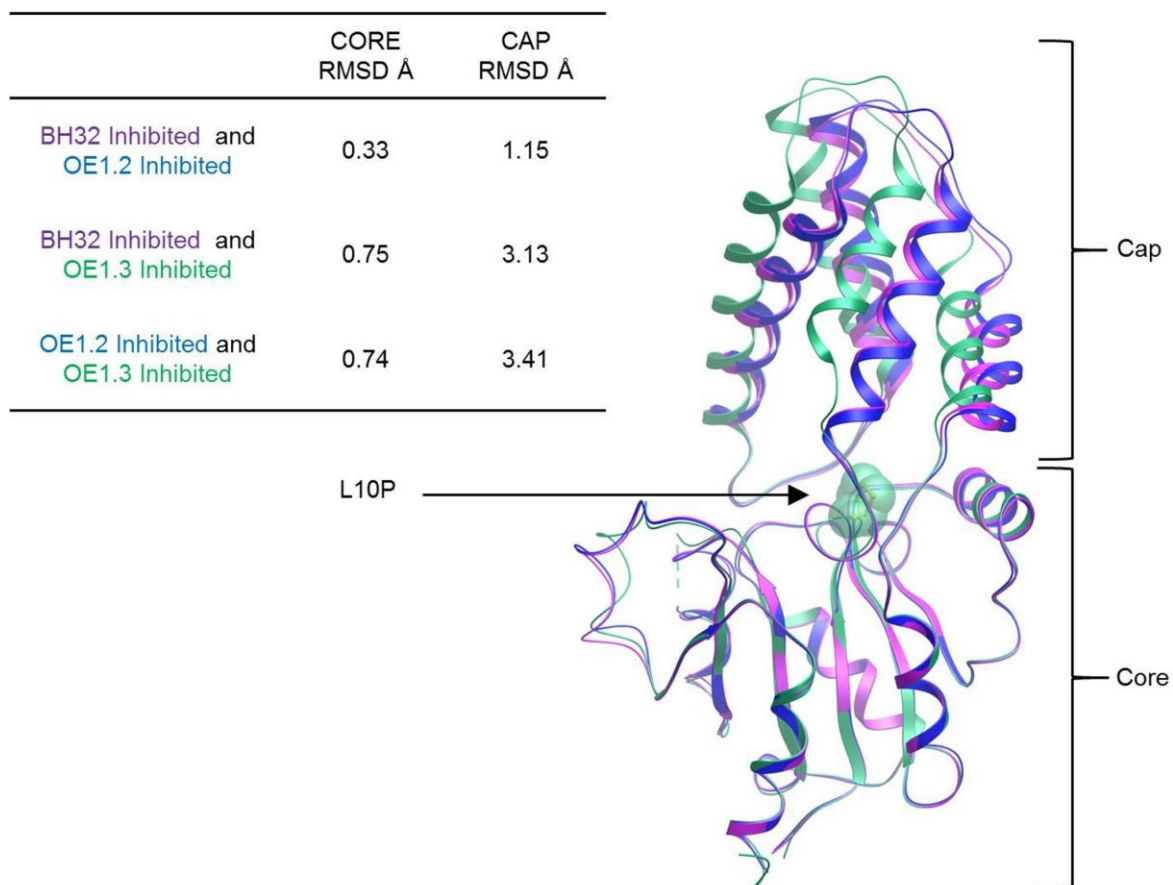
7.4.2.5 Extended Data Figure 5: Rate constants of the hydrolysis of fluorescein 2-phenylacetate catalysed by small-molecule nucleophilic catalysts. a–c) Linear plots showing the rate of hydrolysis of fluorescein 2-phenylacetate catalysed by 3-methylhistidine ($k_{\text{Me-His}} = 0.35 \text{ M}^{-1} \text{ s}^{-1}$, $R^2 = 0.99$) (a), dimethylaminopyridine ($k_{\text{DMAP}} = 1.13 \text{ M}^{-1} \text{ s}^{-1}$, $R^2 = 0.99$) (b) and *N*-methylimidazole ($k_{\text{NMI}} = 1.16 \text{ M}^{-1} \text{ s}^{-1}$, $R^2 = 0.99$) (c). d) Linear plot showing the rate of uncatalysed fluorescein 2-phenylacetate hydrolysis ($k_{\text{obs}} = 5.9 \times 10^{-4} \text{ min}^{-1}$, $R^2 = 0.98$). Data are mean \pm s.d. of measurements made in triplicate.



7.4.2.6 Extended Data Figure 6: Comparison of the ester hydrolysis reaction catalysed by OE1.3 and OE1.3(C186A/C212A). Time course of the hydrolysis of fluorescein 2-phenylacetate (100 μ M) catalysed by OE1.3 (purple) and OE1.3(C186A/C212A) (black) (0.1 μ M) in PBS pH 7.4, 22 $^{\circ}$ C, showing that the Cys186Ala and Cys212Ala mutations have a negligible effect on catalytic activity.

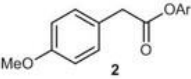
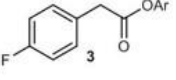
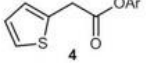
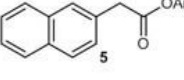
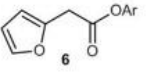
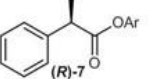
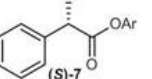


7.4.2.7 Extended Data Figure 7: Structural characterization of inhibited BH32. A ball-and-stick representation of H23 from BH32 inhibited with 2-bromoacetophenone, coloured by atom type with H23 carbon atoms in yellow and acetophenone carbons in white. Clear FEM electron density (blue, contoured at 1σ) extends between the N_{ϵ} of H23 and acetophenone.



7.4.2.8 Extended Data Figure 8: Structural characterization of inhibited BH32, OE1.2 and OE1.3. A global superposition of BH32-inhibited (purple), OE1.2-inhibited (blue) and OE1.3-inhibited (green) structures performed using ICM Pro. The r.m.s.d. values (backbone atoms), derived from the global superposition are calculated separately for the core and cap domains and are reported in the table. BH32-inhibited and OE1.2-inhibited structures retain similar domain orientations, whereas OE1.3 undergoes a reorientation of the cap domain upon inhibition with 2-bromoacetophenone.

7.4.2.9 Extended Data Table 1: Experimental conditions used for substrate profiling of OE1 and OE1.3.

Substrate ^a	Enzyme Variant	Enzyme Conc. (μM)	$v_0/[E]$ (min^{-1})	$\Delta\varepsilon_{500}$ ($\text{mM}^{-1} \text{cm}^{-1}$)	Background hydrolysis ($\mu\text{M min}^{-1}$)
 2	OE1	4	0.16 ± 0.01	48.4	0.07 ± 0.005
	OE1.3	0.25	5.05 ± 0.27		
 3	OE1	4	0.35 ± 0.01	46.7	0.14 ± 0.01
	OE1.3	0.25	4.85 ± 0.17		
 4	OE1	4	0.74 ± 0.03	44.6	0.65 ± 0.03
	OE1.3	0.25	6.46 ± 0.38		
 5	OE1	4	0.04 ± 0.003	50.1	0.05 ± 0.002
	OE1.3	0.5	1.32 ± 0.07		
 6	OE1	4	0.39 ± 0.04	35.2	0.59 ± 0.04
	OE1.3	2	3.31 ± 0.10		
 (R)-7	OE1	10	0.03 ± 0.002	47.0	0.04 ± 0.005
	OE1.3	1	0.62 ± 0.03		
 (S)-7	OE1	4	0.1 ± 0.01	47.0	0.04 ± 0.005
	OE1.3	1	0.41 ± 0.04		

Assay parameters used to determine the initial activity ($v_0/[E]$) for OE1- and OE1.3-catalysed reactions with a range of fluorescein esters.

^aAr, fluorescein.

7.4.2.10 Extended Data Table 2: Experimental and calculated masses of apo and inhibited enzymes.

Variant	Expected Mass	Observed Mass
BH32	27635	27634
BH32 inhibited	27754 (1 modification)	27754
	27873 (2 modifications)	27872
	27992 (3 modifications)	27990
BH32 H23A	27569	27567
OE1	27649	27648
OE1.2	27692	27693
OE1.2 C125A C186A C212A	27596	27597
OE1.2 C125A C186A C212A inhibited	27715 (1 modification)	27715
OE1.3	27630	27630
OE 1.3 C186A C212A	27566	27566
OE 1.3 C186A C212A inhibited	27685 (1 modification)	27685

Mass spectrometry data for BH32 and OE1 variants. Enzymes were alkylated with the mechanistic inhibitor 2-bromoacetophenone.

7.4.3 Supplementary Information

7.4.3.1 DNA and protein sequence of the most active variant OE1.3

Mutations from BH32: L10P A19H S22M **H23Me-His** E46N P63G D125G

ATGATTCGTGCGGTATTCTTTGATAGCCCGGGTACTCTGAATAGCGTTGAAGGTCATGCTAAA
ATGTAGCTGAAAATTATGGAGGAAGTGCTGGGTGACTATCCGCTGAACCCGAAAACCCTTCTT
GACGAATAACAATAAACTGACCCGCGAAGCGTTCTCTAACTATGCGGGCAAACCGTATCGCGG
TCTGCGTGATATCCTGGAAGAAGTAATGCGTAAACTGGCGGAAAAGTACGGTTTTCAAATACCC
TGAAAACCTTCTGGGAAATCTCCCTGCGCATGTCTCAACGCTACGGCGAGCTGTACCCGGAAG
TGGTGGAGTACTGAAATCTCTGAAAGGTAAATATCACGTTGGCATGATCACCGATTCCGGTA
CCGAGCAGGCCATGGCATTCTCTGGACGCACTGGGCATCAAAGACCTGTTTCGATTCCATCACC
ACGTCTGAAGAAGCTGGTTTTCTTTAAACCGCACCCACGCATCTTCGAACTGGCTCTGAAGAAA
GCCGGCGTTAAAGGCGAGGAAGCAGTGTACGTTGGTGACAACCCGGTCAAAGACTGTGGTG
GTTCTAAGAACCTGGGTATGACTAGCATCCTGCTGGATCGTAAAGGTGAGAAACGTGAATTCT
GGGATAAGTGCGACTTTATCGTCTCCGACCTGCGCGAAGTTATTAAGATTGTTGACGAACTGA
ACGGTCAGGGCTCTCTCGAGCACCACCACCACCACCAC

MIRAVFFDSPGTLNSVEGHAK**MMeHis**LKIMEEVLGDYPLNPKTLLDEY**NKL**TREAFSNYAGKPYR
GLRDILEEVMRKLAEKYGFKYPENFWEISLRMSQRYGELYPEVVEVLKSLKGKYHVGMITDS**GTE**
QAMAFLDALGIKDLFDSITTSEEAGFFKPHPRIFELALKKAGVKGEEAVYVGDNPVKDCGGSKNLG
MTSILLDRKGEKREFWDKCDFIVSDLREVIKIVDELNGQGSLEHHHHHH

7.4.3.2 DNA and protein sequence of cutinase CUT190 S226P/R228S

ATGCGTATTCGTCGTCAGGCAGGTACAGGTGCACGTGCGAGCATGGCACGCGCAATTGGTGT
TATGACCACCGCACTGGCAGTTCTGGTTGGTGCAGTTGGTGGTGTGGCCGGTGCAGAAGTTA
GCACCGCACAGGATAATCCGTATGAACGTGGTCCTGATCCGACCGAAGATAGCATTGAAGCA
ATTCGTGGTCCGTTTTAGCGTTGCAACCGAACGTGTTAGCAGCTTTGCAAGCGGTTTTGGTGGT
GGCACCATCTATTATCCGCGTGAAACCGATGAAGGCACCTTTGGTGCCGTTGCAGTTGCACC
GGTTTTTACCGCAAGCCAGGGTAGCATGAGCTGGTATGGTGAACGTGTTGCCAGCCAGGGTT
TTATTGTTTTTACCATTGATACCAACACGCGTCTGGATCAGCCTGGTCAGCGTGGTCGTCAGC
TGCTGGCAGCACTGGATTATCTGGTTGAACGTAGCGATCGTAAAGTTCGTGAACGTCTGGACC
CGAATCGTCTGGCAGTTATGGGTCATAGCATGGGTGGTGGTGGTAGCCTGGAAGCAACCGTT
ATGCGTCCGAGCCTGAAAGCAAGCATTCCGCTGACACCGTGGAATCTGGATAAAACCTGGGG
TCAAGTTCAGGTTCCGACCTTTATCATTGGTGCAGAACTGGATAACCATTGCACCGGTTAGCAC
CCATGCAAAACCGTTTTATGAAAGCCTGCCGAGCAGTCTGCCGAAAGCATATATGGAAGTGA
TGGTGCACCCATTTTGCACCGAATATTCCGAATACCACCATTGCCAAATATGTGATTAGCTGG
CTGAAACGCTTTGTGGATGAAGATACCCGTTATAGCCAGTTTCTGTGTCCGAATCCGACAGAT
CGTGCAATTGAAGAATATCGTAGCACCTGTCCGTATCTCGAGCACCACCACCACCACCAC

MRIRRQAGTGARASMARAIQVMTTALAVLVGAVGGVAGAEVSTAQDNPHYERGPDPTEDESIEAIRG
PFSVATERVSSFASGFGGGTIYYPRETDEGTFGAVAVAPGFTASQGSMSWYGERVASQGFIVFTI
DTNTRLDQPGQRGRQLLAALDYLVERSDRKVRERLDPNRLAVMGHSMGGGGSLEATVMRPSLK
ASIPLTPWNLDKTVGQVQVPTFIIGAELDTIAPVSTHAKPFYESLPSSLPKAYMELDGATHFAPNIP
NTTIAKYVISWLKRFVDEDTRYSQLCPNPTDRAIEEYRSTCPYLEHHHHHH

7.4.3.3 Supplementary Information Table 1: Data collection and refinement statistics

	BH32 Inhibited	OE1	OE1.2 Inhibited	OE1.3	OE1.3 inhibited
Wavelength	0.9795	0.9159	0.9	0.9795	0.9795
Resolution range	41.62 - 2.019 (2.091 - 2.019)	41.43 - 2.0 (2.072 - 2.0)	41.49 - 1.96 (2.03 - 1.96)	40.81 - 1.9 (1.968 - 1.9)	40.74 - 1.5 (1.554 - 1.5)
Space group	P 1 2 1 1	P 1 2 1 1	P 1 2 1 1	P 1 2 1 1	P 2 1 2 1 2 1
Unit cell	34.571 70.549 53.004 90 103.484 90	34.11 70.53 52.82 90 104.24 90	33.98 71.31 52.89 90 105.28 90	33.9519 71.1252 51.9215 90 106.333 90	48.4707 72.9651 75.1683 90 90 90
Total reflections	53729 (5254)	53892 (5384)	58622 (5781)	60932 (5912)	276379 (27371)
Unique reflections	15995 (1586)	16357 (1603)	17448 (1718)	18693 (1841)	43399 (4256)
Multiplicity	3.4 (3.3)	3.3 (3.4)	3.4 (3.4)	3.3 (3.2)	6.4 (6.4)
Completeness (%)	97.97 (98.94)	99.36 (99.38)	99.46 (98.85)	99.61 (97.97)	99.95 (99.91)
Mean I/sigma(I)	17.83 (2.03)	11.53 (2.04)	11.15 (2.06)	11.56 (2.28)	16.63 (2.74)
Wilson B-factor	43.69	36.05	35.32	27.36	17.03
R-merge	0.03619 (0.5781)	0.06056 (0.564)	0.05641 (0.4798)	0.05375 (0.3962)	0.05312 (0.537)
R-meas	0.04311 (0.6888)	0.0723 (0.6713)	0.0671 (0.5697)	0.06441 (0.4787)	0.05791 (0.5846)
R-pim	0.02318 (0.3714)	0.03897 (0.3597)	0.03599 (0.3043)	0.03512 (0.2652)	0.02278 (0.2283)
CC1/2	0.999 (0.837)	0.998 (0.791)	0.998 (0.827)	0.998 (0.804)	0.999 (0.874)
CC*	1 (0.955)	0.999 (0.94)	0.999 (0.951)	0.999 (0.944)	1 (0.966)
Reflections used in refinement	15992 (1584)	16351 (1603)	17442 (1717)	18668 (1834)	43388 (4254)
Reflections used for R-free	765 (74)	822 (80)	906 (98)	865 (92)	2208 (207)

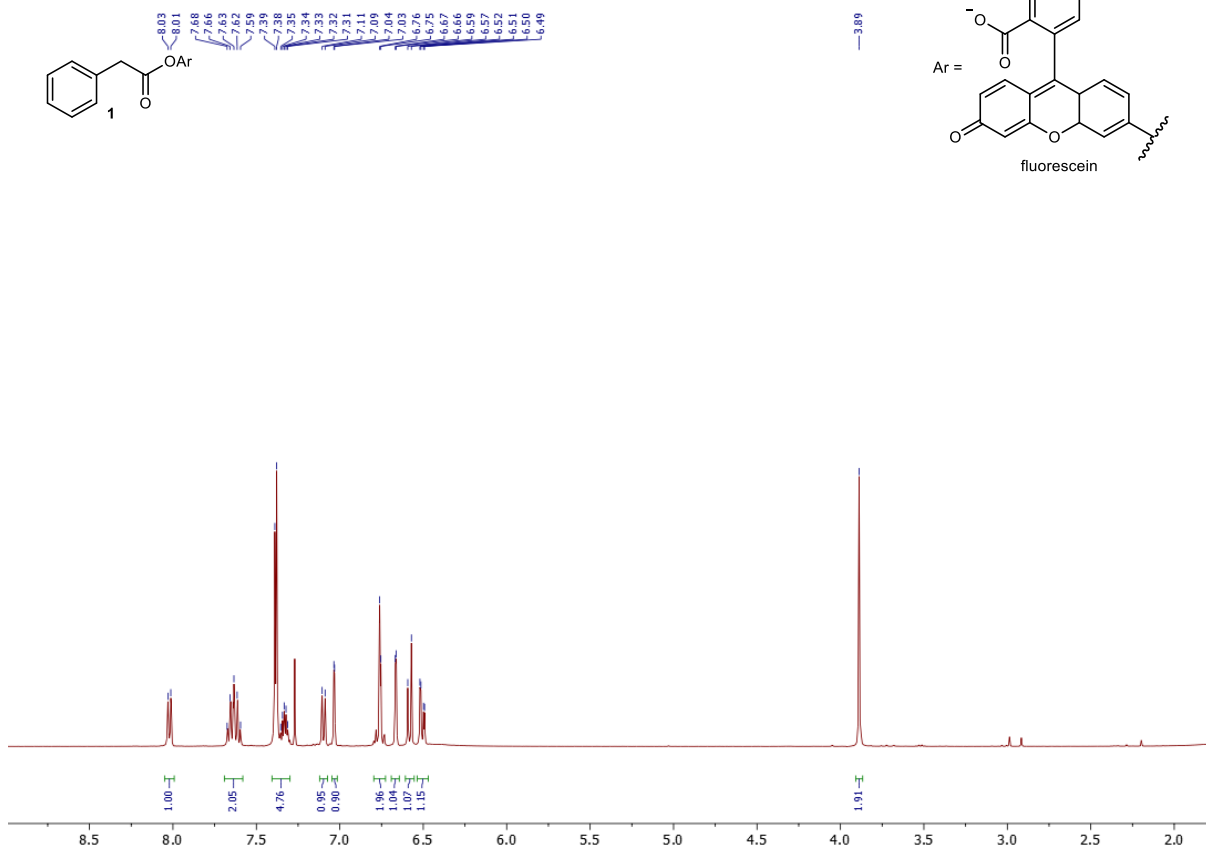
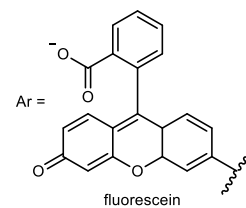
R-work	0.1965 (0.3013)	0.1920 (0.2761)	0.1720 (0.2434)	0.1764 (0.2385)	0.1568 (0.2059)
R-free	0.2360 (0.3454)	0.2283 (0.3356)	0.2136 (0.2735)	0.2247 (0.2664)	0.1797 (0.2374)
CC(work)	0.954 (0.642)	0.948 (0.607)	0.969 (0.892)	0.966 (0.902)	0.970 (0.914)
CC(free)	0.939 (0.625)	0.946 (0.445)	0.970 (0.893)	0.934 (0.793)	0.965 (0.831)
Number of non-hydrogen atoms	1946	2062	2004	2037	2335
macromolecules	1846	1951	1859	1865	2043
ligands	9	1	29	N/A	20
solvent	91	110	116	172	272
Protein residues	230	230	230	229	229
RMS(bonds)	0.002	0.002	0.005	0.008	0.013
RMS(angles)	0.44	0.51	0.74	0.71	1.14
Ramachandran favoured (%)	98.68	99.11	97.78	98.2	98.65
Ramachandran allowed (%)	1.32	0.89	2.22	0.9	1.35
Ramachandran outliers (%)	0	0	0	0.9	0
Rotamer outliers (%)	3.5	1.88	3.54	0.51	1.36
Clash score	1.08	1.53	3.73	2.94	4.58
Average B-factor	56.47	44.41	45.04	35.53	22.59
macromolecules	56.23	44.3	44.76	34.9	20.66
ligands	69.99	38.14	55.44	N/A	36.44
solvent	59.83	46.45	47.03	42.41	36.05
Number of TLS groups	1	1	1	1	1

7.4.3.4 Supplementary Information Table 2: Mother liquor composition used for protein crystallisation of BH32, OE1 and variants

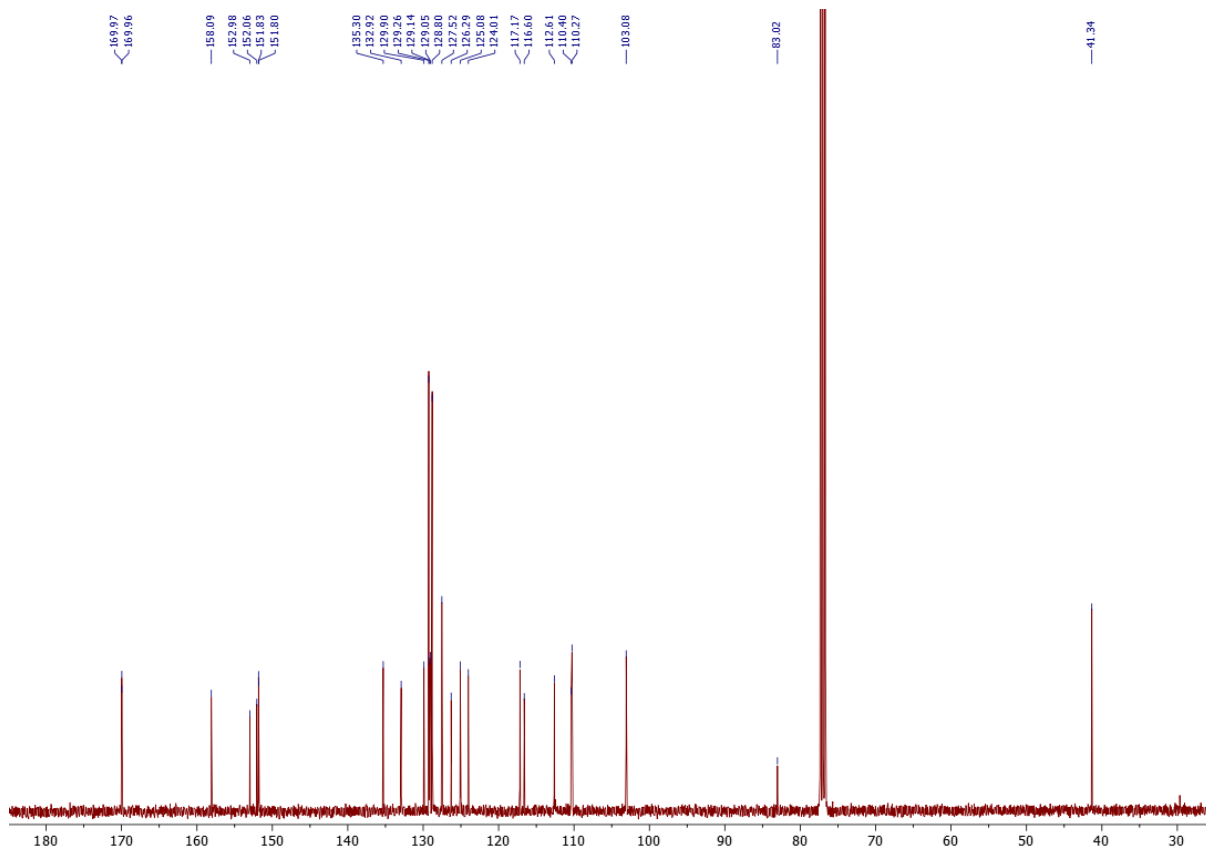
BH32 Inhibited	OE1	OE1.2 Inhibited	OE1.3	OE1.3 Inhibited
0.2 M sodium acetate trihydrate, 0.1 M Tris pH 8.5, 30 % w/v PEG 4000	0.16 M calcium acetate hydrate, 0.08 M sodium cacodylate pH 6.5, 14.4 % w/v PEG 8000	0.05 M magnesium sulfate heptahydrate, 0.1 M HEPES pH 7.5, 28 % v/v PEG Smear Medium	0.2 M magnesium chloride hexahydrate, 0.1 M sodium HEPES pH 7.5, 30 % v/v PEG 400	0.02 M calcium chloride dihydrate 0.1 M sodium acetate pH 4.6, 30 % v/v MPD

7.4.3.5 NMR Spectra

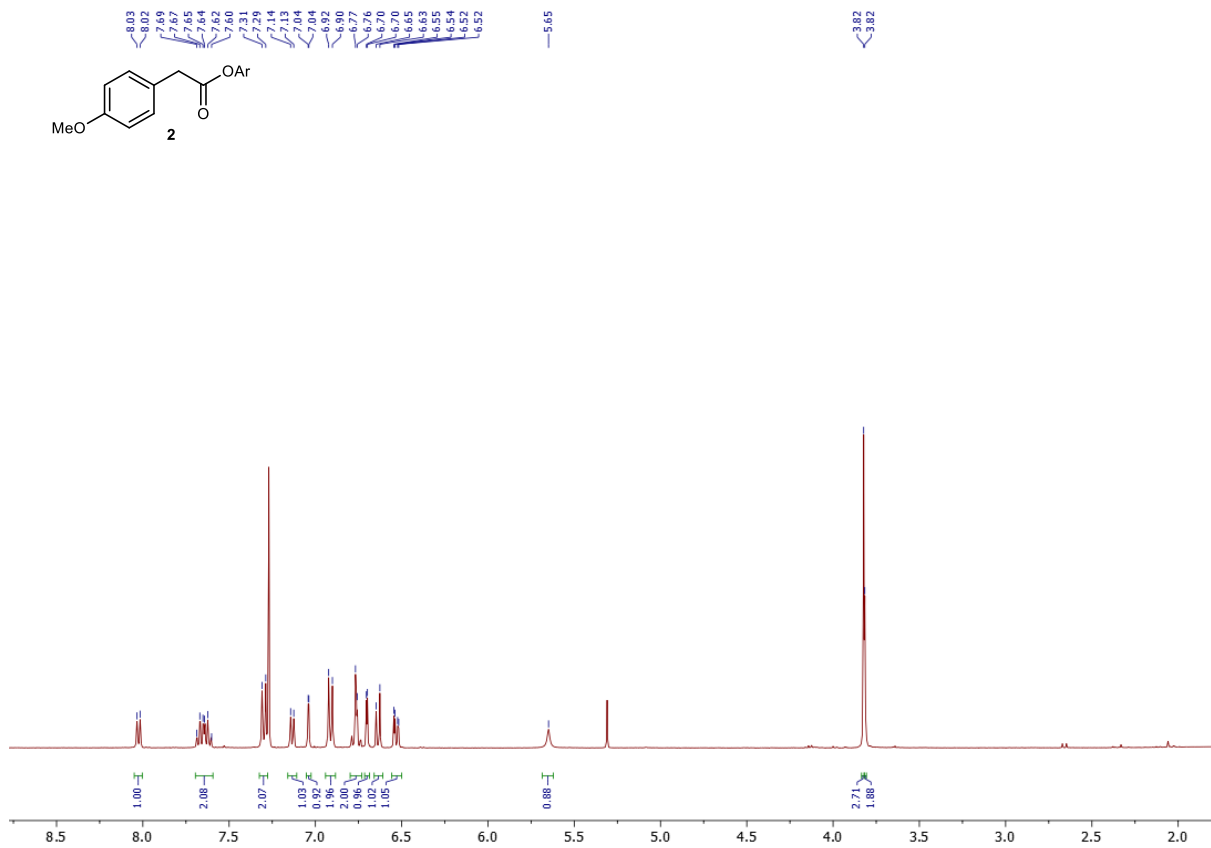
1 – ¹H NMR (400 MHz, CDCl₃)



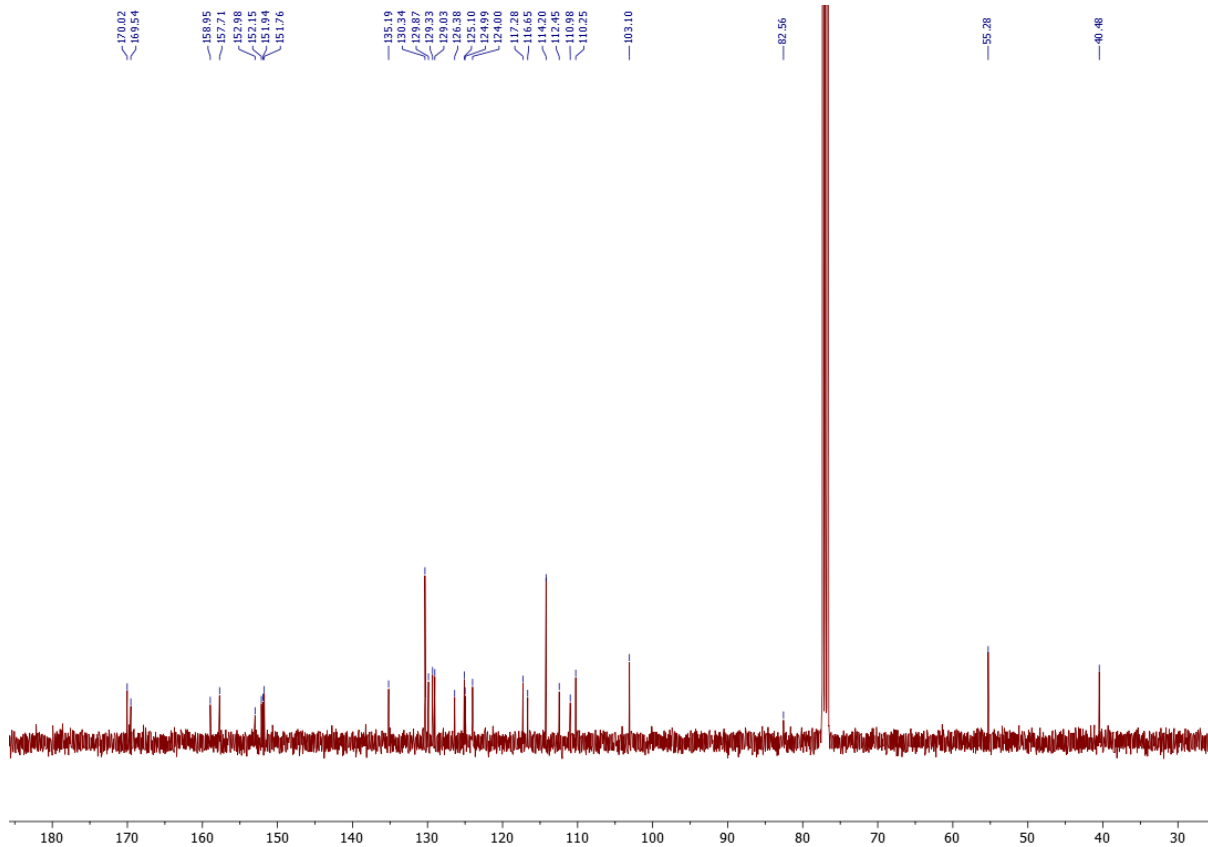
1 – ¹³C NMR (100 MHz, CDCl₃)



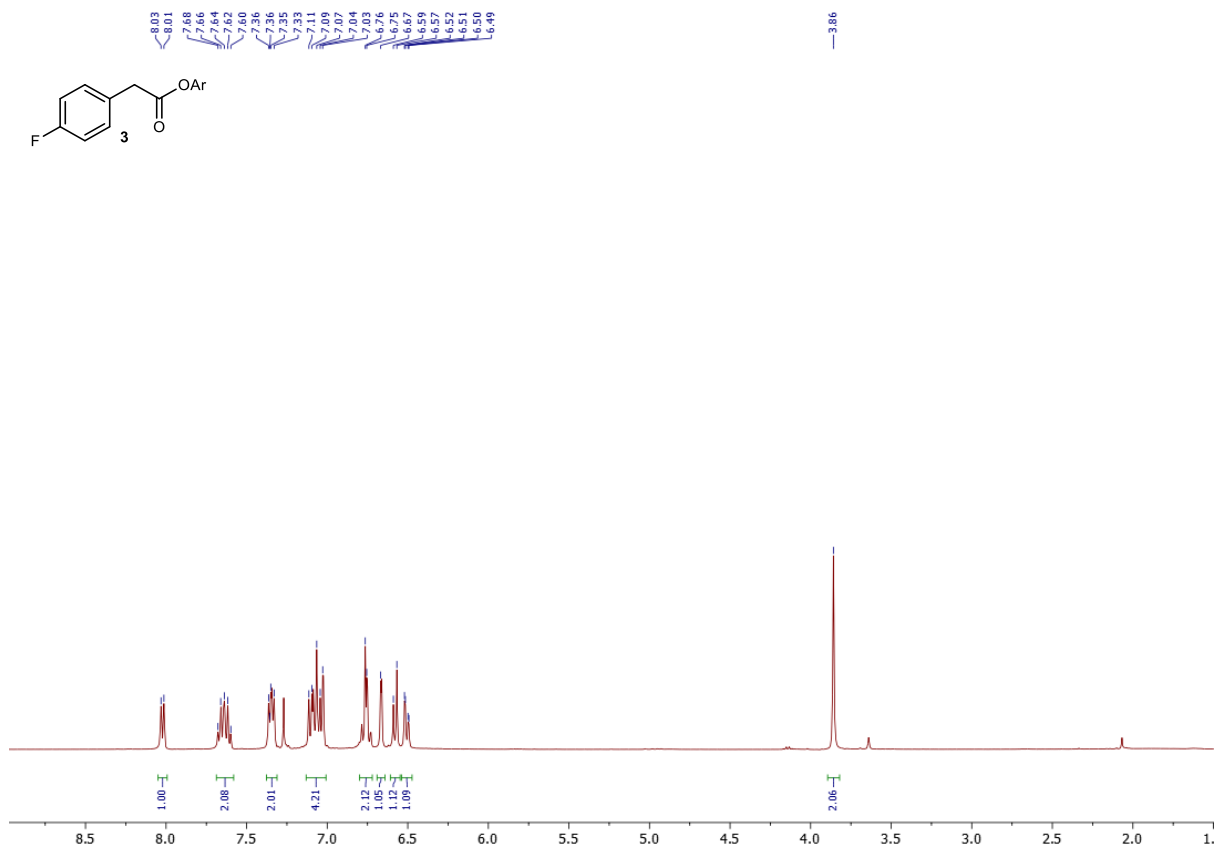
2 – ¹H NMR (400 MHz, CDCl₃)



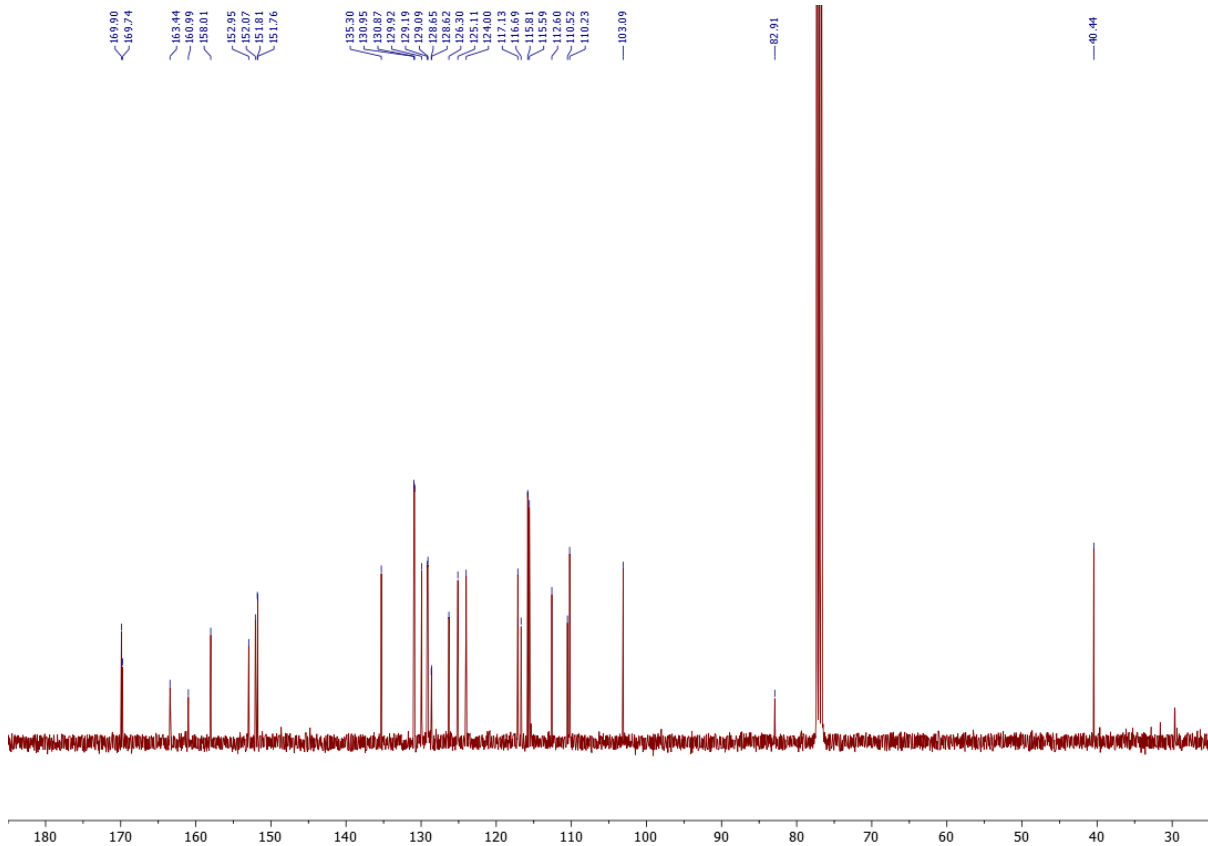
2 – ¹³C NMR (100 MHz, CDCl₃)



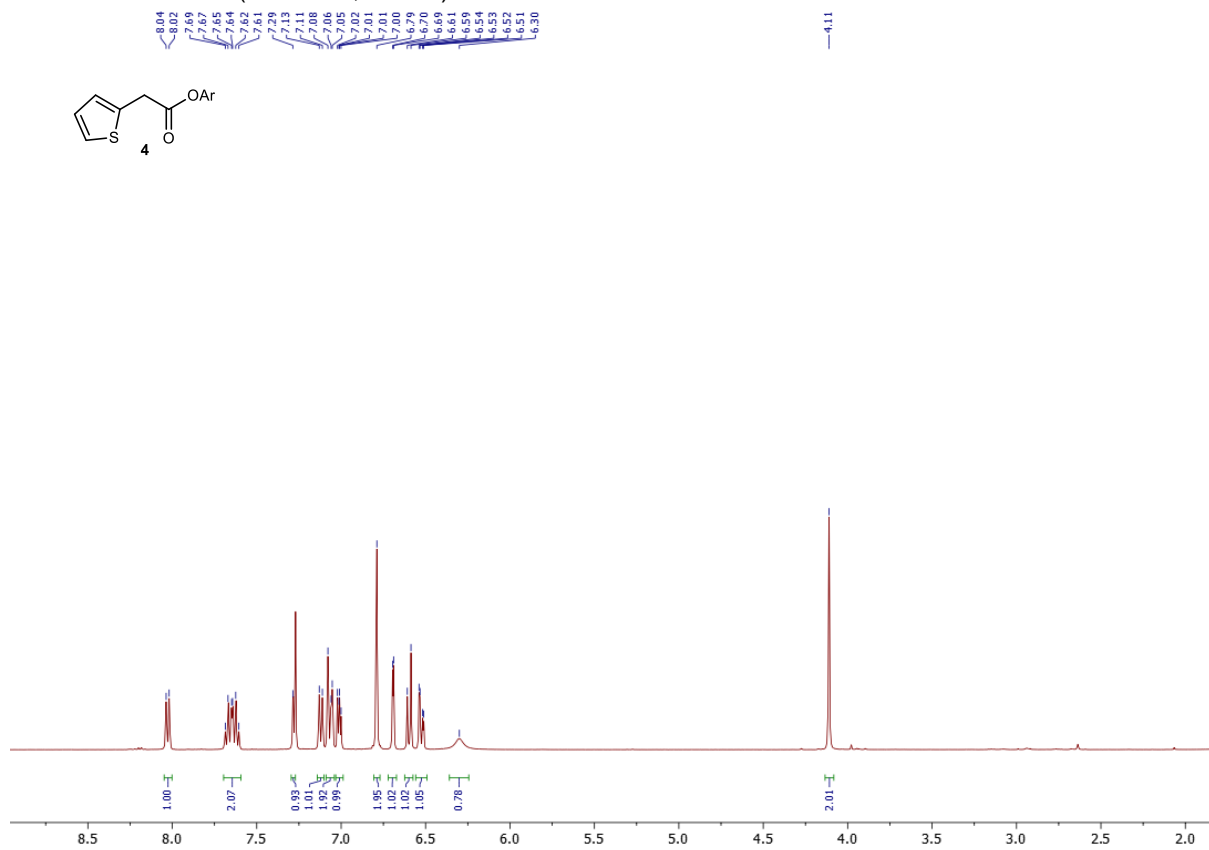
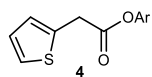
3 – ¹H NMR (400 MHz, CDCl₃)



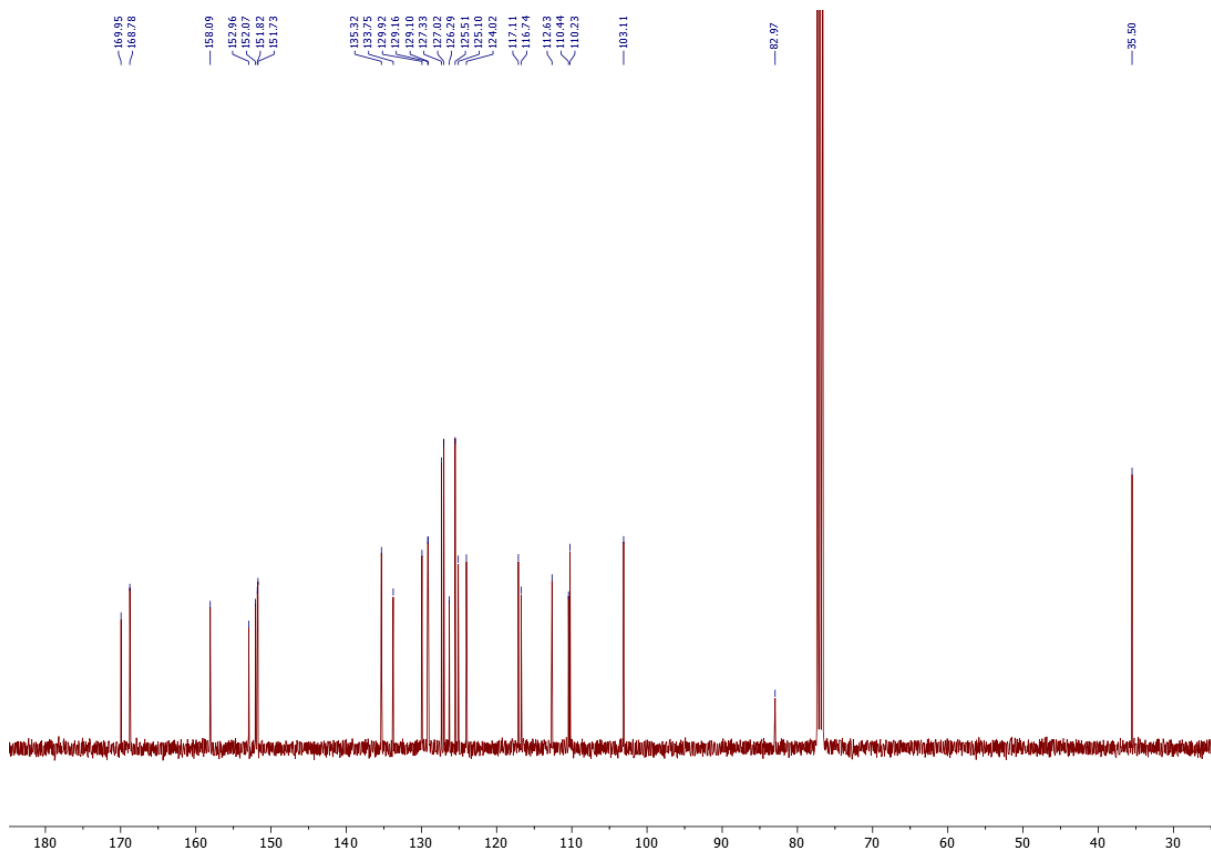
3 – ¹³C NMR (100 MHz, CDCl₃)



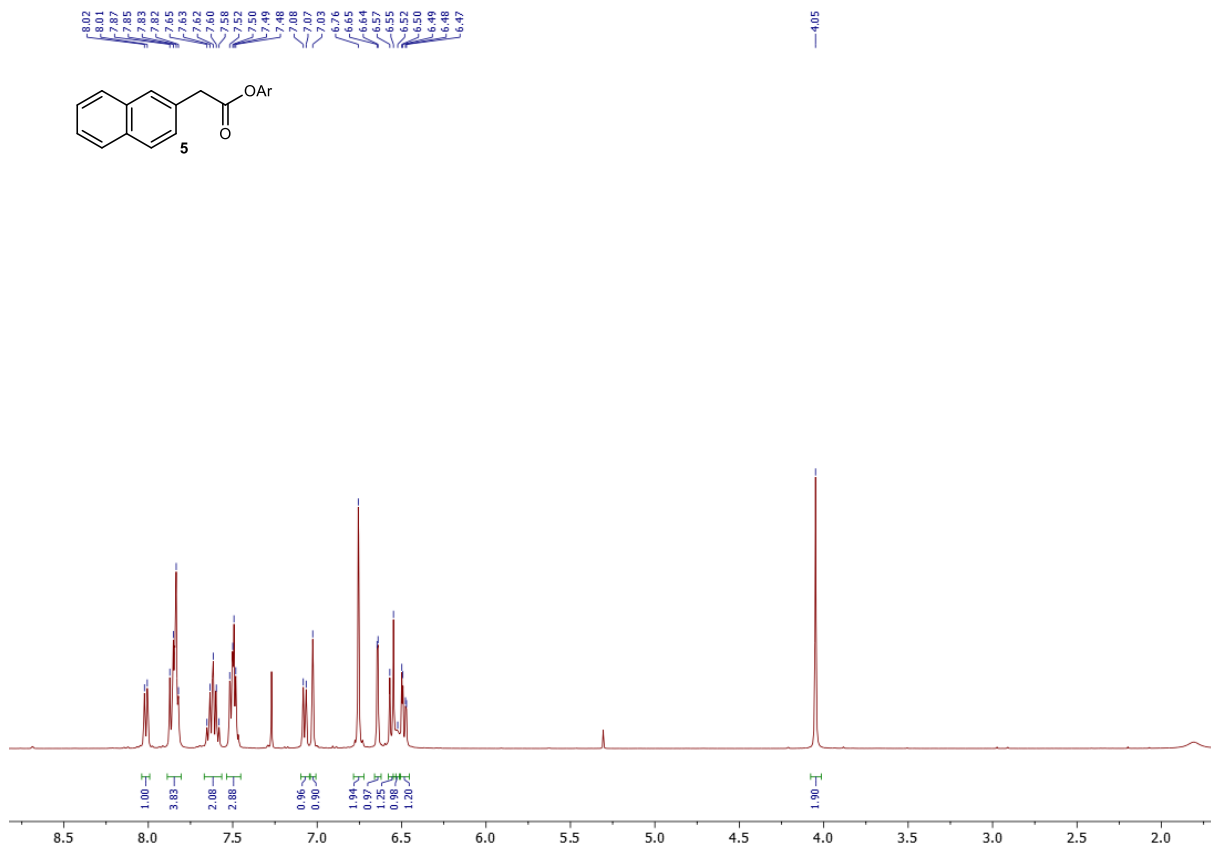
4 – ¹H NMR (400 MHz, CDCl₃)



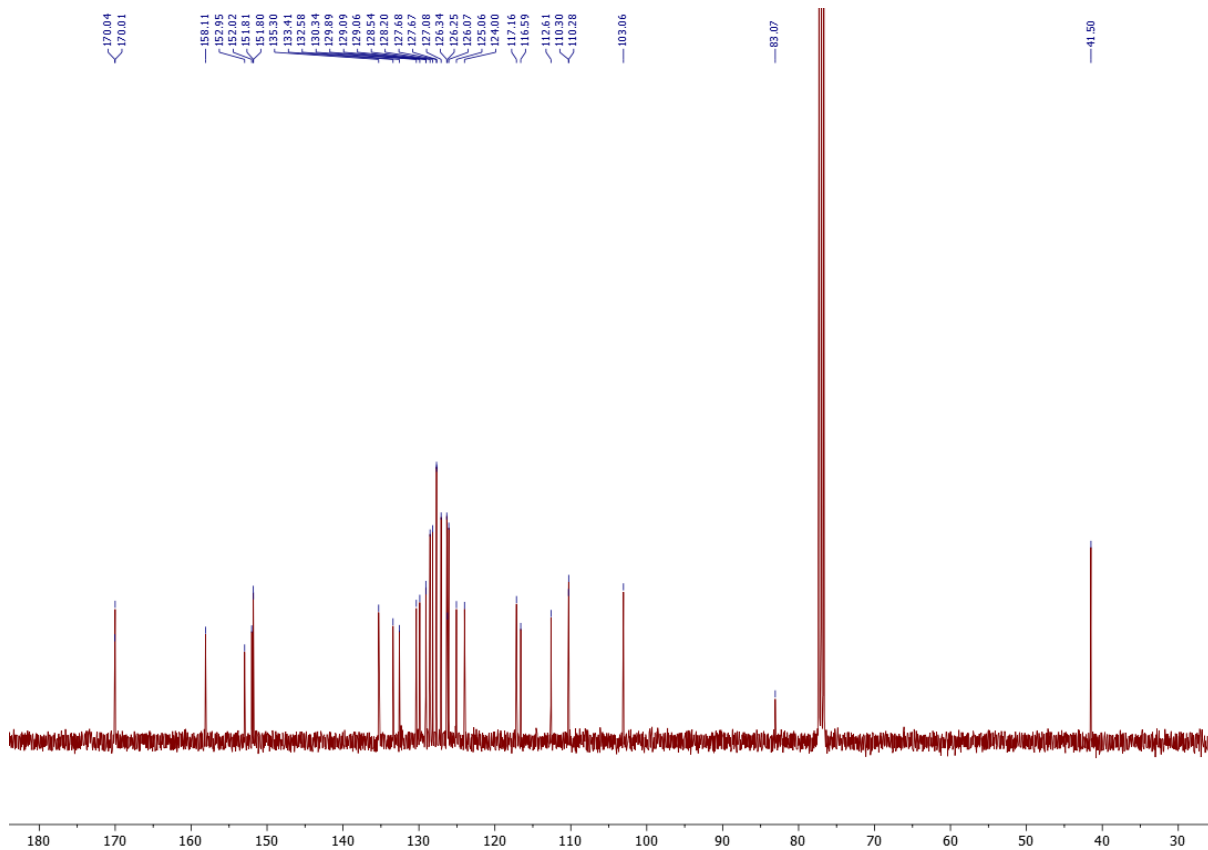
4 – ¹³C NMR (100 MHz, CDCl₃)



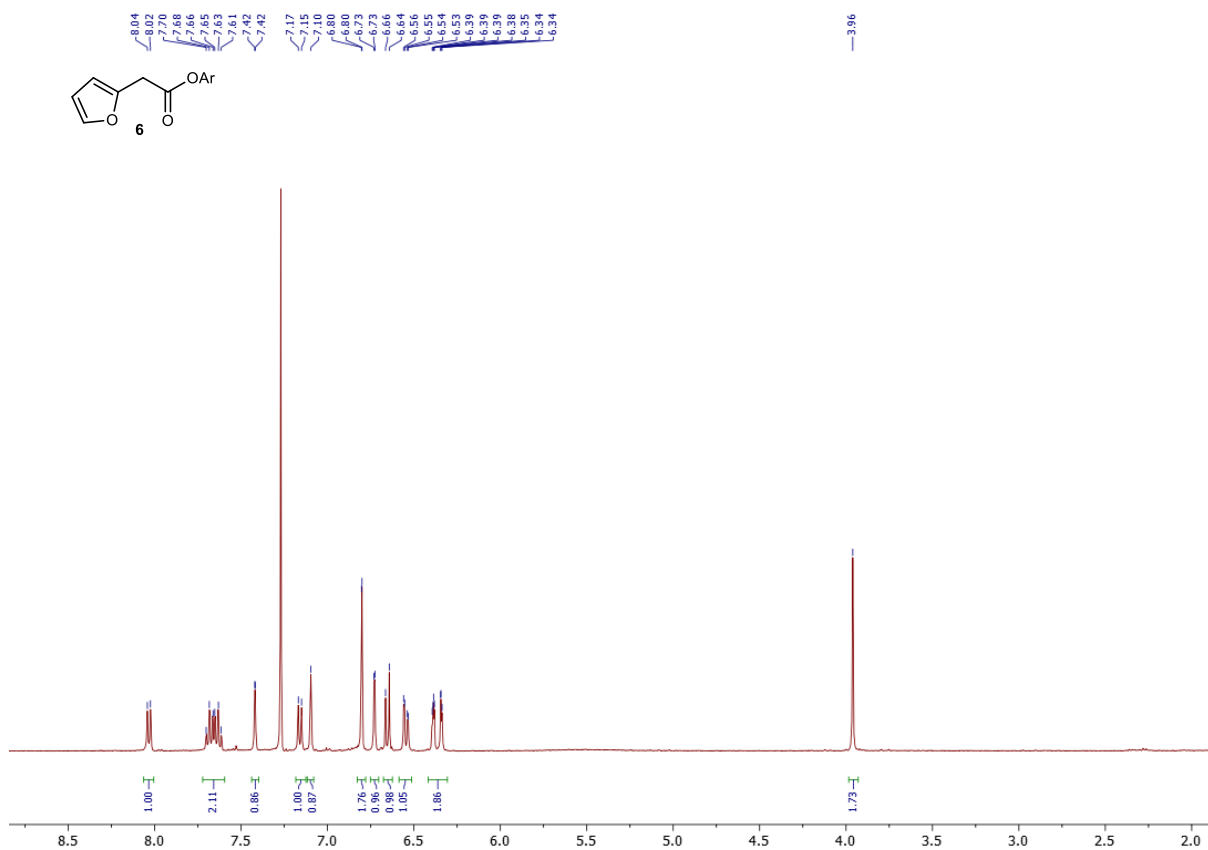
5 – ¹H NMR (400 MHz, CDCl₃)



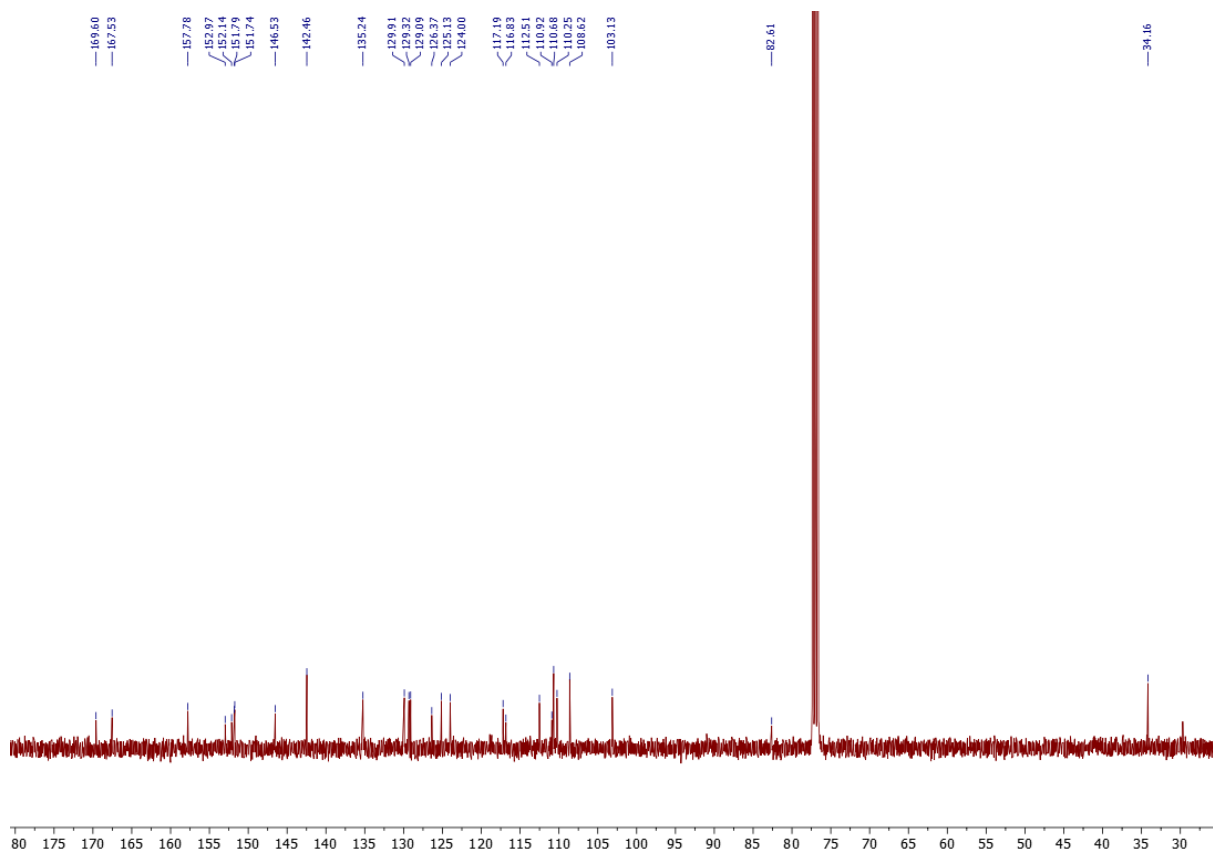
5 – ¹³C NMR (100 MHz, CDCl₃)



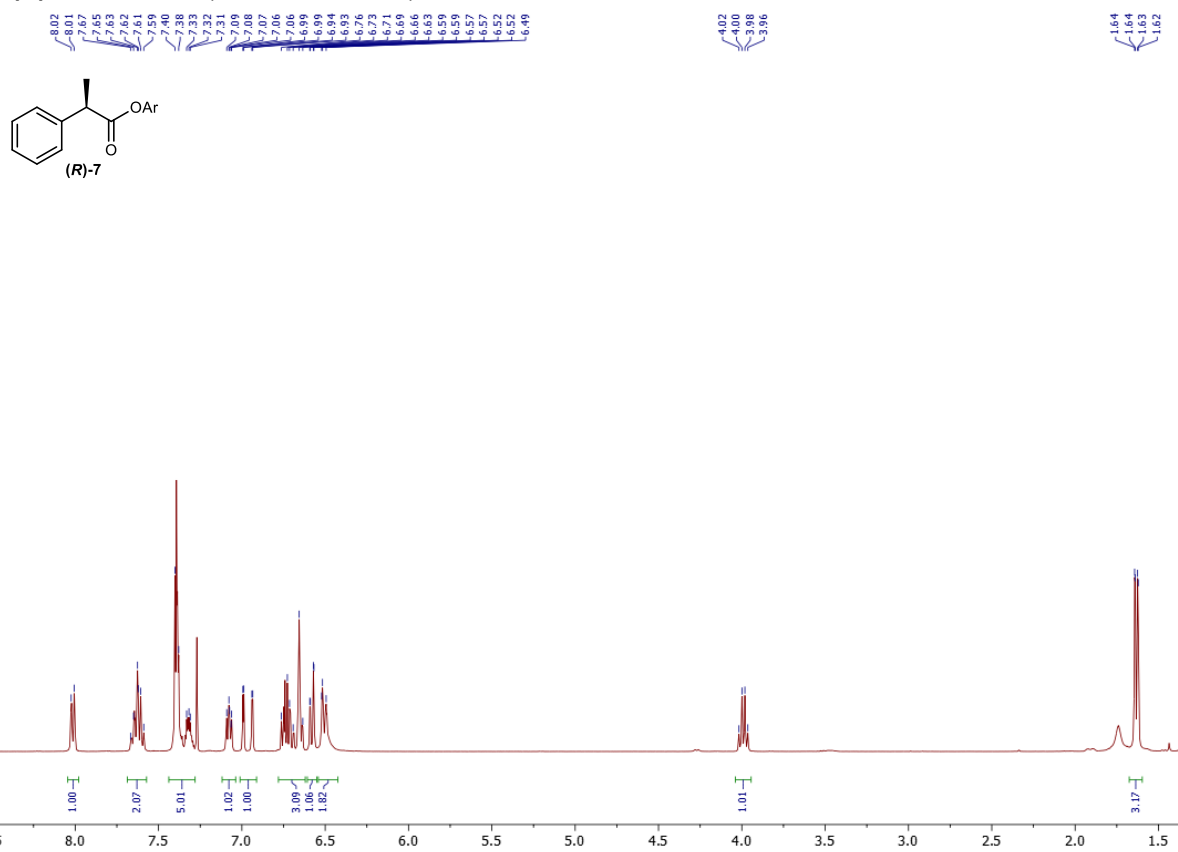
6 – ¹H NMR (400 MHz, CDCl₃)



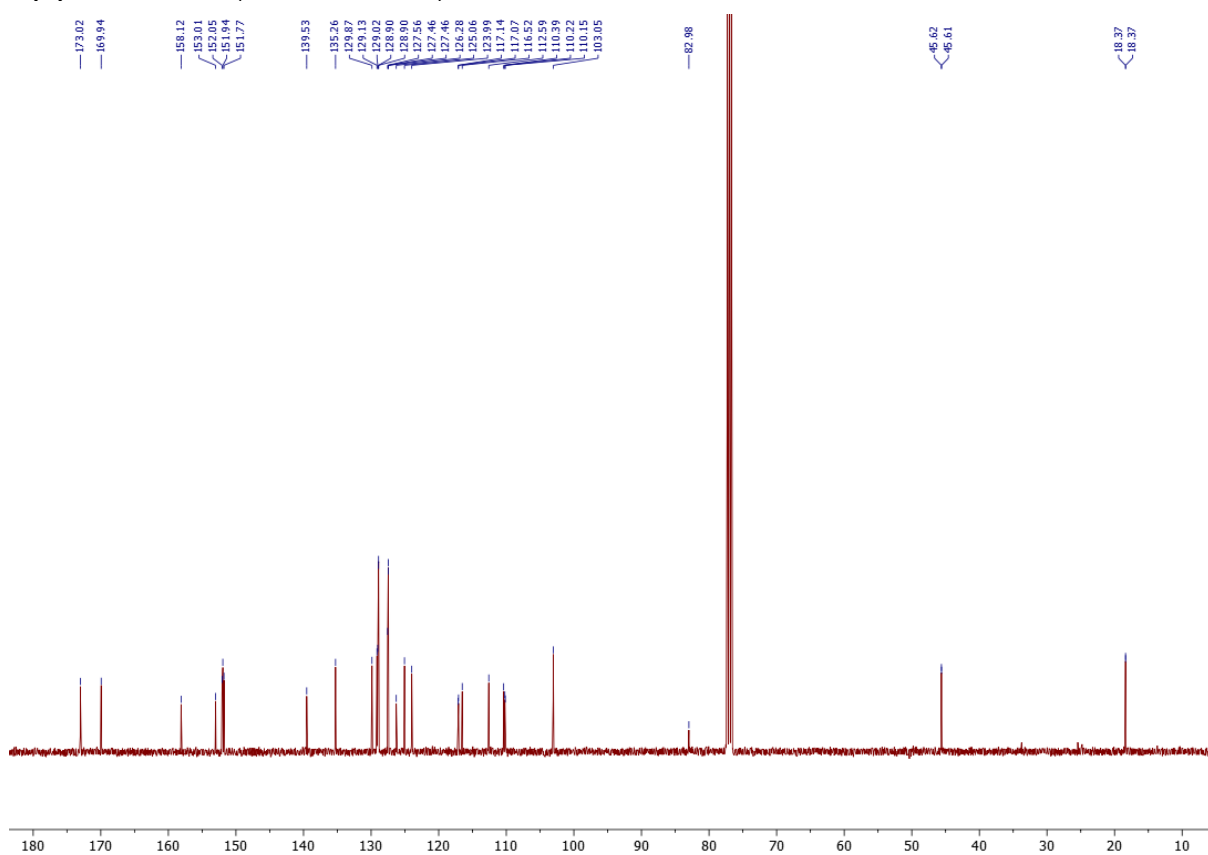
6 – ¹³C NMR (100 MHz, CDCl₃)



(R)-7 – ¹H NMR (400 MHz, CDCl₃)



(R)-7 – ¹³C NMR (100 MHz, CDCl₃)



Chapter 8: Engineering an Efficient and Enantioselective Enzyme for the Morita-Baylis-Hillman Reaction

Manuscript accepted in Nature Chemistry, June 2021

Rebecca Crawshaw¹, Amy E. Crossley¹, Linus Johannissen¹, Ashleigh J. Burke¹, Sam Hay¹, Colin Levy¹, David Baker^{2,3,4}, Sarah L. Lovelock^{1*} and Anthony P. Green^{1*}

¹Manchester Institute of Biotechnology, School of Chemistry, 131 Princess Street, University of Manchester, Manchester M1 7DN, UK. ²Department of Biochemistry, University of Washington, Seattle, WA 98195. ³Institute for Protein Design, University of Washington, Seattle, WA 98195. ⁴Howard Hughes Medical Institute, University of Washington, Seattle, WA 98195.

8.1 Foreword

This chapter consists of a research article accepted in Nature Chemistry in June 2021 and describes the design and evolution of an enantioselective biocatalyst for the Morita-Baylis-Hillman reaction.

8.2 Author Contributions

R.C. carried out molecular biology, protein production, purification, crystallization & kinetic characterization, and directed evolution experiments. A.E.C. and R.C. carried out organic synthesis and substrate profiling of BH32 variants. R.C., A.J.B. and A.E.C. developed spectrophotometric assays and performed enzyme-inhibition experiments. L.J. and S.H. carried out molecular docking and DFT calculations. S.H. interpreted and analysed kinetic data. C.L. interpreted, analysed and presented structural data. D.B. provided the BH32 design model. All authors discussed the results and participated in writing the manuscript. A.P.G. and S.L. directed the research.

8.3 Manuscript

The combination of computational design and directed evolution could offer a general strategy to create enzymes with new functions. To date, this approach has delivered enzymes for a handful of model reactions, selected based on previous achievements with catalytic antibodies. Here we show that new catalytic mechanisms can be engineered into proteins to accelerate valuable chemical transformations for which no natural enzymes or catalytic antibodies are known. Evolutionary optimization of a primitive design afforded a highly efficient and enantioselective enzyme (BH32.14) for the Morita-Baylis-Hillman (MBH) reaction, a valuable multi-step carbon-carbon bond forming process. BH32.14 is suitable for preparative scale transformations, accepts a broad range of aldehyde and enone coupling partners, including challenging MBH substrates such as unsaturated lactones, and is able to promote highly selective mono-functionalizations of dialdehydes. Crystallographic, biochemical and computational studies reveal that the interplay of design and evolution has led to a sophisticated catalytic mechanism comprising a His23 nucleophile paired with a judiciously positioned Arg124. This catalytic arginine shuttles between conformational states to stabilize multiple oxyanion intermediates and serves as a genetically encoded surrogate of privileged bidentate hydrogen bonding catalysts (e.g. thioureas), which promote a wide range of reactions in organic synthesis. This study makes us optimistic about the prospects of designing enzymes for complex multi-step transformations not observed in Nature, but suggests that innovations in multi-state design protocols are needed to account for conformational changes required for efficient catalysis.

The ability to reliably design enzymes would have significant impacts across the chemical industry, allowing the rapid delivery of new biocatalysts in response to diverse societal challenges. Computational enzyme design is conceptually similar to catalytic antibody technology; in that it aims to generate protein catalysts based on fundamental principles of transition state stabilization.¹ However, in principle computational design offers a far more flexible approach, as it is not limited to the antibody fold or reliant on the availability of an imperfect transition state mimic. Thus far, computational algorithms have enabled the design of primitive catalysts for a handful of transformations that have been optimized through laboratory evolution to deliver enzymes with efficiencies approaching natural systems.²⁻⁷ Naturally, early efforts targeted simple model transformations previously achieved with catalytic antibodies.⁸⁻¹⁰ For example, highly effective antibodies and enzymes have been created for the retro-aldol reaction,^{3,7,10} which employ reactive lysine residues reminiscent of natural type I aldolases. If we are to establish 'bottom up' enzyme design as a reliable source of biocatalysts for practical applications, we must now move beyond the functional capabilities of antibodies and develop enzymes for complex bimolecular chemical processes.

The Morita-Baylis-Hillman (MBH) reaction (Figure 1A), involving the coupling of activated alkenes (e.g. α,β -unsaturated carbonyl compounds) with carbon electrophiles (e.g. aldehydes), is an iconic transformation in organic synthesis.¹¹⁻¹³ This transformation provides a versatile and atom economical approach to generate densely functionalized chiral building blocks for synthesis. MBH

reactions are typically promoted by small catalytic nucleophiles such as 1,4-diazabicyclo[2.2.2]octane (DABCO), 4-dimethylaminopyridine (DMAP) and imidazole. Enantioselective versions of the MBH reaction have been developed by employing catalytic peptides, quinidine derivatives, chiral DMAP surrogates or by pairing catalytic nucleophiles with chiral hydrogen bond donors such as thioureas.^{13,14} Although good selectivity can be achieved in favourable cases, in other instances achieving high levels of stereo-control remains a considerable challenge (e.g. with substrates **1** and **2** used in this study).^{15,16} Despite the great synthetic potential, the practical utility of MBH reactions is further compromised by the low efficiencies achieved by existing catalytic systems, which results in prolonged reaction times and the requirement for high catalyst loadings. Given the enormous rate accelerations achieved by enzymes, biological catalysts could offer a plausible solution to these long-standing challenges. However there are no catalytic antibodies or known natural enzymes for the MBH reaction, although thymidylate synthase that catalyzes the conversion of deoxyuridine monophosphate to deoxythymidine monophosphate operates along similar mechanistic principles.¹⁷ Only extremely low levels of promiscuous MBH activity have been reported with a handful of proteins,¹⁸⁻²⁰ with unspecific protein catalysis implicated in a number of these cases.

In the absence of a suitable natural enzyme, we selected a primitive computationally designed protein for the MBH reaction (BH32), as a starting template for evolutionary optimization.²¹ BH32 utilizes a histidine nucleophile (His23) built into the cap domain of haloacid dehalogenase from *Pyrococcus horikoshii* by introducing 12 active site mutations predicted by the Rosetta software suite. Other intended design features (Figure 1A) include: Glu46 to position and activate the His23 catalytic nucleophile; an aromatic aldehyde binding pocket shaped by Phe132 and Leu10; Gln128 to serve as an oxyanion-hole to stabilize the first covalent enzyme-substrate intermediate formed upon reaction with 2-cyclohexen-1-one (**Int 1**); and an ordered water molecule bound through Ser22 designed to stabilize **Int 2**, formed following C-C bond formation, through hydrogen bonding. Despite intensive design efforts, BH32 promotes the coupling of 2-cyclohexen-1-one (**1**) with 4-nitrobenzaldehyde (**2**) with extremely low activity ($k_{\text{cat}} = 0.13 \pm 0.01 \text{ hr}^{-1}$). This activity is dependent on the His23 nucleophile, however comparison of the design model with the structurally characterized protein reveals discrepancies, which compromise the intended design features and likely contribute towards low efficiency. For example, key designed residues including His23 & Ser22 adopt altered conformational states from those predicted by design, while a shift of helix 126-132 alters the position of the designed Gln128 oxyanion hole.

A high-throughput spectrophotometric assay was developed to allow rapid evaluation of large libraries of BH32 derivatives during evolution. This was achieved by modifying the MBH product **3** through acetylation of the C3 secondary alcohol to generate a dual function mechanistic inhibitor and spectroscopic probe (**4**) (Figure 1B). Upon reaction with the His23 nucleophile, it was expected that E1cB elimination of the acetoxy group would generate a stable, conjugated product suitable for spectrophotometric detection. Indeed, incubation of BH32 with **4** resulted in the anticipated time resolved spectral changes. The spectroscopic changes were made more pronounced to improve assay sensitivity, by introducing a 4-OMe substituent to increase the degree of conjugation upon

inhibition. Formation of a stable 1:1 protein-inhibitor complex was confirmed by MS analysis of the intact protein (Table S1). No spectral or mass changes were observed with the BH32 His23Ala variant, confirming the His23 catalytic nucleophile as the site of covalent attachment. Although this assay doesn't report on overall catalytic turnover, we anticipated that it would provide a useful tool for MBHase engineering capable of reporting on key features of MBH catalysis, including nucleophilicity of His23, stabilization of C1 oxyanion intermediates and shape complementarity between the active site and the MBH product.

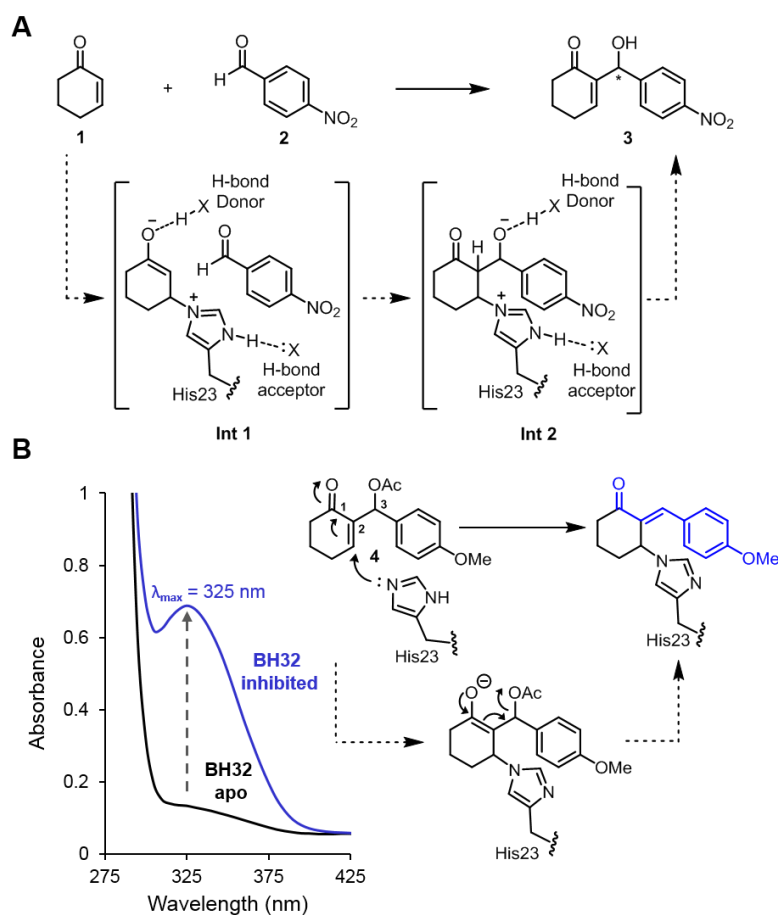


Figure 1: A designed enzyme for the Morita-Baylis-Hillman (MBH) reaction and the development of a dual function mechanistic inhibitor. A) Chemical scheme of the MBH reaction between **1** and **2** catalysed by the computationally designed enzyme BH32.²¹ Intended design features include a His23 nucleophile positioned by a hydrogen bond acceptor, and hydrogen bond donors for oxyanion stabilization. **B)** Chemical scheme of BH32 inhibition with the mechanistic inhibitor **4**. Addition of the His23 nucleophile is followed by E1cB elimination of the acetoxy group, generating a conjugated π -system, which can be monitored by an increase in absorbance at 325 nm. The stereochemistry of the exocyclic double bond in the inhibited complex is unknown. The wavelength scan shows the spectral changes that occur when BH32 (25 μ M) is incubated with inhibitor **4** (250 μ M) for 40 minutes.

The evolutionary strategy used for BH32 optimization included both local and global mutagenesis (Figure S1): error-prone PCR was used to target the entire gene sequence leading to the identification of 'hot spots' that were further interrogated as small focused libraries (Rounds 1-4, 10-11 & 13-14); iterative cassette mutagenesis was used to individually randomize up to twenty positions per round (Rounds 5-6, 8-9 & 12); and combinatorial active site saturation mutagenesis (CASTing) was used to target active site residues (Round 2 & 7). Beneficial diversity identified during each round was combined by DNA shuffling. The aforementioned spectrophotometric assay was used to rapidly evaluate libraries during rounds 1-8 (Figure 2C). The most active (*ca.* 1%) clones identified during each round were further evaluated as purified enzymes for MBH activity using HPLC analysis. The correlation between increased rate of reaction with inhibitor **4** and improving MBH activity was generally excellent. While the reaction of BH32 with inhibitor **4** takes > 60 mins to reach completion, under identical conditions selective modification of BH32.8 is essentially complete within 1.5 minutes (Figure 2C and Table S1). To further refine the catalytic mechanism, BH32.8 was subjected to an additional six rounds of evolution using a HPLC assay to monitor the formation of MBH product **3** catalysed by individual variants arrayed as cell lysates in 96-well plates.

The most active variant to emerge following 14 rounds of evolution (BH32.14) contains 24 mutations (Figure 2A). The relative activities of variants along the evolutionary trajectory were compared in biotransformations of **1** (3 mM) and **2** (0.6 mM) using 3 mol% catalyst (Figure 2B). The starting variant BH32 gave ~0.08 % conversion to product (**3**) after 4.5 hours (Table S2) which increased to only 0.4% following incubation for 22 h (Table 1, Entry 1). Furthermore, product formation was accompanied by a substantial proportion of a competing aldol by-product **S1** (5:1 ratio of **3**:**S1**, Figure S3). In contrast, under identical reaction conditions BH32.14 afforded **3** as the sole product in 58% (Table 1, Entry 2) and 83% conversion (Table 1, Entry 3) after 4.5 hours and 22 hours, respectively. For comparison, with commonly employed small molecule catalytic nucleophiles imidazole, DMAP and DABCO, low but detectable conversions (<0.5%) are only achieved using high catalyst loadings and prolonged reaction times (Table 1, Entry 7-9). This analysis shows how steady improvements across the evolutionary trajectory have afforded an efficient MBHase that is >710-fold more active than the starting design under these assay conditions. This improvement in catalytic performance is primarily achieved through a substantial 160-fold increase in turnover number ($k_{\text{cat}} = 0.35 \pm 0.03 \text{ min}^{-1}$ and $0.13 \pm 0.01 \text{ hr}^{-1}$ for BH32.14 and BH32, respectively, Figure 2D). Although at this stage we cannot differentiate between random and ordered binding mechanisms operating in BH32 and its evolved variants, the magnitude of these k_{cat} values is largely insensitive to the kinetic model used (Table S3). Evolution has also resulted in modest improvements in apparent K_{M} values for both the enone and aldehyde coupling partners ($K_{\text{app}[1]} = 2.6 \pm 0.4 \text{ mM}$ and $8.0 \pm 1.0 \text{ mM}$, $K_{\text{app}[2]} = 1.1 \pm 0.2 \text{ mM}$ and $1.8 \pm 0.2 \text{ mM}$ for BH32.14 and BH32, respectively), meaning that substrate saturation is more readily achieved in the evolved BH32.14 variant (Figure S2 and Table S3).

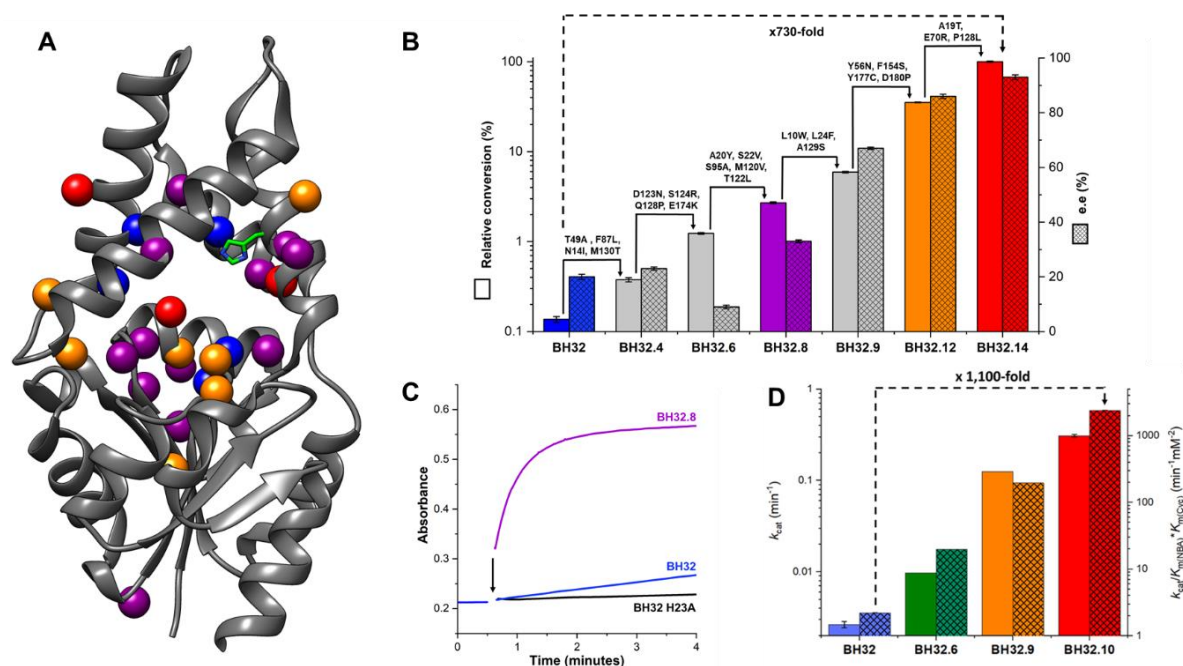


Figure 2: Characterization of BH32, BH32.14 and selected variants. **A)** Structure showing the amino acid positions mutated in BH32.14 (represented as spheres) mapped onto the structure of haloacid dehalogenase from *Pyrococcus horikoshii* (PDB code: 1X42). Mutations introduced during rounds 1-8 are shown in purple, rounds 9-12 in orange and rounds 13-14 in red. Position Asn14 was mutated twice (round 3 & 4) and is shown in purple, position Gln128 was mutated twice (round 5 & 14) and is shown in red. Computationally designed residues remaining following evolution are shown in blue. The His23 catalytic nucleophile is shown in stick representation. **B)** Bar chart showing the relative conversion (solid colour) and enantiomeric excess (hatched) achieved by selected variants along the evolutionary trajectory. Biotransformations were performed using **1** (3 mM), **2** (0.6 mM) and enzyme (18 μM), and analysed following 4.5 hours incubation (see Table S2 for conversion and selectivity data). Error bars represent the standard deviation of measurements made in triplicate. **C)** Time course for the inhibition of BH32.8 (25 μM , purple), BH32 (25 μM , blue) and BH32 H23A (25 μM , black) with inhibitor **4** (250 μM) monitored at 325 nm. The black arrow indicates the time of protein addition. **D)** Bar chart comparing the turnover number (k_{cat}) of BH32 (blue), BH32.8 (purple), BH32.12 (orange) and BH32.14 (red) for the MBH reaction between **1** and **2**. Steady state kinetic data (average of measurements made in triplicate at each substrate concentration) were fitted globally using a kinetic model for two substrates with randomly ordered binding to extract kinetic constants and associated errors (shown as error bars). Representative Michaelis-Menten plots at fixed concentrations of **1** or **2** are also shown in Figure S2.

Although we didn't explicitly select for improvements in enantioselectivity, evolution led to substantial selectivity gains, with reactions catalysed by BH32 and BH32.14 affording (*R*)-**3** in 20% and 93% e.e., respectively (Figure 2B and Table S2). Kinetic improvements were evidently achieved by an increasingly precise recognition of the rate-limiting transition state(s) leading to the formation of the (*R*)-configured product. This selectivity compares favourably with the modest selectivities achieved

for the synthesis of **3** by chiral small molecule catalysts.^{15,16} We also explored the utility of BH32.14 for preparative scale biotransformations (Table 1, Entry 10). Significantly, while the enzyme is rather intolerant to elevated MeCN concentrations, it readily tolerates 20 % DMSO as an organic cosolvent, which allows reactions to be performed with increased substrate loadings (10 mM concentration of **2**). High conversions (94%) and isolated yields (88%) are obtained within 19 h using only 0.5 mol% catalyst loading to allow synthesis of several hundred milligrams of MBH product **3** (Figure S4). Reactions using 0.1 mol% catalyst loading show that the enzyme is able to achieve >530 turnovers (Figure S5). Interestingly, BH32.14 displays reduced, but appreciable levels of activity in up to 40% DMSO (Table S4) and up to 50 °C (Figure S6), highlighting the potential for further reaction intensification in the future. The high degree of solvent tolerance and mutational flexibility of the BH32 scaffold (12% of the protein was mutated during computational design and evolution) is noteworthy, and likely reflects the stability of the starting scaffold, which originates from a hyperthermophilic organism that grows optimally at 98 °C.^{22,23}

Table 1: The MBH reactions of **1 and **2** catalysed by small molecule nucleophiles, BH32, BH32.14 and selected variants.**

Entry	Catalyst	Catalyst Loading (mol%)	Time (h)	Conversion (%)
1	BH32	3	22	<0.5
2	BH32.14	3	4.5	58
3	BH32.14	3	22	83
4	BH32.14 His23Ala	3	4.5	<0.5
5	BH32.14 Arg124Ala	3	4.5	<1
6	BH32.14 Trp10Ala	3	4.5	3.8
7	Imidazole	167	22	<0.5
8	DMAP	167	22	<0.5
9	DABCO	167	22	<0.5
10	BH32.14	0.5	19	94

Entries 1-9 were carried out using **1** (3 mM) and **2** (0.6 mM) in PBS (pH 7.4) with 3% DMSO as a cosolvent. Conversion to product was determined by HPLC analysis. Entry 10 was performed on a preparative scale using **1** (50 mM) and **2** (10 mM) in PBS (pH 7.4) with 20% DMSO as a cosolvent. Conversion to product was determined by HPLC analysis. The final product was isolated in 88% yield following extraction into organic solvent and chromatographic purification.

To further explore synthetic utility, BH32.14 was evaluated for activity towards a range of activated alkene and aldehyde/ketone coupling partners, leading to the synthesis of structurally diverse MBH products **5a-w** (Figure 3). In addition to cyclohexenone **1**, BH32.14 displays high levels of activity in

MBH reactions with cyclopentenone, functionalized cyclopentenones and methyl vinyl ketone. Testament to its catalytic power, BH32.14 can even promote enantioselective transformations of unsaturated lactones (product **5b**), which are notoriously challenging as MBH substrates.^{24,25} BH32.14 also accepts a range of mono- and di- substituted aromatic aldehydes as substrates, although has a clear preference for *para*-substituted derivatives. While a modestly electron-donating *p*-Me substituent is well tolerated (**5i**), introduction of a strongly donating *p*-OMe group leads to a significant reduction in activity (**5j**). The aliphatic aldehydes heptanal, acetaldehyde and cyclohexanecarboxaldehyde are not substrates for BH32.14 (data not shown). Compared with BH32.14, the less highly evolved BH32.8 accepts a broader range of substituents at the 2- and 3-positions, including the activated ketone istatin (product **5o**), albeit with reduced efficiency and minimal selectivity. These results suggests BH32.14 has been highly specialized through evolution to operate efficiently and selectively on specific classes of substrate, whereas its ancestor BH32.8 is more promiscuous and thus provides an attractive starting template for engineering MBHases to produce a broader range of target structures. Similar correlations between improving efficiency and increased substrate specificity have been observed previously during evolutionary optimization of designed enzymes.⁶ These trends can be attributed to improved shape complementarity between the target substrate(s) and the engineered active site, which aids efficient catalysis by maximising productive interactions with the transition states but makes the active site less tolerant of non-native reaction partners. We also recognized the opportunity to perform selective monofunctionalizations of aromatic dialdehydes. Indeed, biotransformations of terephthalaldehyde, thiophene-2,5-dicarboxaldehyde and furan-2,5-dicarboxaldehyde proceed with high conversions to chiral monofunctionalized MBH adducts (**5s-w**). The reaction of cyclohexenone with the unsymmetrical dialdehyde, thiophene-2,4-dicarboxaldehyde delivered enantioenriched monosubstituted products **5v** and **5w** with modest regiocontrol, which could likely be improved through additional rounds of evolution.

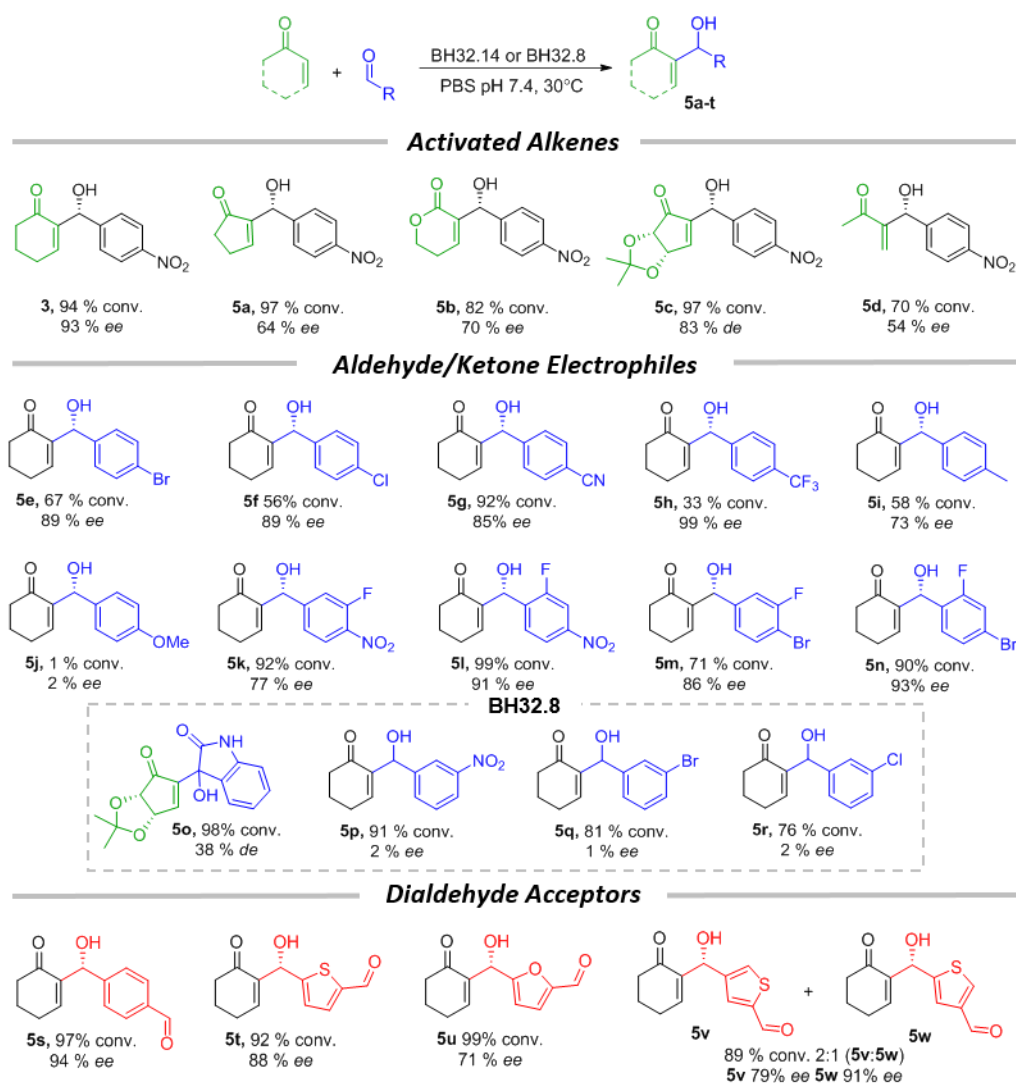


Figure 3: Substrate scope of engineered MBHases. BH32.14 tolerates a range of activated alkenes, aldehydes and dialdehydes as substrates, leading to the production of densely functionalized MBH adducts with high conversions and selectivities. The less highly evolved BH32.8 accepts a broader range of substituents at the 2- and 3- positions, albeit with reduced efficiency and minimal enantioselectivity. Reported conversions and selectivities are an average from biotransformations performed in triplicate. The stereochemistry of **5a-i**, **k-o** & **5s-w** are assigned by analogy to the (*R*)-**3** product formed in BH32.14 mediated biotransformations. Biotransformations were performed using aldehyde/ketone (10 mM), activated alkene (50 mM for **3**, **5a-c**, **5f-h** & **5j-w**, 100 mM for **5d-e** & **5i**) and catalyst (0.5-5 mol%). Specific reaction conditions for the synthesis of **3** & **5a-w** are presented in Table S5.

To understand the origins of improved efficiency following evolution, crystal structures of several evolved BH32 variants were solved for comparison to the original design. The most active variant, BH32.14, proved challenging to crystallize; however we were able to solve the apo structure of BH32.12, which contains 21 out of 24 mutations present in BH32.14, to 2.3 Å resolution (Table S7). Thus far, we have been unable to obtain BH32.12 structures with substrate, product or inhibitor bound. The BH32.12 and BH32 apo-structures superimpose well, with a root-mean-square-deviation of 0.8 Å. However evolution has resulted in extensive remodelling of the active site, including a ~30%

reduction in volume (Figure 4). The designed His23 nucleophile has been preserved and is essential for catalytic activity in BH32.14 (Table 1, Entry 4). In contrast, Gln128 and Ser22 intended to stabilize key oxanion intermediates through hydrogen bonding interactions, have been abandoned during evolution. Instead, an active site Arg124 has emerged which is critical for effective catalysis (Table 1, Entry 5). This catalytic residue emerged in the early rounds of evolutionary optimization, and in the crystal structure of BH32.6 (resolution 1.5 Å, Table S7) adopts a conformation which places the guanidinium motif in close proximity to the amide side chain of the originally designed Gln128. However, subsequent active site remodelling resulted in a substantial repositioning of the arginine side chain leading to a ~5 Å displacement of the guanidinium ion in BH32.12 (Figure S7). The originally designed aldehyde binding site is occluded in BH32.12 by residues Trp10, Leu122, Arg124 & Ser129 which emerged during evolution. Molecular docking of substrates **1** and **2** reveals the presence of a new aldehyde binding pocket shaped by Trp10, Val22, Ile26, Leu64, Trp88, Ser91, Leu92, Phe132, Arg124 & Ser129, and a 2-cyclohexen-1-one binding mode suitable for nucleophilic attack by His23 (Figure 4).

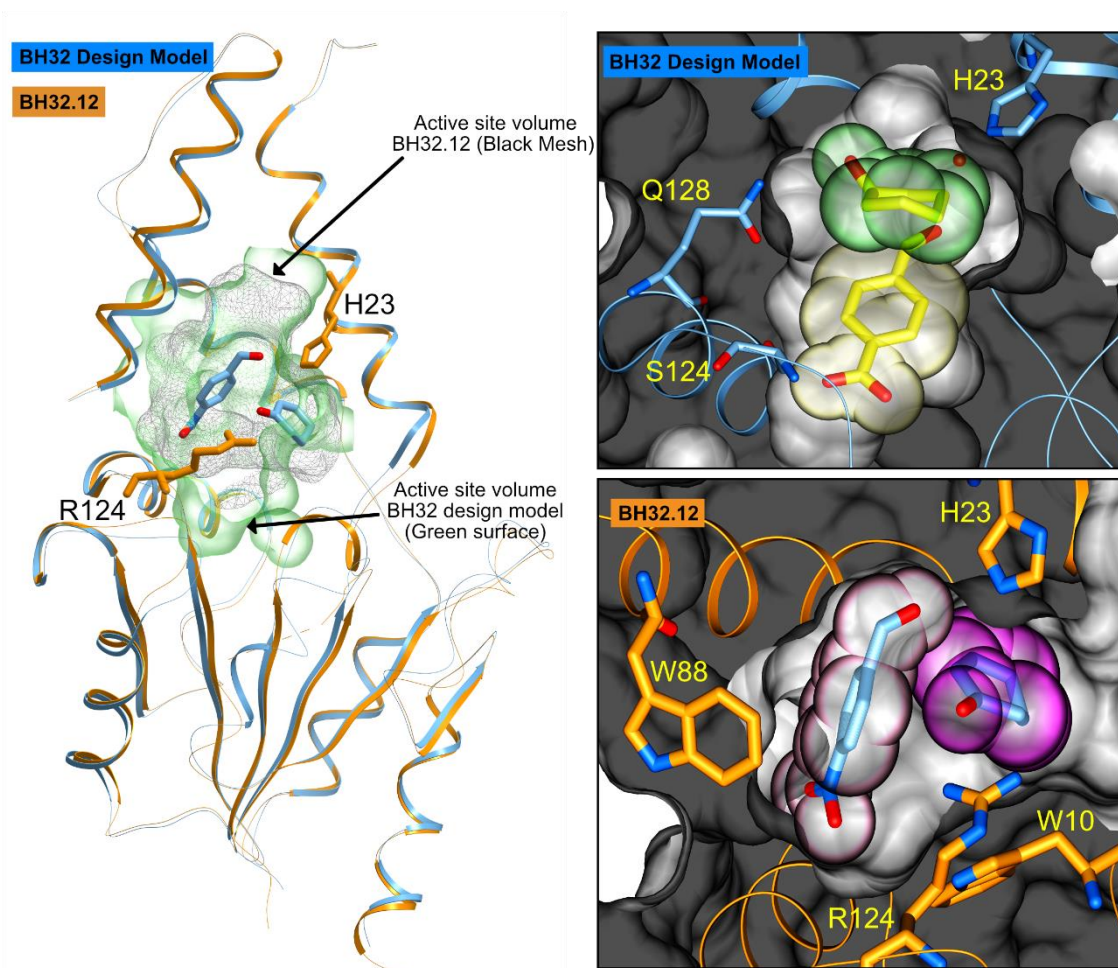


Figure 4: Crystal structures of BH32 and BH32.12. A ribbon representation of the superimposed coordinates of the BH32 design model (blue) and the evolved variant BH32.12 (orange). The His23 nucleophile and catalytic Arg124 from BH32.12 are shown in orange stick representation. Substrates docked into BH32.12 are shown in all atom coloured stick representation. The active site surface

volume of the BH32 design model is shown as a green transparency whilst the equivalent active site surface volume for BH32.12 is shown as a grey mesh. The right hand panels show a close-up representation of the active sites. The top panel shows the substrate binding pocket of BH32 design model highlighting the spatial arrangement of the designed residues Gln128, Ser124 and His23. The protein backbone is shown in ribbon representation (blue) with the protein surface shown in grey. The substrates are derived from the original composite transition state model²¹ with the aldehyde shown in stick representation and transparent yellow CPK spheres. 2-Cyclohexen-1-one is also shown in stick representation with accompanying transparent green CPK spheres. The bottom panel shows the aldehyde and enone binding pocket of BH32.12 highlighting the spatial arrangement of key residues Trp88, Trp10, Arg124 and His23 (stick representation - orange carbon atoms). The protein backbone is shown in ribbon representation (orange) with the protein surface shown in grey. The substrate positions depicted are those obtained from initial docking studies prior to DFT calculations. The aldehyde substrate is shown in stick representation with accompanying transparent pink CPK spheres. 2-Cyclohexen-1-one is shown in stick representation with transparent magenta CPK spheres.

To shed light on the catalytic mechanism, an active site DFT 'cluster' model comprising 273 atoms was constructed from the BH32.12 crystal structure and docked substrates, with peripheral atoms fixed to maintain the crystal structure geometry (Figure S8). A water molecule was also included in the calculations to facilitate proton transfer in the third chemical step. Relaxed potential energy scans were performed to model each step of the proposed mechanism (Figure S9 and S10). During energy minimisation of the reactant state, the aromatic aldehyde forms an edge to face π -stacking interaction with Trp88. The modelling suggests that aldehyde binding is further supported by a hydrogen bonding network involving the *para*-nitro substituent, Ser129 and Trp10, two residues that emerged during the latter stages of evolution. Trp10 lies in close proximity to Arg124 and likely plays an important role in positioning the guanidinium side chain (Figure 4 and S7). A Trp10Ala substitution in BH32.14 leads to a substantial reduction in activity (Table 1, Entry 6), underscoring the importance of this residue to the catalytic mechanism. Nucleophilic addition of His23 to the *si*-face of **1** generates the first oxyanion intermediate (**Int1**) which is stabilized by a bidentate hydrogen bond to the side chain of Arg124. Similar interactions have been observed in natural²⁶ and *de novo* hydrolases,²⁷ as well as catalytic antibodies,²⁸⁻³⁰ and are the hallmark of small molecule hydrogen bonding catalysts such as thiourea and guanidinium ions.^{31,32} While BH32.14 reacts rapidly with inhibitor **4**, this activity is dramatically reduced upon mutation of Arg124 to Ala (Figure S11), supporting the role of this residue in stabilizing oxyanion intermediates at C1. Consistent with its role as the catalytic nucleophile, activity with inhibitor **4** is abolished in BH32.14 His23Ala. DFT modelling shows that inhibitor **4** is well accommodated in the active site with His23 poised for nucleophilic attack and Arg124 suitably positioned for oxyanion stabilization. The enolate of **Int1** is well positioned for subsequent addition to aldehyde **2**. Diastereoselective carbon-carbon bond formation generates a second oxyanion intermediate (**Int2**) with (*R*)-configuration at the C3-position, consistent with the stereochemical outcome of the MBH reactions observed experimentally, and proceeds with transfer of negative charge to the C3-oxygen (Figure 5). Arg124 is ideally positioned to support this charge transfer, and the calculations suggest that this residue can shuttle between bidentate hydrogen

bonding modes to stabilize both **Int1** and **Int2**, via a bridging mode at the transition state involving a single hydrogen bond to each oxygen atom. Consistent with previous models of thiourea promoted MBH reactions,³³ the third chemical step involves water mediated proton transfer from C2 to the C3 alkoxide, leading to the generation of a third oxyanion intermediate (**Int 3**) which again can be stabilized by bidentate hydrogen bonding to Arg124. The final chemical step involves elimination of the His23 nucleophile to generate Morita-Baylis-Hillman product (*R*)-**3**. Our calculations suggest that the third chemical step is rate limiting (or partially rate limiting) (Figure S9), with an energy barrier of 61.9 kJmol⁻¹ compared with barriers of 50.1 kJmol⁻¹ and 47.4 kJmol⁻¹ for steps 1 and 4, respectively. If this were the case, we would expect to observe a solvent kinetic isotope effect (SKIE) as an exchangeable proton is transferred in step 3. Comparison of biotransformations with BH32.14 performed in H₂O and D₂O reveals a modest SKIE of 1.4 ± 0.09 (Figure S13), indicating that proton transfer is involved in the rate-limiting step as suggested by the modelling. Interestingly, no SKIE is observed in biotransformations with BH32 or BH32.8, suggesting that the nature of the rate-limiting step has changed during the course of evolution.

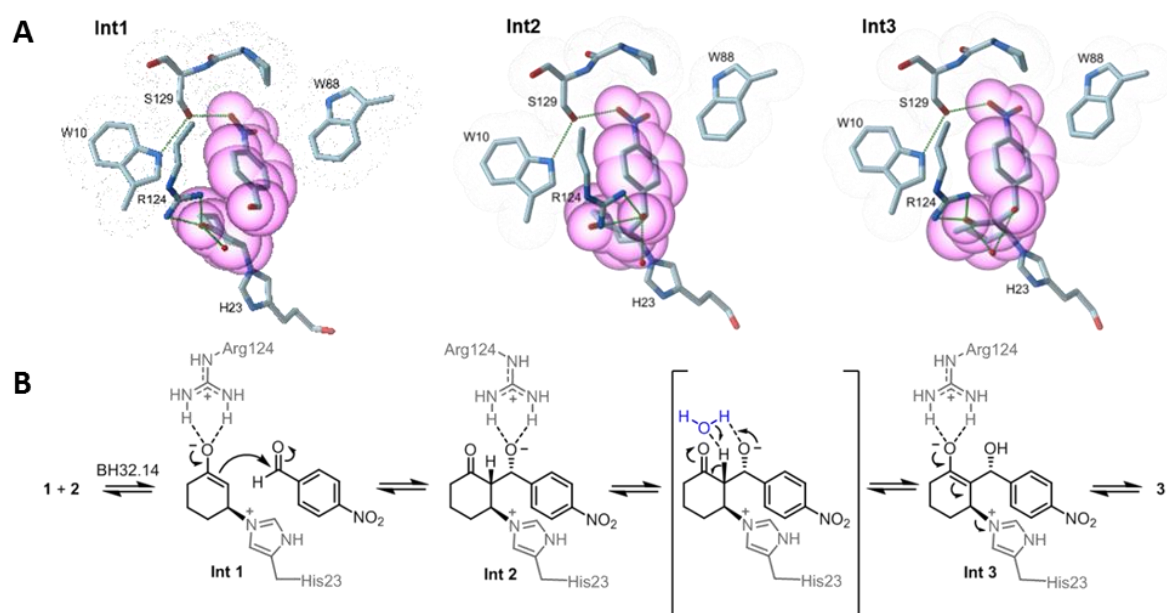


Figure 5: Proposed catalytic mechanism of an engineered MBHase. A) DFT states for intermediates 1, 2 & 3 are shown in all atom coloured stick representation. The images presented show only a subset of the atoms used in the full DFT calculation for greater visual clarity. Atoms derived from several residues that form close packing interactions with substrates **1** and **2** during catalysis (Trp10, Trp88, Arg124 & Ser129) are highlighted with grey dot surfaces. Heavy atoms from the substrates are highlighted with magenta transparent CPK spheres. Atoms from the His23 nucleophile and catalytic Arg124 are shown in all atom coloured stick representation. The hydrogen bonding network that emerged during evolution between Trp10, Ser129 and the aldehyde substrate are shown as black dashed lines. In addition, hydrogen bonds between Arg124 and each intermediate state are shown. **B)** The BH32.14 catalytic mechanism showing the role played by Arg124 in stabilizing three intermediates covalently bound through His23. A catalytic water molecule is shown in blue to facilitate proton transfer from C2 to the C3 alkoxide.

This study provides a remarkable glimpse into the evolution of new catalytic mechanisms in protein active sites, where multiple components work in concert to accelerate valuable and demanding chemical transformations. The development of BH32.14 now allows us to add MBHases to the restricted repertoire of biocatalysts available for C-C bond forming reactions. High-throughput enzyme engineering was facilitated by the development of a spectrophotometric assay, based on an irreversible inhibition reaction with mechanistic similarities to MBH transformations. We anticipate that similar assays will prove valuable for identifying highly active biocatalysts for the MBH reaction or mechanistically related transformations in the future. Beyond its synthetic utility, analysis of the BH32.14 evolution offers valuable lessons to improve enzyme design protocols, to facilitate the design of more efficient catalysts for a broader range of transformations in the future. BH32.14 employs a nucleophilic His23 and a multi-functional Arg124 to accelerate the MBH reaction, in a catalytic mechanism with strong similarities to that observed with small molecule systems.^{31,32} This suggests that in cases where no natural enzyme or catalytic antibodies are available to guide the design of new active site arrangements, we should turn to small molecule catalysis for inspiration. In particular, the observation that an appropriately positioned arginine can serve as a genetically encoded surrogate of privileged bidentate hydrogen bonding catalysts (e.g. thioureas) should inspire the design of biocatalysts for a broad range of non-biological transformations.^{31,32,34,35} Arginine was not considered as a hydrogen bond donor in the original BH32 design constraints and is typically avoided as a catalytic motif during enzyme design due to its high degree of conformational flexibility, which makes accurate positioning of the guanidinium side chain challenging. However, our study shows that in BH32.14 this conformational flexibility is advantageous, with Arg124 providing a highly effective and economical means of stabilizing multiple oxyanion intermediates and transition states. While natural enzymes are inherently dynamic molecules, existing enzyme design protocols generate a static model of the protein-transition state complex. For chemical transformations achieved with catalytic antibodies, it seems reasonable to assume that these single state design protocols could deliver enzymes with comparable or improved efficiencies to antibodies. However, our results suggest that for complex transformations with several high-energy transition states, multi-state enzyme design protocols^{36,37} will be required to account for exchanges between conformational states along the reaction coordinate. The development of these next generation enzyme design methodologies is now underway, using the evolutionary optimization of the BH32.14 catalytic mechanism as inspiration.

8.4 References

1. Hilvert, D. Design of protein catalyts. *Annu. Rev. Biochem.* **82**, 447-470 (2013).
2. Röthlisberger, D. et al. Kemp elimination catalyts by computational enzyme design. *Nature* **453**, 190-195 (2008).
3. Jiang, L. et al. *De novo* computational design of retro-aldol enzymes. *Science* **319**, 1387-1391 (2008).
4. Siegel, J. B. et al. Computational design of an enzyme catalyts for a stereoselective bimolecular Diels-Alder reaction. *Science* **329**, 309-313 (2010).
5. Eiben, C. B. et al. Increased Diels-Alderase activity through backbone remodelling guided by Foldit players. *Nat. Biotechnol.* **30**, 190-192 (2012).
6. Blomberg, R. et al. Precision is essential for efficient catalysis in an evolved Kemp eliminase. *Nature* **503**, 418-421 (2013).
7. Obexer, R. et al. Emergence of a catalytic tetrad during evolution of a highly active artificial aldolase. *Nat. Chem.* **9**, 50-56 (2017).
8. Gouverneur, V. E. et al. Control of the exo and endo pathways of the Diels-Alder reaction by antibody catalysis. *Science* **262**, 204-208 (1993).
9. Stewart, J. D. & Benkovic, S. J. Transition-state stabilization as a measure of the efficiency of antibody catalysis. *Nature* **375**, 388-391 (1995).
10. Barbas III, C. F. et al. Immune versus natural selection: antibody aldolases with enzymic rates but broader scope. *Science* **278**, 2085-2092 (1997).
11. Basavaiah, D., Rao, A. J. & Satyanarayana, T. Recent advances in the Baylis-Hillman reaction and applications. *Chem. Rev.* **103**, 811-892 (2003).
12. Basavaiah, D., Reddy, B. S. Badsara, S. S. Recent contributions from the Baylis-Hillman Reaction to Organic Chemistry. *Chem. Rev.* **9**, 5447-5674 (2010).
13. Wei, Y. & Shi, M. Recent advances in organocatalytic asymmetric Morita-Baylis-Hillman/aza-Morita-Baylis-Hillman Reactions. *Chem. Rev.* **113**, 6659-6690 (2013).
14. Metrano, A. J. et al. Asymmetric catalysis mediated by synthetic peptides, version 2.0: expansion of scope and mechanisms. *Chem. Rev.* **120**, 11479-11615 (2020).
15. Shi, M. & Liu, X.- G. Asymmetric Morita-Baylis-Hillman reaction of arylaldehydes with 2-cyclohexen-1-one and 2-cyclopenten-1-one catalyzed by chiral bis(thio)urea and DABCO. *Org. Lett.* **10**, 1043-1046 (2008).
16. Nakayama, Y., Gotanda, T. & Ito, K. Asymmetric Morita-Baylis-Hillman reactions of 2-cyclohexen-1-one catalyzed by chiral biaryl-based bis(thiourea) organocatalysts. *Tetrahedron Lett.* **52**, 6234-6237 (2011).
17. Islam, Z., Strutzenberg, T. S., Gurevic, I. & Kohen, A. Concerted versus stepwise mechanism in thymidylate synthase. *J. Am. Chem. Soc.* **136**, 9850-9853 (2014).
18. Reetz, M. T., Mondière, R. & Carballeira, J. D. Enzyme promiscuity: first protein-catalyzed Morita-Baylis-Hillman reaction. *Tetrahedron Lett.* **48**, 1679-1681 (2007).

19. López-Iglesias, M., Busto, E., Gotor, V. & Gotor-Fernández, V. Use of protease from *Bacillus licheniformis* as promiscuous catalyst for organic synthesis: applications in C-C and C-N bond formation reactions. *Adv. Synth. Catal.* **353**, 2345-2353 (2011).
20. Joshi, P. N., Purushottam, L., Das, N. K., Mukherjee, S. & Rai, V. Protein self-assembly induces promiscuous nucleophilic biocatalysis in Morita–Baylis–Hillman (MBH) reaction. *RSC Adv.* **6**, 208-211 (2016).
21. Bjelic, S. et al. Computational design of enone-binding proteins with catalytic activity for the Morita-Baylis-Hillman reaction. *ACS Chem. Biol.* **8**, 749-757 (2013).
22. Bloom, J. D., Labthavikul, S. T., Otey, C. R. & Arnold, F. H. Protein stability promotes evolvability. *Proc. Nat. Acad. Sci.* **103**, 5869-5874 (2006).
23. Tokuriki, N. & Tawfik, D. S. Stability effects of mutations and protein evolvability. *Curr. Opin. Struct. Biol.* **19**, 596-604 (2009).
24. Aggarwal, V. K., Emme, I. & Fulford, S. Y. Correlation between p*K*_a and reactivity of quinuclidine-based catalysts in the Baylis–Hillman reaction: Discovery of quinuclidine as optimum catalyst leading to substantial enhancement of scope. *J. Org. Chem.* **3**, 692–700 (2003).
25. Karur, S., Hardin, J., Headley, A. & Li, G. A novel approach to Morita–Baylis–Hillman (MBH) lactones via the Lewis acid-promoted couplings of α,β -unsaturated lactone with aldehydes. *Tetrahedron Lett.* **44**, 2991-2994 (2003).
26. Phillips, M. A., Fletterick, R. & Rutter, W. J. Arginine 127 stabilizes the transition state in carboxypeptidase. *J. Biol. Chem.* **265**, 20692-20698 (1990).
27. Studer, S. et al. Evolution of a highly active and enantiospecific metalloenzyme from short peptides. *Science* **362**, 1285-1288 (2018).
28. Janda, K. D., Schloeder, D., Benkovic, S. J. & Lerner, R. A. Induction of an antibody that catalyzes the hydrolysis of an amide bond. *Science* **241**, 1188-1191 (1988).
29. Thayer, M. M. et al. Structural basis for amide hydrolysis catalyzed by the 43C9 antibody. *J. Mol. Biol.* **291**, 329-345 (1993).
30. Roberts, V. A., Stewart, J., Benkovic, S. J. & Getzoff, E. D. Catalytic antibody model and mutagenesis implicate arginine in transition-state stabilization. *J. Mol. Biol.* **235**, 1098-1116 (1994).
31. Doyle, A. G. & Jacobsen, E. N. Small-molecule H-bond donors in asymmetric catalysis. *Chem Rev.* **107**, 5713-5743 (2007).
32. Taylor, M. S. & Jacobsen, E. N. Asymmetric catalysis by chiral hydrogen-bond donors. *Angew. Chem. Int. Ed.* **45**, 1520-1543 (2006).
33. Amarante, G. W. et al. Brønsted acid catalyzed Morita-Baylis-Hillman reaction: a new mechanistic view for thioureas revealed by ESI-MS(/MS) monitoring and DFT calculations. *Chem. Eur. J.* **15**, 12460-12469 (2009).
34. Knowles, R. R., Lin, S. & Jacobsen, E. N. Enantioselective thiourea-catalyzed cationic polycyclizations. *J. Am. Chem. Soc.* **132**, 5030-5032 (2010).
35. Park, Y. et al. Macrocyclic bis-thioureas catalyze stereospecific glycosylation reactions. *Science* **355**, 162-166 (2017).

36. St-Jacques, A. D., Eyahpaise, M.-E. C. & Chica, R. A. Computational design of multisubstrate enzyme specificity. *ACS Catal.* **9**, 5480-5485 (2019).
37. Davey, J. A., Damry, A. M., Goto, N. K. & Chica, R. A. Rational design of proteins that exchange on functional timescales. *Nat. Chem. Biol.* **13**, 1280-1285 (2017).

Data Availability Statement

Coordinates and structure factors have been deposited in the Protein Data Bank under accession numbers 6Z1K, 7O1D and 6Z1L. The authors declare that the data supporting the findings of this study are available within the paper and its Supplementary Information files. Source data are available from the corresponding author upon reasonable request.

8.5 Supplementary Information

8.5.1 Methods

Materials.

All chemicals and biological materials were obtained from commercial suppliers. Lysozyme, DNase I and kanamycin were purchased from Sigma-Aldrich; polymyxin B sulfate from AlfaAesar; LB agar, LB media, 2xYT media and arabinose from Formedium; *Escherichia coli* (*E. coli*) 5 α , Q5 DNA polymerase, T4 DNA ligase and restriction enzymes from New England BioLabs; and oligonucleotides were synthesized by Integrated DNA Technologies.

Construction of pBbE8k_BH32 and variants.

The original BH32 design²¹ was modified to introduce C186A and C212A mutations to avoid any non-specific alkylations of these positions. These substitutions had no effects on MBH activity. The C186A and C212A double mutant is referred to as BH32 throughout this study. BH32 was subcloned, using *Nde*I and *Xho*I restriction sites, into a pBbE8k vector³⁸ modified to include a 6xHis tag or Strep-tag following the *Xho*I restriction site to yield pBbE8k_BH32_6His or pBbE8k_BH32_Strep. The H23A mutation was introduced into the pBbE8k_BH32 constructs using QuikChange site-directed mutagenesis.

Protein production and purification.

For expression of BH32 and variants, chemically competent *E. coli* 5 α were transformed with the relevant pBbE8k_BH32 constructs. Single colonies of freshly transformed cells were cultured for 18 h in 10 mL LB medium containing 25 $\mu\text{g mL}^{-1}$ kanamycin. Starter cultures (500 μL) were used to inoculate 50 mL 2xYT medium supplemented with 25 $\mu\text{g mL}^{-1}$ kanamycin. Cultures were grown at 37 °C, 200 r.p.m. to an optical density at 600 nm (OD_{600}) of around 0.5. Protein expression was induced with the addition of L-arabinose to a final concentration of 10 mM. Induced cultures were incubated for 20 h at 25 °C and the cells were subsequently collected by centrifugation (3,220g for 10 min). For His-tagged variants, pelleted cells were resuspended in lysis buffer (50 mM HEPES, 300 mM NaCl, pH 7.5 containing 20 mM imidazole) and lysed by sonication. Cell lysates were cleared by centrifugation (27,216g for 30 min), and supernatants were subjected to affinity chromatography using Ni-NTA Agarose (Qiagen). Purified protein was eluted using 50 mM HEPES, 300 mM NaCl, pH 7.5 containing 250 mM imidazole. For Strep-tagged variants, pelleted cells were resuspended in Buffer NP (50 mM NaH_2PO_4 , 300 mM NaCl, pH 8) and lysed by sonication. Cell lysates were cleared by centrifugation (27,216g for 30 min), supernatants were subjected to a *Strep*-Tactin® Superflow Plus resin (Qiagen) and purified protein was eluted using 50 mM NaH_2PO_4 , 300 mM NaCl, 2.5 mM desthiobiotin at pH 8.0. Proteins were desalted using 10DG desalting columns (Bio-Rad) with PBS pH 7.4 and analysed by SDS-PAGE. Proteins were further purified by size-exclusion chromatography using a Superdex 200 column (GE Healthcare) in PBS pH 7.4. Proteins were aliquoted, flash-frozen in liquid nitrogen and stored at -80 °C. Protein concentrations were determined by measuring the absorbance at 280 nm and assuming an extinction coefficient of 31400 $\text{M}^{-1} \text{cm}^{-1}$ for BH32-BH32.7, 32890 $\text{M}^{-1} \text{cm}^{-1}$ for BH32.8, 38390 $\text{M}^{-1} \text{cm}^{-1}$ for BH32.9-BH32.11, and 35410 $\text{M}^{-1} \text{cm}^{-1}$ for BH32.12-BH32.14.

Inhibition of BH32 variants.

Proteins were inhibited under two different reaction conditions (Figure 2C and S11): For comparison of BH32, BH32 H23A and BH32.8, proteins (25 μM) were inhibited following incubation with 4-methoxyphenyl-(6-oxocyclohex-1-en-1-yl)methyl acetate, **4** (250 μM) in PBS pH 7.4 with 3% (v/v) acetonitrile at room temperature. Formation of the covalently modified protein was monitored spectrophotometrically at 325 nm (Figure 2C). Samples were diluted in PBS pH 7.4, excess inhibitor was removed using a Vivaspin® 10k MWCO (Sartorius) and inhibited proteins were characterized by mass spectrometry (Table S1). Under these conditions, inhibition of BH32.12 and BH32.14 was too rapid to be monitored spectrophotometrically. To allow comparison of BH32, BH32 H23A, BH32.8, BH32.12, BH32.14, BH32.14 H23A and BH32.14 R124A (Figure S11), enzyme variants (10 μM) were inhibited following incubation with **4** (25 μM) in PBS pH 7.4 with 3% (v/v) acetonitrile at room temperature.

Mass spectrometry.

Purified protein samples were buffer exchanged into 0.1% acetic acid using a 10k MWCO Vivaspin (Sartorius) and diluted to a final concentration of 0.5 mg mL⁻¹. Mass spectrometry was performed using a 1200 series Agilent LC, with a 5 μL injection into 5% acetonitrile (with 0.1% formic acid) and desalted inline for 1 min. Protein was eluted over 1 min using 95% acetonitrile with 5% water. The resulting multiply charged spectrum was analysed using an Agilent QTOF 6510 and deconvoluted using Agilent MassHunter Software.

Library construction.

Primer sequences used to generate DNA libraries are shown in Table S9.

Rounds 1, 3, 10 & 13: random mutagenesis using error-prone PCR. Random libraries were generated by error-prone PCR of the entire gene using a JBS Error-Prone Kit (Jena Bioscience) according to the manufacturer's protocol. PCR conditions were adjusted to generate an average of 2.5 mutations per gene. The linear library fragments and the modified pBbE8k vector were digested using *NdeI* and *XhoI* endonucleases, gel-purified and subsequently ligated using T4 DNA ligase. Variants with improved activity were sequenced and identified 'hot spots' were subsequently individually randomized by saturation mutagenesis.

Rounds 2, 4-9, 11-12 & 14: saturation mutagenesis. Positions were either individually randomized using NNK codon degeneracy (Rounds 2, 4-6, 8-9, 11-12 & 14), or randomized in pairs using the 22-codon trick³⁹ (Rounds 2 & 7). DNA libraries were constructed by overlap extension PCR and genes were cloned as described above.

Shuffling by overlap extension PCR.

After each round of evolution, beneficial diversity was combined by DNA shuffling of fragments generated by overlap extension PCR. Primers were designed that encoded either the parent amino acid or the identified mutation. These primers were used to generate short fragments (up to 6) which were gel-purified and mixed appropriately in overlap extension PCR to generate genes containing all possible combinations of mutations. Genes were cloned as described above.

Library screening.

For protein expression and screening, all transfer and aliquotting steps were performed using Hamilton liquid-handling robots. Chemically competent *E. coli* 5 α cells were transformed with the ligated libraries. Freshly transformed clones were used to inoculate 180 μ L of 2xYT medium supplemented with 25 μ g mL⁻¹ kanamycin in Corning® Costar® 96-well microtitre round bottom plates. For reference, each plate contained 6 freshly transformed clones of the parent template and 2 clones containing an empty pBbE8k vector. Plates were incubated overnight at 30 °C, 80 % humidity in a shaking incubator at 900 r.p.m. 20 μ L of overnight culture was used to inoculate 480 μ L 2xYT medium supplemented with 25 μ g mL⁻¹ kanamycin. The cultures were incubated at 30 °C, 80 % humidity with shaking at 900 r.p.m. until an OD₆₀₀ of about 0.5 was reached, and L-arabinose was added to a final concentration of 10 mM. Induced plates were incubated for 20 h at 30 °C, 80 % humidity with shaking at 900 r.p.m. Cells were harvested by centrifugation at 2,900 *g* for 5 min. The supernatant was discarded and the pelleted cells were resuspended in 400 μ L of lysis buffer (PBS pH 7.4 buffer supplemented with 1.0 mg mL⁻¹ lysozyme, 0.5 mg mL⁻¹ polymixin B and 10 μ g mL⁻¹ DNase I) and incubated for 2 h at 30 °C, 80 % humidity with shaking at 900 r.p.m. Cell debris was removed by centrifugation at 2,900 *g* for 5 min.

Rounds 1-8: 100 μ L Clarified lysate was transferred to 96-well microtitre plates containing 80 μ L PBS buffer pH 7.4. Reactions were initiated with the addition of 20 μ L inhibitor **4** (Rounds 1-4: 250 μ M final concentration, Rounds 5-6: 100 μ M final concentration) in PBS pH 7.4 containing acetonitrile (3% (v/v) final concentration). Inhibition was monitored spectrophotometrically at 325 nm, over 15 minutes using a CLARIOstar plate reader (BMG Labtech). Reaction rates of individual variants were normalized to the average of the 6 parent clones.

Rounds 9-14: 75 μ L Clarified lysate was transferred to 96-well polypropylene microtitre plates and the reaction was initiated with the addition of 25 μ L assay mix containing 4-nitrobenzaldehyde (0.6 mM final concentration) and 2-cyclohexen-1-one (3 mM final concentration) in PBS pH 7.4. Reactions were heat-sealed and incubated for 18 h at 30 °C, 80 % humidity with shaking at 900 r.p.m. Reactions were quenched with the addition of 100 μ L acetonitrile and incubated for a further 2 h at 30 °C, 80 % humidity with shaking at 900 r.p.m. Precipitated proteins were removed by centrifugation at 2,900*g* for 10 min. 100 μ L of the clarified reaction was transferred to 96-well polypropylene microtitre plates and heat-sealed with pierceable foil. Reactions were evaluated by HPLC analysis as described below.

Following each round, the most active variants were rescreened as purified proteins using the HPLC assay. Proteins were produced and purified as described above, however starter cultures were inoculated from glycerol stocks prepared from the original overnight cultures.

Kinetic characterization.

Initial velocity (V_0) vs [4-nitrobenzaldehyde] kinetic data were measured using strep-tagged purified enzyme (60 μ M BH32, 40 μ M BH32.8, 10 μ M BH32.12 & BH32.14), a fixed concentration of **1** (25 mM) and varying concentrations of **2** (0.25-2 mM for BH32 and 0.1-2 mM for BH32.8, BH32.12 & BH32.14). Reactions were performed in PBS pH 7.4 with 3% acetonitrile and were incubated at 30

°C with shaking (800 r.p.m.). BH32.14 & BH32.12 catalyzed reactions were sampled at 15 minute intervals, BH32.8 was sampled at 35, 80, 120, 150, 180, 225, 270 minutes, and BH32 was sampled at 24 h, 40 h, 49 h, 68 h and 94 h. V_0 vs [2-cyclohexen-1-one] kinetic data were measured using a fixed concentration of **2** (2 mM) and varying concentrations of **1** (1-25 mM for BH32, BH32.8 & BH32.12, and 0.5-25 mM for BH32.14) using the enzyme concentrations and buffer conditions described above. Samples were quenched with 1 volume of acetonitrile and analysed by HPLC as described below (see *chromatographic analysis*).

Linear fits of conversion vs time allowed determination of V_0 at each condition (Figure S2). The combined V_0 vs [4-nitrobenzaldehyde] and V_0 vs [2-cyclohexen-1-one] steady state kinetic data were fitted globally using both the random order binding model (Eq. 1) and a two-substrate ordered binding kinetic model (Eq. 2):

$$v = k_{\text{cat}}[E][A][B]/((K_{\text{mA}} + [A])(K_{\text{mB}} + [B])) \quad (\text{Eq. 1})$$

$$v = k_{\text{cat}}[E][A][B]/([A][B] + K_{\text{mA}}[B] + K_{\text{mB}}[A] + K_{\text{sA}}K_{\text{mB}}) \quad (\text{Eq. 2})$$

Where k_{cat} has its usual meaning, [E] is the total enzyme concentration, [A] and [B] are the initial 2-cyclohexen-1-one and 4-nitrobenzaldehyde concentrations respectively, K_{mA} and K_{mB} are the corresponding *apparent* Michaelis constants, and K_{sA} is the dissociation constant for the enzyme-substrate A complex. Note that Eq. 1 and Eq. 2 are equivalent when $K_{\text{sA}} = K_{\text{mA}}$. Global fitting was performed with shared k_{cat} , K_{mA} , K_{mB} and K_{sA} values (i.e. as a 3D surface fit). Kinetic constants are shown in Table S3.

Kinetic Solvent Isotope Effects

KSIE experiments were performed in PBS (pH/pD 7.4) (Figure S13). Deuterated buffers were prepared using 99.9% D₂O with pD adjusted according to the following relationship: pD = pH_{obs} + 0.38. To compare the activity of BH32, BH32.8 and BH32.14, analytical scale biotransformations were performed using **1** (25 mM), **2** (2 mM) and the relevant biocatalyst (50 μM BH32, 30 μM BH32.8, 10 μM BH32.14) in both deuterated and non-deuterated PBS buffer with 3 % MeCN as a cosolvent. Reactions were performed in triplicate. Reactions in deuterated buffer contained <0.5% H₂O final concentration. All reactions were incubated at 25 °C with shaking (800 r.p.m.) with samples taken every 10 minutes for 1 hour with BH32.8 and BH32.14 and at 15, 21, 24, 40 and 46 hours for BH32. For HPLC analysis, reactions were quenched by the addition of 1 volume of acetonitrile. Samples were vortexed and precipitated proteins removed by centrifugation (14,000 g for 5 minutes).

BH32.14 total turnover numbers

Total turnover numbers achieved by BH32.14 were determined as follows: BH32.14 (0.5 or 0.1 mol%) catalyzed biotransformations were performed in glass vials using **1** (50 mM) and **2** (10 mM) in PBS (pH 7.4) with 20 % DMSO cosolvent (Figure S5). Reactions were incubated at 25 °C with shaking (300 r.p.m.) and samples were taken at 3.0, 28.5, 52.5, 70.25, 100, 159 and 187 hours. For HPLC analysis, reactions were quenched at the stated time points with the addition of 1 volume

acetonitrile. Samples were vortexed and precipitated proteins were removed by centrifugation (14,000 g for 5 minutes).

General procedure for analytical scale biotransformations.

To compare the activity of BH32, BH32.14 and its variants (Table 1), analytical scale biotransformations were performed using **1** (3 mM), **2** (0.6 mM) and the relevant biocatalyst (18 μ M) in PBS (pH 7.4) with 3 % DMSO as a cosolvent. For comparison, reactions were also performed at varying concentrations of small molecule catalytic nucleophiles imidazole, DMAP and DABCO (18 μ M, 60 μ M and 1 mM). For reaction conditions used in the preparation of MBH adducts **5a-w** (Figure 3) see Table S5.

For HPLC analysis, reactions were quenched at the stated time points with the addition of 1 volume acetonitrile. Samples were vortexed and precipitated proteins were removed by centrifugation (14,000 g for 5 minutes). For SFC analysis, the substrates and products were extracted with 3 volumes of ethyl acetate. Precipitated proteins were cleared by centrifugation (14,000 g for 5 minutes), the organic phase was separated and directly injected onto the SFC.

BH32.14 cosolvent tolerance and temperature profile.

To investigate cosolvent tolerance, analytical scale biotransformations were performed using **1** (50 mM), **2** (10 mM) and BH32.14 (50 μ M) in PBS (pH 7.4) with either 20 %, 30 % and 40 % of DMSO or MeCN as a cosolvent (Table S4). All reactions were incubated at 25 °C with shaking (800 r.p.m.) for 5 hours. To evaluate the activity of BH32.14 at elevated temperatures (Figure S6) analytical scale biotransformations were performed using **1** (50 mM), **2** (10 mM) and BH32.14 (50 μ M) in PBS (pH 7.4) with 20 % DMSO as a cosolvent. Enzyme solutions were pre-incubated at the required temperature (25-85 °C at 5 °C intervals) for 15 minutes prior to initiation of the reaction by addition of substrate. Reactions were quenched after 5 hours with the addition of 1 volume MeCN and analysed by HPLC (see below).

Chromatographic analysis.

HPLC analysis was performed on a 1290 Infinity II Agilent LC system with a Kinetex® 5 μ m XB-C18 100 Å LC Column, 50 x 2.1 mm (Phenomenex). For library screening an isocratic method using 25% acetonitrile in water at 1 mL min⁻¹ for 1.5 minutes was used. For substrate profiling reactions, substrates and products (**5a-w**) were eluted over 20 minutes using a gradient of 5-95% acetonitrile in water at 1 mL min⁻¹. Peaks were assigned by comparison to chemically synthesized standards and the peak areas were integrated using Agilent OpenLab software. The extinction coefficients used to calculate the conversion are reported in Table S5.

Chiral analysis was performed using an SFC 1290 Infinity II Agilent system. Enantiomers of the MBH product **3** were separated using a Daicel 80S82 CHIRALPAK® IA-3 SFC column, 3 mm, 50 mm, 3 μ m, and an isocratic method with 35% methanol in CO₂ at 1 mL min⁻¹ for 1 minute. For substrate profiling reactions a range of different SFC methods were used and these are summarized in Table S6. For MBH adducts **5c-d**, **j**, **l**, **n-o**, **r** & **t** the major stereoisomer formed in the biotransformation eluted first; for MBH adducts **3**, **5a-b**, **e-i**, **k**, **m**, **p-q**, **s** & **u-w** the major stereoisomer formed in the

biotransformation eluted second. Peaks were assigned by comparison to chemically synthesized standards and peak areas were integrated using Agilent OpenLabs software.

Preparative scale biotransformation.

A preparative scale biotransformation was performed using **1** (50 mM), **2** (10 mM), strep-tag purified BH32.14 (50 μ M) in PBS (pH 7.4, 72 mL) with 20 % DMSO (18 mL) as a cosolvent. The reaction was incubated at 30 °C with shaking at 100 r.p.m. for 19 hours. An aliquot (100 μ L) was removed and quenched with acetonitrile for HPLC analysis, which showed the reaction had proceeded to 94 % conversion. The reaction mixture was extracted with ethyl acetate (2 x 400 mL), dried over MgSO₄, filtered and the solvent was removed *in vacuo*. The crude product (Figure S4) was purified by flash column chromatography (5:1 cyclohexane:ethyl acetate) to give 2-(hydroxy(4-nitrophenyl)methyl)cyclohex-2-en-1-one, **3** as a light yellow solid (197 mg, 88%). Spectral data is consistent with literature values.⁴⁰ δ_{H} (400 MHz, CDCl₃): 8.21 (m, 2H), 7.56 (m, 2H), 6.82 (t, J = 4.1 Hz, 1H), 5.62 (d, J = 6.1 Hz, 1H), 3.51 (d, J = 6.0 Hz, 1H), 2.46 (m, 4H), 2.03 (m, 2H). ^{13}C NMR (100 MHz, CDCl₃) δ 200.1, 149.3, 148.1, 147.2, 140.2, 127.1, 123.5, 72.0, 38.4, 25.8, 22.3. ESI+ m/z = 270 ([M +Na]⁺,100)

Preparation of product standards **3** and **S1**.⁴⁰

4-Nitrobenzaldehyde (1.5 g, 10 mmol), 2-cyclohexen-1-one (970 μ L, 10 mmol) and imidazole (681 mg, 10 mmol) were stirred in 1M NaHCO₃ (40 mL) and THF (10 mL) for 40 hours at room temperature. The reaction was acidified with 1M HCl and extracted with ethyl acetate (150 mL). The organic layer was dried over MgSO₄, filtered and the solvent was removed *in vacuo*. The reaction yielded a mixture of the Morita-Baylis-Hillman adduct **3** and aldol adduct **S1** which were separated by flash column chromatography (5:1 cyclohexane:ethyl acetate).

2-(hydroxy(4-nitrophenyl)methyl)cyclohex-2-en-1-one **3** (562 mg, 23%). See characterization data above.

6-(hydroxy(4-nitrophenyl)methyl)cyclohex-2-en-1-one **S1** (180 mg, 7%) as a 4:1 mixture of diastereoisomers. Spectral data is consistent with literature values.⁴¹ δ_{H} (400 MHz, CDCl₃): 8.26-8.20 (m, 2H), 7.57-7.51 (m, 2H), 7.10-6.97 (m, 1H), 6.13-6.08 (m, 1H), 5.70 (d, J = 2.3 Hz, 1H_{maj}), 4.99 (d, J = 8.7 Hz, 1H_{min}), 4.95 (br s, OH_{min}), 2.95 (br s, OH_{maj}), 2.72-2.65 (m, 1H_{maj}), 2.62-2.53 (m, 1H_{min}), 2.48-2.25 (m, 2H), 2.06-1.93 (m, 1H), 1.57-1.46 (m, 1H). ESI+ m/z = 270 ([M +Na]⁺,100)

Preparation of **5j** and inhibitor **4**

Anisaldehyde (1.36 g, 10 mmol), 2-cyclohexen-1-one (970 μ L, 10 mmol) and imidazole (681 mg, 10 mmol) were stirred in 1M NaHCO₃ (40 mL) and THF (10 mL) 48 hours at room temperature. The reaction was acidified with 1M HCl and extracted with ethyl acetate (150 mL). The organic layer was dried over MgSO₄, filtered and the solvent was removed *in vacuo*. The product was purified by flash column chromatography (5:1 cyclohexane:ethyl acetate) to yield **5j** (440 mg, 19%). Spectral data is consistent with literature values.⁴² ^1H NMR (400 MHz, CDCl₃) δ 7.30 – 7.25 (m, 2H), 6.90 – 6.85 (m, 2H), 6.74 (t, J = 4.2 Hz, 1H), 5.51 (s, 1H), 3.80 (s, 3H), 3.35 (br s, 1H), 2.48 – 2.42 (m, 2H), 2.42 – 2.35 (m, 2H), 2.03 – 1.96 (m, 2H). ^{13}C NMR (100 MHz, CDCl₃) δ 200.4, 158.9, 147.0, 141.1, 133.8, 127.7, 113.7, 72.0, 55.2, 38.5, 25.7, 22.5. ESI+ m/z = 255 ([M +Na]⁺,100)

5j (50 mg, 0.25 mmol) and acetic anhydride (50 μ L) were stirred in pyridine (1 mL) overnight at room temperature. The reaction was diluted in ethyl acetate (30 mL) and washed with 1M NaHCO₃ (2 x 10 mL), 10% CuSO₄ (2 x 10 mL) and then brine (10 mL). The organic layer was dried over MgSO₄, filtered and the solvent removed *in vacuo*. The product was purified by flash column chromatography (5:1 cyclohexane: ethyl acetate) to give the product (4-methoxyphenyl)(6-oxocyclohex-1-en-1-yl)methyl acetate, **4** (49 mg, 84%). ¹H NMR (400 MHz, CDCl₃) δ 7.30 – 7.24 (m, 2H), 6.96 (t, *J* = 4.3 Hz, 1H), 6.87 – 6.82 (m, 2H), 6.67 (s, 1H), 3.78 (s, 3H), 2.50 – 2.33 (m, 4H), 2.07 (s, 3H), 2.05 – 1.90 (m, 2H). ¹³C NMR (100 MHz, CDCl₃) δ 197.0, 169.5, 159.3, 145.3, 138.9, 130.9, 128.6, 113.7, 71.4, 55.2, 38.3, 25.7, 22.5, 21.2. ESI+ *m/z* = 297 ([M +Na]⁺, 100)

Preparation of chiral standards.

The enantiomers of **3** were separated by preparative chiral HPLC by Reach Separations (Nottingham) to afford (*R*)-**3** (99.5% *e.e*) and (*S*)-**3** (99.9% *e.e*) as white solids. The absolute stereochemistry was determined by measuring the optical rotation ((*R*)-**3** (-52.5°) and (*S*)-**3** (+50.0°) at 0.008 g mL⁻¹ in DCM at 27 °C) and comparison to literature values.⁴³

General procedure for the preparation of racemic product standards (**5a, c, e-i, k-n & p-w**).

Arylaldehyde (3.3 mmol, 1.0 equiv), cyclic enone (3.3 mmol, 1.0 equiv) and imidazole (227 mg, 3.3 mmol, 1.0 equiv) were stirred in 1M NaHCO₃ (13.3 mL) and THF (3.3 mL) for 24h at room temperature. The reaction was acidified with 1M HCl and extracted with ethyl acetate (3 x 50 mL). The organic layer was dried over MgSO₄, filtered and the solvent removed *in vacuo* to give the crude product.

2-((4-nitrophenyl)(hydroxy)methyl)cyclopent-2-en-1-one (5a). Crude product was purified by flash chromatography (2:1 cyclohexane:ethyl acetate) to give the product as a yellow solid (62 mg, 8%). Spectral data is consistent with literature values.¹⁵ ¹H NMR (400 MHz, CDCl₃) δ 8.25-8.20 (m, 2H), 7.62-7.57 (m, 2H), 7.29 (td, *J* = 2.8, 1.2 Hz, 1H), 5.68 (s, 1H), 3.56 (s, 1H), 2.67-2.61 (m, 2H), 2.52-2.46 (m, 2H). ¹³C NMR (101 MHz, CDCl₃) δ 209.5, 159.9, 148.6, 147.9, 146.8, 127.2, 123.9, 69.3, 35.3, 26.9. ESI+ *m/z* = 216.0657 ([M -OH]⁺, 100).

5-(hydroxy(4-nitrophenyl)methyl)-2,2-dimethyl-3a,6a-dihydro-4H-cyclopenta[d][1,3]dioxol-4-one (5c). Crude product was purified by flash chromatography (3:1 cyclohexane:ethyl acetate) to give the two diastereomeric products. Stereoisomer 1 eluted first and was formed as a colourless oil (96 mg, 10%). ¹H NMR (400 MHz, CDCl₃) δ 8.24-8.18 (m, 2H), 7.64-7.57 (m, 2H), 7.40-7.35 (m, 1H), 5.67 (d, *J* = 4.2 Hz, 1H), 5.21 (dd, *J* = 5.4, 2.4 Hz, 1H), 4.50 (d, *J* = 5.4 Hz, 1H), 3.05 (d, *J* = 4.4 Hz, 1H), 1.40 (s, 6H). ¹³C NMR (101 MHz, CDCl₃) δ 201.9, 153.7, 147.9, 147.5, 147.4, 127.3, 124.0, 115.9, 77.8, 77.0, 68.6, 27.6, 26.2. ESI- *m/z* = 304.0844 ([M -H]⁻, 80), 288.08916 (27), 246.0421 (100). Stereoisomer 2 was formed as a colourless oil (75 mg, 8%). ¹H NMR (400 MHz, CDCl₃) δ 8.25-8.19 (m, 2H), 7.61-7.56 (m, 2H), 7.27-7.24 (m, 1H), 5.69 (m, 1H), 5.22 (ddd, *J* = 5.5, 2.4, 1.1 Hz, 1H), 4.55 (d, *J* = 5.4 Hz, 1H), 1.42 (s, 3H), 1.38 (s, 3H). ¹³C NMR (101 MHz, CDCl₃) δ 201.7, 153.8, 147.8, 147.0, 147.0, 127.3, 123.9, 115.7, 77.7, 76.8, 68.5, 27.5, 26.1. ESI- *m/z* = 304.0842 ([M -H]⁻, 85), 288.0892 (33), 246.0423 (100).

2-((4-bromophenyl)(hydroxy)methyl)cyclohex-2-en-1-one (5e). Crude product was purified by flash chromatography (4:1 cyclohexane:ethyl acetate) to give the product as a white solid (128 mg,

14%). Spectral data is consistent with literature values.¹⁵ ¹H NMR (400 MHz, CDCl₃) δ 7.49-7.44 (m, 2H), 7.25-7.21 (m, 2H), 6.73 (t, *J* = 4.2 Hz, 1H), 5.50 (s, 1H), 2.56-2.28 (m, 4H), 2.09-1.89 (m, 2H). ¹³C NMR (101 MHz, CDCl₃) δ 200.5, 147.7, 140.9, 140.8, 131.6, 128.3, 121.5, 72.3, 38.7, 25.9, 22.6. ESI+ *m/z* = 265.0070 ([M ⁸¹Br -OH]⁺, 100), 263.0090 ([M ⁷⁹Br -OH]⁺, 91).

2-((4-chlorophenyl)(hydroxy)methyl)cyclohex-2-en-1-one (5f). Crude product was purified by flash chromatography (4:1 cyclohexane:ethyl acetate) to give the product as a white solid (114 mg, 15%). Spectral data is consistent with literature values.¹⁵ ¹H NMR (400 MHz, CDCl₃) δ 7.30-7.22 (m, 4H), 6.74 (t, *J* = 4.3 Hz, 1H), 5.48 (s, 1H), 3.46 (br s, 1H), 2.45-2.32 (m, 4H), 1.95 (app quint, *J* = 6.3 Hz, 2H). ¹³C NMR (101 MHz, CDCl₃) δ 200.4, 147.6, 140.8, 140.4, 133.2, 128.5, 127.9, 71.8, 38.5, 25.8, 22.5. ESI+ *m/z* = 221.0564 ([M ³⁷Cl -OH]⁺, 30), 219.0591 ([M ³⁵Cl -OH]⁺, 100).

2-((4-cyanophenyl)(hydroxy)methyl)cyclohex-2-en-1-one (5g). Crude product was purified by flash chromatography (3:1 cyclohexane:ethyl acetate) to give the product as a colourless oil (115 mg, 15%). Spectral data is consistent with literature values.⁴⁴ ¹H NMR (400 MHz, CDCl₃) δ 7.62 (d, *J* = 8.3 Hz, 2H), 7.48 (d, *J* = 8.1 Hz, 2H), 6.79 (t, *J* = 4.2 Hz, 1H), 5.55 (d, *J* = 5.9 Hz, 1H), 3.51 (d, *J* = 5.9 Hz, 1H), 2.48-2.38 (m, 4H), 2.05-1.96 (m, 2H). ¹³C NMR (101 MHz, CDCl₃) δ 200.1, 148.0, 147.5, 140.4, 132.5, 127.1, 118.9, 111.3, 72.0, 38.5, 25.8, 22.5. ESI+ *m/z* = 210.0922 ([M -OH]⁺, 100).

2-((4-(trifluoromethyl)phenyl)(hydroxy)methyl)cyclohex-2-en-1-one (5h). Crude product was purified by flash chromatography (4:1 cyclohexane:ethyl acetate) to give the product as a colourless oil (196 mg, 22%). Spectral data is consistent with literature values.⁴⁵ ¹H NMR (400 MHz, CDCl₃) δ 7.58 (d, *J* = 8.1 Hz, 2H), 7.47 (d, *J* = 8.2 Hz, 2H), 6.77 (t, *J* = 4.3 Hz, 1H), 5.57 (d, *J* = 5.4 Hz, 1H), 3.59 (d, *J* = 5.7 Hz, 1H), 2.48-2.37 (m, 4H), 2.04-1.95 (m, 2H). ¹³C NMR (101 MHz, CDCl₃) δ 200.4, 147.9, 145.9, 140.7, 129.6 (q, *J* = 32.3 Hz), 126.8, 125.4 (q, *J* = 3.8 Hz), 122.8, 72.4, 38.6, 25.9, 22.6. ESI+ *m/z* = 253.0853 ([M -OH]⁺, 100).

2-(hydroxy(p-tolyl)methyl)cyclohex-2-en-1-one (5i). Crude product was purified by flash chromatography (3:1 cyclohexane:ethyl acetate) to give the product as a colourless oil (112mg, 16%). Spectral data is consistent with literature values.⁴⁶ ¹H NMR (400 MHz, CDCl₃) δ 7.24 (d, *J* = 8.1 Hz, 2H), 7.15 (d, *J* = 7.9 Hz, 2H), 6.74 (t, *J* = 4.2 Hz, 1H), 5.52 (s, 1H), 3.36 (br s, 1H), 2.48 – 2.42 (m, 2H), 2.42 – 2.35 (m, 2H), 2.34 (s, 3H), 2.04 – 1.95 (m, 2H). ¹³C NMR (126 MHz, CDCl₃) δ 200.6, 147.4, 141.3, 138.8, 137.3, 129.2, 126.5, 72.6, 38.8, 25.9, 22.7, 21.3. ESI+ *m/z* = 239.1050 ([M +Na]⁺, 16), 199.1125 ([M -OH]⁺, 100).

2-((3-fluoro-4-nitrophenyl)(hydroxy)methyl)cyclohex-2-en-1-one (5k). Crude product was purified by flash chromatography (4:1 cyclohexane:ethyl acetate) to give the product as a white solid (53 mg, 6%). ¹H NMR (400 MHz, CDCl₃) δ 8.02 (dd, *J* = 8.5, 7.5 Hz, 1H), 7.34 (dd, *J* = 11.8, 1.8 Hz, 1H), 7.31-7.23 (m, 1H), 6.87 (t, *J* = 4.2 Hz, 1H), 5.54 (s, 1H), 2.54-2.37 (m, 4H), 2.02 (app quint, *J* = 6.2 Hz, 2H). ¹³C NMR (101 MHz, CDCl₃) δ 200.1, 155.7 (d, *J* = 265.2 Hz), 151.6 (d, *J* = 7.7 Hz), 148.7, 139.9, 136.4 (d, *J* = 7.2 Hz), 126.2 (d, *J* = 2.7 Hz), 122.2 (d, *J* = 3.8 Hz), 116.2 (d, *J* = 21.9 Hz), 71.8 (d, *J* = 1.4 Hz), 38.5, 25.9, 22.5. ESI+ *m/z* = 248.0697 ([M -OH]⁺, 100).

2-((2-fluoro-4-nitrophenyl)(hydroxy)methyl)cyclohex-2-en-1-one (5l). Crude product was purified by flash chromatography (4:1 cyclohexane:ethyl acetate) to give the product as a white solid (90 mg, 10%). ¹H NMR (400 MHz, CDCl₃) δ 8.08 (dd, *J* = 8.6, 1.9 Hz, 1H), 7.89 (dd, *J* = 9.8, 2.2 Hz,

1H), 7.83-7.77 (m, 1H), 6.78-6.72 (m, 1H), 5.81 (d, $J = 6.7$ Hz, 1H), 3.92 (d, $J = 6.3$ Hz, 1H), 2.55-2.37 (m, 4H), 2.08-1.93 (m, 2H). ^{13}C NMR (101 MHz, CDCl_3) δ 200.7, 159.0 (d, $J = 251.0$ Hz), 148.5 (d, $J = 1.8$ Hz), 148.1, 138.6, 136.5 (d, $J = 13.3$ Hz), 129.2 (d, $J = 4.4$ Hz), 119.5 (d, $J = 3.7$ Hz), 111.2 (d, $J = 26.9$ Hz), 67.6 (d, $J = 2.5$ Hz), 38.5, 25.9, 22.4. ESI+ $m/z = 248.0717$ ($[\text{M} - \text{OH}]^+$, 100).

2-((3-fluoro-4-bromophenyl)(hydroxy)methyl)cyclohex-2-en-1-one (5m). Crude product was purified by flash chromatography (4:1 cyclohexane:ethyl acetate) to give the product as a colourless oil (43 mg, 4%). ^1H NMR (400 MHz, CDCl_3) δ 7.48 (dd, $J = 8.3, 7.0$ Hz, 1H), 7.16-7.11 (m, 1H), 7.01 (dd, $J = 8.2, 2.0$ Hz, 1H), 6.79 (t, $J = 4.1$, 1H), 5.46 (s, 1H), 3.50 (br s, 1H), 2.49-2.35 (m, 4H), 2.06-1.92 (m, 2H). ^{13}C NMR (101 MHz, CDCl_3) δ 200.3, 159.1 (d, $J = 247.4$ Hz), 147.9, 144.1 (d, $J = 6.2$ Hz), 140.4, 133.3, 123.3 (d, $J = 3.3$ Hz), 114.7 (d, $J = 23.1$ Hz), 107.8 (d, $J = 20.9$ Hz), 71.7 (d, $J = 1.6$ Hz), 38.6, 25.9, 22.5. ESI+ $m/z = 282.9955$ ($[\text{M}^{81}\text{Br} - \text{OH}]^+$, 95), 280.9975 ($[\text{M}^{79}\text{Br} - \text{OH}]^+$, 100).

2-((2-fluoro-4-bromophenyl)(hydroxy)methyl)cyclohex-2-en-1-one (5n). Crude product was purified by flash chromatography (4:1 cyclohexane:ethyl acetate) to give the product as a colourless oil (68 mg, 7%). ^1H NMR (400 MHz, CDCl_3) δ 7.46-7.40 (m, 1H), 7.32 (dd, $J = 8.4, 1.9$ Hz, 1H), 7.20 (dd, $J = 9.7, 1.9$ Hz, 1H), 6.71-6.66 (m, 1H), 5.74 (s, 1H), 3.80 (s, 1H), 2.50-2.35 (m, 4H), 2.05-1.93 (m, 2H). ^{13}C NMR (101 MHz, CDCl_3) δ 200.8, 159.5 (d, $J = 251.1$ Hz), 147.8, 139.3, 129.6 (d, $J = 4.7$ Hz), 127.9 (d, $J = 13.3$ Hz), 127.7 (d, $J = 3.6$ Hz), 121.6 (d, $J = 9.5$ Hz), 118.9 (d, $J = 24.9$ Hz), 67.1 (d, $J = 2.9$ Hz), 38.6, 25.9, 22.5. ESI+ $m/z = 282.9962$ ($[\text{M}^{81}\text{Br} - \text{OH}]^+$, 99), 280.9981 ($[\text{M}^{79}\text{Br} - \text{OH}]^+$, 100).

2-((3-nitrophenyl)(hydroxy)methyl)cyclohex-2-en-1-one (5p). Crude product was purified by flash chromatography (4:1 cyclohexane:ethyl acetate) to give the product as a colourless oil (132 mg, 16%). Spectral data consistent with literature values.¹⁵ ^1H NMR (400 MHz, CDCl_3) δ 8.21 – 8.18 (m, 1H), 8.09 (dd, $J = 8.3, 1.2$ Hz, 1H), 7.70 (d, $J = 7.6$ Hz, 1H), 7.49 (t, $J = 7.9$ Hz, 1H), 6.86 (t, $J = 4.2$ Hz, 1H), 5.58 (d, $J = 5.7$ Hz, 1H), 3.67 (d, $J = 5.8$ Hz, 1H), 2.48 – 2.37 (m, 4H), 2.00 (app quint, $J = 6.3$ Hz, 2H). ^{13}C NMR (101 MHz, CDCl_3) δ 200.2, 148.4, 148.2, 144.4, 140.3, 132.7, 129.3, 122.5, 121.4, 71.9, 38.5, 25.9, 22.5. ESI+ $m/z = 230.08221$ ($[\text{M} - \text{OH}]^+$, 100).

2-((3-bromophenyl)(hydroxy)methyl)cyclohex-2-en-1-one (5q). Crude product was purified by flash chromatography (4:1 cyclohexane:ethyl acetate) to give the product as a colourless oil (67 mg, 7%). Spectral data is consistent with literature values.¹⁵ ^1H NMR (400 MHz, CDCl_3) δ 7.55-7.47 (m, 1H), 7.42-7.36 (m, 1H), 7.31-7.26 (m, 1H), 7.20 (t, $J = 7.8$ Hz, 1H), 6.76 (t, $J = 4.2$ Hz, 1H), 5.50 (d, $J = 5.3$ Hz, 1H), 3.48 (d, $J = 5.6$ Hz, 1H), 2.48-2.38 (m, 4H), 2.04-1.96 (m, 2H). ^{13}C NMR (101 MHz, CDCl_3) δ 200.4, 147.9, 144.3, 140.7, 130.7, 130.0, 129.6, 125.2, 122.7, 72.2, 38.6, 25.9, 22.6. ESI+ $m/z = 265.0051$ ($[\text{M}^{81}\text{Br} - \text{OH}]^+$, 100), 263.0070 ($[\text{M}^{79}\text{Br} - \text{OH}]^+$, 94).

2-((3-chlorophenyl)(hydroxy)methyl)cyclohex-2-en-1-one (5r). Crude product was purified by flash chromatography (4:1 cyclohexane:ethyl acetate) to give the product as a colourless oil (152 mg, 20%). Spectral data consistent is with literature values.¹⁵ ^1H NMR (400 MHz, CDCl_3) δ 7.37-7.34 (m, 1H), 7.30-7.21 (m, 3H), 6.75 (t, $J = 4.2$ Hz, 1H), 5.51 (d, $J = 5.6$ Hz, 1H), 3.46 (d, $J = 5.6$ Hz, 1H), 2.49-2.38 (m, 4H), 2.05-1.97 (m, 2H). ^{13}C NMR (101 MHz, CDCl_3) δ 200.5, 147.9, 143.9, 140.7, 134.5, 129.7, 127.8, 126.7, 124.8, 72.3, 38.7, 25.9, 22.6. ESI+ $m/z = 221.0549$ ($[\text{M}^{37}\text{Cl} - \text{OH}]^+$, 27), 219.0575 ($[\text{M}^{35}\text{Cl} - \text{OH}]^+$, 100).

4-(hydroxy(6-oxocyclohex-1-en-1-yl)methyl)benzaldehyde (5s). Crude product was purified by flash chromatography (3:1 cyclohexane:ethyl acetate) to give the product as a colourless oil (183 mg, 24%). ¹H NMR (400 MHz, CDCl₃) δ 9.96 (s, 1H), 7.82 (d, *J* = 8.0 Hz, 2H), 7.51 (d, *J* = 7.9 Hz, 2H), 6.80 (t, *J* = 4.2 Hz, 1H), 5.58 (d, *J* = 5.5 Hz, 1H), 3.67 (d, *J* = 5.6 Hz, 1H), 2.50-2.30 (m, 4H), 2.07-1.90 (m, 2H). ¹³C NMR (101 MHz, CDCl₃) δ 200.2, 192.1, 148.9, 147.9, 140.6, 135.7, 129.9, 127.0, 72.2, 38.5, 25.9, 22.5. ESI+ *m/z* = 213.0923 ([M -OH]⁺, 20), 185.0976 ([M -OH -CO]⁺, 100).

5-(hydroxy(6-oxocyclohex-1-en-1-yl)methyl)thiophene-2-carbaldehyde (5t). Crude product was purified by flash chromatography (2:1 cyclohexane:ethyl acetate) to give the product as a yellow solid (73 mg, 9%). ¹H NMR (400 MHz, CDCl₃) δ 9.84 (s, 1H), 7.63 (d, *J* = 3.8 Hz, 1H), 7.08 (dd, *J* = 3.8, 1.0 Hz, 1H), 6.99 (t, *J* = 4.2 Hz, 1H), 5.66 (m, 1H), 3.01 (br s, 1H), 2.54-2.40 (m, 4H), 2.13-1.96 (m, 2H). ¹³C NMR (101 MHz, CDCl₃) δ 200.3, 183.1, 158.1, 148.5, 142.9, 139.5, 136.7, 125.4, 70.5, 38.6, 25.9, 22.5. ESI+ *m/z* = 237.0596 ([M + H]⁺, 33), 219.0491 ([M -OH]⁺, 100), 191.0540 ([M -OH -CO]⁺, 21).

5-(hydroxy(6-oxocyclohex-1-en-1-yl)methyl)furan-2-carbaldehyde (5u). Crude product was purified by flash chromatography (2:1 cyclohexane:ethyl acetate) to give the product as a yellow solid (98 mg, 13%). ¹H NMR (400 MHz, CDCl₃) δ 9.55 (s, 1H), 7.20 (d, *J* = 3.6 Hz, 1H), 6.99 (t, *J* = 4.1 Hz, 1H), 6.53 (d, *J* = 3.6 Hz, 1H), 5.51 (s, 1H), 2.53-2.36 (m, 4H), 2.02 (app quint, *J* = 6.2 Hz, 2H). ¹³C NMR (101 MHz, CDCl₃) δ 200.2, 177.7, 161.8, 152.3, 149.4, 137.4, 122.9, 109.8, 68.2, 38.4, 25.9, 22.4. ESI+ *m/z* = 243.0642 ([M + Na]⁺, 78), 203.0716 ([M -OH]⁺, 100), 175.0765 ([M -OH -CO]⁺, 87).

4-(hydroxy(6-oxocyclohex-1-en-1-yl)methyl)thiophene-2-carbaldehyde (5v) and 5-(hydroxy(6-oxocyclohex-1-en-1-yl)methyl)thiophene-3-carbaldehyde (5w). Regioisomers **5v** and **5w** were produced in the same reaction and separated by flash chromatography (3:1 cyclohexane:ethyl acetate). The isomers were assigned based on the chemical shifts of closely related regioisomeric structures.⁴⁷⁻⁴⁸ **5v** was obtained as a yellow oil (10 mg, 2%). ¹H NMR (400 MHz, CDCl₃) δ 9.88 (d, *J* = 1.2 Hz, 1H), 7.69 (d, *J* = 1.5 Hz, 1H), 7.64 (m, 1H), 6.86 (t, *J* = 4.2 Hz, 1H), 5.57 (s, 1H), 2.54-2.39 (m, 4H), 2.09-1.96 (m, 2H). ¹³C NMR (101 MHz, CDCl₃) δ 200.49, 183.12, 147.70, 145.20, 144.2, 140.23, 135.10, 131.11, 69.70, 38.65, 25.89, 22.59. ESI+ *m/z* = 219.0490 ([M -OH]⁺, 100). **5w** was obtained as a yellow oil (23 mg, 3%). ¹H NMR (400 MHz, CDCl₃) δ 9.81 (s, 1H), 8.02 (d, *J* = 1.3 Hz, 1H), 7.28-7.24 (m, 1H), 6.96 (t, *J* = 4.0 Hz, 1H), 5.63 (br s, 1H), 2.54-2.38 (m, 4H), 2.08-1.99 (m, 2H). ¹³C NMR (101 MHz, CDCl₃) δ 200.5, 185.3, 149.7, 148.4, 142.8, 139.4, 136.9, 121.4, 70.2, 38.6, 25.9, 22.5. ESI+ *m/z* = 219.0491 ([M -OH]⁺, 100), 191.0540 ([M -OH -CO]⁺, 15).

Synthesis of 3-(hydroxy(4-nitrophenyl)methyl)-5,6-dihydro-2H-pyran-2-one (5b).

4-Nitrobenzaldehyde (151 mg, 1.0 mmol, 1.0 equiv) and 5,6-dihydro-pyran-2-one (0.1 mL, 1.1 mmol, 1.1 equiv) were stirred under nitrogen in dichloromethane (4.0 mL) and cooled to 0 °C. A solution of diethylaluminium iodide (0.9 M solution in toluene, 1.3 mL, 1.2 mmol, 1.2 equiv) was added dropwise and the resulting brown mixture was stirred for 24h at room temperature. The reaction was quenched with saturated NaHCO₃ (2.0 mL). The dichloromethane layer was separated and the aqueous layer was extracted with dichloromethane (3 x 10 mL). The combined organic layers were dried over MgSO₄, filtered and the solvent was removed *in vacuo*. The crude product was purified by flash column chromatography (1:1 cyclohexane:ethyl acetate) to give the product as an orange solid (23

mg, 9%). Spectral data is consistent with literature values.²⁵ ¹H NMR (400 MHz, CDCl₃) δ 8.27-8.15 (m, 2H), 7.64-7.54 (m, 2H), 6.77 (t, *J* = 4.3 Hz, 1H), 5.66 (d, *J* = 4.9 Hz, 1H), 4.44-4.33 (m, 2H), 3.63 (d, *J* = 5.5 Hz, 1H), 2.62-2.47 (m, 2H). ¹³C NMR (101 MHz, CDCl₃) δ 164.5, 148.3, 147.6, 141.8, 134.2, 127.5, 123.8, 71.8, 66.5, 24.3. ESI- *m/z* = 248.0613 ([M -H]⁻, 100).

Synthesis of 3-(hydroxy(4-nitrophenyl)methyl)but-3-en-2-one (5d).

4-Nitrobenzaldehyde (604mg, 4.0 mmol, 1.0 equiv), DABCO (291 mg, 2.6 mmol, 0.65 equiv), but-3-en-2-one (433 μL, 5.2 mmol, 1.3 equiv) were added to dichloromethane (8 mL) and stirred for 20h at room temperature. The reaction mixture was diluted in dichloromethane (50 mL) and washed with 10% HCl (2 x 30 mL). The organic layer was dried over MgSO₄, filtered and the solvent was removed *in vacuo*. The crude product was purified by flash column chromatography (2:1 cyclohexane:ethyl acetate) to give the product as a white solid (133mg, 15%). Spectral data is consistent with literature values.⁴⁹ ¹H NMR (400 MHz, CDCl₃) δ 8.22 – 8.18 (m, 2H), 7.57 – 7.53 (m, 2H), 6.26 (d, *J* = 1.1 Hz, 1H), 6.03 (d, *J* = 1.1 Hz, 1H), 5.68 (s, 1H), 2.36 (s, 3H). ¹³C NMR (101 MHz, CDCl₃) δ 200.2, 149.1, 149.0, 147.5, 127.9, 127.4, 123.8, 72.5, 26.5. ESI+ *m/z* = 220.0714 ([M -H]⁻, 100), 204.07552 (25).

Preparative biotransformation for the synthesis of 3-(2,2-dimethyl-4-oxo-3α,6α-dihydro-4H-cyclopenta[δ][1,3]dioxol-5-yl)-3-hydroxyindolin-2-one (5o).

A preparative scale biotransformation (10 mL) was performed using (3αS,6αS)-2,2-dimethyl-3α,6α-dihydro-4H-cyclopenta[δ][1,3]dioxol-4-one (50 mM), isatin (10 mM), His-tag purified BH32.8 (60 μM) in PBS (pH 7.0, 8 mL) with DMSO (2 mL) as a cosolvent. The reaction was incubated at 30 °C with shaking at 180 r.p.m. for 1.5 hours. The reaction mixture was extracted with ethyl acetate (2 x 15 mL), dried over MgSO₄, filtered and the solvent removed *in vacuo*. The crude product was purified by flash chromatography (2:1 cyclohexane:ethyl acetate) to give two diastereomeric products. Stereoisomer 1 eluted first as a yellow oil (10 mg, 33%). ¹H NMR (400 MHz, MeOD) δ 7.86 (d, *J* = 2.5 Hz, 1H), 7.25 (t, *J* = 7.8 Hz, 1H), 7.12 (d, *J* = 7.4 Hz, 1H), 6.96 (t, *J* = 7.5 Hz, 1H), 6.91 (d, *J* = 7.8 Hz, 1H), 5.31 (dd, *J* = 5.5, 2.5 Hz, 1H), 4.44 (d, *J* = 5.5 Hz, 1H), 1.37 (s, 3H), 1.34 (s, 3H). ¹³C NMR (101 MHz, MeOD) δ 202.2, 178.6, 156.9, 147.6, 143.9, 131.2, 131.0, 125.4, 123.6, 116.2, 111.4, 79.4, 78.2, 75.5, 28.2, 27.0. ESI+ *m/z* = 324.0842 ([M +Na]⁺, 100). Stereoisomer 2 eluted second as a yellow oil (3 mg, 10%). ¹H NMR (400 MHz, MeOD) δ 7.86 (d, *J* = 2.4 Hz, 1H), 7.27 (t, *J* = 7.7 Hz, 1H), 7.10 (d, *J* = 7.4 Hz, 1H), 6.98 (t, *J* = 7.5 Hz, 1H), 6.92 (d, *J* = 7.7 Hz, 1H), 5.32 (dd, *J* = 5.4, 2.5 Hz, 1H), 4.47 (d, *J* = 5.4 Hz, 1H), 1.36 (s, 3H), 1.30 (s, 3H). ¹³C NMR (101 MHz, MeOD) δ 201.3, 179.1, 156.7, 147.3, 143.8, 131.3, 130.9, 125.2, 123.6, 116.2, 111.6, 79.3, 78.3, 75.4, 28.3, 26.7. ESI+ *m/z* = 324.0844 ([M +Na]⁺, 100).

Crystallization, refinement and model building.

Crystals of BH32.6, BH32.7 and BH32.12 variants were prepared by mixing 200 nL of 20 mg mL⁻¹ protein in PBS buffer pH 7.4 with equal volumes of precipitant. All trials were conducted by sitting-drop vapour diffusion and incubated at 4 °C. Protein crystallization conditions are given in Table S8. BH32.6 and BH32.7 crystals were flash cooled in liquid nitrogen whilst BH32.12 crystals were first cryoprotected by the addition of 10 % PEG 200 to the mother liquor prior to flash cooling. Data were

collected from single crystals at Diamond Light Source and subsequently scaled and reduced with Xia2.⁵⁰ Preliminary phasing was performed by molecular replacement in Phaser using a search model derived from wild-type BH32 (PDB code: 3U26). Iterative cycles of rebuilding and refinement were performed in COOT⁵¹ and Phenix.refine,⁵² respectively. Structure validation with MolProbity and PDBREDO were integrated into the iterative rebuild and refinement process. Complete data collection and refinement statistics can be found in Table S7. Coordinates and structure factors have been deposited in the Protein Data Bank under accession numbers 6Z1K, 7O1D & 6Z1L. All figures and surface representations were generated in ICM Pro (Molsoft).

Molecular Docking.

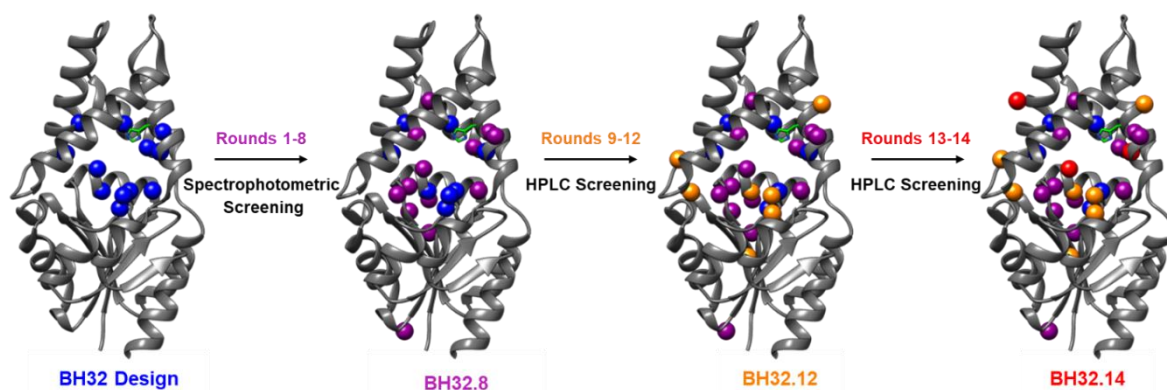
To generate starting structures for DFT modelling, molecular docking was performed with Autodock Vina,⁵³ using AutoDockTools⁵⁴ to assign hydrogen atoms to the crystal structure and generate input files. The protein was kept rigid during docking but all relevant substrate bonds were rotatable. For the product, the highest-scoring pose was selected. For the reactant state, 2-cyclohexen-1-one was docked first and the pose which showed the best overlap with the corresponding fragment of the docked product was selected (this had an estimated binding energy only 0.2 kcal mol⁻¹ higher than the lowest energy pose, which was very similar but rotated around the keto group). The aldehyde was then docked into the 2-cyclohexen-1-one bound structure, and again the binding mode with the best overlap to the corresponding fragment in the docked product was selected (this had an estimated binding energy of 0.8 kcal mol⁻¹ higher than the lowest binding mode).

DFT Modelling.

A cluster model was constructed using the docked conformations for the substrates, including the first-shell amino acids around the substrates (Trp10, Ile14, Ala19, Val22, His23, Ile26, Leu64, Trp88, Ser91, Leu92, Ala95, Arg124, Phe128, Ser129, Phe132). Residues were truncated at the C_β unless their backbone atoms are in near contact with the substrates or involved in hydrogen bonding with the substrates or other amino acids in the cluster model. A water molecule was included in the calculation to facilitate the third chemical step (**Int2** to **Int3**). The models contained a total of 273 atoms as shown in Figure S8. For DFT modelling of the inhibitor **4**-enzyme complex, the energy minimised product state was modified to remove the water molecule and to introduce the acetoxy group present in inhibitor **4**, followed by energy minimization. The coordinates for all energy minimized ground and transition state structures are provided as supplementary files. Calculations were performed using Gaussian16 revision A03,⁵⁵ using the B3LYP functional⁵⁶ and the 6-31G(d,p) basis sets^{57,58} for all atoms except for the Arg124 guanidino nitrogens and the C=O groups of 2-cyclohexen-1-one and aldehyde, for which 6-311+G(d,p) was used. Grimme's D3 dispersion correction with Becke-Johnson damping was employed⁵⁹ and implicit solvation was treated using the polarizable conductor calculation model (CPCM)^{60,61} with a dielectric constant $\epsilon = 5.7$ to mimic the enzyme environment.^{62,63} For comparison, single-point energy calculations were then performed with $\epsilon = 80$. All models have a net charge of +1 (from Arg124) and spin multiplicity 1. Sixteen peripheral atoms were kept fixed during the calculations: the C_α of residues whose backbone was included, and C_β for residues truncated at C_β (atom numbers 16, 26, 31, 36, 43, 52, 54, 57, 60, 71, 77, 85, 89, 97, 104, 245). Each chemical step was modelled by performing a relaxed potential energy scan of the

making/breaking bond for steps 1, 2 and 4. For step 3 (the proton transfer) a simple reaction coordinate, $z = R(\text{C-H}) - R(\text{O-H})$ was scanned where R is distance, C and H are the carbon and hydrogen atoms of the breaking bond and O is the oxygen atom of the water molecule. In each case, the transition state was selected as the structure with the highest potential energy along the scanned coordinate, to within $\pm 0.03 \text{ \AA}$ along the breaking/forming bond or z .

8.5.2 Supplementary Figures S1-S13



Round	Description	Clones Screened	Beneficial mutations	Best Variant ^[1]
1	Random mutagenesis of the entire gene	1800	T49A, A52V, F87L, Q96R, M120L, K167I, V226G	BH32.1 = <i>BH32</i> ^[2] + T49A
2	Saturation mutagenesis of 'hotspots': Y45/T49 and F87/F88 (two sites simultaneously randomized), T49, R50	1980	T49A, T49M, F87L, F87T	BH32.2 = <i>BH32</i> + T49A_F87L
3	Random mutagenesis of the entire gene	1800	N14Y, M130K, E174G	BH32.3 = <i>BH32.2</i> + N14Y
4	Saturation mutagenesis of 'hotspots': N14, M130, E174	270	N14I, M130T, E174G	BH32.4 = <i>BH32.2</i> + N14I_M130T
5	Saturation mutagenesis of active site positions and flexible loop regions: L10, A19, P38, L42, Y45, E46, P60, P63, F81, S91, Q96, S124, D125, Q128, M130, L133, F154, K167, E174, K202	1800	P63C, S124R, D125Q, Q128P, E174K	BH32.5 = <i>BH32.4</i> + S124R_Q128P_E174K
6	Saturation mutagenesis of active site positions and flexible loop regions: V16, E17, G32, Y34, L36, Y61, L64, L68, M120, T122, D123, D125, T126, Q128, E149, G152, L199, E204, K205, E207	1800	D123N, P128L, E204G	BH32.6 = <i>BH32.5</i> + D123N
7	Saturation mutagenesis of positions: S22/S95 and M120/T122 (two sites simultaneously randomized)	2700	S22V_S95A, M120V_T122L	BH32.7 = <i>BH32.6</i> + S22V_S95A_M120V_T122L
8	Saturation mutagenesis of active site positions and flexible loop regions: L10, A20, L24, M27, L42, T45, P63, L64, S91, L92, Q96, D125, E127, A129, I145, T147	1440	A20Y, A129G	BH32.8 = <i>BH32.7</i> + A20Y
9	Saturation mutagenesis of active site positions and flexible loop regions: L10, L24, L42, E46, A129	450	L10W, L24F, L42V, A129S	BH32.9 = <i>BH32.8</i> + L10W_L24F_A129S
10	Random mutagenesis of the entire gene	1800	F154S	BH32.11 = <i>BH32.9</i> + F154S
11	Saturation mutagenesis of F154	90	F154S	BH32.11 = <i>BH32.9</i> + F154S
12	Saturation mutagenesis of active site positions and flexible loop regions: Y20, V30, K47, Y56, I67, E70, F87, S91, R97, F153, K155, F161, L165, K171, V176, Y177, D180, S196, D210, L219, I223	1890	K47E, Y56N, Y177C, D180P, D210G,	BH32.12 = <i>BH32.11</i> + Y56N_Y177C_D180P
13	Random mutagenesis of the entire gene	1800	V16A, A19T, E70R, P128L, S154A	BH32.13 = <i>BH32.12</i> + A19T
14	Saturation mutagenesis of 'hotspots': V16, A19, E70, M72, E89, P128, S154	630	V16P/G, A19T, E70R, P128L/M, S154G/A	BH32.14 = <i>BH32.12</i> + A19T_E70R_P128L

^[1] The gene sequence used as the template for each round of evolution is shown in italics.

^[2] BH32 = haloacid dehalogenase from *Pyrococcus horikoshii* + F9S, V10L, L14N, E19A, T22S, I64L, E68L H91S, H95S, Y128Q, L129A, H132F mutations

Figure S1: Directed evolution of BH32.14. Structures showing the amino acid positions mutated throughout evolution (represented as spheres). The original design contains twelve active site mutations (shown in blue) built into the cap domain of a haloacid dehalogenase from *Pyrococcus horikoshii*.²¹ Fifteen mutations (shown in purple) were introduced during the first eight rounds of evolution, which exploited a spectrophotometric assay. Rounds 9-14 exploited a HPLC assay and led to the accumulation of a further nine mutations (mutations from round 9-12 are shown in orange, and from rounds 13-14 in red). The final variant BH32.14 contains 29 mutations, 5 that remain from the initial computational design and 24 that were installed during evolution. The table describes the method of library generation used, the number of clones evaluated and the sequence of the most improved variant for each round.

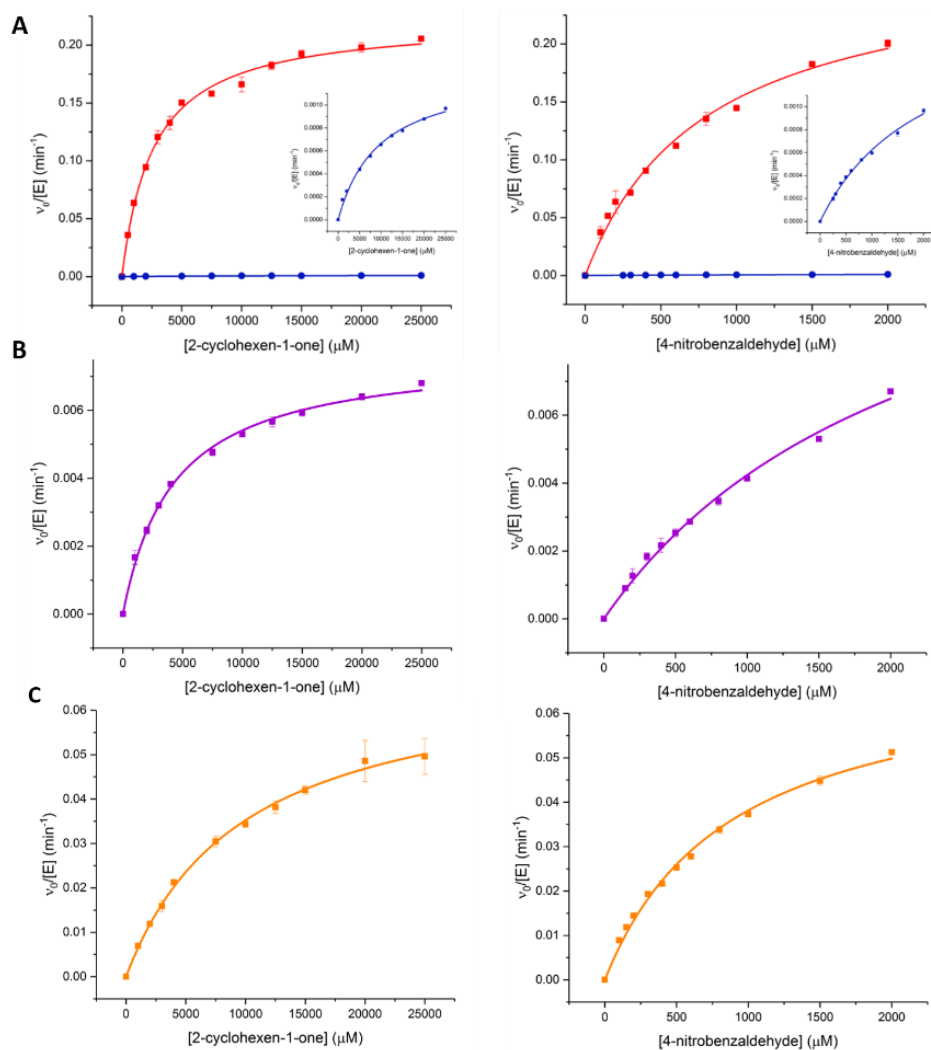


Figure S2: Kinetic characterization of BH32, BH32.8, BH32.12 and BH32.14. Michaelis-Menten plots for the MBH reaction with **1** and **2** catalysed by **A**) BH32 (blue) and BH32.14 (red) **B**) BH32.8 and **C**) BH32.12. Kinetic assays were performed at either a fixed concentration of **1** (25 mM) and various concentrations of **2**, or using a fixed concentration of **2** (2 mM) and various concentrations of **1**. The plots show the averaged initial rates which were fitted to the Michaelis–Menten equation using Origin software. Data are mean \pm s.d. of measurements made in triplicate

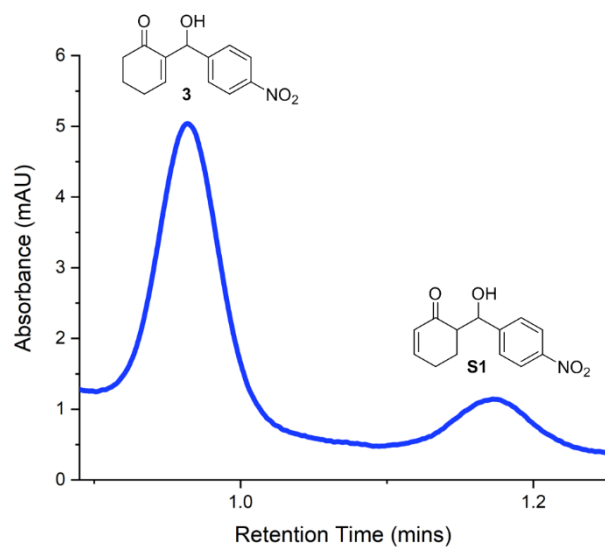


Figure S3: HPLC analysis of the BH32 catalysed MBH reaction. HPLC trace showing product **3** and aldol by-product **S1** (5:1 ratio of **3**:**S1**), formed during the BH32 (3 mol%) catalysed reaction of **1** (3 mM) and **2** (0.6 mM) following 22 hours incubation.

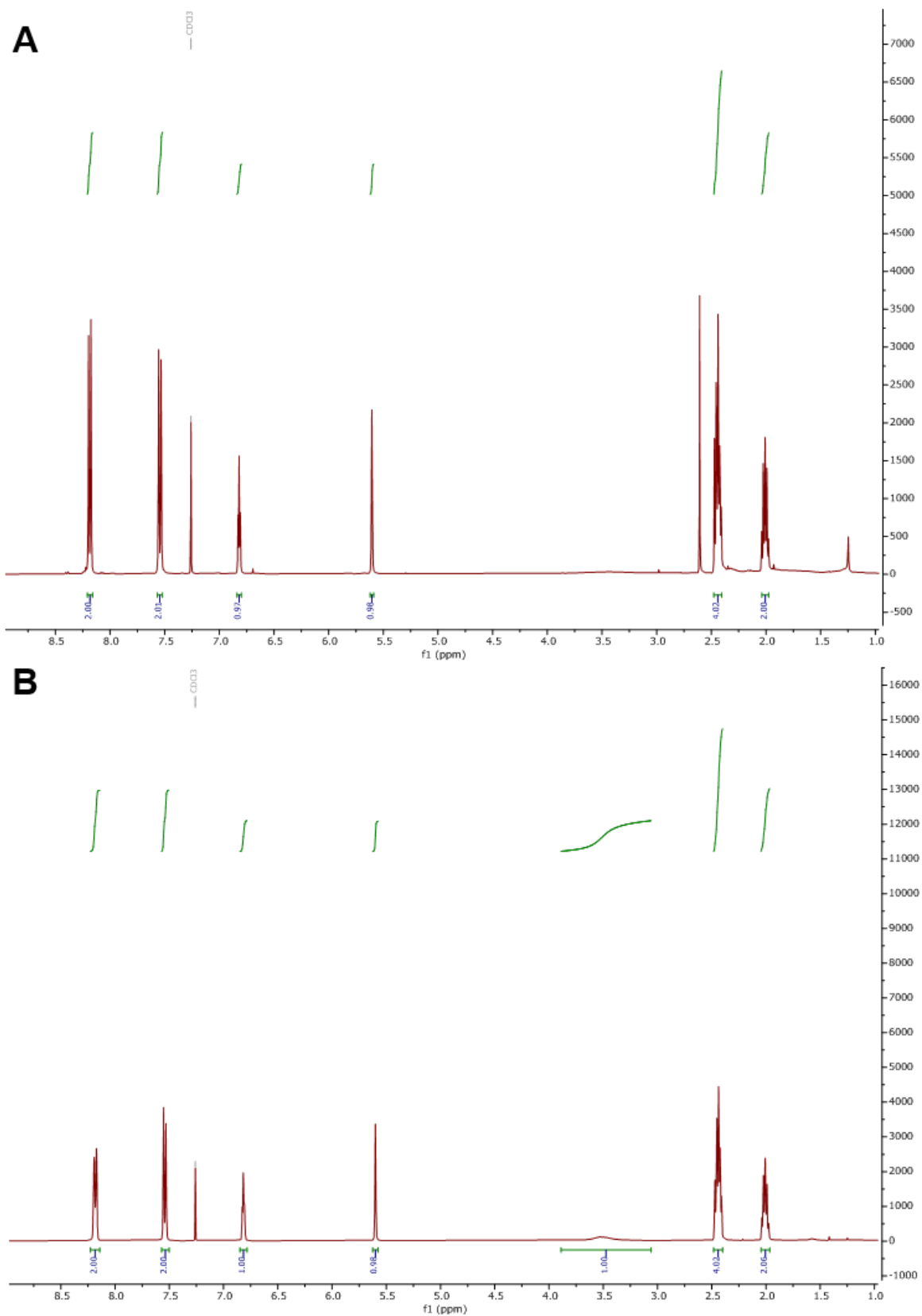


Figure S4: Characterization of product 3 produced from a preparative scale biotransformation. NMR traces (400 MHz; CDCl₃) showing **A**) crude product extracted from the BH32.14 (50 μM) catalysed MBH reaction of **1** (50 mM) and **2** (10 mM) in PBS (pH 7.4) with 20% DMSO as a cosolvent and **B**) product isolated following purification by flash column chromatography.

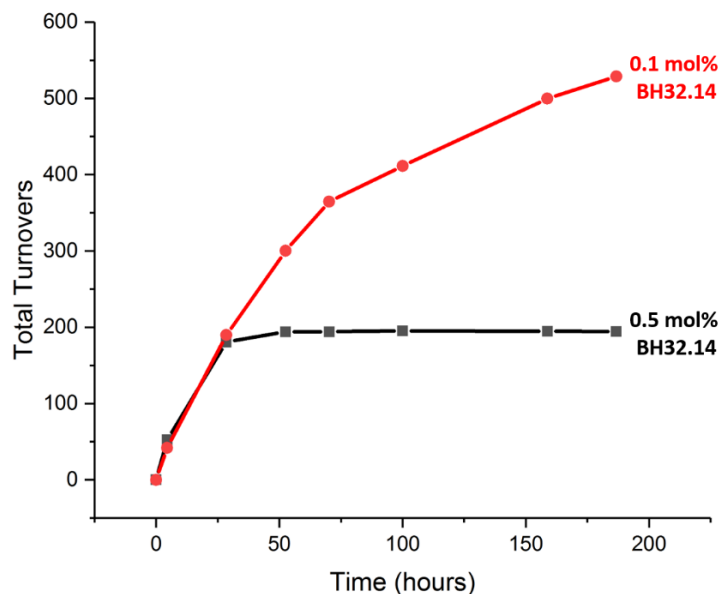


Figure S5: Total turnover numbers achieved by BH32.14. Time-course for the conversion of **1** (50 mM) and **2** (10 mM) in PBS (pH 7.4) with 20 % DMSO cosolvent using 0.5 mol% (black) and 0.1 mol% (red) of BH32.14 as a biocatalyst.

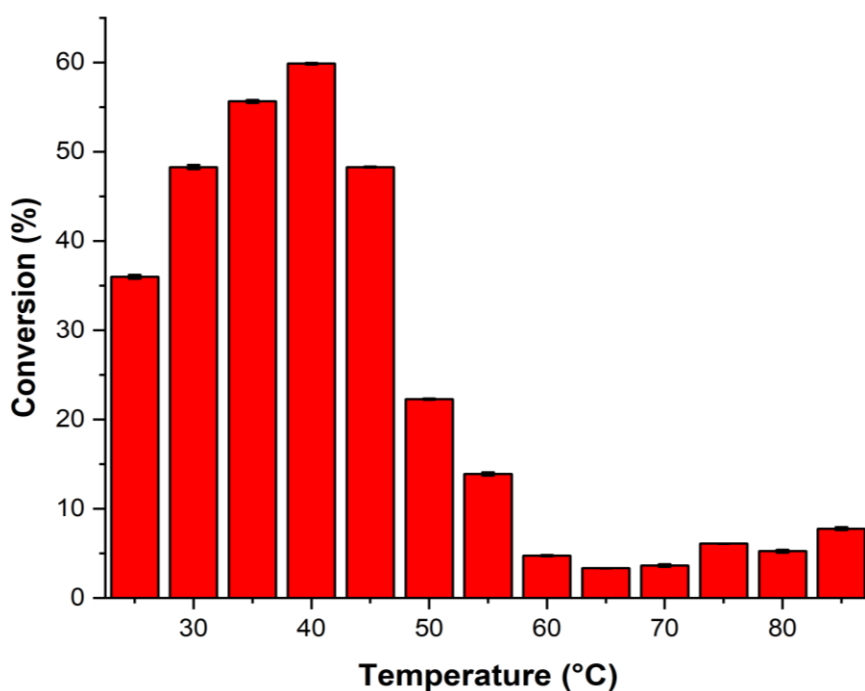


Figure S6: Activity of BH32.14 at varying temperatures. Reaction conversions of BH32.14 mediated biotransformations at temperatures ranging from 25 °C to 85 °C. Biotransformations performed using **1** (50mM), **2** (10mM) and BH32.14 (50 μM) in PBS (pH 7.4) with 20% DMSO as a cosolvent, for 4 hours. The error bars represent the standard deviation of measurements made in triplicate.

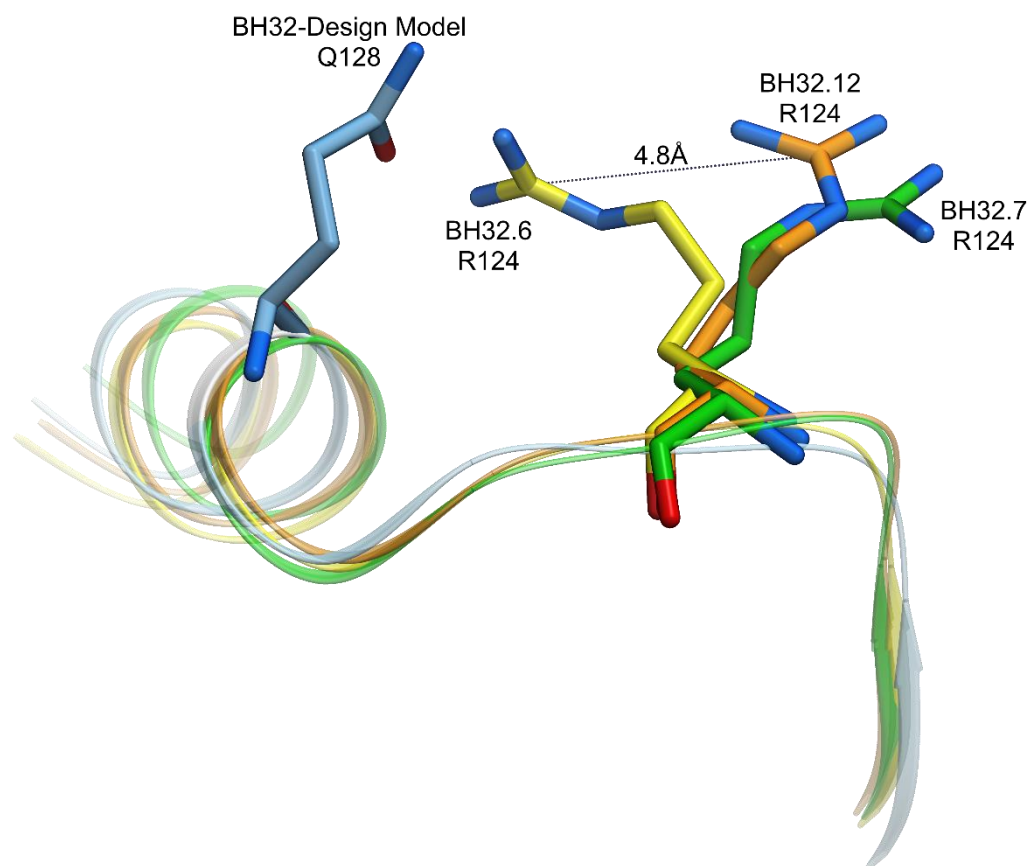


Figure S7: Structural characterization of residues responsible for oxyanion intermediate stabilization in BH32, BH32.6, BH32.7 and BH32.12. Four superimposed structures are displayed, the BH32 design model in blue, BH32.6 in yellow, BH32.7 in green and BH32.12 in orange. Backbone atoms are displayed in cartoon ribbon representation whilst residues are shown as all atom coloured stick models. The catalytic Arg124 in BH32.6 adopts an orientation that places the guanidinium motif in close proximity to the amide side chain of Gln128 designed to interact with the oxyanion of *Int1*. During the evolution process, Arg124 reorientates to adopt a pose ideal to support charge transfer during catalysis (BH32.12 orange).

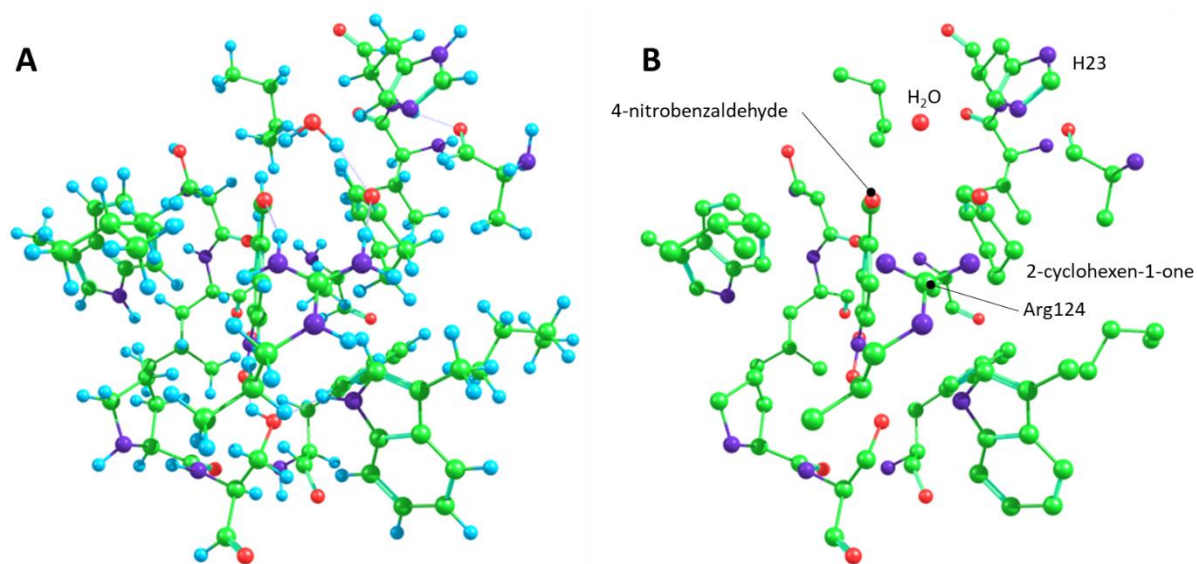


Figure S8. Cluster model used for DFT modelling. Models are shown with **(A)** and without **(B)** hydrogen atoms.

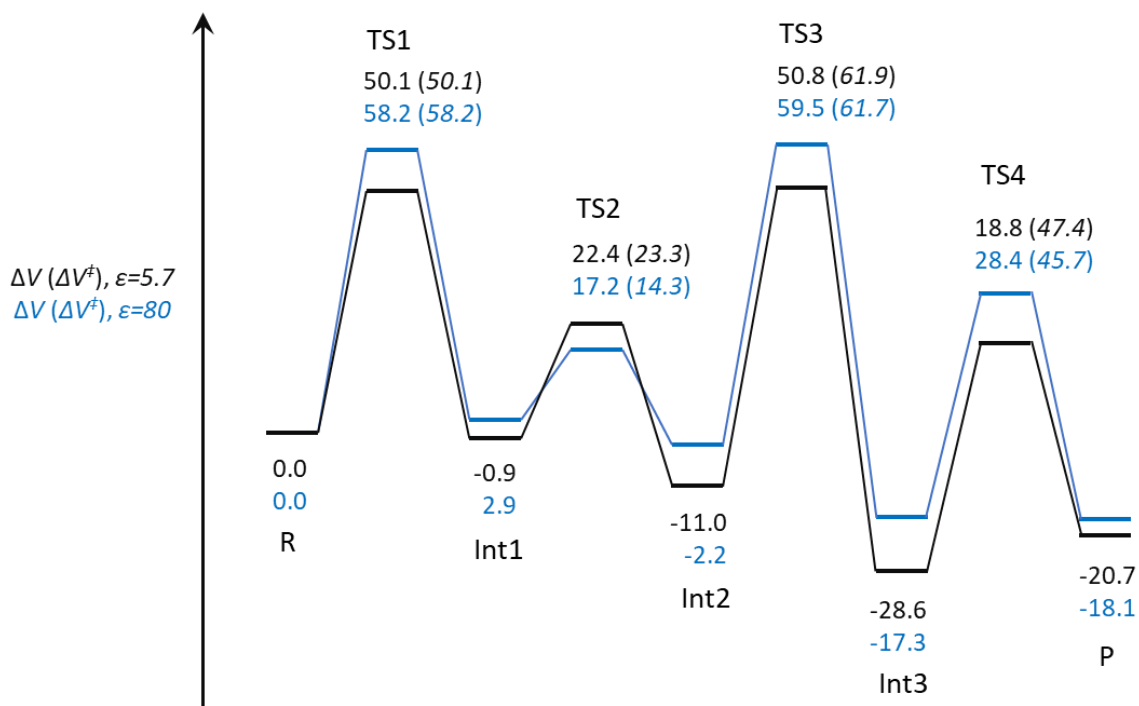


Figure S9: Computed reaction profile for the complete MBH mechanism. The potential energy relative to the reactant (ΔV in kJ mol^{-1}) is shown for each state, and the barrier energy (ΔV^\ddagger in kJ mol^{-1}) for each transition state is shown in parentheses. Geometry optimization was performed using a dielectric, $\epsilon = 5.7$ (black). Single point calculations using $\epsilon = 80$ (blue) show only modest changes in energy of each species, with no change in rate limiting step.

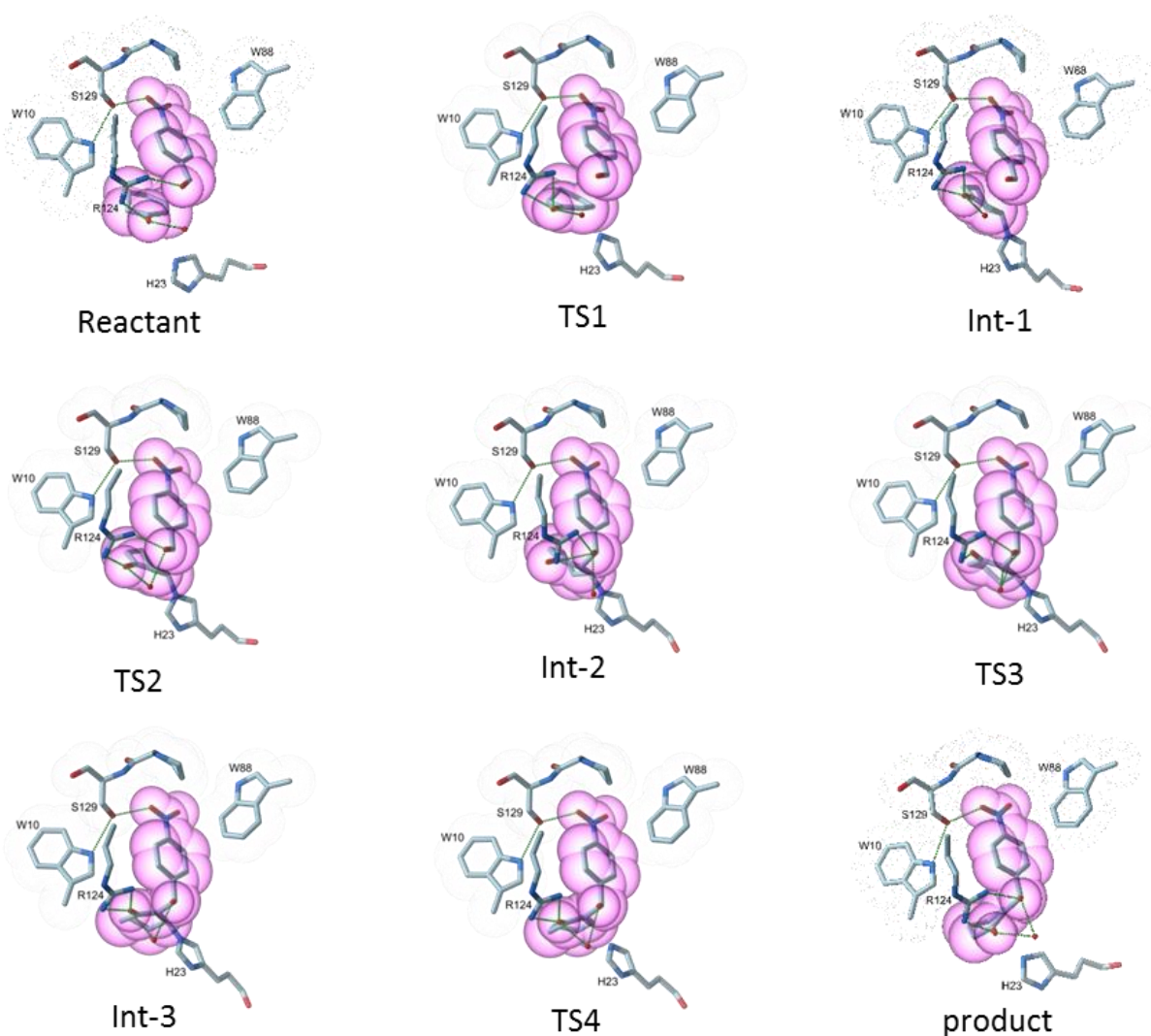


Figure S10: DFT states showing reactants, transition states and intermediates formed along the reaction coordinate. Stick representations of the complete DFT progression from reactant through to products are presented in all atom colours. For clarity a subset of atoms that form close packing interactions with the substrates are shown along with atoms derived from the His23 nucleophile and catalytic Arg124. Atoms derived from residues that provide close packing contacts (Trp10, Trp88 & Ser129) are shown with additional dot surfaces (blue) whilst substrate derived heavy atoms are shown with semi-transparent CPK spheres (magenta). Hydrogen bonds are shown as green dashed lines.

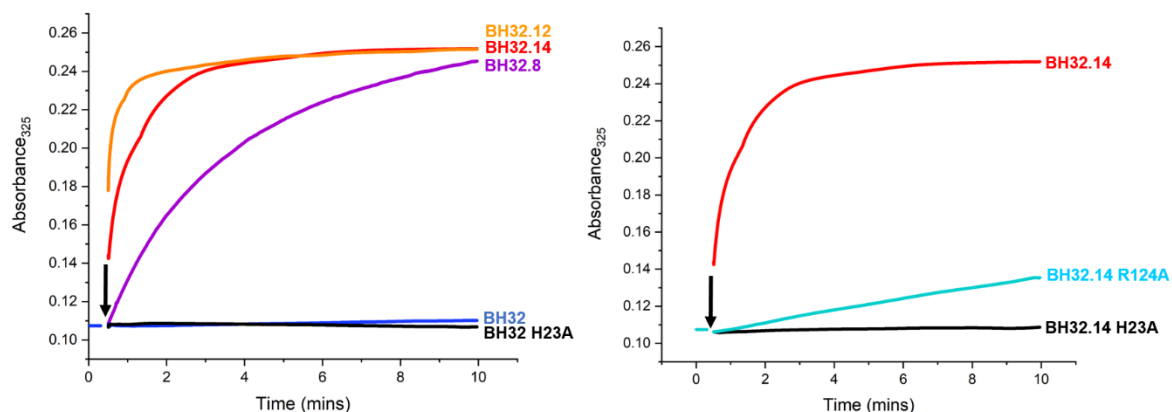


Figure S11: Time course for the inhibition of BH32 and variants. Formation of the covalently modified protein was monitored spectrophotometrically at 325 nm. **A)** Comparison of BH32, BH32 H23A, BH32.8, BH32.12 and BH32.14; **B)** Comparison of BH32.14, BH32.14 R124A and BH32.14 H23A. Reactions were performed using enzyme (10 μ M) and inhibitor **4** (25 μ M) in PBS pH 7.4 with 3% (v/v) acetonitrile at room temperature.

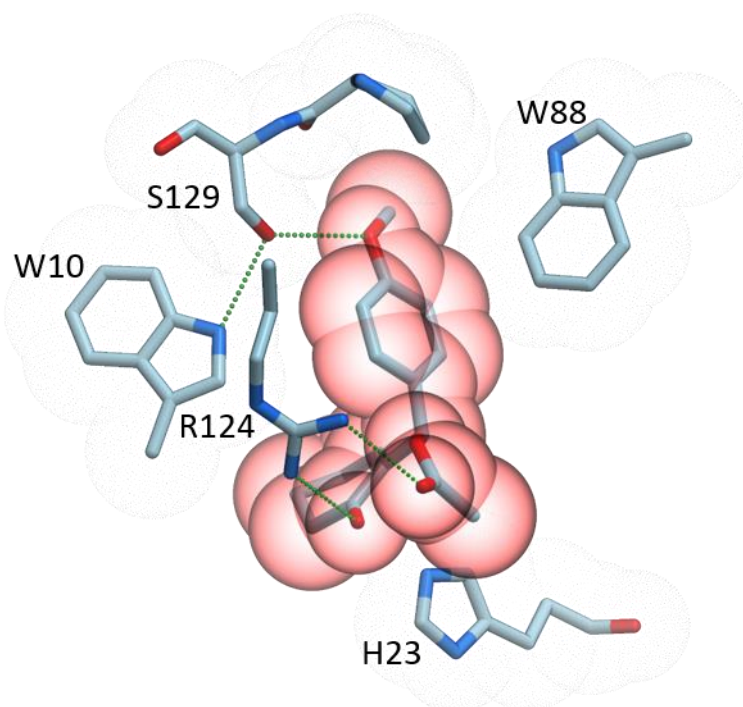


Figure S12: DFT state showing inhibitor **4 bound in the active site of an engineered MBHase.** The DFT model is shown in all atom coloured stick representation. For clarity, only a subset of atoms that form close packing interactions with the inhibitor are shown along with atoms derived from the His23 nucleophile and catalytic Arg124. Atoms derived from residues that provide close packing contacts (Trp10, Trp88 & Ser129) are shown with additional dot surfaces (blue) whilst inhibitor derived heavy atoms are shown with semi-transparent CPK spheres (red). Hydrogen bonds are shown as green dashed lines.

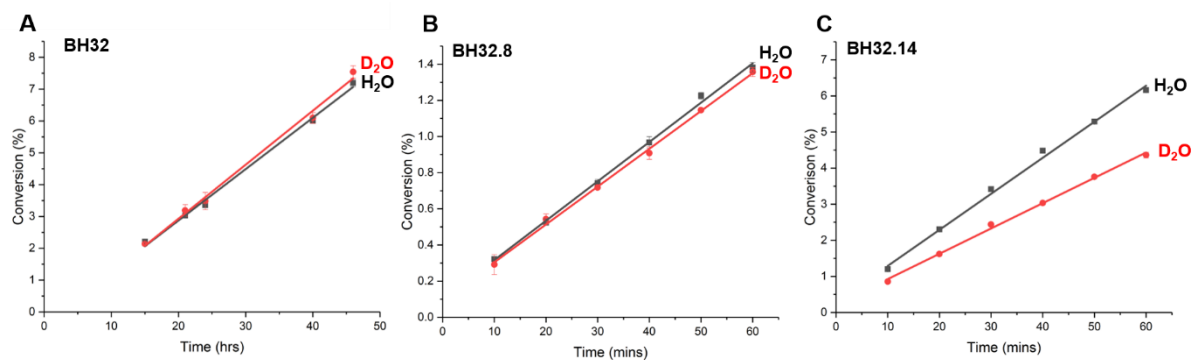


Figure S13: Solvent kinetic isotope effects. Biotransformations were performed using **1** (25 mM), **2** (2 mM) and the relevant biocatalyst (50 μ M BH32, 30 μ M BH32.8, 10 μ M BH32.14) in PBS (pH/pD 7.4) with 3% acetonitrile as a cosolvent. Linear fits of reaction conversion vs time are shown in black (H₂O) and red (D₂O). Error bars represent the standard deviation of measurements made in triplicate.

3. Supplementary Tables S1-S9

Table S1: Experimental and calculated masses of apo and inhibited enzymes. Mass spectrometry data for BH32 and variants. Enzymes were inhibited with mechanistic inhibitor **4**.

Variant	Observed Mass	Expected Mass
BH32	27788	27788
BH32 inhibited (60 minutes incubation)	28003 (80% single modification)	28002
BH32 H23A	27721	27722
BH32 H23A inhibited (60 minutes incubation)	27721 (no modification)	27722
BH32.8*	27580	27579
BH32.8* inhibited (15 minutes incubation)	27793 (95% single modification)	27795
BH32.14	27806	27806
BH32.14 H23A	27740	27739
BH32.14 W10A	27691	27690
BH32.14 R124A	27721	27720

*Variants highlighted contain a C-terminal His-tag. All other proteins contain a strep-tag

Table S2: Conversion and enantiomeric excess achieved by selected variants along the evolutionary trajectory. Biotransformations were performed using **1** (3 mM), **2** (0.6 mM) and enzyme (18 μ M) in PBS (pH 7.4) with 3% MeCN as a cosolvent. To ensure that errors don't arise from determining low conversions achieved by BH32 after 4.5 hours, reactions were monitored over longer timeframes and were shown to be linear throughout this period. All variants preferentially produced the (*R*)-enantiomer. The error bars represent the standard deviation of measurements made in triplicate.

Variant	Time (hours)	Conversion (%)	Relative Conversion	ee
BH32	4.5	0.08 \pm 0.01	0.14 \pm 0.01	-
BH32	22	0.39 \pm 0.01	0.68 \pm 0.02	20 \pm 0.9
BH32	31	0.54 \pm 0.02	0.94 \pm 0.03	-
BH32.4	4.5	0.22 \pm 0.01	0.38 \pm 0.02	23 \pm 0.6
BH32.6	4.5	0.71 \pm 0.02	1.23 \pm 0.03	9 \pm 0.7
BH32.8	4.5	1.56 \pm 0.04	2.71 \pm 0.07	33 \pm 0.5
BH32.9	4.5	3.40 \pm 0.07	5.92 \pm 0.12	67 \pm 0.4
BH32.11	4.5	9.74 \pm 0.11	16.94 \pm 0.20	82 \pm 0.6
BH32.12	4.5	20.30 \pm 0.21	35.33 \pm 0.36	86 \pm 0.8
BH32.14	4.5	57.54 \pm 0.85	100 \pm 1.48	93 \pm 0.9

Table S3: Kinetic characterization of BH32, BH32.8, BH32.12 and BH32.14. Kinetic constants derived from global fitting of the combined V_0 vs [1] and V_0 vs [2] steady state kinetic data (Figure S2) using ordered and/or random order binding models. Fitting did not allow reliable determination of K_{SA} and it was not possible to determine the order of binding. The contribution of K_{SA} on the apparent k_{cat} and K_m values in the ordered binding equation (Eq. 2) was examined by varying $K_{SA}K_{mB}$ over a range of $0.1 \times K_{mA}K_{mB}$ to $10 \times K_{mA}K_{mB}$. The goodness of fit was not significantly different using ordered or random order binding equations across this range of values. While the apparent K_m are sensitive to the value of K_{SA} , the k_{cat} values vary by only ~25% for BH32 and 7% for BH32.14

BH32

Model	k_{cat} (hr ⁻¹)	K_{mA} (μM)	K_{mB} (μM)	$K_{SA}K_{mB}$
Random	0.134 ± 0.012	7998 ± 987	1767 ± 249	-
Ordered	0.170 ± 0.023	16744 ± 3057	2766 ± 517	$0.1 \times K_{mA}K_{mB}$
Ordered	0.134 ± 0.012	7998 ± 987	1767 ± 249	$K_{mA} \times K_{mB}$
Ordered	0.110 ± 0.008	1929 ± 293	1074 ± 178	$10 \times K_{mA}K_{mB}$

BH32.8

Model	k_{cat} (min ⁻¹)	K_{mA} (μM)	K_{mB} (μM)	$K_{SA}K_{mB}$
Random	0.0168 ± 0.001	4173 ± 254	2381 ± 224	-

BH32.12

Model	k_{cat} (min ⁻¹)	K_{mA} (μM)	K_{mB} (μM)	$K_{SA}K_{mB}$
Random	0.100 ± 0.004	9719 ± 640	893 ± 53	-

BH32.14

Model	k_{cat} (min ⁻¹)	K_{mA} (μM)	K_{mB} (μM)	$K_{SA}K_{mB}$
Random	0.349 ± 0.034	2556 ± 444	1137 ± 226	-
Ordered	0.368 ± 0.041	4134 ± 851	1304 ± 280	$0.1 \times K_{mA}K_{mB}$
Ordered	0.349 ± 0.034	2556 ± 444	1137 ± 226	$K_{mA} \times K_{mB}$
Ordered	0.325 ± 0.029	697 ± 128	914 ± 193	$10 \times K_{mA}K_{mB}$

A = 2-cyclohexen-1-one, B = 4-nitrobenzaldehyde

Table S4: Effect of cosolvent on BH32.14 activity. MBH reactions were performed using **1** (50mM), **2** (10mM) and BH32.14 (0.5 mol%) in PBS buffer (pH 7.4) with the stated concentration of MeCN or DMSO as a cosolvent. The percentage conversion was determined after 5 hours by HPLC analysis.

Cosolvent	Conversion (%)
20 % MeCN	2
30 % MeCN	0.3
40 % MeCN	0
20 % DMSO	50
30 % DMSO	43
40 % DMSO	16

Table S5: Reaction conditions for the synthesis of 3 & 5a-w. All reactions were performed using PBS buffer pH 7.4 and 20% DMSO

Product	Enone Conc. (mM) ^[1]	Enzyme	Catalyst loading (mol%)	Reaction time (h)	Mean % Conv. (\pm s.d.)	Wavelength (nm)	extinction coefficient (mM ⁻¹ cm ⁻¹)	
							aldehyde	product
3	50	BH32.14	0.5	18	94 \pm 0.2	280	600	600
5a	50	BH32.14	1.5	18	97 \pm 0.2	220	240	700
5b	50	BH32.14	2.5	48	82 \pm 0.3	220	240	480
5c	50	BH32.14	2.5	1.5	97 \pm 0.1	220	240	400
5d	100	BH32.14	5	48	70 \pm 0.5	220	240	589
5e	100	BH32.14	2.5	18	67 \pm 0.3	220	130	740
5f	50	BH32.14	2.5	48	56 \pm 0.9	220	105	800
5g	50	BH32.14	1.5	18	92 \pm 0.2	254	1000	310
5h	50	BH32.14	5	48	33 \pm 0.4	254	65	190
5i	100	BH32.14	5	48	58 \pm 0.4	220	213	629
5j	50	BH32.14	5	48	1.2 \pm 0.003	220	583	639
5k	50	BH32.14	1.5	18	92 \pm 1.0	220	140	660
5l	50	BH32.14	1.5	18	99 \pm 0.2	220	55	670
5m	50	BH32.14	1.5	48	71 \pm 1.2	220	75	710
5n	50	BH32.14	5	18	90 \pm 0.2	220	80	610
5o ^[2]	50	BH32.8	1.5	0.5	98 \pm 0.1	220	390	80
5p	50	BH32.8	5	48	91 \pm 0.07	220	1000	760
5q	50	BH32.8	5	48	81 \pm 0.2	220	900	590
5r	50	BH32.8	5	48	76 \pm 0.5	220	490	620
5s	50	BH32.14	1.5	18	97 \pm 0.3	220	130	435
5t	50	BH32.14	1.5	18	92 \pm 0.3	254	60	360
5u	50	BH32.14	2.5	48	99 \pm 0.3	220	240	345
5v+5w	50	BH32.14	5	24	89 \pm 0.1	220	300	5v 1000 5w 250

^[1] 10 mM acceptor was used in each reaction

^[2] Reaction was performed in PBS pH 7.0

Table S6: SFC analytical methods for MBH adducts 5a-w

	Column	Flow (mL.min ⁻¹)	Mobile Phase (% MeOH in CO ₂)	Run Time (min)
5a	Daicel 80S82 CHIRALPAK ® IG-3, 3 mm, 50 mm	1	5-10% (3min) 10% (7min)	10
5b	Daicel 80S82 CHIRALPAK ® IA-3, 3 mm, 50 mm	1	25%	2
5c	Daicel 80S82 CHIRALPAK ® IG-3, 3 mm, 50 mm, 3 µm	2	20%	2
5d	Daicel 80S82 CHIRALPAK ® IA-3, 3 mm, 50 mm	1	10%	2
5e	Daicel 80S82 CHIRALPAK ® IA-3, 3 mm, 50 mm, 3 µm	1	35%	1
5f	Daicel 80S82 CHIRALPAK ® IC-3, 3 mm, 50 mm, 3 µm	1	5%	5
5g	Daicel 80S82 CHIRALPAK ® IG-3, 3 mm, 50 mm, 3 µm	1	20%	3
5h	Daicel 80S82 CHIRALPAK ® IG-3, 3 mm, 50 mm, 3 µm	1	5%	4
5i	Daicel 80S82 CHIRALPAK ® IC-3, 3 mm, 50 mm, 3 µm	1	10%	3
5j	Daicel 80S82 CHIRALPAK ® IC-3, 3 mm, 50 mm, 3 µm	1	10	3.4
5k	Daicel 80S82 CHIRALPAK ® IA-3, 3 mm, 50 mm, 3 µm	1.2	3%	7
5l	Daicel 80S82 CHIRALPAK ® IG-3, 3 mm, 50 mm, 3 µm	1	20%	2.2
5m	Daicel 80S82 CHIRALPAK ® IA-3, 3 mm, 50 mm, 3 µm	1.2	3%	6
5n	Daicel 80S82 CHIRALPAK ® IG-3, 3 mm, 50 mm, 3 µm	1	20%	2.2
5o	Daicel 80S82 CHIRALPAK ® IA-3, 3 mm, 50 mm, 3 µm	1	10%	5
5p	Daicel 80S82 CHIRALPAK ® IC-3, 3 mm, 50 mm, 3 µm	1	10%	5
5q	Daicel 80S82 CHIRALPAK ® IC-3, 3 mm, 50 mm, 3 µm	1	20%	2
5r	Daicel 80S82 CHIRALPAK ® IC-3, 3 mm, 50 mm, 3 µm	1	15%	2
5s	Daicel 80S82 CHIRALPAK ® IC-3, 3 mm, 50 mm, 3 µm	2.5	3%	10
5t	Daicel 80S82 CHIRALPAK ® IG-3, 3 mm, 50 mm, 3 µm	1.2	20%	5
5u	Daicel 80S82 CHIRALPAK ® IA-3, 3 mm, 50 mm, 3 µm	1.5	5%	5
5v+ 5w	Daicel 80S82 CHIRALPAK ® IC-3, 3 mm, 50 mm, 3 µm	2	5%	8

Table S7: Data collection and refinement statistics. Entries in parentheses refer to the statistics in the highest resolution bin.

	BH32.6	BH32.7	BH32.12
Wavelength	0.976	0.9763	0.9795
Resolution range	55.26 - 1.48 (1.533 - 1.48)	37.87 - 1.8 (1.864 - 1.8)	42.71 - 2.29 (2.372 - 2.29)
Space group	P 31 2 1	P 1 21 1	P 31 2 1
Unit cell	71.689 71.689 121.272 90 90 120	36.56 69.63 45.72 90 99.29 90	70.9666 70.9666 118.768 90 90 120
Total reflections	578916 (56870)	64699 (6531)	158031 (15120)
Unique reflections	60772 (5941)	20789 (2043)	16121 (1571)
Multiplicity	9.5 (9.6)	3.1 (3.2)	9.8 (9.6)
Completeness (%)	99.90 (99.13)	99.00 (98.55)	99.55 (98.66)
Mean I/sigma(I)	14.64 (1.19)	17.67 (4.27)	10.51 (1.21)
Wilson B-factor	26.4	34.48	65.35
R-merge	0.05985 (1.411)	0.03661 (0.2531)	0.0806 (1.617)
R-meas	0.0634 (1.491)	0.0443 (0.3045)	0.08509 (1.708)
R-pim	0.02062 (0.4776)	0.02464 (0.1674)	0.02701 (0.5474)
CC1/2	0.997 (0.679)	0.998 (0.919)	0.999 (0.603)
CC*	0.999 (0.899)	0.999 (0.979)	1 (0.867)
Reflections used in refinement	60762 (5939)	20802 (2043)	16120 (1551)
Reflections used for R-free	3039 (305)	1067 (117)	824 (95)
R-work	0.1572 (0.2272)	0.2039 (0.3121)	0.2226 (0.3236)
R-free	0.1771 (0.2647)	0.2546 (0.3733)	0.2616 (0.4293)
CC(work)	0.964 (0.872)	0.955 (0.823)	0.946 (0.681)
CC(free)	0.966 (0.831)	0.937 (0.760)	0.925 (0.403)
Number of non-hydrogen atoms macromolecules	2210	1977	1890
ligands	1950	1829	1838
solvent	18	0	9
Protein residues	242	148	43
RMS(bonds)	448	227	226
RMS(angles)	0.009	0.004	0.006
Ramachandran favored (%)	1.12	0.54	1.08
Ramachandran allowed (%)	98.69	99.10	97.75
Ramachandran outliers (%)	1.31	0.90	1.35
Rotamer outliers (%)	0	0	0.9
Clash score	1.43	2.05	2.02
Average B-factor macromolecules	2.76	3.52	8.59
ligands	35.89	44.94	75.73
solvent	34.02	44.77	75.73
Number of TLS groups	60.92		80.84
	49.14	47.07	74.73
	0	1	1

Table S8: Mother liquor composition used for protein crystallization of BH32.6, BH32.7 and BH32.12

Variant	Crystallization conditions (200+200nl drops incubated at 4°C)
BH32.6	0.06 M Divalents [0.3M Magnesium chloride hexahydrate; 0.3M calcium chloride dihydrate] 0.1 M BS1 pH 6.5 [Imidazole; MES monohydrate (acid)] 30% Precipitant mix 2 [40% v/v Ethylene glycol; 20% w/v PEG 8K] Morpheus screen condition A2 (Molecular Dimensions)
BH32.7	0.12 M Monosaccharides [0.2M D-Glucose; 0.2M D-Mannose; 0.2M D-Galactose; 0.2M L-Fucose; 0.2M D-Xylose; 0.2M N-Acetyl-D-Glucosamine] 0.1 M BS2 pH 7.5 [Sodium HEPES; MOPS (acid)] 30 % Precipitant mix 1 [40% v/v PEG 500* MME; 20 % w/v PEG 20000] Morpheus screen condition F5 (Molecular Dimensions)
BH32.12	0.1M SPG pH 9.0, 25% w/v PEG 1500 PACT premier Eco condition A6 (Molecular Dimensions)

Table S9: Primer sequences used to generate DNA libraries

Flanking Primers	
XHO_R	ATGCATGCctcgagagagcct
NDE_F	CATGCATGcatatgattcgtgcgta
Round 2	
Y45x_T49x_F_1	ACCCTGCTGGACGAANDTGAGAACTGNDTCGCGAAGCGTTCTCT
Y45x_T49x_F_2	ACCCTGCTGGACGAAVHGGAGAACTGVHGC GCGAAGCGTTCTCT
Y45x_T49x_F_3	ACCCTGCTGGACGAANDTGAGAACTGVHGC GCGAAGCGTTCTCT
Y45x_T49x_F_4	ACCCTGCTGGACGAAVHGGAGAACTGNDTCGCGAAGCGTTCTCT
Y45x_T49x_F_5	ACCCTGCTGGACGAANDTGAGAACTGTGGCGCGAAGCGTTCTCT
Y45x_T49x_F_6	ACCCTGCTGGACGAATGGGAGAACTGNDTCGCGAAGCGTTCTCT
Y45x_T49x_F_7	ACCCTGCTGGACGAAVHGGAGAACTGTGGCGCGAAGCGTTCTCT
Y45x_T49x_F_8	ACCCTGCTGGACGAATGGGAGAACTGVHGC GCGAAGCGTTCTCT
Y45x_T49x_F_9	ACCCTGCTGGACGAATGGGAGAACTGTGGCGCGAAGCGTTCTCT
Y45x_T49x_R	TTC GTCCAGCAGGGT
F87x_W88x_F_1	AAATACCCTGAAAACNDTNDTGAAATCTCCCTGCGT
F87x_W88x_F_2	AAATACCCTGAAAACVHGVHGGAAATCTCCCTGCGT
F87x_W88x_F_3	AAATACCCTGAAAACNDTVHGGAAATCTCCCTGCGT
F87x_W88x_F_4	AAATACCCTGAAAACVHGNDTGAAATCTCCCTGCGT
F87x_W88x_F_5	AAATACCCTGAAAACNDTTGGGAAATCTCCCTGCGT
F87x_W88x_F_6	AAATACCCTGAAAACGGNDTGAAATCTCCCTGCGT
F87x_W88x_F_7	AAATACCCTGAAAACVHGTGGGAAATCTCCCTGCGT

F87x_W88x_F_8	AAATACCCTGAAAAC TGGVH GAAATCTCCCTGCGT
F87x_W88x_F_9	AAATACCCTGAAAAC TGGTGG GAAATCTCCCTGCGT
F87x_W88x_R	GTTTTCAGGGTATTTGAAACC
T49x_F	GAATACGAGAACT GNNK CGCGAAGCGTTCTCT
T49x_R	CAGTTTCTCGTATTCGTC
R50x_F	GAATACGAGAACTGACC NNK GAAGCGTTCTCTAAC
R50x_R	GGTCAGTTTCTCGTATTC
Round 4	
N14x_F	TTGATAGCCTGGG TACTCTGNNK AGCGTTGAAGGCG
N14x_R	CAGAGTACCCAGGCT
M130x_F	GATACCGAGCAGGCC NNK GCATTCTGGACGCA
M130x_R	GGCCTGCTCGGTATC
E174x_F	GGCGTTAAAGGCGAG NNK GCAGGTACGTTGGT
E174x_R	CTCGCCTTTAACGCC
Round 5	
L10x_F	GCGGTATTCTTTGATAGC NNK GGTACTCTGATTAGC
A19x_F	CTGATTAGCGTTGAAGGC NNK GCTAAATCCCATCTG
P38x_F	GGTGACTATCCGCTGAAC NNK AAAACCCCTGCTGGAC
L42x_F	AACCCGAAAACCC TGNNK GACGAATACGAGAAA
Y45x_F	ACCCTGCTGGACGA NNK GAGAACTGGCTCGC
E46x_F	ACCCTGCTGGACGAATAC NNK AAACTGGCTCGCGAA
P60x_F	AACTATGCGGGCAA NNK TATCGTCCGCTGCGT
P63x_F	GGCAAACCGTATCGT NNK CTGCGTGATATCCTG
F81x_F	GCGGAAAAGTACGGT NNK AAATACCCTGAAAAC
S91x_F	CCTGAAAAC TTGTGGG AAATC NNK CTGCGTATGTCTCAA
Q96x_F	TCCCTGCGTATGTCT NNK CGCTACGGCGAGCTG
S124x_F	GGCATGATCACCGAT NNK GATACCGAGCAGGCC
D125x_F	GGCATGATCACCGATTCT NNK ACCGAGCAGGCCACG
Q128x_F	ACCGATTCTGATACCGAG NNK GCCACGGCATTCTCTG
M130x_F	GATACCGAGCAGGCC NNK GCATTCTGGACGCA
L133x_F	CAGGCCACGGCATT CNNK GACGCACTGGGCATC
F154x_F	TCTGAAGAAGCTGGTT CNNK AAACCGCACCCACGC
K167x_F	TTCGAACTGGCTCTGAAG NNK GCCGGCGTTAAAGGC
E174x_F	GGCGTTAAAGGCGAG NNK GCAGGTACGTTGGT
K202x_F	ATCCTGCTGGATCGT NNK GGTGAGAAACGTGAA
L10x_R	GCTATCAAAGAATACCGC
A19x_R	GCCTTCAACGCTAAT
P38x_R	CGGGTTCAGCGGATA
L42x_R	CAGGGTTTTCGGGTT
Y45x_R	TTCGTCCAGCAGGGT

E46x_R	GTATTCGTCCAGCAG
P60x_R	TTTGCCCGCATAGTT
P63x_R	ACGATACGGTTTGCC
F81x_R	ACCGTACTTTTCCGC
S91x_R	GATTTCCCACAAGTTTTC
Q96x_R	AGACATACGCAGGGA
S124x_R	ATCGGTGATCATGCC
D125x_R	AGAATCGGTGATCATGCC
Q128x_R	CTCGGTATCAGAATCGGT
M130x_R	GGCCTGCTCGGTATC
L133x_R	GAATGCCGTGGCCTG
F154x_R	GAAACCAGCTTCTTCAGA
K167x_R	CTTCAGAGCCAGTTC
E174x_R	CTCGCCTTTAACGCC
K202x_R	ACGATCCAGCAGGAT
Round 6	
V16x_F	GGTACTCTGATTAGC NNK GAAGGCGCTGCTAAA
E17x_F	ACTCTGATTAGCGTT NNK GGCGCTGCTAAATCC
G32x_F	ATGGAGGAAGTGCTG NNK GACTATCCGCTGAACC
Y34x_F	GAAGTGCTGGGTGAC NNK CCGCTGAACCCGAAA
L36x_F	CTGGGTGACTATCCG NNK AACCCGAAAACCCTG
Y61x_F	TATGCGGGCAAACCG NNK CGTCCGCTGCGTGAT
L64x_F	AAACCGTATCGTCCG NNK CGTGATATCCTGGAAGAA
L68x_F	CCGCTGCGTGATATC NNK GAAGAAGTAATGCGTAAACT
M120x_F	AAATATCACGTTGGC NNK ATCACCGATAGGGATACC
T122x_F	CACGTTGGCATGATC NNK GATAGGGATACCGAGC
D123x_F	GTTGGCATGATCAC NNK KAGGGATACCGAGCCG
D125x_F	ATGATCACCGATAGG NNK KACCGAGCCGGCC
T126x_F	ATCACCGATAGGGAT NNK GAGCCGGCCACG
Q128x_F	GATAGGGATACCGAG NNK GCCACGGCATTCTCTG
E149x_F	TCCATCACACGTCT NNK GAAGCTGGTTTCTTTAAACC
G152x_F	ACGTCTGAAGAAGCT NNK TTCTTTAAACCGCACCCA
L199x_F	ATGACTAGCATCCTG NNK GATCGTAAAGGTGAGAAAC
E204x_F	CTGGATCGTAAAGGT NNK AAACGTGAATTCTGGGAT
K205x_F	GATCGTAAAGGTGAG NNK CGTGAATTCTGGGATAAG
E207x_F	AAAGGTGAGAAACGT NNK TTCTGGGATAAGGCG
V16x_R	GCTAATCAGAGTACCCAG
E17x_R	AACGCTAATCAGAGTACC
G32x_R	CAGCACTTCCTCCAT
Y34x_R	GTCACCCAGCACTTC

L36x_R	CGGATAGTCACCCAG
Y61x_R	CGGTTTGCCCGCATA
L64x_R	CGGACGATACGGTTT
L68x_R	GATATCACGCAGCGG
M120x_R	GCCAACGTGATATTTACC
T122x_R	GATCATGCCAACGTG
D123x_R	GGTGATCATGCCAAC
D125x_R	CCTATCGGTGATCATGCC
T126x_R	ATCCCTATCGGTGATCAT
Q128x_R	CTCGGTATCCCTATCG
E149x_R	AGACGTGGTGATGGA
G152x_R	AGCTTCTTCAGACGT
D199x_R	CAGGATGCTAGTCATACC
E204x_R	ACCTTTACGATCCAGCAG
K205x_R	CTCACCTTTACGATCCAG
E207x_R	ACGTTTCTCACCTTTACG
Round 7	
S95x_F1	ATCTCCCTGCGTATG NDT CAACGCTACGGCGAG
S95x_F2	ATCTCCCTGCGTATG VHG CAACGCTACGGCGAG
S95x_F3	ATCTCCCTGCGTATG TGG CAACGCTACGGCGAG
S95x_R	Catacgcaggagat
S22x_F1	GAAGGCGCTGCTAA ANDT CATCTGAAAATTATGGAGGA
S22x_F2	GAAGGCGCTGCTAA VHGC CATCTGAAAATTATGGAGGA
S22x_F3	GAAGGCGCTGCTAA TGGC CATCTGAAAATTATGGAGGA
S22x_R	Tttagcagcgcttc
M120x_T122x_F1	AAATATCACGTTGGC NDT ATC NDT AATAGGGATACCGAG
M120x_T122x_F2	AAATATCACGTTGGC VHG ATC VHGA AATAGGGATACCGAG
M120x_T122x_F3	AAATATCACGTTGGC NDT ATC VHGA AATAGGGATACCGAG
M120x_T122x_F4	AAATATCACGTTGGC VHG ATC NDT AATAGGGATACCGAG
M120x_T122x_F5	AAATATCACGTTGGC NDT ATC TGGA AATAGGGATACCGAG
M120x_T122x_F6	AAATATCACGTTGGC TGG ATC NDT AATAGGGATACCGAG
M120x_T122x_F7	AAATATCACGTTGGC VHG ATC TGGA AATAGGGATACCGAG
M120x_T122x_F8	AAATATCACGTTGGC TGG ATC VHGA AATAGGGATACCGAG
M120x_T122x_F9	AAATATCACGTTGGC TGG ATC TGGA AATAGGGATACCGAG
M120x_T122x_R	GCCAACGTGATATTTAC
Round 8	
L10_F	GTATTCTTTGATAGC NNK GGTACTCTGATTAGCGTT
A20_F	AGCGTTGAAGGCGCT NNK AAAAGTGCATCTGAAAATTATG
L24_F	GCTGCTAAAGTGCAT NNK AAAATTATGGAGGAAGTGCT
M27_F	GTGCATCTGAAAATT NNK GAGGAAGTGCTGGGT

L42_F	AACCCGAAAACCCTG NNK GACGAATACGAGAACTG
T45_F	ACCCTGCTGGACGA NNK GAGAACTGGCTCGC
P63_F	GGCAAACCGTATCGT NNK CTGCGTGATATCCTG
L64_F	AAACCGTATCGTCCG NNK CGTGATATCCTGGAAGAA
S91_F	AACTTGTGGGAAATC NNK CTGCGTATGGCGCAA
L92_F	TTGTGGGAAATCTCC NNK CGTATGGCGCAACG
Q96_F	TCCCTGCGTATGGCG NNK CGCTACGGCGAGC
D125_F	GTGATCCTGAATAGG NNK ACCGAGCCGGC
E127_F	CTGAATAGGGATACC NNK KCCGGCCACGGC
A129_F	AGGGATACCGAGCCG NNK ACGGCATTCTGGAC
I145_F	GACCTGTTCGATTCC NNK ACCACGTCTGAAGAA
T147_F	TTCGATTCCATCAC NNK TCTGAAGAAGCTGGT
L10_R	GCTATCAAAGAATACCGC
A20_R	AGCGCCTTCAACGCT
L24_R	ATGCACTTTAGCAGC
M27_R	AATTTTCAGATGCACTTTAG
L42_R	CAGGGTTTTTCGGGT
T45_R	TTCGTCCAGCAGGGT
P63_R	ACGATACGGTTTGCC
L64_R	CGGACGATACGGTTT
S91_R	GATTTCCCACAAGTTTTC
L92_R	GGAGATTTCCCACAA
Q96_R	CGCCATACGCAGGGA
D125_R	CCTATTCAGGATCACGC
E127_R	GGTATCCCTATTCAGGA
A129_R	CGGCTCGGTATCCCT
I145_R	GGAATCGAACAGGTC
T147_R	GGTGATGGAATCGAA
Round 9	
L10_F	GTATTCTTTGATAGC NNK GGTACTCTGATTAGCGTT
L24_F	GCTTATAAAGTGCAT NNK AAAATTATGGAGGAAGTGCT
L42_F	AACCCGAAAACCCTG NNK GACGAATACGAGAACTG
E46_F	CTGCTGGACGAATAC NNK AAACTGGCTCGCGAA
A129_F	AGGGATACCGAGCCG NNK ACGGCATTCTGGAC
L10_R	GCTATCAAAGAATACCGC
L24_R	ATGCACTTTATAAGC
L42_R	CAGGGTTTTTCGGGT
E46_R	GTATTCGTCCAGCAGGGT
A129_R	CGGCTCGGTATCCCT
Round 11	

F154_F	TCTGAAGAAGCTGGTTTC NNK AAACCGCACCCACGC
F154_R	GAAACCAGCTTCTTCAGA
Round 12	
Y20x_F	AGCGTTGAAGGCGCT NNK AAAAGTGCATTTTAAAATTATGGA
V30x_F	AAAATTATGGAGGA NNK CTGGGTGACTATCCG
K47x_F	CTGGACGAATACGAG NNK CTGGCTCGCGAAGCG
Y46x_F	GAAGCGTTCTTAAC NNK GCGGGCAAACCGTAT
I67x_F	CGTCCGCTGCGTGAT NNK CTGGAAGAAGTAATGCG
E70x_F	CGTGATATCCTGGA NNK GTAATGCGTAAACTGGC
F87x_F	AAATACCCTGAAAAC NNK TGGGAAATCTCCCTG
S91x_F	AACTTGTGGGAAATC NNK CTGCGTATGGCGCAA
R97x_F	CTGCGTATGGCGCA NNK TACGGCGAGCTGTAC
F153x_F	TCTGAAGAAGCTGGT NNK TCTAAACCGCACCCA
K155x_F	GAAGCTGGTTTCTCT NNK CCGCACCCACGCATC
F161x_F	CCGCACCCACGCATC NNK GAACTGGCTCTGAAG
L165x_F	ATCTTCGAACTGGCT NNK AAGAAAGCCGGCGTT
K171x_F	AAGAAAGCCGGCGTT NNK GCGGAGAAAGCAGTG
V176x_F	AAAGGCGAGAAAGC NNK TACGTTGGTGACAAC
Y177x_F	GGCGAGAAAGCAGTG NNK GTTGGTGACAACCCG
D180x_F	GCAGTGTACGTTGGT NNK AACCCGGTCAAAGAC
S196x_F	AACCTGGGTATGACT NNK ATCCTGCTGGATCGT
D210x_F	AAACGTGAATTCTGG NNK AAGGCGGACTTTATC
L219x_F	TTTATCGTCTCCGAC NNK CGCGAAGTTATTAAGATTG
I223x_F	GACCTGCGGAAGTT NNK AAGATTGTTGACGAACTG
Y20x_R	AGCGCCTTCAACGCT
V30x_R	TTCCTCCATAATTTTAAAATGCA
K47x_R	CTCGTATTCGTCCAG
Y56x_R	GTTAGAGAACGCTTCGC
I67x_R	ATCACGCAGCGGACG
E70x_R	TTCCAGGATATCACGCAG
F87x_R	GTTTTCAGGGTATTTGAAA
S91x_R	GATTTCCCACAAGTTTTC
R97x_R	TTGCGCCATACGCAG
F153x_R	ACCAGCTTCTTCAGA
K155x_R	AGAGAAACCAGCTTC
F161x_R	GATGCGTGGGTGCGG
L165x_R	AGCCAGTTCGAAGAT
K171x_R	AACGCCGGCTTTCTT
V176x_R	TGCTTTCTCGCCTTT
Y177x_R	CACTGCTTTCTCGCC

D180x_R	ACCAACGTACACTGC
S196x_R	AGTCATACCCAGGTT
D210x_R	CCAGAATTCACGTTTCT
L219x_R	GTCGGAGACGATAAAGT
I223x_R	AACTTCGCGCAGGTC
Round 14	
V16x_F	GGTACTCTGATTAGC NNK GAAAGGCACTTATAAAAGTG
A19x_F	AATAGCGTTGAAGGC NNK TATAAAAGTGCATTTT
E70x_F	CGTGATATCCTGGA NNK GTAAATGCGTAAA
M72x_F	ATCCTGGAACGTGT NNK CGTAAACTGGCGGAA
E89x_F	CCTGAAAAC T TGTGG NNK ATCTCCCTGCGTATG
P128x_F	AATAGGGATACCGAG NNK TCTACGGCATTCTG
S154x_F	GAAGAAGCTGGTTT CNNK AAACCGCACCCACG
V16x_R	GCTAATCAGAGTACCC
A19x_R	GCCTTCAACGCTAAT
E70x_R	TTCCAGGATATCACG
M72x_R	TACACGTTCCAGGAT
E89x_R	CCACAAGTTTTTCAGG
P128x_R	CTCGGTATCCCTATT
S154x_R	GAAACCAGCTTCTTC

Table S10: Cartesian coordinates for energy minimised cluster models.

R			TS1				
C	2.442144000	-2.750087000	2.346668000	C	1.584125000	-3.435423000	2.735771000
C	1.957197000	-3.759099000	1.338583000	C	1.443880000	-3.976175000	1.329330000
C	1.331559000	-3.085362000	0.114040000	C	1.345721000	-2.845705000	0.299598000
C	2.274618000	-2.049440000	-0.506396000	C	2.523699000	-1.871168000	0.426472000
C	2.943909000	-1.195277000	0.525568000	C	2.780245000	-1.469457000	1.868352000
C	3.009865000	-1.510133000	1.835146000	C	2.206567000	-2.193951000	2.921562000
O	2.379015000	-2.977103000	3.561909000	O	1.108129000	-4.102083000	3.710920000
C	1.063902000	0.507394000	3.232256000	C	0.408984000	-0.030331000	3.867067000
C	0.152415000	0.556049000	2.077198000	C	-0.227147000	0.240390000	2.561683000
C	-1.029743000	-0.203150000	2.055836000	C	-1.474436000	-0.330308000	2.271253000
C	-1.908648000	-0.087838000	0.989465000	C	-2.116820000	-0.022096000	1.083991000
C	-1.576842000	0.787941000	-0.048789000	C	-1.488556000	0.850396000	0.191080000
C	-0.396916000	1.527893000	-0.071695000	C	-0.230988000	1.406954000	0.431390000
C	0.470026000	1.405751000	1.009367000	C	0.394538000	1.093609000	1.637573000
O	0.879888000	-0.173071000	4.228089000	O	-0.110472000	-0.700965000	4.741506000
C	-0.933169000	-7.122602000	1.692388000	C	-1.423394000	-7.022153000	1.348518000
C	-1.855809000	-6.127738000	1.068480000	C	-2.198669000	-5.920714000	0.702112000
C	-1.922815000	-4.767148000	1.273477000	C	-2.264662000	-4.590634000	1.058561000
C	-2.850943000	-6.438153000	0.075028000	C	-3.065746000	-6.079955000	-0.437052000
N	-2.897066000	-4.212728000	0.459174000	N	-3.124545000	-3.917030000	0.207737000
C	-3.483090000	-5.215481000	-0.284662000	C	-3.628665000	-4.803821000	-0.718869000
C	-3.248826000	-7.629982000	-0.555425000	C	-3.415012000	-7.177001000	-1.244588000
C	-4.494428000	-5.161207000	-1.249853000	C	-4.520130000	-4.605267000	-1.777588000
C	-4.254249000	-7.580083000	-1.514376000	C	-4.296877000	-6.981223000	-2.301290000
C	-4.868853000	-6.356046000	-1.855681000	C	-4.843033000	-5.705954000	-2.563022000
C	2.267450000	-7.890944000	-2.331172000	C	1.828570000	-7.906774000	-2.609568000
C	1.553171000	-6.798818000	-1.521476000	C	0.718168000	-6.955504000	-2.135923000

C	2.412936000	-7.555282000	-3.818664000	C	2.647046000	-7.359461000	-3.783999000
C	0.080527000	-6.619399000	-1.896485000	C	-0.377818000	-6.701230000	-3.174828000
N	6.591785000	-5.591382000	0.323696000	N	6.635494000	-6.337701000	-0.210879000
C	6.535803000	-4.675733000	-0.827170000	C	6.282975000	-5.080822000	-0.881072000
C	6.648051000	-3.258942000	-0.325184000	C	6.797818000	-3.908440000	-0.079562000
O	7.599906000	-2.526882000	-0.563478000	O	7.580428000	-3.069116000	-0.499658000
C	5.229035000	-4.879120000	-1.595642000	C	4.763776000	-4.975867000	-1.041430000
N	8.072287000	-0.848451000	-3.048634000	N	8.152090000	-1.322500000	-2.963521000
C	7.056421000	0.157088000	-2.709135000	C	7.227032000	-0.245149000	-2.581464000
C	7.551557000	1.002060000	-1.535568000	C	7.800219000	0.527311000	-1.388024000
O	7.719707000	2.226258000	-1.626102000	O	8.012678000	1.744466000	-1.416859000
C	5.617137000	-0.361719000	-2.430467000	C	5.764724000	-0.681323000	-2.275741000
C	4.667714000	0.807643000	-2.140921000	C	4.884769000	0.522941000	-1.918342000
C	5.103567000	-1.217673000	-3.591361000	C	5.163535000	-1.467026000	-3.444885000
N	7.781708000	0.344209000	-0.377143000	N	8.009937000	-0.193360000	-0.257351000
C	8.151816000	1.086050000	0.810153000	C	8.284139000	0.483660000	0.995797000
C	9.252875000	2.090071000	0.489705000	C	9.619435000	1.217146000	0.941128000
O	9.429317000	3.104899000	1.131724000	O	9.888709000	2.143374000	1.676083000
C	8.709463000	0.136208000	1.888962000	C	8.266454000	-0.523809000	2.154227000
C	7.746532000	-0.934582000	2.296520000	C	6.911603000	-1.143672000	2.274240000
N	8.165738000	-2.162566000	2.769047000	N	6.609127000	-2.185475000	3.133141000
C	6.371458000	-0.996324000	2.337416000	C	5.731842000	-0.857939000	1.628874000
C	7.060104000	-2.898423000	3.074087000	C	5.293557000	-2.490567000	3.003326000
N	5.952527000	-2.221589000	2.823379000	N	4.753996000	-1.706981000	2.087032000
C	6.644487000	4.981941000	0.593782000	C	7.086142000	4.489304000	0.871315000
C	5.491462000	4.352848000	-0.200959000	C	5.886437000	3.933128000	0.092642000
C	6.281655000	6.246487000	1.379492000	C	6.797477000	5.752418000	1.689440000
C	4.456653000	3.626193000	0.665304000	C	4.791448000	3.323446000	0.973977000
C	-3.640458000	2.490302000	7.456810000	C	-3.666159000	2.436240000	7.335334000
C	-2.380798000	1.620952000	7.370065000	C	-2.368320000	1.621606000	7.279122000
C	-2.719302000	0.139633000	7.584983000	C	-2.653589000	0.165916000	6.880520000
C	-1.668005000	1.818729000	6.023650000	C	-1.359732000	2.265346000	6.317192000
C	-2.867980000	9.260412000	2.170184000	C	-2.114854000	9.437861000	2.331388000
C	-2.839791000	7.853618000	1.648277000	C	-2.159003000	8.055742000	1.754265000
C	-3.531951000	7.360032000	0.569313000	C	-2.829681000	7.648107000	0.626841000
C	-2.093809000	6.740908000	2.191105000	C	-1.513816000	6.879399000	2.287939000
N	-3.261078000	6.010055000	0.404284000	N	-2.639820000	6.289736000	0.424689000
C	-2.384966000	5.599181000	1.386332000	C	-1.837495000	5.789298000	1.427449000
C	-1.221991000	6.593684000	3.284383000	C	-0.707402000	6.639116000	3.414438000
C	-1.838732000	4.338571000	1.651980000	C	-1.381655000	4.488904000	1.667299000
C	-0.682113000	5.340483000	3.555864000	C	-0.258563000	5.345986000	3.660290000
C	-0.990350000	4.225169000	2.749182000	C	-0.594885000	4.282995000	2.796158000
N	2.009279000	7.219702000	-1.076264000	N	2.761436000	7.097765000	-0.951541000
C	1.931036000	5.789217000	-0.801410000	C	2.491952000	5.702560000	-0.624239000
C	0.990272000	4.923606000	-1.612657000	C	1.437855000	4.936805000	-1.401446000
O	1.100937000	3.687508000	-1.593190000	O	1.336169000	3.708108000	-1.276284000
C	1.574793000	5.638195000	0.692563000	C	2.125734000	5.648944000	0.873742000
O	2.514645000	6.330978000	1.494346000	O	3.142485000	6.255134000	1.652020000
N	0.013285000	5.570499000	-2.270612000	N	0.613868000	5.680198000	-2.165140000
C	-1.031772000	4.871696000	-2.992421000	C	-0.465449000	5.087293000	-2.925447000
C	-0.479801000	4.567306000	-4.392350000	C	0.094726000	4.712702000	-4.301544000
O	-1.002955000	4.933101000	-5.426886000	O	-0.415027000	5.027477000	-5.359835000
C	-2.344488000	5.660395000	-3.013333000	C	-1.717242000	5.967525000	-2.990639000
C	-3.611401000	4.783897000	-2.987158000	C	-3.041993000	5.180448000	-2.937205000
C	-4.858536000	5.676991000	-2.965736000	C	-4.224349000	6.156146000	-2.980882000
C	-3.694191000	3.786527000	-4.149657000	C	-3.176281000	4.122926000	-4.040671000
N	2.213380000	2.406020000	-4.398265000	N	2.637650000	2.416916000	-4.291817000
C	1.904096000	0.978717000	-4.485538000	C	2.208309000	1.028599000	-4.469594000
C	1.187153000	0.710877000	-5.796294000	C	1.454356000	0.907681000	-5.780798000
O	1.344277000	-0.278531000	-6.483973000	O	1.492294000	-0.060284000	-6.514338000
C	0.947727000	0.590413000	-3.345135000	C	1.232732000	0.644289000	-3.341981000
C	-5.618704000	-2.579417000	4.849235000	C	-5.840607000	-2.233290000	4.528793000
C	-4.262483000	-3.120608000	4.389497000	C	-4.837702000	-3.355262000	4.267082000
C	-3.449775000	-3.639837000	5.581337000	C	-4.141723000	-3.776593000	5.564325000
N	-2.166874000	-4.241706000	5.209374000	N	-3.114176000	-4.801225000	5.366166000
C	-1.044048000	-3.573410000	4.922891000	C	-1.916864000	-4.568183000	4.823569000
N	0.038124000	-4.243177000	4.516773000	N	-1.099483000	-5.572181000	4.501852000
N	-1.001183000	-2.242734000	5.044140000	N	-1.513495000	-3.312097000	4.569783000
N	-7.598589000	2.030436000	0.914829000	N	-7.382459000	2.640454000	0.690902000
C	-7.286066000	2.006759000	-0.528084000	C	-6.991124000	2.637152000	-0.732685000
C	-7.079900000	0.574235000	-1.044579000	C	-6.847277000	1.207687000	-1.279120000
O	-6.894025000	0.327457000	-2.239828000	O	-6.595651000	0.977923000	-2.465671000
C	-5.982451000	2.831035000	-0.684258000	C	-5.628164000	3.373466000	-0.790200000

C	-5.365464000	2.773202000	0.719936000	C	-5.092976000	3.222119000	0.640435000
C	-6.599020000	2.860447000	1.620163000	C	-6.364071000	3.368406000	1.478787000
N	-7.101710000	-0.354075000	-0.062053000	N	-6.999235000	0.254384000	-0.332544000
C	-6.995951000	-1.779788000	-0.261845000	C	-6.998988000	-1.166956000	-0.587870000
C	-8.319405000	-2.457682000	0.076475000	C	-8.370796000	-1.751631000	-0.267282000
O	-8.408284000	-3.552248000	0.591170000	O	-8.541440000	-2.843773000	0.231152000
C	-5.841051000	-2.372097000	0.545376000	C	-5.891386000	-1.882246000	0.178168000
O	-4.578374000	-1.948907000	0.038930000	O	-4.607216000	-1.533467000	-0.331568000
H	3.499417000	-0.866278000	2.555300000	H	2.327537000	-1.838060000	3.937530000
H	2.839024000	-4.343993000	1.037862000	H	2.320797000	-4.605867000	1.122646000
H	1.264412000	-4.451741000	1.820935000	H	0.568066000	-4.628058000	1.286539000
H	0.402278000	-2.587829000	0.413067000	H	0.403710000	-2.306111000	0.452856000
H	1.065183000	-3.846400000	-0.620207000	H	1.316635000	-3.254268000	-0.714186000
H	3.061358000	-2.544412000	-1.096022000	H	3.427947000	-2.331571000	0.018657000
H	1.735329000	-1.414020000	-1.216481000	H	2.337760000	-0.971203000	-0.167412000
H	3.405582000	-0.271105000	0.186935000	H	2.958437000	-0.412953000	2.039059000
H	1.949628000	1.158219000	3.165999000	H	1.386702000	0.449987000	4.030621000
H	-1.260196000	-0.870011000	2.876595000	H	-1.934042000	-1.004538000	2.983169000
H	-0.163545000	2.202714000	-0.885146000	H	0.222657000	2.091240000	-0.278393000
H	1.387837000	1.984087000	1.024437000	H	1.359337000	1.534679000	1.867658000
H	-0.347767000	-7.651762000	0.931428000	H	-0.910961000	-7.639110000	0.603143000
H	-0.224712000	-6.645113000	2.375661000	H	-0.662301000	-6.632160000	2.028487000
H	-1.342599000	-4.140801000	1.935960000	H	-1.771891000	-4.061619000	1.861375000
H	-3.209366000	-3.247496000	0.449506000	H	-3.358750000	-2.931325000	0.231877000
H	-2.774460000	-8.572830000	-0.297988000	H	-2.995945000	-8.159783000	-1.048045000
H	-4.963264000	-4.229587000	-1.534793000	H	-4.945826000	-3.635202000	-1.985479000
H	-4.571277000	-8.492266000	-2.011335000	H	-4.570372000	-7.818486000	-2.936609000
H	-5.646463000	-6.339758000	-2.613672000	H	-5.526549000	-5.571953000	-3.396001000
H	3.264603000	-8.057169000	-1.903634000	H	2.502410000	-8.113178000	-1.768430000
H	2.089887000	-5.848125000	-1.653023000	H	1.169523000	-5.998672000	-1.834944000
H	1.623923000	-7.039724000	-0.452998000	H	0.257907000	-7.370282000	-1.231375000
H	2.962329000	-8.338537000	-4.350920000	H	3.465066000	-8.037012000	-4.049263000
H	2.959304000	-6.613962000	-3.952150000	H	3.086752000	-6.386825000	-3.532979000
H	1.439539000	-7.444843000	-4.306875000	H	2.030286000	-7.220471000	-4.677503000
H	-0.040702000	-6.297624000	-2.934892000	H	0.017490000	-6.216169000	-4.072624000
H	-0.406121000	-5.876735000	-1.260291000	H	-1.162521000	-6.058315000	-2.768431000
H	-0.471520000	-7.557212000	-1.771829000	H	-0.847094000	-7.643152000	-3.481574000
H	5.803667000	-5.427824000	0.948273000	H	6.191426000	-6.391000000	0.704352000
H	7.438384000	-5.434859000	0.866209000	H	7.639917000	-6.396441000	-0.058895000
H	7.396657000	-4.873740000	-1.473308000	H	6.768953000	-5.055500000	-1.861668000
H	5.833755000	-2.916821000	0.340576000	H	6.447356000	-3.870362000	0.970074000
H	5.143096000	-5.924795000	-1.902219000	H	4.392214000	-5.865592000	-1.556130000
H	5.187324000	-4.242974000	-2.483929000	H	4.486154000	-4.089875000	-1.619033000
H	4.366397000	-4.640216000	-0.963971000	H	4.274184000	-4.917749000	-0.063208000
H	8.049745000	-1.617576000	-2.381996000	H	8.027367000	-2.124128000	-2.346321000
H	7.850248000	-1.249072000	-3.955732000	H	7.911900000	-1.644878000	-3.896872000
H	6.999406000	0.856610000	-3.549820000	H	7.205316000	0.479688000	-3.401688000
H	5.657794000	-0.993470000	-1.535543000	H	5.798072000	-1.349579000	-1.406112000
H	4.637121000	1.509127000	-2.981857000	H	4.810343000	1.219736000	-2.760229000
H	4.966578000	1.368704000	-1.251159000	H	5.273723000	1.085735000	-1.065292000
H	3.648408000	0.445781000	-1.981532000	H	3.872638000	0.193375000	-1.665582000
H	5.742971000	-2.088059000	-3.764350000	H	5.730214000	-2.378562000	-3.654163000
H	5.065456000	-0.636640000	-4.520713000	H	5.148089000	-0.860143000	-4.358295000
H	4.093236000	-1.584226000	-3.383208000	H	4.132927000	-1.760283000	-3.219430000
H	7.637854000	-0.663126000	-0.308368000	H	7.851995000	-1.197435000	-0.245663000
H	7.298260000	1.645830000	1.213261000	H	7.524864000	1.253185000	1.180804000
H	9.953628000	1.765776000	-0.305194000	H	10.341750000	0.821063000	0.198499000
H	8.993671000	0.749586000	2.751591000	H	8.531284000	0.006370000	3.075096000
H	9.629772000	-0.325872000	1.511821000	H	9.028155000	-1.296327000	1.994348000
H	9.125349000	-2.464903000	2.862842000	H	7.254826000	-2.637135000	3.767204000
H	5.668535000	-0.235465000	2.031471000	H	5.527007000	-0.121104000	0.870393000
H	7.120278000	-3.902144000	3.468723000	H	4.776152000	-3.244275000	3.576894000
H	7.064811000	4.230707000	1.273676000	H	7.483929000	3.705964000	1.531325000
H	5.916807000	3.644823000	-0.918794000	H	6.254890000	3.176633000	-0.606963000
H	4.996569000	5.137649000	-0.790218000	H	5.459693000	4.741004000	-0.517855000
H	5.946707000	7.042360000	0.703449000	H	6.451662000	6.565233000	1.039825000
H	7.142040000	6.624292000	1.941692000	H	7.694813000	6.098708000	2.212723000
H	5.468185000	6.064946000	2.089709000	H	6.015880000	5.583487000	2.436673000
H	3.655413000	3.203520000	0.048065000	H	3.968468000	2.931423000	0.365244000
H	3.993821000	4.303117000	1.388352000	H	4.370905000	4.066771000	1.656098000
H	4.925764000	2.800886000	1.215770000	H	5.188677000	2.493340000	1.571573000
H	-3.400210000	3.551263000	7.329502000	H	-3.475627000	3.468845000	7.647268000
H	-4.354449000	2.212972000	6.671442000	H	-4.143231000	2.468341000	6.347920000

H	-1.693379000	1.931663000	8.169105000	H	-1.923907000	1.617370000	8.284430000
H	-3.408220000	-0.210122000	6.804220000	H	-3.098007000	0.124782000	5.877555000
H	-3.206728000	-0.028644000	8.550967000	H	-3.354730000	-0.307753000	7.576598000
H	-1.816922000	-0.481852000	7.553243000	H	-1.733989000	-0.427803000	6.860662000
H	-0.748960000	1.225305000	5.967567000	H	-0.413299000	1.715234000	6.308496000
H	-1.405179000	2.868892000	5.855155000	H	-1.148118000	3.303473000	6.595439000
H	-2.316824000	1.505191000	5.195471000	H	-1.751429000	2.271408000	5.292287000
H	-3.525119000	9.889869000	1.564171000	H	-2.697292000	10.136659000	1.724726000
H	-3.227583000	9.297099000	3.205434000	H	-2.518862000	9.460907000	3.350682000
H	-4.207923000	7.867560000	-0.104032000	H	-3.438134000	8.222701000	-0.056941000
H	-3.662439000	5.420676000	-0.306641000	H	-3.032483000	5.755026000	-0.332685000
H	-0.979282000	7.446796000	3.911411000	H	-0.444061000	7.452443000	4.084575000
H	-2.069844000	3.481097000	1.029863000	H	-1.634729000	3.674268000	0.998579000
H	-0.011034000	5.214283000	4.400085000	H	0.361162000	5.146058000	4.529130000
H	-0.554543000	3.260914000	2.985884000	H	-0.227054000	3.286689000	3.012479000
H	2.357627000	7.428995000	-2.005685000	H	3.156316000	7.222159000	-1.877579000
H	1.126383000	7.702388000	-0.930573000	H	1.945420000	7.695417000	-0.848821000
H	2.928478000	5.368569000	-0.949883000	H	3.423530000	5.146501000	-0.759086000
H	0.553964000	6.016132000	0.856842000	H	1.156305000	6.150362000	1.022835000
H	1.588730000	4.585466000	0.976835000	H	2.014540000	4.612099000	1.192975000
H	2.732682000	7.128478000	0.981437000	H	3.462872000	6.991688000	1.102665000
H	0.050890000	6.577946000	-2.329893000	H	0.824730000	6.658922000	-2.297273000
H	-1.162494000	3.906162000	-2.489838000	H	-0.686280000	4.136504000	-2.423179000
H	0.467586000	3.994261000	-4.397262000	H	1.030050000	4.120339000	-4.267881000
H	-2.362993000	6.296163000	-3.905642000	H	-1.690334000	6.562104000	-3.910654000
H	-2.360777000	6.322491000	-2.141844000	H	-1.690760000	6.667864000	-2.149795000
H	-3.582029000	4.190393000	-2.059853000	H	-3.063462000	4.635344000	-1.979842000
H	-4.912534000	6.276145000	-3.881699000	H	-4.224447000	6.709435000	-3.926868000
H	-4.854090000	6.374707000	-2.120941000	H	-4.179727000	6.893465000	-2.171594000
H	-5.772084000	5.078539000	-2.903978000	H	-5.178717000	5.627278000	-2.904219000
H	-3.696932000	4.310954000	-5.110170000	H	-3.108415000	4.583877000	-5.030523000
H	-4.613975000	3.196536000	-4.075827000	H	-4.143513000	3.614925000	-3.962171000
H	-2.857841000	3.084433000	-4.149403000	H	-2.401043000	3.356587000	-3.967512000
H	3.098988000	2.621123000	-4.845824000	H	3.521742000	2.592226000	-4.760369000
H	2.264420000	2.708276000	-3.428431000	H	2.760792000	2.629391000	-3.305349000
H	2.786003000	0.326277000	-4.449754000	H	3.033212000	0.304045000	-4.489038000
H	0.464010000	1.508464000	-6.075907000	H	0.819803000	1.791794000	-6.010983000
H	0.011128000	1.151211000	-3.408380000	H	0.328883000	1.258325000	-3.376203000
H	1.414115000	0.831078000	-2.385592000	H	1.712374000	0.812662000	-2.372806000
H	0.718044000	-0.475251000	-3.373637000	H	0.944534000	-0.404959000	-3.417999000
H	-5.495834000	-1.746382000	5.549503000	H	-5.339514000	-1.338367000	4.914644000
H	-6.203040000	-2.216610000	3.999030000	H	-6.363762000	-1.953124000	3.609994000
H	-3.700703000	-2.337890000	3.865844000	H	-4.088745000	-3.029329000	3.536782000
H	-4.399065000	-3.938450000	3.673161000	H	-5.340583000	-4.228342000	3.836676000
H	-3.274141000	-2.847584000	6.317086000	H	-3.694392000	-2.912338000	6.067217000
H	-4.008739000	-4.417514000	6.105903000	H	-4.862831000	-4.194839000	6.269265000
H	-2.164319000	-5.235221000	5.034122000	H	-3.389862000	-5.764979000	5.480941000
H	0.016202000	-5.249252000	4.474728000	H	-1.415251000	-6.527896000	4.525338000
H	0.915868000	-3.782112000	4.264714000	H	-0.186724000	-5.339827000	4.101929000
H	-0.183850000	-1.689992000	4.804500000	H	-0.545157000	-3.203840000	4.288822000
H	-1.810081000	-1.735446000	5.361458000	H	-1.915154000	-2.536329000	5.071747000
H	-8.546637000	2.343957000	1.087348000	H	-8.312195000	3.020926000	0.822959000
H	-8.090542000	2.431261000	-1.137251000	H	-7.731103000	3.129469000	-1.371607000
H	-5.336239000	2.432918000	-1.468162000	H	-4.968711000	2.958847000	-1.554233000
H	-6.238530000	3.863278000	-0.938323000	H	-5.798196000	4.429938000	-1.015664000
H	-4.655379000	3.578630000	0.917323000	H	-4.336541000	3.964769000	0.902953000
H	-4.848332000	1.820223000	0.870662000	H	-4.655241000	2.228231000	0.780077000
H	-6.421129000	2.475129000	2.628968000	H	-6.269332000	2.934672000	2.479087000
H	-6.923903000	3.906899000	1.709748000	H	-6.617927000	4.431878000	1.593149000
H	-7.322722000	0.046458000	0.852283000	H	-7.246749000	0.642216000	0.580600000
H	-6.834670000	-1.959544000	-1.330977000	H	-6.857276000	-1.305730000	-1.666402000
H	-9.215715000	-1.863036000	-0.196214000	H	-9.219075000	-1.087086000	-0.531325000
H	-5.864993000	-3.459206000	0.475783000	H	-5.999143000	-2.960683000	0.062266000
H	-5.949949000	-2.093939000	1.601567000	H	-5.963757000	-1.641704000	1.246144000
H	-4.576847000	-0.986896000	-0.085067000	H	-4.542883000	-0.570739000	-0.440639000
H	-4.142628000	2.370062000	8.422738000	H	-4.382748000	1.997052000	8.037849000
H	-6.203674000	-3.357660000	5.350168000	H	-6.595586000	-2.537498000	5.261556000
H	-1.869193000	9.713045000	2.163951000	H	-1.087918000	9.818460000	2.388282000
H	7.456499000	5.224476000	-0.103388000	H	7.891525000	4.707628000	0.158289000
H	1.721662000	-8.837178000	-2.216457000	H	1.382224000	-8.870373000	-2.890455000
H	-1.480392000	-7.884544000	2.260409000	H	-2.072047000	-7.695700000	1.923808000
N	-5.732712000	-0.564133000	-5.008653000	N	-5.483400000	0.135172000	-5.203514000
C	-4.694788000	-1.519037000	-4.556770000	C	-4.557261000	-0.948053000	-4.806673000

C	-5.233439000	-2.142150000	-3.293296000	C	-5.221970000	-1.693536000	-3.675720000
O	-5.922014000	-3.149980000	-3.257854000	O	-6.008440000	-2.615573000	-3.822411000
C	-3.384964000	-0.751176000	-4.325143000	C	-3.216005000	-0.320414000	-4.387753000
C	-2.219112000	-1.635703000	-3.952932000	C	-2.134641000	-1.318961000	-4.040000000
C	-1.196329000	-1.885334000	-4.876204000	C	-1.133016000	-1.627901000	-4.969684000
C	-2.140245000	-2.242536000	-2.689729000	C	-2.101382000	-1.955642000	-2.789343000
C	-0.116964000	-2.708524000	-4.549467000	C	-0.121156000	-2.538925000	-4.661042000
C	-1.075543000	-3.082846000	-2.367074000	C	-1.099252000	-2.877155000	-2.480633000
C	-0.054130000	-3.312547000	-3.292601000	C	-0.101163000	-3.167214000	-3.413976000
H	-5.987097000	0.044497000	-4.227797000	H	-5.739290000	0.674035000	-4.373650000
H	-6.579991000	-1.081843000	-5.235817000	H	-6.350699000	-0.280380000	-5.539077000
H	-5.060894000	-1.545701000	-2.382137000	H	-5.026610000	-1.276064000	-2.673398000
H	-3.560544000	-0.005607000	-3.541060000	H	-3.400630000	0.340533000	-3.532934000
H	-1.231484000	-1.412494000	-5.853072000	H	-1.128833000	-1.131098000	-5.935426000
H	-2.909819000	-2.062090000	-1.946538000	H	-2.858554000	-1.730104000	-2.046609000
H	-1.054432000	-3.553773000	-1.391492000	H	-1.102070000	-3.364355000	-1.511348000
H	0.782820000	-3.954985000	-3.038779000	H	0.683719000	-3.876894000	-3.172538000
H	0.679600000	-2.858193000	-5.271183000	H	0.660093000	-2.737494000	-5.387948000
H	-4.568626000	-2.290450000	-5.322480000	H	-4.423162000	-1.624401000	-5.657144000
H	-3.162357000	-0.198058000	-5.241672000	H	-2.886050000	0.315615000	-5.213996000
H	-2.822982000	-0.663072000	0.964761000	H	-3.077452000	-0.457796000	0.859164000
N	-2.521118000	0.974162000	-1.151687000	N	-2.198180000	1.229857000	-1.032837000
O	-3.639193000	0.451151000	-1.068702000	O	-3.374581000	0.865988000	-1.169584000
O	-2.171512000	1.654116000	-2.112794000	O	-1.605873000	1.907838000	-1.866916000
O	3.105195000	-1.234800000	5.650869000	O	1.325573000	-2.787357000	6.216627000
H	2.400956000	-0.596492000	5.462784000	H	0.883753000	-1.967269000	5.943620000
H	2.989177000	-1.869510000	4.920211000	H	1.349692000	-3.317158000	5.394181000

	Int1			TS2			
C	1.110688000	-2.837864000	2.366025000	C	1.455925000	-3.154544000	2.151346000
C	0.736255000	-3.025572000	0.907583000	C	1.021808000	-3.285549000	0.705717000
C	1.518045000	-2.130432000	-0.059790000	C	1.661776000	-2.262317000	-0.238077000
C	2.990479000	-2.068327000	0.338810000	C	3.131272000	-2.055998000	0.126236000
C	3.121031000	-1.450746000	1.737072000	C	3.240030000	-1.441801000	1.530990000
C	2.172604000	-2.047496000	2.720527000	C	2.326249000	-2.090290000	2.547522000
O	0.361589000	-3.431486000	3.244145000	O	0.997796000	-3.953794000	2.999362000
C	0.618724000	-0.010829000	3.710291000	C	1.085405000	-0.719908000	3.386128000
C	-0.040492000	0.272665000	2.416596000	C	0.239323000	-0.218905000	2.254238000
C	-1.312800000	-0.261958000	2.160749000	C	-1.027844000	-0.782623000	2.033310000
C	-1.982559000	0.061713000	0.993261000	C	-1.853460000	-0.300608000	1.031113000
C	-1.363947000	0.924381000	0.082352000	C	-1.400063000	0.755601000	0.234284000
C	-0.089407000	1.456478000	0.294997000	C	-0.142135000	1.337655000	0.416949000
C	0.565808000	1.123037000	1.478347000	C	0.663740000	0.847449000	1.442066000
O	0.043592000	-0.554753000	4.643075000	O	0.511685000	-1.270982000	4.390853000
C	-1.816191000	-6.956180000	1.415531000	C	-1.404354000	-6.985466000	1.495114000
C	-2.622234000	-5.857484000	0.799776000	C	-2.246940000	-5.948045000	0.831151000
C	-2.565226000	-4.507000000	1.065292000	C	-2.384738000	-4.622631000	1.177808000
C	-3.596716000	-6.025028000	-0.247725000	C	-3.099205000	-6.160838000	-0.310146000
N	-3.438585000	-3.824726000	0.235939000	N	-3.273888000	-3.999030000	0.321306000
C	-4.078450000	-4.728402000	-0.585829000	C	-3.725417000	-4.915674000	-0.602799000
C	-4.083547000	-7.142043000	-0.948864000	C	-3.385212000	-7.277994000	-1.114952000
C	-5.015147000	-4.528621000	-1.606281000	C	-4.613406000	-4.767592000	-1.673371000
C	-5.018564000	-6.947824000	-1.959328000	C	-4.265648000	-7.131390000	-2.181662000
C	-5.476322000	-5.652561000	-2.283860000	C	-4.871578000	-5.886174000	-2.457276000
C	1.418570000	-8.068209000	-2.499468000	C	1.837689000	-7.890719000	-2.467888000
C	0.738691000	-6.945361000	-1.701217000	C	0.356699000	-7.586940000	-2.187175000
C	1.731814000	-7.687587000	-3.949907000	C	2.654837000	-6.645569000	-2.832730000
C	-0.667921000	-6.601226000	-2.196239000	C	-0.427158000	-7.103440000	-3.411474000
N	6.311025000	-6.785103000	-0.144107000	N	7.252270000	-5.947722000	-1.394400000
C	6.011069000	-5.485078000	-0.752297000	C	6.283048000	-5.024472000	-0.783501000
C	6.458122000	-4.367955000	0.156373000	C	7.047715000	-4.070897000	0.099073000
O	7.226503000	-3.475515000	-0.167153000	O	7.237202000	-2.893147000	-0.165360000
C	4.510384000	-5.370210000	-1.042306000	C	5.234987000	-5.810174000	0.002885000
N	8.063553000	-1.921387000	-2.774248000	N	8.051700000	-1.361821000	-2.820441000
C	7.249056000	-0.730004000	-2.490796000	C	7.194604000	-0.200498000	-2.533622000
C	7.852562000	0.019887000	-1.298685000	C	7.775980000	0.589639000	-1.354667000
O	8.202126000	1.203435000	-1.350962000	O	8.005285000	1.802203000	-1.405346000
C	5.736511000	-0.989026000	-2.243636000	C	5.703009000	-0.535616000	-2.260472000
C	4.990324000	0.325720000	-1.989095000	C	4.893123000	0.727656000	-1.949581000
C	5.104752000	-1.766113000	-3.402020000	C	5.087224000	-1.309368000	-3.430048000
N	7.935840000	-0.685848000	-0.141662000	N	7.969669000	-0.115567000	-0.210326000

C	8.310905000	-0.025503000	1.089951000	C	8.261547000	0.568153000	1.032334000
C	9.740455000	0.507242000	1.021312000	C	9.638404000	1.225627000	0.997742000
O	10.135935000	1.402936000	1.735475000	O	9.935931000	2.154483000	1.717175000
C	8.145655000	-0.977268000	2.281558000	C	8.159442000	-0.406011000	2.215707000
C	6.716555000	-1.389422000	2.404636000	C	6.789693000	-0.998867000	2.273852000
N	6.278953000	-2.454262000	3.171994000	N	6.498687000	-2.209691000	2.874041000
C	5.595120000	-0.877425000	1.812724000	C	5.610466000	-0.565245000	1.732907000
C	4.948707000	-2.588259000	3.056318000	C	5.204393000	-2.511022000	2.704368000
N	4.517981000	-1.634212000	2.229192000	N	4.645649000	-1.513826000	2.011801000
C	7.347068000	4.040892000	0.912966000	C	7.041558000	4.565998000	0.874281000
C	6.120917000	3.532508000	0.145116000	C	5.842584000	3.991137000	0.109922000
C	7.123597000	5.327111000	1.715354000	C	6.749296000	5.835350000	1.681476000
C	4.981695000	3.031965000	1.039463000	C	4.746956000	3.407675000	1.007890000
C	-3.553036000	2.520561000	7.792771000	C	-3.764714000	2.289587000	7.620434000
C	-2.320076000	1.789732000	7.249283000	C	-2.372503000	1.709330000	7.346163000
C	-2.671910000	0.354939000	6.825823000	C	-2.474764000	0.290539000	6.763989000
C	-1.693442000	2.559479000	6.077646000	C	-1.570205000	2.620851000	6.406760000
C	-1.567427000	9.525774000	2.226872000	C	-2.180178000	9.479126000	2.323129000
C	-1.697321000	8.138576000	1.673239000	C	-2.245266000	8.117540000	1.696081000
C	-2.389187000	7.757776000	0.549228000	C	-2.924829000	7.773205000	0.552823000
C	-1.131198000	6.930511000	2.227384000	C	-1.615136000	6.905467000	2.170581000
N	-2.287656000	6.386966000	0.368502000	N	-2.749400000	6.426135000	0.280540000
C	-1.522735000	5.850745000	1.381983000	C	-1.950759000	5.865638000	1.253363000
C	-0.344870000	6.653656000	3.359736000	C	-0.816921000	6.588729000	3.284687000
C	-1.153985000	4.526637000	1.641696000	C	-1.504351000	4.549042000	1.413958000
C	0.017725000	5.337310000	3.625519000	C	-0.387959000	5.276531000	3.459746000
C	-0.384951000	4.285448000	2.775911000	C	-0.726414000	4.267579000	2.532782000
N	3.173193000	6.889694000	-0.943884000	N	2.702382000	7.133987000	-0.954805000
C	2.845517000	5.500669000	-0.642867000	C	2.435189000	5.740458000	-0.614781000
C	1.795932000	4.781988000	-1.468340000	C	1.381768000	4.969681000	-1.386709000
O	1.670757000	3.550661000	-1.391192000	O	1.300599000	3.738430000	-1.275763000
C	2.418010000	5.448292000	0.839072000	C	2.067746000	5.702325000	0.882231000
O	3.426047000	6.009080000	1.661635000	O	3.082375000	6.320014000	1.655105000
N	0.993274000	5.566695000	-2.210525000	N	0.530157000	5.707488000	-2.127441000
C	-0.119443000	5.032265000	-2.968825000	C	-0.527698000	5.087347000	-2.898501000
C	0.417143000	4.655020000	-4.355162000	C	0.075833000	4.656311000	-4.239704000
O	-0.046010000	5.063150000	-5.402998000	O	-0.420300000	4.889781000	-5.325272000
C	-1.316942000	5.985544000	-3.017274000	C	-1.776340000	5.962490000	-3.044063000
C	-2.687383000	5.279885000	-3.001300000	C	-3.102123000	5.175906000	-2.987571000
C	-3.806858000	6.327589000	-3.040626000	C	-4.286143000	6.143610000	-3.106215000
C	-2.870068000	4.260025000	-4.132722000	C	-3.208051000	4.066467000	-4.042199000
N	2.779718000	2.193013000	-4.277574000	N	2.654434000	2.401868000	-4.295865000
C	2.331125000	0.810401000	-4.444182000	C	2.161833000	1.028425000	-4.414174000
C	1.596449000	0.679447000	-5.765760000	C	1.363157000	0.905049000	-5.698713000
O	1.623127000	-0.305094000	-6.477475000	O	1.337130000	-0.081796000	-6.407585000
C	1.329749000	0.455643000	-3.329240000	C	1.201309000	0.726347000	-3.247392000
C	-5.981315000	-1.887832000	4.501144000	C	-5.834598000	-2.190193000	4.646347000
C	-5.132894000	-3.139191000	4.301083000	C	-4.825134000	-3.291415000	4.339682000
C	-4.483882000	-3.583970000	5.618062000	C	-4.186701000	-3.822093000	5.629704000
N	-3.403564000	-4.552535000	5.418511000	N	-3.036853000	-4.691222000	5.385224000
C	-2.252891000	-4.224438000	4.815843000	C	-1.850123000	-4.247113000	4.948199000
N	-1.423584000	-5.172822000	4.359605000	N	-0.895439000	-5.128013000	4.611537000
N	-1.903055000	-2.945532000	4.668505000	N	-1.603032000	-2.940436000	4.877819000
N	-7.187732000	3.020940000	0.602939000	N	-7.404130000	2.656571000	0.771385000
C	-6.796946000	2.984955000	-0.820457000	C	-7.031610000	2.623479000	-0.656888000
C	-6.745270000	1.546817000	-1.360369000	C	-6.910917000	1.186289000	-1.176613000
O	-6.502990000	1.296520000	-2.544838000	O	-6.726405000	0.941548000	-2.372142000
C	-5.389265000	3.630715000	-0.881444000	C	-5.663304000	3.352514000	-0.745647000
C	-4.862349000	3.445690000	0.548136000	C	-5.135126000	3.286799000	0.694282000
C	-6.119106000	3.673585000	1.390274000	C	-6.412011000	3.457460000	1.517501000
N	-6.964916000	0.613209000	-0.408864000	N	-7.006950000	0.242472000	-0.213887000
C	-7.025482000	-0.810657000	-0.637816000	C	-7.018251000	-1.179061000	-0.475932000
C	-8.432246000	-1.323591000	-0.344827000	C	-8.397649000	-1.757127000	-0.174490000
O	-8.669969000	-2.401474000	0.157330000	O	-8.581862000	-2.865014000	0.282760000
C	-5.975773000	-1.555654000	0.180516000	C	-5.919271000	-1.911042000	0.282642000
O	-4.663669000	-1.313383000	-0.317764000	O	-4.636991000	-1.608410000	-0.254069000
H	2.404763000	-1.936276000	3.773362000	H	2.778007000	-2.251898000	3.519846000
H	0.883464000	-4.085539000	0.659394000	H	1.282319000	-4.306335000	0.398020000
H	-0.337596000	-2.840259000	0.815722000	H	-0.070910000	-3.233552000	0.675822000
H	1.097873000	-1.119279000	-0.059113000	H	1.130894000	-1.307038000	-0.187693000
H	1.423258000	-2.503418000	-1.082968000	H	1.579761000	-2.605428000	-1.271372000
H	3.403816000	-3.081322000	0.366723000	H	3.651498000	-3.019739000	0.116677000
H	3.572878000	-1.491399000	-0.382032000	H	3.628365000	-1.410153000	-0.598119000

H	3.019720000	-0.359712000	1.657877000	H	3.047445000	-0.367105000	1.456156000
H	1.634194000	0.395902000	3.827233000	H	1.949038000	-0.065756000	3.578844000
H	-1.771112000	-0.921346000	2.886688000	H	-1.369986000	-1.589109000	2.668566000
H	0.363045000	2.130284000	-0.424825000	H	0.185442000	2.162841000	-0.206616000
H	1.543622000	1.547600000	1.682585000	H	1.621282000	1.323346000	1.628465000
H	-1.446802000	-7.644060000	0.647122000	H	-0.867576000	-7.590466000	0.755824000
H	-0.942223000	-6.564028000	1.942771000	H	-0.655147000	-6.528848000	2.147364000
H	-1.952416000	-3.973196000	1.776462000	H	-1.909593000	-4.070962000	1.975095000
H	-3.589084000	-2.822313000	0.203179000	H	-3.532533000	-3.017777000	0.316990000
H	-3.728451000	-8.140004000	-0.707518000	H	-2.919612000	-8.237651000	-0.909252000
H	-5.361039000	-3.541412000	-1.882012000	H	-5.077322000	-3.817415000	-1.895650000
H	-5.400970000	-7.801580000	-2.511145000	H	-4.490707000	-7.984533000	-2.814838000
H	-6.198013000	-5.524469000	-3.085209000	H	-5.545739000	-5.787142000	-3.301869000
H	2.351729000	-8.350275000	-1.994891000	H	2.280002000	-8.360776000	-1.580406000
H	1.373101000	-6.047405000	-1.732512000	H	0.289195000	-6.832005000	-1.391034000
H	0.683693000	-7.240036000	-0.645427000	H	-0.125097000	-8.489806000	-1.790442000
H	2.254238000	-8.497332000	-4.469597000	H	3.713068000	-6.888059000	-2.976875000
H	2.371743000	-6.797924000	-3.988401000	H	2.591003000	-5.891993000	-2.038066000
H	0.822109000	-7.464692000	-4.516274000	H	2.295730000	-6.181475000	-3.757020000
H	-0.659482000	-6.234775000	-3.227031000	H	-0.039339000	-6.155640000	-3.796253000
H	-1.130520000	-5.830694000	-1.575596000	H	-1.481517000	-6.951369000	-3.163174000
H	-1.320825000	-7.480242000	-2.160011000	H	-0.372944000	-7.838426000	-4.223462000
H	5.790568000	-6.904312000	0.723207000	H	7.720203000	-6.502928000	-0.679767000
H	7.299061000	-6.858166000	0.087122000	H	7.972641000	-5.434676000	-1.897820000
H	6.575822000	-5.394917000	-1.686088000	H	5.811411000	-4.441052000	-1.580938000
H	6.071132000	-4.425121000	1.193223000	H	7.511480000	-4.524381000	0.998300000
H	4.201813000	-6.214687000	-1.664253000	H	4.786033000	-6.563732000	-0.648240000
H	4.279982000	-4.440045000	-1.568489000	H	4.442076000	-5.156616000	0.376285000
H	3.926528000	-5.400794000	-0.115511000	H	5.689632000	-6.320144000	0.859269000
H	7.824716000	-2.670128000	-2.124472000	H	7.793571000	-2.133632000	-2.206947000
H	7.831029000	-2.266805000	-3.701195000	H	7.864162000	-1.683750000	-3.765776000
H	7.350078000	-0.046692000	-3.339859000	H	7.252108000	0.480276000	-3.388670000
H	5.659466000	-1.613996000	-1.344242000	H	5.686841000	-1.191470000	-1.380917000
H	5.059358000	0.989550000	-2.857466000	H	4.906709000	1.418884000	-2.798774000
H	5.392481000	0.869684000	-1.130689000	H	5.282653000	1.267077000	-1.083256000
H	3.929524000	0.142872000	-1.798036000	H	3.848514000	0.479393000	-1.741955000
H	5.582876000	-2.739293000	-3.543554000	H	5.619046000	-2.245482000	-3.620479000
H	5.187315000	-1.207073000	-4.341678000	H	5.110530000	-0.712612000	-4.349613000
H	4.041784000	-1.944278000	-3.209071000	H	4.042956000	-1.560182000	-3.217383000
H	7.687291000	-1.669217000	-0.110725000	H	7.796279000	-1.114090000	-0.186429000
H	7.679603000	0.856932000	1.248748000	H	7.550350000	1.389334000	1.182236000
H	10.396523000	-0.003095000	0.287378000	H	10.354047000	0.775800000	0.279827000
H	8.478081000	-0.463061000	3.188666000	H	8.389299000	0.138113000	3.136838000
H	8.777699000	-1.863402000	2.155138000	H	8.899279000	-1.207215000	2.113673000
H	6.862352000	-3.042156000	3.754526000	H	7.155925000	-2.791979000	3.378491000
H	5.471547000	-0.057186000	1.127859000	H	5.374870000	0.321011000	1.169651000
H	4.338278000	-3.333436000	3.536719000	H	4.711574000	-3.399182000	3.061510000
H	7.706325000	3.248368000	1.584911000	H	7.448357000	3.793183000	1.541842000
H	6.449442000	2.730351000	-0.522945000	H	6.214148000	3.218491000	-0.569837000
H	5.751154000	4.339348000	-0.502609000	H	5.415829000	4.781219000	-0.523341000
H	6.803392000	6.144235000	1.058092000	H	6.387794000	6.637095000	1.026724000
H	8.042079000	5.642092000	2.221100000	H	7.649128000	6.196283000	2.190211000
H	6.346936000	5.201660000	2.476264000	H	5.978426000	5.666572000	2.439696000
H	4.154293000	2.634925000	0.440035000	H	3.937027000	2.970765000	0.412446000
H	4.582102000	3.838424000	1.659166000	H	4.308173000	4.177530000	1.647251000
H	5.329232000	2.233426000	1.706524000	H	5.151318000	2.620592000	1.656652000
H	-3.301839000	3.535127000	8.120526000	H	-3.698866000	3.290819000	8.059680000
H	-4.325628000	2.601321000	7.018160000	H	-4.338746000	2.370164000	6.689089000
H	-1.574542000	1.730817000	8.054880000	H	-1.833404000	1.645310000	8.301726000
H	-3.418749000	0.366809000	6.020861000	H	-3.012733000	0.309531000	5.806894000
H	-3.090584000	-0.217882000	7.660653000	H	-3.016992000	-0.380690000	7.439529000
H	-1.785593000	-0.170846000	6.454437000	H	-1.481915000	-0.136675000	6.582894000
H	-0.797968000	2.052052000	5.703554000	H	-0.563585000	2.224320000	6.232281000
H	-1.410568000	3.576839000	6.368754000	H	-1.467693000	3.630445000	6.819235000
H	-2.402218000	2.639464000	5.243917000	H	-2.066833000	2.709574000	5.432460000
H	-2.102287000	10.248740000	1.604952000	H	-2.765739000	10.202486000	1.749286000
H	-1.973006000	9.592283000	3.243575000	H	-2.569129000	9.469578000	3.348445000
H	-2.956858000	8.360310000	-0.145473000	H	-3.528423000	8.388238000	-0.099489000
H	-2.709093000	5.866734000	-0.383374000	H	-3.173977000	5.926965000	-0.483434000
H	-0.030111000	7.457266000	4.019356000	H	-0.544554000	7.358123000	4.001590000
H	-1.458714000	3.720039000	0.984653000	H	-1.753024000	3.783327000	0.687679000
H	0.621281000	5.110557000	4.499156000	H	0.223841000	5.021028000	4.319721000
H	-0.084170000	3.269739000	3.007035000	H	-0.364356000	3.256090000	2.686902000

H	3.591816000	7.011586000	-1.859759000	H	3.087850000	7.249440000	-1.885985000
H	2.376615000	7.514666000	-0.851435000	H	1.884591000	7.729522000	-0.853327000
H	3.762094000	4.914347000	-0.746403000	H	3.367156000	5.184441000	-0.745124000
H	1.463656000	5.985464000	0.955429000	H	1.097588000	6.203026000	1.024419000
H	2.255632000	4.414132000	1.144939000	H	1.958140000	4.669070000	1.213101000
H	3.791938000	6.740448000	1.134060000	H	3.400963000	7.051306000	1.097527000
H	1.220091000	6.546423000	-2.302155000	H	0.732618000	6.686008000	-2.273280000
H	-0.388395000	4.089996000	-2.475736000	H	-0.768001000	4.157825000	-2.367935000
H	1.291529000	3.975559000	-4.337454000	H	1.030020000	4.101357000	-4.157036000
H	-1.242671000	6.605524000	-3.917730000	H	-1.723700000	6.509650000	-3.991915000
H	-1.258936000	6.656811000	-2.154602000	H	-1.773312000	6.704880000	-2.239882000
H	-2.758385000	4.716263000	-2.057261000	H	-3.148086000	4.673397000	-2.009178000
H	-3.758346000	6.899096000	-3.974385000	H	-4.274484000	6.641258000	-4.082538000
H	-3.730130000	7.044644000	-2.215768000	H	-4.256419000	6.927827000	-2.341179000
H	-4.792753000	5.856937000	-2.988516000	H	-5.239654000	5.615487000	-3.011579000
H	-2.766441000	4.741266000	-5.109874000	H	-3.120430000	4.478365000	-5.051942000
H	-3.865556000	3.806763000	-4.075381000	H	-4.174305000	3.557341000	-3.958894000
H	-2.141175000	3.448575000	-4.072908000	H	-2.431100000	3.308654000	-3.915449000
H	3.686850000	2.343119000	-4.708309000	H	3.525511000	2.526503000	-4.803306000
H	2.853567000	2.433900000	-3.292389000	H	2.826022000	2.636380000	-3.322173000
H	3.144162000	0.073255000	-4.440815000	H	2.951557000	0.267151000	-4.434119000
H	0.987102000	1.573173000	-6.025474000	H	0.760018000	1.809583000	-5.933664000
H	0.451532000	1.105871000	-3.368350000	H	0.329885000	1.387569000	-3.271995000
H	1.802911000	0.597375000	-2.353027000	H	1.713677000	0.894669000	-2.295788000
H	1.001345000	-0.580756000	-3.415154000	H	0.857496000	-0.307899000	-3.286325000
H	-5.363165000	-1.043632000	4.825833000	H	-5.346051000	-1.330484000	5.117936000
H	-6.482713000	-1.599318000	3.572716000	H	-6.323238000	-1.837481000	3.733509000
H	-4.351767000	-2.939473000	3.559974000	H	-4.047985000	-2.905454000	3.670650000
H	-5.738692000	-3.962240000	3.906471000	H	-5.303380000	-4.123743000	3.811986000
H	-4.091800000	-2.722719000	6.169943000	H	-3.876428000	-2.998746000	6.283565000
H	-5.215293000	-4.055604000	6.276478000	H	-4.908045000	-4.405799000	6.204425000
H	-3.638361000	-5.532828000	5.461966000	H	-3.209106000	-5.682585000	5.315881000
H	-1.777230000	-6.102026000	4.196513000	H	-1.160881000	-6.096762000	4.519692000
H	-0.621873000	-4.847612000	3.811439000	H	-0.144289000	-4.800032000	4.001502000
H	-1.011366000	-2.752932000	4.204475000	H	-0.701883000	-2.520618000	4.599134000
H	-2.329446000	-2.221361000	5.221931000	H	-2.307812000	-2.286545000	5.175051000
H	-8.086915000	3.469395000	0.733244000	H	-8.350017000	2.995393000	0.904503000
H	-7.503245000	3.522217000	-1.461391000	H	-7.773282000	3.110462000	-1.298585000
H	-4.759296000	3.171960000	-1.645178000	H	-4.995231000	2.890918000	-1.474084000
H	-5.491153000	4.695431000	-1.108941000	H	-5.828816000	4.393095000	-1.038741000
H	-4.060639000	4.139214000	0.810314000	H	-4.390285000	4.053381000	0.917716000
H	-4.486122000	2.426507000	0.685146000	H	-4.685161000	2.307696000	0.888007000
H	-6.051114000	3.230531000	2.388741000	H	-6.314704000	3.089197000	2.543537000
H	-6.299308000	4.751355000	1.509755000	H	-6.690014000	4.520678000	1.563648000
H	-7.186939000	1.024048000	0.500764000	H	-7.220940000	0.630972000	0.706390000
H	-6.860005000	-0.983802000	-1.707617000	H	-6.866017000	-1.293283000	-1.556785000
H	-9.239637000	-0.620902000	-0.636882000	H	-9.237807000	-1.073704000	-0.414818000
H	-6.150059000	-2.629089000	0.112314000	H	-6.061321000	-2.987420000	0.182341000
H	-6.052316000	-1.261822000	1.234943000	H	-5.968646000	-1.657795000	1.349097000
H	-4.516171000	-0.360038000	-0.428347000	H	-4.499034000	-0.646894000	-0.290966000
H	-3.989059000	1.987767000	8.644783000	H	-4.332720000	1.654555000	8.308862000
H	-6.755683000	-2.045531000	5.259797000	H	-6.617542000	-2.544516000	5.325488000
H	-0.518627000	9.841429000	2.281956000	H	-1.149347000	9.849411000	2.377909000
H	8.160653000	4.208067000	0.195608000	H	7.841188000	4.781644000	0.154024000
H	0.777559000	-8.960004000	-2.481265000	H	1.908729000	-8.629615000	-3.277321000
H	-2.399728000	-7.559328000	2.123690000	H	-2.001403000	-7.679237000	2.100750000
N	-5.394724000	0.345886000	-5.260968000	N	-5.604918000	0.047253000	-4.976101000
C	-4.533422000	-0.777189000	-4.832599000	C	-4.594360000	-0.987456000	-4.705613000
C	-5.222261000	-1.426108000	-3.656437000	C	-5.223554000	-2.055742000	-3.840674000
O	-6.032093000	-2.335969000	-3.739026000	O	-5.688991000	-3.101479000	-4.258451000
C	-3.147764000	-0.224487000	-4.453108000	C	-3.369163000	-0.346967000	-4.029680000
C	-2.141657000	-1.282197000	-4.056694000	C	-2.252668000	-1.333855000	-3.771517000
C	-1.148486000	-1.686312000	-4.958077000	C	-1.241017000	-1.528654000	-4.721115000
C	-2.173718000	-1.883330000	-2.787696000	C	-2.222589000	-2.099631000	-2.596320000
C	-0.206954000	-2.655201000	-4.605127000	C	-0.222858000	-2.458964000	-4.504258000
C	-1.242760000	-2.861475000	-2.434966000	C	-1.216422000	-3.043956000	-2.382121000
C	-0.251338000	-3.247104000	-3.341210000	C	-0.209906000	-3.223217000	-3.334436000
H	-5.611923000	0.927147000	-4.448880000	H	-5.952717000	0.431526000	-4.096053000
H	-6.288573000	-0.026447000	-5.576941000	H	-6.403044000	-0.371455000	-5.449276000
H	-5.021922000	-0.939253000	-2.687681000	H	-5.307384000	-1.780813000	-2.769843000
H	-3.279764000	0.489115000	-3.631249000	H	-3.690941000	0.116027000	-3.090735000
H	-1.094180000	-1.219456000	-5.937144000	H	-1.235452000	-0.932306000	-5.628836000
H	-2.925245000	-1.585787000	-2.064838000	H	-2.991914000	-1.957831000	-1.846057000

H	-1.294260000	-3.318611000	-1.452170000	H	-1.222491000	-3.636484000	-1.472959000
H	0.479118000	-4.000029000	-3.063133000	H	0.580892000	-3.947266000	-3.163089000
H	0.570482000	-2.928806000	-5.311553000	H	0.568112000	-2.565441000	-5.239732000
H	-4.457005000	-1.496793000	-5.653786000	H	-4.300888000	-1.450582000	-5.654214000
H	-2.777462000	0.344050000	-5.310876000	H	-3.024393000	0.461751000	-4.681429000
H	-2.959291000	-0.351918000	0.795135000	H	-2.831159000	-0.730842000	0.875369000
N	-2.093720000	1.314772000	-1.118232000	N	-2.281687000	1.293569000	-0.786613000
O	-3.284186000	0.980980000	-1.224766000	O	-3.434622000	0.841693000	-0.881818000
O	-1.509321000	1.972340000	-1.976827000	O	-1.865191000	2.191533000	-1.518918000
O	1.219159000	-2.933753000	5.840660000	O	1.949243000	-3.245195000	5.643811000
H	0.905779000	-2.015705000	5.827405000	H	1.503214000	-2.405692000	5.401726000
H	0.994925000	-3.223586000	4.928169000	H	1.779912000	-3.760358000	4.836110000

Int2			TS3				
C	1.358708000	-2.987511000	1.705510000	C	1.354032000	-3.054400000	1.758730000
C	1.033357000	-3.106646000	0.230884000	C	1.694377000	-3.867216000	0.525110000
C	1.983251000	-2.326244000	-0.688370000	C	2.558835000	-3.107057000	-0.475139000
C	3.383596000	-2.259708000	-0.067287000	C	3.765263000	-2.540792000	0.262632000
C	3.291488000	-1.379646000	1.181930000	C	3.320393000	-1.491678000	1.286247000
C	2.273171000	-1.891549000	2.211805000	C	2.195295000	-1.948176000	2.205112000
O	0.895373000	-3.783639000	2.506014000	O	0.388101000	-3.424624000	2.444564000
C	1.476427000	-0.687075000	2.895692000	C	1.466345000	-0.728431000	2.857277000
C	0.407126000	-0.172751000	1.942235000	C	0.380440000	-0.183186000	1.955182000
C	-0.861729000	-0.775705000	1.934337000	C	-0.905816000	-0.750675000	1.933977000
C	-1.842502000	-0.362453000	1.045192000	C	-1.862399000	-0.309332000	1.033077000
C	-1.545625000	0.670401000	0.148318000	C	-1.531824000	0.715833000	0.141704000
C	-0.302135000	1.307700000	0.138045000	C	-0.272499000	1.321648000	0.147161000
C	0.661636000	0.879328000	1.048734000	C	0.671539000	0.864574000	1.064457000
O	0.996755000	-1.049820000	4.123470000	O	0.957100000	-1.019824000	4.156280000
C	-0.867541000	-7.013866000	1.914729000	C	-0.928038000	-7.061866000	1.630401000
C	-1.785757000	-6.122786000	1.144447000	C	-1.844721000	-6.170457000	0.856417000
C	-2.026208000	-4.784993000	1.360491000	C	-2.065138000	-4.825710000	1.054774000
C	-2.615326000	-6.510994000	0.031967000	C	-2.693809000	-6.565106000	-0.237954000
N	-2.959655000	-4.318036000	0.454049000	N	-3.002763000	-4.360241000	0.151824000
C	-3.339952000	-5.352448000	-0.373740000	C	-3.405819000	-5.401840000	-0.655454000
C	-2.812123000	-7.717688000	-0.662448000	C	-2.917277000	-7.780965000	-0.907799000
C	-4.240701000	-5.378155000	-1.443792000	C	-4.323394000	-5.433620000	-1.710267000
C	-3.702153000	-7.743434000	-1.731626000	C	-3.823107000	-7.813028000	-1.962880000
C	-4.407770000	-6.583232000	-2.117600000	C	-4.518453000	-6.649895000	-2.357780000
C	2.413603000	-7.849988000	-2.032157000	C	2.371101000	-7.783742000	-2.324020000
C	0.901745000	-7.740822000	-1.773970000	C	0.953060000	-7.415216000	-1.856267000
C	3.063964000	-6.517459000	-2.424592000	C	3.278891000	-6.567324000	-2.537329000
C	0.070798000	-7.446241000	-3.026577000	C	0.099643000	-6.723647000	-2.923686000
N	7.580780000	-5.351716000	-1.330023000	N	7.407865000	-5.209992000	-1.740618000
C	6.630682000	-4.570723000	-0.523195000	C	6.600792000	-4.587533000	-0.678322000
C	7.415364000	-3.546015000	0.263577000	C	7.476778000	-3.591330000	0.044957000
O	7.475500000	-2.360538000	-0.028688000	O	7.390730000	-2.380140000	-0.094975000
C	5.836193000	-5.502243000	0.388619000	C	6.061758000	-5.662278000	0.261823000
N	8.113042000	-0.872704000	-2.711559000	N	8.169345000	-0.772297000	-2.770946000
C	7.152506000	0.222359000	-2.503923000	C	7.166397000	0.267373000	-2.489187000
C	7.623265000	1.130601000	-1.370051000	C	7.625612000	1.123037000	-1.311936000
O	7.613353000	2.361239000	-1.459803000	O	7.657478000	2.355903000	-1.362516000
C	5.694573000	-0.237681000	-2.238286000	C	5.727424000	-0.259503000	-2.234254000
C	4.749942000	0.945890000	-2.006526000	C	4.745989000	0.878574000	-1.930816000
C	5.183350000	-1.128677000	-3.375086000	C	5.225978000	-1.111249000	-3.404172000
N	7.981574000	0.500120000	-0.222297000	N	7.932619000	0.445466000	-0.174966000
C	8.175750000	1.237802000	1.012909000	C	8.175224000	1.153738000	1.066482000
C	9.569217000	1.863596000	1.035111000	C	9.583309000	1.750551000	1.069571000
O	10.291340000	1.874787000	2.009051000	O	10.269424000	1.854273000	2.064043000
C	7.955586000	0.352580000	2.240482000	C	7.961733000	0.273725000	2.294722000
C	6.644376000	-0.359341000	2.218988000	C	6.590455000	-0.302787000	2.377645000
N	6.404145000	-1.477899000	2.998417000	N	6.214042000	-1.149270000	3.408102000
C	5.503522000	-0.176090000	1.487621000	C	5.515427000	-0.256416000	1.537048000
C	5.181576000	-1.962759000	2.756971000	C	4.976101000	-1.616620000	3.205487000
N	4.610753000	-1.180892000	1.833595000	N	4.529443000	-1.078668000	2.063542000
C	6.646612000	5.117007000	0.680686000	C	6.673997000	5.052549000	0.859696000
C	5.502124000	4.480506000	-0.121460000	C	5.530344000	4.441011000	0.037321000
C	6.260559000	6.396427000	1.430602000	C	6.291965000	6.307899000	1.651150000
C	4.459521000	3.766047000	0.745298000	C	4.481895000	3.701810000	0.876380000
C	-3.694429000	2.779131000	7.377834000	C	-3.703312000	2.580577000	7.380401000
C	-2.479379000	1.843697000	7.364101000	C	-2.513601000	1.613168000	7.373292000

C	-2.870724000	0.433280000	7.820911000	C	-2.918789000	0.240617000	7.924135000
C	-1.830994000	1.812163000	5.972218000	C	-1.928739000	1.476481000	5.959389000
C	-2.922647000	9.360664000	1.984638000	C	-2.874462000	9.314205000	2.254298000
C	-2.868282000	8.007710000	1.339797000	C	-2.831349000	7.981443000	1.567180000
C	-3.486044000	7.638346000	0.170438000	C	-3.444521000	7.656383000	0.382128000
C	-2.173254000	6.832111000	1.817236000	C	-2.154256000	6.782925000	0.2012495000
N	-3.208037000	6.312767000	-0.119178000	N	-3.181325000	6.336749000	0.053878000
C	-2.410428000	5.788013000	0.874560000	C	-2.397283000	5.771549000	1.036062000
C	-1.393256000	6.547545000	2.952820000	C	-1.386065000	6.453611000	3.144069000
C	-1.890751000	4.498269000	1.033488000	C	-1.894895000	4.470988000	1.158810000
C	-0.890308000	5.261178000	3.125048000	C	-0.899392000	5.156586000	3.279425000
C	-1.135741000	4.247101000	2.174786000	C	-1.150417000	4.175526000	2.296528000
N	2.052384000	7.283728000	-1.117652000	N	2.100119000	7.313830000	-0.878798000
C	1.954417000	5.858539000	-0.818871000	C	1.995932000	5.877555000	-0.640395000
C	1.008698000	4.993712000	-1.636598000	C	1.055242000	5.050837000	-1.502477000
O	1.110441000	3.756941000	-1.619272000	O	1.162044000	3.815125000	-1.548454000
C	1.580511000	5.737666000	0.670942000	C	1.608703000	5.694978000	0.839773000
O	2.515664000	6.440608000	1.471399000	O	2.538560000	6.360468000	1.677522000
N	0.036751000	5.629171000	-2.320840000	N	0.080173000	5.715168000	-2.154297000
C	-0.960989000	4.870066000	-3.042643000	C	-0.912583000	4.986452000	-2.913790000
C	-0.313871000	4.201113000	-4.256627000	C	-0.256418000	4.366025000	-4.147934000
O	-0.754314000	3.209818000	-4.799134000	O	-0.700845000	3.405259000	-4.739671000
C	-2.170413000	5.751277000	-3.439103000	C	-2.118153000	5.884284000	-3.284404000
C	-3.539552000	5.048928000	-3.323051000	C	-3.489128000	5.181222000	-3.201431000
C	-4.666049000	6.082789000	-3.451345000	C	-4.612475000	6.221696000	-3.301737000
C	-3.749307000	3.905742000	-4.322222000	C	-3.695771000	4.073165000	-4.239910000
N	2.424819000	2.377354000	-4.371073000	N	2.497837000	2.510808000	-4.344572000
C	2.029074000	0.965936000	-4.392854000	C	2.059471000	1.110837000	-4.380833000
C	1.313198000	0.685385000	-5.702033000	C	1.320194000	0.878131000	-5.686503000
O	1.441658000	-0.332207000	-6.358757000	O	1.463281000	-0.097327000	-6.401434000
C	1.052723000	0.667551000	-3.240959000	C	1.098493000	0.826228000	-3.213603000
C	-5.641243000	-2.435631000	4.880665000	C	-5.688819000	-2.556109000	4.725164000
C	-4.255427000	-3.053192000	4.696738000	C	-4.442094000	-3.429433000	4.634348000
C	-3.551157000	-3.234892000	6.046465000	C	-3.720920000	-3.524412000	5.984783000
N	-2.175229000	-3.715758000	5.925259000	N	-2.410902000	-4.169025000	5.870171000
C	-1.155045000	-2.972171000	5.476515000	C	-1.365601000	-3.588953000	5.267030000
N	0.041934000	-3.545728000	5.240162000	N	-0.274706000	-4.312487000	4.944246000
N	-1.260202000	-1.659864000	5.294797000	N	-1.365074000	-2.285211000	4.999565000
N	-7.497251000	2.106667000	0.821048000	N	-7.500267000	2.134234000	0.812463000
C	-7.240003000	2.015839000	-0.629322000	C	-7.224855000	2.093789000	-0.636792000
C	-7.037488000	0.567338000	-1.081810000	C	-7.031599000	0.659453000	-1.138960000
O	-6.960564000	0.270550000	-2.277485000	O	-6.943094000	0.401321000	-2.342657000
C	-5.971657000	2.880718000	-0.883075000	C	-5.941055000	2.948633000	-0.840920000
C	-5.379616000	3.075446000	0.520779000	C	-5.356573000	3.064112000	0.574562000
C	-6.626667000	3.146906000	1.400423000	C	-6.610138000	3.125763000	1.445867000
N	-6.959816000	-0.328111000	-0.071387000	N	-6.974230000	-0.270445000	-0.158346000
C	-6.929509000	-1.761093000	-0.271462000	C	-6.941664000	-1.695293000	-0.407890000
C	-8.248838000	-2.375025000	0.186436000	C	-8.278501000	-2.322825000	-0.026722000
O	-8.340477000	-3.451495000	0.737320000	O	-8.392663000	-3.420833000	0.475371000
C	-5.735221000	-2.417058000	0.411440000	C	-5.775028000	-2.378297000	0.296275000
O	-4.512404000	-2.075434000	-0.231104000	O	-4.529610000	-2.003532000	-0.279292000
H	2.790998000	-2.341519000	3.054782000	H	2.597975000	-2.518268000	3.308261000
H	1.053128000	-4.177007000	0.002720000	H	2.229270000	-4.763059000	0.871925000
H	-0.006148000	-2.792765000	0.095943000	H	0.748795000	-4.221946000	0.105526000
H	1.607966000	-1.307727000	-0.850484000	H	1.985886000	-2.296023000	-0.940046000
H	2.021984000	-2.800125000	-1.670641000	H	2.884433000	-3.768285000	-1.282426000
H	3.731324000	-3.264968000	0.197740000	H	4.283784000	-3.346005000	0.793302000
H	4.103937000	-1.836394000	-0.767183000	H	4.482672000	-2.092485000	-0.425873000
H	3.005329000	-0.379583000	0.849995000	H	3.028507000	-0.585802000	0.743382000
H	2.244430000	0.105508000	2.975605000	H	2.232211000	0.050557000	2.958467000
H	-1.075967000	-1.572531000	2.634828000	H	-1.150163000	-1.556351000	2.609014000
H	-0.093129000	2.116862000	-0.552821000	H	-0.035968000	2.129888000	-0.536054000
H	1.620777000	1.387499000	1.069578000	H	1.646424000	1.341381000	1.089832000
H	-0.134042000	-7.499487000	1.259237000	H	-0.228187000	-7.590380000	0.972321000
H	-0.315602000	-6.445965000	2.668790000	H	-0.337305000	-6.484236000	2.347681000
H	-1.578193000	-4.125660000	2.088787000	H	-1.586942000	-4.159642000	1.756729000
H	-3.301400000	-3.365583000	0.367337000	H	-3.345823000	-3.406218000	0.083925000
H	-2.270488000	-8.613531000	-0.371931000	H	-2.384269000	-8.679135000	-0.608068000
H	-4.783216000	-4.494146000	-1.750005000	H	-4.859522000	-4.549720000	-2.029438000
H	-3.857442000	-8.667803000	-2.280258000	H	-3.999790000	-8.744446000	-2.493072000
H	-5.090589000	-6.622137000	-2.960564000	H	-5.217191000	-6.698001000	-3.187611000
H	2.903456000	-8.230534000	-1.126873000	H	2.833171000	-8.443763000	-1.579137000
H	0.719967000	-6.958017000	-1.023988000	H	1.024866000	-6.768788000	-0.970618000

H	0.546326000	-8.677210000	-1.325251000	H	0.435090000	-8.324265000	-1.525497000
H	4.146822000	-6.621147000	-2.552448000	H	4.287296000	-6.863180000	-2.844955000
H	2.891702000	-5.757945000	-1.651663000	H	3.372546000	-5.992465000	-1.608913000
H	2.658927000	-6.129243000	-3.364960000	H	2.884411000	-5.893440000	-3.305034000
H	0.338527000	-6.487047000	-3.478891000	H	0.556743000	-5.793974000	-3.273311000
H	-0.995761000	-7.410567000	-2.786546000	H	-0.891631000	-6.479405000	-2.532091000
H	0.222597000	-8.223307000	-3.785180000	H	-0.032917000	-7.374679000	-3.795918000
H	8.230635000	-5.857501000	-0.730594000	H	8.207225000	-5.703981000	-1.347382000
H	8.133481000	-4.744022000	-1.930236000	H	7.770693000	-4.507924000	-2.381132000
H	5.965295000	-4.030339000	-1.204490000	H	5.784187000	-4.037699000	-1.153904000
H	8.017678000	-3.945282000	1.104844000	H	8.282678000	-4.028576000	0.668798000
H	5.311349000	-6.245112000	-0.216756000	H	5.479096000	-6.386238000	-0.312189000
H	5.102361000	-4.951618000	0.983339000	H	5.423017000	-5.232440000	1.038324000
H	6.503179000	-6.029042000	1.079961000	H	6.882504000	-6.193802000	0.755558000
H	7.884877000	-1.647457000	-2.090804000	H	8.013349000	-1.571083000	-2.159082000
H	8.007460000	-1.231520000	-3.655952000	H	8.030600000	-1.118292000	-3.716289000
H	7.163502000	0.854822000	-3.397271000	H	7.145074000	0.949963000	-3.344564000
H	5.737361000	-0.845236000	-1.325874000	H	5.800198000	-0.913204000	-1.357812000
H	4.677027000	1.569606000	-2.902606000	H	4.609642000	1.521607000	-2.806050000
H	5.080009000	1.595742000	-1.192893000	H	5.084665000	1.523383000	-1.115552000
H	3.741640000	0.594877000	-1.769502000	H	3.763279000	0.479591000	-1.660945000
H	5.804083000	-2.019358000	-3.502596000	H	5.871821000	-1.975282000	-3.582523000
H	5.174737000	-0.580860000	-4.324628000	H	5.181478000	-0.521799000	-4.327386000
H	4.160753000	-1.463776000	-3.173808000	H	4.218660000	-1.488036000	-3.198654000
H	8.011071000	-0.512703000	-0.180395000	H	7.938895000	-0.569566000	-0.157994000
H	7.472609000	2.082543000	1.010101000	H	7.493277000	2.015763000	1.095307000
H	9.872775000	2.313777000	0.071243000	H	9.932110000	2.092598000	0.077057000
H	8.043282000	0.973237000	3.136937000	H	8.186455000	0.870683000	3.182826000
H	8.759282000	-0.389192000	2.301800000	H	8.687489000	-0.548885000	2.285790000
H	7.051055000	-1.878675000	3.666048000	H	6.777437000	-1.374678000	4.218031000
H	5.253505000	0.566161000	0.751090000	H	5.377626000	0.259916000	0.605981000
H	4.737996000	-2.804338000	3.259337000	H	4.411859000	-2.272776000	3.868427000
H	7.037017000	4.377784000	1.394854000	H	7.064672000	4.291260000	1.550084000
H	5.931439000	3.768193000	-0.830269000	H	5.961600000	3.747332000	-0.688856000
H	5.013406000	5.263174000	-0.718139000	H	5.046559000	5.241463000	-0.539441000
H	5.949493000	7.176858000	0.726189000	H	5.977906000	7.110634000	0.973577000
H	7.100688000	6.786927000	2.014261000	H	7.135314000	6.678942000	2.242760000
H	5.422903000	6.227106000	2.114660000	H	5.457607000	6.117504000	2.333811000
H	3.675947000	3.313966000	0.126415000	H	3.693900000	3.284297000	0.238954000
H	3.974044000	4.457219000	1.438694000	H	4.002821000	4.368806000	1.597490000
H	4.926798000	2.965659000	1.332708000	H	4.940164000	2.870530000	1.426641000
H	-3.416107000	3.796063000	7.081429000	H	-3.412142000	3.571357000	7.015383000
H	-4.461321000	2.425148000	6.677780000	H	-4.506395000	2.208256000	6.732368000
H	-1.737892000	2.236242000	8.073811000	H	-1.732635000	2.026061000	8.026585000
H	-3.620406000	0.008406000	7.139928000	H	-3.699167000	-0.204790000	7.294289000
H	-3.312115000	0.443048000	8.822892000	H	-3.316498000	0.314632000	8.941789000
H	-2.004087000	-0.236336000	7.843373000	H	-2.066837000	-0.448546000	7.945212000
H	-0.925841000	1.195073000	5.965780000	H	-1.044278000	0.829734000	5.953193000
H	-1.553905000	2.817070000	5.635287000	H	-1.638580000	2.449134000	5.546197000
H	-2.528107000	1.401107000	5.229843000	H	-2.671018000	1.039688000	5.277956000
H	-3.541118000	10.047075000	1.400157000	H	-3.480275000	10.026088000	1.687286000
H	-3.342812000	9.308131000	2.996348000	H	-3.302822000	9.234879000	3.260738000
H	-4.110402000	8.223275000	-0.489877000	H	-4.056756000	8.269065000	-0.264235000
H	-3.604350000	5.791370000	-0.883331000	H	-3.571111000	5.846196000	-0.733723000
H	-1.192562000	7.320764000	3.688951000	H	-1.181438000	7.201184000	3.905219000
H	-2.072584000	3.729177000	0.291561000	H	-2.080504000	3.727044000	0.392538000
H	-0.289774000	5.032063000	4.000340000	H	-0.308007000	4.893047000	4.151261000
H	-0.718978000	3.256553000	2.328613000	H	-0.746313000	3.175742000	2.421706000
H	2.398611000	7.469113000	-2.053058000	H	2.454014000	7.535726000	-1.803373000
H	1.172318000	7.775495000	-0.984558000	H	1.219460000	7.801447000	-0.734633000
H	2.946306000	5.421299000	-0.955116000	H	2.987481000	5.442865000	-0.786931000
H	0.562028000	6.127253000	0.814667000	H	0.590100000	6.081267000	0.991053000
H	1.581850000	4.689980000	0.974601000	H	1.604555000	4.635274000	1.098857000
H	2.752168000	7.221606000	0.941544000	H	2.782816000	7.161745000	1.182617000
H	0.035159000	6.637404000	-2.366407000	H	0.074096000	6.724397000	-2.150963000
H	-1.303756000	4.061011000	-2.390082000	H	-1.261478000	4.152639000	-2.297432000
H	0.605674000	4.699080000	-4.624042000	H	0.672365000	4.870668000	-4.482391000
H	-2.044731000	6.151858000	-4.452606000	H	-1.985790000	6.321870000	-4.281602000
H	-2.173388000	6.614432000	-2.764216000	H	-2.123833000	6.722130000	-2.578374000
H	-3.586917000	4.591506000	-2.323064000	H	-3.544354000	4.690899000	-2.217601000
H	-4.661163000	6.531065000	-4.451218000	H	-4.599951000	6.703944000	-4.285620000
H	-4.565342000	6.899393000	-2.727956000	H	-4.514712000	7.012793000	-2.550111000
H	-5.643253000	5.614290000	-3.299484000	H	-5.591761000	5.750746000	-3.172382000

H	-3.687710000	4.276986000	-5.352012000	H	-3.628475000	4.479099000	-5.256150000
H	-4.741319000	3.464129000	-4.181256000	H	-4.689523000	3.629524000	-4.118675000
H	-3.001034000	3.122159000	-4.203458000	H	-2.949863000	3.284156000	-4.144396000
H	3.380486000	2.494492000	-4.690514000	H	3.460072000	2.601872000	-4.652477000
H	2.350702000	2.761876000	-3.432834000	H	2.424295000	2.888528000	-3.403737000
H	2.877354000	0.273365000	-4.324748000	H	2.890396000	0.395091000	-4.341398000
H	0.629500000	1.501908000	-6.011436000	H	0.612151000	1.692858000	-5.939842000
H	0.142581000	1.265136000	-3.335568000	H	0.208418000	1.456601000	-3.278561000
H	1.525761000	0.927097000	-2.289688000	H	1.603581000	1.056395000	-2.271779000
H	0.780637000	-0.388575000	-3.225967000	H	0.792078000	-0.219838000	-3.204133000
H	-5.572803000	-1.440144000	5.332306000	H	-5.428925000	-1.527754000	5.000577000
H	-6.156065000	-2.332891000	3.920863000	H	-6.214873000	-2.523896000	3.766810000
H	-3.646370000	-2.416321000	4.044912000	H	-3.757441000	-3.019852000	3.882650000
H	-4.328711000	-4.027669000	4.201070000	H	-4.700843000	-4.440954000	4.302259000
H	-3.553321000	-2.300444000	6.618158000	H	-3.594337000	-2.536230000	6.437586000
H	-4.084872000	-3.964591000	6.658663000	H	-4.301759000	-4.110897000	6.698982000
H	-2.015166000	-4.706924000	6.019181000	H	-2.394223000	-5.176404000	5.930789000
H	0.048949000	-4.531225000	5.023452000	H	-0.367565000	-5.317641000	4.973545000
H	0.671781000	-2.980904000	4.667206000	H	0.227811000	-3.956854000	4.123276000
H	-0.457145000	-1.186402000	4.805879000	H	-0.522069000	-1.821076000	4.627978000
H	-2.109221000	-1.169316000	5.515864000	H	-2.127855000	-1.701407000	5.298177000
H	-8.477890000	2.275869000	1.016180000	H	-8.478817000	2.320833000	1.001745000
H	-8.076466000	2.388396000	-1.231496000	H	-8.048091000	2.499125000	-1.235776000
H	-5.278970000	2.405032000	-1.578276000	H	-5.251687000	2.496220000	-1.554734000
H	-6.270712000	3.845351000	-1.303829000	H	-6.221499000	3.937877000	-1.215039000
H	-4.757236000	3.968024000	0.604803000	H	-4.713100000	3.936051000	0.704702000
H	-4.775449000	2.207130000	0.800462000	H	-4.776057000	2.168973000	0.818104000
H	-6.424309000	2.934023000	2.454730000	H	-6.423020000	2.860739000	2.491138000
H	-7.076701000	4.149224000	1.336876000	H	-7.035413000	4.140494000	1.423841000
H	-7.105403000	0.090187000	0.848487000	H	-7.134230000	0.116698000	0.772793000
H	-6.870982000	-1.916942000	-1.356720000	H	-6.840307000	-1.812661000	-1.495096000
H	-9.138476000	-1.747473000	-0.027069000	H	-9.158386000	-1.683912000	-0.247084000
H	-5.833673000	-3.501466000	0.350388000	H	-5.864368000	-3.459320000	0.181783000
H	-5.712829000	-2.137919000	1.472817000	H	-5.797297000	-2.147137000	1.369003000
H	-4.410356000	-1.109324000	-0.280634000	H	-4.432578000	-1.035960000	-0.297063000
H	-4.148229000	2.828215000	8.373430000	H	-4.115335000	2.698146000	8.388434000
H	-6.268809000	-3.055611000	5.529814000	H	-6.389677000	-2.936200000	5.476002000
H	-1.924367000	9.805097000	2.078403000	H	-1.871664000	9.743143000	2.369119000
H	7.476409000	5.341038000	-0.001279000	H	7.503931000	5.296999000	0.184775000
H	2.594514000	-8.595504000	-2.817991000	H	2.306008000	-8.365553000	-3.253296000
H	-1.413008000	-7.816487000	2.426841000	H	-1.478618000	-7.829130000	2.189404000
N	-5.634847000	-0.620824000	-4.778254000	N	-5.694207000	-0.514050000	-4.900231000
C	-4.549922000	-1.580753000	-4.529589000	C	-4.535387000	-1.384427000	-4.643461000
C	-5.099655000	-2.720764000	-3.700566000	C	-4.982017000	-2.514695000	-3.742850000
O	-5.399114000	-3.818574000	-4.135925000	O	-5.351685000	-3.603391000	-4.149965000
C	-3.376050000	-0.873972000	-3.829987000	C	-3.397653000	-0.555040000	-4.025600000
C	-2.182576000	-1.783819000	-3.653881000	C	-2.157995000	-1.374590000	-3.747019000
C	-1.145491000	-1.792143000	-4.594982000	C	-1.189299000	-1.566835000	-4.740931000
C	-2.117960000	-2.681684000	-2.578601000	C	-1.966185000	-1.987815000	-2.500743000
C	-0.066317000	-2.668561000	-4.465160000	C	-0.056566000	-2.344546000	-4.496251000
C	-1.056664000	-3.580630000	-2.459135000	C	-0.838623000	-2.772604000	-2.252264000
C	-0.022967000	-3.570515000	-3.399362000	C	0.123728000	-2.948160000	-3.249161000
H	-6.014318000	-0.274910000	-3.895025000	H	-6.059727000	-0.146233000	-4.020130000
H	-6.399259000	-1.085660000	-5.263749000	H	-6.442737000	-1.058759000	-5.323488000
H	-5.290146000	-2.454628000	-2.640788000	H	-5.027157000	-2.264816000	-2.663738000
H	-3.722876000	-0.498171000	-2.861416000	H	-3.762133000	-0.094804000	-3.100915000
H	-1.171763000	-1.095640000	-5.427967000	H	-1.310137000	-1.085642000	-5.707393000
H	-2.904278000	-2.675830000	-1.833010000	H	-2.707103000	-1.855869000	-1.722225000
H	-1.042029000	-4.284852000	-1.633989000	H	-0.724025000	-3.246500000	-1.282679000
H	0.812444000	-4.256112000	-3.298022000	H	1.012222000	-3.539179000	-3.054230000
H	0.743536000	-2.625471000	-5.186231000	H	0.699343000	-2.444411000	-5.267970000
H	-4.216274000	-1.993258000	-5.488230000	H	-4.207685000	-1.822379000	-5.592868000
H	-3.112750000	-0.000650000	-4.434517000	H	-3.171923000	0.260377000	-4.719701000
H	-2.812906000	-0.836661000	1.039884000	H	-2.841521000	-0.764912000	1.015309000
N	-2.566465000	1.108174000	-0.785313000	N	-2.531870000	1.172488000	-0.803556000
O	-3.676247000	0.549630000	-0.765299000	O	-3.639057000	0.607502000	-0.824350000
O	-2.310051000	2.026421000	-1.565921000	O	-2.261507000	2.108952000	-1.556790000
O	3.153431000	-2.108679000	5.245028000	O	2.759807000	-2.771149000	4.610217000
H	3.214265000	-1.963036000	6.197375000	H	2.416038000	-3.656356000	4.791723000
H	2.320833000	-1.639714000	4.953910000	H	1.615968000	-1.672208000	4.557579000

TS4			P				
C	1.665950000	-3.181607000	2.110894000	C	2.643969000	-2.602341000	2.464843000
C	2.168866000	-4.204363000	1.108976000	C	3.065423000	-3.825158000	1.683479000
C	2.445554000	-3.610904000	-0.268424000	C	2.806847000	-3.759994000	0.182517000
C	3.371706000	-2.400974000	-0.142633000	C	3.254508000	-2.402572000	-0.361716000
C	2.850663000	-1.425495000	0.895907000	C	2.636544000	-1.298463000	0.430763000
C	1.928491000	-1.822871000	1.896635000	C	2.299895000	-1.376941000	1.739426000
O	1.024600000	-3.645802000	3.114869000	O	2.632818000	-2.686445000	3.702477000
C	1.344087000	-0.650567000	2.701030000	C	1.610579000	-0.156762000	2.392314000
C	0.240103000	-0.051546000	1.858177000	C	0.389497000	0.183576000	1.563787000
C	-1.039794000	-0.627797000	1.869238000	C	-0.746791000	-0.633727000	1.670492000
C	-2.016272000	-0.189983000	0.991440000	C	-1.859774000	-0.401020000	0.882600000
C	-1.699715000	0.828228000	0.084352000	C	-1.816626000	0.650897000	-0.037796000
C	-0.447697000	1.446918000	0.069758000	C	-0.705562000	1.482703000	-0.164812000
C	0.511493000	1.004964000	0.975712000	C	0.395349000	1.245706000	0.655413000
O	0.826827000	-0.958727000	3.986526000	O	1.166970000	-0.345190000	3.730983000
C	-0.842639000	-7.113312000	1.457491000	C	-0.019792000	-7.189111000	1.685935000
C	-1.703661000	-6.093557000	0.792538000	C	-0.984715000	-6.247654000	1.045159000
C	-1.833182000	-4.753650000	1.086758000	C	-1.352158000	-4.989598000	1.469228000
C	-2.605093000	-6.363616000	-0.296073000	C	-1.752550000	-6.517031000	-0.143234000
N	-2.767810000	-4.176703000	0.243700000	N	-2.310321000	-4.464853000	0.619321000
C	-3.257359000	-5.138991000	-0.612583000	C	-2.576806000	-5.380377000	-0.374303000
C	-2.911191000	-7.519099000	-1.036809000	C	-1.823128000	-7.605162000	-1.031629000
C	-4.198074000	-5.051510000	-1.643735000	C	-3.462975000	-5.315511000	-1.452988000
C	-3.841838000	-7.431333000	-2.065963000	C	-2.695159000	-7.537015000	-2.113287000
C	-4.478228000	-6.207216000	-2.364281000	C	-3.509220000	-6.401545000	-2.319045000
C	2.468109000	-7.710288000	-2.507734000	C	3.261318000	-7.486195000	-2.337688000
C	1.136551000	-7.172337000	-1.958824000	C	1.790704000	-7.111548000	-2.091234000
C	3.338002000	-6.644701000	-3.183171000	C	4.105357000	-6.337915000	-2.903906000
C	0.164822000	-6.675419000	-3.033209000	C	1.011262000	-6.750130000	-3.358994000
N	7.653258000	-5.252880000	-1.589012000	N	7.828253000	-4.423093000	-1.854702000
C	6.668432000	-4.520193000	-0.777220000	C	7.064399000	-3.750777000	-0.789647000
C	7.421231000	-3.535100000	0.088211000	C	7.969199000	-2.723822000	-0.141167000
O	7.491748000	-2.338203000	-0.145277000	O	7.973447000	-1.536634000	-0.426978000
C	5.847954000	-5.499971000	0.056368000	C	6.554411000	-4.778461000	0.212812000
N	8.173023000	-0.684274000	-2.741898000	N	8.063753000	0.251254000	-2.996134000
C	7.195784000	0.382263000	-2.467546000	C	6.943286000	1.127980000	-2.620671000
C	7.652471000	1.216423000	-1.273330000	C	7.368883000	2.034208000	-1.460429000
O	7.655004000	2.451394000	-1.293261000	O	7.324191000	3.268430000	-1.525797000
C	5.737626000	-0.114610000	-2.253394000	C	5.615452000	0.397719000	-2.269577000
C	4.773424000	1.040471000	-1.959642000	C	4.522597000	1.389171000	-1.852282000
C	5.255410000	-0.926729000	-3.460429000	C	5.148462000	-0.474408000	-3.439109000
N	7.996060000	0.518940000	-0.161152000	N	7.759073000	1.406060000	-0.324360000
C	8.191971000	1.189463000	1.110398000	C	7.901358000	2.156443000	0.910685000
C	9.583511000	1.817311000	1.167868000	C	8.969623000	3.230500000	0.770560000
O	10.238112000	1.921605000	2.183603000	O	8.999413000	4.227216000	1.461639000
C	7.960929000	0.249845000	2.294074000	C	8.274037000	1.207624000	2.066103000
C	6.576206000	-0.304567000	2.317085000	C	7.329809000	0.049145000	2.207352000
N	6.134180000	-1.188645000	3.286194000	N	7.722054000	-1.127793000	2.813621000
C	5.517857000	-0.163905000	1.453823000	C	6.028861000	-0.184510000	1.806508000
C	4.863647000	-1.562455000	3.003495000	C	6.680336000	-2.004419000	2.755896000
N	4.480038000	-0.948890000	1.895365000	N	5.635634000	-1.464438000	2.150463000
C	6.658452000	5.079547000	0.996737000	C	5.892980000	5.821286000	0.729554000
C	5.524242000	4.491418000	0.144396000	C	4.833331000	5.043482000	-0.062435000
C	6.264695000	6.311884000	1.818113000	C	5.364935000	7.018604000	1.526918000
C	4.473558000	3.721680000	0.952499000	C	3.907282000	4.184760000	0.805068000
C	-3.983321000	1.713088000	7.696370000	C	-4.087694000	0.964432000	7.795494000
C	-2.509418000	1.404787000	7.408712000	C	-2.617915000	1.226166000	7.446510000
C	-2.348260000	-0.014578000	6.841085000	C	-2.001757000	0.011204000	6.740571000
C	-1.905673000	2.441179000	6.450485000	C	-2.469383000	2.484670000	6.580448000
C	-2.927505000	9.225691000	2.479295000	C	-4.104015000	8.787977000	2.322943000
C	-2.881501000	7.916540000	1.750890000	C	-3.924546000	7.483660000	1.606799000
C	-3.475725000	7.630334000	0.546373000	C	-4.502707000	7.117566000	0.416111000
C	-2.219752000	6.702332000	2.173503000	C	-3.125793000	6.355832000	2.031624000
N	-3.212660000	6.319525000	0.183583000	N	-4.101278000	5.839441000	0.062766000
C	-2.452083000	5.721150000	1.164947000	C	-3.264338000	5.341985000	1.038491000
C	-1.475312000	6.336702000	3.309752000	C	-2.328776000	6.088953000	3.159602000
C	-1.963284000	4.413915000	1.262333000	C	-2.632798000	4.098332000	1.143374000
C	-1.002713000	5.032195000	3.419433000	C	-1.715040000	4.845249000	3.277574000
C	-1.244080000	4.080440000	2.405762000	C	-1.865356000	3.859408000	2.279052000
N	2.068991000	7.343930000	-0.693891000	N	0.996326000	7.454416000	-0.863450000
C	1.975807000	5.901821000	-0.490436000	C	1.116165000	6.012776000	-0.670320000

C	1.050697000	5.086544000	-1.379976000	C	0.308190000	5.080790000	-1.557477000
O	1.162185000	3.851955000	-1.446126000	O	0.612781000	3.880801000	-1.658564000
C	1.571202000	5.679808000	0.980554000	C	0.757035000	5.726932000	0.801970000
O	2.481818000	6.337576000	1.845109000	O	1.566977000	6.506697000	1.664544000
N	0.080070000	5.758362000	-2.028867000	N	-0.778741000	5.595758000	-2.160523000
C	-0.921916000	5.042719000	-2.789658000	C	-1.696478000	4.734166000	-2.878599000
C	-0.276613000	4.419927000	-4.027127000	C	-0.989609000	4.140941000	-4.095185000
O	-0.718102000	3.448532000	-4.604124000	O	-1.310272000	3.095329000	-4.620183000
C	-2.107808000	5.968353000	-3.157503000	C	-2.973900000	5.513976000	-3.277914000
C	-3.493053000	5.289464000	-3.129646000	C	-4.279219000	4.693185000	-3.237115000
C	-4.593275000	6.357060000	-3.200380000	C	-5.484263000	5.637796000	-3.341967000
C	-3.702471000	4.237475000	-4.224376000	C	-4.367516000	3.596860000	-4.304513000
N	2.482289000	2.639435000	-4.280704000	N	1.978059000	2.723797000	-4.355785000
C	2.084889000	1.229080000	-4.346525000	C	1.730993000	1.279319000	-4.402905000
C	1.362143000	0.997541000	-5.661238000	C	1.004187000	0.937075000	-5.691574000
O	1.529212000	0.033162000	-6.385730000	O	1.202102000	-0.068127000	-6.349798000
C	1.117240000	0.894241000	-3.197309000	C	0.842148000	0.832955000	-3.228608000
C	-5.645748000	-2.724671000	4.653760000	C	-5.268595000	-3.338885000	4.874914000
C	-4.495188000	-3.704710000	4.444485000	C	-3.862717000	-3.791993000	4.467228000
C	-3.722837000	-3.936123000	5.747220000	C	-2.924402000	-3.815157000	5.679515000
N	-2.552308000	-4.797463000	5.567991000	N	-1.598160000	-4.373427000	5.401160000
C	-1.446450000	-4.419993000	4.912397000	C	-0.528606000	-3.703693000	4.956641000
N	-0.548628000	-5.337263000	4.526873000	N	0.613302000	-4.363610000	4.729303000
N	-1.203848000	-3.131663000	4.664355000	N	-0.588460000	-2.391805000	4.718053000
N	-7.514933000	2.037129000	0.850395000	N	-7.823994000	1.020738000	0.984386000
C	-7.212916000	2.042275000	-0.595056000	C	-7.520237000	1.042000000	-0.460677000
C	-6.974291000	0.627471000	-1.132838000	C	-7.091846000	-0.339241000	-0.975411000
O	-6.823600000	0.409084000	-2.337947000	O	-6.885000000	-0.559406000	-2.171962000
C	-5.964614000	2.952024000	-0.758777000	C	-6.401447000	2.102392000	-0.639645000
C	-5.393718000	3.034542000	0.664512000	C	-5.823378000	2.247696000	0.775364000
C	-6.655147000	3.027800000	1.526942000	C	-7.063659000	2.094817000	1.655661000
N	-6.964105000	-0.331183000	-0.179180000	N	-6.982139000	-1.270433000	-0.000003000
C	-6.898236000	-1.748812000	-0.458401000	C	-6.732635000	-2.675256000	-0.231374000
C	-8.231464000	-2.411948000	-0.129054000	C	-7.982741000	-3.488497000	0.086776000
O	-8.335599000	-3.525801000	0.339149000	O	-7.962560000	-4.581948000	0.611115000
C	-5.736625000	-2.416579000	0.270025000	C	-5.528810000	-3.162922000	0.572758000
O	-4.487178000	-1.987750000	-0.257789000	O	-4.333932000	-2.516317000	0.149987000
H	2.090289000	-3.296885000	4.505996000	H	4.139804000	-3.913904000	1.883477000
H	3.076038000	-4.662519000	1.527570000	H	2.586307000	-4.692165000	2.149363000
H	1.414262000	-4.994891000	1.059537000	H	1.736263000	-3.890689000	-0.013683000
H	1.499967000	-3.301330000	-0.723333000	H	3.329279000	-4.575552000	-0.323232000
H	2.893485000	-4.357222000	-0.930610000	H	4.347469000	-2.301629000	-0.290739000
H	4.373130000	-2.731853000	0.144032000	H	2.993464000	-2.286314000	-1.417480000
H	3.477501000	-1.885652000	-1.100669000	H	2.454632000	-0.363855000	-0.094019000
H	2.768797000	-0.400026000	0.549655000	H	2.310180000	0.684755000	2.362953000
H	2.142413000	0.096326000	2.804148000	H	-0.755558000	-1.463680000	2.364702000
H	-1.262504000	-1.431545000	2.558996000	H	-0.676842000	2.288205000	-0.886002000
H	-0.221463000	2.247610000	-0.624467000	H	1.263782000	1.890088000	0.566960000
H	1.483963000	1.486432000	0.985723000	H	0.788575000	-7.469047000	0.999234000
H	-0.316447000	-7.730000000	0.720653000	H	0.439121000	-6.743838000	2.573969000
H	-0.082380000	-6.647495000	2.089812000	H	-1.000516000	-4.423767000	2.318994000
H	-1.319523000	-4.160124000	1.829486000	H	-2.788417000	-3.575151000	0.703889000
H	-3.104507000	-3.219979000	0.262788000	H	-1.202651000	-8.483082000	-0.876069000
H	-2.421152000	-8.462185000	-0.811462000	H	-4.088732000	-4.450803000	-1.606766000
H	-4.683693000	-4.118435000	-1.884520000	H	-2.754436000	-8.368222000	-2.809720000
H	-4.083429000	-8.313848000	-2.651115000	H	-4.184555000	-6.365685000	-3.168438000
H	-5.193241000	-6.152425000	-3.178735000	H	3.703199000	-7.822213000	-1.390934000
H	3.034311000	-8.162749000	-1.683657000	H	1.745446000	-6.270830000	-1.385459000
H	1.340993000	-6.360175000	-1.247746000	H	1.288328000	-7.949950000	-1.592855000
H	0.646904000	-7.965672000	-1.380225000	H	5.161757000	-6.615442000	-2.980377000
H	4.288341000	-7.066365000	-3.526506000	H	4.044350000	-5.451350000	-2.261716000
H	3.570892000	-5.829994000	-2.487571000	H	3.767943000	-6.040546000	-3.901803000
H	2.839345000	-6.202588000	-4.051525000	H	1.420461000	-5.861615000	-3.849270000
H	0.583424000	-5.845247000	-3.609130000	H	-0.037966000	-6.547438000	-3.125738000
H	-0.769640000	-6.328696000	-2.583218000	H	1.042098000	-7.573218000	-4.083021000
H	-0.079881000	-7.479075000	-3.737871000	H	8.630469000	-4.912830000	-1.461184000
H	8.288956000	-5.778958000	-0.991528000	H	8.190611000	-3.740954000	-2.517433000
H	8.219344000	-4.608899000	-2.136935000	H	6.232654000	-3.214943000	-1.258807000
H	6.025118000	-3.948449000	-1.454455000	H	8.722771000	-3.130095000	0.564285000
H	7.992678000	-3.976463000	0.930041000	H	5.931569000	-5.517044000	-0.297620000
H	5.341112000	-6.209026000	-0.602817000	H	5.968561000	-4.295485000	0.996697000
H	5.097821000	-4.978250000	0.655627000	H	7.389603000	-5.303070000	0.689932000
H	6.492857000	-6.063483000	0.739343000	H	8.093945000	-0.546284000	-2.362344000

H	7.961703000	-1.493532000	-2.159837000	H	7.883433000	-0.133055000	-3.919660000
H	8.058758000	-0.996540000	-3.701918000	H	6.755442000	1.808776000	-3.457181000
H	7.205944000	1.073720000	-3.316126000	H	5.827167000	-0.263474000	-1.418944000
H	5.761394000	-0.787722000	-1.387206000	H	4.304133000	2.101385000	-2.655865000
H	4.687381000	1.708390000	-2.822517000	H	4.802376000	1.963635000	-0.965295000
H	5.091540000	1.653696000	-1.113312000	H	3.592403000	0.860685000	-1.625467000
H	3.772639000	0.657647000	-1.738682000	H	5.883420000	-1.244706000	-3.689248000
H	5.881309000	-1.806091000	-3.634183000	H	4.974486000	0.133088000	-4.335505000
H	5.264780000	-0.316177000	-4.371264000	H	4.210319000	-0.980707000	-3.190690000
H	4.229956000	-1.277385000	-3.304913000	H	7.774783000	0.393222000	-0.278782000
H	7.984404000	-0.495232000	-0.163801000	H	6.961817000	2.669326000	1.152223000
H	7.489557000	2.034678000	1.156081000	H	9.756076000	3.006883000	0.020985000
H	9.953134000	2.187219000	0.192153000	H	8.308919000	1.804577000	2.984018000
H	8.179963000	0.802640000	3.212179000	H	9.287181000	0.819755000	1.902782000
H	8.684622000	-0.573928000	2.250148000	H	8.629788000	-1.311614000	3.217850000
H	6.667704000	-1.501491000	4.086142000	H	5.365523000	0.481511000	1.273476000
H	5.439288000	0.419444000	0.555411000	H	6.733534000	-2.999650000	3.172462000
H	4.261566000	-2.220607000	3.614841000	H	6.418589000	5.131463000	1.402863000
H	7.040984000	4.298889000	1.669617000	H	5.347614000	4.400262000	-0.782692000
H	5.964093000	3.823766000	-0.600798000	H	4.236634000	5.755967000	-0.649239000
H	5.041577000	5.308634000	-0.409724000	H	4.910231000	7.760302000	0.859357000
H	5.961348000	7.133987000	1.159120000	H	6.170324000	7.513524000	2.079428000
H	7.098564000	6.665543000	2.433378000	H	4.596620000	6.719914000	2.247939000
H	5.419852000	6.102324000	2.482124000	H	3.178316000	3.650813000	0.184936000
H	3.692487000	3.318301000	0.297715000	H	3.349653000	4.793534000	1.521543000
H	3.985253000	4.364185000	1.689630000	H	4.483504000	3.435087000	1.361780000
H	4.932943000	2.877381000	1.480919000	H	-4.528935000	1.816668000	8.323103000
H	-4.103727000	2.713758000	8.125087000	H	-4.675360000	0.794024000	6.884851000
H	-4.572905000	1.672072000	6.772185000	H	-2.066338000	1.388646000	8.382920000
H	-1.957004000	1.454219000	8.357417000	H	-2.542995000	-0.184706000	5.804420000
H	-2.889302000	-0.106505000	5.889804000	H	-2.062640000	-0.886021000	7.366424000
H	-2.748127000	-0.767121000	7.530044000	H	-0.948392000	0.181706000	6.492972000
H	-1.294028000	-0.249950000	6.655204000	H	-1.417057000	2.691488000	6.356360000
H	-0.844378000	2.241230000	6.265102000	H	-2.887374000	3.364637000	7.080819000
H	-1.991952000	3.456054000	6.853442000	H	-2.994477000	2.363242000	5.624867000
H	-2.421976000	2.423246000	5.482615000	H	-4.781127000	9.446752000	1.772500000
H	-3.518339000	9.960701000	1.925999000	H	-4.520067000	8.641715000	3.327046000
H	-3.373807000	9.116850000	3.475143000	H	-5.177522000	7.673992000	-0.218730000
H	-4.072984000	8.265448000	-0.092244000	H	-4.459193000	5.315453000	-0.718976000
H	-3.603708000	5.850161000	-0.616472000	H	-2.202298000	6.841278000	3.932960000
H	-1.279925000	7.061584000	4.094911000	H	-2.744553000	3.354771000	0.364300000
H	-2.143268000	3.694222000	0.472816000	H	-1.105227000	4.627198000	4.149196000
H	-0.433914000	4.738258000	4.296509000	H	-1.368396000	2.901286000	2.392859000
H	-0.854310000	3.073260000	2.512846000	H	1.306322000	7.756085000	-1.781254000
H	2.436569000	7.590634000	-1.606758000	H	0.051641000	7.795516000	-0.704228000
H	1.181507000	7.820061000	-0.553768000	H	2.162615000	5.739720000	-0.824524000
H	2.973306000	5.480371000	-0.633761000	H	-0.310883000	5.941733000	0.955759000
H	0.545333000	6.049268000	1.127463000	H	0.920850000	4.672973000	1.031610000
H	1.578064000	4.614298000	1.214830000	H	1.679923000	7.351751000	1.195448000
H	2.720591000	7.153627000	1.371905000	H	-0.966228000	6.585068000	-2.092992000
H	0.065523000	6.767062000	-1.998854000	H	-1.974540000	3.897558000	-2.231692000
H	-1.289074000	4.213868000	-2.177339000	H	-0.154193000	4.752152000	-4.489922000
H	0.640302000	4.932622000	-4.380182000	H	-2.853069000	5.971929000	-4.267646000
H	-1.944646000	6.437937000	-4.135606000	H	-3.075650000	6.341441000	-2.566619000
H	-2.116079000	6.781490000	-2.423025000	H	-4.315624000	4.180011000	-2.264475000
H	-3.577412000	4.754705000	-2.171654000	H	-5.493396000	6.140967000	-4.315468000
H	-4.554909000	6.883166000	-4.160935000	H	-5.468066000	6.417378000	-2.572248000
H	-4.492067000	7.111160000	-2.412115000	H	-6.422235000	5.083006000	-3.242483000
H	-5.583707000	5.900993000	-3.107565000	H	-4.301151000	4.031046000	-5.309291000
H	-3.597115000	4.688711000	-5.218180000	H	-5.327364000	3.075609000	-4.225758000
H	-4.711155000	3.817735000	-4.149923000	H	-3.566902000	2.865080000	-4.199641000
H	-2.981740000	3.423815000	-4.145626000	H	2.932113000	2.936580000	-4.627036000
H	3.433940000	2.765911000	-4.608989000	H	1.823429000	3.088434000	-3.419244000
H	2.423659000	2.987045000	-3.327302000	H	2.654460000	0.686805000	-4.382644000
H	2.934046000	0.535349000	-4.309337000	H	0.239050000	1.687389000	-5.977584000
H	0.638061000	1.800150000	-5.909462000	H	-0.130845000	1.328488000	-3.266971000
H	0.200788000	1.484142000	-3.275656000	H	1.324357000	1.110592000	-2.287882000
H	1.591737000	1.139578000	-2.243321000	H	0.689368000	-0.247184000	-3.244127000
H	0.858150000	-0.164912000	-3.201658000	H	-5.252048000	-2.326666000	5.293112000
H	-5.274705000	-1.744468000	4.972667000	H	-5.942590000	-3.334198000	4.013786000
H	-6.213641000	-2.582977000	3.729644000	H	-3.457994000	-3.129447000	3.692868000
H	-3.813664000	-3.323609000	3.675372000	H	-3.899316000	-4.797044000	4.032180000
H	-4.870714000	-4.668718000	4.083274000	H	-2.808674000	-2.815876000	6.109662000

H	-3.407385000	-2.987043000	6.194152000	H	-3.353436000	-4.434760000	6.470783000
H	-4.357204000	-4.422337000	6.490845000	H	-1.503777000	-5.374391000	5.484530000
H	-2.692481000	-5.790193000	5.683311000	H	0.701271000	-5.332561000	4.989074000
H	-0.820360000	-6.306858000	4.496981000	H	1.452746000	-3.862565000	4.440301000
H	0.202620000	-5.019538000	3.908492000	H	0.212090000	-1.840302000	4.399094000
H	-0.360420000	-2.864626000	4.151983000	H	-1.440806000	-1.885044000	4.887022000
H	-1.783649000	-2.409860000	5.057264000	H	-8.818856000	1.100332000	1.152047000
H	-8.499657000	2.203919000	1.025438000	H	-8.394996000	1.308814000	-1.064573000
H	-8.043568000	2.433423000	-1.193902000	H	-5.663670000	1.802073000	-1.383549000
H	-5.257760000	2.555754000	-1.487714000	H	-6.847403000	3.048853000	-0.960662000
H	-6.282284000	3.944573000	-1.092610000	H	-5.310661000	3.197633000	0.936158000
H	-4.777102000	3.919540000	0.831103000	H	-5.116819000	1.437662000	0.982461000
H	-4.790491000	2.148450000	0.884348000	H	-6.827364000	1.811865000	2.686180000
H	-6.467273000	2.729115000	2.562977000	H	-7.624452000	3.040530000	1.683800000
H	-7.108723000	4.030136000	1.539570000	H	-7.241219000	-0.911418000	0.921258000
H	-7.152040000	0.031947000	0.756786000	H	-6.553660000	-2.802904000	-1.304514000
H	-6.764312000	-1.842302000	-1.543992000	H	-8.932521000	-2.995040000	-0.205810000
H	-9.118299000	-1.785557000	-0.357117000	H	-5.388709000	-4.233196000	0.418907000
H	-5.789929000	-3.496988000	0.134085000	H	-5.707287000	-2.992173000	1.642249000
H	-5.801315000	-2.204191000	1.345051000	H	-4.492798000	-1.562259000	0.060527000
H	-4.468704000	-1.018123000	-0.333201000	H	-4.194525000	0.079506000	8.432126000
H	-4.412269000	0.990012000	8.398469000	H	-5.693850000	-4.008812000	5.629447000
H	-6.341332000	-3.084993000	5.419288000	H	-3.150874000	9.315865000	2.448464000
H	-1.924030000	9.643495000	2.625591000	H	6.657251000	6.180434000	0.028213000
H	7.496183000	5.343831000	0.339145000	H	3.306259000	-8.345116000	-3.020732000
H	2.261716000	-8.520373000	-3.220249000	H	-0.510274000	-8.120264000	1.994779000
H	-1.427107000	-7.798301000	2.085142000	N	-5.597436000	-1.107290000	-4.875749000
N	-5.625861000	-0.417038000	-4.948798000	C	-4.466186000	-1.954306000	-4.445969000
C	-4.488395000	-1.314017000	-4.681160000	C	-4.959455000	-2.841188000	-3.310800000
C	-4.977863000	-2.429387000	-3.788717000	O	-5.587877000	-3.874242000	-3.470753000
O	-5.373070000	-3.508771000	-4.194626000	C	-3.300122000	-1.046729000	-4.017013000
C	-3.341098000	-0.509871000	-4.048687000	C	-2.035832000	-1.779564000	-3.621294000
C	-2.111925000	-1.346005000	-3.773811000	C	-1.042394000	-2.043046000	-4.575340000
C	-1.119754000	-1.496104000	-4.751937000	C	-1.818515000	-2.204402000	-2.302393000
C	-1.951005000	-2.013876000	-2.551173000	C	0.133125000	-2.708488000	-4.223938000
C	0.006578000	-2.285656000	-4.515885000	C	-0.643786000	-2.870409000	-1.944918000
C	-0.831047000	-2.813707000	-2.313343000	C	0.337057000	-3.124501000	-2.905239000
C	0.154788000	-2.946962000	-3.294113000	H	-5.985076000	-0.636537000	-4.055660000
H	-6.000781000	-0.060538000	-4.067648000	H	-6.342570000	-1.709905000	-5.220973000
H	-6.375115000	-0.943418000	-5.393657000	H	-4.786546000	-2.435883000	-2.297542000
H	-5.038417000	-2.166385000	-2.713706000	H	-3.650683000	-0.424610000	-3.186732000
H	-3.707945000	-0.055896000	-3.122555000	H	-1.177711000	-1.699115000	-5.596742000
H	-1.217886000	-0.972213000	-5.698590000	H	-2.572953000	-2.018088000	-1.547436000
H	-2.709444000	-1.914037000	-1.783450000	H	-0.506171000	-3.193844000	-0.918073000
H	-0.739235000	-3.333318000	-1.364529000	H	1.250425000	-3.643074000	-2.631289000
H	1.034185000	-3.554661000	-3.106547000	H	0.897607000	-2.879977000	-4.975187000
H	0.779577000	-2.353835000	-5.274169000	H	-4.170113000	-2.592356000	-5.285606000
H	-4.160599000	-1.757781000	-5.627811000	H	-3.094431000	-0.371554000	-4.852795000
H	-3.102209000	0.310044000	-4.732995000	H	-2.732405000	-1.030406000	0.970080000
H	-2.996427000	-0.641836000	0.999030000	N	-2.958691000	0.871467000	-0.901752000
N	-2.700732000	1.253367000	-0.868681000	O	-3.909760000	0.077465000	-0.848927000
O	-3.777868000	0.635389000	-0.921367000	O	-2.948029000	1.833320000	-1.673204000
O	-2.461775000	2.212803000	-1.605042000	H	1.946629000	-0.290870000	4.331671000
O	2.640653000	-2.715709000	5.076092000	O	3.386991000	-0.539281000	5.212024000
H	1.521148000	-1.430657000	4.489822000	H	3.225608000	-0.623166000	6.161736000
H	2.513389000	-3.026680000	5.982057000	H	3.327337000	-1.446776000	4.852282000

4. DNA and protein sequence for the most active variant BH32.14

Mutations from the BH32 Design: L10W, N14I, A19T, A20Y, S22V, L24F, T49A, Y56N, E70R, F87L, S95A, M120V, T122L, D123N, S124R, Q128L, A129S, M130T, F154S, E174K, Y177C, D180P, C186A, C212A

ATGATTCGTGCGGTATTCTTTGATAGCTGGGGTACTCTGATTAGCGTTGA
AGGCACTTATAAAGTGCATTTTAAAATTATGGAGGAAGTCTGGGGTACT
ATCCGCTGAACCCGAAAACCCTGCTGGACGAATACGAGAAACTGGCTCGC
GAAGCGTTCTCTAACAAATGCGGGCAAACCGTATCGTCCGCTGCGTGATAT
CCTGGAACGTGTAATGCGTAAACTGGCGGAAAAGTACGGTTTCAAATACC
CTGAAAACCTTGTGGGAAATCTCCCTGCGTATGGCGCAACGCTACGGCGAG
CTGTACCCGGAAGTGGTGAAGTACTGAAATCTCTGAAAGGTAAATATCA
CGTTGGCGTGATCCTGAATAGGGATACCGAGCTGTCTACGGCATTCTGG
ACGCACTGGGCATCAAAGACCTGTTGACTCCATCACCACGTCTGAAGAA
GCTGGTTTCTCTAAACCGCACCCACGCATCTTCGAACTGGCTCTGAAGAA
AGCCGGCGTTAAAGGCGAGAAAGCAGTGTGTGTTGGTCCTAACCCGGTCA
AAGACGCGGGTGGTTCTAAGAACCTGGGTATGACTAGCATCCTGCTGGAT
CGTAAAGGTGAGAAACGTGAATTCTGGGATAAGGCGGACTTTATCGTCTC
CGACCTGCGCGAAGTTATTAAGATTGTTGACGAACTGAACGGTCAGGGCT
CTCTCGAGTGGAGTCACCCACAGTTTGAGAAA

MIRAVFFDSWGLTISVEGTYKVHFKIMEEVLGDYPLNPKLLDEYEKLAR
EAFSNNAGKPYRPLRDILERVMRKLAEKYGFKYPENLWEISLRMAQRYGE
LYPEVVEVLKSLKGYHVG**VILNR**DEL**ST**AFLDALGIKDLFDSITTSEE
AGF**SK**PHPRIFELALKKAGVKGE**KAVCVGPN**PVKD**AGG**SKNLGMTSILLD
RKGEKREFWDK**AD**FIVSDLREVIVDELNGQGSLEWSHPQFEK

5. Supplementary References

38. Lee, T. S. et al. BglBrick vectors and datasheets: A synthetic biology platform for gene expression. *J. Biol. Eng.* **5**, 12 (2011).
39. Kille, S. et al. Reducing codon redundancy and screening effort of combinatorial protein libraries created by saturation mutagenesis. *ACS Synth. Biol.* **2**, 83-92 (2013).
40. Luo, S., Wang, P. G. & Cheng, J.-P. Remarkable rate acceleration of imidazole-promoted Baylis-Hillman reaction involving cyclic enones in basic water solution. *J. Org. Chem.* **69**, 555-558 (2004).
41. Kataoka, T., Iwama, T., Tsujiyama, S., Iwamura, T. & Watanabe, S. The Chalcogeno-Baylis-Hillman reaction: a new preparation of allylic alcohols from aldehydes and electron-deficient alkenes. *Tetrahedron* **54**, 11813-11824 (1998).

42. Vazquez-Chavez, J. et al. Effect of chiral N-substituents with methyl and trifluoromethyl groups on the catalytic performance of mono- and bifunctional thioureas. *Org. Biomol. Chem.* **17**, 10045-10051 (2019).
43. Wang, F. et al. A highly efficient kinetic resolution of Morita–Baylis–Hillman adducts achieved by N–Ar axially chiral Pd-complexes catalyzed asymmetric allylation. *Chem. Commun.* **47**, 12813–12815 (2011).
44. Kwong, C. K.- W., Huang, R., Zhang, M., Shi, M. & Toy, P. H. Bifunctional polymeric organocatalysts and their application in the cooperative catalysis of Morita-Baylis-Hillman reaction. *Chemistry* **13**, 2369-2376 (2007).
45. Li, G., Wei, H.- X. Gao, J. J. & Caputo, T. D. TiCl₄-mediated Baylis–Hillman and aldol reactions without the direct use of a Lewis base. *Tetrahedron Lett.* **41**, 1-5 (2000).
46. Yang, J. et al. Endohedral functionalized cage as a tool to create frustrated lewis pairs. *Angew. Chem. Int. Ed.* **57**, 14212-14215 (2018).
47. Venable, J. D. et al. Preparation and Biological Evaluation of Indole, Benzimidazole, and Thienopyrrole Piperazine Carboxamides: Potent Human Histamine H₄ Antagonists. *J. Med. Chem.* **48**, 8289-8298 (2005).
48. Comins, D. L. & Killpack, M. O. Lithiation of heterocycles directed by -amino alkoxides. *J. Org. Chem.* **52**, 104-109 (1987).
49. Coelho, F. et al. Ultrasound in Baylis–Hillman reactions with aliphatic and aromatic aldehydes: scope and limitations. *Tetrahedron* **58**, 7437-7447 (2002).
50. Winter, G. et al. DIALS: implementation and evaluation of a new integration package. *Acta Crystallogr. D.* **74**, 85-97 (2018).
51. Emsley, P., Lohkamp, B., Scott, W. G. & Cowtan, K. Features and development of Coot. *Acta Crystallogr. D Biol. Crystallogr.* **66**, 486-501 (2010).
52. Afonine, P. V. et al. Towards automated crystallographic structure refinement with phenix.refine. *Acta Crystallogr. D Biol. Crystallogr.* **68**, 352-67 (2012).
53. Trott, O. & Olson, A. J. AutoDock Vina: improving the speed and accuracy of docking with a new scoring function, efficient optimization, and multithreading. *J Comput. Chem.* **31**, 455-61 (2010).
54. Morris, G. M. et al. AutoDock4 and AutoDockTools4: Automated docking with selective receptor flexibility. *J Comput. Chem.* **30**, 2785-91 (2009).
55. Frisch, M. J. et al. *Gaussian 16* Rev A.03, Wallingford, CT (2016).
56. Becke, A. D. Density-functional thermochemistry. III. The role of exact exchange. *J. Chem. Phys.* **98**, 5648-5652 (1993).
57. Hehre, W., Ditchfield, R. & Pople, J. Further extensions of gaussian-type basis sets for use in molecular orbital studies of organic molecules. *J. Chem. Phys.* **56**, 2257-2261 (1972)
58. Francl, M. et al. Self-consistent molecular orbital methods. XXIII. A polarization-type basis set for 2nd-row elements. *J. Chem. Phys.* **77**, 3654-3665 (1982).
59. Grimme, S., Ehrlich, S. & Goerigk, L. Effect of the damping function in dispersion corrected density functional theory. *J. Comput. Chem.* **32**, 1456-65 (2011).
60. Barone, V. & Cossi, M. Quantum calculation of molecular energies and energy gradients in solution by a conductor solvent model. *J. Phys. Chem.* **102**, 1995-2001 (1998).

61. Cossi, M., Rega, N., Scalmani, G. & Barone, V. Energies, structures, and electronic properties of molecules in solution with the C-PCM solvation model. *J. Comput. Chem.* **24**, 669-681 (2003).
62. Shaik, S., Kumar, D., de Visser, S. P., Altun, A. & Thiel, W. Theoretical perspective on the structure and mechanism of cytochrome P450 enzymes. *Chem. Rev.* **105**, 2279–2328 (2005).
63. Heyes, D. J., Sakuma, M., de Visser, S. P. & Scrutton, N. S. Nuclear quantum tunneling in the light-activated enzyme protochlorophyllide oxidoreductase. *J. Biol. Chem.* **284**, 3762-3767 (2009).

Chapter 9: Enzyme Design and Engineering Pave the Road to Fully Programmable Protein Catalysis

Sarah L. Lovelock¹, Rebecca Crawshaw¹, Sophie Basler², Colin Levy¹, David Baker^{3,4,5}, Donald Hilvert², Anthony P. Green¹

¹Manchester Institute of Biotechnology, School of Chemistry, 131 Princess Street, University of Manchester, Manchester M1 7DN, UK. ²Laboratory of Organic Chemistry, ETH Zürich, Zürich, Switzerland. ³Department of Biochemistry, University of Washington, Seattle, WA 98195. ⁴Institute for Protein Design, University of Washington, Seattle, WA 98195. ⁵Howard Hughes Medical Institute, University of Washington, Seattle, WA 98195.

9.1 Foreword

This chapter consists of a review article submitted to Nature in April 2021, discussing recent progress in the field, including the development of artificial metalloenzymes, enzymes with non-canonical organocatalytic groups and the computational design of *de novo* enzymes from first principles.

9.2 Abstract

We have entered an era where protein structures can be designed with near atomic level precision based on fundamental biophysical principles. The next key challenge is how to embed catalytic sites and substrate binding pockets with the same level of accuracy, to rapidly deliver *de novo* biocatalysts in response to diverse societal demands. At first glance this ambition may appear a distant dream but there are reasons to be optimistic. The interplay of *in silico* design and high-throughput experimentation has afforded artificial enzymes containing metal cofactors and non-canonical organocatalytic groups, shedding light on how protein structure can be optimized to harness the reactivity of non-proteinogenic elements. If we are to capitalize on these advances, we must learn how to reliably design enzymes based on the fundamental principles of transition state stabilization that underpin catalysis. Computational algorithms have enabled the design of primitive catalysts for a narrow, but increasingly complex, series of chemical transformations; however at present extensive laboratory evolution is required to deliver efficient enzymes. Here, we review recent developments in the field and highlight opportunities for innovation to allow us to transition beyond the current state-of-the-art, to a scenario where *in silico* methods can operate in isolation to provide *de novo* biocatalysts suitable for practical applications.

9.3 Introduction

Enzymes are exceptionally powerful catalysts that employ sophisticated active sites to process chemical transformations. The enormous rate accelerations and unrivalled selectivities achievable with enzymes make them attractive catalysts for use in sustainable manufacturing processes.¹⁻³ The field of biocatalysis has advanced to the stage where it is now viewed as a key enabling technology

for the development of a greener and more efficient chemical industry.^{4,5} Rapid progress has been underpinned by several major methodological innovations, including: the availability of rapid, accurate and low cost DNA synthesis and sequencing services; the development of advanced bioinformatics tools and computational modelling methods; and increasingly sophisticated experimental workflows for high-throughput structural and biochemical enzyme characterization.⁶ These advances have led to the availability of an increasingly diverse portfolio of natural enzymes with interesting catalytic functions, which can in principle be exploited by synthetic chemists when devising routes to target molecules. However, natural enzymes are seldom suitable for direct use in chemical processes and protein engineering is typically required to optimize their properties for practical applications. Recent years have seen the emergence of high-throughput protein engineering strategies, most notably directed evolution, for developing biocatalysts that process non-native substrates with high efficiency and selectivity, and that operate effectively under commercially viable process conditions (Figure 1A).^{5,7-9}

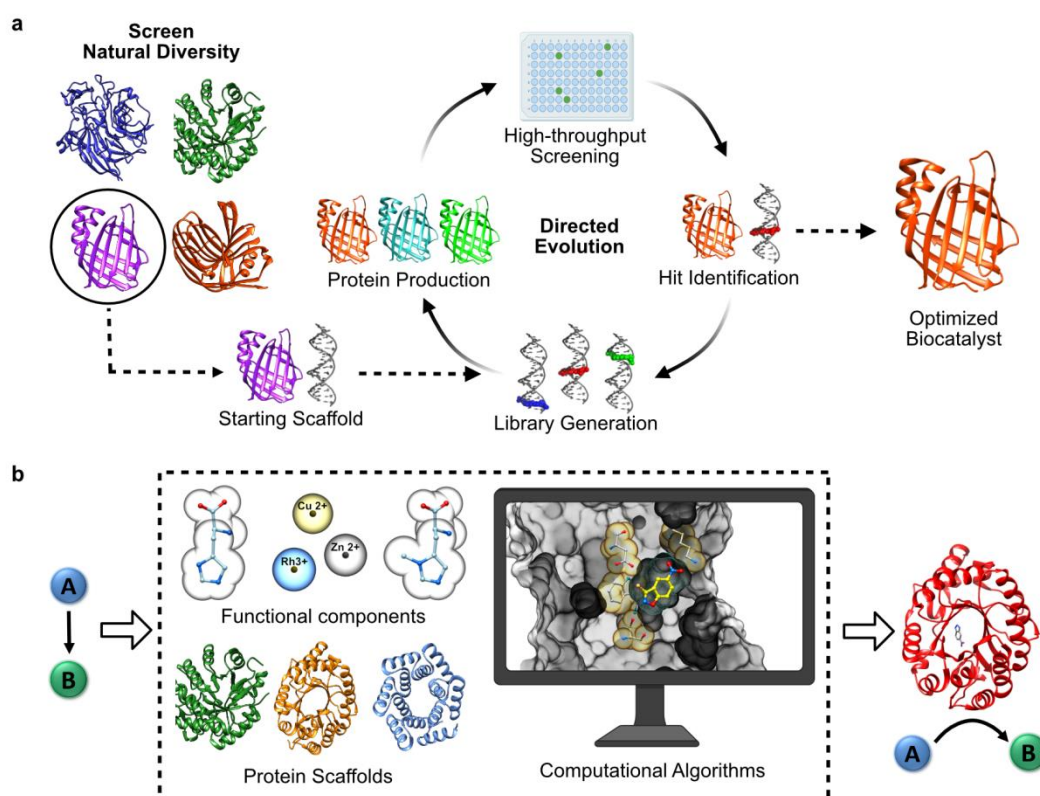


Figure 1. Top down enzyme engineering vs bottom up design. A) Workflow for the development of practically useful biocatalysts. Natural enzymes with desired catalytic activities are identified and their properties optimized via directed evolution. B) Ambition of *de novo* enzyme design. Following selection of a target transformation, computational methods can be used to predict protein sequences with desired catalytic function. Both natural and *de novo* proteins can serve as host scaffolds for new catalytic sites. Canonical & non-canonical amino acid side chains and metal ion cofactors can serve as key functional components in *de novo* active sites.

Although powerful, directed evolution is costly and time consuming which restricts the potential impact of biocatalysis on many industrial processes. Furthermore, for many desirable chemical transformations there are no known enzymes that can serve as starting templates for evolutionary optimization. To address these limitations, ultra-high throughput screening methods¹⁰⁻¹³ and continuous evolution platforms have been developed which offer exciting avenues to accelerate protein engineering,¹⁴⁻¹⁶ while the discovery of mechanistically promiscuous enzymes provides a gateway to catalytic functions not found in Nature.¹⁷⁻²⁰ However these strategies are only amenable to a handful of chemical transformations and do not offer general solutions.

In light of these limitations it is timely to consider how we will deliver a step change in the field, to allow rapid, reliable and cost-effective development of biocatalysts for a broad range of applications. While top-down engineering of natural enzymes undoubtedly remains the gold standard for biocatalyst development, this approach can only take us so far. In our view bottom-up or *de novo* enzyme design, where entirely new catalytic centres are created within protein hosts, could offer a general solution to both the speed and scope of biocatalyst delivery in the future (Figure 1B).²¹⁻²³ Here, we will review key developments to illustrate recent progress in this nascent field, including the development of artificial metalloenzymes, enzymes with non-canonical organocatalytic groups and the computational design of *de novo* enzymes from first principles. This analysis serves as a platform to discuss the limitations of current design approaches, and how we hope to address these challenges moving forward.

9.3.1 Artificial Metalloenzymes

The functional capabilities of natural enzymes are greatly expanded by the recruitment of metal ion cofactors that facilitate redox chemistry, radical processes and challenging functional group conversions. These metalloenzymes benefit from the synergistic action of the metal cofactor and protein scaffold to accelerate some of the most challenging transformations in Nature. The enviable catalytic properties of these systems have inspired the development of complementary approaches to design artificial metalloenzymes. A strategy that has proven particularly versatile involves anchoring pre-assembled transition metal complexes into selected protein scaffolds. This approach has given rise to active catalysts for a wide range of non-biological transformations, including alkene metathesis and transfer hydrogenations.²⁴⁻²⁶ In general though, designing productive interactions between the protein, substrate and transition metal complex has proven challenging, and consequently the catalytic efficiencies achieved by these hybrid systems are often lower than the isolated small-molecule complex. A notable exception involved the design of an enantioselective benzannulase comprising a biotinylated rhodium(III) complex bound to a streptavidin scaffold (Figure 2A).²⁷ This artificial metalloenzyme accelerates the coupling of benzamides and alkenes by *ca.* 100-fold over the isolated complex to generate dihydroisoquinolone products with enantiomeric ratios as high as 93:7. This rate acceleration can be attributed to a designed aspartate or glutamate which serves as a catalytic base and works in tandem with the rhodium cofactor to promote the key C-H activation/orthometallation process.

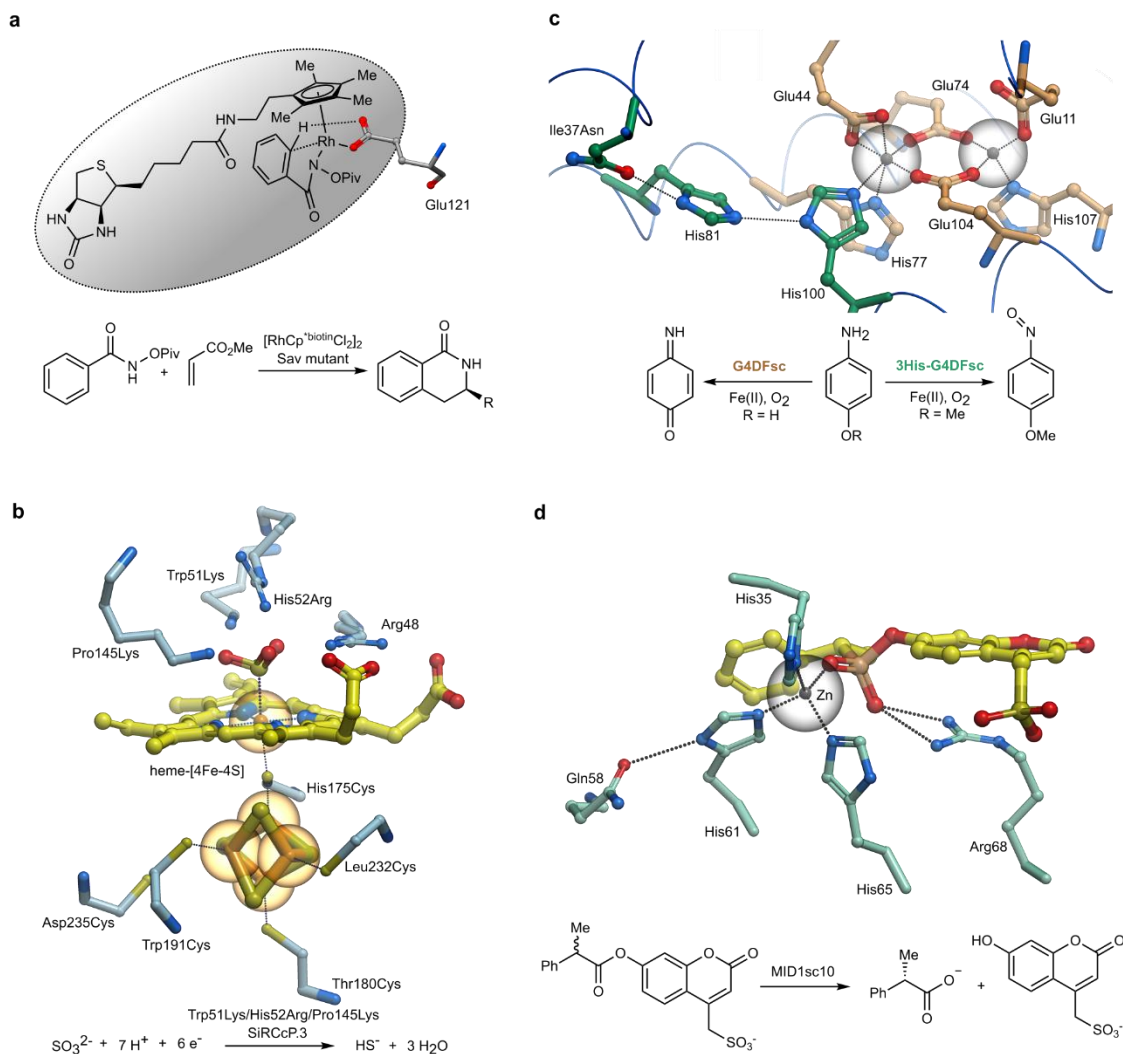


Figure 2. Approaches to *de novo* metalloenzymes. A) Supramolecular anchoring of pre-assembled transition metal complexes into host scaffolds. This approach was used for the development of an enantioselective benzannulase comprising a biotinylated rhodium(III) complex bound to streptavidin. A designed aspartate or glutamate serves as a catalytic base and works in tandem with the rhodium cofactor to promote the key C-H activation/orthometallation process. B) Introduction of new functional components into existing metalloenzymes can lead to new functions. For example, the design of a [4Fe-4S] cluster into an engineered myoglobin gave rise to an artificial sulfite reductase. C) New protein scaffolds have been designed from scratch to bind metal cofactors and modulate catalysis. The ‘Due Ferri’ protein G4DFsc (gold) is a hydroquinone oxidase that employs a carboxylate bridged diiron cofactor as a catalytic centre. Introduction of a third histidine ligand (green) into the metal binding cavity transforms G4DFsc from a hydroquinone oxidase to an arylamine N-hydroxylase. D) A designed homodimeric peptide (MID1) containing two interfacial zinc binding sites served as a starting point for evolutionary optimization to afford an efficient and enantioselective zinc hydrolase MID1sc10.

An alternative approach to metalloenzyme design that has proven particularly effective involves reengineering natural metalloproteins to install new functional elements that work in concert with the native cofactor. Key examples include the development of functional mimics of heme copper oxidases and nitric oxide reductases by engineering copper (Cu_B) and non-heme iron (Fe_B) binding sites, respectively, into the distal pocket of the heme protein myoglobin.^{28,29} In contrast to the native enzymes, the heteronuclear centres of these *de novo* metalloenzymes are built into a small and robust protein scaffold that can be easily produced, engineered and crystallized for high-resolution structural characterization. Such systems provide an ideal basis for elucidating key structural and mechanistic features giving rise to the high efficiencies and selectivities achieved by natural metalloenzymes. The power of this approach was recently exemplified through the design of an artificial enzyme that catalyzes sulfite reduction, a transformation that has thus far eluded synthetic catalysts (Figure 2B).³⁰ Rosetta *Matcher* and *Enzyme Design* algorithms were used to design an iron sulphur cluster into the proximal pocket of cytochrome *c* peroxidase, along with a bridging cysteine ligand which coordinates the native heme cofactor and the designed [4Fe-4S] cluster. The sulfite reductase activity of the initial design was improved by >60-fold through the targeted introduction of positively charged Arg and Lys residues in the substrate binding pocket and a Cys235 residue close to the [4Fe-4S] cluster. The activity of this optimized variant is only *ca.* 5-fold lower than the native sulfite reductase from *Mycobacterium tuberculosis*, with approximately 10% of the products formed arising from complete (6 electron and 7 proton) reduction to hydrogen sulfide.

Creating metalloenzymes 'from scratch', where new protein scaffolds are designed to bind metal cofactors and modulate catalysis, offers the prospect of complete control over metalloprotein sequence, structure and function. Most research in this area has focussed on introducing binding sites for metal ions and metalloporphyrin cofactors into designed α -helical bundles, giving rise to protein catalysts for hydrolytic reactions, redox processes and carbene transfers.³¹⁻³⁶ The introduction of complex dinuclear cofactors such as carboxylate-bridged diiron centres has led to a family of 'Due Ferri' (DF) proteins with a variety of O_2 -dependent activities, including the substrate-gated 4-electron reduction of oxygen to water.^{33,37-39} Interestingly, the catalytic function of these DF proteins can be altered through rational reprogramming of the metal coordination environment (Figure 2C). Specifically, G4DFsc was successfully transformed from a hydroquinone oxidase to an arylamine N-hydroxylase by introducing a third His ligand to the metal binding cavity.³⁹

Metal binding sites have also been designed at the interface of polypeptides or protein subunits to direct the assembly of higher-order structures.⁴⁰ In one instance, a designed homodimeric peptide containing two interfacial zinc binding sites was found to display serendipitous activity for ester bond hydrolysis resulting from a vacant metal coordination site adjacent to a hydrophobic pocket.^{41, 42} Fusion of the N and C termini of the dimer subunits and removal of one of the two zinc binding sites afforded a single chain variant, which was subjected to extensive laboratory evolution to deliver a highly efficient ($k_{\text{cat}}/K_M \sim 10^6 \text{ M}^{-1} \text{ s}^{-1}$) and enantioselective zinc hydrolase (Figure 2D).⁴³ A high resolution crystal structure of the evolved enzyme complexed with a transition state analogue sheds light on the catalytic mechanism, revealing that the catalytic zinc ion is coordinated by 3 histidine ligands and activates the nucleophilic water as a metal hydroxide, while an active site Arg64

stabilizes the anionic transition states through bidentate hydrogen bonding. This simple helical bundle scaffold was subsequently transformed into a proficient catalyst for a bimolecular hetero-Diels-Alder reaction.⁴⁴ Evolution afforded the chemo- and stereoselective metalloenzyme DA7 which uses Lewis acid catalysis and a strategically positioned hydrogen bond network for effective transition state stabilization.

9.3.2 Enzymes with Non-Canonical Amino Acids as Catalytic Elements

Enzyme design strategies are typically reliant on Nature's alphabet of twenty canonical amino acids, which contain a narrow range of functional groups. This limited functionality restricts the range of catalytic mechanisms that can be installed into *de novo* active sites. However, a wider range of functional components can now be accessed using genetic code expansion methods which allow the selective incorporation of structurally diverse non-canonical amino acids (ncAA) into proteins.^{45,46} These methods typically employ an orthogonal aminoacyl-tRNA synthetase (aaRS)-tRNA pair to direct the incorporation of a ncAA in response to an unassigned codon (most commonly UAG) introduced into the gene of interest (Figure 3A). Genetically encoded ncAAs provide new avenues to explore how enzymes operate at the molecular level,⁴⁷⁻⁵¹ and have been used to improve biocatalyst activity and stability.^{52,53} The availability of an expanded set of amino acid building blocks also provides exciting opportunities to design enzymes with new catalytic mechanisms not observed in Nature.⁵⁴

This approach was recently showcased through the design of a *de novo* hydrolase (OE1) that employs *N*_ε-methyl histidine (Me-His) as a non-canonical catalytic nucleophile with a similar mode of reactivity to the widely employed nucleophilic catalyst DMAP (Figure 3B).⁵⁵ Histidine methylation was essential for catalytic function, as it prevented the accumulation of unreactive acyl-enzyme intermediates that compromised the catalytic activity of earlier *de novo* hydrolases equipped with canonical nucleophiles.⁵⁶⁻⁶⁰ Optimization of OE1 was achieved over iterative rounds of evolution using workflows adapted to an expanded genetic code to afford a variant OE1.3, which is 4 orders of magnitude more efficient than equivalent small molecule catalysts in promoting ester hydrolysis, and OE1.4 which is able to promote enantioselective transformations.

A related approach was used to generate *de novo* enzymes to promote the synthesis of oximes and hydrazones (Figure 3C). A *p*-azidophenylalanine residue introduced into the transcriptional regulator protein LmrR was reduced with tris(2-carboxyethyl)phosphine to unmask a *p*-aminophenylalanine residue containing a reactive aniline side chain.⁶¹ While the initial LmrR_pAF variant gave modest activity improvements over the parent protein LmrR, subsequent optimization through targeted rounds of directed evolution afforded a quadruple mutant with a 55-fold improvement in k_{cat} and a 26,000 fold increased efficiency over aniline in solution.⁶² Combined, these studies suggest that the introduction of 'organocatalytic' motifs into evolvable protein scaffolds can offer a general strategy to deliver enzymes which are orders of magnitude more efficient than small organic catalysts used in isolation.

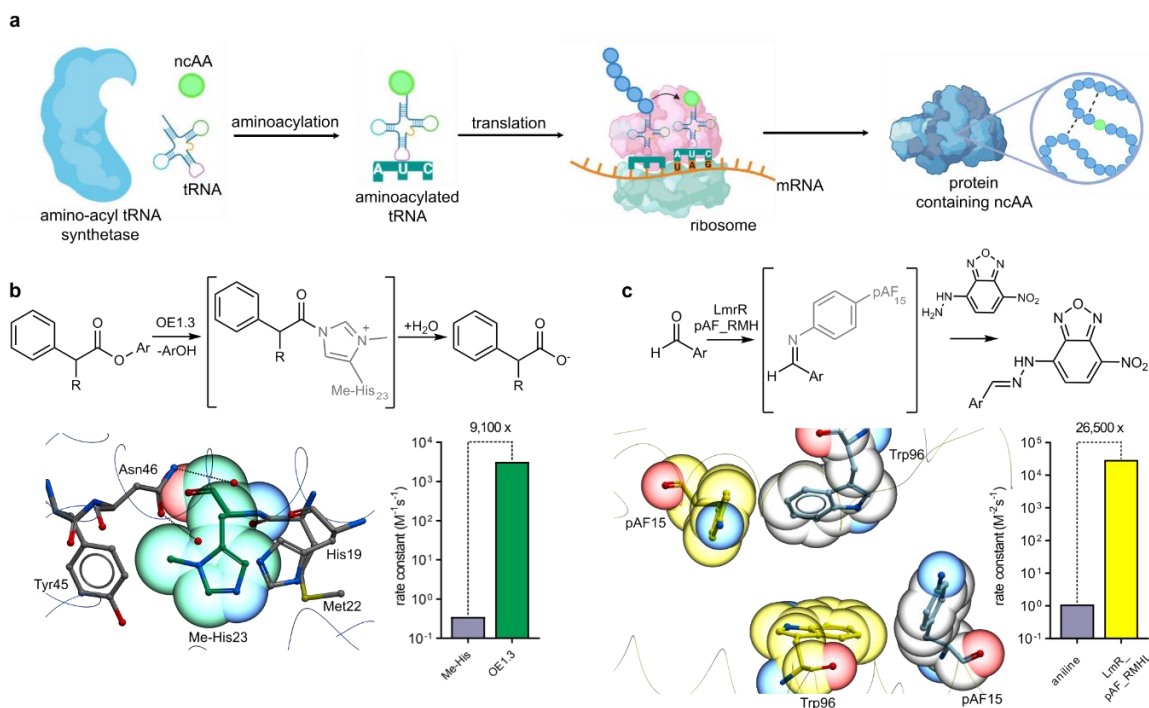


Figure 3. Enzymes with an expanded amino acid alphabet. A) An orthogonal aminoacyl-tRNA synthetase (aaRS) aminoacylates its cognate tRNA with a non-canonical amino acid (ncAA). The aminoacylated tRNA is decoded on the ribosome in response to a UAG codon in the mRNA during translational elongation, leading to the addition of an ncAA to the growing polymer. B) Genetically encoded Me-His residues can serve as non-canonical catalytic nucleophiles to promote enantioselective ester hydrolysis in *de novo* active sites. Histidine methylation is essential for catalytic function as it prevents the formation of unreactive acyl-enzyme intermediates derived from canonical histidine nucleophiles. The bar chart shows the *ca.* 9000-fold rate acceleration achieved by OE1.3 compared with free Me-His in solution. C) Post-translational chemical reduction of a *p*-azidophenylalanine (pAzF) residue installed into an engineered LmrR unmasks a *p*-aminophenylalanine (pAF) catalytic nucleophile designed to promote hydrazone formation.

9.3.3 Designing Enzymes to Stabilize Rate-Limiting Transition States

If we are to capitalize on our ability to install new functional components into proteins, we must learn how to reliably design enzymes based on the fundamental principles of transition state stabilization that underpin catalysis. To this end, early efforts exploited the mammalian immune system to raise antibodies towards stable transition state analogues.⁶³⁻⁶⁸ This approach has delivered catalytic antibodies for a wide range of chemical transformations. However, in general antibodies fail to achieve the efficiencies of natural enzymes and many energetically demanding reactions have proved intractable to this approach.

More recently computational enzyme design has emerged as a powerful and more flexible approach that does not depend on the availability of imperfect transition state analogues and is not restricted to the antibody fold (Figure 4).²¹⁻²³ The design process involves the following general steps; 1) Design and generation of a 'theozyme' – an idealized active site model comprising a quantum mechanically

calculated transition state (TS) and key functional groups from amino acid side chains required for TS stabilization. 2) Docking of the theozyme into structurally characterized proteins to identify sterically complementary scaffolds which can accommodate the key catalytic groups as amino acid side chains linked to the protein backbone. 3) Redesign of residues in and around the active site to optimize packing of the theozyme. To date, this process has allowed the design of primitive protein catalysts for a handful of model transformations.⁶⁹⁻⁷³ Although the activities of the starting designs are typically low, similar to catalytic antibodies, they can be optimized through laboratory evolution.⁷⁴⁻⁷⁷ In favourable cases, this combination of computational design and directed evolution has afforded biocatalysts with efficiencies comparable to natural enzymes. A comprehensive understanding of the molecular changes giving rise to improved activity can then be used to inform the development of improved design protocols.

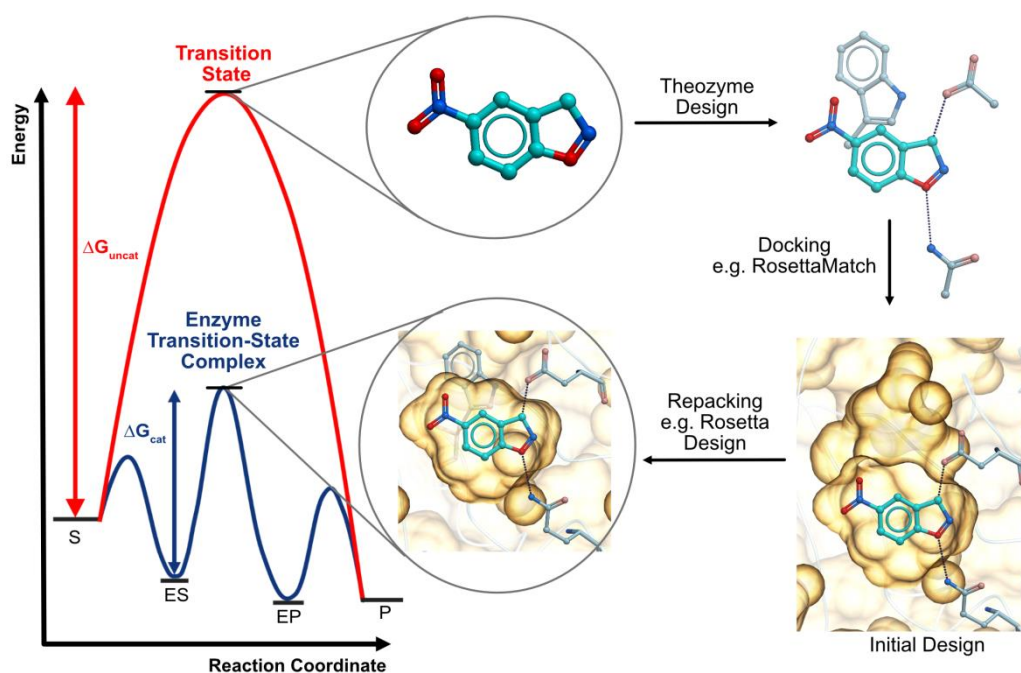


Figure 4. Computational design of enzymes. Reaction profiles of an uncatalyzed (red) and enzyme catalyzed (blue) single-step reaction are shown. Computational methods are used to design new active sites in proteins based on their ability to stabilize rate-limiting transitions states. A typical procedure begins with a quantum mechanically calculated transition state (TS) of a target transformation, termed the theozyme. Key functional groups, such as surrogates of amino acid chains required to stabilize the TS, are explicitly included in the calculation. The resulting ensemble, which represents an idealized model of a minimal active site, is then docked into structurally characterized protein scaffolds using programs such as RosettaMatch. The selected binding pockets are then computationally repacked, for example with RosettaDesign, to optimize interactions between the substrate and the transition state. The designs are subsequently ranked and tested experimentally. Promising designs can be optimized experimentally using directed evolution. The Kemp elimination, involving the conversion of benzisoxazoles into salicylonitriles, has proven a popular target transformation for enzyme designers and provides a valuable model system for

studying proton transfers from carbon (Figure 5A).^{70,71} The evolved enzyme HG3.17 is the most efficient Kemp eliminase reported to date and catalyzes the deprotonation of 5-nitrobenzisoxazole with a $k_{\text{cat}} \sim 700 \text{ s}^{-1}$, which represents a 1000-fold improvement over the parent design (HG3) and is in the range of proton transfer rates observed in many naturally occurring enzymes.⁷⁴ This extraordinary activity can be attributed to highly effective bifunctional catalysis, involving a designed Asp127 catalytic base and a Gln50 that emerged during evolution to stabilize developing negative charge on the phenoxide leaving group, within an active site that is perfectly tuned to accommodate the substrate in a productive pose for catalysis. Subsequent characterization of HG3, HG3.17 and the intermediate variant HG3.7 using a combination of cryo- and high-temperature crystallography, and nuclear magnetic resonance (NMR) spectroscopy reveals that the conformational ensemble of the protein backbone is altered during evolution, to minimize unproductive conformers observed in the HG3 design in favour of a highly active conformational sub-state.^{78,79} Interestingly, this active conformer is not present in the original xylanase scaffold used as the template for design. This analysis suggests that more efficient catalyst sequences could be predicted using improved design protocols that explicitly sample energetically accessible backbone conformers.

Beyond simple proton transfer reactions, the interplay of computational design and directed evolution has afforded highly efficient catalysts for bimolecular aldol^{72,76,80,81} and Diels-Alder reactions.^{73,75,82} The most active aldolase to date, RA95.5-8F, was generated following extensive evolution of the RA95 design (Figure 5B). It cleaves the fluorogenic substrate (*R*)-methadol with a k_{cat} of 10.5 s^{-1} , which is in the range of natural type-I aldolases.⁷⁶ Here the discovery of highly efficient enzymes was facilitated by ultra-high throughput screening of variant libraries by fluorescence activated droplet sorting, allowing evaluation of *ca.* 2000 sequences per second. Interestingly, the originally designed catalytic Lys210, which operates via the formation of Schiff-base intermediates along the reaction coordinate, was abandoned during the course of evolution in favour of Lys83, which is a more reactive catalytic nucleophile. Structural and biochemical characterization of RA95.5-8F reveals that Lys83 forms part of a sophisticated catalytic centre comprising a Lys-Tyr-Asn-Tyr tetrad that emerged adjacent to a designed hydrophobic pocket during laboratory evolution.

In contrast to extensive active site changes observed during optimization of RA95 and HG3, the structure of the most highly evolved Diel-Alderase CE20, which promotes selective cycloaddition of 4-carboxybenzyl*trans*-1,3-butadiene-1-carbamate and *N,N*-dimethylacrylamide, shows good overall agreement to the original design model DA20_00 (Figure 5C).⁷⁵ In particular, the orientation of the bound product and the conformations of the catalytic side chains of Gln208 and Tyr134, which form hydrogen bonding interactions with the diene and dienophile to reduce the HOMO-LUMO energy gap, closely match the design model and changed minimally over the entire evolutionary trajectory. Instead, molecular changes introduced during enzyme optimization gradually reshaped the active site pocket to achieve more effective preorganization of the reactants into productive conformations for the bimolecular reaction. Notably, substantial activity gains were achieved through the introduction of a designed 24-residue helix-turn-helix motif, which was generated in a crowdsourcing experiment using the problem solving skills of online game players and serves as a lid element to close off the solvent exposed active site.⁸²

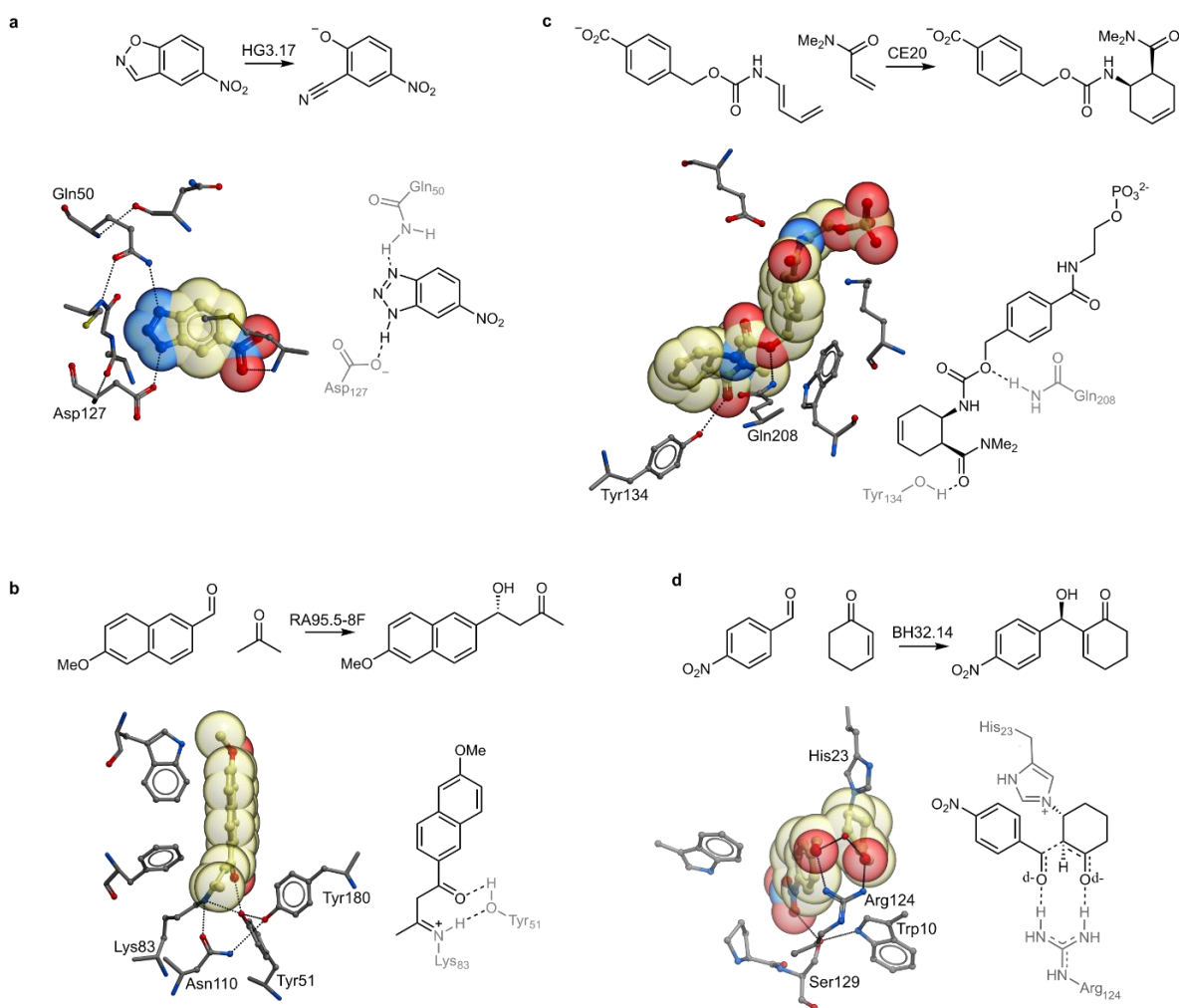


Figure 5. *De novo* enzymes through computational design and directed evolution. A) The Kemp Eliminase HG3.17 employs a designed Asp107 catalytic base and Gln50 as an oxyanion hole to catalyze the deprotonation of 5-nitrobenzisoxazole. B) The evolved retro-aldolase RA95.5-8F utilizes a Lys-Tyr-Asn-Tyr catalytic tetrad to cleave fluorogenic substrate (*R*)-methadol. C) The Diels Alder reaction of 4-carboxybenzyl*trans*-1,3-butadiene-1-carbamate and *N,N*-dimethylacrylamide is accelerated by CE20. Catalytic side chains Gln208 and Tyr134 form hydrogen bonding interactions with the diene and dienophile to reduce the HOMO-LUMO energy gap. D) The enantioselective Morita-Baylis-Hillmanase BH32.14 employs a designed His23 nucleophile and catalytic Arg124 to promote the coupling of 4-nitrobenzaldehyde and 2-cyclohexen-1-one. Arg124 shuttles between conformational states to stabilize multiple oxyanion intermediates and transition states along the complex reaction coordinate.

Given the conceptual similarities between computational enzyme design and catalytic antibody technology, early computational design efforts targeted chemical transformations that were previously achieved with antibodies. If we are to establish design as a useful source of biocatalysts for practical applications, we must move beyond the functional capabilities of antibodies and develop enzymes for more complex chemical processes for which no effective protein catalysts are known.

To this end, an efficient and enantioselective enzyme (BH32.14) for bimolecular Morita-Baylis-Hillman (MBH) reactions was recently developed following extensive evolutionary optimization of a primitive computational design (Figure 5D).^{77,83} Crystallographic, biochemical and computational studies reveal that selective catalysis by BH32.14 is achieved through a sophisticated active site arrangement comprising a designed His23 paired with a judiciously positioned Arg124 which emerged during evolution. This catalytic arginine shuttles between conformational states to provide a highly economical means of stabilizing multiple oxyanion intermediates and transition states along the complex reaction coordinate. Arg124 serves as a genetically encoded surrogate of privileged bidentate hydrogen bonding catalysts commonly employed in organic synthesis to promote a wealth of chemical transformations including the MBH reaction.

9.3.4 A Roadmap to Better Designer Enzymes

The examples presented in this review illustrate great progress made in the field of enzyme design and engineering over the past decade and offer a glimpse into the exciting opportunities that lie ahead. If design is to achieve, or even surpass, the level of practical utility achieved by more established top-down approaches to biocatalyst development there are two central challenges that the community must now address (Figure 6).

First, we must learn how to design highly active enzymes with efficiencies more akin to natural systems. At present, even for relatively simple transformations many designs must be produced and experimentally tested to identify a few displaying desired activity, and extensive evolutionary optimization is required to bridge the efficiency gap to natural enzymes. The development of ultrahigh-throughput enzyme design and screening protocols would facilitate the search for more potent catalysts and could offer a practical route to highly active designs in the medium term. However if we are to overcome our reliance on high-throughput experimentation, we must consider the factors that make enzyme design so challenging. Efficient protein catalysis requires an extremely high degree of precision to achieve effective discrimination of the transition state from the ground state, and even angstrom level inaccuracies in side chain positioning can have a catastrophic impact on catalysis. The design challenge is amplified when targeting multi-step reactions, where carefully orchestrated conformational adjustments are needed for precise recognition of multiple chemical states. Striking the balance between active site preorganization and conformational dynamics will be critical to the future success of enzyme design.

The low success rates and modest activities achieved thus far can, in part, be attributed to the coarse-grained sampling methods and approximate energy calculations employed by existing design algorithms. While these design methods allow for rapid exploration of protein sequence space, this increased speed inevitably comes at the expense of accuracy. Structural characterization of designed enzymes reveals that key catalytic elements are often not positioned as intended.^{57,72,74,83} Accurate placement of polar side chains and the generation of hydrogen bonding networks have proven especially challenging. To address these limitations more sophisticated molecular force fields, that allow accurate treatment of electrostatics and interactions with solvent, are needed to increase model accuracy. Likewise, more intensive calculations, including QM/MM hybrid methods

and MD simulations with explicit solvent, can play an important role in evaluating and refining computational designs to allow more effective discrimination of the transition state relative to the ground state.⁸⁴⁻⁸⁶ Although too slow for routine screening of hundreds of designs, as computational power increases we can expect these methods to be more widely integrated into enzyme design processes in the future.

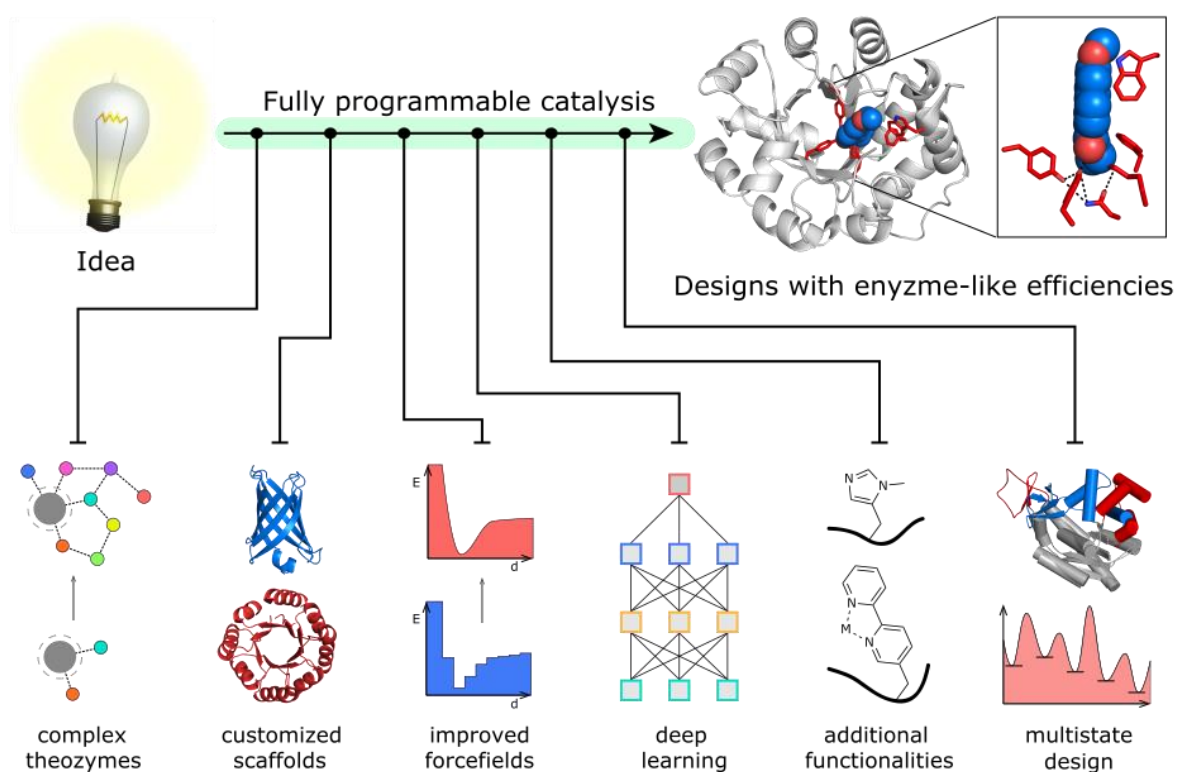


Figure 6. A roadmap to better designer enzymes. The figure illustrates anticipated methodological innovations that will facilitate the design of protein catalysts with enzyme-like efficiencies for a broad range of chemical transformations.

More efficient designs could also be generated through the use of more sophisticated theozyme arrangements. To date, designs have been generated based on simple theozymes containing a small number of functional side chains. In all cases, evolutionary optimization of these designs led to complex arrangements of secondary and tertiary interactions to orientate and fine-tune the reactivity of key catalytic residues, underscoring the importance of extended networks of active site residues.^{74-77,87} While the transition to more complex theozymes could provide a gateway to more active designs, it will be more challenging to identify protein scaffolds with suitable backbone geometries to accommodate the increased number of functional components. New ensemble based design methods that account for backbone flexibility along with methods for sculpting protein backbones could facilitate this search.^{88,89} More ambitious is the design of new protein folds with backbone geometries specifically tailored to accommodate complex theozyme arrangements.⁹⁰ Although yet to be applied to catalysis, the recent design of a fluorescence-activating beta-barrel with a backbone custom built to bind a small fluorescent cofactor,⁹¹ and the design of proteins that undergo

conformational exchanges reminiscent of those observed in natural enzymes,^{88,92} hints at the future potential of this approach.

The emergence of deep learning algorithms that allow accurate prediction of protein structure directly from primary sequence provides exciting new opportunities to design such customized scaffolds.⁹³⁻⁹⁷ Beyond the prediction of protein structure, machine learning has been used to more intelligently navigate sequence space during directed evolution of protein function,⁹⁸⁻¹⁰¹ and to produce proteins from scratch satisfying sets of constraints associated with binding interfaces.¹⁰² A data driven strategy using evolutionary sequence information was also recently employed to generate active mutases that convert chorismate to prephenate.¹⁰³ Interestingly, this transformation has thus far proved intractable to computational approaches based on free energy calculations. A crucial next step is to understand how these 'big-data' approaches can be adapted to tackle new chemical transformations where extensive evolutionary sequence information is lacking. To this end, deep learning methods are now being extended to design proteins containing active sites defined by a collection of residues and their relative geometries. Given a description of such a site and a structure prediction method such as RoseTTAFold⁹⁵ or AlphaFold,^{93,96} sequences that fold to proteins harboring the site might be generated by explicitly optimizing a loss function assessing the extent to which the active site is recapitulated, or by filling in the missing sequence and structure information in a forward pass through versions of the networks optimized to recover both sequence and structure information. Moving forward, we anticipate that hybrid design strategies that combine beneficial aspects of deep learning and fundamental biophysical understanding will prove a fruitful avenue for exploration. Irrespective of the particular design method employed, it is clear that in the search for enzyme-like efficiencies, directed evolution will continue to play a central role in refining the catalytic sites of *de novo* enzymes for the foreseeable future.

Second, we must expand the range of chemistries achievable with *de novo* enzymes, and develop catalysts for valuable chemical processes that can be implemented at scale. To maximize synthetic utility, particular emphasis should be placed on non-biological classes of reaction for which no natural enzymes are known. In these instances, mechanistic strategies employed in small molecule catalysis can be used to inspire theozyme design. Here, broader collaboration between organic chemists and protein designers will prove especially valuable to identify suitable active site arrangements for new target transformations. The range of accessible chemistries can be greatly extended by engineering cellular translation to introduce new functional amino acids into proteins, that can be used to modulate catalysis by metal ion cofactors or that serve as genetically encoded surrogates of small molecule organic catalysts.^{50,55,61,62,104,105} In the field of organocatalysis, large numbers of chemical transformations can be accelerated using a handful of generic activation modes.¹⁰⁶⁻¹¹⁰ Consequently, the addition of a few key amino acids to the genetic code could lead to an explosion of new activities in designed active sites. In the future, enzyme designers and engineers will continue to push the boundaries of the field by developing catalysts for increasingly complex transformations. Here it is likely that existing design protocols that use a single transition structure to approximate all species along the reaction coordinate and generate a static model of the protein-transition state complex will become progressively less effective. Instead, more comprehensive design methods that model

multiple chemical states along the reaction coordinate will be needed to tackle complex reactions involving multiple high-energy transition states.^{111,112}

In summary, although there remain considerable challenges to overcome, we are cautiously optimistic that fully programmable catalysis - where new protein sequences can be predicted from scratch to achieve a desired catalytic function - will become a reality in the future. In our view, this ambitious goal can only be achieved through a collaborative and multidisciplinary effort drawing on expertise in computational chemistry & biology, organic chemistry, enzymology, structural biology, protein design, directed evolution and beyond.

9.4 References

- 1 Savile, C. K. *et al.* Biocatalytic asymmetric synthesis of chiral amines from ketones applied to sitagliptin manufacture. *Science* **329**, 305-309 (2010).
- 2 Huffman, M. A. *et al.* Design of an in vitro biocatalytic cascade for the manufacture of islatravir. *Science* **366**, 1255-1259 (2019).
- 3 Schober, M. *et al.* Chiral synthesis of LSD1 inhibitor GSK2879552 enabled by directed evolution of an imine reductase. *Nat. Catal.* **2**, 909–915 (2019).
- 4 Devine, P.N. *et al.* Extending the application of biocatalysis to meet the challenges of drug development. *Nat. Rev. Chem.* **2**, 409-421 (2018).
- 5 Turner, N. J. Directed evolution drives the next generation of biocatalysts. *Nat. Chem. Biol.* **5**, 567-573 (2009).
- 6 Bornscheuer, U. T. *et al.* Engineering the third wave of biocatalysis. *Nature* **485**, 185-194 (2012).
- 7 Zeymer, C. & Hilvert, D. Directed Evolution of Protein Catalysts. *Annu. Rev. Biochem.* **87**, 131-157 (2018).
- 8 Arnold, F. H. Directed Evolution: Bringing New Chemistry to Life. *Angew. Chem. Int. Ed. Engl* **57**, 4143-4148 (2018).
- 9 Qu, G., Li, A., Acevedo-Rocha, C. G., Sun, Z. & Reetz, M. T. The Crucial Role of Methodology Development in Directed Evolution of Selective Enzymes. *Angew. Chem. Int. Ed. Engl.* **59**, 13204-13231 (2020).
- 10 Fernandez-Gacio, A., Uguen, M. & Fastrez, J. Phage display as a tool for the directed evolution of enzymes. *Trends Biotechnol.* **21**, 408-414 (2003).
- 11 Becker, S., Schmoldt, H. U., Adams, T. M., Wilhelm, S. & Kolmar, H. Ultra-high-throughput screening based on cell-surface display and fluorescence-activated cell sorting for the identification of novel biocatalysts. *Curr. Opin. Biotechnol.* **15**, 323-329 (2004).
- 12 Agresti, J. J. *et al.* Ultrahigh-throughput screening in drop-based microfluidics for directed evolution. *Proc. Natl. Acad. Sci. USA* **107**, 4004-4009 (2010).
- 13 Debon, A., Pott, M., Obexer, R., Green, A.P., Friedrich, L., Griffiths, A.D. & Hilvert, D. Ultrahigh-throughput screening enables efficient single-round oxidase remodelling. *Nat. Catal.* **2**, 740-747 (2019).
- 14 Esvelt, K. M., Carlson, J. C. & Liu, D. R. A system for the continuous directed evolution of biomolecules. *Nature* **472**, 499-503 (2011).
- 15 Bryson, D. I. *et al.* Continuous directed evolution of aminoacyl-tRNA synthetases. *Nat. Chem. Biol.* **13**, 1253-1260 (2017).
- 16 Ravikumar, A., Arzumanyan, G. A., Obadi, M. K. A., Javanpour, A. A. & Liu, C. C. Scalable, Continuous Evolution of Genes at Mutation Rates above Genomic Error Thresholds. *Cell* **175**, 1946-1957 (2018).
- 17 Zhang, R. K. *et al.* Enzymatic assembly of carbon–carbon bonds via iron-catalysed sp³ C-H functionalization. *Nature* **565**, 67-72 (2018).

- 18 Chen, K., Huang, X., Kan, S. B. J., Zhang, R. K. & Arnold, F. H. Enzymatic construction of highly strained carbocycles. *Science* **360**, 71-75 (2018).
- 19 Biegasiewicz, K. F. *et al.* Photoexcitation of flavoenzymes enables a stereoselective radical cyclization. *Science* **364**, 1166-1169 (2019).
- 20 Ji, P., Park, J., Gu, Y., Clark, D. S. & Hartwig, J. F. Abiotic reduction of ketones with silanes catalysed by carbonic anhydrase through an enzymatic zinc hydride. *Nat. Chem.* **13**, 312-318 (2021).
- 21 Kiss, G., Celebi-Olcum, N., Moretti, R., Baker, D. & Houk, K. N. Computational enzyme design. *Angew. Chem. Int. Ed. Engl.* **52**, 5700-5725 (2013).
- 22 Hilvert, D. Design of protein catalysts. *Annu. Rev. Biochem.* **82**, 447-470 (2013).
- 23 Baker, D. An exciting but challenging road ahead for computational enzyme design. *Protein Sci.* **19**, 1817-1819 (2010).
- 24 Jeschek, M. *et al.* Directed evolution of artificial metalloenzymes for in vivo metathesis. *Nature* **537**, 661-665 (2016).
- 25 Zhao, J. *et al.* Genetic Engineering of an Artificial Metalloenzyme for Transfer Hydrogenation of a Self-Immolative Substrate in Escherichia coli's Periplasm. *J. Am. Chem. Soc.* **140**, 13171-13175 (2018).
- 26 Rebelein, J. G. & Ward, T. R. In vivo catalyzed new-to-nature reactions. *Curr. Opin. Biotechnol.* **53**, 106-114 (2018).
- 27 Hyster, T. K., Knorr, L., Ward, T. R. & Rovis, T. Biotinylated Rh(III) complexes in engineered streptavidin for accelerated asymmetric C-H activation. *Science* **338**, 500-503 (2012). **Development of an artificial benzannulase in which a designed carboxylate works in tandem with the rhodium cofactor to promote the key C-H activation/orthometallation process.**
- 28 Bhagi-Damodaran, A., Michael, M., Zhu, Q. *et al.* Why copper is preferred over iron for oxygen activation and reduction in haem-copper oxidases. *Nat. Chem.* **9**, 257-263 (2017).
- 29 Yeung, N. *et al.* Rational design of a structural and functional nitric oxide reductase. *Nature* **462**, 1079-1082 (2009).
- 30 Mirts, E. N., Petrik, I. D., Hosseinzadeh, P., Nilges, M. J. & Lu, Y. A designed heme-[4Fe-4S] metalloenzyme catalyzes sulfite reduction like the native enzyme. *Science* **361**, 1098-1101 (2018). **Installation of an iron sulphur cluster into cytochrome c peroxidase affords an artificial enzyme for sulphite reduction, a transformation that has thus far eluded synthetic catalysts.**
- 31 Hill, R. B., Raleigh, D. P., Lombardi, A. & DeGrado, W. F. De novo design of helical bundles as models for understanding protein folding and function. *Acc. Chem. Res.* **33**, 745-754 (2000).
- 32 Koder, R. L. & Dutton, P. L. Intelligent design: the de novo engineering of proteins with specified functions. *Dalton Trans.* **25**, 3045-3051 (2006).
- 33 Faiella, M. *et al.* An artificial di-iron oxo-protein with phenol oxidase activity. *Nat. Chem. Biol.* **5**, 882-884 (2009).

- 34 Smith, B. A. & Hecht, M. H. Novel proteins: from fold to function. *Curr. Opin. Chem. Biol.* **15**, 421-426 (2011).
- 35 Zastrow, M. L., Peacock, A. F., Stuckey, J. A. & Pecoraro, V. L. Hydrolytic catalysis and structural stabilization in a designed metalloprotein. *Nat. Chem.* **4**, 118-123 (2011).
- 36 Stenner, R., Steventon, J. W., Seddon, A. & Anderson, J. L. R. A de novo peroxidase is also a promiscuous yet stereoselective carbene transferase. *Proc. Natl. Acad. Sci. USA* **117**, 1419-1428 (2020).
- 37 Chino, M. *et al.* A De Novo Heterodimeric Due Ferri Protein Minimizes the Release of Reactive Intermediates in Dioxygen-Dependent Oxidation. *Angew. Chem. Int. Ed.* **56**, 15580–15583 (2017).
- 38 Lombardi, A., Pirro, F., Maglio, O., Chino, M. & DeGrado, W. F. De Novo Design of Four-Helix Bundle Metalloproteins: One Scaffold, Diverse Reactivities. *Acc. Chem. Res.* **52**, 1148-1159 (2019).
- 39 Reig, J. A. *et al.* Alteration of the oxygen-dependent reactivity of *de novo* Due Ferri proteins. *Nat. Chem.* **4**, 900-906 (2012). **Demonstration that the catalytic function of de novo Due Ferri proteins can be altered through rational reprogramming of the metal coordination environment.**
- 40 Salgado, E. N., Faraone-Mennella, J., & Tezcan, F. A. Controlling protein-protein interactions through metal coordination: assembly of a 16-helix bundle protein. *J. Am. Chem. Soc.* **129**, 13374–13375 (2007).
- 41 Der, B. S. *et al.* Metal-mediated affinity and orientation specificity in a computationally designed protein homodimer. *J. Am. Chem. Soc.* **134**, 375–385 (2012).
- 42 Der, B. S., Edwards, D. R. & Kuhlman, B. Catalysis by a de novo zinc-mediated protein interface: implications for natural enzyme evolution and rational enzyme engineering. *Biochemistry* **51**, 3933-3940 (2012).
- 43 Studer, S. *et al.* Evolution of a highly active and enantiospecific metalloenzyme from short peptides. *Science* **362**, 1285-1288, (2018). **Design and evolution transforms a designed zinc-binding peptide into a globular metalloenzyme that accelerates ester hydrolysis with high efficiency.**
- 44 Basler, S. *et al.* Efficient Lewis acid catalysis of an abiological reaction in a de novo protein scaffold. *Nat. Chem.* **13**, 231-235 (2021). **Engineering a de novo metalloenzyme to accelerate a bimolecular hetero-Diels-Alder reaction with high specificity.**
- 45 Chin, J. W. Expanding and reprogramming the genetic code. *Nature* **550**, 53-60 (2017).
- 46 Liu, C. C. & Schultz, P. G. Adding new chemistries to the genetic code. *Annu. Rev. Biochem.* **79**, 413-444 (2010).
- 47 Seyedsayamdost, M. R., Xie, J., Chan, C. T. Y., Schultz, P. G. & Stubbe, J. Site-Specific Insertion of 3-Aminotyrosine into Subunit $\alpha 2$ of E. coli Ribonucleotide Reductase: Direct Evidence for Involvement of Y730 and Y731 in Radical Propagation. *J. Am. Chem. Soc.* **129**, 15060–15071 (2007).
- 48 Faraldos, J. A. *et al.* Probing Eudesmane Cation- π Interactions in Catalysis by

- Aristolochene Synthase with Non-canonical Amino Acids. *J. Am. Chem. Soc.* **133**, 13906–13909 (2011).
- 49 Wu, Y. & Boxer, S. G. A Critical Test of the Electrostatic Contribution to Catalysis with Noncanonical Amino Acids in Ketosteroid Isomerase. *J. Am. Chem. Soc.* **138**, 11890–11895 (2016).
- 50 Ortmayer, M. *et al.* Rewiring the "Push-Pull" Catalytic Machinery of a Heme Enzyme Using an Expanded Genetic Code. *ACS Catal.* **10**, 2735-2746 (2020).
- 51 Ortmayer, M. *et al.* A Noncanonical Tryptophan Analogue Reveals an Active Site Hydrogen Bond Controlling Ferryl Reactivity in a Heme Peroxidase. *JACS Au* **1**, 913-918 (2021).
- 52 Li, J. C., Liu, T., Wang, Y., Mehta, A. P. & Schultz, P. G. Enhancing Protein Stability with Genetically Encoded Noncanonical Amino Acids. *J. Am. Chem. Soc.* **140**, 15997–16000 (2018).
- 53 Green, A. P., Hayashi, T., Mittl, P. R. & Hilvert, D. A Chemically Programmed Proximal Ligand Enhances the Catalytic Properties of a Heme Enzyme. *J. Am. Chem. Soc.* **138**, 11344-11352 (2016).
- 54 Zhao, J., Burke, A. J. & Green, A. P. Enzymes with noncanonical amino acids. *Curr. Opin. Chem. Biol.* **55**, 136-144 (2020).
- 55 Burke, A. J. *et al.* Design and evolution of an enzyme with a non-canonical organocatalytic mechanism. *Nature* **570**, 219-223 (2019). **The development of a hydrolytic enzyme that uses a non-canonical amino acid as the key catalytic nucleophile.**
- 56 Bolon, D. N. & Mayo, S. L. Enzyme-like proteins by computational design. *Proc. Natl Acad. Sci. USA* **98**, 14274–14279 (2001).
- 57 Richter, F. *et al.* Computational design of catalytic dyads and oxyanion holes for ester hydrolysis. *J. Am. Chem. Soc.* **134**, 16197–16206 (2012).
- 58 Rajagopalan, S. *et al.* Design of activated serine-containing catalytic triads with atomic-level accuracy. *Nat. Chem. Biol.* **10**, 386–391 (2014).
- 59 Moroz, Y. S. *et al.* New tricks for old proteins: single mutations in a nonenzymatic protein give rise to various enzymatic activities. *J. Am. Chem. Soc.* **137**, 14905–14911 (2015).
- 60 Burton, A. J., Thomson, A. R., Dawson, W. M., Brady, R. L. & Woolfson, D. N. Installing hydrolytic activity into a completely de novo protein framework. *Nat. Chem.* **8**, 837–844 (2016).
- 61 Drienovska, I., Mayer, C., Dulson, C. & Roelfes, G. A designer enzyme for hydrazone and oxime formation featuring an unnatural catalytic aniline residue. *Nat. Chem.* **10**, 946-952 (2018). **Development of an artificial enzyme that uses an unnatural aniline residue to promote oxime and hydrazone formations.**
- 62 Mayer, C., Dulson, C., Reddem, E., Thunnissen, A. W. H. & Roelfes, G. Directed Evolution of a Designer Enzyme Featuring an Unnatural Catalytic Amino Acid. *Angew. Chem. Int. Ed. Engl.* **58**, 2083-2087 (2019).

- 63 Tramontano, A., Janda, K. D. & Lerner, R. A. Catalytic antibodies. *Science* **234**, 1566-1570 (1986).
- 64 Wagner, J., Lerner, R. A. & Barbas, C. F., 3rd. Efficient aldolase catalytic antibodies that use the enamine mechanism of natural enzymes. *Science* **270**, 1797-1800 (1995).
- 65 Gouverneur, V. E. *et al.* Control of the exo and endo pathways of the Diels-Alder reaction by antibody catalysis. *Science* **262**, 204-208 (1993).
- 66 Wentworth, P., Jr. *et al.* Antibody catalysis of the oxidation of water. *Science* **293**, 1806-1811 (2001).
- 67 Hsieh, L. C., Yonkovich, S., Kochersperger, L. & Schultz, P. G. Controlling chemical reactivity with antibodies. *Science* **260**, 337-339 (1993).
- 68 Hilvert, D. Critical analysis of antibody catalysis. *Annu Rev Biochem* **69**, 751-793 (2000).
- 69 Bolon, D. N. & Mayo, S. L. Enzyme-like proteins by computational design. *Proc. Natl. Acad. Sci. USA* **98**, 14274-14279 (2001).
- 70 Rothlisberger, D. *et al.* Kemp elimination catalysts by computational enzyme design. *Nature* **453**, 190-195 (2008).
- 71 Privett, H. K. *et al.* Iterative approach to computational enzyme design. *Proc. Natl. Acad. Sci. USA* **109**, 3790-3795 (2012).
- 72 Jiang, L. *et al.* De novo computational design of retro-aldol enzymes. *Science* **319**, 1387-1391 (2008).
- 73 Siegel, J. B. *et al.* Computational design of an enzyme catalyst for a stereoselective bimolecular Diels-Alder reaction. *Science* **329**, 309-313 (2010). **Computational design and experimental characterization of enzymes catalyzing a bimolecular Diels-Alder reaction, an important carbon-carbon bond forming process.**
- 74 Blomberg, R. *et al.* Precision is essential for efficient catalysis in an evolved Kemp eliminase. *Nature* **503**, 418-421 (2013). **Demonstrates that artificial enzymes can be evolved to accelerate elementary chemical reactions with efficiencies comparable to natural enzymes.**
- 75 Preiswerk, N. *et al.* Impact of scaffold rigidity on the design and evolution of an artificial Diels-Alderase. *Proc. Natl. Acad. Sci. USA* **111**, 8013-8018 (2014).
- 76 Obexer, R. *et al.* Emergence of a catalytic tetrad during evolution of a highly active artificial aldolase. *Nat. Chem.* **9**, 50-56 (2017). **Ultra-high throughput screening facilitates the development of an artificial aldolase with efficiencies comparable to natural class I aldolases.**
- 77 Crawshaw *et al.* Engineering an Efficient and Enantioselective Enzyme for the Morita-Baylis-Hillman Reaction. *Nature Chemistry*, manuscript accepted. **Demonstration that laboratory evolution of designed enzymes can deliver sophisticated active sites to accelerate complex non-biological transformations.**
- 78 Otten, R. *et al.* How directed evolution reshapes the energy landscape in an enzyme to boost catalysis. *Science* **370**, 1442-1446 (2020).

- 79 Broom, A. *et al.* Ensemble-based enzyme design can recapitulate the effects of laboratory directed evolution in silico. *Nat. Commun.* **11**, 4808 (2020).
- 80 Althoff, E. A. *et al.* Robust design and optimization of retroaldol enzymes. *Protein Sci.* **21**, 717-726 (2012).
- 81 Giger, L. *et al.* Evolution of a designed retro-aldolase leads to complete active site remodeling. *Nat. Chem. Biol.* **9**, 494-498 (2013).
- 82 Eiben, C. B. *et al.* Increased Diels-Alderase activity through backbone remodeling guided by Foldit players. *Nat. Biotechnol.* **30**, 190-192 (2012).
- 83 Bjelic, S. *et al.* Computational design of enone-binding proteins with catalytic activity for the Morita-Baylis-Hillman reaction. *ACS Chem. Biol.* **8**, 749-757 (2013).
- 84 Kiss, G., Rothlisberger, D., Baker, D. & Houk, K. N. Evaluation and ranking of enzyme designs. *Protein Sci.* **19**, 1760–1773 (2010).
- 85 Frushicheva, M. P., Cao, J., Chu, Z. T. & Warshel, A. Exploring challenges in rational enzyme design by simulating the catalysis in artificial Kemp eliminase. *Proc. Natl. Acad. Sci. USA* **107**, 16869–16874 (2010).
- 86 Bunzel, H.A. *et al.* Evolution of dynamical networks enhances catalysis in a designer enzyme. *Nat. Chem.* **13**, 1017–1022 (2021).
- 87 Weitzner, B. D., Kipnis, Y., Daniel, A. G., Hilvert, D. & Baker, D. A computational method for design of connected catalytic networks in proteins. *Protein Sci.* **28**, 2036-2041 (2019).
- 88 Davey, J. A., Damry, A. M., Goto, N. K. & Chica, R. A. Rational design of proteins that exchange on functional timescales. *Nat. Chem. Biol.* **13**, 1280-1285 (2017).
- 89 Pan, X. *et al.* Expanding the space of protein geometries by computational design of de novo fold families. *Science* **369**, 1132-1136 (2021).
- 90 Huang, P. S., Boyken, S. E. & Baker, D. The coming of age of de novo protein design. *Nature* **537**, 320-327, (2016).
- 91 Dou, J. *et al.* De novo design of a fluorescence-activating beta-barrel. *Nature* **561**, 485-491 (2018).
- 92 Wei, K. Y. *et al.* Computational design of closely related proteins that adopt two well-defined but structurally divergent folds. *Proc. Natl. Acad. Sci. USA* **117**, 7208-7215 (2020).
- 93 Senior, A. W. *et al.* Improved protein structure prediction using potentials from deep learning. *Nature* **577**, 706-710 (2020). **Development of AlphaFold, a deep learning algorithm for accurate prediction of protein structure from primary sequence.**
- 94 Hiranuma, N. *et al.* Improved protein structure refinement guided by deep learning based accuracy estimation. *Nat. Commun.* **12**, 1340 (2021).
- 95 Baek, M. *et al.* Accurate prediction of protein structures and interactions using a 3-track network. *Science* **373**, 871-876 (2021). **Development of RoseTTAFold, a freely available deep learning program for fast and accurate prediction of protein structure.**

- 96 Jumper, J. *et al.* Highly accurate protein structure prediction with AlphaFold. *Nature* **596**, 583-589 (2021).
- 97 Anishchenko, I., Chidyausiku, T. M., Ovchinnikov, S., Pellock, S. J. & Baker, D. De novo protein design by deep network hallucination. <https://www.biorxiv.org/content/10.1101/2020.07.22.211482v1>.
- 98 Mazurenko, S., Prokop, Z. & Damborsky, J. Machine Learning in Enzyme Engineering. *ACS Catal.* **10**, 1210-1223 (2020).
- 99 Ma, E. J. *et al.* Machine-Directed Evolution of an Imine Reductase for Activity And Stereoselectivity. *ACS Catal.* **11**, 12433-12445 (2021).
- 100 Bedbrook, C. N., Yang, K. K., Rice, A. J., Gradinaru, V. & Arnold, F. A. Machine learning to design integral membrane channelrhodopsins for efficient eukaryotic expression and plasma membrane localization. *PLoS Comput. Biol.* **13**, e1005786 (2017).
- 101 Wu, Z., Kan, S. B. J., Lewis, R. D., Wittmann, B. J. & Arnold, F. H. Machine learning-assisted directed protein evolution with combinatorial libraries. *Proc. Natl. Acad. Sci. USA* **116**, 8852-8858 (2019).
- 102 Tischer, D. *et al.* Design of proteins presenting discontinuous functional sites using deep learning. <https://www.biorxiv.org/content/10.1101/2020.11.29.402743v1>.
- 103 Russ, W. P. *et al.* An evolution-based model for designing chorismate mutase enzymes. *Science* **369**, 440-445 (2020).
- 104 Hayashi, T. *et al.* Capture and characterization of a reactive haem–carbenoid complex in an artificial metalloenzyme. *Nat. Catal.* **1**, 578-584 (2018).
- 105 Carminati, D. M. & Fasan, R. Stereoselective Cyclopropanation of Electron-Deficient Olefins with a Cofactor Redesign Carbene Transferase Featuring Radical Reactivity. *ACS Catal.* **9**, 9683-9687 (2019).
- 106 Erkkila, A., Majander, I. & Pihko, P. M. Iminium catalysis. *Chem. Rev.* **107**, 5416-5470 (2007).
- 107 Mukherjee, S., Yang, J. W., Hoffmann, S. & List, B. Asymmetric enamine catalysis. *Chem. Rev.* **107**, 5471-5569 (2007).
- 108 Doyle, A. G. & Jacobsen, E. N. Small-molecule H-bond donors in asymmetric catalysis. *Chem. Rev.* **107**, 5713-5743 (2007).
- 109 Wurz, R. P. Chiral dialkylaminopyridine catalysts in asymmetric synthesis. *Chem. Rev.* **107**, 5570–5595 (2007).
- 110 Beeson, T. D., Mastracchio, A., Hong, J. B., Ashton, K. & Macmillan, D. W. Enantioselective organocatalysis using SOMO activation. *Science* **316**, 582-585 (2007).
- 111 St-Jacques, A.D., Eyahpaise, M.-E. C. & Chica, R.A. Computational Design of Multisubstrate Enzyme Specificity. *ACS Catal.* **9**, 5480-5485 (2019).
- 112 Davey, J. A. & Chica, R. A. Multistate approaches in computational protein design. *Protein Sci.* **21**, 1241-1252 (2012).